



biomedicines

Hypoxia-Inducible Factors

Regulation and Therapeutic Potential

Edited by

Kiichi Hirota

Printed Edition of the Special Issue Published in *Biomedicines*

Hypoxia-Inducible Factors: Regulation and Therapeutic Potential

Hypoxia-Inducible Factors: Regulation and Therapeutic Potential

Editor

Kiichi Hirota

MDPI • Basel • Beijing • Wuhan • Barcelona • Belgrade • Manchester • Tokyo • Cluj • Tianjin



Editor

Kiichi Hirota
Kansai Medical University
Japan

Editorial Office

MDPI
St. Alban-Anlage 66
4052 Basel, Switzerland

This is a reprint of articles from the Special Issue published online in the open access journal *Biomedicines* (ISSN 2227-9059) (available at: https://www.mdpi.com/journal/biomedicines/special_issues/hypoxia-inducible_factors).

For citation purposes, cite each article independently as indicated on the article page online and as indicated below:

LastName, A.A.; LastName, B.B.; LastName, C.C. Article Title. <i>Journal Name</i> Year , <i>Volume Number</i> , Page Range.
--

ISBN 978-3-0365-2912-7 (Hbk)

ISBN 978-3-0365-2913-4 (PDF)

© 2022 by the authors. Articles in this book are Open Access and distributed under the Creative Commons Attribution (CC BY) license, which allows users to download, copy and build upon published articles, as long as the author and publisher are properly credited, which ensures maximum dissemination and a wider impact of our publications.

The book as a whole is distributed by MDPI under the terms and conditions of the Creative Commons license CC BY-NC-ND.

Contents

About the Editor	vii
Preface to "Hypoxia-Inducible Factors: Regulation and Therapeutic Potential"	ix
Kiichi Hirota Special Issue: Hypoxia-Inducible Factors: Regulation and Therapeutic Potential Reprinted from: <i>Biomedicines</i> 2021, 9, 1768, doi:10.3390/biomedicines9121768	1
Hidemasa Bono and Kiichi Hirota Meta-Analysis of Hypoxic Transcriptomes from Public Databases Reprinted from: <i>Biomedicines</i> 2020, 8, 10, doi:10.3390/biomedicines8010010	5
Philipp Moog, Katharina Kirchhoff, Sanjar Bekeran, Anna-Theresa Bauer, Sarah von Isenburg, Ulf Dornseifer, Hans-Günther Machens, Arndt F. Schilling and Ektoras Hadjipanayi Comparative Evaluation of the Angiogenic Potential of Hypoxia Preconditioned Blood-Derived Secretomes and Platelet-Rich Plasma: An In Vitro Analysis Reprinted from: <i>Biomedicines</i> 2020, 8, 16, doi:10.3390/biomedicines8010016	17
Kiichi Hirota Basic Biology of Hypoxic Responses Mediated by the Transcription Factor HIFs and Its Implication for Medicine Reprinted from: <i>Biomedicines</i> 2020, 8, 32, doi:10.3390/biomedicines8020032	41
Philipp Moog, Maryna Jensch, Jessica Hughes, Burak Salgin, Ulf Dornseifer, Hans-Günther Machens, Arndt F. Schilling and Ektoras Hadjipanayi Use of Oral Anticoagulation and Diabetes Do Not Inhibit the Angiogenic Potential of Hypoxia Preconditioned Blood-Derived Secretomes Reprinted from: <i>Biomedicines</i> 2020, 8, 283, doi:10.3390/biomedicines8080283	67
Philipp Moog, Rahmin Schams, Alexander Schneidinger, Arndt F. Schilling, Hans-Günther Machens, Ektoras Hadjipanayi and Ulf Dornseifer Effect of Hypoxia Preconditioned Secretomes on Lymphangiogenic and Angiogenic Sprouting: An in Vitro Analysis Reprinted from: <i>Biomedicines</i> 2020, 8, 365, doi:10.3390/biomedicines8090365	89
Shuoyu Wei, Takayuki Isagawa, Masamichi Eguchi, Daisuke Sato, Hiroto Tsukano, Keishi Miyata, Yuichi Oike, Norihiko Takeda, Satoshi Ikeda, Hiroaki Kawano and Koji Maemura Febuxostat, a Xanthine Oxidase Inhibitor, Decreased Macrophage Matrix Metalloproteinase Expression in Hypoxia Reprinted from: <i>Biomedicines</i> 2020, 8, 470, doi:10.3390/biomedicines8110470	105
Yuling Chen and Timo Gaber Hypoxia/HIF Modulates Immune Responses Reprinted from: <i>Biomedicines</i> 2021, 9, 260, doi:10.3390/biomedicines9030260	119
Kiichi Hirota HIF- α Prolyl Hydroxylase Inhibitors and Their Implications for Biomedicine: A Comprehensive Review Reprinted from: <i>Biomedicines</i> 2021, 9, 468, doi:10.3390/biomedicines9050468	151

Yoko Ono and Hidemasa Bono

Multi-Omic Meta-Analysis of Transcriptomes and the Bibliome Uncovers Novel
Hypoxia-Inducible Genes

Reprinted from: *Biomedicines* **2021**, *9*, 582, doi:10.3390/biomedicines9050582 **177**

About the Editor

Kiichi Hirota is a member of the Institute of Biomedical Science, Head of the Department of Human Stress Response Science, and a professor at Kansai Medical University, Hirakata, Japan. After receiving a Ph.D. in redox biology in the laboratory of Junji Yodoi, Institute for Virus Research, Kyoto, Japan, he started a career as a physician–scientist at Kyoto University Hospital. Then, he was involved in the search for hypoxia biology in the laboratory of Gregg L. Semenza, Johns Hopkins University. As a board-certified anesthesiologist and physician-scientist, he is involved in critical care medicine from the perspective of oxygen metabolism in his own laboratory at Kansai Medical University, Hirakata, Japan.

Preface to "Hypoxia-Inducible Factors: Regulation and Therapeutic Potential"

The role of oxygen as an essential molecule in our survival as mammals is indisputable.

The Special Issue Editor is an anesthesiologist. For anesthesiologists and intensivists, an important goal of patient management is to maintain oxygen homeostasis in patients admitted to the operating room or intensive care unit. For this purpose, it is essential to understand the organism's strategies against oxygen imbalance, especially concerning oxygen deprivation (hypoxia). Adaptation to hypoxia and the maintenance of oxygen homeostasis involves a wide range of responses that occur at different tissue levels in the body. On the other hand, oxygen produces cellular damage through the production of reactive oxygen species. Thus, living organisms are built on a precarious balance surrounding oxygen.

Reactive oxygen species and hypoxic conditions produce a signal in the body. In other words, the constantly fluctuating partial pressure of oxygen serves as a cue for the biological response, and a system for rapid response was constructed in the process of evolution. In this way, an *in vivo* system that senses the dysregulation of oxygen metabolism was developed, and attempts were made to understand this system through comprehensive gene expression analysis. Various endogenous and exogenous stimuli generate reactive oxygen species (ROS), which cause oxidative stress to the organism. Due to the ease of experimental techniques, gene expression studies have accumulated a vast amount of data. However, research on hypoxia using molecular biology has lagged, since molecular oxygen is a gas under atmospheric pressure and normal temperature. The solution to this problem remained an open question until the beginning of the 21st century, when the molecular mechanisms that explain the maintenance and induction of erythropoietin (EPO) expression were discovered. In the early 1990s, the transcription factor hypoxia-inducible factor 1 (HIF-1) was isolated as a factor that explains the molecular mechanism of the maintenance and the induction of erythropoietin (EPO) expression. After cDNA cloning in 1995, a line of research into HIF-1 activation elucidated the molecular mechanism of its regulation of activity in an oxygen partial-pressure-dependent manner. Three enzymes responsible for the hydroxylation of proline residues and one enzyme responsible for the hydroxylation of asparagine residues in the α -subunit of HIF (HIF- α), are now known to play an essential role in this process. There is a consensus that these are cellular "hypoxia sensors". The 2019 Nobel Prize in Physiology or Medicine was awarded to three researchers for their outstanding work in identifying HIF, isolating the molecule, and studying its activation mechanism.

Oxygen is an essential molecule for ATP production in cells, and a scheme is assumed in which the maintenance of biological functions becomes impossible due to the lack of energy caused by its deficiency. It has been thought that a lack of oxygen leads to cell death, the malfunction of biological functions, and death of the individual. However, the classical view of oxygen has been completely revised in the last 20 years. Oxygen is an essential molecule for the maintenance of life. Still, we mammals do not have a mechanism to biosynthesize oxygen in our bodies, and higher organisms such as vertebrates, which are composed of various tissues and organs, are always "deficient" in oxygen. The mainstream view is that the body has evolved mechanisms to respond to the lack of essential molecules or hypoxia and has actively used them to maintain bodily integrity.

This e-book is a collection of research and review papers covering various areas of oxygen biology research that focus on, among other factors, the fundamental understanding of HIF signaling pathways and related gene expression profiling; epigenetic regulation; diagnostics, prognostics, and pharmacogenomic biomarkers; molecular targets driving the regulation of human physiology and pathophysiology; clinical trials with new agents; and validation in animal models.

Kiichi Hirota

Editor



Editorial

Special Issue: Hypoxia-Inducible Factors: Regulation and Therapeutic Potential

Kiichi Hirota

Department of Human Stress Response Science, Institute of Biomedical Science, Kansai Medical University, Hirakata 573-1010, Osaka, Japan; khirota-kyt@umin.ac.jp; Tel.: +81-72-804-2526

Oxygen (O₂) is an essential molecule [1] in the production of adenosine triphosphate (ATP) in cells, and a lack of energy due to O₂ deficiency makes the maintenance of biological functions and human life improbable. Since oxygen functions as the final electron acceptor in the series of ATP synthesis reactions in conjunction with oxidative phosphorylation in mitochondria, its deficiency causes the oxidation of a series of coenzymes such as nicotinamide and flavin adenine dinucleotide and the reduction in oxygen molecules to water molecules (H₂O). Persistent deficiency has been believed to cause to the loss of biological functions, even resulting in death. This classical view of oxygen has been completely revised over the last 20 years. Mammals do not have a mechanism for biosynthesizing oxygen in their bodies. In higher organisms such as vertebrates, which possess many organs, oxygen in the body is always “scarce,”; therefore, the dominant view is that organisms have evolved mechanisms to respond to the lack of this essential molecule (hypoxia), and actively use it to maintain body integrity [2,3].

Anatomically complex, higher multicellular organisms are equipped with specialized mechanisms to enable all cells to obtain sufficient oxygen. The respiratory system consists of lungs, which provide oxygen to be transferred to hemoglobin in red blood cells, the diaphragm, other respiratory support muscles, and neuroepithelial cells that sense the partial pressure of oxygen. The cardiovascular system consists of red blood cells, oxygen-carrying medium, the heart, the transport engine, blood vessels, and transport channels. The proper development and preservation of these systems require the harmonious expression of thousands of genes. The transcription factor responsible for such gene expression is hypoxia-inducible factor 1 (HIF-1) [3].

In the late 1980s, a team at Johns Hopkins University in Baltimore, USA, searched for an intracellular factor involved in the hypoxia-induced expression of erythropoietin (Epo) and isolated the complementary DNA (cDNA) of a transcription factor in 1995 [4]. This transcription factor was named HIF-1 [5–7]. A closely related gene, hypoxia-inducible factor 2 α (HIF2A) or endothelial PAS domain protein 1 (EPAS1), was identified and cloned in 1997, followed by hypoxia inducible factor 3 α (HIF3A) in 1998 [8]. A series of genes, including those coding for various glycolytic enzymes, glucose transport proteins, vascular endothelial growth factor, and hematopoietic factor Epo, are regulated by HIFs at the transcriptional level. Therefore, HIFs play a role in the activation of “hypoxia-inducible” genes, and we can refer to the term “HIF” as “Highly Involved Factor” [9].

In 2019, the Nobel Prize in Physiology or Medicine was awarded to three researchers for outstanding achievements in this field [10–12].

In this Special Issue, we invited research and review papers in various areas of oxygen biology research that focused on the fundamental understanding of HIF signaling pathways and related gene expression profiling, as well as pharmacogenomic biomarkers, molecular targets driving the regulation of human physiology and pathophysiology, and validation in animal models. As a result, we published six original papers and three review articles in this Special Issue [1,13–20].

Changes in gene expression in response to hypoxic stimuli were studied, with the discovery of hypoxia response systems represented by HIFs. Bono et al. performed a

Citation: Hirota, K. Special Issue: Hypoxia-Inducible Factors: Regulation and Therapeutic Potential. *Biomedicines* **2021**, *9*, 1768. <https://doi.org/10.3390/biomedicines9121768>

Received: 26 October 2021

Accepted: 29 October 2021

Published: 25 November 2021

Publisher’s Note: MDPI stays neutral with regard to jurisdictional claims in published maps and institutional affiliations.



Copyright: © 2021 by the author. Licensee MDPI, Basel, Switzerland. This article is an open access article distributed under the terms and conditions of the Creative Commons Attribution (CC BY) license (<https://creativecommons.org/licenses/by/4.0/>).

meta-analysis of RNA-sequencing data from hypoxic transcriptomes archived in public databases. In addition, meta-analyzed hypoxic transcriptome data were integrated with public chromatin immunoprecipitation-sequencing data on the known human HIFs, HIF-1, and HIF-2, to provide insights into hypoxia-responsive pathways involving direct transcription factor binding. This study serves as a useful resource for hypoxia research [13]. However, Bono and Ono hypothesized that some hypoxia-responsive genes might not have yet been discovered, hiding behind famous genes. Furthermore, they searched for novel hypoxia-responsive genes in a data-driven manner by utilizing biodigital transformation [19], where data accumulated in a public database (DB) were used for research. They constructed a meta-analysis method to evaluate variations in the expression levels of all genes collected from public databases, before and after hypoxic stimulation, and discovered several novel hypoxia-responsive genes using a multi-omics analysis that integrated information on all genes in the article database. They also created a data-driven meta-analysis method to evaluate alterations in the expression information (transcriptome) of all genes with and without hypoxic stimulation collected from public databases. Thus, they discovered several novel hypoxia-responsive genes through a multi-omics analysis that integrated the collected transcriptome information with genes published in all papers (bibliome) in the public DB.

The secretome is expected to be useful in biomarker discovery because it contains abundant proteins and fragments of membrane proteins secreted and released by cancer cells, unlike blood samples, which do not contain secretions from various tissues.

The term “secretome” is a general term that includes not only soluble proteins released from cells via the endoplasmic reticulum (ER)-Golgi pathway, but also extracellular matrix proteins and cleaved fragments of membrane proteins. Moog et al. have shown that the properties of the secretome are affected by hypoxia in a series of studies [16–18].

It has been reported that HIF-1 regulates the induction of matrix metalloproteinases (MMPs). Wei et al. found that xanthine oxidase-derived reactive oxygen species (ROS) induced MMP-3, MMP-10, and MMP-13 in mouse macrophages upon hypoxic exposure. Induction was not inhibited by HIF-1 α -deficient macrophages, but was HIF-1-independent. Additionally, induction was found to be inhibited by febuxostat, a xanthine oxidase inhibitor. Febuxostat administration is a potential therapeutic option for disease management in atherosclerotic patients [20].

The role of oxygen metabolism in the regulation of inflammation and immune responses has attracted attention. Humoral factors, including cytokines and chemokines, and physical stimuli such as heat and tissue breakdown induce ROS and generate oxidative stress, while impaired blood vessels, impaired blood flow, increased oxygen consumption by infiltrating cells, and impaired oxygen diffusion due to edema reducing the oxygen concentration in tissues. Inflammatory cells, which work “in the field” of inflammation, adapt to these changes in the oxygen environment to maintain cellular functions and contribute to biological defense and homeostasis [21,22]. Chen and Gaber summarized the effects of physiological and pathophysiological hypoxia on innate and adaptive immune activity. We provide an overview on the control of immune response by cellular hypoxia-induced pathways, with a focus on the role of HIFs, and discuss the opportunity to target hypoxia-sensitive pathways for the treatment of cancer and autoimmunity [14].

HIF plays an essential role in this process; it is a transcription factor that mediates Epo induction at the transcriptional level under hypoxic conditions. In 2001, cDNA cloning of dioxygenases acting on prolines and asparagine residues, which play essential roles in this process, was reported. HIF-prolyl hydroxylases (PHs) constitute the core molecular mechanism for detecting a decrease in the partial pressure of oxygen, or hypoxia, in the cells, and are known as oxygen sensors [23–26]. In this review, I discuss the process of the molecular cloning of HIF and HIF-PHs, which explains hypoxia-induced Epo expression, the development of HIF-PH inhibitors that artificially or exogenously activate HIF by inhibiting HIF-PH, and the significance and implications of medical intervention using HIF-PH inhibitors [15].

We hope that this Special Issue will reflect the current exciting researches concerning HIFs and their applications in medicine and health science.

Funding: This research received no external funding.

Conflicts of Interest: The authors declare no conflict of interest.

References

- Hirota, K. Basic Biology of Hypoxic Responses Mediated by the Transcription Factor HIFs and its Implication for Medicine. *Biomedicines* **2020**, *8*, 32. [[CrossRef](#)] [[PubMed](#)]
- West, J.B. Physiological Effects of Chronic Hypoxia. *N. Engl. J. Med.* **2017**, *376*, 1965–1971. [[CrossRef](#)] [[PubMed](#)]
- Semenza, G.L. Oxygen sensing, homeostasis, and disease. *N. Engl. J. Med.* **2011**, *365*, 537–547. [[CrossRef](#)] [[PubMed](#)]
- Semenza, G.L.; Neffelt, M.K.; Chi, S.M.; Antonarakis, S.E. Hypoxia-inducible nuclear factors bind to an enhancer element located 3' to the human erythropoietin gene. *Proc. Natl. Acad. Sci. USA* **1991**, *88*, 5680–5684. [[CrossRef](#)]
- Wang, G.; Semenza, G. Characterization of hypoxia-inducible factor 1 and regulation of DNA binding activity by hypoxia. *J. Biol. Chem.* **1993**, *268*, 21513–21518. [[CrossRef](#)]
- Wang, G.; Jiang, B.; Rue, E.; Semenza, G. Hypoxia-inducible factor 1 is a basic-helix-loop-helix-PAS heterodimer regulated by cellular O₂ tension. *Proc. Natl. Acad. Sci. USA* **1995**, *92*, 5510–5514. [[CrossRef](#)]
- Wang, G.; Semenza, G. Purification and characterization of hypoxia-inducible factor 1. *J. Biol. Chem.* **1995**, *270*, 1230–1237. [[CrossRef](#)]
- Keith, B.; Johnson, R.S.; Simon, M.C. HIF1alpha and HIF2alpha: Sibling rivalry in hypoxic tumour growth and progression. *Nat. Rev. Cancer* **2011**, *12*, 9–22. [[CrossRef](#)] [[PubMed](#)]
- Semenza, G.L. HIF-1 and human disease: One highly involved factor. *Genes Dev.* **2000**, *14*, 1983–1991. [[CrossRef](#)]
- Shimoda, L.A. Raise your glass: Celebrating the 2019 Nobel Prize in Physiology or Medicine. *Am. J. Physiol. Lung Cell Mol. Physiol.* **2020**, *318*, L147–L148. [[CrossRef](#)]
- Moslehi, J.; Rathmell, W.K. The 2019 Nobel Prize honors fundamental discoveries in hypoxia response. *J. Clin. Investig.* **2020**, *130*, 4–6. [[CrossRef](#)] [[PubMed](#)]
- Ledford, H.; Callaway, E. Biologists who decoded how cells sense oxygen win medicine Nobel. *Nature* **2019**, *574*, 161–162. [[CrossRef](#)] [[PubMed](#)]
- Bono, H.; Hirota, K. Meta-Analysis of Hypoxic Transcriptomes from Public Databases. *Biomedicines* **2020**, *8*, 10. [[CrossRef](#)] [[PubMed](#)]
- Chen, Y.; Gaber, T. Hypoxia/HIF Modulates Immune Responses. *Biomedicines* **2021**, *9*, 260. [[CrossRef](#)]
- Hirota, K. HIF-alpha Prolyl Hydroxylase Inhibitors and Their Implications for Biomedicine: A Comprehensive Review. *Biomedicines* **2021**, *9*, 468. [[CrossRef](#)]
- Moog, P.; Jensch, M.; Hughes, J.; Salgin, B.; Dornseifer, U.; Machens, H.G.; Schilling, A.F.; Hadjipanayi, E. Use of Oral Anticoagulation and Diabetes Do Not Inhibit the Angiogenic Potential of Hypoxia Preconditioned Blood-Derived Secretomes. *Biomedicines* **2020**, *8*, 283. [[CrossRef](#)]
- Moog, P.; Kirchhoff, K.; Bekeran, S.; Bauer, A.T.; von Isenburg, S.; Dornseifer, U.; Machens, H.G.; Schilling, A.F.; Hadjipanayi, E. Comparative Evaluation of the Angiogenic Potential of Hypoxia Preconditioned Blood-Derived Secretomes and Platelet-Rich Plasma: An In Vitro Analysis. *Biomedicines* **2020**, *8*, 16. [[CrossRef](#)]
- Moog, P.; Schams, R.; Schneidinger, A.; Schilling, A.F.; Machens, H.G.; Hadjipanayi, E.; Dornseifer, U. Effect of Hypoxia Preconditioned Secretomes on Lymphangiogenic and Angiogenic Sprouting: An in Vitro Analysis. *Biomedicines* **2020**, *8*, 365. [[CrossRef](#)]
- Ono, Y.; Bono, H. Multi-Omic Meta-Analysis of Transcriptomes and the Bibliome Uncovers Novel Hypoxia-Inducible Genes. *Biomedicines* **2021**, *9*, 582. [[CrossRef](#)]
- Wei, S.; Isagawa, T.; Eguchi, M.; Sato, D.; Tsukano, H.; Miyata, K.; Oike, Y.; Takeda, N.; Ikeda, S.; Kawano, H.; et al. Febuxostat, a Xanthine Oxidase Inhibitor, Decreased Macrophage Matrix Metalloproteinase Expression in Hypoxia. *Biomedicines* **2020**, *8*, 470. [[CrossRef](#)]
- Nizet, V.; Johnson, R.S. Interdependence of hypoxic and innate immune responses. *Nat. Rev. Immunol.* **2009**, *9*, 609–617. [[CrossRef](#)] [[PubMed](#)]
- Taylor, C.T.; Colgan, S.P. Regulation of immunity and inflammation by hypoxia in immunological niches. *Nat. Rev. Immunol.* **2017**, *17*, 774–785. [[CrossRef](#)] [[PubMed](#)]
- Epstein, A.; Gleadle, J.; McNeill, L.; Hewitson, K.; O'Rourke, J.; Mole, D.; Mukherji, M.; Metzen, E.; Wilson, M.; Dhanda, A.; et al. *C. elegans* EGL-9 and mammalian homologs define a family of dioxygenases that regulate HIF by prolyl hydroxylation. *Cell* **2001**, *107*, 43–54. [[CrossRef](#)]
- Lando, D.; Peet, D.J.; Gorman, J.J.; Whelan, D.A.; Whitelaw, M.L.; Bruick, R.K. FIH-1 is an asparaginyl hydroxylase enzyme that regulates the transcriptional activity of hypoxia-inducible factor. *Genes Dev.* **2002**, *16*, 1466–1471. [[CrossRef](#)] [[PubMed](#)]
- Mahon, P.C.; Hirota, K.; Semenza, G.L. FIH-1: A novel protein that interacts with HIF-1alpha and VHL to mediate repression of HIF-1 transcriptional activity. *Genes Dev.* **2001**, *15*, 2675–2686. [[CrossRef](#)]

26. Lando, D.; Peet, D.J.; Whelan, D.A.; Gorman, J.J.; Whitelaw, M.L. Asparagine hydroxylation of the HIF transactivation domain a hypoxic switch. *Science* **2002**, *295*, 858–861. [[CrossRef](#)]



Article

Meta-Analysis of Hypoxic Transcriptomes from Public Databases

Hidemasa Bono ^{1,*} and Kiichi Hirota ^{2,*}

¹ Database Center for Life Science (DBCLS), Joint Support-Center for Data Science Research, Research Organization of Information and Systems, 1111 Yata, Mishima, Shizuoka 411-8540, Japan

² Department of Human Stress Response Science, Institute of Biomedical Science, Kansai Medical University, Hirakata 573-1010, Japan

* Correspondence: bono@dbcls.rois.ac.jp (H.B.); hif1@mac.com (K.H.); Tel.: +81-4-7135-5508 (H.B.)

Received: 30 November 2019; Accepted: 8 January 2020; Published: 9 January 2020

Abstract: Hypoxia is the insufficiency of oxygen in the cell, and hypoxia-inducible factors (HIFs) are central regulators of oxygen homeostasis. In order to obtain functional insights into the hypoxic response in a data-driven way, we attempted a meta-analysis of the RNA-seq data from the hypoxic transcriptomes archived in public databases. In view of methodological variability of archived data in the databases, we first manually curated RNA-seq data from appropriate pairs of transcriptomes before and after hypoxic stress. These included 128 human and 52 murine transcriptome pairs. We classified the results of experiments for each gene into three categories: upregulated, downregulated, and unchanged. Hypoxic transcriptomes were then compared between humans and mice to identify common hypoxia-responsive genes. In addition, meta-analyzed hypoxic transcriptome data were integrated with public ChIP-seq data on the known human HIFs, HIF-1 and HIF-2, to provide insights into hypoxia-responsive pathways involving direct transcription factor binding. This study provides a useful resource for hypoxia research. It also demonstrates the potential of a meta-analysis approach to public gene expression databases for selecting candidate genes from gene expression profiles generated under various experimental conditions.

Keywords: hypoxia; transcriptome; RNA-seq; ChIP-seq; public database; meta-analysis

1. Introduction

The development of high-throughput sequencing technology has enabled cost-effective reading of tens of millions of base pairs in a single run. RNA-seq takes advantage of this technology to elucidate the expression profiles of genes and transcriptomes assayed under particular conditions by producing counts of sequences corresponding to genes of interest.

Published transcriptome data have been archived to two large public databases (DBs), the Gene Expression Omnibus (GEO) in the US National Center for Biotechnology Information (NCBI) [1] and ArrayExpress (AE) in the European Bioinformatics Institute (EBI) [2]. The number of records in these DBs is now over two million in samples and near a hundred thousand in data series. They are freely accessible and thus ready to be reused for data-driven research. Nevertheless, large-scale comparison among archived data has not often been carried out because of the technical challenges presented by the magnitude, complexity, and cumbersome nature of the data. Even if very large amounts of data can be successfully downloaded, it can be difficult to interpret data from different laboratories, as experimental protocols used are not uniform.

Even though oxygen is an essential molecule for life support, higher organisms such as mammals do not have a mechanism to biosynthesize oxygen in the body. Organs and tissues are regularly exposed to risk of “oxygen deficiency”, and living organisms have evolved mechanisms to respond to hypoxia. The supply and consumption of oxygen determine its intracellular partial pressure, which is kept in a

relatively narrow range. Oxygen deficiency (hypoxia) and oxygen excess (hyperoxia) cause an adaptive response to maintain oxygen homeostasis at the cellular level. This includes adjustments to the energy metabolism system according to changes in oxygen partial pressure. In addition, higher organisms that are anatomically complex have specialized mechanisms to acquire necessary and sufficient oxygen for all cells. Proper functioning and regulation of these systems require the coordinated expression of many genes, and this is thought to be controlled by transcription factors known as hypoxia-inducible factors (HIFs, HIF-1 and HIF-2) [3]. The differential regulation of gene expression by HIF-1 and HIF-2 has been studied. Both HIF-1 and HIF-2 control the gene expression of glucose transporter 1 (GLUT1) and vascular endothelial growth factor A (VEGFA). Gene expression of glycolytic enzymes such as hexokinases (HK1 and HK2), phosphofructokinase (PFK), fructose-bisphosphate aldolase A (ALDOA), phosphoglycerate kinase 1 (PGK1), and lactate dehydrogenase (LDHA) controlled by mainly HIF-1. On the other hand, gene expression of erythropoietin (EPO) and POU5F1 (OCT4) is HIF-2-dependent [4].

Various groups have published comprehensive data on gene expression in response to hypoxic stress, but have not produced uniform results, and because of this the pathways involved are not entirely clear. In addition, there may be other data on hypoxia-related genes that have not been reported as such, due to the main experimental target not being hypoxic stress [5]. Collective analysis of gene expression and transcription factor binding information obtained from multiple studies that also introduces comparative analysis between species has not previously been attempted in this field. Further, although the analysis of many comprehensive datasets should enable the elucidation of novel control pathways, comprehensive methods to achieve this are lacking.

Based on the above background, this study aimed to develop a comparative data analysis method to identify expression fluctuations and transcription factor binding regions associated with hypoxic stress, and to use it to perform a meta-analysis of available data in the public DBs, and gene functional analyses. We first curated hypoxic RNA-seq transcriptome data from GEO and AE to make a list of hypoxia-normoxia transcriptome pairs. We then did systematic transcriptome quantification analysis on the datasets we collected. By introducing a new metric that counts instances of upregulation, downregulation, or unresponsiveness of genes, we determined the average effect of hypoxia on genes under different experimental conditions. We also compared these values between genes orthologous in humans and mice. In addition, we examined data from chromatin immunoprecipitation sequencing (ChIP-seq), which comprehensively elucidates the regions in which transcription factors bind to genomic DNA.

2. Materials and Methods

2.1. Curation of Public Gene Expression Data

In order to screen hypoxia-related gene expression data from public databases, we used a graphical web tool called All Of gene Expression (AOE; <https://aoe.dbcls.jp/>) [6]. AOE not only integrates metadata from the NCBI Gene Expression Omnibus (GEO) [1], EBI ArrayExpress (AE) [2], and DDBJ Genomic Expression Archive (GEA) [7], but also those of RNA-seq data archived only in the Sequence Read Archive (SRA) [8]. Conventional search by the keywords 'hypoxia' or 'hypoxic' in AOE was adopted to scan the databases initially. The curation of the data, which included paired 'hypoxia' and 'normoxia' experiment entries, and descriptions of cell line and experimental conditions (oxygen concentration) used, was done manually.

In our previous pilot study, we investigated the human and mouse data produced by Affymetrix GeneChip [9], but the subsequent accumulation of RNA-seq data enabled this study to be focused only on RNA-seq. In order to minimize the noise from different sequencing platforms, it was necessary to exclude data from older sequencing platforms. Consequently, nearly all data were the product of Illumina sequencing platforms. The complete lists of these paired data are available from figshare

(human: <https://doi.org/10.6084/m9.figshare.5811987.v2>; mouse: <https://doi.org/10.6084/m9.figshare.9948158.v1>).

2.2. Gene Expression Quantification

After we searched hypoxia-related entries using AOE, corresponding run data were downloaded from SRA in the DDBJ FTP site (<ftp://ftp.ddbj.nig.ac.jp/>). Since the downloaded data were in the SRA format, these files were transferred to FASTQ formatted files for expression quantification using the fasterq-dump program in the SRA Toolkit (<https://www.ncbi.nlm.nih.gov/sra/docs/toolkitsoft/>). Both single-end and paired-end reads were re-used for the analysis. RNA-seq reads were then quantified using ikra (v1.2.0) [10], an RNA-seq pipeline centered on Salmon [11]. Ikra automates the RNA-seq data analysis process, which includes quality control of reads (Trim Galore version 0.4.1 [12] with Cutadapt version 1.9.1 [13]) and transcript quantification (Salmon version 0.14.0 with reference transcript sets in GENCODE release 30 for human and M21 for mouse). These tools were used with default parameters in ikra. The workflow presented here was selected because we aimed to extract hypoxia inducible genes from heterogeneous RNA-seq data (single-end and paired-end) archived in SRA from various laboratories by counting upregulated and downregulated genes. In this study, the data acquisition and quality control process took around six weeks for the current data set. Processed transcript quantification from RNA-seq data was also uploaded to figshare and are publicly available (human: <https://doi.org/10.6084/m9.figshare.9948170.v1>; mouse: <https://doi.org/10.6084/m9.figshare.9948200.v1>).

Where hypoxia and normoxia transcriptome data were paired, the ratio of all gene pairs (termed the HN ratio) was calculated.

$$\text{HN ratio} = \frac{(\text{Gene expression value in hypoxia}) + 1}{(\text{Gene expression value in normoxia}) + 1} \quad (1)$$

Values of HN ratios for all paired samples were then classified into three groups. When the HN ratio was over the threshold for upregulation, the gene was regarded as upregulated. Similarly, when the HN ratio was below the threshold for downregulation, the gene was regarded as downregulated. If the gene was labeled as neither upregulated nor downregulated, it was classified as ‘unchanged’. Finally, the numbers of counts for up, down, and unchanged were calculated for all genes. For the up-/downregulated gene classification, several thresholds were tested to optimize the calibration. For this study, we adopted a two-fold threshold after several parameters (1.5, 2, 5, and 10-fold) was tested to classify up/downregulated genes. The number of paired samples in which genes were up/down regulated was counted for all genes in the human genome.

For the evaluation of hypoxia-inducible genes, a hypoxia-and-normoxia score (HN-score) was calculated for all genes in humans and mice respectively. HN-score was the count of (count of human RNA-seq UP) – (count of human RNA-seq DOWN). HN-scores for all genes were also calculated in mice. Orthologous genes between humans and mice and the functional annotations of genes were downloaded from Ensembl Biomart [14]. Full lists of counts (up/down/unchanged) with HN-scores for all genes were accessible from figshare (human: <https://doi.org/10.6084/m9.figshare.5812710.v3>; mouse: <https://doi.org/10.6084/m9.figshare.9948233.v2>).

All codes used for processing the data are freely available from GitHub (<https://github.com/bonohu/chypoxia/>).

2.3. Meta-Analysis of ChIP-Seq Data

Public ChIP-seq data were collected, curated, and pre-calculated for reuse in the ChIP-Atlas database [15]. Average MACS2 scores for all genes were retrieved using the ‘Target Genes’ tool in ChIP-Atlas for hypoxia-inducible factor 1- α (HIF1A) and Endothelial PAS domain-containing protein 1 (EPAS1, also known as hypoxia-inducible factor-2 α (HIF-2 α)) as ‘Antigens’ with \pm 5k for the ‘Distance from TSS’ parameter. For the integration of ChIP-seq data into RNA-seq data produced above, the names of genes were used to join two datasets.

2.4. Visualization and the Integrated Functional Analysis of Genes

For producing scatter plots, we used TIBCO Spotfire Desktop version 7.6.0 (TIBCO Spotfire, Inc., Palo Alto, CA, USA) with TIBCO Spotfire's "Better World" program license (<http://spotfire.tibco.com/better-world-donation-program/>) in this study.

Metascape was used for the gene set enrichment analysis [16]. Conventional 'express analysis' in Metascape was used to draw histograms. In the gene set enrichment analysis of genes upregulated and downregulated in hypoxic transcriptomes (Supplementary Figure S1), the HN-scores described above were used for the extraction of a gene list for Metascape input. Two lists of genes were generated by extracting genes whose HN-score was over (or below) a threshold, where roughly 1% of all genes could be listed. These HN-score thresholds were 32 for upregulation (374 genes) and -34 for downregulation (324 genes), respectively.

3. Results

3.1. Curation of Hypoxic Transcriptome Data in Public Databases

We initially mined hypoxia-related gene expression data from public databases using an integrated graphical web tool for gene expression data called AOE, which has been maintained as an index of public gene expression databases. Using the conventional keyword search by 'hypoxia' in AOE, we showed that the number of paired samples was very few in most model organisms except humans and mice.

Pairs of samples before and after hypoxic stress were made after careful curation of dataset descriptions. We were able to obtain 128 pairs from 35 data series in humans and 53 pairs from 10 data series in mice in 2018. The complete list of pairs in RNA-seq data by Illumina sequencers is also accessible from figshare (human: <https://doi.org/10.6084/m9.figshare.5811987.v2>; mouse: <https://doi.org/10.6084/m9.figshare.9948158.v1>).

The overall procedure of the work described above is depicted in Figure 1.

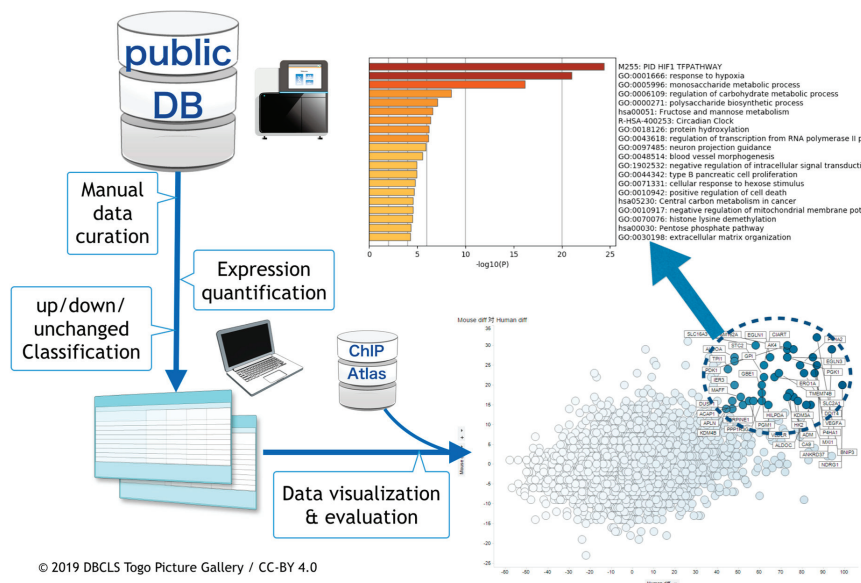


Figure 1. Schematic view of hypoxic transcriptome meta-analysis. Public databases were searched and hypoxia-related RNA-seq data were manually curated. Following this, meta-analysis was done. In conjunction with meta-analyzed data from ChIP-Atlas, data were visualized and evaluated.

3.2. Meta-Analysis of Hypoxia-Responsive Genes

After the quantification of gene expression from RNA-seq data, the number of conditions under which each gene was upregulated, downregulated, and unchanged were counted. The reason for this three-way categorization is that the data are highly series-specific owing to various cell lines and experimental conditions. Complete lists of the meta-analyzed results are accessible from figshare (human: <https://doi.org/10.6084/m9.figshare.5812710.v3>; mouse: <https://doi.org/10.6084/m9.figshare.9948233.v2>).

In order to visualize differentially expressed genes, we introduced a value called HN-score. HN-score is the number of UP counts minus the number of DOWN counts and was calculated for all genes. Using this score, we were able to quantify the degree to which each gene was affected by hypoxia. For example, *VEGFA* had 92 UP, 6 DOWN, and 30 unchanged counts. Its HN-score was thus 86 (= 92 – 6).

Following this, genes orthologous between humans and mice were related utilizing an orthologous gene table generated from Ensembl Biomart. This operation yields a list of genes concurrently upregulated in humans and mice. In order to sort the table, the sum of human and mouse HN-scores was calculated (called total HN-score). For example, the score for *VEGFA* (human) was 86 and that for *Vegfa* (mouse) was 23, so the total HN-score for *VEGF* gene was 109. Table 1 shows the top 25 genes with high total HN-score, and a complete merged list is available from figshare (<https://doi.org/10.6084/m9.figshare.9958169.v1>).

Table 1. List of top 25 hypoxia inducible genes. Top 25 genes with high hypoxia-and-normoxia-score (HN-score; human + mouse) with the number of paired samples that were judged as up-regulated and down-regulated after hypoxic stress. For the calculation of HN-score, see the text.

Human Gene	Human Up	Human Down	Human HN-Score	Mouse Gene	Mouse Up	Mouse Down	Mouse HN-Score	Total HN-Score
<i>ANKRD37</i>	101	7	94	<i>Ankrd37</i>	35	6	29	123
<i>NDRG1</i>	104	5	99	<i>Ndrp1</i>	22	2	20	119
<i>BNIP3</i>	92	5	87	<i>Bnip3</i>	33	1	32	119
<i>P4HA1</i>	92	5	87	<i>P4ha1</i>	27	2	25	112
<i>DDIT4</i>	94	9	85	<i>Ddit4</i>	29	2	27	112
<i>VEGFA</i>	92	6	86	<i>Vegfa</i>	23	0	23	109
<i>FAM162A</i>	82	6	76	<i>Fam162a</i>	30	1	29	105
<i>SLC2A1</i>	88	7	81	<i>Slc2a1</i>	28	5	23	104
<i>P4HA2</i>	83	4	79	<i>P4ha2</i>	27	2	25	104
<i>PDK1</i>	80	7	73	<i>Pdk1</i>	32	2	30	103
<i>AK4</i>	82	9	73	<i>Ak4</i>	31	2	29	102
<i>PGK1</i>	78	5	73	<i>Pgk1</i>	30	3	27	100
<i>EGLN3</i>	82	9	73	<i>Egln3</i>	29	2	27	100
<i>ALDOC</i>	93	9	84	<i>Aldoc</i>	17	2	15	99
<i>MXI1</i>	88	6	82	<i>Mxi1</i>	16	1	15	97
<i>ENO2</i>	99	5	94	<i>Eno2</i>	13	11	2	96
<i>CA9</i>	88	10	78	<i>Car9</i>	21	5	16	94
<i>ANGPTL4</i>	98	6	92	<i>Angptl4</i>	8	6	2	94
<i>ADM</i>	83	7	76	<i>Adm</i>	20	3	17	93
<i>TMEM74B</i>	76	7	69	<i>Tmem74b</i>	24	1	23	92
<i>HK2</i>	82	8	74	<i>Hk2</i>	21	3	18	92
<i>EGLN1</i>	69	4	65	<i>Egln1</i>	27	0	27	92
<i>BNIP3L</i>	84	5	79	<i>Bnip3l</i>	12	0	12	91
<i>KDM3A</i>	78	5	73	<i>Kdm3a</i>	18	1	17	90
<i>C4orf47</i>	91	5	86	<i>1700029J07Rik</i>	7	3	4	90

Figure 2 visualizes this table as a scatter plot of HN-score values for humans and mice. Genes located in the upper right are those upregulated after hypoxia both in humans and mice. Genes in that category included previously reported typical hypoxia-responsive genes, for example *PGK1*, *VEGFA*, and *EGLN3*, supporting the validity of our method. On the other hand, genes downregulated both in humans and mice included some not previously identified as hypoxia-related.

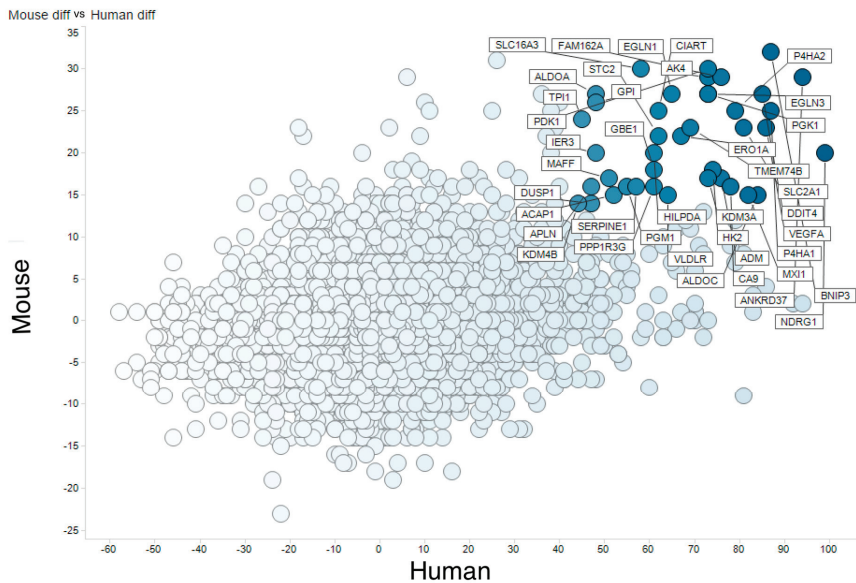


Figure 2. Meta-analysis of hypoxic transcriptomes by RNA-seq. Comparison of human and mouse hypoxic transcriptomes analyzed by RNA-seq. The X axis shows (count of human RNA-seq UP) – (count of human RNA-seq DOWN) and the Y axis shows (count of mouse RNA-seq UP) – (count of mouse RNA-seq DOWN).

We then performed set enrichment analysis using Metascape. The analysis clearly revealed that some genes upregulated in many samples with high HN-scores are well-known hypoxia-responsive genes, while some are not (Supplementary Figure S1A). The latter can be novel candidates for hypoxia-responsive genes to study signaling pathways in hypoxia research. Metascape also clearly depicted the functions of downregulated genes with low HN-scores (Supplementary Figure S1B). Those genes were apparently related to DNA repair and replication [17].

3.3. Integration of Meta-Analyzed ChIP-Seq Data

In order to investigate expression regulation of genes of interest by direct transcription factor binding, we studied ChIP-seq data. In addition to the public nucleotide sequence databases, ChIP-seq data processed by the MACS2 program are also available from the ChIP-Atlas database, which is a database for meta-analysis results from publicly available ChIP-seq data [15]. Thus, we retrieved ChIP-seq data for hypoxia-inducible factor 1-alpha (HIF1A) and endothelial PAS domain-containing protein 1 (EPAS1, also known as hypoxia-inducible factor-2alpha (HIF-2alpha)) from ChIP-Atlas.

We integrated meta-analysis results of human RNA-seq (hypoxic transcriptome) described above and human ChIP-seq data for HIF1A and EPAS1. Then, we visualized the results by conventional scatterplot (Figure 3). The source data are available from figshare (<https://doi.org/10.6084/m9.figshare.9958181.v2>). In addition to reported hypoxia-responsive genes such as *ANKRD37* [18], novel HIF1-target candidate genes were found with high HN-score and high ChIP-seq score (Figure 3A). In Figure 3A, genes with high HN-score but low ChIP-seq score were also found, and these may belong to the non-HIF1 regulation pathway. *NDRG1*, which encodes a cytoplasmic protein involved in stress responses, hormone responses, cell growth, and differentiation, is a typical gene with such a pattern. Furthermore, we found HIF1-specific and HIF2-specific genes in the scatter plots for HIF1A (Figure 3A) and EPAS1 (Figure 3B). Genes with high ChIP-scores in EPAS1 but not in HIF1A could be HIF2 targets, but there were no distinct genes in this category.

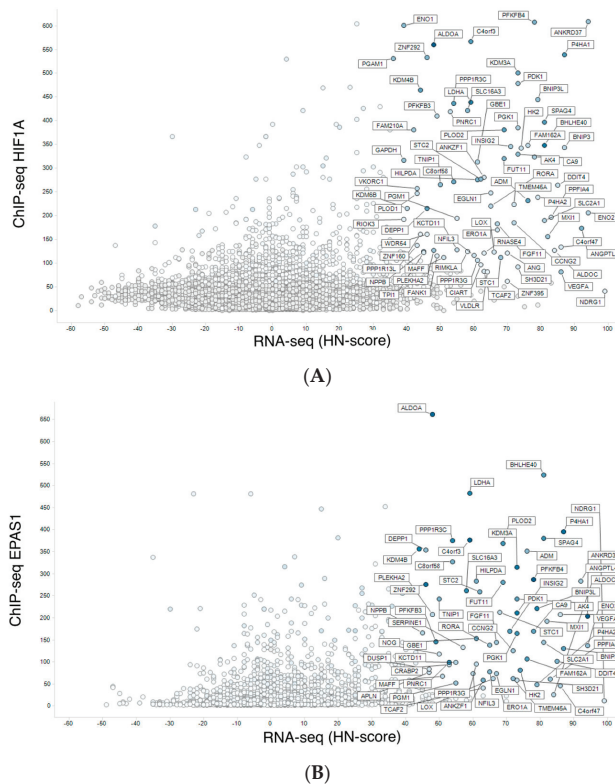


Figure 3. Integration of meta-analyzed ChIP-seq peak values to hypoxic transcriptomes. **(A)** Meta-analyzed hypoxic transcriptomes (RNA-seq) vs. average of HIF1A ChIP-seq peak values. **(B)** RNA-seq and EPAS1 ChIP-seq.

In order to study the differences between HIF1A and EPAS1 more thoroughly, we then investigated genes with high MACS2 score for HIF1A and EPAS1 (with positive HN-score). Surprisingly, the top 100 genes for HIF1A and EPAS1 were exactly the same, and we therefore increased the number of genes to 300. The top 300 genes for HIF1A (<https://doi.org/10.6084/m9.figshare.9958235.v1>) and EPAS1 (<https://doi.org/10.6084/m9.figshare.9958250.v1>) were generated and compared to identify the differences. The two gene lists were analyzed and visualized using the ‘calculate and draw custom Venn diagrams’ website (<http://bioinformatics.psb.ugent.be/webtools/Venn/>; Figure 4A). Gene set enrichment analysis of the intersection of the two gene lists revealed typical features of hypoxia-inducible genes (Figure 4B), while analysis of the HIF1A-specific and EPAS1-specific portions also showed interesting features (Figure 4C,D). Genes with the functional annotations ‘M00001: glycolysis (Embden-Meyerhof pathway)’ and ‘GO:0031167: rRNA methylation’ were enriched among HIF1A-specific genes (Figure 4C). This preferential regulation of glycolysis by HIF1A was previously described from microarray data [19]. On the other hand, genes with ‘GO:0040008: regulation of growth’ and ‘GO:0003151: outflow tract morphogenesis’ were enriched among EPAS1-specific genes (Figure 4D). These observations may reflect target gene differences between these two transcription factors.

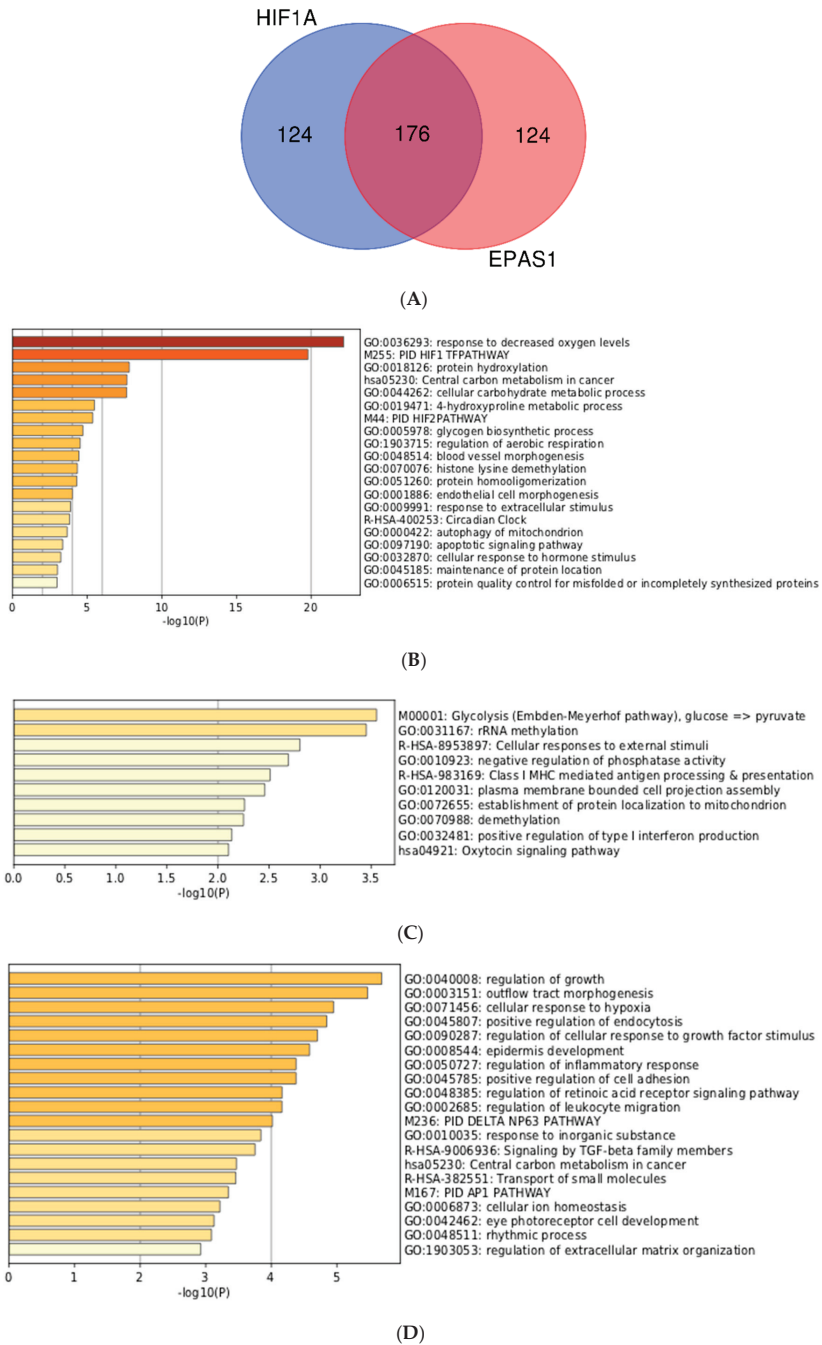


Figure 4. Comparison and gene set enrichment analysis of HIF1A-specific and EPAS1-specific genes. (A) Venn-diagram of the top 300 genes. (B) Enrichment analysis for 176 intersecting genes. (C) Enrichment analysis for 124 HIF1A-specific genes. (D) Enrichment analysis for 124 EPAS1-specific genes.

4. Discussion

While over two million transcriptome samples have been archived in public databases (NCBI Gene Expression Omnibus and EBI ArrayExpress), these data were reported by various laboratories and are thus derived from different populations, analysis platforms, and sampling conditions. The resultant variability can compromise meaningful comparisons, and it is indispensable to curate the data manually to do meta-analysis for the study of specific biological stresses.

Using AOE, we made a complete survey of hypoxia-related gene expression data in the public databases. The large quantity of relevant data available made it possible to do meta-analysis at the level of transcriptome sequences. In our previous study, only 23 hypoxia-normoxia pairs could be analyzed due to a lack of available human RNA-seq, and no relevant murine RNA-seq data could be found. However, although the amount of microarray data available is much greater, most RNA-seq data are from Illumina platforms (for example HiSeq2500, HiSeq2000, and NextSeq500), simplifying comparison. Thus, we decided to use data only from RNA-seq for our meta-analysis on the hypoxic transcriptome in the public databases.

We manually curated data by reference to recorded metadata and made pairs of hypoxia-normoxia data from human and mouse cell lines. It is often troublesome to handle ratio data that contains a very large number of columns. Thus, we tentatively set the threshold for upregulation and downregulation in hypoxia, and reduced the ratio information for all samples into a cumulative upregulation/downregulation count. This conversion made it substantially easier to interpret genes biologically. After optimization, we determined a threshold of two-fold for this study to filter genes for up/downregulated although it is not a process to extract statistically significant differentially expressed genes.

Gene set enrichment analysis for genes with high HN-scores showed that genes involved in 'HIF-1 alpha transcription factor network' (GSEA Gene Set: PID_HIF1_TFPATHWAY) and 'response to oxygen levels' (Gene Ontology: GO:0070482) were reasonably enriched (Figure S1). This evidence justifies our meta-analysis on hypoxic transcriptomes. Detailed analyses of hypoxia-inducible genes in humans and mice (Table 1) identified a series of hypoxia-inducible genes in a data-driven manner.

In addition, our integration of ChIP-seq into RNA-seq data added substantial information on hypoxia-inducible genes (Figure 3). HIF binding directly mediates gene upregulation, but not for gene downregulation as described in previous works [20,21]. High ChIP-seq scores, based on the MACS2 program via the ChIP-Atlas database, indicated genes whose regulatory regions were directly bound by transcription factors. For example, *ANKRD37* showed both high HN-score and high ChIP-seq score (Figure 3A), while *NDRG1* had a high HN-score but a low ChIP-seq score. By differentiating genes in this way, we can generate additional hypotheses about pathways regulating differential regulation until the hypothesis that the transcription factor binds near to the transcription start site (TSS) is valid. For example, EPAS1/HIF2A preferentially binds to distant regulatory regions [22]. In this case, we cannot use meta-analyzed ChIP-seq data for further analyses. In other cases where transcription factor binds to genomic region near TSS, the integration of meta-analyzed ChIP-seq and RNA-seq data clearly filtered genes with direct and indirect regulation, and this information can be a valuable resource for the functional analysis of hypoxia-inducible genes.

Our future work will involve detailed analyses of co-upregulated genes across many more species, which will be possible after the compilation of such transcriptome data. In view of the insights enabled by the integration of ChIP-seq with RNA-seq data, another potential future approach is the inclusion of additional types of omics data.

All data described in the manuscript are archived in figshare as a collection (Bono, H. figshare <https://doi.org/10.6084/m9.figshare.c.4690397.v1> (2019)). Source codes to replicate our study are freely available from GitHub (<https://github.com/bonohu/chypoxia>).

Supplementary Materials: Supplementary materials can be found at <http://www.mdpi.com/2227-9059/8/1/10/s1>.

Author Contributions: Conceptualization, H.B. and K.H.; methodology, H.B.; software, H.B.; validation, H.B.; formal analysis, H.B.; investigation, H.B.; resources, H.B.; data curation, H.B.; writing—original draft preparation, H.B.; writing—review and editing, K.H.; visualization, H.B.; supervision, H.B.; project administration, H.B.; funding acquisition, H.B. All authors have read and agreed to the published version of the manuscript.

Funding: This work was supported by the National Bioscience Database Center of the Japan Science and Technology Agency (JST).

Acknowledgments: Computing was partly provided by the super computer system at the National Institute of Genetics (NIG), Research Organization of Information and Systems (ROIS), Japan.

Conflicts of Interest: The authors declare no conflict of interest. The funders had no role in the design of the study; in the collection, analyses, or interpretation of data; in the writing of the manuscript, or in the decision to publish the results.

References

1. Barrett, T.; Wilhite, S.E.; Ledoux, P.; Evangelista, C.; Kim, I.F.; Tomashevsky, M.; Marshall, K.A.; Phillippy, K.H.; Sherman, P.M.; Holko, M.; et al. NCBI GEO: Archive for functional genomics data sets—Update. *Nucleic Acids Res.* **2013**, *41*, D991–D995. [[CrossRef](#)] [[PubMed](#)]
2. Athar, A.; Füllgrabe, A.; George, N.; Iqbal, H.; Huerta, L.; Ali, A.; Snow, C.; Fonseca, N.A.; Petryszak, R.; Papatheodorou, I.; et al. ArrayExpress update—From bulk to single-cell expression data. *Nucleic Acids Res.* **2018**, *47*, D711–D715. [[CrossRef](#)] [[PubMed](#)]
3. Hirota, K. An intimate crosstalk between iron homeostasis and oxygen metabolism regulated by the hypoxia-inducible factors (HIFs). *Free Radic. Biol. Med.* **2019**, *133*, 118–129. [[CrossRef](#)] [[PubMed](#)]
4. Keith, B.; Johnson, R.; Simon, M. HIF1 α and HIF2 α : Sibling rivalry in hypoxic tumour growth and progression. *Nat. Rev. Cancer* **2012**, *12*, 9–22. [[CrossRef](#)] [[PubMed](#)]
5. Hill, D.R.; Huang, S.; Nagy, M.S.; Yadagiri, V.K.; Fields, C.; Mukherjee, D.; Bons, B.; Dedhia, P.H.; Chin, A.M.; Tsai, Y.-H.; et al. Bacterial colonization stimulates a complex physiological response in the immature human intestinal epithelium. *elife* **2017**, *6*, e29132. [[CrossRef](#)] [[PubMed](#)]
6. Bono, H. All of gene expression (AOE): An integrated index for public gene expression databases. *BioRxiv* **2019**, 626754. [[CrossRef](#)]
7. Kodama, Y.; Mashima, J.; Kosuge, T.; Ogasawara, O. DDBJ update: The Genomic Expression Archive (GEA) for functional genomics data. *Nucleic Acids Res.* **2019**, *47*, D69–D73. [[CrossRef](#)] [[PubMed](#)]
8. Kodama, Y.; Shumway, M.; Leinonen, R.; International Nucleotide Sequence Database Collaboration. The Sequence Read Archive: Explosive growth of sequencing data. *Nucleic Acids Res.* **2012**, *40*, D54–D56. [[CrossRef](#)] [[PubMed](#)]
9. Bono, H. Meta-analysis of hypoxic transcriptomes from public databases. *BioRxiv* **2018**, 267310. [[CrossRef](#)]
10. Hiraoka, Y.; Yamada, K.; Kawasaki, Y.; Hirose, H.; Matsumoto, Y.; Ishikawa, K.; Yasumizu, Y. Ikra: Rnaseq Pipeline Centered on Salmon. 2019. Available online: <https://doi.org/10.5281/zenodo.3352573> (accessed on 9 January 2020).
11. Patro, R.; Duggal, G.; Love, M.I.; Irizarry, R.A.; Kingsford, C. Salmon provides fast and bias-aware quantification of transcript expression. *Nat. Methods* **2017**, *14*, 417–419. [[CrossRef](#)] [[PubMed](#)]
12. Krueger, F. Trim Galore. 2015. Available online: https://www.bioinformatics.babraham.ac.uk/projects/trim_galore/ (accessed on 9 January 2020).
13. Martin, M. Cutadapt removes adapter sequences from high-throughput sequencing reads. *EMBnet. J.* **2011**, *17*, 10–12. [[CrossRef](#)]
14. Kinsella, R.J.; Kähäri, A.; Haider, S.; Zamora, J.; Proctor, G.; Spudich, G.; Almeida-King, J.; Staines, D.; Derwent, P.; Kerhornou, A.; et al. Ensembl BioMart: A hub for data retrieval across taxonomic space. *Database* **2011**, *2011*, bar030. [[CrossRef](#)] [[PubMed](#)]
15. Oki, S.; Ohta, T.; Shioi, G.; Hatanaka, H.; Ogasawara, O.; Okuda, Y.; Kawaji, H.; Nakaki, R.; Sese, J.; Meno, C. ChIP-Atlas: A data-mining suite powered by full integration of public ChIP-seq data. *EMBO Rep.* **2018**, *19*, e46255. [[CrossRef](#)] [[PubMed](#)]
16. Zhou, Y.; Zhou, B.; Pache, L.; Chang, M.; Khodabakhshi, A.H.; Tanaseichuk, O.; Benner, C.; Chanda, S.K. Metascape provides a biologist-oriented resource for the analysis of systems-level datasets. *Nat. Commun.* **2019**, *10*, 1523. [[CrossRef](#)] [[PubMed](#)]

17. Nakamura, H.; Bono, H.; Hiyama, K.; Kawamoto, T.; Kato, Y.; Nakanishi, T.; Nishiyama, M.; Hiyama, E.; Hirohashi, N.; Sueoka, E.; et al. Differentiated embryo chondrocyte plays a crucial role in DNA damage response via transcriptional regulation under hypoxic conditions. *PLoS ONE* **2018**, *13*, e0192136. [[CrossRef](#)] [[PubMed](#)]
18. Benita, Y.; Kikuchi, H.; Smith, A.D.; Zhang, M.Q.; Chung, D.C.; Xavier, R.J. An integrative genomics approach identifies Hypoxia Inducible Factor-1 (HIF-1)-target genes that form the core response to hypoxia. *Nucleic Acids Res.* **2009**, *37*, 4587–4602. [[CrossRef](#)]
19. Hu, C.J.; Wang, L.Y.; Chodosh, L.A.; Keith, B.; Simon, M.C. Differential roles of hypoxia-inducible factor 1alpha (HIF-1alpha) and HIF-2alpha in hypoxic gene regulation. *Mol. Cell. Biol.* **2003**, *23*, 9361–9374. [[CrossRef](#)]
20. Mole, D.R.; Blancher, C.; Copley, R.R.; Pollard, P.J.; Gleadle, J.M.; Ragoussis, J.; Ratcliffe, P.J. Genome-wide association of hypoxia-inducible factor (HIF)-1alpha and HIF-2alpha DNA binding with expression profiling of hypoxia-inducible transcripts. *J. Biol. Chem.* **2009**, *284*, 16767–16775. [[CrossRef](#)]
21. Ortiz-Barahona, A.; Villar, D.; Pescador, N.; Amigo, J.; del Peso, L. Genome-wide identification of hypoxia-inducible factor binding sites and target genes by a probabilistic model integrating transcription-profiling data and in silico binding site prediction. *Nucleic Acids Res.* **2010**, *38*, 2332–2345. [[CrossRef](#)] [[PubMed](#)]
22. Smythies, J.A.; Sun, M.; Masson, N.; Salama, R.; Simpson, P.D.; Murray, E.; Neumann, V.; Cockman, M.E.; Choudhry, H.; Ratcliffe, P.J.; et al. Inherent DNA-binding specificities of the HIF-1 α and HIF-2 α transcription factors in chromatin. *EMBO Rep.* **2019**, *20*, e46401. [[CrossRef](#)] [[PubMed](#)]



© 2020 by the authors. Licensee MDPI, Basel, Switzerland. This article is an open access article distributed under the terms and conditions of the Creative Commons Attribution (CC BY) license (<http://creativecommons.org/licenses/by/4.0/>).



Article

Comparative Evaluation of the Angiogenic Potential of Hypoxia Preconditioned Blood-Derived Secretomes and Platelet-Rich Plasma: An In Vitro Analysis

Philipp Moog¹, Katharina Kirchhoff¹, Sanjar Bekeran¹, Anna-Theresa Bauer¹, Sarah von Isenburg², Ulf Dornseifer^{1,3}, Hans-Günther Machens^{1,*}, Arndt F. Schilling^{4,†} and Ektoras Hadjipanayi^{1,†}

¹ Experimental Plastic Surgery, Clinic for Plastic, Reconstructive and Hand Surgery, Klinikum Rechts der Isar, Technische Universität München, D-81675 Munich, Germany; philippmoog@web.de (P.M.); katharina.kirchhoff@icloud.com (K.K.); sanjar.bekeran@gmx.de (S.B.); anna.theresa.bauer@googlemail.com (A.-T.B.); dornseifer@ustransplant.de (U.D.); e.hadjipanayi@googlemail.com (E.H.)

² Department of Plastic, Reconstructive, Hand and Burn Surgery, Bogenhausen Hospital, D-81925 Munich, Germany; dr.isenburg@neuhannlorenz-isenburg.com

³ Department of Plastic, Reconstructive and Aesthetic Surgery, Isar Klinikum, D-80331 Munich, Germany

⁴ Department of Trauma Surgery, Orthopedics and Plastic Surgery, Universitätsmedizin Göttingen, D-37075 Göttingen, Germany; arndt.schilling@med.uni-goettingen.de

* Correspondence: Hans-Guenther.Machens@mri.tum.de

† These authors contributed equally to this work.

Received: 4 November 2019; Accepted: 10 January 2020; Published: 16 January 2020

Abstract: Blood-derived factor preparations are being clinically employed as tools for promoting tissue repair and regeneration. Here we set out to characterize the in vitro angiogenic potential of two types of frequently used autologous blood-derived secretomes: platelet-rich plasma (PRP) and hypoxia preconditioned plasma (HPP)/serum (HPS). The concentration of key pro-angiogenic (VEGF) and anti-angiogenic (TSP-1, PF-4) protein factors in these secretomes was analyzed via ELISA, while their ability to induce microvessel formation and sprouting was examined in endothelial cell and aortic ring cultures, respectively. We found higher concentrations of VEGF in PRP and HPP/HPS compared to normal plasma and serum. This correlated with improved induction of microvessel formation by PRP and HPP/HPS. HPP had a significantly lower TSP-1 and PF-4 concentration than PRP and HPS. PRP and HPP/HPS appeared to induce similar levels of microvessel sprouting; however, the length of these sprouts was greater in HPP/HPS than in PRP cultures. A bell-shaped angiogenic response profile was observed with increasing HPP/HPS dilutions, with peak values significantly exceeding the PRP response. Our findings demonstrate that optimization of peripheral blood cell-derived angiogenic factor signalling through hypoxic preconditioning offers an improved alternative to simple platelet concentration and release of growth factors pre-stored in platelets.

Keywords: peripheral blood cells; blood-derived therapy; hypoxia; angiogenesis; platelet rich plasma (PRP); hypoxia preconditioned plasma; hypoxia preconditioned serum

1. Introduction

Over the past decade, there has been a growing interest in the therapeutic application of autologous blood-derived products for the treatment of various skin pathologies and chronic wounds [1–5]. Under physiological conditions, a wound can rapidly regenerate through a series of well-defined wound healing stages, namely haemostasis, inflammation, proliferation and angiogenesis, and eventually tissue remodelling [6,7]. The efficiency and reliability of this complex system of cellular

responses, which are powered by a myriad of molecular cascades, suggests that targeted reproduction of the basic foundation underlying the natural process would provide a useful tool for promoting tissue repair and regeneration on-demand. These treatments could be readily applied in the clinical setting, despite an incomplete understanding of the precise set of rules that govern such mechanisms, at present. This rationale has given rise to the clinical use of peripheral blood cell-derived growth factor mixtures, which in effect represent cumulative samples of the molecular output of the key cell types that participate in the wound healing program. During the haemostatic phase, platelets play a paramount role by concentrating at the site of injury, and releasing a plethora of growth factors through degranulation [8–11]. The clot fibrin matrix thereafter provides a scaffold for migrating peripheral blood cells (PBCs), e.g., neutrophils, macrophages, lymphocytes, and other cell types (e.g., fibroblasts, endothelial cells) [12–14]. As a result of vascular trauma and the consequent disruption in oxygen supply, PBCs are exposed to local hypoxia, which leads to the production and release of pro-angiogenic growth factors that stimulate new vessel formation and reestablishment of the wound bed's microcirculation [15–18]. Thus, the main purpose of the application of blood-derived secretomes in wounded or ischaemic tissues is the targeted stimulation and support of the cellular responses that naturally drive angiogenesis and tissue repair, via protein growth factor signalling. The utilization of autologous growth factors provides a means of offering a personalised treatment to each individual patient, while autologous blood-derived products present unique advantages compared to allogeneic/xenogeneic therapies, by minimizing the risk of infection and adverse immunological reactions [2,5,16,19–21].

Platelet-rich plasma (PRP), currently accepted as the gold-standard of blood-based regenerative therapies [3,4], is a firmly defined fraction of the plasma component of peripheral blood, with a platelet concentration significantly above the normal limit (normal human plasma platelet count: 150,000–450,000 platelets/ μL) [22–26]. The aim of the PRP procedure is to achieve an increased concentration of platelet-derived protein growth factors by increasing the plasma concentration of platelets (Figure 1A). Typically, the concentration of platelets in PRP is about three to six times the normal platelet concentration in peripheral blood [27,28], and can therefore generate an elevated concentration of growth factors [11,27,29]. This supraphysiological factor concentration in PRP is achieved through platelet activation, degranulation and release of their stored growth factors [11,29–31], e.g., VEGF (vascular endothelial growth factor), PDGF (platelet-derived growth factor), EGF (epidermal growth factor), IGF-1 (insulin-like growth factor-1), bFGF (basic fibroblast growth factor), TGF- β 1 (transforming growth factor beta-1), TSP-1 (thrombospondin-1) and PF-4 (platelet factor-4) [23,31–35]. Evidently, PRP is a composite mixture of both angiogenesis-promoting (e.g., VEGF, PDGF) and angiogenesis-inhibiting (e.g., TSP-1, PF-4) protein factors, which makes the analysis of this secretome's net angiogenic effect(s) inherently complex. Indeed, the functional utility of PRP as a regenerative agent has not yet been fully clarified, despite its almost 20 years of use [3,4]. At an *in vitro* level, PRP is known to stimulate many cell types involved in wound repair, such as dermal fibroblasts and endothelial cells [36–39]. The clinical data on the efficacy of PRP for skin regeneration and treatment of chronic wounds are so far inconclusive [35,40].

Vascularization of the wound bed is achieved through angiogenesis, which is required for adequate supply of nutrients/oxygen and maintenance of cell viability. Following platelet aggregation and haemostasis, hypoxia (i.e., low oxygen tension) acts as the strongest stimulus for angiogenic induction [17,18,41]. Utilization of hypoxia as a tool to stimulate angiogenesis on-demand harnesses the innate biological mechanism that naturally promotes new vessel formation in the body, in both physiological (e.g., embryogenesis) and pathological states (e.g., ischemia, wound healing, tumour formation) [16–18,42,43]. Hypoxia preconditioned blood-derived secretomes can be generated through the process of “extracorporeal wound simulation”, which entails peripheral blood incubation under physiological temperature (37 °C) and hypoxia (1–10% O_2) (Figure 1B) [2,5,19,44]. As previously demonstrated, pericellular hypoxia can be achieved *in situ* within the blood incubation chamber, by adjusting the blood volume per unit area (BVUA), i.e., the PBC seeding density, and hence cellular

O₂ consumption, thus overcoming the need for an oxygen-controlling incubator [2,13,19]. It is already established that PBCs respond to stress (e.g., hypoxia, ischemia, inflammation, ultrasound) by upregulating a range of pro-angiogenic growth factors such as VEGF [2,5,45–48], bFGF [46–48], IL-8 [2,47,48] and MMP-9 [2,47]. For the purpose of a personalised therapeutic approach, PBCs represent an ideal autologous cell type, since their simple harvest and ample availability makes them easy to employ [2,5,19]. The provision of a standardized ex vivo hypoxic microenvironment for PBCs, that simulates the one normally found in an in vivo wound, could thus enable obtaining physiological growth factor mixtures, of naturally-occurring protein factor concentrations and ratios [5,19,44]. These growth factors can be delivered in the form of hypoxia preconditioned plasma (HPP) or hypoxia preconditioned serum (HPS), depending on whether peripheral blood is, respectively, anticoagulated or allowed to clot before conditioning (Figure 1B) [2,19,44].

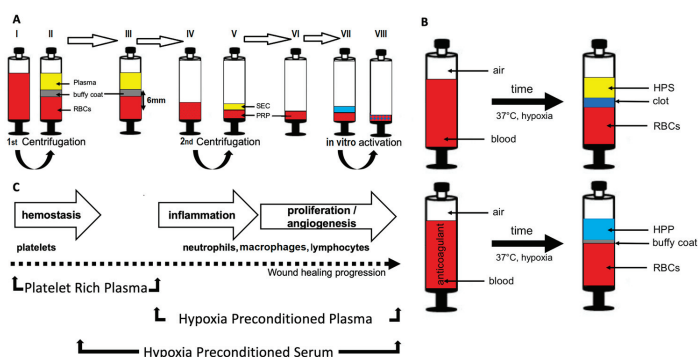


Figure 1. Method of preparation of different blood-derived secretomes and their correlation with the physiological wound healing phases. (A) Preparation of platelet-rich plasma (PRP). Main procedure steps are shown by arrows. (I) Tube with anticoagulant after blood sampling. (II) After 1st centrifugation, blood has been separated into the shown layers. (III) Collection of all content (including the buffy coat) above the mark (6 mm), and (IV) transfer to another tube without anticoagulant before re-centrifugation. (V) After 2nd centrifugation, there is a division into serum component (SEC) and PRP. (VI) Separation of PRP (0,5 mL) from the SEC. (VII) Activation of PRP with Thrombin and CaCl₂, or by CaCl₂ only. (VIII) Activated PRP as a final product (blue dots represent released growth factors in PRP). (B) Preparation of hypoxia preconditioned secretomes (HPS, HPP). Blood is allowed to clot (top), or anticoagulated (bottom), and PBCs (in clot or buffy coat) are preconditioned under pericellular (local) hypoxia (~1% O₂) and physiological temperature (37 °C) for 4 to 7 days. Sedimentation passively separates growth factor-rich hypoxia preconditioned serum (HPS) or hypoxia preconditioned plasma (HPP) from clot or buffy coat, respectively, and red blood cells (RBCs) at the bottom (C) Overview of the correlation of the two categories of blood-derived secretomes with the key cell types involved in wound healing, and the corresponding wound healing phases. PRP comprises an increased concentration of platelet-derived growth factors, which is naturally achieved during hemostasis through platelet concentration within the fibrin clot, while HPS and HPP mostly comprise hypoxia-induced factors, which are naturally produced by PBCs during the inflammatory and proliferative phases.

By following the natural sequence of the wound healing stages, which progresses from haemostasis through to angiogenesis, it becomes readily apparent that the above described peripheral blood-derived secretomes, i.e., platelet-rich plasma (PRP) and hypoxia preconditioned products (HPP/HPS), not only differ in their method of preparation, but also correspond to, and essentially mirror distinct phases of the wound healing program (Figure 1C). Thus, while PRP contains a high concentration of platelet-derived factors by employing platelet concentration via blood centrifugation [29], something that also naturally happens during haemostasis through platelet aggregation within the fibrin clot, HPS and HPP comprise mostly protein factors that are newly produced by PBCs as a result of hypoxic

exposure during blood conditioning [2,44]. A comparative evaluation of these two secretome categories, with respect to their angiogenic potential, is therefore a reasonable attempt towards understanding the relative contribution of these different cell types (platelets vs. PBCs) towards wound angiogenesis, as well as essential for gaining a greater insight into their specific clinical utility in wound healing and tissue repair therapies.

In the current study, we aimed to characterize these peripheral blood-derived secretomes, in terms of their key pro-angiogenic factor (VEGF) and anti-angiogenic factor (PF-4, TSP-1) composition, and analyse in vitro their ability to induce microvessel formation and sprouting in endothelial cell and aortic ring cultures, respectively. Furthermore, the effect of secretome freeze-storage on growth factor concentration and bioactivity, as well as the effect of secretome dilution on angiogenic potential were tested, parameters that are ultimately relevant for clinical application.

2. Materials and Methods

2.1. Preparation of Platelet-Derived Secretomes—Platelet Rich Plasma (PRP)

All blood donors provided written informed consent as directed by the ethics committee of the Technical University Munich, Germany, which approved this study (File Nr.: 497/16S). The preparation of PRP followed an established, double-centrifugation protocol [49] (see Figure 1A). In the first step, 6.5 mL venous blood was collected in blood tubes pre-filled with citrate anticoagulant (BD Vacutainer, Becton, Dickinson and Company, USA), under sterile and standardized conditions. Next, the blood was centrifuged at $160 \times g$ for 20 min. After centrifugation, the blood was separated into three layers, from top to bottom: platelet-poor plasma (PPP), buffy coat (platelets and white blood cells) and red blood cells (RBCs). A mark was then placed 6 mm below the upper edge of the blood cell component (BCC), and all content above the mark (containing the buffy coat) was pipetted and transferred into a new sterile tube without anticoagulant, then centrifuged again for 15 min at $400 \times g$. This second centrifugation resulted into separation of PRP and serum component (SEC). The PRP (approx. 0.5 mL) was separated from the SEC. The in vitro activation of PRP was carried out either with 0.5 mL of 1 I.U. Thrombin/mL and 1.7 mg/mL CaCl_2 (Tisseel, Baxter, Germany) or with CaCl_2 only in a concentration of 3.4 mg/mL. After an incubation period of 30 min at 37°C , a third centrifugation (20 min, $160 \times g$) was carried out. Then, 0.5 mL of the activated PRP supernatant was analyzed.

2.2. Preparation of Hypoxia Preconditioned Secretomes—Hypoxia Preconditioned Serum (HPS)/Plasma (HPP)

In the first step, 20 mL venous blood was collected in a 30 mL polypropylene syringe (Omnifix®, B Braun AG, Germany) that contained no additive or was pre-filled with 1 mL heparin (Medunasal®–Heparin 500 I.U. 5 mL ampoules), or in blood tubes pre-filled with EDTA anticoagulant (BD Vacutainer, Becton, Dickinson and Company, USA), under sterile and standardized conditions (Blood Collection Set; Safety-Lok, CE 0050, BD Vacutainer, Becton, Dickinson and Company, USA). Then, a 0.2 μm pore filter was attached (Sterifix®, CE 0123, Braun Melsungen AG, Germany) and by pulling the plunger, 5 mL air was drawn into the syringe. Subsequently, the filter was removed and the capped syringe was placed upright in an incubator ($37^\circ\text{C}/5\% \text{CO}_2$) and incubated for 4 or 7 days (blood incubation time), without any prior centrifugation. Pericellular local hypoxia ($\sim 1\% \text{O}_2$) was induced in situ through cell-mediated O_2 consumption, by controlling the blood volume per unit area ($\text{BVUA} > 1 \text{ mL}/\text{cm}^2$), and consequently the PBC seeding density in the blood container [13,19]. After the predefined incubation time, the blood was passively separated into three layers, from top to bottom; plasma/serum, clot/buffy coat, red blood cell component, so that the top layer comprising hypoxia preconditioned plasma or serum (HPP/HPS) could be filtered (0.2 μm pore filter, Sterifix®, B Braun AG, Germany) into a new syringe (see Figure 1B), removing cells/cellular debris. Through the step of filtration, the serum/plasma was rendered cell-free. HPP and HPS secretomes were then sampled, and partially diluted as required with phosphate buffered saline (PBS) at dilutions of 1:1; 1:2; 1:5; 1:10; 1:50; 1:100; 1:500; 1:1000, before being analyzed.

2.3. Preparation of Blood-Derived Secretomes

In the first step 20 mL venous blood was collected in a 30 mL polypropylene syringe (Omnifix[®], B Braun AG, Germany) that contained no additive or was pre-filled with 1 mL heparin (Medunasal[®]–Heparin 500 I.U. 5 mL ampoules), or in blood tubes pre-filled with EDTA anticoagulant (BD Vacutainer, Becton, Dickinson and Company, USA), under sterile and standardized conditions (Blood Collection Set; Safety-Lok, CE 0050, BD Vacutainer, Becton, Dickinson and Company, USA). Blood with EDTA or heparin anticoagulant was centrifuged for 10 min at 160× g to obtain plasma samples. Plasma samples were also prepared with heparin anticoagulant and simple sedimentation for 60 min, without centrifugation. After sedimentation or centrifugation, the blood was separated into the known layers (see Sections 2.1 and 2.2), so that the top layer (plasma or serum) could be filtered into a new syringe. Plasma or serum samples were collected and partially diluted with PBS at dilutions of 1:1; 1:2; 1:5; 1:10; 1:50; 1:100; 1:500; 1:1000, before being analyzed.

To test the anticoagulant EDTA for its angiogenic effect, 5 mL of PBS was added to the vacutainers containing EDTA and analyzed after sufficient mixing. Furthermore, the anticoagulant heparin and the PRP activators Thrombin and CaCl₂ were tested at the previously mentioned concentrations (see Section 2.1). PBS medium and recombinant VEGF (90 ng/mL) were also tested as negative and positive controls, respectively.

2.4. Quantitative Analysis of VEGF, TSP-1 and PF-4 Concentration in Blood-Derived Secretomes

Blood-derived secretomes were sampled and analyzed by ELISA for VEGF, TSP-1 and PF-4 (R&D, USA), according to manufacturer's instructions. Factor concentrations in blood-derived secretomes were measured immediately after the predefined incubation period (4 or 7 days), and after storage for 4 or 12 weeks at −20 °C degrees, as indicated. Five samples were tested per condition.

2.5. Analysis of the Effect of Blood-Derived Secretomes on In Vitro Microvessel Formation

The angiogenic potential of blood-derived secretomes was tested in an in vitro angiogenesis assay, by assessing their ability to induce tube formation in human umbilical vein endothelial cells (HUVECs, CellSystems, Germany), seeded on factor-reduced Matrigel (BD, Germany). HUVECS were seeded at a density of 10×10^3 well, with 50 µL of test or control media added per well (µ-Slide Angiogenesis, Ibidi, Germany), and cultured in 5% CO₂/37 °C for 12 h. Cells were then stained with Calcein AM (PromoKine, Germany), and tube formation was observed with fluorescence and phase contrast microscopy. Assessment of the extent of capillary-like network formation was carried out by counting the number of tubes and nodes (a node was defined as the point of intersection of two or more tubules), and quantification of tube length was carried out with image analysis using imageJ software (NIH, USA). Blood-derived secretomes were tested immediately after the predefined incubation period (4 or 7 days), and after storage for 4 or 12 weeks at −20 °C degrees, as indicated. At least three wells were tested per sample ($n = 5$), per condition.

2.6. Analysis of the Effect of Blood-Derived Secretomes on In Vitro Microvessel Sprouting

Blood-derived secretomes were tested in the aortic ring assay, to assess their ability to induce microvessel sprouting. Aortic rings were dissected from female adult mice as previously described [50], underwent overnight serum starvation in opti-MEM reduced serum medium (Life Technologies, Germany) and embedded into Matrigel bilayer matrix (50 µL/layer in 96-well plates) (BD, Germany). Test and control secretomes, and control media were added (150 µL/well) to the rings, before culturing them in 5% CO₂/37 °C. Medium change was carried out every 3 days, while rings were observed with phase contrast microscopy at 0, 3, 6 and 8 days and photographed, with all 4 quarters per ring analyzed for sprouting (formation of structures of connected cells that were attached, at their base, to the ring). Furthermore, tube length was quantified after a culture period of 8 days with image analysis using imageJ software (NIH, USA). At least three aortic rings were tested per sample ($n = 5$).

2.7. Statistical Analysis

For each experimental condition, $n = 5$ subjects were tested (in certain cases $n = 3$ or 4 subjects were tested, as noted). Data are expressed as mean \pm standard deviation. Statistical analysis was carried out using Student's independent t-test where a maximum of two groups was compared or repeated-measures ANOVA with Bonferroni adjustment, accompanied by post-hoc pairwise comparisons for analysis of three or more groups, using SPSS 14 software. Mauchly's test was used to assess violation of sphericity in repeated-measures ANOVA, and in instances where Mauchly's test was significant, degrees of freedom were corrected using Greenhouse–Geisser estimates of sphericity. The probability of a type one error was set to 5% ($\alpha = 0.05$), unless noted otherwise.

3. Results

3.1. Quantitative Analysis of Pro- (VEGF) and Anti-Angiogenic (TSP-1, PF-4) Growth Factor Concentration in Blood-Derived Secretomes

To establish a growth factor concentration baseline, we first quantitatively analyzed via ELISA the concentration of key angiogenesis-related protein factors (VEGF, TSP-1, PF-4) in normal plasma and serum, before proceeding to test their concentration in PRP and HPP/HPS. As shown in Figure 2A, the concentration of the pro-angiogenic factor VEGF in hypoxia preconditioned secretomes and platelet-derived secretomes showed a significant 3- to 5-fold increase compared to their baseline level in fresh plasma ($p < 0.01$) and fresh serum ($p < 0.05$). Due to a large standard deviation in factor levels, no statistically significant differences could be observed between the three tested secretomes, except for HPP prepared with EDTA as anticoagulant, which had a significantly lower VEGF concentration ($p < 0.001$). The concentration of the platelet-derived angiogenic inhibitors TSP-1 and PF-4 in both fresh plasma and HPP (prepared with either EDTA or heparin anticoagulant) was significantly lower than that in HPS and PRP ($p < 0.01$) (Figure 2A), indicating that the process of blood conditioning used for HPP preparation did not significantly increase platelet activation. Indeed, no significant difference in the concentration of any of the factors tested could be observed when plasma preparation (following heparin anticoagulation) was carried out through passive sedimentation of blood, as also used for HPP preparation, or conventionally through blood centrifugation (Figure 2A). The method of blood anticoagulation used for HPP preparation (EDTA vs. heparin) appeared to influence VEGF and TSP-1 levels (lower levels with EDTA than heparin anticoagulation), but not PF-4, suggesting that EDTA primarily influenced hypoxia-regulated factor expression, rather than platelet activation, in HPP. The type of PRP activation used (CaCl_2 vs. thrombin + CaCl_2) did not appear to exert any significant influence on the concentration of these three factors being released in PRP (Figure 2A).

Based on these findings, a more detailed characterization of hypoxia preconditioned secretomes was undertaken, in terms of the effect of varying the duration of blood incubation time on factor levels. Physiological hypoxia (1% O_2) was generated in situ through cell-mediated O_2 consumption, as previously described [13,19] (see Materials and Methods Section 2.2). The positive effect of hypoxia on VEGF upregulation was evident over the tested incubation period of 7 days (Figure 2B). Indeed, as it had been expected from the data of Figure 2A, a 3- to 4-fold increase in the VEGF concentration of HPP and HPS was observed following 4 and 7 days blood incubation, compared to baseline values in fresh plasma and serum (no blood incubation), respectively ($p < 0.05$) (Figure 2B). In direct comparison, the VEGF concentration of 7 days -incubated HPS was significantly greater than that in HPP ($p < 0.01$), although this difference was absent at 4 days incubation (Figure 2B). With respect to the anti-angiogenic factors, TSP-1 and PF-4 concentrations in 4 days -incubated HPP were more than threefold lower than those in fresh plasma, an effect persisting over 7 days of blood incubation ($p < 0.01$) (Figure 2B). In contrast, TSP-1 concentration in HPS was threefold higher compared to fresh serum after 4 and 7 days incubation ($p < 0.01$). No significant difference was seen in PF-4 levels between HPS (either incubation period) and fresh serum. Nonetheless, significant differences could be recorded between

HPP and HPS with respect to both TSP-1 and PF-4 concentration, at 4 and 7 days incubation ($p < 0.05$) (Figure 2B).

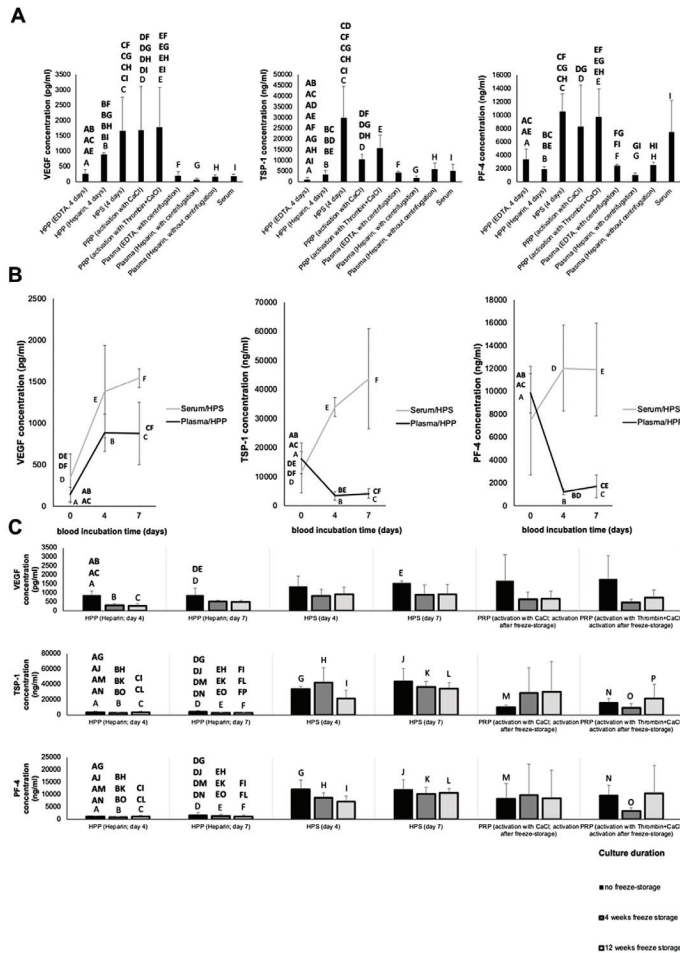


Figure 2. Quantitative analysis of pro- (VEGF) and anti-angiogenic (TSP-1, PF-4) factor storage concentration in blood-derived secretomes. (A) Plot showing the concentration of VEGF (pg/mL); TSP-1 (ng/mL) and PF-4 (ng/mL) in the various blood-derived secretomes tested ($n = 5$). Note that HPP and HPS were prepared without centrifugation. EDTA and heparin were used as blood anticoagulants in HPP and plasma preparation. (B) Effect of blood incubation time (days) on pro- (VEGF) and anti- (TSP-1, PF-4) angiogenic factor concentration in hypoxia preconditioned secretomes over 4 and 7 days preconditioning ($n = 5$). (C) Effect of freeze-storage on factor bioavailability. Plots comparing the VEGF, TSP-1 and PF-4 concentrations in fresh blood-derived secretomes and in secretomes stored for 4 and 12 weeks at $-20\text{ }^{\circ}\text{C}$ before testing ($n = 5$). Capital letter pairs over plots indicate statistical comparison of corresponding data points. For all pair comparisons, $p < 0.05$, unless otherwise indicated. Error bars represent s.d.

To examine whether the tested blood-derived secretomes could maintain their proteomic bioavailability when stored at low temperature ($-20\text{ }^{\circ}\text{C}$), what would admittedly be a clinically useful property for off-the shelf clinical application, HPP/HPS and PRP samples were frozen for 4 and

12 weeks following preparation, before factor protein levels were quantified via ELISA. As shown in Figure 2C, there was a significant drop in the HPP concentration of bioavailable VEGF in samples obtained after 4 days blood incubation ($p < 0.01$), but not 7 days, suggesting an initially more robust VEGF upregulation following 7 days blood preconditioning. Nonetheless, VEGF remained detectable in all frozen HPP samples tested, even after 12 weeks freeze-storage. Furthermore, neither 4 nor 12 weeks freeze-storage seemed to significantly affect VEGF bioavailability in HPS and PRP. Importantly, no differences could be seen in TSP-1 and PF-4 levels between fresh and frozen secretomes (HPP, HPS, PRP). This could be indirectly confirmed, through the maintenance of a significantly higher TSP-1 and PF-4 concentration in frozen HPS and PRP samples compared to frozen HPP samples ($p < 0.05$) (Figure 2C).

3.2. Analysis of the Ability of Blood-Derived Secretomes to Induce Microvessel Formation In Vitro

Following an analysis of pro- and anti-angiogenic factor concentration in blood-derived secretomes, we moved on to investigate their ability to induce microvessel formation in human umbilical vein endothelial cell (HUVEC) in vitro cultures. We found a 3- to 4-fold increase in the number of tubes ($p < 0.05$), and a 4- to 5-fold increase in the number of nodes ($p < 0.05$) in hypoxia preconditioned and platelet-derived secretomes compared to baseline levels in fresh plasma and serum (Figure 3A,B). No significant difference in the induced angiogenic response was observed between hypoxia preconditioned and platelet-derived secretomes, except for HPP prepared with EDTA as anticoagulant, which showed minimal tube formation. In support of our ELISA results, the omission of centrifugation in plasma preparation, as well as the method used for PRP activation (CaCl₂ vs. thrombin + CaCl₂) did not significantly influence the degree of tube formation.

An assessment of microvessel formation in cultures with hypoxia preconditioned secretomes that were prepared with a varying blood incubation time (4 vs. 7 days) showed that preconditioning improved the angiogenic potential of serum, which was initially less angiogenic than fresh plasma ($p < 0.001$) (Figure 3A,C). In particular, HPS prepared with both 4 and 7 days blood incubation generated 3 to 4 times as many tubes ($p < 0.001$) and nodes ($p < 0.05$) as fresh serum, although no significant differences were observed between the two incubation periods. In HPP cultures, 4 days of blood preconditioning had a positive effect on the number of nodes formed compared to fresh plasma ($p < 0.001$), although no significant difference was found in terms of tube formation (Figure 3A,C).

We also tested the functional bioactivity of freeze-stored secretomes in the in vitro angiogenesis assay. As expected from our VEGF data (see Figure 2C), freezing hypoxia preconditioned and platelet-derived secretomes did not appear to impair their angiogenicity, with all secretomes inducing significantly greater tube formation than phosphate buffered saline (PBS), used here as negative control ($p < 0.001$) (Figure 4A,B). Moreover, no difference in bioactivity was detected between secretomes, for any of the two freeze-storage periods tested.

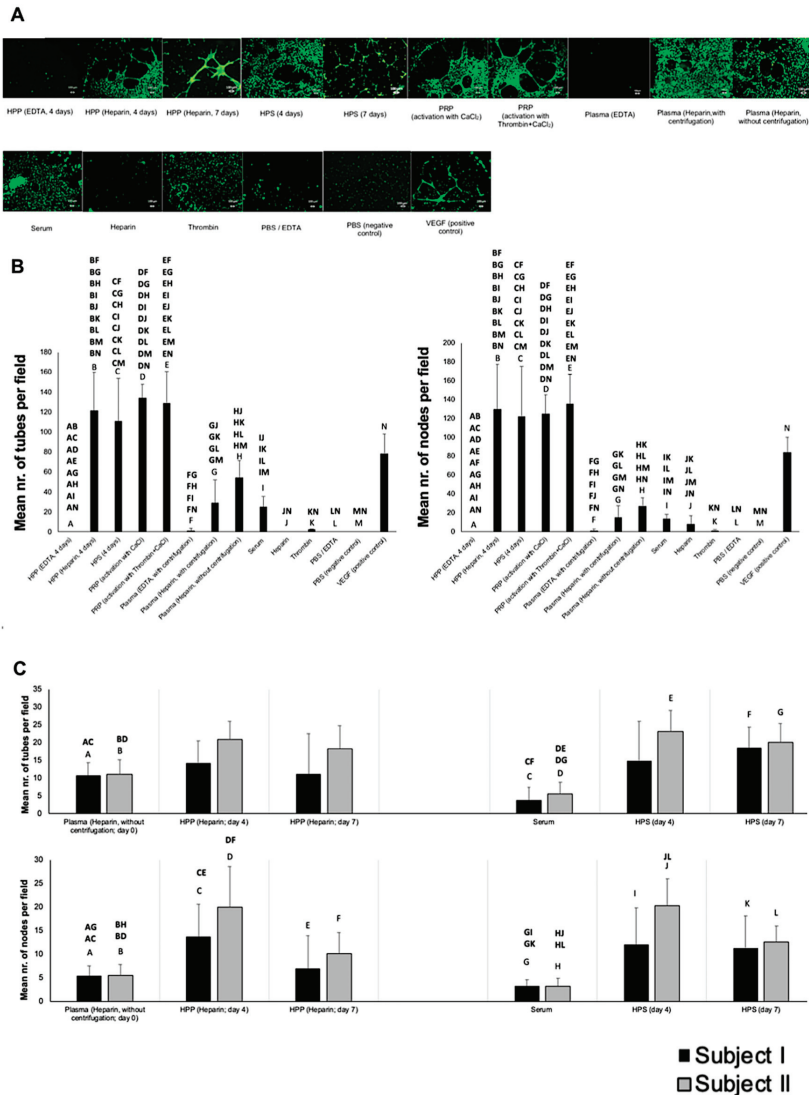


Figure 3. Effect of blood-derived secretomes on microvessel formation in human umbilical vein endothelial cell (HUVEC) cultures in vitro. (A) Panel showing representative images of the tube formation assay (12 h), carried out in the presence of the shown blood-derived secretomes (Bars = 100 μ m). (B) Plot showing the mean number of tubes (left) and nodes (right) formed in different blood-derived secretome cultures ($n = 5$). (C) Effect of blood incubation time (4 and 7 days) on the angiogenic activity of hypoxia preconditioned secretomes. Plot showing the mean number of tubes (top) and nodes (bottom) formed in 4 and 7 days incubated -HPP and -HPS cultures, with blood obtained from two subjects ($n = 3$ per subject). Capital letter pairs over plots indicate statistical comparison of corresponding data points. For all pair comparisons $p < 0.05$, unless otherwise indicated. Error bars represent s.d.

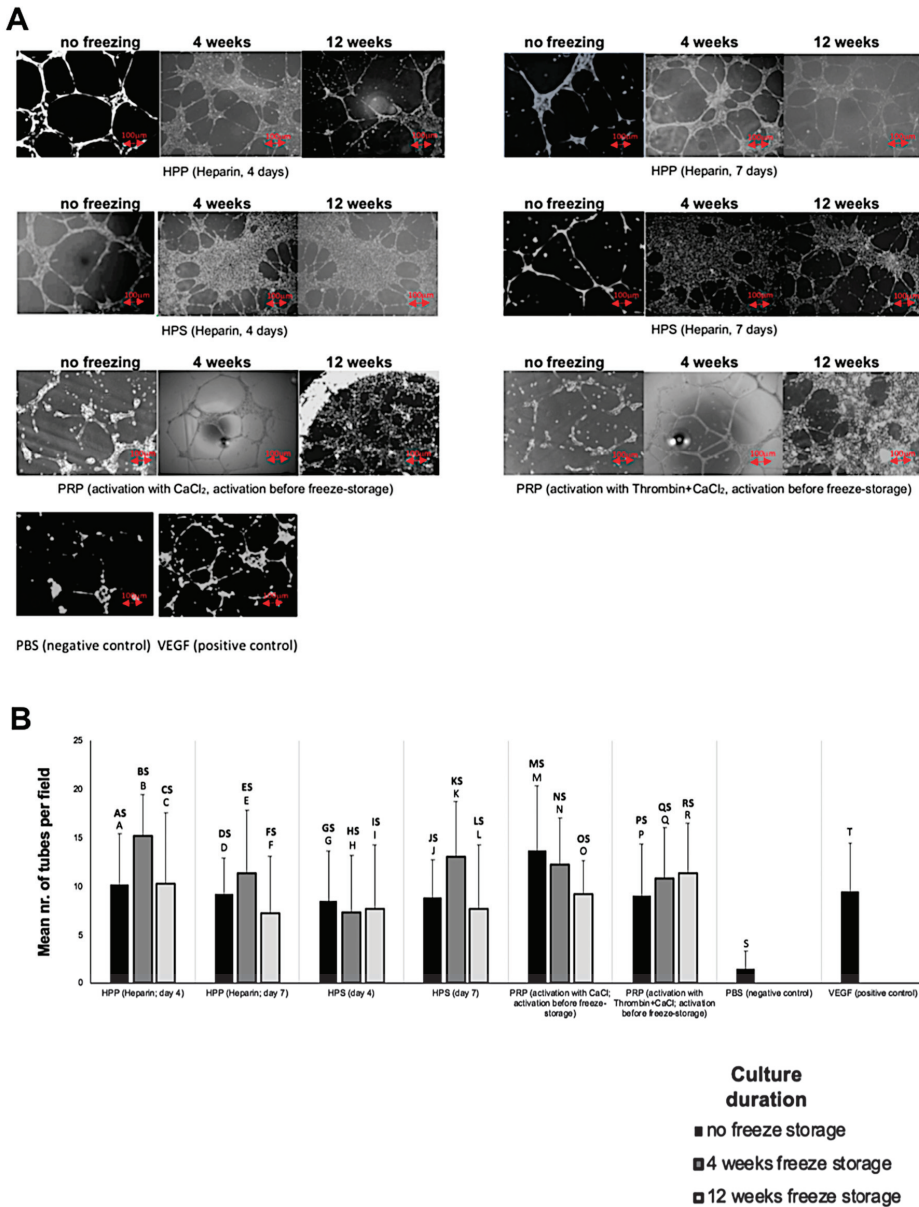


Figure 4. Effect of blood-derived secretome freeze-storage on angiogenic activity. (A) Panel showing representative images of the tube formation assay carried out with HPP, HPS and PRP secretomes that underwent freeze storage for 4 and 12 weeks (Bars = 100 μ m). (B) Plot comparing the mean number of tubes formed in endothelial cell cultures in the presence of fresh blood-derived secretomes or secretomes that underwent freeze-storage for 4 and 12 weeks at -20°C ($n = 5$) ($p < 0.001$). Capital letter pairs over plots indicate statistical comparison of corresponding data points. For all pair comparisons $p < 0.05$, unless otherwise indicated. Error bars represent s.d.

3.3. Analysis of the Ability of Blood-Derived Secretomes to Induce Microvessel Sprouting In Vitro

Having assessed the ability of the various blood-derived secretomes to induce microvessel formation in vitro, an analysis of microvessel sprouting was carried out using the mouse aortic ring assay. Screening for sprouting angiogenesis only showed small differences between hypoxia preconditioned and platelet-derived secretomes (Figure 5A,B). In all secretome cultures, we observed a trend for an increasing number of sprouts as culture duration increased (3, 6 and 8 days), although such differences were again non-significant, due to the high standard deviation seen between samples (Figure 5B). Similar to the tube formation assay, fresh plasma and HPP prepared with EDTA as anticoagulant induced significantly a smaller number of sprouts than their heparin-anticoagulated counterparts ($p < 0.001$).

In contrast to the sprout number, hypoxia preconditioned secretomes (heparin- anticoagulated HPP, and HPS) generated a 2- to 3-fold greater mean sprout length than platelet-derived secretomes ($p < 0.01$) after a culture period of 8 days, when the longest microvessels could be observed (Figure 5C). Moreover, heparin-anticoagulated HPP induced significantly longer sprouts than pure VEGF, used here as positive control ($p < 0.05$). In agreement with our analysis of sprout number, sprout length was found to be negatively impacted when EDTA was used as anticoagulant in fresh plasma and HPP (Figure 5C). Fresh serum generated equally long sprouts as HPS, but significantly longer sprouts than PRP ($p < 0.05$), indicating that while both hypoxia-induced and platelet-derived factors seemed to be important for sprout lengthening, an oversupply of platelet-derived factors appeared to limit sprout extension.

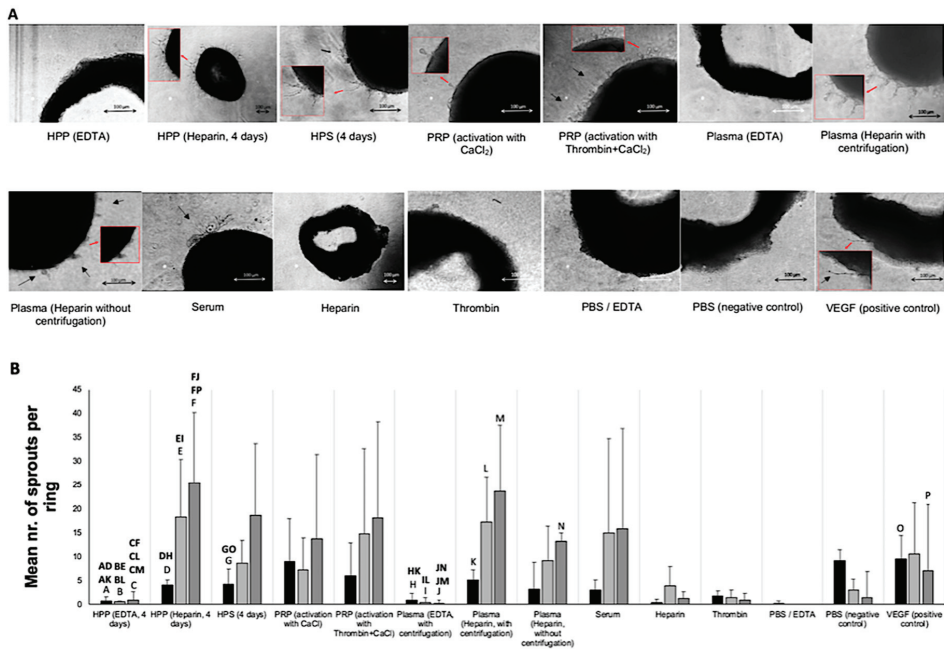


Figure 5. Cont.

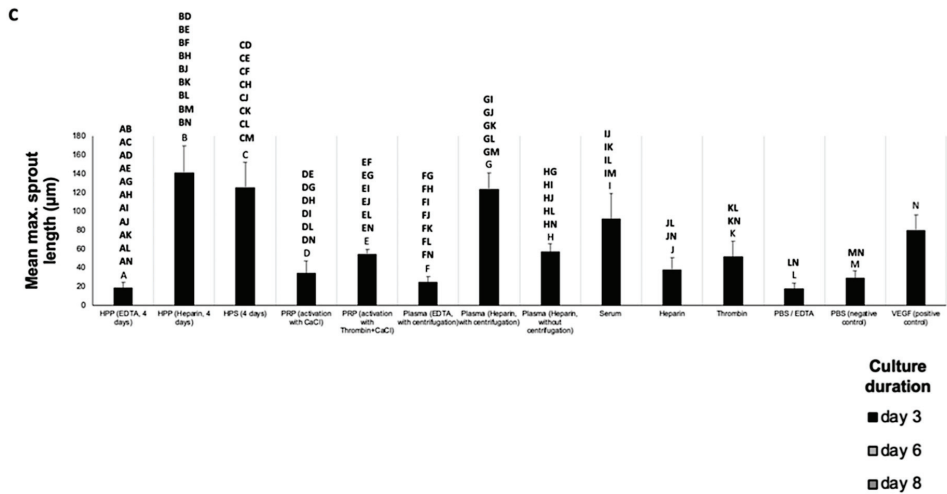


Figure 5. Effect of blood-derived secretomes on microvessel sprouting in the aortic ring assay in vitro. (A) Panel showing representative images of aortic rings, embedded in Matrigel and cultured in the presence of the shown blood-derived secretomes for 3, 6 and 8 days. (Bars = 100 µm). Microvessels sprouting from aortic rings are indicated by black arrows. Enlarged image sections are indicated by red insets. (B) Plot showing the mean number of sprouts per ring over a culture duration of 3, 6 and 8 days ($n = 3$). (C) Plot showing the mean maximum sprout length after a culture period of 8 days ($n = 3$). Capital letter pairs over plots indicate statistical comparison of corresponding data points. For all pair comparisons, $p < 0.05$, unless otherwise indicated. Error bars represent s.d.

3.4. Effect of Hypoxia Preconditioned Secretome Dilution on Angiogenic Activity

With the assumption that following in vivo secretome delivery, growth factor release and diffusion into the surrounding microenvironment would evidently result in some degree of reduction in the local protein factor concentration, we moved on to test the angiogenic potential of increasing dilutions (1:1 to 1:1000) of hypoxia preconditioned secretomes and basal plasma/serum controls, as this could be informative towards potentially identifying clinically effective dosage. In this experiment, we deliberately avoided diluting PRP, as this is per definition a concentrated secretome (i.e., diluted PRP would resemble normal plasma). Increasing the dilution of HPP and HPS up to 1:100 produced a progressively stronger angiogenic response in terms of the number of tubes and nodes formed in endothelial cell cultures (Figure 6A–C). Beyond this dilution level, however, the angiogenic response diminished rapidly ($p < 0.01$). The distinct bell-shaped profile observed in HPP/HPS was not clearly evident within the range of dilutions tested for fresh plasma and serum, implying a delay phenomenon in the dilution effect, as confirmed by the significantly greater response induced by 1:100 diluted HPP and HPS compared to 1:100 diluted plasma ($p < 0.001$) and serum ($p < 0.05$), respectively (Figure 6B,C). HPP and HPS with a 1:2 dilution demonstrated similar mean number of tubes and nodes as platelet-derived secretomes. Significant differences could be revealed, however, in the range of 1:5–1:100 dilution, with HPP/HPS surpassing the PRP angiogenic response ($p < 0.01$) (Figure 6B,C). Higher HPP/HPS dilutions (1:500 and 1:1000), on the other hand, generated less tubes and nodes than PRP ($p < 0.001$) (Figure 6B,C). Importantly, no significant difference could be observed between the angiogenic response induced by PRP and fresh plasma or serum diluted by 1:50 to 1:1000 (Figure 6B,C).

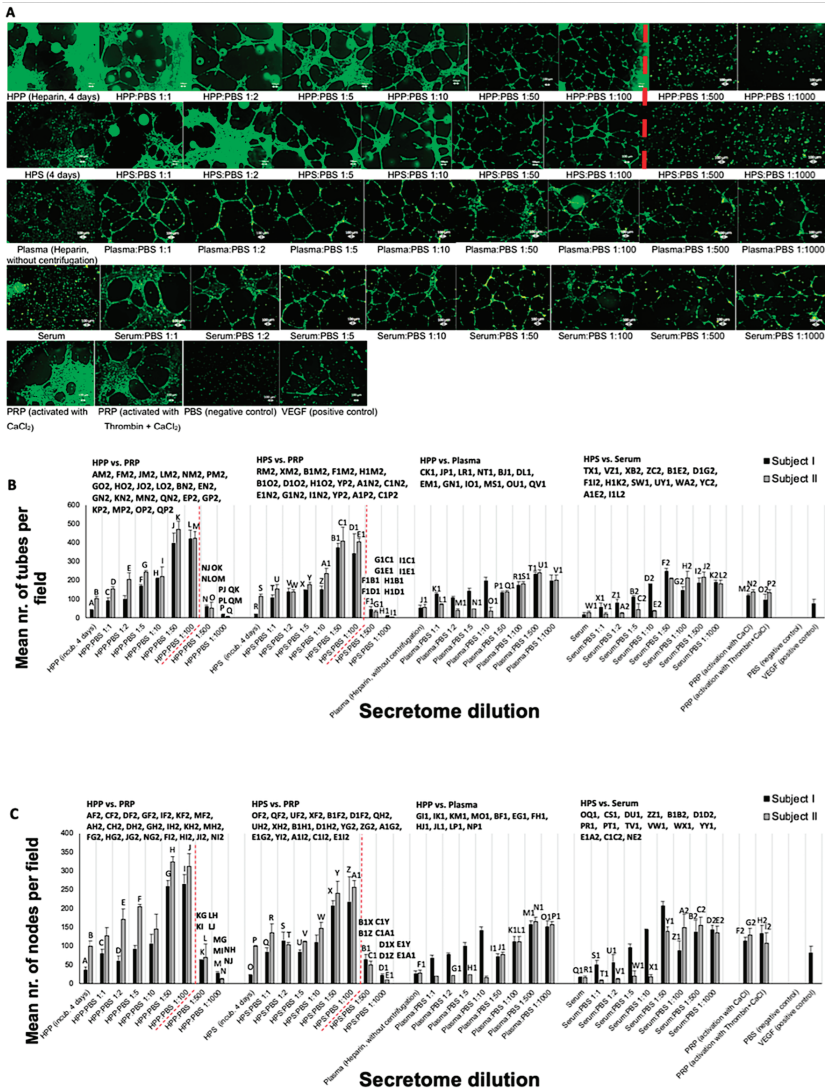


Figure 6. Effect of hypoxia preconditioned secretome dilution on microvessel formation in HUVEC cultures in vitro. **(A)** Panel showing representative images of the tube formation assay (12 h), carried out in the presence of the shown diluted blood-derived secretomes (Bars = 100 μ m). **(B,C)** Plot showing the mean number of tubes **(B)** and nodes **(C)** formed in cultures with different blood-derived secretome and basal control dilutions (1:1 to 1:1000), for blood obtained from two individual subjects ($n = 3$ per subject). The red dashed line indicates the statistically significant cut-off point of dilution. Capital letter pairs shown directly above histograms indicate intra-condition statistical comparison of corresponding data points, while HPP/HPS vs. Plasma/Serum and HPP/HPS vs. PRP statistical comparisons are shown on the upper part of plot B and C. For all pair comparisons $p < 0.05$, unless otherwise indicated. Error bars represent s.d.

The effect of secretome dilution was also tested in the aortic ring assay, which showed that microvessel sprouting increased with a more prolonged culture time (3, 6 and 8 days), and behaved in a similar manner to tube formation, with increasing dilutions generating a gradually greater response, although here differences were less significant due to the high standard deviation seen between samples (Figure 7A,B). HPS, as well as fresh serum and plasma produced the previously seen bell-shaped profile, but with the cut-off point being observed earlier, at the 1:10 dilution (Figure 7A,B). No distinct peak was observed in the HPP dilution series, although here dilutions equal to or greater than 1:500 also generated only a very small response. According to our previous data, HPS and PRP generated a similar mean number of sprouts, however, HPS dilutions of 1:1 to 1:10 generally produced a larger number of sprouts than PRP ($p < 0.05$) (Figure 7A,B). In addition, fresh plasma dilutions of 1:1 to 1:10 performed better in terms of sprouting than PRP ($p < 0.05$). With respect to the length of sprouts, no clear bell-shaped profile could be observed in any of the tested secretomes (Figure 7C). HPP and HPS generated significantly longer sprouts than PRP, up to dilutions of 1:1 and 1:50, respectively ($p < 0.01$). PRP also appeared to underperform diluted fresh plasma and serum, up to dilutions of 1:10 ($p < 0.05$).

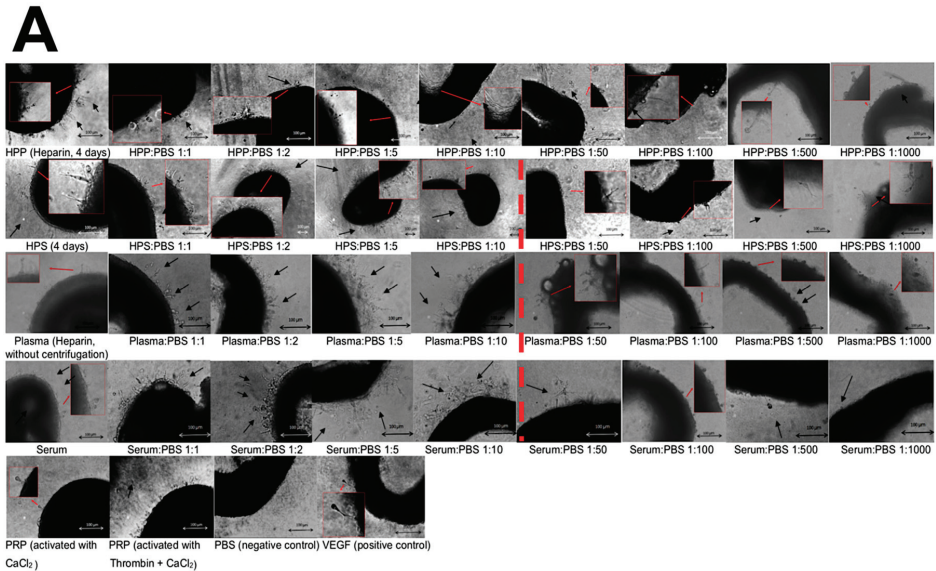
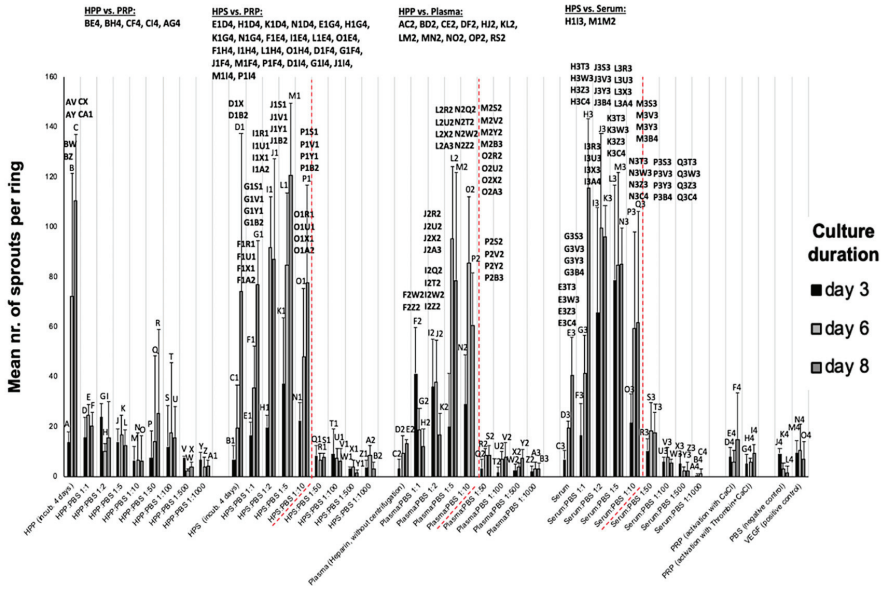


Figure 7. Cont.

B



C

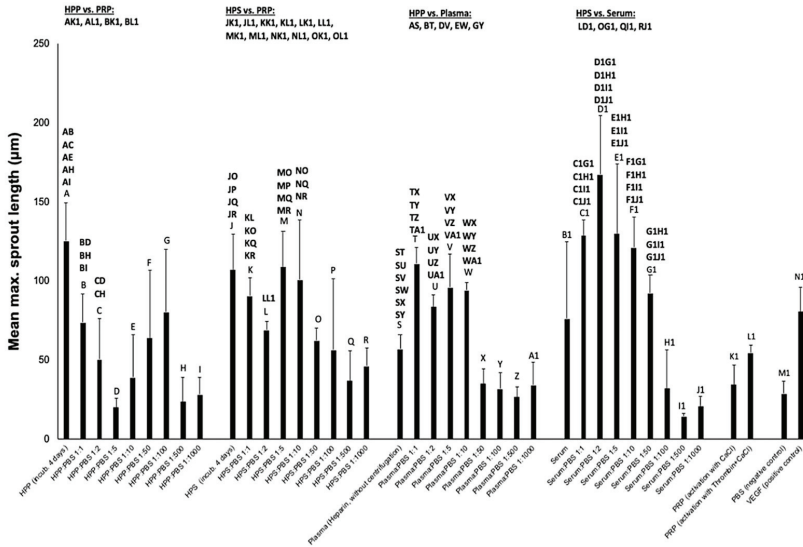


Figure 7. Effect of hypoxia preconditioned secretome dilution on microvessel sprouting in vitro. (A) Panel showing representative images of aortic rings, embedded in Matrigel and cultured in the presence of diluted blood-derived secretomes for 3, 6 and 8 days (Bars = 100 µm). Microvessels sprouting from aortic rings are indicated by black arrows. Enlarged image sections are shown by red insets. (B) Plot showing the mean number of sprouts per ring over a culture duration of 3, 6 and 8 days ($n = 3$). (C) Plot showing the mean maximum sprout length after a culture period of 8 days ($n = 3$). Red dashed lines on plots and images indicate statistically significant cut-off points of dilution. Capital letter pairs shown directly above histograms indicate intra-condition statistical comparison of corresponding data points, while HPP/HPS vs. Plasma/Serum and HPP/HPS vs. PRP statistical comparisons are shown on the upper part of plot B and C. For all pair comparisons $p < 0.05$, unless otherwise indicated. Error bars represent s.d.

4. Discussion

Peripheral blood has been, for considerable time, thought of as a suitable source of growth factor proteins that can be used to aid tissue repair and regeneration [2,5,8,44,51,52]. This is indeed a sound rationale, given the interwoven participation of peripheral blood cells in all stages of the wound healing process [6,8,53,54]. Among the various blood-based products that have been clinically tested, platelet-derived secretomes such as platelet-rich plasma (PRP) and platelet-rich fibrin matrix (PRFM) have received by far the greatest attention [3,4,55]. Hypoxia preconditioned blood-derived secretomes (HPP and HPS) represent a newer development in the field of autologous growth factor preparations, and offer a novel alternative to platelet-derived secretomes [2,5,19,44]. The basic idea underlying the proposed functionality of all these products is the *ex vivo* recapitulation of the physiological cellular responses involved in wound repair, by employing protein factor signalling that is naturally emitted by key cell types, namely platelets in the PRP approach, and peripheral blood cells (PBCs: neutrophils, macrophages, lymphocytes) in HPP/HPS (see Figure 1C). In contrast to simple blood centrifugation and subsequent concentration of cells (platelets), and their growth factors, blood preconditioning under physiological temperature and hypoxia (i.e., extracorporeal wound simulation) offers a means of optimizing the angiogenic potential of blood-based products through hypoxia-induced temporal changes in PBC growth factor expression, without merely relying on the release of factors already stored within platelets at the time of blood collection [2,5,19,44]. Furthermore, by allowing PBCs to regulate their O₂ microenvironment, as employed in this work, instead of exposing them to an artificial one (i.e., fixed/global hypoxia produced within an O₂ controlling incubator), it may even be possible to better simulate the conditions encountered within an *in vivo* wound [16–19], since the direct correlation of pericellular O₂ tension with hypoxia-regulated gene expression [5,13] suggests that a more physiological angiogenic response could be achieved through cell-mediated hypoxia. Importantly, beyond the obvious differences in cell type employed (i.e., platelets vs. PBCs) and method of preparation used (i.e., centrifugation vs. hypoxic preconditioning), PRP and HPP/HPS organically differ with respect to their specific correlation with the wound healing phases, the former having a direct correlation with the haemostatic phase, while the latter being more closely correlated with the angiogenesis-driven proliferative phase (see Figure 1C). It could thus be argued that the development of hypoxia preconditioned secretomes represents a true paradigm shift in the evolution of blood-based products, since it offers a logical progression along the wound healing pathway itself, pushing the focus away from the initial trauma-induced signalling phase, towards the more specific hypoxia-driven angiogenic response.

In this work we hypothesized that the aforementioned fundamental differences in the preparation of these secretomes would translate into measurable differences in the concentration of key pro- (VEGF) and anti- (TSP-1, PF-4) angiogenic factor proteins. We deliberately chose to focus on hypoxia-regulated factors (VEGF, TSP-1) and platelet-derived factors (VEGF, TSP-1, PF-4), in order to identify whether the method of secretome preparation, i.e., hypoxic preconditioning vs platelet concentration, influenced their angiogenic composition. We found that both PRP and HPP/HPS had a significantly higher VEGF concentration compared to their baseline controls, i.e., fresh plasma and fresh serum (see Figure 2A), while the levels of the platelet-derived factors TSP-1 and PF-4 in HPP were significantly lower than those in HPS and PRP, indicating minimal platelet activation during blood conditioning in HPP (see Figure 2A). Indeed, the method of blood anticoagulation used for HPP preparation, i.e., EDTA vs. heparin, appeared to only influence the levels of the hypoxia-regulated factors VEGF and TSP-1 (EDTA likely interfered with hypoxia-inducible factor (HIF) signalling [56]), but not PF-4, which is solely derived from platelets. The increased concentration of VEGF in HPP, which must therefore be primarily of non-platelet origin, thus supports the positive influence of hypoxic blood conditioning on PBC pro-angiogenic factor expression [2,5]. It should, of course, not be forgotten that the three factors tested here, while important in angiogenesis, only represent a tiny portion of the plethora of pro- and anti-angiogenic factor proteins that are known to exist in blood-derived secretomes [2,13,17,57], therefore, the differences between the growth factor profiles of these secretomes might be vastly greater

than what can be inferred from our current results. For example, differences in their content and composition of matrix metalloproteinases (MMPs), which are known to be released by platelets and leukocytes, could significantly affect their utility in preventing/treating scar formation in traumatic and chronic wounds, with significant clinical implications. Previous work from our group had employed mass spectrometry to analyse the proteomic composition of peripheral blood cell-derived secretomes in an *in vitro* wound model utilizing hypoxic stress stimulation [13]. Further proteome profiling using similar approaches might indeed highlight a greater degree of dissimilarity in their growth factor composition, and by extension in their *in vivo* functionality.

The statistically significant correlation of HPP/HPS VEGF concentration with an increasing blood incubation time of 4 to 7 days (see Figure 2B) confirmed our previous findings of hypoxia-induced pro-angiogenic factor upregulation in hypoxia preconditioned secretomes [2,5]. The higher VEGF concentration measured in 7 days-incubated HPS, compared to that measured in HPP, likely represents the additional platelet-derived VEGF that had been released into HPS following blood coagulation. In these experiments, HPP not only had a lower concentration of VEGF than HPS, but also a lower concentration of the platelet-derived angiogenesis inhibitors TSP-1 and PF-4, in agreement with the data of Figure 2A. The finding that TSP-1 and PF-4 concentrations in 4 and 7 days-incubated HPP were significantly lower than those in fresh plasma (see Figure 2B) might be explained by a net protein breakdown occurring during blood incubation, in the absence of continuous factor release from platelets. In contrast, hypoxia-induced upregulation of TSP-1 expression in HPS [2] resulted in a higher TSP-1 concentration in 4 and 7 days-incubated HPS than that in fresh serum, a difference not seen in the levels of PF-4 (see Figure 2B). Therefore, while HPP appears to comprise primarily hypoxia-induced pro-angiogenic signalling, and can be thus considered an angiogenesis-targeting growth factor mixture, HPS represents a more ‘complete’ secretome, since it provides both the coagulation-generated, as well as the hypoxia-induced phase of the wound healing cascade (see Figure 1C). Despite their differences, both HPP and HPS are characterized by the physiological optimization of their growth factor composition, which is achieved through hypoxia, rather than an artificial fortification in the concentration of platelet-derived factors, as in PRP. This, by definition, makes HPP and HPS more physiological secretomes than platelet-based products, with significant implications towards their functionality as promoters of tissue-regeneration.

An analysis of the ability of these blood-derived secretomes to induce microvessel formation in endothelial cell cultures *in vitro* revealed that both hypoxia preconditioned and platelet-derived secretomes were more potent than their corresponding baseline controls (fresh plasma and serum), with no significant difference in either the number of tubes or nodes being observed between the two secretome types (see Figure 3A,B). The latter is important, given the previously discussed differences in the concentration of anti-angiogenic factors between HPP and HPS/PRP, and highlights the dependence of new vessel formation on the presence of an adequate amount of pro-angiogenic factors, at least at the *in vitro* level. In accordance to our ELISA results (see Figure 2A), HPP prepared with EDTA as anticoagulant showed minimal tube formation, likely due to its low concentration of pro-angiogenic factors (e.g., VEGF). The positive effect of hypoxia on secretome angiogenic potential could be confirmed by the finding that hypoxic preconditioning improved the angiogenic activity of serum (4 and 7 days-incubated HPS), which was initially less angiogenic than fresh plasma (see Figure 3A,C), an observation that is consistent with the fact that serum has a higher concentration of anti-angiogenic factors (e.g., TSP-1, PF-4). The length of blood conditioning (4 vs. 7 days) did not appear to significantly influence the angiogenic potency of HPP or HPS (see Figure 3A,C), in agreement with the plateau seen in VEGF concentration (see Figure 2B).

Assessment of the functional bioactivity of freeze-stored secretomes in the *in vitro* angiogenesis assay provided evidence that low-temperature storage did not negatively impact their ability to promote microvessel formation (see Figure 4A,B), which was in agreement with our ELISA data showing preservation of VEGF protein in all secretomes, following 4 and 12 weeks freeze storage (see Figure 2C). As in the case of fresh secretomes, no difference in angiogenic potency was detected

between freeze-stored hypoxia preconditioned and platelet-derived secretomes (see Figure 4A,B). We note, however, that only the platelet-derived secretomes that had been activated *in vitro* before freezing, and were thus rendered cell-free, could be tested in this assay, since freezing caused cell haemolysis and prevented evaluation of PRP that had been activated after freeze-storage. This problem of platelet haemolysis might, however, present more than just a technical hurdle, since the presence of cellular debris in the final product might prohibit the freezing of PRP immediately after its preparation, in the clinical setting.

With respect to microvessel sprouting, no significant differences could be detected between hypoxia preconditioned and platelet-derived secretomes, while neither secretome type appeared to induce more sprouting in aortic ring cultures than fresh plasma or serum (see Figure 5A,B). Hypoxia preconditioned secretomes did, however, promote the formation of longer sprouts than PRP (see Figure 5C). This finding, together with the fact that fresh serum generated equally long sprouts as HPS, and significantly longer sprouts than PRP (see Figure 5C), seems to suggest that while both hypoxia-induced and platelet-derived factors are important for sprout lengthening, as previously suggested [58], an oversupply of platelet-derived factors, more specifically angiogenic inhibitors (e.g., PF-4), appears to limit sprout extension. Previous work from our group, and others, has demonstrated that microvessel formation and sprouting are two distinct cellular responses, which appear to rely on different sets of growth factor signalling rules [13,59]. In particular, while microvessel formation is strongly inhibited by the platelet-derived angiostatic factor PF-4, this factor seems to play an important role in sprouting angiogenesis [13,60]. Our new data indicate that while an abundance of PF-4, even at the supraphysiological concentrations found in PRP, does not limit microvessel sprouting, it might have a negative impact on the average extension of new sprouts. Further work is, however, required to fully clarify these effects, before a precise factor concentration range that optimally supports these responses can be defined.

Interestingly, diluting hypoxia preconditioned secretomes appeared to *increase* their ability to promote microvessel formation in the *in vitro* angiogenesis assay, rather than decrease it. This effect persisted up to a 100-fold dilution, beyond which a reduced angiogenic response was observed (see Figure 6). Furthermore, both HPP and HPS of 1:5 to 1:100 dilution were more potent than PRP, which is by its nature a concentrated product, and is known to contain large amounts of angiogenesis-inhibiting growth factors (e.g., PF4, TSP-1) [11,29,61]. Similar effects were observed in the sprouting assay, although here the maximum HPP/HPS dilution that could support sprouting was lower, at 1:10 (see Figure 7). Importantly, PRP was not found to be more angiogenic (microvessel formation and sprouting) than analogous dilutions of fresh plasma or serum (see Figures 6 and 7), which casts doubt on the actual utility of concentrating platelet-derived secretomes as a power-tool for stimulating angiogenesis *in vivo*. When taken together into consideration, these findings suggest that physiological microvessel formation and sprouting are dependent on the fine balance of pro- and anti-angiogenic factors, rather than an oversupply of any single factor. As an oversimplification, the most favourable growth factor composition seems to be one that allows a relative reduction of angiogenesis-inhibitory factors, while maintaining an adequate amount of pro- angiogenic factors. Predictably, and as shown by our data, when the latter becomes too low, the response sharply declines. This mechanism would be in support of angiogenic disinhibition, instead of direct pro-angiogenic stimulation, as the primary switch that physiologically triggers hypoxia-induced angiogenesis *in vivo* (Figure 8A,B), and it is in agreement with the findings of our previous work which employed PF-4 blocking experiments in an *in vitro* wound healing model [13]. The proposed two-step optimization of PBC-derived secretomes, i.e., first through hypoxic stimulation, and subsequent controlled dilution, mirrors in fact the spatiotemporal evolution of growth factor signalling that powers the angiogenesis-driven proliferative phase of wound healing, and forms the foundation of tissue repair following haemostasis (Figure 8A,B).

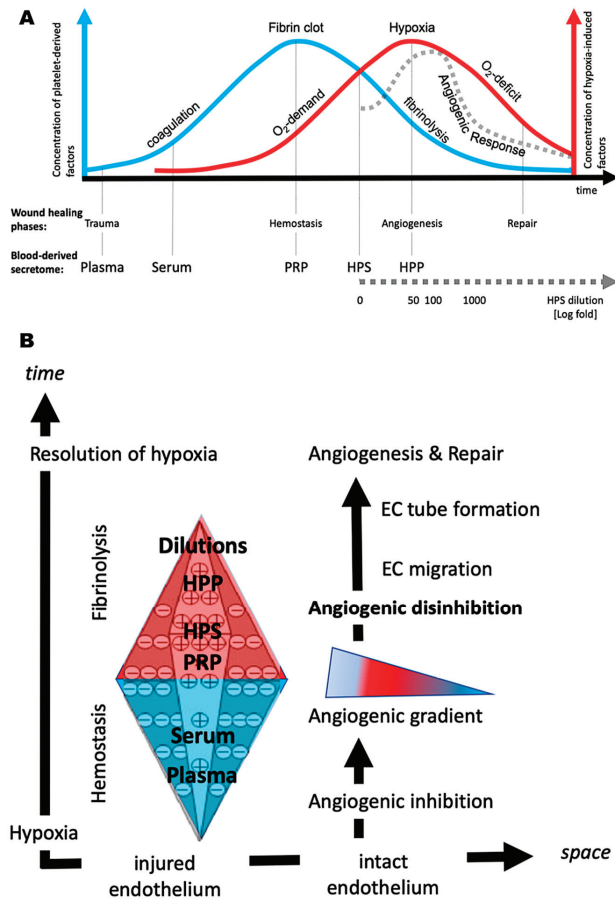


Figure 8. Biological basis underlying the utilization of different blood-derived secretomes. (A) Plot showing the representative correlation of different types of blood-derived secretomes (plasma, serum, PRP, HPS, HPP) with the progressive phases of wound repair. The coagulation-induced signaling phase (platelet-derived growth factors; blue curve) that supports haemostasis, correlates with PRP since it depends on the maximum concentration of platelets, while the hypoxia-induced signaling phase (PBC-derived growth factors; red curve) that drives angiogenesis, correlates initially with HPS, and eventually with HPP and HPS dilutions. The shape of the dotted gray curve represents the net angiogenic response, and is theoretically defined by subtracting anti-angiogenic platelet-derived signaling (blue curve) from pro-angiogenic hypoxia-induced signaling (red curve). (B) Proposed mechanism for the biochemical control of wound angiogenesis, and correlation of the various blood-derived secretomes (plasma, serum, PRP, HPS, HPP) with the different wound healing phases. Following completion of the haemostatic phase, the fibrin matrix undergoes controlled degradation through fibrinolysis, leading to depletion in the local pool of anti-angiogenic factors (e.g., PF-4) which are bound to fibrin (indicated by “-” sign), while up-regulation of pro-angiogenic factors (e.g., VEGF) through hypoxia (indicated by “+” sign) leads to the formation of chemoattractive gradients that direct endothelial cell (EC) migration towards the injured site. Angiogenic disinhibition enables vascularization of the matrix through fibrinolysis-mediated EC invasion, which facilitates resolution of hypoxia and tissue repair.

From a cell-biological perspective, hypoxic preconditioning of peripheral blood may offer an additional advantage, beyond the direct hypoxia-induced upregulation and optimization of angiogenic

growth factor signaling that we have presented and discussed here. Previous work has indeed demonstrated that hypoxic preconditioning increases the survival and angiogenic potency of peripheral blood mononuclear cells via oxidative stress resistance and reduced reactive oxygen species (ROS) accumulation, compared to normoxic culture [62]. Powered with that knowledge, it might be possible in the future to develop more advanced therapeutic strategies around the HPP/HPS concept, by combining peripheral blood hypoxic preconditioning together with hypoxia/reoxygenation (H/R) protocols, since it is known that H/R (but not hypoxia alone) enhances the activation of ROS-dependent intracellular signaling and as a result accelerates the rate of neovascularization in vivo [63]. The combination of hypoxia-induced pro-angiogenic growth factor signaling with ROS generation could potentially offer a more physiological, and by extension robust angiogenic response than either approach in isolation.

5. Conclusions

The findings of this study highlight the fact that the angiogenic potential of blood-derived secretomes is defined by the complex stoichiometry of their component pro- and anti-angiogenic factor proteins, rather than the concentration of one or more growth factors. This understanding, then establishes a basis that, at its core, strongly opposes the rationale of concentrating cells (e.g., platelets) and their stored growth factors, as a means of optimizing the composition of a blood-derived product. In contrast to the PRP approach, hypoxic conditioning of peripheral blood generates compositions that are characterized by the physiological upregulation of hypoxia-induced pro-angiogenic signalling, and which can further be fine-tuned through controlled secretome dilution. By employing this method, complex compositions can be obtained that are relatively rich in pro-angiogenic growth factors (e.g., VEGF), but have a lower concentration of anti-angiogenic factors (e.g., PF-4), compared to PRP. Our data indicate that such optimized secretomes promote a stronger angiogenic response than PRP in vitro, and therefore merit further clinical investigation as useful tools for promoting tissue repair and regeneration. The ability to administer hypoxia preconditioned products as cell-free preparations further differentiates these from platelet-based products, since it makes them safe and suitable for off-the-shelf application via freeze-storage.

Author Contributions: Conceptualization, E.H., A.F.S. and P.M.; methodology, E.H., P.M., K.K. and A.F.S.; software, P.M., S.B. and A.-T.B.; validation, P.M., S.B., K.K. and A.-T.B.; formal analysis, P.M., K.K., S.B.; investigation, P.M., K.K., S.B. and A.-T.B.; resources, H.-G.M.; data curation, P.M., K.K., S.B. and U.D.; writing—original draft preparation, P.M., E.H., and A.F.S.; writing—review and editing, P.M., E.H., A.F.S., U.D. and S.v.I.; visualization, P.M., E.H.; supervision, E.H., and A.F.S.; project administration, H.-G.M., E.H.; funding acquisition, H.-G.M. All authors have read and agreed to the published version of the manuscript.

Funding: This research received no external funding.

Conflicts of Interest: The authors declare no conflict of interest. The blood donors involved in this study do not have any direct relationship with the authors. In the past 5 years AFS has provided consulting services to IPB and has received institutional support by Biomet, Curasan. No royalties. This study was carried out under the umbrella of the EmaCure Project (for more info please visit www.emacure.org).

Abbreviations

PBC	peripheral blood cells
HPS	hypoxia preconditioned serum
HPP	hypoxia preconditioned plasma
PRP	platelet-rich plasma
PRFM	platelet-rich fibrin matrix
VEGF	vascular endothelial growth factor
TSP-1	thrombospondin-1
PF-4	platelet factor-4
IL-8	interleukin-8
FGF	fibroblast growth factor
MMP-9	matrix metalloproteinase-9
PBS	phosphate buffered saline

References

- Hesseler, M.J.; Shyam, N. Platelet-rich plasma and its utility in medical dermatology: A systematic review. *J. Am. Acad. Dermatol.* **2019**, *81*, 834–846. [[CrossRef](#)] [[PubMed](#)]
- Hadjipanayi, E.; Moog, P.; Bekeran, S.; Bereznoi, A.; Aguir, J.; Bauer, A.T.; Kükrek, H.; Schmauss, D.; Isenburg, S.; Ntziachristos, V.; et al. In vitro characterization of hypoxia preconditioned serum (HPS)-Fibrin hydrogels: Basis for an injectable biomimetic tissue regeneration therapy. *J. Funct. Biomater.* **2019**, *10*, 22. [[CrossRef](#)] [[PubMed](#)]
- Sampson, S.; Gerhardt, M.; Mandelbaum, B. Platelet rich plasma injection grafts for musculoskeletal injuries: A review. *Curr. Rev. Musculoskelet. Med.* **2008**, *1*, 165–174. [[CrossRef](#)] [[PubMed](#)]
- Carter, M.J.; Fyelling, C.; Parnell, L.K. Use of platelet rich plasma gel on wound healing: A systematic review and meta-analysis. *Eplasty* **2011**, *11*, e38.
- Hadjipanayi, E.; Bauer, A.T.; Moog, P.; Salgin, B.; Kükrek, H.; Fersch, B.; Hopfner, U.; Meissner, T.; Schlüter, A.; Ninkovic, M.; et al. Cell-free Carrier System for Localised Delivery of Peripheral Blood Cell-Derived Engineered Factor Signaling: Towards Development of a One-Step Device for Autologous Angiogenic Therapy. *J. Control. Release* **2013**, *169*, 91–102. [[CrossRef](#)]
- Reinke, J.M.; Sorg, H. Wound repair and regeneration. *Eur. Surg. Res.* **2012**, *49*, 35–43. [[CrossRef](#)]
- Stadelmann, W.K.; Digenis, A.; Tobin, G.R. Physiology and healing dynamics of chronic cutaneous wounds. *Am. J. Surg.* **1998**, *176*, 26S–38S. [[CrossRef](#)]
- Chicharro-Alcántara, D.; Rubio-Zaragoza, M.; Damiá-Giménez, E.; Carrillo-Poveda, J.M.; Cuervo-Serrato, B.; Peláez-Gorra, P.; Sopena-Juncosa, J.J. Platelet Rich Plasma: New Insights for Cutaneous Wound Healing Management. *J. Funct. Biomater.* **2018**, *9*, 10. [[CrossRef](#)]
- Golebiewska, E.M.; Poole, A. Platelet secretion: From haemostasis to wound healing and beyond. *Blood Rev.* **2015**, *29*, 153–162. [[CrossRef](#)]
- Italiano, J.E.; Richardson, J.L.; Patel-Hett, S.; Battinelli, E.; Zaslavsky, A.; Short, S. Angiogenesis is regulated by a novel mechanism: Pro-and antiangiogenic proteins are organized into separate platelet α granules and differentially released. *Blood* **2008**, *111*, 1227–1233. [[CrossRef](#)]
- Masoudi, E.; Ribas, J.; Kaushik, G.; Leijten, J.; Khademhosseini, A. Platelet-Rich Blood Derivatives for Stem Cell-Based Tissue Engineering and Regeneration. *Curr. Stem Cell Rep.* **2016**, *2*, 33–42. [[CrossRef](#)] [[PubMed](#)]
- Tonnesen, M.G.; Feng, X.; Clark, R.A. Angiogenesis in wound healing. *J. Investig. Dermatol. Symp. Proc.* **2000**, *5*, 40–46. [[CrossRef](#)] [[PubMed](#)]
- Hadjipanayi, E.; Kuhn, P.H.; Moog, P.; Bauer, A.T.; Kuekrek, H.; Mirzoyan, L.; Hummel, A.; Kirchhoff, K.; Salgin, B.; Isenburg, S.; et al. The Fibrin Matrix regulates Angiogenic Responses within the Hemostatic Microenvironment through Biochemical Control. *PLoS ONE* **2015**, *10*, e0135618. [[CrossRef](#)] [[PubMed](#)]
- Feng, X.; Tonnesen, M.G.; Mousa, S.A.; Clark, R.A. Fibrin and collagen differentially but synergistically regulate sprout angiogenesis of human dermal microvascular endothelial cells in 3-dimensional matrix. *Int. J. Cell Biol.* **2013**, *2013*, 231279. [[CrossRef](#)]
- Bogdanovski, D.A.; DiFazio, L.T.; Bogdanovski, A.K.; Csóka, B.; Jordan, G.B.; Paul, E.R.; Antonioli, L.; Pilip, S.A.; Nemeth, Z.H. Hypoxia-inducible-factor-1 in trauma and critical care. *J. Crit. Care* **2017**, *42*, 207–212. [[CrossRef](#)]
- Hadjipanayi, E.; Schilling, A.F. Hypoxia-based strategies for angiogenic induction. *Organogenesis* **2013**, *9*, 261–272. [[CrossRef](#)]
- Hickey, M.M.; Simon, M.C. Regulation of angiogenesis by hypoxia and hypoxia-inducible factors. *Curr. Top. Dev. Biol.* **2006**, *76*, 217–257.
- Simon, M.C.; Keith, B. The role of oxygen availability in embryonic development and stem cell function. *Nat. Rev. Mol. Cell Biol.* **2008**, *9*, 285–296. [[CrossRef](#)]
- Hadjipanayi, E.; Schilling, A.F. Regeneration through autologous hypoxia preconditioned plasma. *Organogenesis* **2014**, *10*, 164–169. [[CrossRef](#)]
- Muñoz, M.; García-Vallejo, J.; Ruiz, M.D.; Romero, R.; Olalla, E.; Sebastián, C. Transfusion of post-operative shed blood: Laboratory characteristics and clinical utility. *Eur. Spine J.* **2004**, *1*, 107–113. [[CrossRef](#)]
- Sikorski, R.A.; Rizkalla, N.A.; Yang, W.W.; Frank, S.M. Autologous blood salvage in the era of patient blood management. *Vox Sang.* **2017**, *112*, 499–510. [[CrossRef](#)] [[PubMed](#)]

22. Eppley, B.L.; William, S.; Pietrzak, M.B. Platelet- rich plasma:a review of biology and Applications in Plastic Surgery. *Plast. Reconstr. Surg.* **2006**, *118*, 147–159. [[CrossRef](#)] [[PubMed](#)]
23. Marx, R.E. Platelet-rich plasma (PRP): What ist PRP and what is not PRP? *Implant Dent.* **2001**, *10*, 225–228. [[CrossRef](#)] [[PubMed](#)]
24. Akhundov, K.; Pietramaggiore, G.; Waselle, L.; Darwiche, S.; Guerid, S.; Scaletta, C.; Hirt-Burri, N.; Applegate, L.A.; Raffoul, W.V. Development of a cost- effective method for platelet- rich plasma (PRP) preparation for topical wound healing. *Ann. Burns Fire Dis.* **2012**, *25*, 207–213.
25. Abu-Ghname, A.; Perdanasari, A.T.; Davis, M.J.; Reece, E.M. Platelet-Rich Plasma: Principles and Applications in Plastic Surgery. *Semin Plast. Surg.* **2019**, *33*, 155–161. [[CrossRef](#)]
26. Marx, R.E. Platelet-rich plasma: Evidence to support its use. *J. Oral Maxillofac. Surg.* **2004**, *62*, 489–496. [[CrossRef](#)] [[PubMed](#)]
27. Scalfani, A.P.; McCormick, S.A. Induction of dermal collagenesis, angiogenesis, and adipogenesis in human skin by injection of platelet-rich fibrin matrix. *Arch. Facial Plast. Surg.* **2012**, *14*, 132–136.
28. Raeissadat, S.A.; Rayegani, S.; Hassanabadi, H.; Fathi, M.; Ghorbani, E.; Babae, M.; Azma, K. Knee Osteoarthritis Injection Choices: Platelet- Rich Plasma (PRP) Versus Hyaluronic Acid (A one-year randomized clinical trial). *Clin. Med. Insights Arthritis Musculoskelet. Disord.* **2015**, *8*, 1–8. [[CrossRef](#)]
29. Amable, P.R.; Caias, R.; Teixeira, M.V.T.; da Cruz Pacheco, I.; Corrêa do Amaral, R.J.F.; Granjeiro, J.M.; Borojevic, R. Platelet-rich plasma preparation for regenerative medicine: Optimization and quantification of cytokines and growth factors. *Stem Cell Res. Ther.* **2013**, *4*, 67. [[CrossRef](#)]
30. Pachito, D.V.; Latorraca, C.O.C.; Riera, R. Efficacy of platelet-rich plasma for non-transfusion use: Overview of systematic reviews. *Int. J. Clin. Pract.* **2019**, *13*, e13402. [[CrossRef](#)]
31. Scalfani, A.P. Applications of platelet-rich fibrin matrix in facial plastic surgery. *Facial Plast. Surg.* **2009**, *25*, 270–276. [[CrossRef](#)] [[PubMed](#)]
32. Hom, D.B. New Developments in wound healing relevant to facial plastic surgery. *Arch. Facial Plast. Surg.* **2008**, *10*, 402–406. [[CrossRef](#)] [[PubMed](#)]
33. van den Dolder, J.; Mooren, R.; Vloon, A.P.; Stoeltinga, P.J.; Jansen, J.A. Platelet-Rich Plasma: Quantification of Growth Factor Levels and the Effect on Growth and Differentiation of Rat Bone Marrow Cells. *Tissue Eng.* **2006**, *12*, 3067–3073. [[CrossRef](#)] [[PubMed](#)]
34. Aghaloo, T.L.; Moy, P.K.; Freymiller, D.E.G. Investigation of platelet-rich plasma in rabbit cranial defects: A pilot study. *J. Oral Maxillofac. Surg.* **2002**, *60*, 1176–1181. [[CrossRef](#)]
35. Kuffler, D.P. Platelet-Rich Plasma Promotes Axon Regeneration, Wound Healing, and Pain Reduction: Fact or Fiction. *Mol. Neurobiol.* **2015**, *52*, 990–1014. [[CrossRef](#)]
36. Cervelli, V.; Gentile, P.; Scioli, M.G.; Grimaldi, M.; Casciani, C.U.; Spagnoli, L.G.; Orlandi, A. Application of platelet-rich plasma in plastic surgery: Clinical and in vitro evaluation. *Tissue Eng. Part C Methods* **2009**, *15*, 625–634. [[CrossRef](#)]
37. Cho, E.B.; Park, G.S.; Park, S.S.; Jang, Y.J.; Kim, K.H.; Kim, K.J.; Park, E.J. Effect of platelet-rich plasma on proliferation and migration in human dermal fibroblasts. *J. Cosmet. Dermatol.* **2019**, *18*, 1105–1112. [[CrossRef](#)]
38. Martinez, C.E.; Smith, P.; Palma Alvarado, V.A. The influence of platelet-derived products on angiogenesis and tissue repair: A concise update. *Front. Physiol.* **2015**, *6*, 290. [[CrossRef](#)]
39. Kim, D.H.; Je, Y.J.; Kim, C.D.; Lee, Y.H.; Seo, Y.J.; Lee, J.H.; Lee, Y. Can Platelet-rich Plasma Be Used for Skin Rejuvenation? Evaluation of Effects of Platelet-rich Plasma on Human Dermal Fibroblast. *Ann. Dermatol.* **2011**, *23*, 424–431. [[CrossRef](#)]
40. Martinez-Zapata, M.J.; Marti-Carvajal, A.J.; Sola, I.; Expósito, J.A.; Bolibar, I.; Rodriguez, L.; Garcia, J.; Zaror, C. Autologous platelet-rich plasma for treating chronic wounds. *AR Cochrane Database Syst. Rev.* **2016**, *25*, 1–56. [[CrossRef](#)]
41. Kimmel, H.M.; Grant, A.; Ditata, J. The Presence of Oxygen in Wound Healing. *Wounds* **2016**, *28*, 264–270.
42. Carmeliet, P. Angiogenesis in life, disease and medicine. *Nature* **2005**, *174*, 2336–2342. [[CrossRef](#)]
43. Ribatti, D.; Folkman, J. A pioneer in the study of angiogenesis. *Angiogenesis* **2008**, *11*, 3–10. [[CrossRef](#)]
44. Hadjipanayi, E.; Bekeran, S.; Moog, P. Extracorporeal Wound Simulation as a Foundation for Tissue Repair and Regeneration Therapies. *Int. J. Transp. Plast. Surg.* **2018**, *2*, 1–10.
45. Burke, B.; Giannoudis, A.; Corke, K.P.; Gill, D.; Wells, M.; Ziegler-Heitbrock, L.; Lewis, C.E. Hypoxia-induced gene expression in human macrophages: Implications for ischemic tissues and hypoxia-regulated gene therapy. *Am. J. Pathol.* **2003**, *163*, 1233–1243. [[CrossRef](#)]

46. Panutosopulos, D.; Zafiroopoulos, A.; Krambovitis, E.; Kochiadakis, G.E.; Igoumenidis, N.E.; Spandidos, D.A. Peripheral monocytes from diabetic patients with coronary artery disease display increased bFGF and VEGF mRNA expression. *J. Transl. Med.* **2003**, *1*, 6. [[CrossRef](#)] [[PubMed](#)]
47. Lichtenauer, M.; Mildner, M.; Hoetzenecker, K.; Zimmermann, M.; Podesser, B.K.; Sipos, W.; Berényi, E.; Dworschak, M.; Tschachler, E.; Gyöngyösi, M.; et al. Secretome of apoptotic peripheral blood cells (APOSEC) confers cytoprotection to cardiomyocytes and inhibits tissue remodelling after acute myocardial infarction: A preclinical study. *Basic Res. Cardiol.* **2011**, *106*, 1283–1297. [[CrossRef](#)] [[PubMed](#)]
48. Reher, P.; Doan, N.; Bradnock, B.; Meghji, S.; Harris, M. Effect of ultrasound on the production of IL-8, basic FGF and VEGF. *Cytokine* **1999**, *11*, 416–423. [[CrossRef](#)]
49. Nagata, M.J.; Messora, M.R.; Furlaneto, F.A.; Fucini, S.E.; Bosco, A.F.; Garcia, V.G.; Deliberador, T.M.; de Melo, L.G. Effectiveness of two methods for preparation of autologous platelet-rich plasma: An experimental study in rabbits. *Eur. J. Dent.* **2010**, *4*, 395–402. [[CrossRef](#)]
50. Baker, M.; Robinson, S.D.; Lechertier, T.; Barber, P.R.; Tavora, B.; D’Amico, G.; Jones, D.T.; Vojnovic, B.; Hodivala-Dilke, K. Use of the mouse aortic ring assay to study angiogenesis. *Nat. Protoc.* **2011**, *7*, 89–104. [[CrossRef](#)]
51. Wahl, S.M.; Wong, H.; McCartney-Francis, N. Role of growth factors in inflammation and repair. *J. Cell Biochem.* **1989**, *40*, 193–199. [[CrossRef](#)]
52. Samadi, P.; Sheykhhasan, M.; Khoshinani, H.M. The Use of Platelet-Rich Plasma in Aesthetic and Regenerative Medicine: A Comprehensive Review. *Aesth. Plast. Surg.* **2019**, *43*, 803–814. [[CrossRef](#)]
53. Cañedo-Dorantes, L.; Cañedo-Ayala, M. Skin Acute Wound Healing: A Comprehensive Review. *Int. J. Inflamm.* **2019**, *2019*, 3706315. [[CrossRef](#)]
54. Guo, S.; DiPietro, L.A. Factors Affecting Wound Healing. *J. Dent. Res.* **2010**, *89*, 219–229. [[CrossRef](#)] [[PubMed](#)]
55. Alser, O.H.; Goutos, I. The evidence behind the use of platelet-rich plasma (PRP) in scar management: A literature review. *Scars Burn Heal.* **2018**, *4*, 1–15. [[CrossRef](#)] [[PubMed](#)]
56. Malairaman, U.; Dandapani, K.; Katyal, A. Effect of Ca2EDTA on Zinc Mediated Inflammation and Neuronal Apoptosis in Hippocampus of an In Vivo Mouse Model of Hypobaric Hypoxia. *PLoS ONE* **2014**, *9*, e110253. [[CrossRef](#)] [[PubMed](#)]
57. Senzel, L.; Gnatenko, D.; Bahou, W.F. The Platelet Proteome. *Curr. Opin. Hematol.* **2009**, *16*, 329–333. [[CrossRef](#)]
58. Go, R.S.; Ritman, E.L.; Owen, W.G. Angiogenesis in rat aortic rings stimulated by very low concentrations of serum and plasma. *Angiogenesis* **2003**, *6*, 25–29. [[CrossRef](#)]
59. Nowak-Sliwinska, P.; Alitalo, K.; Allen, E.; Anisimov, A.; Aplin, A.C.; Auerbach, R.; Augustin, H.G.; Bates, D.O.; van Beijnum, J.R.; Bender, R.H.; et al. Consensus guidelines for the use and interpretation of angiogenesis assays. *Angiogenesis* **2018**, *21*, 425–532. [[CrossRef](#)]
60. Hang, T.C.; Tedford, N.C.; Reddy, R.J.; Rimchala, T.; Wells, A.; White, F.M.; Kamm, R.D.; Lauffenburger, D.A. Vascular Endothelial Growth Factor (VEGF) and Platelet (PF-4) Factor 4 Inputs Modulate Human Microvascular Endothelial Signaling in a Three-Dimensional Matrix Migration Context. *Mol. Cell Proteom.* **2013**, *12*, 3704–3718. [[CrossRef](#)]
61. El-Sharkawy, H.; Kantarci, A.; Deady, J.; Hasturk, H.; Liu, H.; Alshahat, M.; Van Dyke, T.E. Platelet-rich plasma: Growth factors and pro- and anti-inflammatory properties. *J. Periodontol.* **2007**, *78*, 661–669. [[CrossRef](#)] [[PubMed](#)]
62. Kubo, M.; Li, T.S.; Suzuki, R.; Shirasawa, B.; Morikage, N.; Ohshima, M.; Qin, S.L.; Hamano, K. Hypoxic preconditioning increases survival and angiogenic potency of peripheral blood mononuclear cells via oxidative stress resistance. *Am. J. Physiol. Heart Circ. Physiol.* **2008**, *294*, H590–H595. [[CrossRef](#)] [[PubMed](#)]
63. Lelkes, P.I.; Hahn, K.L.; Sukovich, D.A.; Karmiol Schmidt, D.H. On the possible role of reactive oxygen species in angiogenesis. *Adv. Exp. Med. Biol.* **1998**, *454*, 295–310. [[PubMed](#)]



© 2020 by the authors. Licensee MDPI, Basel, Switzerland. This article is an open access article distributed under the terms and conditions of the Creative Commons Attribution (CC BY) license (<http://creativecommons.org/licenses/by/4.0/>).

Review

Basic Biology of Hypoxic Responses Mediated by the Transcription Factor HIFs and Its Implication for Medicine

Kiichi Hirota

Department of Human Stress Response Science, Institute of Biomedical Science, Kansai Medical University, Hirakata, Osaka 573-1010, Japan; khirota-kyt@umin.ac.jp; Tel.: +81-72-804-2526

Received: 5 January 2020; Accepted: 12 February 2020; Published: 13 February 2020

Abstract: Oxygen (O₂) is essential for human life. Molecular oxygen is vital for the production of adenosine triphosphate (ATP) in human cells. O₂ deficiency leads to a reduction in the energy levels that are required to maintain biological functions. O₂ acts as the final acceptor of electrons during oxidative phosphorylation, a series of ATP synthesis reactions that occur in conjunction with the electron transport system in mitochondria. Persistent O₂ deficiency may cause death due to malfunctioning biological processes. The above account summarizes the classic view of oxygen. However, this classic view has been reviewed over the last two decades. Although O₂ is essential for life, higher organisms such as mammals are unable to biosynthesize molecular O₂ in the body. Because the multiple organs of higher organisms are constantly exposed to the risk of “O₂ deficiency,” living organisms have evolved elaborate strategies to respond to hypoxia. In this review, I will describe the system that governs oxygen homeostasis in the living body from the point-of-view of the transcription factor hypoxia-inducible factor (HIF).

Keywords: hypoxia; transcription factor; hypoxia-inducible factor 1; HIF-1; hypoxia sensing

1. Introduction

The theory of phlogiston was proposed before the discovery of O₂ [1,2]. It was believed that substances burned in air were rich in phlogiston. The fact that combustion soon ceased in an enclosed space was taken as clear-cut evidence for air having the capacity to absorb only a finite amount of phlogiston [3,4]. When air became completely “phlogisticated,” it was no longer able to support the combustion of any material. This led to the concept that “burning” was a process, which released a substance termed phlogiston. According to this theory, fresh air does not contain phlogiston. Thus, oxygen was “discovered” as a so-called anti-phlogiston substance. Thus, from the very beginning of its discovery, oxygen was considered because of its deficiency [3]. Unlike gas molecules such as nitric oxide (NO), carbon monoxide (CO) and hydrogen sulfide (H₂S), oxygen is not produced in vivo and easily becomes “deficient” when supply is discontinued or diminished. In clinical settings, hypoxemia, defined as a drop in the partial pressure of O₂ in blood, leads to hypoxia. However, according to experimental as well as clinical evidence, the concept of a “normal” blood O₂ concentration cannot be unitarily defined. Hypoxia is conceptually defined as a lack of O₂ in the whole body or specific tissues/organs. Under hypoxic conditions, O₂ metabolism is suppressed. Usually, a decrease in absolute O₂ supply is indicated, but in clinical settings, a negative mismatch between O₂ supply to tissues/cells and O₂ demand is considered as a hypoxic state. When O₂ metabolism is suppressed, a biological response resembling an hypoxic response may be induced even when O₂ is amply available. When O₂ consumption rises beyond the limits of cardiopulmonary capacity for supplying O₂, or when an organ is exposed to inflammatory mediators due to sepsis or conditions involving disturbed O₂ utilization due to drugs or mitochondrial disorders, a response resembling a hypoxic state is observed at the

tissue/cell level. On the other hand, erythropoietin (EPO)-producing cells (REP cells), believed to be present in kidney stroma, may sense discrepancies between supply of, and demand for, oxygen and regulate erythrocyte production by modulating EPO secretion. EPO concentrations change constantly. Evidently, physiological “hypoxic regions” exist and play an important role in signal transduction in vivo. Reactive oxygen species (ROS) generated by oxygen exert toxic effects, but also play an essential role as secondary messengers in intracellular signal transduction. Thus, O₂ plays a role in both energy production and signal transduction in the body. This field of study may be termed investigative hypoxia biology. The partial pressure of O₂ in the cells is kept within a relatively narrow range. In humans, the O₂ partial pressure in the alveoli is about 110 mmHg, and the partial pressure of O₂ in the heart, kidney and brain is partially about 20 mmHg. The O₂ partial pressure of all cells is determined by the supply and consumption of O₂. Deviations such as hypoxia and hyperoxia trigger an adaptive response to maintain O₂ homeostasis at the cellular level. For the proper function and regulation of these systems, a harmonious expression of thousands of genes is probably required. In this review, I will describe the system which governs the O₂ homeostasis in the living body from the point of view of the transcription factors hypoxia-inducible factor (HIF).

2. Hypoxic Conditions in the Living Body

Hypoxic conditions in the living body in which O₂ metabolism is suppressed may be classified according to the underlying mechanism as follows [5–7] (Figure 1).

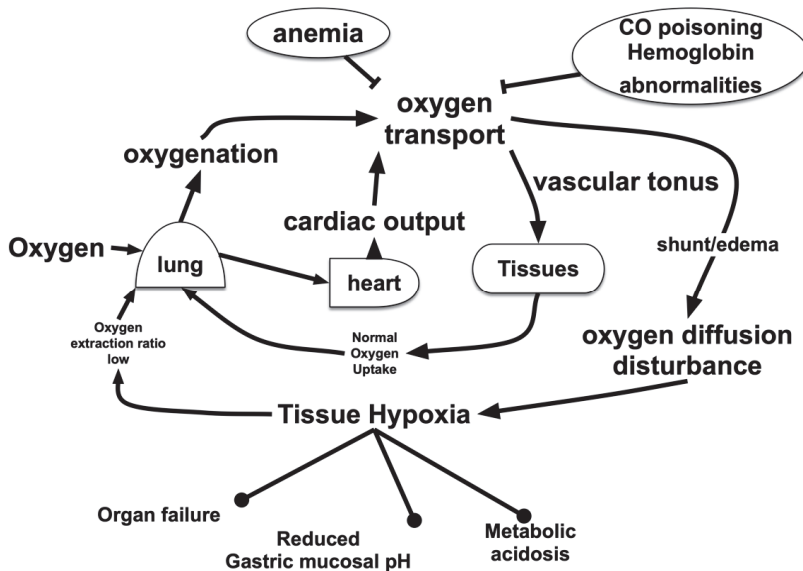


Figure 1. Oxygen (O₂) flow in the living body. O₂ is carried from the lungs to peripheral organs and tissues by red blood cells through blood vessels. Impaired oxygenation due to lung injury, disorders in transport due to anemia or blood clots and/or disturbance of transition from blood vessels to cells due to interstitial edema result in tissue hypoxia. In addition, O₂-related metabolic disturbances due to suppression of O₂ utilization, such as drug-induced mitochondrial suppression, might have an effect on the living body, which is equivalent to that of hypoxia.

2.1. Hypoxic Hypoxia

Hypoxemia is a state of reduced oxygen partial pressure in the blood, the onset mechanisms of which are a low O₂ partial pressure (caused by high altitudes or enclosed spaces), alveolar hypoventilation (drug effects and sleep apnea), loss of gas exchange efficiency in alveoli (pulmonary edema and acute lung injury), presence of pulmonary or intra-organic shunt (liver cirrhosis, congenital malformation) and ventilation decrease of the blood flow ratio (body position, artificial respiration). Hypoxemia can be assessed via a pulse oximeter even without drawing blood. Arterial blood gas analyses have been performed under extreme conditions (e.g., at atmospheric pressure of 253 mmHg, found at altitudes of 8400 m above the Everest summit, the PiO₂ was 43.1 mmHg; the average value of four individuals) [8–10].

2.2. Hypemic Hypoxia

Apart from being due to hypoxemia, the O₂ transport capacity of blood may decline for various other reasons, such as carbon monoxide poisoning [11,12], methemoglobinemia [13,14], congenital hemoglobin disorders [15–17] and impairment of O₂ transport capacity to tissues/organs. O₂ partial pressure in the blood is maintained. It may be determined by analyzing blood via a CO-oximeter. Anemia, in which the oxygen-carrying capacity is reduced due to a decrease in the red blood cell count and hemoglobin levels, is also included in this category. Hematopoietic disorders or iron deficiency may act as an onset mechanism for anemia. Anemia can be diagnosed via blood tests. Few studies have explicitly elucidated the actual impact of anemia, even though hemoglobin in red blood cells is known to be responsible for the oxygen-transporting ability of blood. We examined the difference in EPO expression between hypoxemia in 12.9-week-old C57BL mice exposed to a 10% oxygen environment (approximately 82% SpO₂) and an anemia group (200 µL of blood removed from the orbital vein for a decrease in the hematocrit from 44% to 33%) [18,19]. The plasma erythropoietin concentration was measured via ELISA 3 h later. The hypoxemia group contained 1000 pg/mL and the anemic group contained 1400 pg/mL, compared with 50 pg/mL for the control group. Thus, the anemic state induces a robust hypoxia-inducible gene response in not only the kidneys but also in the brain and the liver.

2.3. Tissue Hypoperfusion and Ischemia

Ischemia occurs because of low blood pressure, a thrombus or an embolus. Ischemia (hypoxia + low glucose + low amino acid) and hypoxia elicit completely different responses at the cellular level. Enhanced activation of hypoxia-inducible factor 1 was observed under hypoxic conditions (a 1% oxygen environment). However, activation was drastically attenuated under conditions that imitated ischemia (low oxygen + low glucose + low amino acid). Failure of blood flow in the limbs and skin can be easily detected, but visceral blood flow failure can only be assessed via ultrasonography, contrast CT or a similar technique [20,21].

2.4. Tissue Oxygen Metabolism Disorder

Even if O₂ supply is maintained above a certain level, O₂ burden may occur when O₂ consumption in the tissues/organs increases. Such a disease state may be caused by tissue O₂ metabolism disorder. Conditions that suppress O₂ metabolism in cells, such as cytotoxicity, mitochondrial suppression via therapeutic drugs or cyanide poisoning [22,23], biguanide-induced lactate acidosis [24,25] and propofol infusion syndrome [26,27], are classified in this category. However, oxygen metabolism disorder cannot be accurately diagnosed in real-time prior to organ dysfunction or some such effect becoming apparent. Only estimation methods based on the concentration of marker substances, such as lactic acid, are effective.

3. Hypoxia-Sensing Mechanisms

Molecular O₂ is essential for the development and growth of multicellular organisms. Mammals have evolved a sophisticated physiological network, which involves the capture, binding, transport, and delivery of molecular oxygen in order to maintain O₂ homeostasis at the tissue level. A critical aspect of this network is the ability to sense and respond to low O₂ conditions (Figure 2).

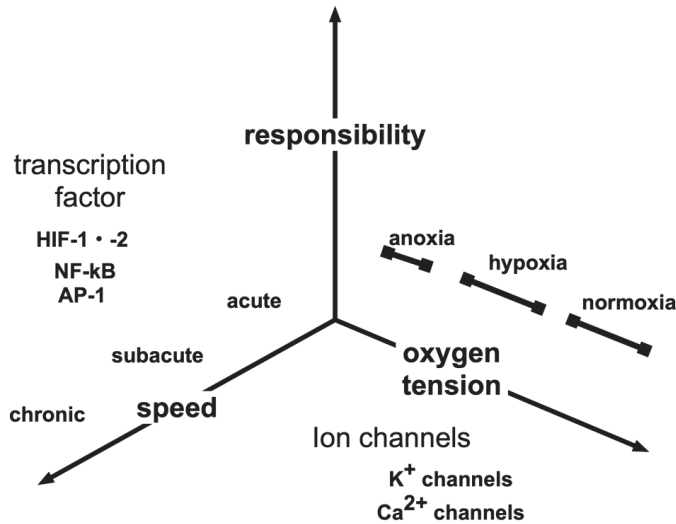


Figure 2. Various hypoxic responses. The hypoxic response of a living body may be classified in various ways according to the presence or absence of the gene response, rapidity and oxygen partial pressure that induces the response. In addition to HIF-1, transcription factors responsible for hypoxic responses include NF-κB and AP-1, which are master transcription factors for inflammatory responses. Hypoxic responses may vary from those that are triggered quickly, within minutes, such as hypoxic pulmonary vasospasm responses, to those involving several hours, such as erythropoietin induction. In addition, high altitude adaptation may occur over a few weeks.

Hypoxic responses by the body are not uniform. Therefore, hypoxic sensing mechanisms are not unique (Figure 3). When a biological system senses a reduction in arterial oxygen partial pressure at the carotid and aorta bodies, signals are transmitted to the respiratory center in response [28,29]. Glomus type I cells in the carotid and aortic bodies act as sensing cells of this system. Type I glomus cells depolarize when O₂ partial pressure decreases. This opens voltage-gated calcium channels resulting in a flow of calcium ions into the cytoplasm, which causes exocytosis of vesicles containing neurotransmitters [30–32]. In the event of hypoxic pulmonary artery contraction, sensor cells detect O₂ tension [33–35]. Renal EPO-producing (REP) cells in kidney stroma sense O₂ concentrations in renal arteries [36,37]. Thus, each of these hypoxic responses is associated with a sensing mechanism that may be defined via molecular biology. However, there is no consensus on whether molecular mechanisms underlying ion channel-based hypoxia signaling represent a universal strategy. It is not known whether similar or different O₂-sensing mechanisms are utilized during acute and chronic responses in depolarizable and nondepolarizable cells. A priori, one may postulate a variety of mechanisms by which cells may sense oxygen concentration levels. In the simplest model, the sensor binds oxygen directly, causing the fraction of sensor molecules bound to ligands to decline with the oxygen concentration. The bacterium, *Rhizobium meliloti*, exhibits a two-component signaling system consisting of FixL, a hemoprotein kinase that is active in the deoxy state, and FixJ, a transcription factor that becomes active when phosphorylated by FixL [38,39]. Hemoglobin also acts as an O₂ sensor.

The 3D structure of hemoglobin allosterically changes in response to O₂ tension. Although there is a lack of experimental support for a ligand model, it is possible that mammalian O₂ sensing involves molecular interactions with one or more hemoproteins. Besides heme, iron-sulfur clusters represent another intracellular target for O₂. In the presence of O₂, iron regulatory protein 2 is degraded via iron-sulfur cluster formation [40].

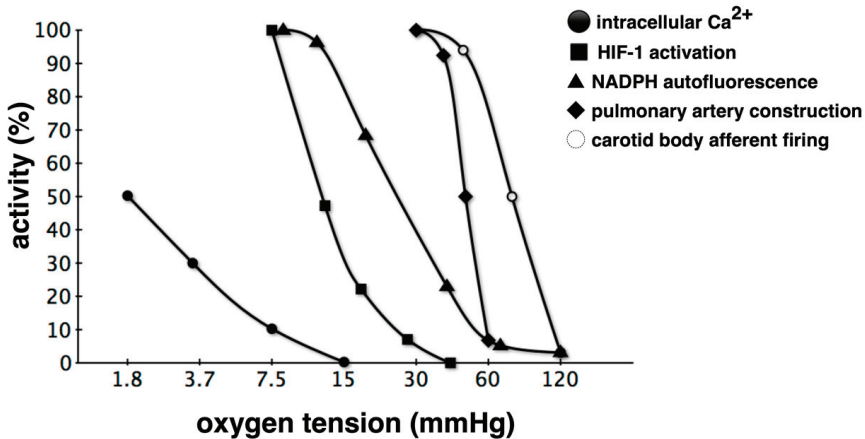


Figure 3. Relationship between oxygen tension and activities of hypoxic responses. Classification based on the partial pressure of O₂ that triggers a response is also possible. Hypoxic pulmonary vasospasm reactions begin at a higher oxygen partial pressure compared to HIF-1 activation, and intracellular Ca²⁺ elevation is mostly observed under anoxic conditions. Such varying hypoxic responses are probably due to differences in the corresponding O₂ partial pressure sensing mechanisms [28,31,34,41–44]. Hypoxia detected via several sensors is triggered as a hypoxic response through various effectors, but crosstalk occurs during the transduction of such signals. For example, some voltage-dependent K⁺ channel subtypes are regulated by HIF-1. NADPH: nicotinamide adenine dinucleotide phosphate.

Reportedly, mice display a mechanism by which the odor receptor, *Olfir78*, is able to sense an increase in lactic acid due to a decrease in oxygen, resulting in the excitation of the glomus I cells of arteriolar bodies [32,45]. A hypoxic response may be categorized by the threshold at which the reaction is triggered as well as by the mechanism of the reaction or the speed of the reaction. These differences may be due to differences in oxygen partial pressure sensors.

Although research using classical biochemical methods has a long history, molecular biology methods were introduced only in the 1990s. cDNA cloning of hypoxia-inducible factor 1 (HIF-1) became an important turning point in modern oxygen biology [46].

This review will focus on the biology of hypoxia-inducible factors in relationship with medicine.

4. Hypoxia-Inducible Factors

Evidently, hypoxia is not only sensed by specialized tissues and organelles, such as the carotid body and pulmonary artery smooth muscle, but also by all nucleated cells. A cellular factor that plays an essential role in hypoxia-elicited gene responses has been identified. It is the transcription factor hypoxia-inducible factor 1 (HIF-1). HIF-1 was originally isolated as the factor responsible for inducing erythropoietin under hypoxic conditions [47–51]. HIF-1 is a heterodimer consisting of an alpha subunit (HIF-1 α) and a beta subunit (HIF-1 β , ARNT) [50]. When cells sense hypoxia and HIF-1 is activated, HIF-1 recognizes and binds to a special sequence (hypoxia response element) in the regulatory domain of the target genes, thereby activating or silencing the transcription of an entire line of genes [48]. Early studies using cell lines indicate that HIF-1 increases erythrocyte production via

erythropoietin, vasculogenesis via vascular endothelial cell growth factor and glycolysis via a series of glycolytic enzymes. Although HIF-1 was originally isolated as the factor responsible for EPO induction, it has in the meantime been shown that EPO is a target of HIF-2 [52,53]. Consider metabolism as an example as well [54–57]. When oxygen concentrations are normal, mitochondria maintain oxidative phosphorylation at a level that is sufficient to produce ATP (aerobic metabolism) efficiently. However in environments that are low in oxygen, metabolism shifts to glycolysis (anaerobic metabolism). HIF-1 activates a gene set encoding the enzymes responsible for glycolysis (9 of the 12 glycolytic enzymes regulate HIF-1 expression), and conversely, another gene set that suppresses oxidative phosphorylation to facilitate metabolic reprogramming [58,59]. The body attempts to adapt more to hypoxic stress by mobilizing a large number of genes via HIF-1 at cellular, tissue, organ, and systemic levels to maintain cellular energy, blood flow, and oxygen transportation competence. A comprehensive analysis of gene expression revealed that hypoxia-inducible expression of over 5000 genes (at least 20% of all genes) was controlled by HIF-1 [60].

There are three isoforms of HIF: HIF-1, HIF-2, and HIF-3. The three types of HIF- α subunits have a basic helix–loop–helix (bHLH) region at the N-terminus and a Per-ARNT-Sim homology (PAS). Among the HIF- α subunits, HIF-1 α and HIF-2 α are N-terminal transactivation domain (N-TAD) and a C-terminal transactivation domain (C-TAD). These two subtypes control the expression of common sets of genes and expression of subtype-specific sets of genes due to the differences in post-translational modifications and the expression among cells and tissues [61,62]. The subtype-specific controls confer the diversity of the hypoxic response. On the other hand, HIF-3 α lacks the component of C-TAD.

HIF-1 α and HIF-2 α have 48% homology at the amino acid sequence level [61]. Homology in the functional domains is higher. The topic is how HIF-1 and HIF-2, which have high homology to the primary structure, play differential roles in each cell and body.

HIF-1 was originally isolated from liver and cervical cancer cell lines as a transcription factor responsible for the induction of EPO expression. According to genetic engineering analysis using mice thereafter, HIF-2 but not HIF-1 is a transcription factor that mainly works in EPO-producing cells in the stroma of the kidney [37,63,64]. The genetic variation of EPAS1 (HIF-2 α) has been reported by pedigree analysis of human familial polycythemia [52]. Although HIFs are thought to play an important role in cancer progression, the role of privileged HIF-2 in renal and adrenal cancer has been elucidated [61]. On the other hand, molecules closely related to energy metabolism often depend on HIF-1 for the regulation of expression [61].

The ontology of the differences is ensured by various molecular mechanisms. Although HIF-1 α and HIF-2 α have considerable homology, there is directivity for post-translational modification of proteins and binding to DNA, and each has a specific set of genes. There is also an explanation that the transcription of HIF-1 α and HIF-2 α is regulated in organs and tissues, and there is a bias in expression in certain cells [61]. A HIF-2 α -specific inhibitor PT2385 has also been developed and is under clinical trial as a therapeutic agent for renal cancer [65–68].

O₂ supply to cells takes place via simple diffusion. However, advanced multicellular organisms that are anatomically complex are specialized in a manner in which all cells may receive sufficient oxygenation. The respiratory system consists of the lung, the diaphragm, muscles aiding respiration, and neuroepithelial cells that sense the partial pressure of O₂ to maintain O₂ transfer to hemoglobin in red blood cells. The circulatory system is composed of red blood cells as O₂ carriers, the heart as the carrier engine and blood vessels as the carrier. For proper development and maintenance of these systems, coordinated expression of several thousand genes is required. HIF-1 is a molecule that changes its activity specifically to suit conditions involving hypoxia and participates in the expression of many hypoxia-inducible genes [54] (Figure 4).

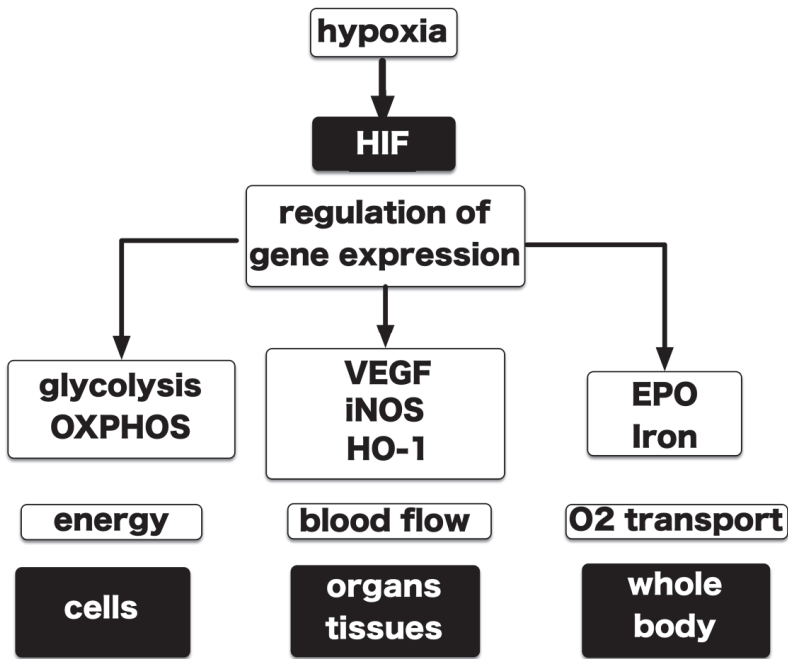


Figure 4. The network of transcription factors and hypoxic responses. Gene responses that depend on HIF-1 and HIF-2 (HIFs) are an important element of the response to low-oxygen by the living body and form an elaborate network. Responses are generated at the cellular, tissue, organ or whole-body level. At each level, a low oxygen response appears as the sum of the responses of individual cells. HIFs have been identified as a key transcription factor in this network. HIFs are present in all nucleated cells, and its activation depends on the partial pressure of oxygen to which cells are exposed. However, activation may be modified by factors specific to cells and tissues. iNOS: inducible nitric oxide synthase; HO-1: heme oxygenase 1.

5. Central Dogma of the Molecular Mechanism of HIF-1 Activation

Although preliminary studies indicated that HIF-1 contained non-heme iron [69,70], the results of these studies could not be reproduced. HIF-1 α is a basic helix–loop–helix PAS protein, wherein its PAS domain is extensively utilized for O₂ and redox sensing by archaea bacteria, such as FixL [39,71], suggesting that HIF-1 activity may be directly affected by changes in O₂ concentration. However, these hypotheses have been rejected.

An outline of the oxygen partial pressure sensing mechanism has been presented in order to explain molecular mechanisms underlying HIF-1 activation under hypoxic conditions [72–75]. The HIF-1 α protein is translated from messenger RNA and undergoes modification via oxygenases (hydroxylases). In the presence of sufficient oxygen, its proline residues are hydroxylated and HIF-1 α ubiquitination modification is dependent on hydroxylation of its proline residue by the E3 ligase, VHL, because of which the modified, poly-ubiquitinated HIF-1 α protein is transported to the proteasome, an intracellular protein destroying entity, and degraded. On the other hand, independent of protein stabilization, the ability of HIF-1 α to activate transcription is also controlled by hydroxylation modification of the asparagine residue [76–78]. Hydroxylated HIF-1 α is inactive as a transcription factor. Under hypoxic conditions, molecular oxygen is deficient as a substrate for this enzyme reaction, and because of which hydroxylation of proline residues and asparagine residues is suppressed, protein destruction is reduced, and HIF-1 α accumulates in the cell. It has been shown that HIF-1 α , HIF-2 α , and HIF-1 β enter into the nucleus by the action of nuclear transport receptors importins α/β . HIF-1 α ,-1 β and

HIF-2 α are binding to importin α 1, α 3, α 5, and α 7 [79–81]. It is also reported that importin α 4 and α 7 is involved in the nuclear transport of the HIF-1 α subunit [82]. In the nucleus, HIF- α dimerizes with HIF-1 β and exerts an activity as a transcription factor. Two types of dioxygenases play an essential role in this scheme. Proline hydroxylases have three types of isozymes, which are prolyl hydroxylase domains (PHD) 1 to 3 [55,83]. Asparagine residue hydroxylase was isolated as a factor inhibiting HIF (FIH)-1 [84,85]. Subsequent analyses demonstrated that these enzymes catalyze the oxidation of proline or asparagine residues, which require molecular oxygen and α -ketoglutarate as a substrate. Divalent iron (Fe^{2+}) and ascorbic acid act as essential co-factors for such enzymatic activity. Thus, a signal indicating a decrease in the partial pressure of the oxygen substrate is converted to a decrease in the activity of the oxygenated enzyme. As a result, the proportion of the hydroxylated product among newly formed HIF-1 α decreases in association with VHL and decreases ubiquitination [86]. The “Central dogma” declaring the existence of a balance between protein destruction and neogenesis shifts and HIF-1 α protein accumulation in the cell, was established in 2001. A particular finding in this field was awarded the Nobel Prize in Physiology or Medicine in 2019 [46,74] (Figure 5).

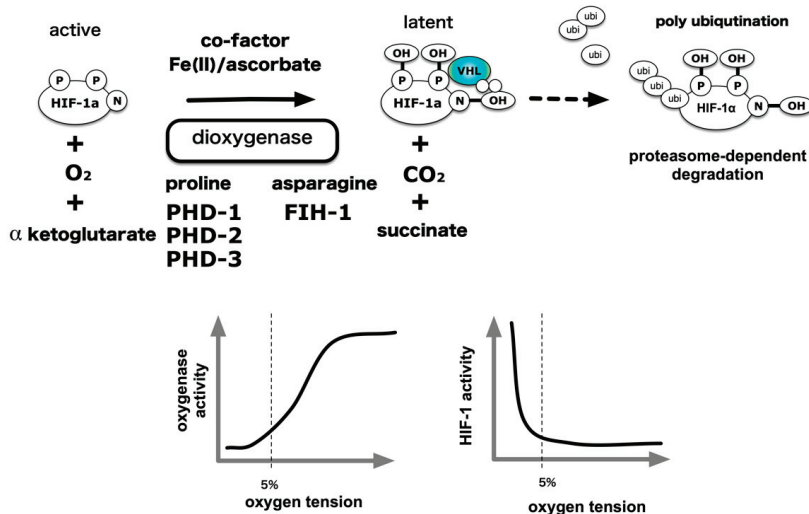


Figure 5. Molecular mechanism of hypoxia-elicited HIFs activation. Mainstream HIF-1 and HIF-2 activation is due to the hydroxylation reaction by the prolyl hydroxylase domain (PHD) protein, which is a HIF- α prolyl hydroxylase and factor inhibiting HIF-1 (FIH-1) protein, which is HIF- α asparaginyl hydroxylase. O_2 acts as a substrate for these enzymatic reactions. Thus, a decrease in O_2 concentration results in a decrease in enzymatic reactions, resulting in an accumulation of HIF- α proteins in the cell, which in turn activates it as a transcription factor, thereby resulting in gene expression. Intracellular processes that influence this reaction can be regulators of HIF-1 activity independent of O_2 tension. In addition, certain intracellular signals can increase the translation of HIF-1 α protein and promote HIF-1 activation. P: Proline, N: Asparagine VHL: von Hippel-Lindau.

Hydroxyl modification activity was examined using recombinant PHD1 prepared in vitro by an in vitro transcription-translation methodology, and the activity of PHD1 was suppressed from 21% to 0% O_2 conditions following a decrease in oxygen partial pressure [83]. Using the 20-amino acid polypeptide as a substrate for recombinant protein increase in insect cells, it was found that the K_m of PHDs for oxygen as a substrate was in the range of 230–250 μM , while the K_m of FIH-1 was 90 μM [87,88] (Table 1). Physiologically, the partial pressure of oxygen in human alveoli is slightly less than 100 mmHg, or approximately 13%, at 1 atmosphere. It was reported to be about 40–20 mmHg (5%–3%) in the interstitium, which causes diffusion from the capillaries through the arteries, where the

intracellular partial pressure further decreases to 20–10 mmHg (3%–1.3%). Another study indicates that the established hepatoma cell line HepG2 cells derived from human hepatocellular carcinoma are exposed to an oxygen partial pressure of 2 mmHg or less, under culture conditions of 20% oxygen [89]. O₂ solubility in pure water at 20 °C, and 100, 20 and 2 mmHg are equivalent to approximately 36, 7.2 and 0.7 μM, respectively. Considering the above evidence, and the intracellular concentration of α-ketoglutarate, ascorbic acid and divalent iron, the activity of PHD is continuously suppressed from 20% O₂ to 0% anoxia. The evidence goes against the dogma that HIF-1α hydroxylase is a bona fide hypoxic sensor. When oxygen, the final electron acceptor in the electron transport system, decreases in a low oxygen environment (1%–5% O₂), the electrons that have lost the acceptor react with oxygen without passing through the cytochrome C-respiratory chain enzyme complex to generate superoxide (O²⁻). O²⁻ is converted to hydrogen peroxide by Mn-SOD or Cu/Zn SOD present in mitochondria and goes out of mitochondria to oxidize divalent irons into trivalent irons, inhibiting HIF-α-hydroxylase enzymatic activity [90–92]. Based on the above experimental facts, there are claims that the bona fide hypoxia sensor is a mitochondrion, and that the HIF-α hydroxylation system is an execution system located downstream of mitochondria [93].

Table 1. Enzymatic properties of HIF-α hydroxylases and type I collagen hydroxylase.

Gene	Protein	Substrate		Km (μM)			
		Pro-402	Pro-564	O ₂	α-ketoglutarate	Ascorbate	Fe(II)
<i>EGLN1</i>	PHD2/HPH-2	+	+	230	60	170	0.03
<i>EGLN2</i>	PHD-1/HPH-3	+	+	250	60	180	0.1
<i>EGLN3</i>	PHD3/HPH-1	–	+	230	55	140	0.03
<i>HIF1AN</i>	FIH-1	Asp-803		90	25	260	0.5
<i>P4HA1</i>	C-P4H-I	collagen		40	20	300	

HIF-α subunits are post-translationally regulated by the hydroxylation of prolines (catalyzed by PHDs) and the hydroxylation of asparagine (catalyzed by FIH-1). In addition to hydroxylation, both HIF-1α and HIF-2α are subject to a range of distinct, O₂-dependent and independent post-translational modifications. Early work showed that both HIF-1α and HIF-2α are phosphorylated [94,95]. HIF-1α is phosphorylated by MAPK [94], casein kinase 1 (CK1) [96], ataxia telangiectasia mutated (ATM) [97], glycogen synthase kinase 3 (GSK3) [98], Polo-like kinase 3 (Plk3) [99] and protein kinase A (PKA) [100,101] under hypoxic and normoxic conditions. Phosphorylation affects HIF-α protein expression through regulation of translation and regulation of intracellular stability. In addition, it modulates HIF activity by altering intracellular localization and controlling transcriptional activation. HIF-2α is also a substrate of these kinases [95,102,103].

The activity of HIF-α proteins is also modulated by sirtuins, a family of redox-sensitive, NAD⁺-dependent deacetylases and/or ADP-ribosyltransferases. Mammalian cells express a family of sirtuins (SIRT1–7) that regulate complex changes in gene expression, metabolism and the cellular redox status [104]. SIRT1 forms a complex with HIF-2α and deacetylates conserved lysine residues in the N-TAD to enhance HIF-2α transcriptional activity [105]. SIRT1 was also reported to deacetylate lysine residues in HIF-1α, which resulted in HIF-1α transcriptional repression [106]. The apparently opposing effects of SIRT1 on HIF-1α and HIF-2α could skew cells toward either HIF-1α or HIF-2α transcriptional programs in response to changing metabolic activity in hypoxic tumors. It is possible that other acetylation and deacetylation events regulate HIF activity. For example, in mice, arrest defective 1 (ARD1) was reported to destabilize HIF-1α by acetylating Lys532 [107], an event that is apparently reversed by the recruitment of histone deacetylase 1 (HDAC1) to HIF1α by metastasis-associated protein 1 (MTA1) [108]. Finally, a growing number of reports indicate that HIFα proteins are subject to numerous other post-translational modifications, including sumoylation, S-nitrosylation and neddylation [109–113], although whether any of these modifications differentially regulate HIF-1α and HIF-2α is as yet unknown.

6. ROS Generation under Hypoxic Conditions and Its Involvement in HIF-1 Activation

Moderate hypoxic conditions (1–5%) cause a dearth of oxygen, the final electron acceptor of the electron transport system, whereby electrons lose their acceptor and are unable to pass through the cytochrome C-respiratory enzyme chain complex. These electrons then react to produce superoxide (O_2^-) [92,93,114]. Mn-SOD or Cu/Zn SOD in mitochondria convert O_2^- to hydrogen peroxide, which subsequently leaves the mitochondria to oxidize divalent irons into a trivalent status or to modify the hydroxylase of the HIF-1 α subunit, thereby inhibiting the HIF-1 α hydroxylation system. Inhibition of the HIF-1 α subunit hydroxylation converts it to an activated form. Cells cultured under special conditions produce live $\rho 0$ cells that are deficient in mitochondrial DNA. Intracellular accumulation of HIF-1 α protein and HIF-1-dependent gene expression is not observed under experimental conditions even when these $\rho 0$ cells are exposed to 1% hypoxia. Furthermore, when the cell is exposed to a hypoxic environment, ROS generate from the mitochondria. The theory that the true hypoxia sensor is in mitochondria is based on the experimental fact that ROS are produced, and that HIF activation occurs in a ROS-dependent manner [90,91,115,116].

There is also a counterargument to this opposition scheme. The deletion of PHDs causes losses in HIF-1 regulation to become insensitive to oxygen partial pressure control. There has been no counter-example of this phenomenon until now. However, this only confirms that hydroxylation modification is an essential process in HIF-1 α regulation by oxygen partial pressure and does not indicate that PHD is only a bona fide oxygen partial pressure sensor. Several reports have indicated that, in $\rho 0$ cells, HIF-1 α protein expression is regulated in an oxygen partial pressure-dependent manner [93].

7. Response to Intermittent Hypoxia

Hypoxia is not exclusively persistent. Intermittent hypoxia may normally occur in vivo. Persistent hypoxemia, characteristic of congenital heart disease, causes pulmonary arteries to contract and causes pulmonary hypertension. On the other hand, intermittent hypoxia occurring in excess of 100 times per night, such as during sleep apnea, is known to induce an increase in systemic blood pressure. A process that begins with ROS has been proposed as the mechanism underlying the onset of the above condition [117]. Intermittent hypoxia accompanied by recurrent oxygenation is typical of the sleep apnea syndrome. Generated ROS cause an increase in the intracellular calcium ion (Ca^{2+}) concentration. The increase in Ca^{2+} activates HIF-1, that induces NADPH oxidase 2 (NOX2) expression. Thus, the current study focused on ROS production. On the other hand, ROS suppress the activation of HIF-2, which induces the expression of Mn-SOD, which has the effect of eliminating ROS. Sustained ROS production suppresses heme oxygenase-2 (HO-2) activity, promotes the production of carbon monoxide and hydrogen sulfide, and stimulates sympathetic nerves in order to facilitate the entry of ROS into the circulatory system [118–121]. In this manner, the response of the body to continuous hypoxia is different from its response to intermittent hypoxia [122].

8. Induction of HIF-1 Activity under Non-Hypoxic Conditions

It is reported that deletion and mutations of tumor suppressor genes, such as p53, PTEN, and VHL, confer HIFs activation even under non-hypoxic conditions [123–127]. Receptor stimulation by growth factors, such as HER2, insulin-like growth factor 1, and insulin, induced HIF-1 activation under non-hypoxic conditions [128–130]. Muscarinic receptors and nicotinic receptors are also known [131]. Furthermore, there is a report that prostaglandin E1 and E2, which are inflammatory mediators, also activate HIF-1 in an EP receptor-dependent manner [132,133]. PI3K (phosphoinositide 3-kinase) is activated by a signal from the receptor; a signal is transmitted to mTOR (mammalian target of rapamycin) and S6 kinase via Akt, and translation of the HIF-1 α protein from mRNA is enhanced [134,135]. As a result, HIF-1 α protein accumulates in the cell and activates HIF-1. In parallel with this pathway, translation enhancement via MAPK (mitogen-activated protein kinase) has been

reported. Treatment with cigarette smoke extract and smoking resulted in the expression of HIF-1 α protein and promoted the expression of pro-inflammatory factors such as VEGF and HO-1 in established cell lines derived from the alveolar epithelium and in vivo mice. Smoking also promotes the expression of the Rtp801 (REDD1) gene and matrix metalloproteinase (MMP), which are attracting attention as molecules that promote alveolar damage and changes in emphysema [136]. This activation requires the production of ROS. In other words, the generated ROS may lead to the activation of HIF-1 regardless of the oxygen partial pressure of the environment.

Cytokines and chemokines mediate inflammation. These regulate phagocyte activity and recruit leukocytes. These also cause fever, which is a typical symptom of local and systemic inflammation. Both proinflammatory cytokines, TNF- α and IL-1 β , reportedly activate HIF-1 [137–139]. TNF- α and IL-1 β activate HIF-1 via multiple pathways, including ROS and nitric oxide (NO) production and phosphoinositide 3-kinase (PI3K) and/or nuclear factor κ B (NF- κ B) activation. Moreover, mediators of the inflammatory microenvironment, including adenosine and lipopolysaccharide (LPS), also activate HIF-1. HIF-1 α protein expression is induced following stimulation of the adenosine receptor and toll-like receptor 4 (TLR-4) in a PI3K-dependent and ROS-dependent manner [140]. Increases in protein translation shift the balance by overwhelming the degradation system, resulting in increased HIF-1 α protein. The steady-state of HIF-1 α expression is mainly determined by the hydroxylation-mediated degradation system in the proteasome (Figure 6).

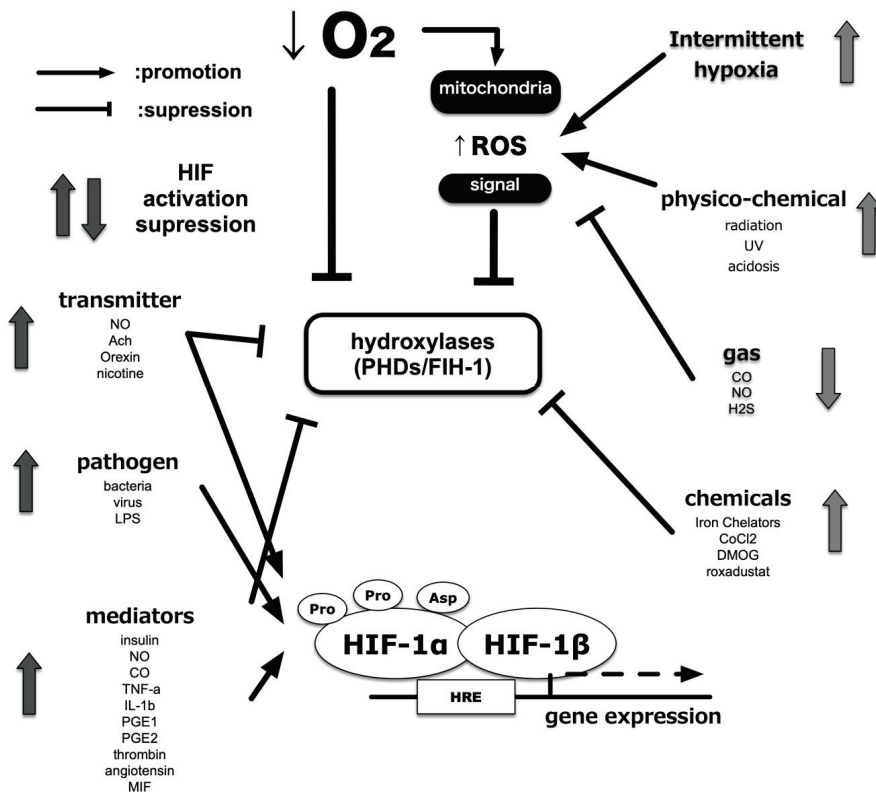


Figure 6. Alternatives to HIF activity regulation. In addition to the partial pressure of O₂, other factors related to HIF activity have been identified. Various intracellular processes affect HIF activity independently of O₂ partial pressure and via crosstalk with low O₂ signals. In addition, certain intracellular signals result in enhanced translation of HIF-1 α protein and promote HIF-1 activation.

NO, regardless of whether exogenously added or endogenously produced, increases HIF-1 α protein and causes transactivation of HIF-1 even under normoxic conditions [141–143]. NO decreases PHD activity and inhibits HIF-1 α ubiquitination, suggesting that hypoxia and NO adopt synergistic intracellular pathways to stabilize and increase HIF-1 α [144,145]. Another study using the NO donor, NOC-18, reported that NO increases PI3K activity and HIF-1 α protein translation in a mTOR-dependent manner, even under normoxic conditions [146,147]. By contrast, when HIF-1 α expression was analyzed under conditions of 1% O₂, treatment with a NO donor, DETA/NO, suppressed the accumulation of the HIF-1 α protein by affecting the mitochondrial electron transfer chain [148,149]. This paradox can be explained by the observation that NO competes with O₂ for binding to mitochondrial cytochrome oxidase, which consumes most of the O₂ within the cell [148,149]. Inhibition of PHDs by NADPH oxidase-mediated ROS production is proposed as the underlying regulatory principle. In fact, exogenous H₂O₂ also induces the expression of HIF-1 α protein and increases HIF-1 activity. It is reported that ROS oxidize Fe (II) at the catalytic site of PHDs, thus blocking such activity [149]. Another possibility is that ROS inhibits PHDs via the oxidation of active site amino acids [148]. These possibilities indicate that an increase in ROS during inflammation may contribute to HIF-1 α accumulation and its activation.

A Close Interaction between NF- κ B and HIFs

HIFs play a crucial role in the cellular hypoxic response. However, these are not the only molecules that regulate sensitivity to environmental O₂. At present, over 20 different transcription factors have been reported as mediating different forms of hypoxic response, either directly or indirectly.

Members of the nuclear factor κ B (NF- κ B) family of transcription factors regulate inflammation and orchestrate immune response and tissue homeostasis. Members of this family interact with members of the PHD–HIF pathway in a manner that links inflammation to hypoxia [150–152]. Studies conducted on mouse inflammatory bowel disease models indicate that PHDs play a regulatory role in the antiapoptotic effect exerted by NF- κ B during intestinal inflammation [153]. Hypoxia during intestinal ischemia–reperfusion activates NF- κ B in intestinal epithelial cells, which increase TNF- α production but also simultaneously attenuate intestinal epithelial apoptosis. Additional interaction between hypoxia and inflammation involves the I κ B kinase complex, a regulatory component of NF- κ B, which regulates HIF-1 α transcription before and during inflammation. Hypoxia amplifies the NF- κ B pathway by increasing the expression and signaling of TLRs, which in turn enhances the production of antimicrobial factors and stimulates phagocytosis, leukocyte recruitment, and adaptive immunity.

NF- κ B activity is regulated by inhibitors of NF- κ B (I κ B) kinases (IKKs), mainly IKK β , which induce phosphorylation-dependent degradation of I κ B inhibitors in response to infectious or inflammatory stimuli. HIF mediates NF- κ B activation in neutrophils under anoxic conditions and promotes the expression of NF- κ B-regulated cytokines in macrophages stimulated by LPS in a TLR4-dependent manner [138,154]. Interestingly, hypoxia itself can stimulate NF- κ B activation by inhibiting prolyl hydroxylases that negatively modulate IKK β catalytic activity [150].

NF- κ B contributes to increased HIF-1 α mRNA transcription under hypoxic conditions. Activation of HIF-1 α transcription by bacteria or LPS under normoxic as well as hypoxic conditions has recently been reported by a study using mice deficient in IKK β [152]. Macrophages infected with Gram-positive or Gram-negative bacteria, and mice subjected to hypoxia, exhibited a marked defect in HIF-1 α expression, following the deletion of the gene encoding IKK β [152]. These results confirmed that transcriptional activation of HIF-1 α by IKK β -responsive NF- κ B is a crucial precursor to post-transcriptional stabilization and accumulation of the HIF-1 α protein.

9. Pathophysiological Role of HIFs in Human Diseases

9.1. Kidney and Iron Metabolism

Kidneys perform a large amount of glomerular filtration and reabsorb approximately 99% of urine via transporters. This process requires energy and therefore results in ATP consumption. Thus,

in order to meet the high demand for energy, kidneys consume a large amount of oxygen [53,155]. In fact, the kidney is in such a low oxygen concentration state that HIF is activated even under normoxic conditions [156,157]. Renal tubule tissues, which extend from the glomerulus to the collective duct in the kidney, undergo resorption and secretion of the glomerular filtrate. The renal tubule is surrounded by capillaries that extend from the glomerulus and reabsorbs most of the water and inorganic salts of the raw urine components discharged into the Bowman's sac via the renal corpuscles. Even at the highest cortical surface layer, O₂ partial pressure is between 40 and 60 mmHg but is kept as low as 15 mmHg in the medulla under physiological conditions. Reportedly, a decrease in oxygen partial pressure plays an important role in the progression of acute and chronic renal disorders [156,158]. For example, in contrast agent nephropathy, the hypoxic state that occurs due to an increase in the reabsorption of solute, and a decrease in blood flow in the medulla, plays a critical role in the development of renal failure. An animal experiment indicated that administration of diuretics to suppress Na⁺ reabsorption during acute renal failure reduced oxygen consumption and increased oxygen partial pressure, thereby alleviating kidney damage [159,160]. Angiotensin II caused a marked decrease in oxygen partial pressure during chronic renal failure, increased oxidative stress, decreased NO, and changed oxygen consumption of mitochondria causing relative hypoxia [161]. Thus, the hypoxic state is involved in the etiology of renal failure [53,155].

EPO, a major target gene of HIFs, is produced in fibroblast cells (renal EPO producing cells) in the renal cortex in a HIF-2-dependent manner [52]. Since HIF-2 α is decomposed by hydroxylation in the presence of oxygen molecules, an inhibitor of this hydroxylase domain-containing protein (PHD) has been developed as a new hematopoietic stimulator (ESA). PHD inhibitors may show potential benefits in terms of cost and invasiveness compared to conventional EPO formulations. In fact, the HIF-PH inhibitor, roxadustat, is commercially available in Japan.

When hematopoiesis in the bone marrow increases resulting in an increased demand for iron, the expression of various genes involved in iron utilization and absorption is induced. Because many of these inductions are brought about by HIF-1 and HIF-2, activation of HIFs is thought to accelerate the hematopoietic response via the efficient use of iron [162,163]. Hepcidin is important as an internal defense mechanism that suppresses excessive iron uptake [164–167]. Hepcidin, produced in hepatocytes, is a small peptide with a molecular weight of 2.8 kDa. It promotes cellular uptake and degradation through phosphorylation of the iron excretion pump ferroportin and suppresses iron absorption, storage, release, and recycling. Hepcidin, which is induced by BMP-SMAD and IL6-STAT3 signaling, causes iron refractory anemia during inflammation. Patients undergoing hemodialysis therapy have high blood hepcidin levels due to various factors such as chronic inflammation and infection, which contributes to the anemia refractory to EPO. On the other hand, hypoxia suppresses hepcidin expression, thereby promoting the uptake and release of iron from reticuloendothelial cells. Although the molecular mechanism underlying this reaction remains unknown, recent studies have shown that HIF directly suppresses hepcidin via bone marrow hematopoiesis by EPO. Furthermore, HIF degrades hemojuvelin, a cofactor of the BMP receptor, via transcription of matriptase-2, and suppresses hepcidin expression. The mechanism of hepcidin suppression by hypoxia at the molecular level as well as the individual level is becoming increasingly clear. Treating anemia via HIF activation is expected to effectively improve anemia associated with chronic inflammation, which is a condition often seen in hemodialysis patients [168–170].

9.2. Cancer Progression

In solid cancerous tumor tissue, cancer cells grow at a very high rate. In contrast, the rate of angiogenesis inside the tumor is slow, the tumor vessels are extremely fragile and meandering, and frequent occlusion and blood regurgitation occur [171,172]. These result in hypoxic regions where tumor tissue is not supplied with sufficient oxygen, which is known to activate HIFs. In addition, VHL deletion in clear cell carcinoma of the kidney and many other HIF may be activated independently

of hypoxia, such as activation of the phosphoinositide 3-kinase (PI3K)/Akt pathway [173]. There is a positive correlation between HIFs expression and poor prognosis.

HIFs contribute to the adaptation to hypoxia in metabolic reprogramming and angiogenesis in cancer cells as well as normal cells, and in particular, cancer cells generate ATP by glycolysis even under normal oxygen conditions [173]. Many studies have shown that HIF-1 is deeply involved in this phenomenon (Warburg effect) [174–176]. Furthermore, cancer tissues do not have sufficient blood flow. Thus cancer cells are also undernutrition. Not only do cancer cells adapt to their hypoxia and hyponutrition environment through HIFs, but they also change the cells that make up cancer tissues [177,178]. In recent years, the relationship between cancer metastasis and HIFs has been elucidated [179]. Metastasis consists of many steps, and epithelial–mesenchymal transition (EMT) is a particularly essential phenomenon [180,181]. HIFs induces the expression of the transcription factor TWIST, which regulates EMT, and induces nuclear translocation of the EMT regulator SNAIL. In addition, HIFs cooperates with transforming growth factor (TGF)- β to produce Sma and Mad Related Activates the Family (SMAD) pathway and causes EMT, including a decrease in E-cadherin. In addition, in breast cancer, HIF-1-induced angiopoietin-related protein 4 (ANGPTL4) inhibits adhesion between vascular endothelial cells and promotes cancer extravasation. In addition, HIF-1 produces lysyl oxidase (LOX) and LOX-like proteins from cancer cells. It has also been reported that the outer matrix is remodeled to promote cancer cell invasion [182,183].

9.3. Lactate and Hypoxia Response

High serum lactate (> 2 mmol/L) constitutes a diagnostic criterion for septic shock in the “International consensus definition of sepsis and septic shock in third edition (Sepsis-3)”. The established consensus is that lactic acidosis indicates a negative mismatch between the demand for oxygen and its supply in the peripheral tissues. However, this consensus has now been revised. A classification of hyperlactatemia was proposed: With tissue oxygenation deficiency and without tissue oxygenation deficiency as Type A and Type B, respectively [184].

Propofol is widely used as intravenous anesthesia. Propofol infusion syndrome (PRIS) is a manifestation of propofol toxicity [185–187]. Propofol infusion syndrome is usually detected in those who have been administered high doses of propofol for an extended time. When propofol reaches toxic levels, it uncouples oxidative phosphorylation in the mitochondrial electron transport chain, causing severe acidosis [186]. Propofol also inhibits carnitine palmitoyltransferase, which is involved in fatty acid metabolism. Fatty acid accumulation can lead to arrhythmia and poor energy availability [26]. An imbalance in demand for energy and its supply may lead to organ dysfunction. The authors used an extracellular flux analyzer that measures the oxygen consumption rate (OCR) of cells and extracellular pH change (ECAR), which reflects lactic acid production [27,188]. Exposure to hypoxia for approximately 2 h may lead to metabolic reprogramming, resulting in switching from oxidative phosphorylation to glycolysis in a HIF-1 dependent manner [27,188]. OCR is suppressed and ECAR is enhanced. On the other hand, propofol, which is used for anesthesia and sedation, also suppresses oxygen consumption and stimulates lactic acid production in approximately 4 h when cells are exposed to a concentration of approximately 25 μ M. Drug-induced mitochondrial disorder is an example of promoting lactic acid production. In addition, clinical concentrations of propofol facilitate the conversion of cellular metabolic mode easily when mitochondrial function is suppressed for unknown reasons.

9.4. Cardiac Hypertrophy and Heart Failure

Takeda and a colleague established a mouse cardiac fibrosis and remodeling model induced by narrowing the transverse aorta. They found that myocardial tissue was hypoxic and that there was an accumulation of macrophages in the hypoxic regions of the heart, by examination via a phosphorescent probe as well as an analysis based on flow cytometry [189,190]. Furthermore, by analyzing mice with suppressed HIF-1 α signaling of macrophages, they found that HIF-1 α signaling induced macrophage

accumulation in the heart [191]. As fibrosis of mice hearts increased with suppressed HIF-1 α signaling, it was believed that macrophage accumulation in the heart suppressed fibrosis [190,192]. Next, they investigated the mechanism by which macrophage accumulation in the heart inhibited fibrosis, and reported that macrophage associated HIF-1 α signaling produced oncostatin M, a cytokine, which inhibited the activation of cardiac fibroblasts by suppressing TGF- β /Smad signaling, thereby suppressing the fibrosis of myocardial tissue. This revealed that macrophage accumulation in the heart suppresses excessive fibrosis of the heart by producing oncostatin M [190]. Heart fibrosis prevention effect of oncostatin M may indicate a new therapeutic target for heart fibrosis and heart failure. The central fructose-metabolizing enzyme is ketohexokinase (KHK), which exists in two isoforms: KHK-A and KHK-C, generated through mutually exclusive alternative splicing of KHK pre-mRNAs. It was demonstrated that splice factors as HIF-1 α targets, which prompted the analysis of their RNA targets, unveiling mechanistic and functional linkages between HIF-1 α , splice factor 3b subunit 1 (SF3B1), KHK-C splice isoform production and fructose metabolism in cardiac hypertrophy. Myocardial hypoxia enhances fructose metabolism in human and mouse models of pathological cardiac hypertrophy through HIF-1 α activation of SF3B and SF3B1-mediated splice switching of KHK-A to KHK-C [193]. Thus, HIF-1 has been shown to have important roles under various pathways for hypertrophy and heart failure.

9.5. Placenta Formation and Oxygen Tension-Pregnancy Induced Hypertension and Intrauterine Growth Retardation

The placenta is a target for the elucidation of the pathogenesis of pregnancy-induced hypertension (PIH), intrauterine growth retardation (IUGR) and therapeutic intervention [194,195]. The etiology of PIH was presumed to be “toxins” produced in the placenta and other organs of pregnant women, which caused hypertension and proteinuria, leading to the onset of PIH [196]. Lately, impairment of placental circulation has come to be considered as the new etiology. Histological findings closely associated with PIH have indicated its causes as the shallowness of infiltration of the trophoblast into the muscle layer and the smallness of the vasculature in the placenta of PIH cases. In this context, the association between hypoxia and trophoblast proliferation/infiltration was stressed. Reportedly, infiltration of the trophoblast and its proliferation are enhanced under hypoxic conditions. This suggests that oxygen metabolism may be involved in the etiology of PIH, IUGR, or eclampsia, and therefore considered a target in the treatment of these conditions [197].

Implantation disorders are a major issue in reproductive medicine, but effective diagnosis and treatment have not yet been established. Implantation is achieved by embryos entering the uterus and adhering to the endometrium (embryo adhesion) and the process of embryos entering the endometrium (embryo infiltration) [198,199]. Although precise interaction between the uterus and the embryo is supposedly essential for the establishment of implantation, details of the underlying mechanism remain unknown. It is demonstrated by using reports that it is HIF-2, and not HIF-1, that exclusively acts in the endometrium to regulate the process of embryonic invasion [199,200]. Due to the role played by endometrial stromal HIFs, the endometrial luminal epithelium is peeled off to expose the endometrial stroma, enabling easier entry of the embryo into the endometrial stroma. Simultaneously, they also clarified that the endometrial stroma was in close contact with the embryo and that the embryo was laboring to survive. As a result, the mechanism of implantation occurring in the uterus has been elucidated, and the cause of infertility due to implantation failure may be clarified in the near future. It is hoped that future examinations of the effect of HIFs on human endometrium may lead to the development of new diagnostic and therapeutic methods for implantation disorders.

9.6. Immunity

It has been reported that stimulation of the T-cell receptor/CD3 antigen complex may also activate HIF-1 in T-cell lymphocytes [201,202]. This suggests that not only innate immunity but also acquired immunity elicited by antigens are affected by oxygen partial pressure and HIF-1 [139,203]. Cellular

glucose metabolism and fat metabolism play a major role in the process of naive T-cell differentiation into helper T cells/17/regulatory T Treg cells, which are vital for regulating the immune system. Cells producing IFN- γ , which modulates processes associated with cellular immunity, such as viral exclusion, are produced by different cytokines. Th2 cells produce IL-4, which regulates processes related to humoral immunity, such as the elimination of parasites, and Th17 cells produce IL-17 and Treg cells that suppress the immune system. Of these, it has been suggested that the RAR-related orphan receptor (ROR) γ t, the main regulator of Th17 cell differentiation, produces IL-17 with the cooperation of HIF-1 α . On the other hand, under Th17 cell-inducing conditions, ubiquitinated HIF-1 α binds to Foxp3, a major regulator of Treg cell differentiation, and is degraded along with Foxp3 in the proteasome. These results suggest that HIF-1 regulates the balance between Th17 and Treg cells. These findings indicate the importance of oxygen metabolism to many processes, including the maintenance of antibody quality and class switching, which even applies to processes such as B-cell activation.

9.7. Role of Hypoxia on Autophagy and Cellular Damage

Autophagy is a system in which lysosomes degrade proteins and organelles in the cytoplasm. The ubiquitin–proteasome system is also used to degrade intracellular components, but the ubiquitin–proteasome system is used to degrade relatively short-lived proteins [204–206]. Intracellular proteins and organelles are degraded by autophagy when they are no longer needed or as needed, and their components are reused in the cells. Autophagy activity is low in normal cells but becomes upregulated and activated when cells are exposed to an environment such as starvation or hypoxia [207]. Autophagy is a tightly controlled pathway, an important and clever system built into the cell to sustain its life under stress.

HIF-1-induced B-cell lymphoma 2 (BCL2)/adenovirus E1B19kDa protein-interacting protein 3 (BNIP3) competes with BCL2 to release Beclin1 involved in autophagosome formation. BNIP3 promotes autophagy by binding to and inhibiting Ras homolog enriched in brain (Rheb), which is important for activation of the mTOR pathway [208–210]. As a result, mitophagy (mitochondrial autophagy) is triggered, and dysfunctional mitochondria are removed. A mechanism for maintaining ATP production and a mechanism for adapting to a hypoxic environment by suppressing ATP consumption have been reported. Regulated in development and DNA damage response 1 (REDD1) induced by HIF-1 inhibits the binding of tuberous sclerosis protein 2 (TSC2), a suppressor of mTOR, to 14–3-3 protein [211]. The released TSC2 suppresses ATP consumption by suppressing the mTOR pathway and reducing gene translation efficiency [209,210].

10. Conclusions

In this review, I described the current state of researches on hypoxia response and oxygen metabolism in a living body and explained the relationship between various biological phenomena and the HIF system.

Funding: This work was supported by a research grant from the Kansai Medical University (KMU) research consortium and the branding program as a world-leading research university on intractable immune and allergic diseases from MEXT Japan.

Acknowledgments: I would like to thank Editage (www.editage.com) for English language editing.

Conflicts of Interest: The author declares no conflict of interest.

References

1. Severinghaus, J.W. Eight sages over five centuries share oxygen's discovery. *Adv. Physiol. Educ.* **2016**, *40*, 370–376. [[CrossRef](#)] [[PubMed](#)]
2. Severinghaus, J.W. The Most Important Discovery of Science. *Adv. Exp. Med. Biol.* **2016**, *876*, 1–16. [[CrossRef](#)] [[PubMed](#)]

3. West, J.B. Joseph Priestley, oxygen, and the enlightenment. *Am. J. Physiol. Lung Cell Mol. Physiol.* **2014**, *306*, L111–L119. [[CrossRef](#)] [[PubMed](#)]
4. Fara, P. Joseph Priestley: Doctor Phlogiston or Reverend Oxygen? *Endeavour* **2010**, *34*, 84–86. [[CrossRef](#)] [[PubMed](#)]
5. Leach, R.M.; Treacher, D.F. The pulmonary physician in critical care * 2: Oxygen delivery and consumption in the critically ill. *Thorax* **2002**, *57*, 170–177. [[CrossRef](#)] [[PubMed](#)]
6. Bateman, N.T.; Leach, R.M. ABC of oxygen. Acute oxygen therapy. *BMJ* **1998**, *317*, 798–801. [[CrossRef](#)]
7. Evans, T.W.; Smithies, M. ABC of intensive care: Organ dysfunction. *BMJ* **1999**, *318*, 1606–1609. [[CrossRef](#)]
8. Williams, A.J. ABC of oxygen: Assessing and interpreting arterial blood gases and acid-base balance. *BMJ* **1998**, *317*, 1213–1216. [[CrossRef](#)]
9. Grocott, M.P.; Martin, D.S.; Levett, D.Z.; McMorrow, R.; Windsor, J.; Montgomery, H.E.; Caudwell Xtreme Everest Research Group. Arterial blood gases and oxygen content in climbers on Mount Everest. *N. Engl. J. Med.* **2009**, *360*, 140–149. [[CrossRef](#)]
10. Griva, K.; Stygall, J.; Wilson, M.H.; Martin, D.; Levett, D.; Mitchell, K.; Mythen, M.; Montgomery, H.E.; Grocott, M.P.; Aref-Adib, G.; et al. Caudwell Xtreme Everest: A prospective study of the effects of environmental hypoxia on cognitive functioning. *PLoS ONE* **2017**, *12*, e0174277. [[CrossRef](#)] [[PubMed](#)]
11. Ernst, A.; Zibrak, J.D. Carbon monoxide poisoning. *N. Engl. J. Med.* **1998**, *339*, 1603–1608. [[CrossRef](#)] [[PubMed](#)]
12. Rose, J.J.; Wang, L.; Xu, Q.; McTiernan, C.F.; Shiva, S.; Tejero, J.; Gladwin, M.T. Carbon Monoxide Poisoning: Pathogenesis, Management, and Future Directions of Therapy. *Am. J. Respir. Crit. Care Med.* **2017**, *195*, 596–606. [[CrossRef](#)] [[PubMed](#)]
13. Curry, S. Methemoglobinemia. *Ann. Emerg. Med.* **1982**, *11*, 214–221. [[CrossRef](#)]
14. Wright, R.O.; Lewander, W.J.; Woolf, A.D. Methemoglobinemia: Etiology, pharmacology, and clinical management. *Ann. Emerg. Med.* **1999**, *34*, 646–656. [[CrossRef](#)]
15. Haley, K. Congenital Hemolytic Anemia. *Med. Clin. North. Am.* **2017**, *101*, 361–374. [[CrossRef](#)] [[PubMed](#)]
16. Taher, A.T.; Weatherall, D.J.; Cappellini, M.D. Thalassaemia. *Lancet* **2018**, *391*, 155–167. [[CrossRef](#)]
17. Higgs, D.R.; Engel, J.D.; Stamatoyannopoulos, G. Thalassaemia. *Lancet* **2012**, *379*, 373–383. [[CrossRef](#)]
18. Tanaka, T.; Kai, S.; Koyama, T.; Daijo, H.; Adachi, T.; Fukuda, K.; Hirota, K. General Anesthetics Inhibit Erythropoietin Induction under Hypoxic Conditions in the Mouse Brain. *PLoS ONE* **2011**, *6*, e29378. [[CrossRef](#)] [[PubMed](#)]
19. Kai, S.; Tanaka, T.; Matsuyama, T.; Suzuki, K.; Hirota, K. The volatile anesthetic isoflurane differentially suppresses the induction of erythropoietin synthesis elicited by acute anemia and systemic hypoxemia in mice in an hypoxia-inducible factor-2-dependent manner. *Eur. J. Pharmacol.* **2014**, *732C*, 43–49. [[CrossRef](#)] [[PubMed](#)]
20. Harada, H.; Itasaka, S.; Kizaka-Kondoh, S.; Shibuya, K.; Morinibu, A.; Shinomiya, K.; Hiraoka, M. The Akt/mTOR pathway assures the synthesis of HIF-1alpha protein in a glucose- and reoxygenation-dependent manner in irradiated tumors. *J. Biol. Chem.* **2009**, *284*, 5332–5342. [[CrossRef](#)]
21. Dayan, F.; Bilton, R.L.; Laferriere, J.; Trottier, E.; Roux, D.; Pouyssegur, J.; Mazure, N.M. Activation of HIF-1alpha in exponentially growing cells via hypoxic stimulation is independent of the Akt/mTOR pathway. *J. Cell Physiol.* **2009**, *218*, 167–174. [[CrossRef](#)] [[PubMed](#)]
22. Gracia, R.; Shepherd, G. Cyanide poisoning and its treatment. *Pharmacotherapy* **2004**, *24*, 1358–1365. [[CrossRef](#)] [[PubMed](#)]
23. Tshala-Katumbay, D.D.; Ngombe, N.N.; Okitundu, D.; David, L.; Westaway, S.K.; Boivin, M.J.; Mumba, N.D.; Banea, J.P. Cyanide and the human brain: Perspectives from a model of food (cassava) poisoning. *Ann. N Y Acad. Sci.* **2016**, *1378*, 50–57. [[CrossRef](#)] [[PubMed](#)]
24. Inzucchi, S.E.; Lipska, K.J.; Mayo, H.; Bailey, C.J.; McGuire, D.K. Metformin in patients with type 2 diabetes and kidney disease: A systematic review. *JAMA* **2014**, *312*, 2668–2675. [[CrossRef](#)]
25. Kreisberg, R.A. Lactate homeostasis and lactic acidosis. *Ann. Intern. Med.* **1980**, *92*, 227–237. [[CrossRef](#)]
26. Fudickar, A.; Bein, B. Propofol infusion syndrome: Update of clinical manifestation and pathophysiology. *Minerva Anesthesiol.* **2009**, *75*, 339–344.

27. Sumi, C.; Okamoto, A.; Tanaka, H.; Nishi, K.; Kusunoki, M.; Shoji, T.; Uba, T.; Matsuo, Y.; Adachi, T.; Hayashi, J.I.; et al. Propofol induces a metabolic switch to glycolysis and cell death in a mitochondrial electron transport chain-dependent manner. *PLoS ONE* **2018**, *13*, e0192796. [[CrossRef](#)]
28. Chang, A.J. Acute oxygen sensing by the carotid body: From mitochondria to plasma membrane. *J. Appl. Physiol. (1985)* **2017**, *123*, 1335–1343. [[CrossRef](#)]
29. Piskuric, N.A.; Nurse, C.A. Expanding role of ATP as a versatile messenger at carotid and aortic body chemoreceptors. *J. Physiol.* **2013**, *591*, 415–422. [[CrossRef](#)]
30. Conde, S.V.; Sacramento, J.F.; Guarino, M.P. Carotid body: A metabolic sensor implicated in insulin resistance. *Physiol. Genomics* **2018**, *50*, 208–214. [[CrossRef](#)]
31. Prabhakar, N.R.; Peng, Y.J. Oxygen Sensing by the Carotid Body: Past and Present. *Adv. Exp. Med. Biol.* **2017**, *977*, 3–8. [[CrossRef](#)] [[PubMed](#)]
32. Chang, A.J.; Ortega, F.E.; Riegler, J.; Madison, D.V.; Krasnow, M.A. Oxygen regulation of breathing through an olfactory receptor activated by lactate. *Nature* **2015**, *527*, 240–244. [[CrossRef](#)] [[PubMed](#)]
33. Dunham-Snary, K.J.; Wu, D.; Sykes, E.A.; Thakrar, A.; Parlow, L.R.G.; Mewburn, J.D.; Parlow, J.L.; Archer, S.L. Hypoxic Pulmonary Vasoconstriction: From Molecular Mechanisms to Medicine. *Chest* **2017**, *151*, 181–192. [[CrossRef](#)] [[PubMed](#)]
34. Lumb, A.B.; Slinger, P. Hypoxic pulmonary vasoconstriction: Physiology and anesthetic implications. *Anesthesiology* **2015**, *122*, 932–946. [[CrossRef](#)] [[PubMed](#)]
35. Sylvester, J.T.; Shimoda, L.A.; Aaronson, P.I.; Ward, J.P. Hypoxic pulmonary vasoconstriction. *Physiol. Rev.* **2012**, *92*, 367–520. [[CrossRef](#)] [[PubMed](#)]
36. Souma, T.; Nezu, M.; Nakano, D.; Yamazaki, S.; Hirano, I.; Sekine, H.; Dan, T.; Takeda, K.; Fong, G.H.; Nishiyama, A.; et al. Erythropoietin Synthesis in Renal Myofibroblasts Is Restored by Activation of Hypoxia Signaling. *J. Am. Soc. Nephrol.* **2016**, *27*, 428–438. [[CrossRef](#)]
37. Suzuki, N.; Yamamoto, M. Roles of renal erythropoietin-producing (REP) cells in the maintenance of systemic oxygen homeostasis. *Pflugers. Arch.* **2016**, *468*, 3–12. [[CrossRef](#)]
38. Yamawaki, T.; Ishikawa, H.; Mizuno, M.; Nakamura, H.; Shiro, Y.; Mizutani, Y. Regulatory Implications of Structural Changes in Tyr201 of the Oxygen Sensor Protein FixL. *Biochemistry* **2016**, *55*, 4027–4035. [[CrossRef](#)]
39. Wright, G.S.A.; Saeki, A.; Hikima, T.; Nishizono, Y.; Hisano, T.; Kamaya, M.; Nukina, K.; Nishitani, H.; Nakamura, H.; Yamamoto, M.; et al. Architecture of the complete oxygen-sensing FixL-FixJ two-component signal transduction system. *Sci. Signal.* **2018**, *11*. [[CrossRef](#)]
40. Iwai, K.; Drake, S.K.; Wehr, N.B.; Weissman, A.M.; LaVaute, T.; Minato, N.; Klausner, R.D.; Levine, R.L.; Rouault, T.A. Iron-dependent oxidation, ubiquitination, and degradation of iron regulatory protein 2: Implications for degradation of oxidized proteins. *Proc. Natl. Acad. Sci. USA* **1998**, *95*, 4924–4928. [[CrossRef](#)]
41. Starkov, A.A.; Fiskum, G. Regulation of brain mitochondrial H₂O₂ production by membrane potential and NAD(P)H redox state. *J. Neurochem.* **2003**, *86*, 1101–1107. [[CrossRef](#)] [[PubMed](#)]
42. Strielkov, I.; Pak, O.; Sommer, N.; Weissmann, N. Recent advances in oxygen sensing and signal transduction in hypoxic pulmonary vasoconstriction. *J. Appl. Physiol. (1985)* **2017**, *123*, 1647–1656. [[CrossRef](#)] [[PubMed](#)]
43. Ortega-Saenz, P.; Lopez-Barneo, J. Physiology of the Carotid Body: From Molecules to Disease. *Annu. Rev. Physiol.* **2019**. [[CrossRef](#)] [[PubMed](#)]
44. Jiang, B.H.; Semenza, G.L.; Bauer, C.; Marti, H.H. Hypoxia-inducible factor 1 levels vary exponentially over a physiologically relevant range of O₂ tension. *Am. J. Physiol.* **1996**, *271*, C1172–C1180. [[CrossRef](#)] [[PubMed](#)]
45. Torres-Torrel, H.; Ortega-Saenz, P.; Macias, D.; Omura, M.; Zhou, T.; Matsunami, H.; Johnson, R.S.; Mombaerts, P.; Lopez-Barneo, J. The role of Olf78 in the breathing circuit of mice. *Nature* **2018**, *561*, E33–E40. [[CrossRef](#)] [[PubMed](#)]
46. Ledford, H.; Callaway, E. Biologists who decoded how cells sense oxygen win medicine Nobel. *Nature* **2019**, *574*, 161–162. [[CrossRef](#)]
47. Semenza, G.L.; Neufeld, M.K.; Chi, S.M.; Antonarakis, S.E. Hypoxia-inducible nuclear factors bind to an enhancer element located 3' to the human erythropoietin gene. *Proc. Natl. Acad. Sci. USA* **1991**, *88*, 5680–5684. [[CrossRef](#)]
48. Wang, G.; Semenza, G. Characterization of hypoxia-inducible factor 1 and regulation of DNA binding activity by hypoxia. *J. Biol. Chem.* **1993**, *268*, 21513–21518.

49. Wang, G.; Jiang, B.; Rue, E.; Semenza, G. Hypoxia-inducible factor 1 is a basic-helix-loop-helix-PAS heterodimer regulated by cellular O₂ tension. *Proc. Natl. Acad. Sci. USA* **1995**, *92*, 5510–5514. [[CrossRef](#)]
50. Wang, G.; Semenza, G. Purification and characterization of hypoxia-inducible factor 1. *J. Biol. Chem.* **1995**, *270*, 1230–1237. [[CrossRef](#)]
51. Semenza, G.L. Serendipity, Generosity, and Inspiration. *Cell* **2016**, *167*, 20–24. [[CrossRef](#)] [[PubMed](#)]
52. Percy, M.J.; Furlow, P.W.; Lucas, G.S.; Li, X.; Lappin, T.R.; McMullin, M.F.; Lee, F.S. A gain-of-function mutation in the HIF2A gene in familial erythrocytosis. *N. Engl. J. Med.* **2008**, *358*, 162–168. [[CrossRef](#)] [[PubMed](#)]
53. Nangaku, M.; Eckardt, K.U. Hypoxia and the HIF system in kidney disease. *J. Mol. Med. (Berl)* **2007**, *85*, 1325–1330. [[CrossRef](#)] [[PubMed](#)]
54. Semenza, G.L. HIF-1 and human disease: One highly involved factor. *Genes Dev.* **2000**, *14*, 1983–1991. [[PubMed](#)]
55. Semenza, G.L. HIF-1, O(2), and the 3 PHDs: How animal cells signal hypoxia to the nucleus. *Cell* **2001**, *107*, 1–3. [[CrossRef](#)]
56. Hirota, K.; Semenza, G.L. Regulation of angiogenesis by hypoxia-inducible factor 1. *Crit. Rev. Oncol. Hematol.* **2006**, *59*, 15–26. [[CrossRef](#)]
57. Hirota, K. Involvement of hypoxia-inducible factors in the dysregulation of oxygen homeostasis in sepsis. *Cardiovasc. Hematol. Disord. Drug Targets* **2015**, *15*, 29–40. [[CrossRef](#)]
58. Hirota, K. Hypoxia-inducible factor 1, a master transcription factor of cellular hypoxic gene expression. *J. Anesth.* **2002**, *16*, 150–159. [[CrossRef](#)]
59. Dang, C.V.; Semenza, G.L. Oncogenic alterations of metabolism. *Trends Biochem Sci* **1999**, *24*, 68–72. [[CrossRef](#)]
60. Manalo, D.J.; Rowan, A.; Lavoie, T.; Natarajan, L.; Kelly, B.D.; Ye, S.Q.; Garcia, J.G.; Semenza, G.L. Transcriptional regulation of vascular endothelial cell responses to hypoxia by HIF-1. *Blood* **2005**, *105*, 659–669. [[CrossRef](#)]
61. Keith, B.; Johnson, R.S.; Simon, M.C. HIF1alpha and HIF2alpha: Sibling rivalry in hypoxic tumour growth and progression. *Nat. Rev. Cancer* **2011**, *12*, 9–22. [[CrossRef](#)] [[PubMed](#)]
62. Lee, K.E.; Simon, M.C. From stem cells to cancer stem cells: HIF takes the stage. *Curr. Opin. Cell Biol.* **2012**, *24*, 232–235. [[CrossRef](#)] [[PubMed](#)]
63. Suzuki, N.; Hirano, I.; Pan, X.; Minegishi, N.; Yamamoto, M. Erythropoietin production in neuroepithelial and neural crest cells during primitive erythropoiesis. *Nat. Commun.* **2013**, *4*, 2902. [[CrossRef](#)] [[PubMed](#)]
64. Souma, T.; Suzuki, N.; Yamamoto, M. Renal erythropoietin-producing cells in health and disease. *Front. Physiol.* **2015**, *6*, 167. [[CrossRef](#)] [[PubMed](#)]
65. Cho, H.; Du, X.; Rizzi, J.P.; Liberzon, E.; Chakraborty, A.A.; Gao, W.; Carvo, I.; Signoretti, S.; Bruick, R.K.; Josey, J.A.; et al. On-target efficacy of a HIF-2alpha antagonist in preclinical kidney cancer models. *Nature* **2016**, *539*, 107–111. [[CrossRef](#)] [[PubMed](#)]
66. Chen, W.; Hill, H.; Christie, A.; Kim, M.S.; Holloman, E.; Pavia-Jimenez, A.; Homayoun, F.; Ma, Y.; Patel, N.; Yell, P.; et al. Targeting renal cell carcinoma with a HIF-2 antagonist. *Nature* **2016**, *539*, 112–117. [[CrossRef](#)]
67. Courtney, K.D.; Infante, J.R.; Lam, E.T.; Figlin, R.A.; Rini, B.L.; Brugarolas, J.; Zojwalla, N.J.; Lowe, A.M.; Wang, K.; Wallace, E.M.; et al. Phase I Dose-Escalation Trial of PT2385, a First-in-Class Hypoxia-Inducible Factor-2alpha Antagonist in Patients With Previously Treated Advanced Clear Cell Renal Cell Carcinoma. *J. Clin. Oncol.* **2018**, *36*, 867–874. [[CrossRef](#)]
68. Wehn, P.M.; Rizzi, J.P.; Dixon, D.D.; Grina, J.A.; Schlachter, S.T.; Wang, B.; Xu, R.; Yang, H.; Du, X.; Han, G.; et al. Design and Activity of Specific Hypoxia-Inducible Factor-2alpha (HIF-2alpha) Inhibitors for the Treatment of Clear Cell Renal Cell Carcinoma: Discovery of Clinical Candidate (S)-3-((2,2-Difluoro-1-hydroxy-7-(methylsulfonyl)-2,3-dihydro-1 H-inden-4-yl)oxy)-5-fluorobenzonitrile (PT2385). *J. Med. Chem.* **2018**, *61*, 9691–9721. [[CrossRef](#)]
69. Srinivas, V.; Zhu, X.; Salceda, S.; Nakamura, R.; Caro, J. Hypoxia-inducible factor 1alpha (HIF-1alpha) is a non-heme iron protein. Implications for oxygen sensing. *J. Biol. Chem.* **1998**, *273*, 18019–18022. [[CrossRef](#)]
70. Srinivas, V.; Zhu, X.; Salceda, S.; Nakamura, R.; Caro, J. Hypoxia-inducible factor 1alpha (HIF-1alpha) is a non-heme iron protein. Implications for oxygen sensing. *J. Biol. Chem.* **1999**, *274*, 1180.

71. Taylor, B.L.; Zhulin, I.B. PAS domains: Internal sensors of oxygen, redox potential, and light. *Microbiol. Mol. Biol. Rev.* **1999**, *63*, 479–506. [[CrossRef](#)] [[PubMed](#)]
72. Semenza, G.L. Oxygen sensing, homeostasis, and disease. *N. Engl. J. Med.* **2011**, *365*, 537–547. [[CrossRef](#)] [[PubMed](#)]
73. West, J.B. Physiological Effects of Chronic Hypoxia. *N. Engl. J. Med.* **2017**, *376*, 1965–1971. [[CrossRef](#)] [[PubMed](#)]
74. Fandrey, J.; Schodel, J.; Eckardt, K.U.; Katschinski, D.M.; Wenger, R.H. Now a Nobel gas: Oxygen. *Pflügers. Arch.* **2019**. [[CrossRef](#)] [[PubMed](#)]
75. Semenza, G.L. Oxygen sensing, hypoxia-inducible factors, and disease pathophysiology. *Annu. Rev. Pathol.* **2014**, *9*, 47–71. [[CrossRef](#)] [[PubMed](#)]
76. Maxwell, P.H.; Wiesener, M.S.; Chang, G.W.; Clifford, S.C.; Vaux, E.C.; Cockman, M.E.; Wykoff, C.C.; Pugh, C.W.; Maher, E.R.; Ratcliffe, P.J. The tumour suppressor protein VHL targets hypoxia-inducible factors for oxygen-dependent proteolysis. *Nature* **1999**, *399*, 271–275. [[CrossRef](#)] [[PubMed](#)]
77. Ivan, M.; Kondo, K.; Yang, H.; Kim, W.; Valiando, J.; Ohh, M.; Salic, A.; Asara, J.M.; Lane, W.S.; Kaelin, W.G., Jr. HIF α targeted for VHL-mediated destruction by proline hydroxylation: Implications for O₂ sensing. *Science* **2001**, *292*, 464–468. [[CrossRef](#)]
78. Jaakkola, P.; Mole, D.R.; Tian, Y.M.; Wilson, M.I.; Gielbert, J.; Gaskell, S.J.; Kriegsheim, A.; Hebestreit, H.F.; Mukherji, M.; Schofield, C.J.; et al. Targeting of HIF- α to the von Hippel-Lindau ubiquitylation complex by O₂-regulated prolyl hydroxylation. *Science* **2001**, *292*, 468–472. [[CrossRef](#)]
79. Kallio, P.J.; Okamoto, K.; O'Brien, S.; Carrero, P.; Makino, Y.; Tanaka, H.; Poellinger, L. Signal transduction in hypoxic cells: Inducible nuclear translocation and recruitment of the CBP/p300 coactivator by the hypoxia-inducible factor-1 α . *EMBO J.* **1998**, *17*, 6573–6586. [[CrossRef](#)]
80. Luo, J.C.; Shibuya, M. A variant of nuclear localization signal of bipartite-type is required for the nuclear translocation of hypoxia inducible factors (1 α , 2 α and 3 α). *Oncogene* **2001**, *20*, 1435–1444. [[CrossRef](#)]
81. Depping, R.; Steinhoff, A.; Schindler, S.G.; Friedrich, B.; Fagerlund, R.; Metzen, E.; Hartmann, E.; Kohler, M. Nuclear translocation of hypoxia-inducible factors (HIFs): Involvement of the classical importin α / β pathway. *Biochim. Biophys. Acta.* **2008**, *1783*, 394–404. [[CrossRef](#)] [[PubMed](#)]
82. Chachami, G.; Paraskeva, E.; Mingot, J.M.; Braliou, G.G.; Gorlich, D.; Simos, G. Transport of hypoxia-inducible factor HIF-1 α into the nucleus involves importins 4 and 7. *Biochem. Biophys. Res. Commun.* **2009**, *390*, 235–240. [[CrossRef](#)] [[PubMed](#)]
83. Epstein, A.; Gleadle, J.; McNeill, L.; Hewitson, K.; O'Rourke, J.; Mole, D.; Mukherji, M.; Metzen, E.; Wilson, M.; Dhanda, A.; et al. C. elegans EGL-9 and mammalian homologs define a family of dioxygenases that regulate HIF by prolyl hydroxylation. *Cell* **2001**, *107*, 43–54. [[CrossRef](#)]
84. Mahon, P.C.; Hirota, K.; Semenza, G.L. FIH-1: A novel protein that interacts with HIF-1 α and VHL to mediate repression of HIF-1 transcriptional activity. *Genes Dev* **2001**, *15*, 2675–2686. [[CrossRef](#)] [[PubMed](#)]
85. Lando, D.; Peet, D.J.; Whelan, D.A.; Gorman, J.J.; Whitelaw, M.L. Asparagine hydroxylation of the HIF transactivation domain a hypoxic switch. *Science* **2002**, *295*, 858–861. [[CrossRef](#)]
86. Hirota, K.; Semenza, G.L. Regulation of hypoxia-inducible factor 1 by prolyl and asparaginyl hydroxylases. *Biochem Biophys. Res. Commun.* **2005**, *338*, 610–616. [[CrossRef](#)]
87. Hirsila, M.; Koivunen, P.; Gunzler, V.; Kivirikko, K.I.; Myllyharju, J. Characterization of the human prolyl 4-hydroxylases that modify the hypoxia-inducible factor. *J. Biol. Chem.* **2003**, *278*, 30772–30780. [[CrossRef](#)]
88. Koivunen, P.; Hirsila, M.; Gunzler, V.; Kivirikko, K.I.; Myllyharju, J. Catalytic properties of the asparaginyl hydroxylase (FIH) in the oxygen sensing pathway are distinct from those of its prolyl 4-hydroxylases. *J. Biol. Chem.* **2004**, *279*, 9899–9904. [[CrossRef](#)]
89. Metzen, E.; Wolff, M.; Fandrey, J.; Jelkmann, W. Pericellular PO₂ and O₂ consumption in monolayer cell cultures. *Respir. Physiol.* **1995**, *100*, 101–106. [[CrossRef](#)]
90. Guzy, R.D.; Hoyos, B.; Robin, E.; Chen, H.; Liu, L.; Mansfield, K.D.; Simon, M.C.; Hammerling, U.; Schumacker, P.T. Mitochondrial complex III is required for hypoxia-induced ROS production and cellular oxygen sensing. *Cell Metab.* **2005**, *1*, 401–408. [[CrossRef](#)]

91. Brunelle, J.K.; Bell, E.L.; Quesada, N.M.; Vercauteren, K.; Tiranti, V.; Zeviani, M.; Scarpulla, R.C.; Chandel, N.S. Oxygen sensing requires mitochondrial ROS but not oxidative phosphorylation. *Cell Metab.* **2005**, *1*, 409–414. [[CrossRef](#)] [[PubMed](#)]
92. Mansfield, K.D.; Guzy, R.D.; Pan, Y.; Young, R.M.; Cash, T.P.; Schumacker, P.T.; Simon, M.C. Mitochondrial dysfunction resulting from loss of cytochrome c impairs cellular oxygen sensing and hypoxic HIF- α activation. *Cell Metab.* **2005**, *1*, 393–399. [[CrossRef](#)] [[PubMed](#)]
93. Kaelin, W. ROS: Really involved in oxygen sensing. *Cell Metab.* **2005**, *1*, 357–358. [[CrossRef](#)] [[PubMed](#)]
94. Richard, D.E.; Berra, E.; Gothie, E.; Roux, D.; Pouyssegur, J. p42/p44 mitogen-activated protein kinases phosphorylate hypoxia-inducible factor 1 α (HIF-1 α) and enhance the transcriptional activity of HIF-1. *J. Biol. Chem.* **1999**, *274*, 32631–32637. [[CrossRef](#)]
95. Conrad, P.W.; Freeman, T.L.; Beitner-Johnson, D.; Millhorn, D.E. EPAS1 trans-activation during hypoxia requires p42/p44 MAPK. *J. Biol. Chem.* **1999**, *274*, 33709–33713. [[CrossRef](#)]
96. Kalousi, A.; Mylonis, I.; Politou, A.S.; Chachami, G.; Paraskeva, E.; Simos, G. Casein kinase 1 regulates human hypoxia-inducible factor HIF-1. *J. Cell Sci.* **2010**, *123*, 2976–2986. [[CrossRef](#)]
97. Bencokova, Z.; Kaufmann, M.R.; Pires, I.M.; Lecane, P.S.; Giaccia, A.J.; Hammond, E.M. ATM activation and signaling under hypoxic conditions. *Mol. Cell Biol.* **2009**, *29*, 526–537. [[CrossRef](#)]
98. Flugel, D.; Gorlach, A.; Michiels, C.; Kietzmann, T. Glycogen synthase kinase 3 phosphorylates hypoxia-inducible factor 1 α and mediates its destabilization in a VHL-independent manner. *Mol. Cell Biol.* **2007**, *27*, 3253–3265. [[CrossRef](#)]
99. Xu, D.; Yao, Y.; Lu, L.; Costa, M.; Dai, W. Plk3 functions as an essential component of the hypoxia regulatory pathway by direct phosphorylation of HIF-1 α . *J. Biol. Chem.* **2010**, *285*, 38944–38950. [[CrossRef](#)]
100. Bullen, J.W.; Tchernyshyov, I.; Holewinski, R.J.; DeVine, L.; Wu, F.; Venkatraman, V.; Kass, D.L.; Cole, R.N.; Van Eyk, J.; Semenza, G.L. Protein kinase A-dependent phosphorylation stimulates the transcriptional activity of hypoxia-inducible factor 1. *Sci. Signal.* **2016**, *9*, ra56. [[CrossRef](#)]
101. McNamee, E.N.; Vohwinkel, C.; Eltzschig, H.K. Hydroxylation-independent HIF-1 α stabilization through PKA: A new paradigm for hypoxia signaling. *Sci. Signal.* **2016**, *9*, fs11. [[CrossRef](#)]
102. Gkotinakou, I.M.; Befani, C.; Simos, G.; Liakos, P. ERK1/2 phosphorylates HIF-2 α and regulates its activity by controlling its CRM1-dependent nuclear shuttling. *J. Cell Sci.* **2019**, *132*. [[CrossRef](#)]
103. Pangou, E.; Befani, C.; Mylonis, I.; Samiotaki, M.; Panayotou, G.; Simos, G.; Liakos, P. HIF-2 α phosphorylation by CK1 δ promotes erythropoietin secretion in liver cancer cells under hypoxia. *J. Cell Sci.* **2016**, *129*, 4213–4226. [[CrossRef](#)] [[PubMed](#)]
104. Finkel, T.; Deng, C.X.; Mostoslavsky, R. Recent progress in the biology and physiology of sirtuins. *Nature* **2009**, *460*, 587–591. [[CrossRef](#)] [[PubMed](#)]
105. Dioum, E.M.; Chen, R.; Alexander, M.S.; Zhang, Q.; Hogg, R.T.; Gerard, R.D.; Garcia, J.A. Regulation of hypoxia-inducible factor 2 α signaling by the stress-responsive deacetylase sirtuin 1. *Science* **2009**, *324*, 1289–1293. [[CrossRef](#)]
106. Lim, J.H.; Lee, Y.M.; Chun, Y.S.; Chen, J.; Kim, J.E.; Park, J.W. Sirtuin 1 modulates cellular responses to hypoxia by deacetylating hypoxia-inducible factor 1 α . *Mol. Cell* **2010**, *38*, 864–878. [[CrossRef](#)]
107. Jeong, J.W.; Bae, M.K.; Ahn, M.Y.; Kim, S.H.; Sohn, T.K.; Bae, M.H.; Yoo, M.A.; Song, E.J.; Lee, K.J.; Kim, K.W. Regulation and destabilization of HIF-1 α by ARD1-mediated acetylation. *Cell* **2002**, *111*, 709–720. [[CrossRef](#)]
108. Yoo, Y.G.; Kong, G.; Lee, M.O. Metastasis-associated protein 1 enhances stability of hypoxia-inducible factor-1 α protein by recruiting histone deacetylase 1. *EMBO J.* **2006**, *25*, 1231–1241. [[CrossRef](#)]
109. Li, J.; Xu, Y.; Jiao, H.; Wang, W.; Mei, Z.; Chen, G. Sumoylation of hypoxia inducible factor-1 α and its significance in cancer. *Sci. China Life Sci.* **2014**, *57*, 657–664. [[CrossRef](#)]
110. Bae, S.H.; Jeong, J.W.; Park, J.A.; Kim, S.H.; Bae, M.K.; Choi, S.J.; Kim, K.W. Sumoylation increases HIF-1 α stability and its transcriptional activity. *Biochem. Biophys. Res. Commun.* **2004**, *324*, 394–400. [[CrossRef](#)]
111. Li, F.; Sonveaux, P.; Rabbani, Z.N.; Liu, S.; Yan, B.; Huang, Q.; Vujaskovic, Z.; Dewhirst, M.W.; Li, C.Y. Regulation of HIF-1 α stability through S-nitrosylation. *Mol. Cell* **2007**, *26*, 63–74. [[CrossRef](#)] [[PubMed](#)]
112. Ryu, J.H.; Li, S.H.; Park, H.S.; Park, J.W.; Lee, B.; Chun, Y.S. Hypoxia-inducible factor α subunit stabilization by NEDD8 conjugation is reactive oxygen species-dependent. *J. Biol. Chem.* **2011**, *286*, 6963–6970. [[CrossRef](#)] [[PubMed](#)]

113. Ema, M.; Hirota, K.; Mimura, J.; Abe, H.; Yodoi, J.; Sogawa, K.; Poellinger, L.; Fujii-Kuriyama, Y. Molecular mechanisms of transcription activation by HLF and HIF1alpha in response to hypoxia: Their stabilization and redox signal-induced interaction with CBP/p300. *EMBO J.* **1999**, *18*, 1905–1914. [[CrossRef](#)]
114. Papandreou, I.; Cairns, R.A.; Fontana, L.; Lim, A.L.; Denko, N.C. HIF-1 mediates adaptation to hypoxia by actively downregulating mitochondrial oxygen consumption. *Cell Metab.* **2006**, *3*, 187–197. [[CrossRef](#)]
115. Chandel, N.S.; McClintock, D.S.; Feliciano, C.E.; Wood, T.M.; Melendez, J.A.; Rodriguez, A.M.; Schumacker, P.T. Reactive oxygen species generated at mitochondrial complex III stabilize hypoxia-inducible factor-1alpha during hypoxia: A mechanism of O2 sensing. *J. Biol. Chem.* **2000**, *275*, 25130–25138. [[CrossRef](#)]
116. Schumacker, P.T. Hypoxia, anoxia, and O2 sensing: The search continues. *Am. J. Physiol. Lung Cell Mol. Physiol.* **2002**, *283*, L918–L921. [[CrossRef](#)]
117. Yuan, G.; Khan, S.A.; Luo, W.; Nanduri, J.; Semenza, G.L.; Prabhakar, N.R. Hypoxia-inducible factor 1 mediates increased expression of NADPH oxidase-2 in response to intermittent hypoxia. *J. Cell Physiol.* **2011**, *226*, 2925–2933. [[CrossRef](#)]
118. Nanduri, J.; Makarenko, V.; Reddy, V.D.; Yuan, G.; Pawar, A.; Wang, N.; Khan, S.A.; Zhang, X.; Kinsman, B.; Peng, Y.J.; et al. Epigenetic regulation of hypoxic sensing disrupts cardiorespiratory homeostasis. *Proc. Natl. Acad. Sci. USA* **2012**, *109*, 2515–2520. [[CrossRef](#)]
119. Prabhakar, N.R.; Peng, Y.J.; Yuan, G.; Nanduri, J. Reactive oxygen radicals and gaseous transmitters in carotid body activation by intermittent hypoxia. *Cell Tissue Res.* **2018**, *372*, 427–431. [[CrossRef](#)]
120. Yuan, G.; Peng, Y.J.; Khan, S.A.; Nanduri, J.; Singh, A.; Vasavda, C.; Semenza, G.L.; Kumar, G.K.; Snyder, S.H.; Prabhakar, N.R. H2S production by reactive oxygen species in the carotid body triggers hypertension in a rodent model of sleep apnea. *Sci. Signal.* **2016**, *9*, ra80. [[CrossRef](#)]
121. Nanduri, J.; Peng, Y.J.; Wang, N.; Khan, S.A.; Semenza, G.L.; Kumar, G.K.; Prabhakar, N.R. Epigenetic regulation of redox state mediates persistent cardiorespiratory abnormalities after long-term intermittent hypoxia. *J. Physiol.* **2017**, *595*, 63–77. [[CrossRef](#)] [[PubMed](#)]
122. Prabhakar, N.R.; Semenza, G.L. Adaptive and maladaptive cardiorespiratory responses to continuous and intermittent hypoxia mediated by hypoxia-inducible factors 1 and 2. *Physiol. Rev.* **2012**, *92*, 967–1003. [[CrossRef](#)] [[PubMed](#)]
123. Ravi, R.; Mookerjee, B.; Bhujwalla, Z.M.; Sutter, C.H.; Artemov, D.; Zeng, Q.; Dillehay, L.E.; Madan, A.; Semenza, G.L.; Bedi, A. Regulation of tumor angiogenesis by p53-induced degradation of hypoxia-inducible factor 1alpha. *Genes Dev.* **2000**, *14*, 34–44. [[PubMed](#)]
124. Semenza, G.L. VHL and p53: Tumor suppressors team up to prevent cancer. *Mol. Cell* **2006**, *22*, 437–439. [[CrossRef](#)]
125. An, W.G.; Kanekal, M.; Simon, M.C.; Maltepe, E.; Blagosklonny, M.V.; Neckers, L.M. Stabilization of wild-type p53 by hypoxia-inducible factor 1alpha. *Nature* **1998**, *392*, 405–408. [[CrossRef](#)]
126. Amelio, I.; Mancini, M.; Petrova, V.; Cairns, R.A.; Vikhrev, P.; Nicolai, S.; Marini, A.; Antonov, A.A.; Le Quesne, J.; Baena Acevedo, J.D.; et al. p53 mutants cooperate with HIF-1 in transcriptional regulation of extracellular matrix components to promote tumor progression. *Proc. Natl. Acad. Sci. USA* **2018**, *115*, E10869–E10878. [[CrossRef](#)]
127. D’Orazi, G.; Cirone, M. Mutant p53 and Cellular Stress Pathways: A Criminal Alliance That Promotes Cancer Progression. *Cancers (Basel)* **2019**, *11*. [[CrossRef](#)]
128. Laughner, E.; Taghavi, P.; Chiles, K.; Mahon, P.C.; Semenza, G.L. HER2 (neu) signaling increases the rate of hypoxia-inducible factor 1alpha (HIF-1alpha) synthesis: Novel mechanism for HIF-1-mediated vascular endothelial growth factor expression. *Mol. Cell Biol.* **2001**, *21*, 3995–4004. [[CrossRef](#)]
129. Fukuda, R.; Hirota, K.; Fan, F.; Jung, Y.D.; Ellis, L.M.; Semenza, G.L. Insulin-like growth factor 1 induces hypoxia-inducible factor 1-mediated vascular endothelial growth factor expression, which is dependent on MAP kinase and phosphatidylinositol 3-kinase signaling in colon cancer cells. *J. Biol. Chem.* **2002**, *277*, 38205–38211. [[CrossRef](#)]
130. Treins, C.; Giorgetti-Peraldi, S.; Murdaca, J.; Semenza, G.L.; Van Obberghen, E. Insulin stimulates hypoxia-inducible factor 1 through a phosphatidylinositol 3-kinase/target of rapamycin-dependent signaling pathway. *J. Biol. Chem.* **2002**, *277*, 27975–27981. [[CrossRef](#)]

131. Hirota, K.; Fukuda, R.; Takabuchi, S.; Kizaka-Kondoh, S.; Adachi, T.; Fukuda, K.; Semenza, G.L. Induction of hypoxia-inducible factor 1 activity by muscarinic acetylcholine receptor signaling. *J. Biol. Chem.* **2004**, *279*, 41521–41528. [[CrossRef](#)] [[PubMed](#)]
132. Fukuda, R.; Kelly, B.; Semenza, G.L. Vascular endothelial growth factor gene expression in colon cancer cells exposed to prostaglandin E2 is mediated by hypoxia-inducible factor 1. *Cancer Res.* **2003**, *63*, 2330–2334. [[PubMed](#)]
133. Suzuki, K.; Nishi, K.; Takabuchi, S.; Kai, S.; Matsuyama, T.; Kurosawa, S.; Adachi, T.; Maruyama, T.; Fukuda, K.; Hirota, K. Differential roles of prostaglandin E-type receptors in activation of hypoxia-inducible factor 1 by prostaglandin E1 in vascular-derived cells under non-hypoxic conditions. *PeerJ* **2013**, *1*, e220. [[CrossRef](#)]
134. Zhong, H.; Chiles, K.; Feldser, D.; Laughner, E.; Hanrahan, C.; Georgescu, M.M.; Simons, J.W.; Semenza, G.L. Modulation of hypoxia-inducible factor 1 α expression by the epidermal growth factor/phosphatidylinositol 3-kinase/PTEN/AKT/FRAP pathway in human prostate cancer cells: Implications for tumor angiogenesis and therapeutics. *Cancer Res.* **2000**, *60*, 1541–1545.
135. Jiang, B.H.; Liu, L.Z. PI3K/PTEN signaling in tumorigenesis and angiogenesis. *Biochim. Biophys. Acta* **2008**, *1784*, 150–158. [[CrossRef](#)]
136. Daijo, H.; Hoshino, Y.; Kai, S.; Suzuki, K.; Nishi, K.; Matsuo, Y.; Harada, H.; Hirota, K. Cigarette smoke reversibly activates hypoxia-inducible factor 1 in a reactive oxygen species-dependent manner. *Sci. Rep.* **2016**, *6*, 34424. [[CrossRef](#)]
137. Peyssonnaud, C.; Datta, V.; Cramer, T.; Doedens, A.; Theodorakis, E.A.; Gallo, R.L.; Hurtado-Ziola, N.; Nizet, V.; Johnson, R.S. HIF-1 α expression regulates the bactericidal capacity of phagocytes. *J. Clin. Invest.* **2005**, *115*, 1806–1815. [[CrossRef](#)]
138. Walmsley, S.R.; Print, C.; Farahi, N.; Peyssonnaud, C.; Johnson, R.S.; Cramer, T.; Sobolewski, A.; Condliffe, A.M.; Cowburn, A.S.; Johnson, N.; et al. Hypoxia-induced neutrophil survival is mediated by HIF-1 α -dependent NF-kappaB activity. *J. Exp. Med.* **2005**, *201*, 105–115. [[CrossRef](#)]
139. Cramer, T.; Johnson, R.S. A novel role for the hypoxia inducible transcription factor HIF-1 α : Critical regulation of inflammatory cell function. *Cell Cycle* **2003**, *2*, 192–193. [[CrossRef](#)]
140. Nishi, K.; Oda, T.; Takabuchi, S.; Oda, S.; Fukuda, K.; Adachi, T.; Semenza, G.L.; Shingu, K.; Hirota, K. LPS induces hypoxia-inducible factor 1 activation in macrophage-differentiated cells in a reactive oxygen species-dependent manner. *Antioxid Redox Signal.* **2008**, *10*, 983–996. [[CrossRef](#)]
141. Wang, F.; Sekine, H.; Kikuchi, Y.; Takasaki, C.; Miura, C.; Heiwa, O.; Shuin, T.; Fujii-Kuriyama, Y.; Sogawa, K. HIF-1 α -prolyl hydroxylase: Molecular target of nitric oxide in the hypoxic signal transduction pathway. *Biochem. Biophys. Res. Commun.* **2002**, *295*, 657–662. [[CrossRef](#)]
142. Sandau, K.B.; Fandrey, J.; Brune, B. Accumulation of HIF-1 α under the influence of nitric oxide. *Blood* **2001**, *97*, 1009–1015. [[CrossRef](#)]
143. Sandau, K.B.; Faus, H.G.; Brune, B. Induction of hypoxia-inducible-factor 1 by nitric oxide is mediated via the PI 3K pathway. *Biochem. Biophys. Res. Commun.* **2000**, *278*, 263–267. [[CrossRef](#)]
144. Metzén, E.; Zhou, J.; Jelkmann, W.; Fandrey, J.; Brune, B. Nitric oxide impairs normoxic degradation of HIF-1 α by inhibition of prolyl hydroxylases. *Mol. Biol. Cell* **2003**, *14*, 3470–3481. [[CrossRef](#)]
145. Brune, B.; Zhou, J. The role of nitric oxide (NO) in stability regulation of hypoxia inducible factor-1 α (HIF-1 α). *Curr. Med. Chem.* **2003**, *10*, 845–855. [[CrossRef](#)]
146. Kasuno, K.; Takabuchi, S.; Fukuda, K.; Kizaka-Kondoh, S.; Yodoi, J.; Adachi, T.; Semenza, G.L.; Hirota, K. Nitric oxide induces hypoxia-inducible factor 1 activation that is dependent on MAPK and phosphatidylinositol 3-kinase signaling. *J. Biol. Chem.* **2004**, *279*, 2550–2558. [[CrossRef](#)]
147. Palmer, L.A.; Gaston, B.; Johns, R.A. Normoxic stabilization of hypoxia-inducible factor-1 expression and activity: Redox-dependent effect of nitrogen oxides. *Mol. Pharmacol.* **2000**, *58*, 1197–1203. [[CrossRef](#)]
148. Mateo, J.; Garcia-Lecea, M.; Cadenas, S.; Hernandez, C.; Moncada, S. Regulation of hypoxia-inducible factor-1 α by nitric oxide through mitochondria-dependent and -independent pathways. *Biochem. J.* **2003**, *376*, 537–544. [[CrossRef](#)]
149. Sumbayev, V.V.; Yasinska, I.M. Peroxynitrite as an alternative donor of oxygen in HIF-1 α proline hydroxylation under low oxygen availability. *Free Radic. Res.* **2006**, *40*, 631–635. [[CrossRef](#)]

150. Cummins, E.P.; Berra, E.; Comerford, K.M.; Ginouves, A.; Fitzgerald, K.T.; Seeballuck, F.; Godson, C.; Nielsen, J.E.; Moynagh, P.; Pouyssegur, J.; et al. Prolyl hydroxylase-1 negatively regulates I κ B kinase-beta, giving insight into hypoxia-induced NF κ B activity. *Proc. Natl. Acad. Sci. USA* **2006**, *103*, 18154–18159. [[CrossRef](#)]
151. Dehne, N.; Brune, B. HIF-1 in the inflammatory microenvironment. *Exp. Cell Res.* **2009**, *315*, 1791–1797. [[CrossRef](#)] [[PubMed](#)]
152. Rius, J.; Guma, M.; Schachtrup, C.; Akassoglou, K.; Zinkernagel, A.S.; Nizet, V.; Johnson, R.S.; Haddad, G.G.; Karin, M. NF-kappaB links innate immunity to the hypoxic response through transcriptional regulation of HIF-1alpha. *Nature* **2008**, *453*, 807–811. [[CrossRef](#)]
153. Colgan, S.P.; Taylor, C.T. Hypoxia: An alarm signal during intestinal inflammation. *Nat. Rev. Gastroenterol. Hepatol.* **2010**, *7*, 281–287. [[CrossRef](#)]
154. Walmsley, S.R.; Cadwallader, K.A.; Chilvers, E.R. The role of HIF-1alpha in myeloid cell inflammation. *Trends Immunol.* **2005**, *26*, 434–439. [[CrossRef](#)]
155. Nangaku, M. Chronic hypoxia and tubulointerstitial injury: A final common pathway to end-stage renal failure. *J. Am. Soc. Nephrol.* **2006**, *17*, 17–25. [[CrossRef](#)]
156. Matsumoto, M.; Tanaka, T.; Yamamoto, T.; Noiri, E.; Miyata, T.; Inagi, R.; Fujita, T.; Nangaku, M. Hypoperfusion of peritubular capillaries induces chronic hypoxia before progression of tubulointerstitial injury in a progressive model of rat glomerulonephritis. *J. Am. Soc. Nephrol.* **2004**, *15*, 1574–1581. [[CrossRef](#)]
157. Manotham, K.; Tanaka, T.; Matsumoto, M.; Ohse, T.; Miyata, T.; Inagi, R.; Kurokawa, K.; Fujita, T.; Nangaku, M. Evidence of tubular hypoxia in the early phase in the remnant kidney model. *J. Am. Soc. Nephrol.* **2004**, *15*, 1277–1288. [[CrossRef](#)]
158. Tanaka, T.; Miyata, T.; Inagi, R.; Fujita, T.; Nangaku, M. Hypoxia in renal disease with proteinuria and/or glomerular hypertension. *Am. J. Pathol.* **2004**, *165*, 1979–1992. [[CrossRef](#)]
159. Katavetin, P.; Miyata, T.; Inagi, R.; Tanaka, T.; Sassa, R.; Ingelfinger, J.R.; Fujita, T.; Nangaku, M. High glucose blunts vascular endothelial growth factor response to hypoxia via the oxidative stress-regulated hypoxia-inducible factor/hypoxia-responsible element pathway. *J. Am. Soc. Nephrol.* **2006**, *17*, 1405–1413. [[CrossRef](#)]
160. Katavetin, P.; Inagi, R.; Miyata, T.; Tanaka, T.; Sassa, R.; Ingelfinger, J.R.; Fujita, T.; Nangaku, M. Albumin suppresses vascular endothelial growth factor via alteration of hypoxia-inducible factor/hypoxia-responsive element pathway. *Biochem. Biophys. Res. Commun.* **2008**, *367*, 305–310. [[CrossRef](#)]
161. Izuhara, Y.; Nangaku, M.; Inagi, R.; Tominaga, N.; Aizawa, T.; Kurokawa, K.; van Ypersele de Strihou, C.; Miyata, T. Renoprotective properties of angiotensin receptor blockers beyond blood pressure lowering. *J. Am. Soc. Nephrol.* **2005**, *16*, 3631–3641. [[CrossRef](#)]
162. Hirota, K. An intimate crosstalk between iron homeostasis and oxygen metabolism regulated by the hypoxia-inducible factors (HIFs). *Free Radic. Biol. Med.* **2019**, *133*, 118–129. [[CrossRef](#)]
163. Peyssonnaud, C.; Zinkernagel, A.S.; Schuepbach, R.A.; Rankin, E.; Vaulont, S.; Haase, V.H.; Nizet, V.; Johnson, R.S. Regulation of iron homeostasis by the hypoxia-inducible transcription factors (HIFs). *J. Clin. Invest.* **2007**, *117*, 1926–1932. [[CrossRef](#)]
164. Hentze, M.W.; Muckenthaler, M.U.; Galy, B.; Camaschella, C. Two to tango: Regulation of Mammalian iron metabolism. *Cell* **2010**, *142*, 24–38. [[CrossRef](#)]
165. Simpson, R.J.; McKie, A.T. Regulation of intestinal iron absorption: The mucosa takes control? *Cell Metab.* **2009**, *10*, 84–87. [[CrossRef](#)]
166. Nemeth, E.; Ganz, T. Regulation of iron metabolism by hepcidin. *Annu Rev. Nutr.* **2006**, *26*, 323–342. [[CrossRef](#)]
167. Nemeth, E.; Tuttle, M.S.; Powelson, J.; Vaughn, M.B.; Donovan, A.; Ward, D.M.; Ganz, T.; Kaplan, J. Hepcidin regulates cellular iron efflux by binding to ferroportin and inducing its internalization. *Science* **2004**, *306*, 2090–2093. [[CrossRef](#)]
168. Chen, N.; Hao, C.; Liu, B.C.; Lin, H.; Wang, C.; Xing, C.; Liang, X.; Jiang, G.; Liu, Z.; Li, X.; et al. Roxadustat Treatment for Anemia in Patients Undergoing Long-Term Dialysis. *N. Engl. J. Med.* **2019**, *381*, 1011–1022. [[CrossRef](#)]
169. Kaplan, J. Roxadustat and Anemia of Chronic Kidney Disease. *N. Engl. J. Med.* **2019**, *381*, 1070–1072. [[CrossRef](#)]

170. Chen, N.; Hao, C.; Peng, X.; Lin, H.; Yin, A.; Hao, L.; Tao, Y.; Liang, X.; Liu, Z.; Xing, C.; et al. Roxadustat for Anemia in Patients with Kidney Disease Not Receiving Dialysis. *N. Engl. J. Med.* **2019**, *381*, 1001–1010. [[CrossRef](#)]
171. Brown, J.M.; Wilson, W.R. Exploiting tumour hypoxia in cancer treatment. *Nat. Rev. Cancer* **2004**, *4*, 437–447. [[CrossRef](#)] [[PubMed](#)]
172. Semenza, G.L. Hypoxia-inducible factors: Mediators of cancer progression and targets for cancer therapy. *Trends Pharmacol. Sci.* **2012**, *33*, 207–214. [[CrossRef](#)] [[PubMed](#)]
173. Keith, B.; Simon, M.C. Hypoxia-inducible factors, stem cells, and cancer. *Cell* **2007**, *129*, 465–472. [[CrossRef](#)] [[PubMed](#)]
174. Liberti, M.V.; Locasale, J.W. The Warburg Effect: How Does it Benefit Cancer Cells? *Trends Biochem. Sci.* **2016**, *41*, 211–218. [[CrossRef](#)] [[PubMed](#)]
175. Koppenol, W.H.; Bounds, P.L.; Dang, C.V. Otto Warburg’s contributions to current concepts of cancer metabolism. *Nat. Rev. Cancer* **2011**, *11*, 325–337. [[CrossRef](#)] [[PubMed](#)]
176. Kim, J.W.; Dang, C.V. Cancer’s molecular sweet tooth and the Warburg effect. *Cancer Res.* **2006**, *66*, 8927–8930. [[CrossRef](#)] [[PubMed](#)]
177. Rattigan, Y.I.; Patel, B.B.; Ackerstaff, E.; Sukenick, G.; Koutcher, J.A.; Glod, J.W.; Banerjee, D. Lactate is a mediator of metabolic cooperation between stromal carcinoma associated fibroblasts and glycolytic tumor cells in the tumor microenvironment. *Exp. Cell Res.* **2012**, *318*, 326–335. [[CrossRef](#)]
178. Fiaschi, T.; Marini, A.; Giannoni, E.; Taddei, M.L.; Gandellini, P.; De Donatis, A.; Lanciotti, M.; Serni, S.; Cirri, P.; Chiarugi, P. Reciprocal metabolic reprogramming through lactate shuttle coordinately influences tumor-stroma interplay. *Cancer Res.* **2012**, *72*, 5130–5140. [[CrossRef](#)]
179. Rankin, E.B.; Giaccia, A.J. Hypoxic control of metastasis. *Science* **2016**, *352*, 175–180. [[CrossRef](#)]
180. Lamouille, S.; Xu, J.; Derynck, R. Molecular mechanisms of epithelial-mesenchymal transition. *Nat. Rev. Mol. Cell Biol.* **2014**, *15*, 178–196. [[CrossRef](#)]
181. Haase, V.H. Oxygen regulates epithelial-to-mesenchymal transition: Insights into molecular mechanisms and relevance to disease. *Kidney Int.* **2009**, *76*, 492–499. [[CrossRef](#)] [[PubMed](#)]
182. Liu, Z.J.; Semenza, G.L.; Zhang, H.F. Hypoxia-inducible factor 1 and breast cancer metastasis. *J. Zhejiang Univ. Sci. B* **2015**, *16*, 32–43. [[CrossRef](#)] [[PubMed](#)]
183. Semenza, G.L. Molecular mechanisms mediating metastasis of hypoxic breast cancer cells. *Trends Mol. Med.* **2012**, *18*, 534–543. [[CrossRef](#)] [[PubMed](#)]
184. Suetrong, B.; Walley, K.R. Lactic Acidosis in Sepsis: It’s Not All Anaerobic: Implications for Diagnosis and Management. *Chest* **2016**, *149*, 252–261. [[CrossRef](#)]
185. Cray, S.H.; Robinson, B.H.; Cox, P.N. Lactic acidemia and bradyarrhythmia in a child sedated with propofol. *Crit. Care Med.* **1998**, *26*, 2087–2092. [[CrossRef](#)]
186. Finsterer, J.; Frank, M. Propofol Is Mitochondrion-Toxic and May Unmask a Mitochondrial Disorder. *J. Child. Neurol.* **2016**, *31*, 1489–1494. [[CrossRef](#)]
187. Krajcova, A.; Waldauf, P.; Andel, M.; Duska, F. Propofol infusion syndrome: A structured review of experimental studies and 153 published case reports. *Crit. Care* **2015**, *19*, 398. [[CrossRef](#)]
188. Sumi, C.; Okamoto, A.; Tanaka, H.; Kusunoki, M.; Shoji, T.; Uba, T.; Adachi, T.; Iwai, T.; Nishi, K.; Harada, H.; et al. Suppression of mitochondrial oxygen metabolism mediated by the transcription factor HIF-1 alleviates propofol-induced cell toxicity. *Sci. Rep.* **2018**, *8*, 8987. [[CrossRef](#)]
189. Abe, H.; Semba, H.; Takeda, N. The Roles of Hypoxia Signaling in the Pathogenesis of Cardiovascular Diseases. *J. Atheroscler. Thromb.* **2017**, *24*, 884–894. [[CrossRef](#)]
190. Abe, H.; Takeda, N.; Isagawa, T.; Semba, H.; Nishimura, S.; Morioka, M.S.; Nakagama, Y.; Sato, T.; Soma, K.; Koyama, K.; et al. Macrophage hypoxia signaling regulates cardiac fibrosis via Oncostatin M. *Nat. Commun.* **2019**, *10*, 2824. [[CrossRef](#)]
191. Semba, H.; Takeda, N.; Isagawa, T.; Sugiura, Y.; Honda, K.; Wake, M.; Miyazawa, H.; Yamaguchi, Y.; Miura, M.; Jenkins, D.M.; et al. HIF-1 α -PDK1 axis-induced active glycolysis plays an essential role in macrophage migratory capacity. *Nat. Commun.* **2016**, *7*, 11635. [[CrossRef](#)] [[PubMed](#)]
192. Sano, M.; Minamino, T.; Toko, H.; Miyauchi, H.; Orimo, M.; Qin, Y.; Akazawa, H.; Tateno, K.; Kayama, Y.; Harada, M.; et al. p53-induced inhibition of Hif-1 causes cardiac dysfunction during pressure overload. *Nature* **2007**, *446*, 444–448. [[CrossRef](#)] [[PubMed](#)]

193. Mirtschink, P.; Krishnan, J.; Grimm, F.; Sarre, A.; Horl, M.; Kayikci, M.; Fankhauser, N.; Christinat, Y.; Cortijo, C.; Feehan, O.; et al. HIF-driven SF3B1 induces KHK-C to enforce fructolysis and heart disease. *Nature* **2015**, *522*, 444–449. [[CrossRef](#)] [[PubMed](#)]
194. Caniggia, I.; Winter, J.; Lye, S.J.; Post, M. Oxygen and placental development during the first trimester: Implications for the pathophysiology of pre-eclampsia. *Placenta* **2000**, *21*, S25–S30. [[CrossRef](#)] [[PubMed](#)]
195. Red-Horse, K.; Zhou, Y.; Genbacev, O.; Prakobphol, A.; Foulk, R.; McMaster, M.; Fisher, S.J. Trophoblast differentiation during embryo implantation and formation of the maternal-fetal interface. *J. Clin. Invest.* **2004**, *114*, 744–754. [[CrossRef](#)]
196. Cross, J.C.; Baczyk, D.; Dobric, N.; Hemberger, M.; Hughes, M.; Simmons, D.G.; Yamamoto, H.; Kingdom, J.C. Genes, development and evolution of the placenta. *Placenta* **2003**, *24*, 123–130. [[CrossRef](#)] [[PubMed](#)]
197. Caniggia, I.; Mostachfi, H.; Winter, J.; Gassmann, M.; Lye, S.J.; Kuliszewski, M.; Post, M. Hypoxia-inducible factor-1 mediates the biological effects of oxygen on human trophoblast differentiation through TGFbeta(3). *J. Clin. Invest.* **2000**, *105*, 577–587. [[CrossRef](#)]
198. Hirota, Y. Progesterone governs endometrial proliferation-differentiation switching and blastocyst implantation. *Endocr. J.* **2019**, *66*, 199–206. [[CrossRef](#)]
199. Fukui, Y.; Hirota, Y.; Matsuo, M.; Gebril, M.; Akaeda, S.; Hiraoka, T.; Osuga, Y. Uterine receptivity, embryo attachment, and embryo invasion: Multistep processes in embryo implantation. *Reprod. Med. Biol.* **2019**, *18*, 234–240. [[CrossRef](#)]
200. Matsumoto, L.; Hirota, Y.; Saito-Fujita, T.; Takeda, N.; Tanaka, T.; Hiraoka, T.; Akaeda, S.; Fujita, H.; Shimizu-Hirota, R.; Igaue, S.; et al. HIF2alpha in the uterine stroma permits embryo invasion and luminal epithelium detachment. *J. Clin. Invest.* **2018**, *128*, 3186–3197. [[CrossRef](#)]
201. Nakamura, H.; Makino, Y.; Okamoto, K.; Poellinger, L.; Ohnuma, K.; Morimoto, C.; Tanaka, H. TCR engagement increases hypoxia-inducible factor-1 alpha protein synthesis via rapamycin-sensitive pathway under hypoxic conditions in human peripheral T cells. *J. Immunol.* **2005**, *174*, 7592–7599. [[CrossRef](#)] [[PubMed](#)]
202. Makino, Y.; Nakamura, H.; Ikeda, E.; Ohnuma, K.; Yamauchi, K.; Yabe, Y.; Poellinger, L.; Okada, Y.; Morimoto, C.; Tanaka, H. Hypoxia-inducible factor regulates survival of antigen receptor-driven T cells. *J. Immunol.* **2003**, *171*, 6534–6540. [[CrossRef](#)] [[PubMed](#)]
203. Oda, T.; Hirota, K.; Nishi, K.; Takabuchi, S.; Oda, S.; Yamada, H.; Arai, T.; Fukuda, K.; Kita, T.; Adachi, T.; et al. Activation of hypoxia-inducible factor 1 during macrophage differentiation. *Am. J. Physiol. Cell Physiol.* **2006**, *291*, C104–C113. [[CrossRef](#)] [[PubMed](#)]
204. Ohsumi, Y. Historical landmarks of autophagy research. *Cell Res.* **2014**, *24*, 9–23. [[CrossRef](#)] [[PubMed](#)]
205. Nam, T.; Han, J.H.; Devkota, S.; Lee, H.W. Emerging Paradigm of Crosstalk between Autophagy and the Ubiquitin-Proteasome System. *Mol. Cells* **2017**, *40*, 897–905. [[CrossRef](#)]
206. Saha, S.; Panigrahi, D.P.; Patil, S.; Bhutia, S.K. Autophagy in health and disease: A comprehensive review. *Biomed. Pharmacother.* **2018**, *104*, 485–495. [[CrossRef](#)]
207. Levine, B.; Kroemer, G. Biological Functions of Autophagy Genes: A Disease Perspective. *Cell* **2019**, *176*, 11–42. [[CrossRef](#)]
208. Chourasia, A.H.; Macleod, K.F. Tumor suppressor functions of BNIP3 and mitophagy. *Autophagy* **2015**, *11*, 1937–1938. [[CrossRef](#)]
209. Zhao, Y.; Xiong, X.; Jia, L.; Sun, Y. Targeting Cullin-RING ligases by MLN4924 induces autophagy via modulating the HIF1-REDD1-TSC1-mTORC1-DEPTOR axis. *Cell Death Dis.* **2012**, *3*, e386. [[CrossRef](#)]
210. Wolff, N.C.; Vega-Rubin-de-Celis, S.; Xie, X.J.; Castrillon, D.H.; Kabbani, W.; Brugarolas, J. Cell-type-dependent regulation of mTORC1 by REDD1 and the tumor suppressors TSC1/TSC2 and LKB1 in response to hypoxia. *Mol. Cell Biol.* **2011**, *31*, 1870–1884. [[CrossRef](#)]
211. Brugarolas, J.; Lei, K.; Hurley, R.L.; Manning, B.D.; Reiling, J.H.; Hafen, E.; Witters, L.A.; Ellisen, L.W.; Kaelin, W.G., Jr. Regulation of mTOR function in response to hypoxia by REDD1 and the TSC1/TSC2 tumor suppressor complex. *Genes Dev.* **2004**, *18*, 2893–2904. [[CrossRef](#)] [[PubMed](#)]





Article

Use of Oral Anticoagulation and Diabetes Do Not Inhibit the Angiogenic Potential of Hypoxia Preconditioned Blood-Derived Secretomes

Philipp Moog¹, Maryna Jensch¹, Jessica Hughes¹, Burak Salgin², Ulf Dornseifer^{1,3}, Hans-Günther Machens^{1,*}, Arndt F. Schilling^{4,†} and Ektoras Hadjipanayi^{1,†}

¹ Experimental Plastic Surgery, Clinic for Plastic, Reconstructive and Hand Surgery, Klinikum Rechts der Isar, Technische Universität München, D-81675 Munich, Germany; philippmoog@web.de (P.M.); marinajensch@gmx.de (M.J.); Jessica.Hughes@gmx.de (J.H.); ulf.dornseifer@isarklinikum.de (U.D.); e.hadjipanayi@gmail.com (E.H.)

² Centre for Neuroscience, Surgery and Trauma, Blizzard Institute, Barts and The London School of Medicine and Dentistry, Queen Mary University of London, London E1 4NS, UK; b.salgin@qmul.ac.uk

³ Department of Plastic, Reconstructive and Aesthetic Surgery, Isar Klinikum, D-80331 Munich, Germany

⁴ Department of Trauma Surgery, Orthopedics and Plastic Surgery, Universitätsmedizin Göttingen, D-37075 Göttingen, Germany; arndt.schilling@med.uni-goettingen.de

* Correspondence: Hans-Guenther.Machens@mri.tum.de; Tel.: +49-089-4140-2271

† These Authors contributed equally to this work.

Received: 7 July 2020; Accepted: 9 August 2020; Published: 11 August 2020

Abstract: Patients suffering from tissue ischemia, who would greatly benefit from angiogenesis-promoting therapies such as hypoxia preconditioned blood-derived secretomes commonly receive oral anticoagulation (OA) and/or have diabetes mellitus (DM). In this study, we investigated the effect of OA administration on the *in vitro* angiogenic potential of hypoxia preconditioned plasma (HPP) and serum (HPS), prepared from nondiabetic/diabetic subjects who did not receive OA ($n = 5$) or were treated with acetylsalicylic acid (ASA, $n = 8$), ASA + clopidogrel ($n = 10$), or nonvitamin K antagonist oral anticoagulants ($n = 7$) for longer than six months. The effect of DM was differentially assessed by comparing HPP/HPS obtained from nondiabetic ($n = 8$) and diabetic ($n = 16$) subjects who had not received OA in the past six months. The concentration of key proangiogenic (vascular endothelial growth factor or VEGF) and antiangiogenic (thrombospondin-1 or TSP-1 and platelet factor-4 or PF-4) protein factors in HPP/HPS was analyzed via ELISA, while their ability to induce microvessel formations was examined in endothelial cell cultures. We found that OA use significantly reduced VEGF levels in HPP, but not HPS, compared to non-OA controls. While HPP and HPS TSP-1 levels remained largely unchanged as a result of OA usage, HPS PF-4 levels were significantly reduced in samples obtained from OA-treated subjects. Neither OA administration nor DM appeared to significantly reduce the ability of HPP or HPS to induce microvessel formations *in vitro*. These findings indicate that OA administration does not limit the angiogenic potential of hypoxia preconditioned blood-derived secretomes, and therefore, it does not prohibit the application of these therapies for supporting tissue vascularization and wound healing in healthy or diabetic subjects.

Keywords: acetylsalicylic acid; angiogenesis; blood-derived therapy; COX-1; clopidogrel; drug anticoagulation; hypoxia; hypoxia preconditioned plasma; hypoxia preconditioned serum; NOACs; peripheral blood cells; oral anticoagulation; VEGF

1. Introduction

Wounds normally heal via a set of complex and interactive phases that include hemostasis, inflammation, proliferation, and remodeling [1–4]. This well-orchestrated wound-healing process can

be impaired by various local and systemic factors, causing further complications and a lower quality of life for patients [4]. A chronic wound results when the healing program, which becomes activated following tissue injury, does not orderly progress through the aforementioned stages and is thus unable to complete the sequence of biological events that physiologically lead to angiogenic induction [4,5]. This failure to stimulate vascularization, and supply traumatized tissue with oxygen and nutrients, is what forces the development of chronic wounds, which clinically are directly related to poor tissue perfusion [6]. Chronic tissue ischemia, frequently manifested in the form of atherosclerotic or diabetes-induced wound-healing disorders, is a leading disease in the Western world and is associated with high morbidity and mortality [7,8], while its prevalence is steadily increasing [2,4,7,9].

Atherosclerosis is a progressive inflammatory disease leading to atherosclerotic plaques that cause narrowing of the arterial lumen [7,10–13]. Restriction of the vessel lumen and the presence of atherosclerotic plaques are linked to an increased risk of cardiovascular events such as myocardial infarction, stroke, and peripheral ischemia [7,10,11,13,14]. Among those suffering from peripheral ischemia, 20% to 70% have chronic leg ulcers [15]. Without timely, appropriate interventions, progressive atherosclerotic plaque-related ischemia increases the one-year risk of lower limb wound deterioration by 35% [15,16]. Similar to atherosclerosis, the dysregulation of wound healing in diabetes is mainly characterized by a series of micro- and macrovascular changes, chronic inflammation, disruption of angiogenic processes, and an imbalance in extracellular matrix regulation [4,8,17–19]. The persistent hyperglycemic state in diabetic patients results in endothelial dysfunction and smooth muscle abnormalities, followed by vasoconstriction due to the reduction of vasodilators [20]. Moreover, hyperglycemia correlates with stiffer blood vessels, which causes alterations in blood flow and, consequently, reduced tissue oxygenation [8,18,21]. Vascular pathology also contributes to reduced leukocyte migration into the wound, which becomes more vulnerable to infections [18,22]. Importantly, diabetic wounds are negatively impacted by insufficient angiogenesis (new vessel formation), as they show decreased vascularity and capillary density [23,24].

While the etiology of chronic, nonhealing wounds is multifaceted and specific pathology-dependent, the progression to a nonhealing phenotype is consistently closely linked to poor tissue perfusion [23,25,26], which, consequently, leads to tissue ischemia. As a means of normalizing the blood flow profile, oral anticoagulation (OA) is often necessary when treating patients suffering from atherosclerotic and/or diabetic microangiopathies [27], and it is commonly administered as an adjuvant therapy for vascular stenosis in the context of vascular interventions such as vascular dilation and stenting [28]. For example, in symptomatic peripheral arterial disease, single antiplatelet therapy with acetylsalicylic acid (ASA) or clopidogrel is indicated [29]. In patients undergoing percutaneous peripheral interventions for significantly stenosed blood vessels, at least four weeks of dual antiplatelet therapy with ASA and clopidogrel is recommended after infrainguinal stent implantation, while stenting below-the-knee arteries is often followed by an even longer period of dual antiplatelet therapy [29]. Often, however, these treatments are unsatisfactory, and there are, so far, no established therapeutic options that can improve local tissue perfusion by actively supporting angiogenesis in the wound microenvironment [8,30–35].

Our previous work provided evidence that hypoxia preconditioned blood-derived secretomes could constitute a new generation of autologous and bioactive topically applied/injectable compositions that can supply the necessary biochemical signals for initiating and supporting dermal fibroblast proliferation/migration and angiogenesis in injured tissue, thus driving wound healing to completion [34–37]. Our latest data also suggest that, beyond promoting angiogenesis, hypoxia preconditioned secretomes also have the ability to induce lymphangiogenesis, another important biological process in wound healing (work in progress). These angiogenic growth factor mixtures can be obtained through extracorporeal wound simulation (EWS), a method that employs peripheral blood conditioning outside the body [34,37,38]. Conditioning peripheral blood cells (PBCs) under the very same conditions that are normally encountered within a healing wound, i.e., physiological temperature and hypoxia, offers a means of optimizing the angiogenic potential of hypoxia

preconditioned secretomes, i.e., hypoxia preconditioned plasma (HPP) and hypoxia preconditioned serum (HPS), which can be readily and selectively prepared in the clinical setting by adjusting blood coagulation prior to hypoxic conditioning [34,37–39]. HPP and HPS constitute phase-specific growth factor secretomes, since each corresponds to a different phase of the wound-healing cascade—specifically, HPP being more closely correlated with the hypoxia-induced upregulation of proangiogenic growth factors that are produced by leukocytes, while HPS comprising a combination of coagulation-mediated platelet-derived protein factors and hypoxia-induced signaling [34,38,39]. The differences in proteomic composition that result from this selective adjustment of blood coagulation have already been extensively characterized by our group, showing that, while HPP has a comparable concentration of the proangiogenic factor vascular endothelial growth factor (VEGF) to HPS, it has a lower concentration of the platelet-derived angiogenic inhibitors thrombospondin-1 (TSP-1) and platelet factor-4 (PF-4) [37,39]. Despite these differences in protein factor concentrations, both HPP and HPS appear to induce similar levels of microvessel formation and sprouting *in vitro* [39].

As previously mentioned, many patients requiring angiogenesis-promoting therapies for central/peripheral vasculopathy and chronic wounds, who would greatly benefit from new generation bioactive treatments such as hypoxia preconditioned blood-derived secretomes, routinely receive OA [27,40,41]. A better understanding of the effects that OA administration may have on the angiogenic potential of blood-derived secretomes is therefore a key prerequisite for advancing their clinical utility. Moreover, the high frequency of the coprevalence of atherosclerotic disease and diabetes in this target patient group necessitates a differential investigation of the effects that OA administration and diabetic pathology may have on peripheral blood cell angiogenic functions. In the current study, we aimed to characterize the proteomic composition of HPP and HPS derived from peripheral blood that was obtained from nondiabetic and diabetic subjects receiving OA medications, specifically acetylsalicylic acid (ASA), a combination of ASA and clopidogrel, and nonvitamin K antagonist oral anticoagulants (NOACs), in terms of key proangiogenic (VEGF) and antiangiogenic (PF-4 and TSP-1) growth factors. Furthermore, an attempt was made to differentially analyze the influence of OA administration and diabetic pathology on the secretomes' ability to induce microvessel formations *in vitro*. Beyond providing useful insights into the clinical utility of these potentially therapeutic products, this work could also enhance our scientific understanding of the interactive roles that coagulation-mediated and hypoxia-induced protein factor signaling may have in wound angiogenesis.

2. Experimental Section

2.1. Study Collective

All blood donors provided written informed consent as directed by the ethics committee of the Technical University Munich, Germany, which approved this study (File Nr.: 497/16S; Amendment; date of approval: 19 of August 2017). The use of oral anticoagulation (OA) was due to previous comorbidities (2 subjects: strokes, 18 subjects: cardiac disease, 4 subjects: peripheral arterial diseases, and 5 subjects: thromboembolic events; note: some subjects received OA due to multiple comorbidities, which led to 29 comorbidities in 25 subjects). Subjects were recruited in our clinic in 2018–2019, while inclusion of subjects in the study was done on a voluntary basis. All subjects were screened for drug-mediated blood anticoagulation and diabetes mellitus and exclusion criteria. We excluded subjects who were under a non-consistent blood anticoagulation regime in the past 6 months or had a diagnosis for diabetic disease for less than one year, as well as subjects who suffered from mental disorders (e.g., dementia and psychosis). Further comorbidities such as heart disease were not considered as exclusion criteria. Smokers were defined as those who had smoked more than one cigarette in the past three months.

For OA experiments, we included and evaluated 25 subjects with an average age of 70.64 ± 7.22 years (Table 1A). Subjects were divided into three groups, according to the type of OA administered. We tested the effect of three of the most widely used oral blood anticoagulants:

Group 1, acetylsalicylic acid (ASA) (100 mg/day), group 2, a combination of ASA + clopidogrel (Plavix) (100 mg + 75 mg/day), and group 3, nonvitamin K antagonist oral anticoagulants/factor-Xa-inhibitors (NOACs) (e.g., Apixaban and Rivaroxaban; dose was dependent on pathology and drug type). All subjects were under a consistent blood anticoagulation regime in the past 6 months. Seven subjects who took oral anticoagulation (OA) suffered from type 2 diabetes (T2D) (Table 1A).

Table 1. Demographic data.

A	No OA	ASA	ASA + Clopidogrel	NOACs
Total number	5	8	10	7
Male/Female	4/1	6/2	9/1	5/2
Mean age ± SD (years)	26.0 ± 3.8	71.8 ± 5.9	71.5 ± 6.4	67.0 ± 8.6
Smoking (number of subjects)	0	1	4	0
Diabetes Mellitus (number of subjects)	0	4	2	1
B	No DM(No OA)	T1D(No OA)	T2D(No OA)	
Total number	8	6	10	
Male/Female	4/4	4/2	1/9	
Mean age ± SD (years)	30.75 ± 3.99	39.0 ± 5.88	62.4 ± 18.55	
BMI (kg/m²)	20.87 ± 2.50	26.34 ± 4.92	40.7 ± 15.16	
Blood glucose at the time of blood collection (mg/dL)	98.75 ± 5.58	126.84 ± 37.74	122.2 ± 31.58	

Patient demographics of different subject groups included in (A) oral anticoagulation (OA) experiments to assess the effects of three of the most widely used oral blood anticoagulants: group 1, acetylsalicylic acid (ASA) (100 mg/day), group 2, a combination of ASA + clopidogrel (Plavix) (100 mg + 75 mg/day), and group 3, nonvitamin K antagonist oral anticoagulants (NOACs) (e.g., Apixaban and Rivaroxaban) (dose was dependent on the pathology and drug type). All subjects were under a consistent blood anticoagulation regime in the past 6 months and (B) diabetes mellitus (DM) experiments, further differentiated into type 1 (T1D) and type 2 (T2D) diabetes, in order to assess the effect of DM independently of OA use. Subjects had a clinical diagnosis of DM for longer than one year prior to initiation of the study. BMI = body mass index and SD = standard deviation.

To assess the effect of diabetes mellitus (DM) independently of OA use, we included and evaluated 16 diabetic subjects with an average age of 52.09 ± 18.86 years, of which 6 subjects had a clinical diagnosis of type 1 diabetes (T1D) and 10 subjects of type 2 diabetes (T2D) for longer than one year prior to the initiation of the study (Table 1B). None of the 16 DM subjects had received oral anticoagulation in the past 6 months, but all took medication to control blood sugar. Blood glucose was determined immediately after taking blood for HPP/HPS preparation. The timing of drawing blood was independent of prior food intake.

Control subjects were young healthy adults who were not taking any medication, including oral anticoagulation (OA), and without any known comorbidities. A total of 13 subjects were included: 5 of them serving as a control group for examining OA administration and 8 as a control group for examining the effects of DM. Table 1 provides information on the patient demographics.

2.2. Preparation of Blood Plasma/Serum and Hypoxia Preconditioned Plasma (HPP)/Serum (HPS) Samples

Peripheral venous blood (10 mL) was collected from all study participants ($n = 54$) into a 10-mL polypropylene syringe (Omnifix[®], Braun AG, Melsungen, Germany) that contained no additive for normal serum and HPS preparation or was pre-filled with 1-mL heparin (Medunasal[®], Heparin 500 I.U. 5-mL ampoules, Sintetica[®], Münster, Germany) for normal plasma and HPP preparation, under sterile and standardized conditions (Blood Collection Set 0.8 × 19 mm × 178 mm; Safety-Lok, CE 0050, BD Vacutainer, BD, NJ, USA). For normal plasma/serum preparation, following passive sedimentation for 60 min at room temperature (25 °C, no centrifugation) the blood was separated into three layers, from bottom to top: red blood cell component (RBCs), clot/buffy coat, and serum/plasma, so that the top layer (serum or plasma) could be filtered into a new syringe. For HPP/HPS preparation, following blood sampling a 0.2- μ m pore filter was attached to the syringe (Sterifix[®], CE 0123, Braun AG, Melsungen, Germany), and by pulling the plunger, 2 mL of air was drawn into the syringe through the filter (note that the 10-mL polypropylene syringe has a 13-mL capacity when pulled up to the stop). Subsequently,

the filter was removed, and the capped syringe was placed upright in an incubator (37 °C/5% CO₂) and incubated for 4 days (blood incubation time) without any prior centrifugation (Figure 1). Pericellular local hypoxia (~1% O₂) was induced in situ through cell-mediated O₂ consumption by controlling the blood volume per unit area (BVUA > 1 mL/cm²) and, consequently, the PBC seeding density in the blood container [34,42]. After the predefined incubation time, the blood was passively separated into three layers (Figure 1), from top to bottom: HPP/HPS, buffy coat/clot, and red blood cell (RBC) component, so that the top layer comprising hypoxia preconditioned plasma or serum could be filtered (0.2-µm pore filter, Sterifix[®], Braun AG, Melsungen, Germany) into a new syringe, removing cells/cellular debris.

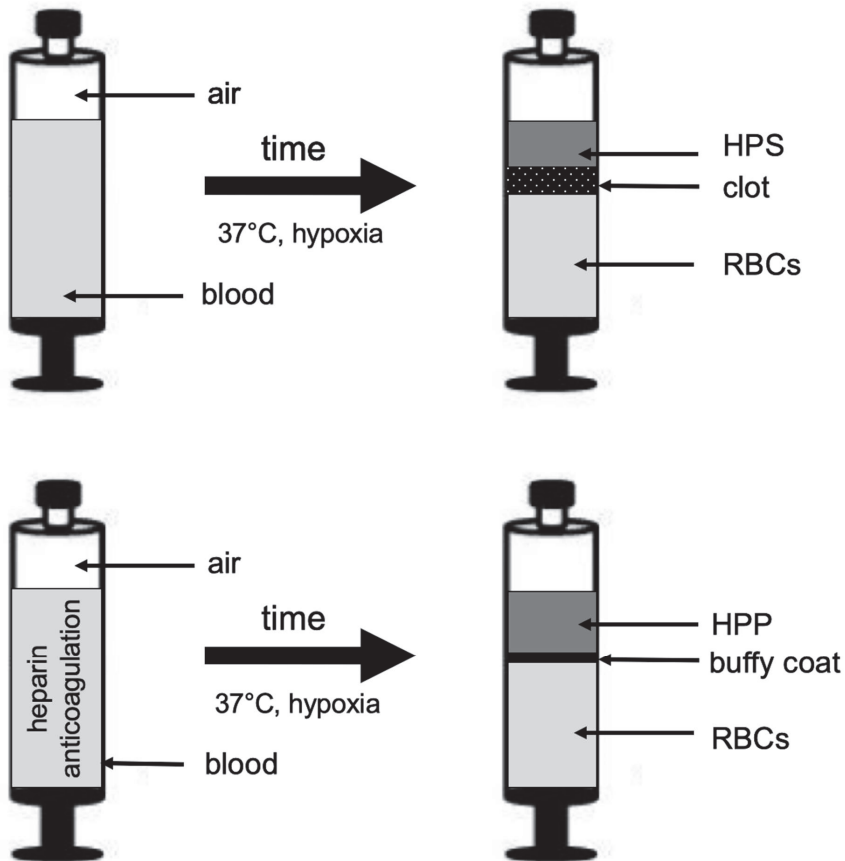


Figure 1. Method of preparation of hypoxia preconditioned plasma and serum (HPP and HPS). Peripheral venous blood obtained from subjects that received no oral anticoagulation (OA) or were on treatment with oral anticoagulants (acetylsalicylic acid (ASA), ASA + clopidogrel, or nonvitamin K antagonist oral anticoagulants (NOACs)) was allowed to clot (upper schematic) or additionally anticoagulated with heparin (bottom schematic) for HPS and HPP preparation, respectively. Peripheral blood cells (in clot or buffy coat) were conditioned under pericellular (local) hypoxia (~1% O₂) and physiological temperature (37 °C) for 4 days. Sedimentation passively separated growth factor-rich HPS and HPP from clot and buffy coat, respectively, while red blood cells (RBCs) collected at the bottom of the chamber.

2.3. Quantitative Analysis of VEGF, TSP-1, and PF-4 Concentrations in Blood-Derived Secretomes

Blood-derived secretomes (normal plasma/serum, HPP, and HPS) were sampled and analyzed by ELISA for VEGF, TSP-1, and PF-4 (R&D Systems, Inc., Minneapolis, MN, USA), according to the manufacturer's instructions. Factor concentrations in hypoxia preconditioned blood-derived secretomes (HPP/HPS) were measured immediately after the predefined incubation period (4 days). At least one well was tested per subject per condition.

2.4. Analysis of the Effect of Blood-Derived Secretomes on Microvessel Formation In Vitro

The angiogenic potential of blood-derived secretomes was tested in an in vitro angiogenesis assay by assessing their ability to induce microvessel formations in human umbilical vein endothelial cells (HUVECs, CellSystems, Troisdorf, Germany) seeded on factor-reduced Matrigel (BD, Heidelberg, Germany). HUVECs were seeded at a density of 10×10^3 /well, with 50 μ L of test or control media added per well (μ -Slide angiogenesis, Ibidi, Gräfelfing, Germany), and cultured in a 5% CO₂/37 °C incubator for 12 h. Cells were then stained with Calcein AM (PromoKine, Heidelberg, Germany), and endothelial cell tube formation was observed with fluorescence and phase contrast microscopy. Assessment of the extent of capillary-like network formation was carried out by counting the number of tubes and nodes (a node was defined as the point of intersection of two or more tubules). Hypoxia preconditioned blood-derived secretomes (HPP/HPS) were tested immediately after the predefined incubation period (4 days). Phosphate-buffered saline (PBS) medium and recombinant VEGF (90 ng/mL) were also tested as negative and positive controls, respectively. At least three wells were tested per sample per condition.

2.5. Statistical Analysis

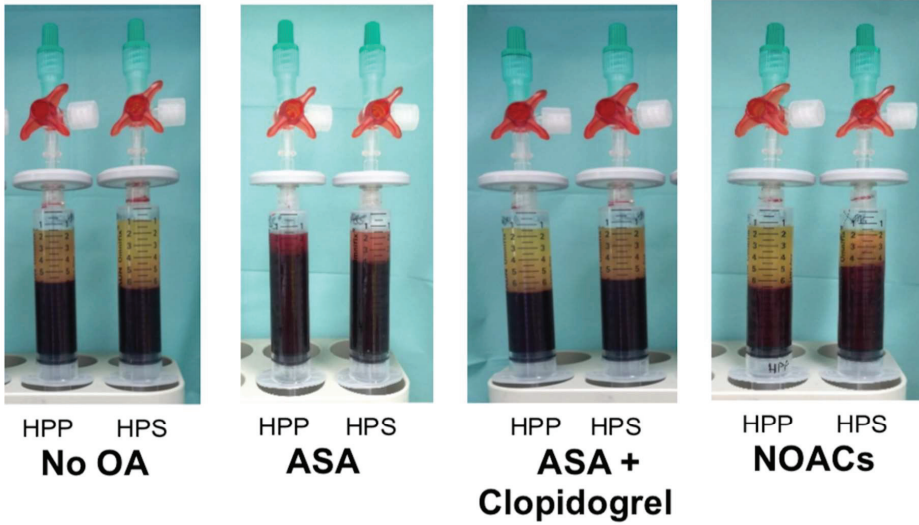
Statistical analysis was carried out using a Student's independent *t*-test, where a maximum of two groups was compared, or one-way ANOVA with Bonferroni adjustment, accompanied by post-hoc pairwise comparisons for analyses of more than two groups, using SPSS 14 software (version 14, IBM, Ehningen, Germany). The probability of a type-one error was set to 5% ($\alpha = 0.05$), unless noted otherwise. For each experimental condition, blood-derived secretome samples from at least 5 subjects were tested, as noted in Table 1. Data are expressed as mean \pm standard deviation.

3. Results

3.1. Effect of Oral Anticoagulation on Pro- (VEGF) and Anti-(TSP-1 and PF-4)Angiogenic Growth Factor Concentrations in Hypoxia Preconditioned Blood-Derived Secretomes

The primary aim of this study was to examine whether the administration of oral anticoagulation (OA) influences the angiogenic properties of blood-derived hypoxia preconditioned secretomes. The first question we sought to answer was whether the use of OA prevents clotting in situ during the preparation of hypoxia preconditioned serum (HPS) from peripheral venous blood. As can be seen in Figure 2, clotting occurred normally in all HPS samples, after four days of blood incubation, regardless of the type of OA administered, although slightly smaller clots were present in HPS samples obtained from patients receiving a combination of ASA and clopidogrel.

Day 0



Day 4

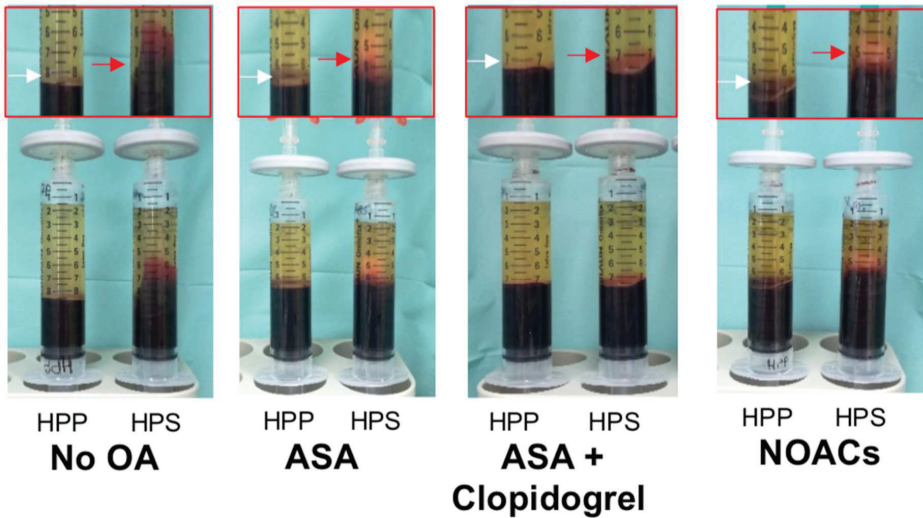


Figure 2. Representative images of hypoxia preconditioned plasma and serum (HPP and HPS) samples, obtained from subjects not receiving oral anticoagulation (OA) or subjects using acetylsalicylic acid (ASA), ASA + clopidogrel, or nonvitamin K antagonist oral anticoagulants (NOACs). Upper panel shows samples immediately after blood collection (day 0), while lower panel shows samples following 4 days of blood conditioning (sedimentation and hypoxic incubation). Enlarged image sections, indicated by red insets on day 4 images, show an enlarged view of the buffy coat layer (white arrow) and clot (red arrow) in 4-day incubated-HPP and -HPS samples, respectively.

To establish a growth factor concentration baseline, we quantitatively analyzed via ELISA the concentration of key pro- and antiangiogenic protein factors (VEGF, TSP-1, and PF-4) in normal plasma and serum and compared them to their hypoxia-conditioned counterparts, obtained from healthy subjects that did not receive OA. As shown in Figure 3A, the concentration of the proangiogenic factor VEGF in hypoxia preconditioned plasma (HPP) and serum (HPS) showed a three-to-five-fold increase compared to its baseline level in fresh plasma ($p > 0.05$) and fresh serum ($p < 0.05$), respectively. There was no significant difference between HPP and HPS VEGF levels in these subjects ($p > 0.05$). In contrast, for subjects receiving OA (ASA, ASA + clopidogrel, or NOACs), HPP appeared to consistently have a significantly lower VEGF concentration than HPS ($p < 0.05$), regardless of the type of OA administered, but, also, a lower VEGF concentration compared to HPP obtained with no OA ($p < 0.05$), as well as fresh plasma, although this difference was only significant for HPP obtained from subjects receiving ASA or NOACs ($p < 0.05$).

Examination of the angiogenic inhibitor TSP-1 in these secretomes showed a significantly lower concentration in HPP compared to HPS ($p < 0.05$). This difference was present with or without OA administration (Figure 3B). Moreover, HPS obtained from all subjects had a significantly higher TSP-1 concentration compared to normal serum ($p < 0.05$). In contrast, the TSP-1 concentration of HPP obtained with or without OA appeared to be somewhat lower than that of normal plasma, although this difference was not significant ($p > 0.05$).

Quantification of the PF-4 concentration yielded similar results to TSP-1, with HPP having a significantly lower concentration compared to HPS, regardless of whether blood had been obtained with or without OA intake ($p < 0.05$) (Figure 3C). In contrast to the TSP-1 concentration, however, the HPP PF-4 concentration was significantly below that of normal plasma for all conditions tested ($p < 0.05$). Furthermore, HPS obtained from subjects not receiving OA appeared to have a two-to-three-fold higher PF-4 concentration compared to HPS obtained with OA administration, as well as normal serum ($p < 0.05$).

3.2. Quantitative Analysis of Blood-Derived Secretome Pro- (VEGF) and Anti-(TSP-1 and PF-4) Angiogenic Growth Factor Concentrations in Diabetic Subjects

Oral anticoagulation is commonly prescribed to patients suffering from peripheral vascular pathology [43], which is commonly associated with diabetes mellitus [44]. Indeed, in our study collective, seven subjects receiving OA had concomitant type 2 diabetes (T2D) (see Table 1A). In order to assess whether the presence of diabetes exerted a bias in our analysis of the influence of OA administration on blood-derived secretome angiogenic composition (note; all subjects not receiving OA were non-diabetic), we examined the concentration of VEGF, TSP-1 and PF-4 in hypoxia preconditioned plasma and serum (HPP, HPS) samples, derived from non-diabetic and diabetic subjects who had not taken OA in the past 6 months. As shown in Figure 4A–C, no significant differences could be seen in the levels of these three protein factors between diabetic and non-diabetic subjects, in either HPP or HPS. Furthermore, the HPP/HPS concentration of these three factors was not significantly different in subjects suffering from type 1 or type 2 diabetes (Figure 4). Examination of the platelet-derived angiogenic inhibitors TSP-1 and PF-4 in these secretomes did show a significantly lower concentration in HPP compared to HPS ($p < 0.05$), in agreement with our previous data (Figure 3B,C), while this difference was present with or without T1D/T2D (Figure 4B,C), except for T1D subjects who had similar levels of TSP-1 in HPP and HPS. These results indicated that diabetes mellitus was likely not a confounding factor in the investigation of the effect of OA administration on HPP/HPS angiogenic potential.

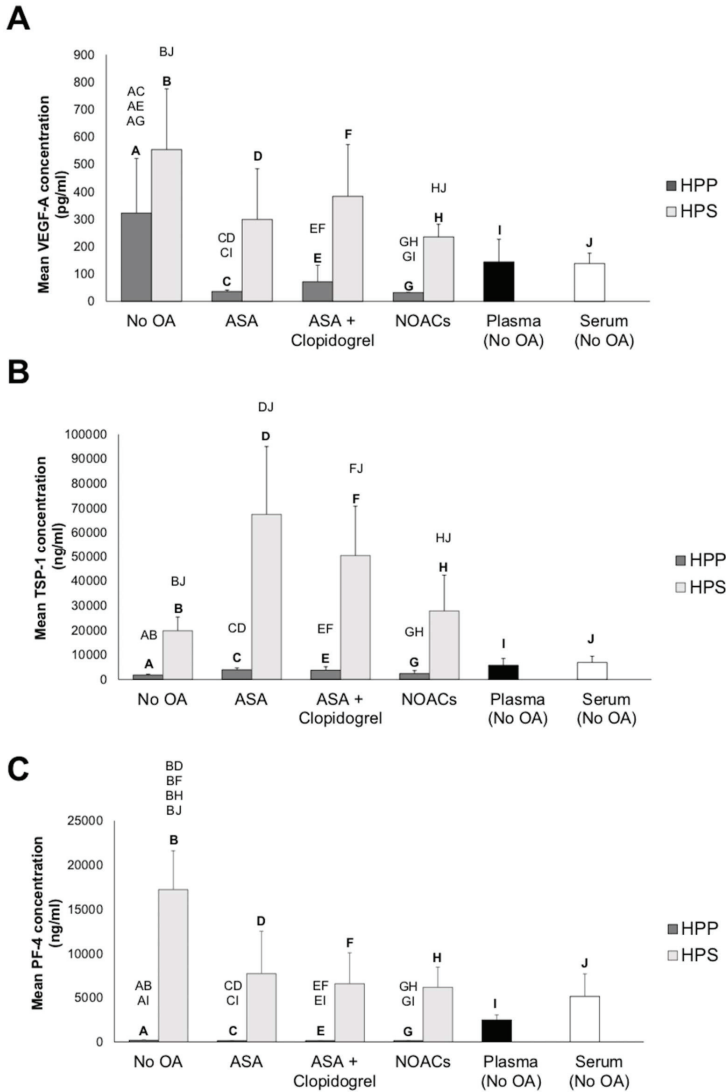


Figure 3. Quantitative analysis of pro- (vascular endothelial growth factor or VEGF) and antiangiogenic (thrombospondin-1 or TSP-1 and platelet factor-4 or PF-4) factor concentrations in blood-derived secretomes obtained with or without oral anticoagulation (OA). Plots showing the concentrations of (A) VEGF (pg/mL), (B) TSP-1 (ng/mL), and (C) PF-4 (ng/mL) in blood-derived secretomes: hypoxia preconditioned plasma (HPP), hypoxia preconditioned serum (HPS), normal plasma, and normal serum. HPP and HPS samples were obtained from subjects that received no oral anticoagulation (OA) or were on treatments with acetylsalicylic acid (ASA), ASA + clopidogrel, or nonvitamin K antagonist oral anticoagulants (NOACs). Capital letter pairs over plots indicate statistical comparisons of the corresponding data points. For all pair comparisons, $p < 0.05$, unless otherwise indicated. Error bars represent s.d.; number of subjects tested: no OA, $n = 5$; ASA, $n = 8$; ASA + clopidogrel, $n = 10$; NOACs, $n = 7$; normal plasma (no OA), $n = 5$; and normal serum (no OA), $n = 5$. At least one assay well was tested per subject per condition.

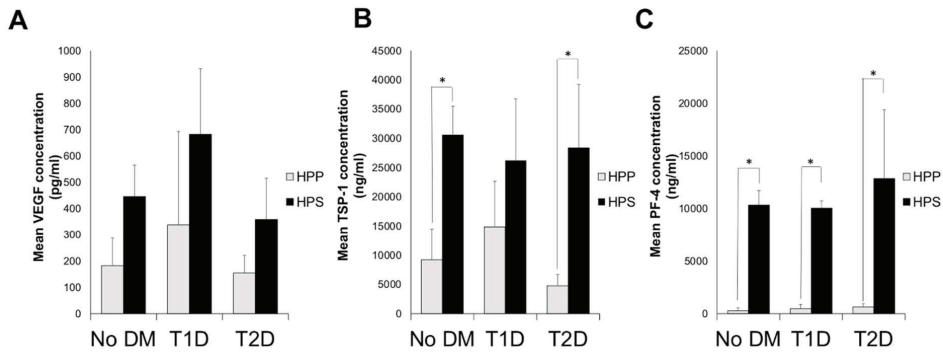


Figure 4. Comparative analysis of pro- (VEGF) and antiangiogenic (TSP-1 and PF-4) factor concentrations in hypoxia preconditioned blood-derived secretomes obtained from diabetic and nondiabetic subjects. Plot showing the concentrations of (A) VEGF (pg/mL), (B) TSP-1 (ng/mL), and (C) PF-4 (ng/mL) in HPP and HPS samples obtained from subjects suffering from type 1 (T1D) or type 2 (T2D) diabetes mellitus (DM) and nondiabetic subjects (no DM). For all pair comparisons, * $p < 0.05$, unless otherwise indicated. Error bars represent s.d.; number of subjects tested: no DM, $n = 8$; T1D, $n = 6$; and T2D, $n = 10$. At least one assay well was tested per subject per condition.

3.3. Effects of Oral Anticoagulation on the Ability of Hypoxia Preconditioned Blood-Derived Secretomes to Induce Angiogenesis In Vitro

Following an analysis of key pro- and antiangiogenic protein factors in blood-derived secretomes obtained from subjects receiving OA, we moved on to investigate the effects of OA administration on the secretomes' ability to induce microvessel formations in human umbilical vein endothelial cell (HUVEC) in vitro cultures. In subjects not receiving OA, HPP and HPS induced two-to-three times as many tubes and nodes (microvessel intersections) as fresh plasma and serum, respectively ($p < 0.05$) (Figure 5A–C). Additionally, HPS obtained from these subjects, but not HPP, appeared to perform somewhat better than pure recombinant VEGF, tested here as a positive control, in terms of the number of tubes formed ($p < 0.05$) (Figure 5B). In subjects receiving OA, however, only HPS appeared to be more angiogenic than fresh serum ($p < 0.05$), with HPP samples evoking a weaker angiogenic response that was comparable to that of normal plasma (Figure 5A–C). Notably, HPS obtained from ASA-treated subjects generated less tubes (although a similar number of nodes) compared to control HPS. Moreover, HPS obtained from subjects receiving OA failed to surpass the response produced by pure VEGF, while HPP obtained from ASA- and NOAC-treated subjects generated a significantly lower response than control HPP and positive control VEGF samples ($p < 0.05$) (Figure 5B,C). Importantly, no significant differences were observed in the number of tubes or nodes formed in cultures incubated with HPP or HPS, regardless of whether subjects were receiving OA or not (Figure 5A–C).

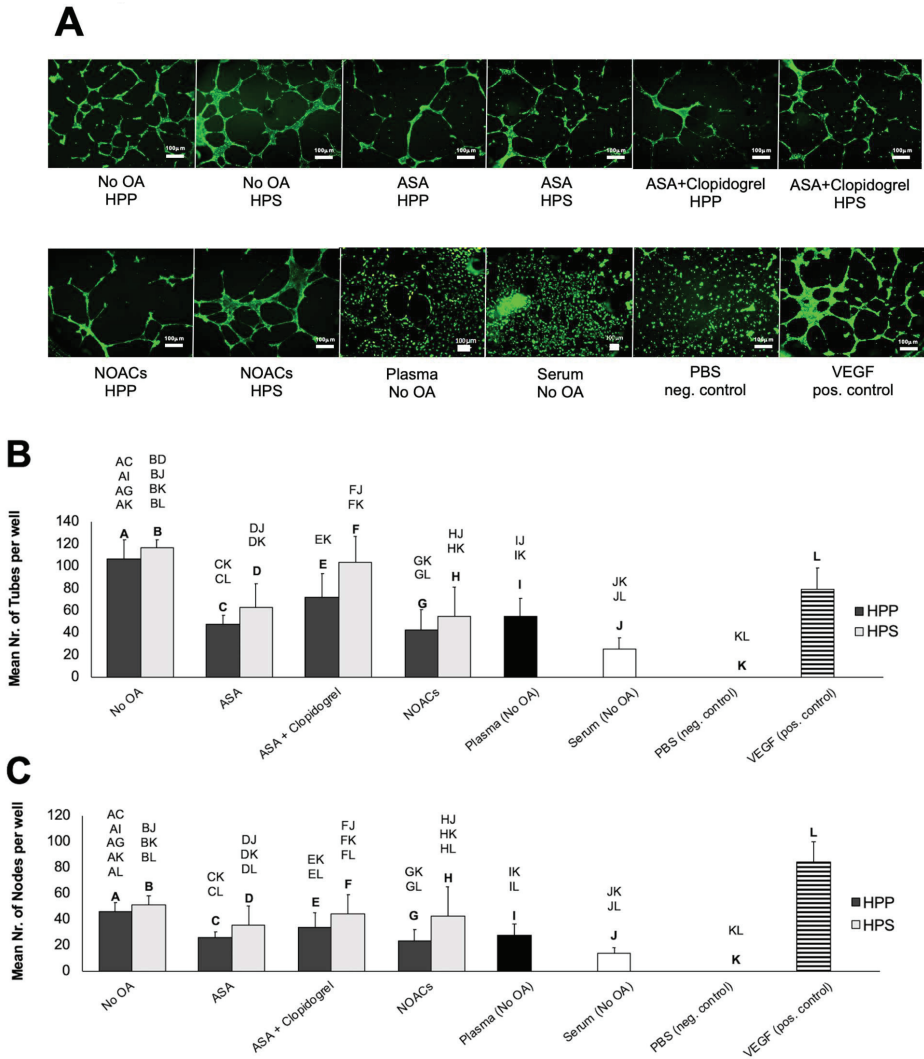


Figure 5. Effects of hypoxia preconditioned blood-derived secretomes obtained with or without oral anticoagulation (OA) on microvessel formations in human umbilical vein endothelial cell (HUVEC) cultures in vitro. (A) Panel showing representative images of the tube formation assay (12 h) carried out in the presence of blood-derived secretomes (HPP, HPS, normal plasma, and normal serum) obtained from subjects that did not receive oral anticoagulation (OA) or were treated with acetylsalicylic acid (ASA), ASA + clopidogrel, or nonvitamin K antagonist oral anticoagulants (NOACs) (Bars = 100 μ m). (B) Plots showing the mean number of tubes and (C) nodes formed in HUVEC cultures that were incubated for 12 h with blood-derived secretomes. Capital letter pairs over plots indicate statistical comparisons of the corresponding data points. For all pair comparisons, $p < 0.05$, unless otherwise indicated. Error bars represent s.d.; number of subjects tested: no OA, $n = 5$; ASA, $n = 8$; ASA + clopidogrel, $n = 10$; NOACs, $n = 7$; normal plasma (no OA), $n = 5$; normal serum (no OA), $n = 5$; phosphate-buffered saline (PBS), $n = 3$; and VEGF, $n = 3$. Three samples were tested per subject per condition.

3.4. Influence of Diabetes Mellitus on the Ability of Hypoxia Preconditioned Blood-Derived Secretomes to Induce Angiogenesis In Vitro

After having shown that the presence of diabetes does not significantly influence the concentration of key pro- and antiangiogenic factors in HPP/HPS, we proceeded by examining whether this translated into an equal ability of hypoxia preconditioned secretomes, obtained from diabetic and nondiabetic subjects who did not receive OA in the past six months, to induce microvessel formations in vitro. As shown in Figure 6A–C, no significant differences could be seen as a result of diabetic pathology in the mean number of tubes and nodes formed in human umbilical vein endothelial cell (HUVEC) cultures following 12-h incubation with either HPP or HPS. While all samples induced a stronger angiogenic response than the negative control ($p < 0.05$), all conditions underperformed pure VEGF (positive control) in terms of node formation ($p < 0.05$) (Figure 6B and Figure 5C). Furthermore, and in agreement with our ELISA results, HPP/HPS-induced microvessel formations did not significantly differ between T1D and T2D subjects (Figure 6A–C).

A

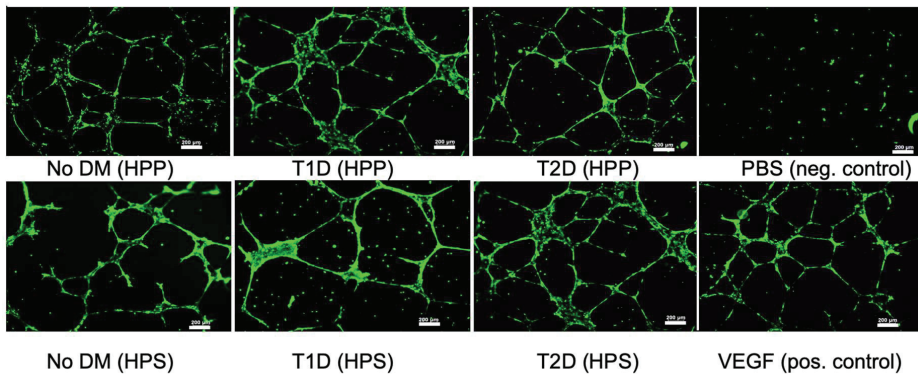


Figure 6. Cont.

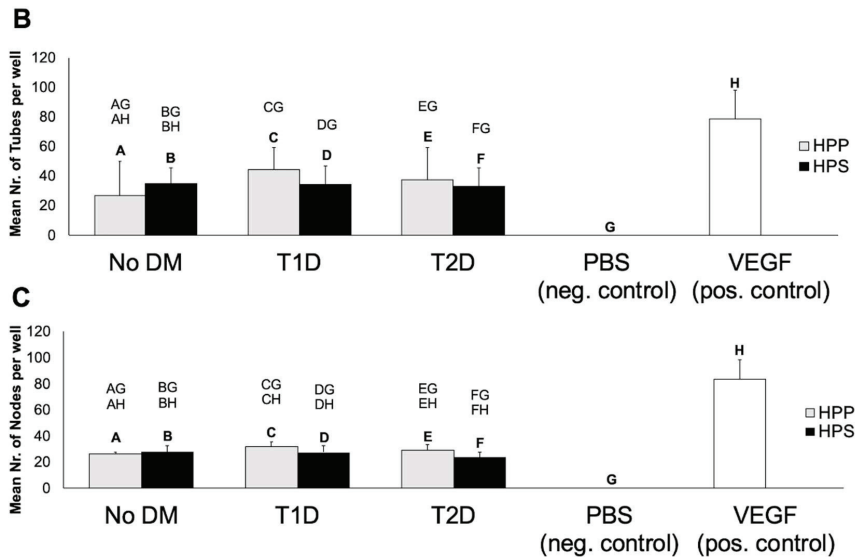


Figure 6. Effects of hypoxia preconditioned blood-derived secretomes obtained from diabetic subjects on microvessel formations in human umbilical vein endothelial cell (HUVEC) cultures in vitro. (A) Panel showing representative images of the tube formation assay (12 h), carried out in the presence of hypoxia preconditioned plasma and serum (HPP and HPS) obtained from subjects suffering from type 1 (T1D) or type 2 (T2D) diabetes, as well as nondiabetic subjects (no DM) (Bars = 200 μ m). (B) Plots showing the mean number of tubes and (C) nodes formed in HUVEC cultures that were incubated for 12 h with HPP and HPS samples obtained from the above test conditions. Capital letter pairs over plots indicate statistical comparisons of the corresponding data points. For all pair comparisons, $p < 0.05$, unless otherwise indicated. Error bars represent s.d.; number of subjects tested: no DM, $n = 8$; T1D, $n = 6$; T2D, $n = 10$; PBS, $n = 3$; and VEGF, $n = 3$. Three samples were tested per subject per condition.

4. Discussion

Hypoxia preconditioned blood-derived secretomes represent a new development in the field of autologous growth factor therapies that could prove to be beneficial to many patients requiring angiogenesis-promoting treatments for central/peripheral ischemia and chronic/diabetic wounds [34–39]. These autologous growth factor preparations are produced through the extracorporeal conditioning of peripheral blood cells (PBCs) under wound-simulating conditions [34,38]. We previously described the use of hypoxia preconditioned plasma (HPP), i.e., plasma derived after conditioning anticoagulated blood under a physiological temperature (37 °C) and physiological hypoxia (1–10% O₂) for four days (Figure 1) as a tool for stimulating microvessel formation and sprouting [34,39]. Similarly, conditioning blood in a nonanticoagulated state yields hypoxia preconditioned serum (HPS) (Figure 1), which (at least, in vitro) was found to be equally angiogenic as HPP [37,39]. In terms of the growth factor composition, while HPP comprises primarily PBC-derived hypoxia-induced signaling, HPS represents a more “complete” secretome, since it provides both coagulation-mediated platelet-derived factors, as well as hypoxia-induced signaling [37–39]. These secretomes therefore represent a developmental progression to platelet-based blood-derived products, such as platelet-rich plasma (PRP), which comprises exclusively platelet-derived growth factors and is currently accepted as the gold standard of blood-based regenerative therapies [45,46]. Instead of merely providing the initial (i.e., hemostasis-generated) phase of the wound-healing cascade, HPP and HPS supply angiogenesis-specific signaling that is naturally produced through hypoxia and, as a result, appear to be more angiogenic in vitro than PRP [39].

We have previously demonstrated that hypoxia preconditioned plasma (HPP), prepared using heparin anticoagulation, has approximately the same VEGF concentration as hypoxia preconditioned serum (HPS) but a much lower concentration of the platelet-derived angiogenesis inhibitors TSP-1 and PF-4 [39]. Here, we could confirm these findings in a larger sample of healthy subjects not using oral anticoagulation (Figure 3). Importantly, the current data verifies the positive effect of hypoxic conditioning on optimizing the proangiogenic composition of blood-derived secretomes, shown here by the significant increase in the HPS VEGF level compared to the normal serum (Figure 3). This difference translated into a more potent angiogenic response induced in endothelial cell cultures by HPP and HPS compared to the normal plasma and serum, respectively (Figure 5). These results suggest that the enrichment of blood-derived secretomes with hypoxia-induced protein factor signaling, beyond the level that can normally be obtained through platelet factor release, could enhance their angiogenic potency, thus making these therapies suitable for treating chronic wounds and ischemic tissues and possibly be more effective than solely platelet-based products such as PRP [39].

The primary question tested in this study was whether the long-term (six months) use of oral anticoagulation influences the angiogenic composition of hypoxia preconditioned secretomes. In our past work, we showed that the concentrations of the platelet-derived angiogenic inhibitors TSP-1 and PF-4 in both fresh plasma and HPP were significantly lower than that in HPS and platelet-rich plasma (PRP), indicating that the anticoagulation of blood prior to incubation effectively reduces platelet activation, even after static blood conditioning for four days [39]. Furthermore, the method of blood anticoagulation used for HPP preparation (EDTA vs. heparin) appeared to have an influence on the VEGF and TSP-1 protein levels, with lower concentrations observed in HPP obtained through EDTA compared to heparin anticoagulation but not PF-4 levels [39]. These previous findings provided a solid basis for developing our formal hypothesis, namely that long-term OA administration might alter the proteomic compositions of HPP and/or HPS. To examine this, the subjects were divided into three groups, representing three of the most widely used oral blood anticoagulants: (1) acetylsalicylic acid (ASA), (2) a combination of ASA + clopidogrel, and (3) nonvitamin K antagonist oral anticoagulants (NOACs) (Table 1A). The ELISA results presented here show that all three OA regimes significantly reduced the concentration of VEGF in HPP (compared to the control HPP), but not in HPS, to the extent that the HPP VEGF appeared significantly lower than that of HPS (something that was not observed either here or in previous studies when no OA was used [39]) (Figure 3). Furthermore, while clotting appeared macroscopically intact in all HPS samples obtained from subjects using OA (Figure 2), PF-4 levels in these samples were significantly lower than those in HPS obtained from subjects not using OA (Figure 3), suggesting a possible interference of OA administration with platelet activation in situ, and factor release. Nonetheless, given that VEGF, TSP-1, and PF-4 concentrations in HPS samples were significantly higher than in HPP samples obtained with all three OA regimes, it is safe to infer that OA administration does not completely abolish platelet activation during blood conditioning (provided that the extra amount of protein in HPS was platelet-derived). On the other hand, when considered in combination, the observed reductions in the HPP VEGF level and HPS PF-4 level suggest that OA use might influence both the PBC-generated hypoxia-induced signaling phase, as well as the platelet-derived factor release.

With respect to the angiogenicity of hypoxia preconditioned secretomes, we found that OA administration did not abolish the ability of HPP and HPS to stimulate microvessel formations in vitro (Figure 5). Indeed, HPP and HPS samples prepared from subjects using any of the three OA regimes tested could induce a complex capillary-like network in endothelial cell cultures following 12-h incubation. We did observe, however, that OA administration had a weakening effect (significant in samples obtained from ASA- and NOAC-treated subjects) on the angiogenic potential of HPP, which appeared reduced by half in comparison to HPP samples obtained without OA use (Figure 5), suggesting that the observed reduction in the OA-associated HPP VEGF level (Figure 3) might be responsible for this change. This finding may not be surprising, after all, given that the HPP concentrations of the angiogenic inhibitors TSP-1 and PF-4 were comparable with and without OA use

(Figure 3), potentially making room for the concentrations of proangiogenic factors, such as VEGF, to assume a more determining role on the secretome's net angiogenic effect. These results provide useful insight into the clinical utility of hypoxia preconditioned blood-derived secretomes in patients receiving OA, since they suggest that HPS may be a better alternative to HPP when choosing a tool to stimulate/support tissue angiogenesis and perfusion.

A large number of studies have already been published on the aforementioned OAs. ASA, a classical NSAID, has been used in broad conditions, including fever, pain, and inflammatory disease [47]. ASA inhibits cyclooxygenase-1 (COX-1) in platelets, thereby blocking the production of prostaglandins [48] and the production of thromboxan-A₂ (TXA₂), leading to reduced platelet activation and aggregation [49]. Previous studies have demonstrated that ASA and its derivatives can alter the VEGF expression, leading to suppressed angiogenesis as a consequence, although how ASA decreases the VEGF expression remains unknown [50–53]. For example, in hypertensive patients who had significantly higher plasma levels of VEGF, there were significant reductions in VEGF plasma concentrations while following the treatment with ASA for three months, indicating that the use of ASA leads to a reduction in intraplatelet angiogenic growth factors and platelet activation [54]. ASA has also previously been shown to decrease the plasma levels of VEGF in patients with ischemic heart disease who were undergoing coronary artery bypass grafting [55]. Furthermore, a daily use of low-dose ASA has been reported to reduce VEGF, platelet-derived growth factor (PDGF)-AB, and transforming growth factor beta-1 (TGF-beta1) expressions in freshly isolated human PRP [56]. These changes, also encountered in our data, can be attributed to alterations in the platelet activation and degranulation-mediated release of stored growth factors, e.g., VEGF, PDGF, EGF, insulin-like growth factor-1 (IGF-1), basic fibroblast growth factor (bFGF), TGF-beta1, TSP-1, and PF-4 [57–61]. ASA might affect other blood cell types, as well. For example, ASA was found to block the differentiation of macrophages from bone marrow cells *in vitro* and decrease cell numbers, phagocytosis, and immunogenicity of mouse macrophages *in vivo* [62]. ASA was also shown to inhibit the tissue recruitment of monocytes/macrophages by impeding their adhesion process through COX-independent mechanisms [63]. Moreover, ASA may exert significant anti-inflammatory effects by suppressing the production of macrophage-derived inflammatory mediators [64]. As suggested by our results, such alterations in the PBC behaviors and growth factor expression affect the proteomic composition of PBC-derived secretomes, which further influences their angiogenic activity. Beyond that, the presence of ASA in the blood might also have direct effects on the endothelial cell function. Indeed, NSAIDs have been shown to inhibit angiogenesis in rodent models [47,65], while ASA significantly blocks the *in vitro* migration and capillary-like structure formation by endothelial cells [66]. It is therefore likely that the observed effects of ASA administration on the HPP angiogenic function might stem from a combination of reduced proangiogenic factor levels, as well as the direct inhibition of endothelial cells. Further studies are required before the relative significance of these mechanisms can be clarified.

A typical clinical combination of oral anticoagulants is that of ASA and clopidogrel. Clopidogrel targets the ADP P2Y₁₂ receptor on platelets, responsible for irreversible platelet aggregation in response to ADP [67]. It has been shown that a seven-day intake of clopidogrel does not significantly modify the plasma concentrations of angiogenic factors VEGF-A, placenta growth factor, and stromal cell-derived factor-1 or biomarkers of endothelial cell activation [67]. On the other hand, clopidogrel inhibits the angiogenesis of gastric ulcer healing at least partially through inhibition of the VEGF-VEGFR2-ERK signal transduction pathway and, also, inhibits VEGF-stimulated HUVEC proliferation via the downregulation of VEGFR-2 and pERK [68]. Here, we did not include a clopidogrel-only group, as it is clinically rare, which makes it difficult to examine the isolated effect of clopidogrel on HPP/HPS angiogenic functions. Our results indicate that a combination of ASA and clopidogrel does not significantly alter the secretomes' angiogenic composition (with respect to the three protein factors tested) compared to the ASA-only treatment, although the angiogenic response produced was somewhat stronger, effectively preventing the significant reduction in tube formation relative to

the control HPP/HPS samples induced by ASA-only administration (Figure 5B). This is particularly interesting, since the daily ASA dose (100mg) in the combination group was the same as with the ASA-only group. Whether this effect is due to an interaction between ASA and clopidogrel or a direct effect of clopidogrel needs to be further examined.

Following the launch of nonvitamin K antagonist oral anticoagulants (NOACs), taking Warfarin (vitamin-K antagonist) became rather rare, so that a sufficient number of Warfarin-treated subjects could not be recruited for this study. Over the past 50 years, Warfarin has been used as the mainstream drug for the prevention of stroke and systemic thrombo-embolism, before being surpassed by NOACs due to some clinical benefits (e.g., fewer drug interactions) [69,70]. NOACs, such as Rivaroxaban and Apixaban, are factor Xa inhibitors that block the generation of thrombin [71]. Factor Xa occupies a central position within the coagulation cascade as a convergence point between the intrinsic and extrinsic pathways and might play a key role in the regulation of angiogenesis [72]. Thrombin is known to inhibit the growth and branching of vascular tubules in vitro [39,72,73], while recombinant FX/FXa inhibits angiogenesis in HUVEC cultures in vitro [72] and was also found to be antiangiogenic when tested in in vivo models such as the zebrafish intersegmental vasculature (ISV) formation assay and the chick embryo chorioallantoic membrane (CAM) assay [72]. Furthermore, it has been demonstrated that the antiangiogenic effect of FXa is mediated through protease-activated receptor-1 (PAR-1) [72], which, in itself, has been reported to be both pro- and antiangiogenic; PAR-1 activation, when accompanied by low levels of thrombin, enhances angiogenesis in HUVEC cultures [72,74], while high concentrations of thrombin inhibit angiogenesis [72,75]. Our results indicate that HPP and HPS obtained from NOAC-treated subjects had a similar proteomic composition and angiogenic activity in the tube formation assay as HPP/HPS prepared from ASA-treated subjects (Figures 3 and 5). As with the other two OA groups tested, the NOAC treatment appeared, on one hand, to reduce HPP angiogenicity; on the other, it did not significantly reduce the angiogenic effectiveness of HPS, which remained more potent than that of the normal serum. It is possible that any FXa/thrombin-mediated effects of the NOAC treatment on cultured endothelial cells, that might well be angiogenesis-supporting [72], are counterbalanced by the reduction in platelet activation and proangiogenic factor release in HPP/HPS, although this requires further investigation.

In this study, the presence of diabetes mellitus (DM) in the OA-treated subject population (7 out of the 25 subjects tested) was identified as a potential bias for the observed results, since DM is known to affect both leukocyte and platelet functions [76,77]. Indeed, chronic and acute hyperglycemia can trigger platelet activation [78,79], while, in diabetic patients, the production of several growth factors involved in initiating and sustaining the healing process are compromised [18]; for example, VEGF and TGF-beta protein expressions are reduced in diabetic dermal wounds [80,81]. Here, we examined the effects of DM independently of OA administration. We found no significant differences in either the proteomic composition or angiogenic activity of HPP and HPS obtained from diabetic subjects, compared to nondiabetic controls (Figures 3 and 5). The type of diabetes (type 1 vs. type 2) did not appear to have an effect, either. These findings suggest that the application of hypoxia preconditioning as a tool for improving the angiogenic potency of blood-derived secretomes may be able to bypass aberrances in angiogenic functions that are a direct consequence of the disease state of diabetes.

A major limitation of this study is that, compared to the healthy, young subjects not using OA, OA-treated subjects were older and suffered from cardiovascular disease (Table 1A). Furthermore, none of the healthy subjects smoked, while one in five OA-treated subjects was a smoker. It is indeed known, by virtue of clinical observations, that an advanced age affects wound healing and is accompanied by the impairment of angiogenesis [82–84], while various wound-healing cellular processes demonstrate characteristic age-related changes [85]. For example, leukocytes display an age-related increase in the secretion of many inflammatory mediators [85–88], while the infiltration of macrophages and B-lymphocytes into wounds is delayed in models of wound healing in middle-aged and elderly mice [85,89]. The production of growth factors by macrophages declines with age as well [85,90]. As for the effect of smoking, several angiogenic factors have been found to be enhanced

by nicotine [91]. For instance, nicotine induces the expression of proangiogenic growth factors bFGF, PDGF, and VEGF in endothelial cells [91–95]. In our study, nicotine in the plasma/serum of smokers might have also directly influenced the angiogenic response, since it is known that nicotine stimulates proliferation and tube formation by endothelial cells in vitro [94]. It is thus not possible to say with certainty that the observed differences in the secretome proteomic composition and angiogenic activity were the result of OA use or a consequence of other factors (e.g., old age, comorbidities, and smoking). Further studies, using larger patient samples (e.g., >20–30 subjects per group, based on similar studies), are therefore required before the effects of such confounding factors can be individually assessed, so that the findings of this study can be clearly validated. Nonetheless, based on the data presented in this work, it is reasonably safe to argue that OA administration, even in older patients who smoke, does not inhibit the angiogenic activity of hypoxia-preconditioned blood-derived secretomes, and therefore, it does not prohibit their potential application as tools for promoting therapeutic angiogenesis.

5. Conclusions

The findings of this study highlight the fact that neither OA administration nor DM (T1D or T2D) appear to inhibit the ability of HPP or HPS to induce microvessel formations in vitro, despite the significantly reduced VEGF concentrations in HPP and PF-4 levels in HPS, compared to non-OA controls. These findings also, once again, confirm the positive effect of hypoxic conditioning on optimizing the angiogenic potential of blood-derived secretomes and suggests that OA use does not prohibit the application of these products for supporting tissue vascularization and wound healing. Therefore, patients requiring angiogenesis-promoting therapies for central/peripheral ischemia and chronic wounds could potentially still benefit from these new-generation autologous and bioactive treatments.

Author Contributions: Conceptualization, P.M., A.F.S., and E.H.; methodology, P.M., M.J., J.H., U.D., and E.H.; software, P.M., M.J., J.H., U.D., and E.H.; validation, P.M., M.J., and J.H.; formal analysis, P.M., J.M., J.H., and E.H.; investigation, P.M., M.J., and J.H.; resources, H.-G.M.; data curation, P.M., M.J., J.H., and U.D.; writing—original draft preparation, P.M. and E.H.; writing—review and editing, P.M., E.H., and B.S.; visualization, P.M. and E.H.; supervision, E.H.; project administration, H.-G.M. and E.H.; and funding acquisition, H.-G.M. All authors have read and agreed to the published version of the manuscript.

Funding: This study received no specific financial support from a public, commercial, or nonprofit financing agency.

Conflicts of Interest: The authors declare no conflicts of interest. The blood donors involved in this study did not have any direct relationship or dependency relationship with the project leader. This study was carried out under the umbrella of the EmaCure Project (for more info, please visit www.emacure.org).

Abbreviations

ASA	Acetylsalicylic acid
bFGF	basic fibroblast growth factor
COX1	Cyclooxygenase-1
EGF	epidermal growth factor
EWS	Extracorporeal Wound Simulation
HPP	hypoxia preconditioned plasma
HPS	hypoxia preconditioned serum
HUVECs	human umbilical vein endothelial cells
IGF-1	insulin-like growth factor-1
NOACs	Nonvitamin K antagonist oral anticoagulants
OA	oral anticoagulation
PAR1	Protease-activated receptor-1
PBC	peripheral blood cells
PBS	phosphate buffered saline
PDGF	platelet-derived growth factor
PF-4	platelet factor-4
TGF-beta1	transforming growth factor beta-1
TSP-1	thrombospondin-1
TXA2	thromboxan-A ₂
VEGF	vascular endothelial growth factor

References

1. Reinke, J.M.; Sorg, H. Wound repair and regeneration. *Eur. Surg. Res.* **2012**, *49*, 35–43. [[CrossRef](#)] [[PubMed](#)]
2. Han, G.; Ceilley, R. Chronic Wound Healing: A Review of Current Management and Treatments. *Adv. Ther.* **2017**, *34*, 599–610. [[CrossRef](#)]
3. Stadelmann, W.K.; Digenis, A.G.; Tobin, G.R. Physiology and healing dynamics of chronic cutaneous wounds. *Am. J. Surg.* **1998**, *176*, 26–38. [[CrossRef](#)]
4. Avishai, E.; Yeghiazaryan, K.; Golubnitschaja, O. Impaired wound healing: Facts and hypotheses for multi-professional considerations in predictive, preventive and personalised medicine. *EPMA J.* **2017**, *8*, 23–33. [[CrossRef](#)] [[PubMed](#)]
5. Lazarus, G.S.; Cooper, D.M.; Knighton, D.R.; Margolis, D.J.; Pecoraro, R.E.; Rodeheaver, G.; Robson, M.C. Definitions and guidelines for assessment of wounds and evaluation of healing. *Arch. Dermatol.* **1994**, *130*, 489–493. [[CrossRef](#)]
6. Woo, K.; Brandys, T.; Marin, J. Assessing chronic wound perfusion in the lower extremity: Current and emerging approaches. *Chronic Wound Care Manag. Res.* **2015**, *2*, 149–157. [[CrossRef](#)]
7. Thiruvoipati, T.; Kielhorn, C.E.; Armstrong, E.J. Peripheral artery disease in patients with diabetes: Epidemiology, mechanisms, and outcomes. *World J. Diabetes* **2015**, *6*, 961–969. [[CrossRef](#)] [[PubMed](#)]
8. Tuttolomondo, A.; Maida, C.; Pinto, A. Diabetic foot syndrome: Immune-inflammatory features as possible cardiovascular markers in diabetes. *World J. Orthop.* **2015**, *6*, 62–76. [[CrossRef](#)]
9. Skelly, C.L.; Cifu, A.S. Screening, Evaluation, and Treatment of Peripheral Arterial Disease. *JAMA* **2016**, *316*, 1486–1487. [[CrossRef](#)] [[PubMed](#)]
10. Emini Veseli, B.; Perotta, P.; De Meyer, G.R.A.; Roth, L.; Van der Donckt, C.; Martinet, W.; De Meyer, G.R.Y. Animal models of atherosclerosis. *Eur. J. Pharmacol.* **2017**, *5*, 3–13. [[CrossRef](#)] [[PubMed](#)]
11. Luisis, A.J. Atherosclerosis. *Nature* **2000**, *407*, 233–241. [[CrossRef](#)] [[PubMed](#)]
12. Rafieian-Kopaei, M.; Setorki, M.; Douidi, M.; Baradaran, A.; Nasri, H. Atherosclerosis: Process, Indicators, Risk Factors and New Hopes. *Int. J. Prev. Med.* **2014**, *5*, 927–946. [[PubMed](#)]
13. Bentzon, J.F.; Otusua, F.; Virmani, R.; Falk, E. Mechanisms of Plaque Formation and Rupture. *Circ. Res.* **2014**, *114*, 1852–1866. [[CrossRef](#)] [[PubMed](#)]
14. Aronson, D.; Edelman, E.R. Revascularization for coronary artery disease in diabetes mellitus: Angioplasty, stents and coronary artery bypass grafting. *Rev. Endocr. Metab. Disord.* **2010**, *11*, 75–86. [[CrossRef](#)]
15. Bolton, L. Peripheral arterial disease: Scoping review of patient-centred outcomes. *Int. Wound J.* **2019**, *16*, 1521–1532. [[CrossRef](#)]
16. Abu Dabrh, A.M.; Steffen, M.W.; Undavalli, C.; Asi, N.; Wang, Z.; Elamin, M.B.; Conte, M.S.; Murad, M.H. The natural history of untreated severe or critical limb ischemia. *J. Vasc. Surg.* **2015**, *62*, 1642–1651. [[CrossRef](#)]
17. Lim, J.Z.; Ng, N.S.; Thomas, C. Prevention and treatment of diabetic foot ulcers. *J. R. Soc. Med.* **2017**, *110*, 104–109. [[CrossRef](#)]
18. Spampinato, D.F.; Caruso, G.J.; De Pasquale, R.; Sortino, M.A.; Merlo, S. The Treatment of Impaired Wound Healing in Diabetes: Looking among Old Drugs. *Pharmaceuticals* **2020**, *3*, 60. [[CrossRef](#)]
19. Petrie, J.R.; Guzik, T.J.; Touyz, R.M. Diabetes, Hypertension and Cardiovascular Disease: Clinical Insights and Vascular Mechanisms. *Can. J. Cardiol.* **2018**, *34*, 575–584. [[CrossRef](#)]
20. Davis, F.M.; Kimball, A.; Boniakowski, A.; Gallagher, K. Dysfunctional Wound Healing in Diabetic Foot Ulcers: New Crossroads. *Curr. Diabetes Rep.* **2018**, *18*, 2. [[CrossRef](#)]
21. Dinh, T.; Elder, S.; Veves, A. Delayed wound healing in diabetes: Considering future treatments. *Diabetes Manag.* **2011**, *1*, 509–519. [[CrossRef](#)]
22. Greenhalgh, D.G. Wound healing and diabetes mellitus. *Clin. Plast. Surg.* **2003**, *30*, 37–45. [[CrossRef](#)]
23. Okonkwo, U.A.; DiPietro, L. Diabetes and Wound Angiogenesis. *Int. J. Mol. Sci.* **2017**, *18*, 1419. [[CrossRef](#)] [[PubMed](#)]
24. Dinh, T.; Veves, A. Microcirculation of the Diabetic Foot. *Curr. Pharm. Des.* **2005**, *11*, 2301–2309. [[CrossRef](#)]
25. Honnegowda, T.M.; Kumar, P.; Udupa, E.G.; Kumar, S.; Kumar, U.; Rao, P. Role of angiogenesis and angiogenic factors in acute and chronic wound healing. *Plast. Aesthet. Res.* **2015**, *2*, 243–249.
26. Mustoe, T.A.; Tae, A.S.; Tarpley, J.E.; Pierce, G.F. Role of hypoxia in growth factor responses: Differential effects of basic fibroblast growth factor and platelet-derived growth factor in an ischemic wound model. *Wound Repair Regen.* **1994**, *2*, 277–283. [[CrossRef](#)] [[PubMed](#)]

27. Al Said, S.; Bode, C.; Duerschmied, D. Anticoagulation in Atherosclerotic Disease. *Hamostaseologie* **2018**, *38*, 240–246.
28. Krankenberg, K. Recommended interventions for the treatment of peripheral artery disease: Keep the patients moving. *Internist* **2019**, *60*, 1235–1239. [[CrossRef](#)]
29. Olinic, D.M.; Tataru, D.; Homorodean, C.; Spinu, M.; Olinic, M. Antithrombotic treatment in peripheral artery disease. *VASA* **2018**, *47*, 99–108. [[CrossRef](#)]
30. Phelps, E.A.; Garcia, A.J. Update on therapeutic vascularization strategies. *Regen Med.* **2009**, *4*, 65–80. [[CrossRef](#)]
31. Kosaric, N.; Kiwanuka, H.; Gurtner, G.C. Stem cell therapies for wound healing. *Expert Opin. Biol. Ther.* **2019**, *19*, 575–585. [[CrossRef](#)] [[PubMed](#)]
32. Bauer, S.M.; Bauer, R.J.; Velazquez, O.C. Angiogenesis, vasculogenesis, and induction of healing in chronic wounds. *Vasc. Endovasc. Surg.* **2005**, *39*, 293–306. [[CrossRef](#)] [[PubMed](#)]
33. Frykberg, R.G.; Banks, J. Challenges in the Treatment of Chronic Wounds. *Adv. Wound Care* **2015**, *4*, 560–582. [[CrossRef](#)] [[PubMed](#)]
34. Hadjipanayi, E.; Schilling, A.F. Regeneration through autologous hypoxia preconditioned plasma. *Organogenesis* **2014**, *10*, 164–169. [[CrossRef](#)]
35. Hadjipanayi, E.; Schilling, A.F. Hypoxia- based strategies for angiogenic induction. *Organog. Landes Biosci.* **2013**, *9*, 1–12. [[CrossRef](#)]
36. Hadjipanayi, E.; Bauer, A.T.; Moog, P.; Salgin, B.; Kükrek, H.; Fersch, B.; Hopfner, U.; Meissner, T.; Schlüter, A.; Ninkovic, M.; et al. Cell-free Carrier System for Localised Delivery of Peripheral Blood Cell-Derived Engineered Factor Signaling: Towards Development of a One-Step Device for Autologous Angiogenic Therapy. *J. Control. Release* **2013**, *169*, 91–102. [[CrossRef](#)]
37. Hadjipanayi, E.; Moog, P.; Bekeran, S.; Kirchhoff, K.; Bereznoi, A.; Aguirre, J.; Bauer, A.T.; Kükrek, H.; Schmauss, D.; Hopfner, U.; et al. In Vitro Characterization of Hypoxia Preconditioned Serum (HPS)-Fibrin Hydrogels: Basis for an Injectable Biomimetic Tissue Regeneration Therapy. *J. Funct. Biomater.* **2019**, *10*, 22. [[CrossRef](#)]
38. Hadjipanayi, E.; Bekeran, S.; Moog, P. Extracorporeal Wound Simulation as a Foundation for Tissue Repair und Regeneration Therapies. *Int. J. Transpl. Plast. Surg.* **2018**, *2*, 1–10.
39. Moog, P.; Kirchhoff, K.; Bekeran, S.; Bauer, A.T.; Isenburg, S.; Dornseifer, U.; Machens, H.G.; Schilling, A.F.; Hadjipanayi, E. Comparative Evaluation of the Angiogenic Potential of Hypoxia Preconditioned Blood-Derived Secretomes and Platelet-Rich Plasma: An In Vitro Analysis. *Biomedicines* **2020**, *8*, 16. [[CrossRef](#)]
40. Koutsoumpelis, A.; Argyriou, C.; Tasopoulou, K.M.; Georgakarakos, E.I.; Georgiadis, G.S. Novel Oral Anticoagulants in Peripheral Artery Disease: Current Evidence. *Curr. Pharm. Des.* **2018**, *24*, 4511–4515. [[CrossRef](#)]
41. Gupta, A.; Lee, M.S.; Gupta, K.; Kumar, V.; Reddy, S. A Review of Antithrombotic Treatment in Critical Limb Ischemia After Endovascular Intervention. *Cardiol. Ther.* **2019**, *8*, 193–209. [[CrossRef](#)] [[PubMed](#)]
42. Hadjipanayi, E.; Kuhn, P.H.; Moog, P.; Bauer, A.T.; Kuekrek, H.; Mirzoyan, L.; Hummel, A.; Kirchhoff, K.; Salgin, B.; Isenburg, S.; et al. The Fibrin Matrix regulates Angiogenic Responses within the Hemostatic Microenvironment through Biochemical Control. *PLoS ONE* **2015**, *10*, e0135618. [[CrossRef](#)] [[PubMed](#)]
43. Simon, E.M.; Streitz, M.J.; Sessions, D.J.; Kaide, C.G. Anticoagulation Reversal. *Emerg. Med. Clin. N. Am.* **2018**, *36*, 585–601. [[CrossRef](#)] [[PubMed](#)]
44. Tickner, A.; Klinghard, C.; Arnold, J.F.; Marmolejo, V. Total Contact Cast Use in Patients With Peripheral Arterial Disease: A Case Series and Systematic Review. *Wounds* **2018**, *30*, 49–56.
45. Sampson, S.; Gerhardt, M.; Mandelbaum, B. Platelet rich plasma injection grafts for musculoskeletal injuries: A review. *Curr. Rev. Musculoskelet. Med.* **2008**, *1*, 165–174. [[CrossRef](#)]
46. Carter, M.J.; Fyelling, C.P.; Parnell, L.K. Use of platelet rich plasma gel on wound healing: A systematic review and meta-analysis. *Eplasty* **2011**, *11*, e38.
47. Thun, M.J.; Henley, S.J.; Patrono, C. Nonsteroidal anti-inflammatory drugs as anticancer agents: Mechanistic, pharmacologic, and clinical issues. *J. Natl. Cancer Inst.* **2002**, *94*, 252–266. [[CrossRef](#)]
48. Jacobs, E.J.; Newton, C.; Stevens, V.L.; Campbell, P.T.; Freedland, S.J.; Gapstur, S.M. Daily aspirin use and prostate cancer-specific mortality in a large cohort of men with nonmetastatic prostate cancer. *J. Clin. Oncol.* **2014**, *32*, 3716–3722. [[CrossRef](#)]

49. Li, H.; Liu, K.; Boardman, L.A.; Zhao, Y.; Wang, L.; Sheng, Y.; Oi, N.; Limburg, P.J.; Bode, A.M.; Dong, Z. Circulating prostaglandin biosynthesis in colorectal cancer and potential clinical significance. *Ebiomedicine* **2015**, *2*, 165–171. [[CrossRef](#)]
50. Dai, X.; Yan, J.; Fu, X.; Pan, Q.; Sun, D.; Xu, Y.; Wang, J.; Nie, L.; Tong, L.; Shen, A.; et al. Aspirin Inhibits Cancer Metastasis and Angiogenesis via Targeting Heparanase. *Clin. Cancer Res.* **2017**, *23*, 6267–6278. [[CrossRef](#)]
51. Zhang, H.; Lu, J.; Jiao, Y.; Chen, Q.; Li, M.; Wang, Z.; Yu, Z.; Huang, X.; Yao, A.; Gao, Q.; et al. Aspirin Inhibits Natural Killer/T-Cell Lymphoma by Modulation of VEGF Expression and Mitochondrial Function. *Front. Oncol.* **2018**, *8*, 679. [[CrossRef](#)] [[PubMed](#)]
52. Ouyang, N.; Williams, J.; Rigas, B. NO-donating Aspirin Inhibits Angiogenesis by Suppressing VEGF Expression in HT-29 Human Colon Cancer Mouse Xenografts. *Carcinogenesis* **2008**, *29*, 1794–1798. [[CrossRef](#)] [[PubMed](#)]
53. Zhang, X.; Wang, Z.; Wang, Z.; Zhang, Y.; Jia, Q.; Wu, L.; Zhang, W. Impact of Acetylsalicylic Acid on Tumor Angiogenesis and Lymphangiogenesis Through Inhibition of VEGF Signaling in a Murine Sarcoma Model. *Oncol. Rep.* **2013**, *29*, 1907–1913. [[CrossRef](#)] [[PubMed](#)]
54. Nadar, S.; Blann, A.D.; Lip, G.Y.H. Effects of Aspirin on Intra-Platelet Vascular Endothelial Growth Factor, Angiopoietin-1, and P-Selectin Levels in Hypertensive Patients. *Am. J. Hypertens.* **2006**, *19*, 970–977. [[CrossRef](#)]
55. Gerrah, R.; Fogel, M.; Gilon, D. Aspirin decreases vascular endothelial growth factor release during myocardial ischemia. *Int. J. Cardiol.* **2004**, *94*, 25–29. [[CrossRef](#)]
56. Jayaram, P.; Yeh, P.; Patel, S.J.; Sela, R.; Shybut, T.B.; Grol, M.W.; Lee, B.H. Effects of Aspirin on Growth Factor Release From Freshly Isolated Leukocyte-Rich Platelet-Rich Plasma in Healthy Men: A Prospective Fixed-Sequence Controlled Laboratory Study. *Am. J. Sports Med.* **2019**, *47*, 1223–1229. [[CrossRef](#)]
57. Marx, R.E.; Carlson, E.R.; Eichstaedt, R.M.; Schimmele, S.R.; Strauss, J.E.; Georgeff, K.R. Platelet-rich plasma: Growth factor enhancement for bone grafts. *Oral Surg. Endod.* **1998**, *85*, 638–646.
58. Hom, D.B. New Developments in wound healing relevant to facial plastic surgery. *Arch. Facial Plast. Surg.* **2008**, *10*, 402–406. [[CrossRef](#)]
59. Van den Dolder, J.; Mooren, R.; Vloon, A.P.; Stoelinga, P.J.; Jansen, J.A. Platelet-Rich Plasma: Quantification of Growth Factor Levels and the Effect on Growth and Differentiation of Rat Bone Marrow Cells. *Tissue Eng.* **2006**, *12*, 3067–3073. [[CrossRef](#)]
60. Aghaloo, T.L.; Moy, P.K.; Freymiller, E.G. Investigation of platelet-rich plasma in rabbit cranial defects: A pilot study. *J. Oral Maxillofac. Surg.* **2002**, *60*, 1176–1181. [[CrossRef](#)]
61. Kuffler, D.P. Platelet-Rich Plasma Promotes Axon Regeneration, Wound Healing, and Pain Reduction: Fact or Fiction. *Mol. Neurobiol.* **2015**, *52*, 990–1014. [[CrossRef](#)] [[PubMed](#)]
62. Javeed, A.; Hou, Y.; Duan, K.; Zhang, B.; Shen, H.; Cao, Y.; Zhao, Y. Aspirin Significantly Decreases the Nonopsonic Phagocytosis and Immunogenicity of Macrophages in Mice. *Inflamm. Res.* **2011**, *60*, 389–398. [[CrossRef](#)] [[PubMed](#)]
63. Hussain, M.; Javeed, A.; Ashraf, M.; Zhao, Y.; Mukhtar, M.M.; Rehman, M.U. Aspirin and immune system. *Int. Immunopharmacol.* **2012**, *12*, 10–20. [[CrossRef](#)] [[PubMed](#)]
64. Shackelford, R.E.; Alford, P.B.; Xue, Y.; Thai, S.F.; Adams, D.O.; Pizzo, S. Aspirin inhibits tumor necrosis factoralpha gene expression in murine tissue macrophages. *Mol. Pharmacol.* **1997**, *52*, 421–429. [[CrossRef](#)]
65. Jones, M.K.; Wang, H.; Peskar, B.M.; Levin, E.; Itani, R.M.; Sarfeh, I.J.; Tarnawski, A.S. Inhibition of angiogenesis by nonsteroidal anti-inflammatory drugs: Insight into mechanisms and implications for cancer growth and ulcer healing. *Nat. Med.* **1999**, *5*, 1418–1423. [[CrossRef](#)]
66. Maity, G.; Chakraborty, J.; Ghosh, A.; Haque, I.; Banerjee, S.; Banerjee, S.K. Aspirin suppresses tumor cell-induced angiogenesis and their incongruity. *J. Cell Commun. Signal.* **2019**, *13*, 491–502. [[CrossRef](#)]
67. Smadja, D.M.; Bura, A.; Szymezak, J.; Blanchard, A.; Remones, V.; Azizi, M.; Gaussem, P. Effect of clopidogrel on circulating biomarkers of angiogenesis and endothelial activation. *J. Cardiol.* **2012**, *59*, 30–35. [[CrossRef](#)]
68. Luo, J.C.; Peng, Y.C.; Chen, T.S.; Huo, T.I.; Hou, M.C.; Huang, H.C.; Lin, H.C.; Lee, F.Y. Clopidogrel inhibits angiogenesis of gastric ulcer healing via downregulation of vascular endothelial growth factor receptor 2. *J. Formos. Med. Assoc.* **2016**, *115*, 764–772. [[CrossRef](#)]
69. Verdecchia, P.; Angeli, F.; Aita, A.; Bartolini, C.; Reboldi, G. Why Switch From Warfarin to NOACs? *Intern. Emerg. Med.* **2016**, *11*, 289–293. [[CrossRef](#)]

70. Hart, R.G.; Pearce, L.A.; Aguilar, M.I. Meta-analysis: Antithrombotic therapy to prevent stroke in patients who have nonvalvular atrial fibrillation. *Ann. Intern. Med.* **2007**, *146*, 857–867. [[CrossRef](#)]
71. Gómez-Outes, A.; Suarez-Gea, M.L.; Lecumberri, R.; Terleira-Fernández, A.I.; Vargas-Castrillón, E.; Rocha, E. Potential role of new anticoagulants for prevention and treatment of venous thromboembolism in cancer patients. *Vasc. Health Risk Manag.* **2013**, *9*, 207–228. [[CrossRef](#)] [[PubMed](#)]
72. Lange, S.; Gonzales, I.; Pinto, M.P.; Arce, M.; Valenzuela, R.; Aranda, E.; Elliot, M.; Alvarez, M.; Henriquez, S.; Velasquez, E.V.; et al. Independent anti-angiogenic capacities of coagulation factors X and Xa. *J. Cell Physiol.* **2014**, *229*, 1673–1680. [[CrossRef](#)] [[PubMed](#)]
73. Wang, B.; Pearson, T.; Manning, G.; Donnelly, R. In vitro study of thrombin on tubule formation and regulators of angiogenesis. *Clin. Appl. Thromb. Hemost.* **2010**, *16*, 674–678. [[CrossRef](#)] [[PubMed](#)]
74. Haralabopoulos, C.; Grant, D.S.; Kleinman, H.K.; Maragoudakis, M.E. Thrombin promotes endothelial cell alignment in Matrigel In Vitro and angiogenesis in vivo. *Am. J. Physiol.* **1997**, *273*, C239–C245. [[CrossRef](#)] [[PubMed](#)]
75. Chan, B.; Merchan, J.R.; Kale, S.; Sukhatme, V.P. Antiangiogenic property of human thrombin. *Microvasc. Res.* **2003**, *66*, 1–14. [[CrossRef](#)]
76. Sabor, M.; Moinuddin, S.; Ilyas, S. Platelets structural, functional and metabolic alterations in diabetes mellitus. *Pak. J. Physiol.* **2012**, *8*, 40–43.
77. Szablewski, L.; Sulima, A. The Structural and Functional Changes of Blood Cells and Molecular Components in Diabetes Mellitus. *Biol. Chem.* **2017**, *398*, 411–423. [[CrossRef](#)]
78. Kaur, R.; Kaur, M.; Singh, J. Endothelial dysfunction and platelet hyperactivity in type 2 diabetes mellitus: Molecular insights and therapeutic strategies. *Cardiovasc. Diabetol.* **2018**, *17*, 121. [[CrossRef](#)]
79. Assert, R.; Scherk, G.; Bumbure, A.; Pirags, V.; Schatz, H.; Pfeiffer, A.F. Regulation of protein kinase C by short term hyperglycaemia in human platelets in vivo and in vitro. *Diabetologia* **2001**, *44*, 188–195. [[CrossRef](#)]
80. Kampfer, H.; Pfeilchifter, J.; Frank, S. Expressional regulation of angiopoietin-1 and -2 and the tie-1 and -2 receptor tyrosine kinases during cutaneous wound healing: A comparative study of normal and impaired repair. *Lab. Investig.* **2001**, *81*, 361–373. [[CrossRef](#)]
81. Bitar, M.S.; Labbad, Z. Transforming growth factor-beta and insulin-like growth factor-1 in relation to diabetes-induced impairment of wound healing. *J. Surg. Res.* **1996**, *61*, 113–119. [[CrossRef](#)] [[PubMed](#)]
82. Rivard, A.; Fabre, J.E.; Silver, M.; Chen, D.; Murohara, T.; Kearney, M.; Magner, M.; Asahara, T.; Isner, J.M. Age-dependent impairment of angiogenesis. *Circulation* **1999**, *99*, 111–120. [[CrossRef](#)] [[PubMed](#)]
83. Nakae, I.; Fujita, M.; Miwa, K.; Hasegawa, K.; Kihara, Y.; Nohara, R.; Miyamoto, S.; Ueda, K.; Tamaki, S.; Sasayama, S. Age-dependent impairment of coronary collateral development in humans. *Heart Vessel.* **2000**, *15*, 176–180. [[CrossRef](#)] [[PubMed](#)]
84. Ouriel, K.; Veith, F.J. Acute lower limb ischemia: Determinants of outcome. *Surgery* **1998**, *124*, 336–341. [[CrossRef](#)]
85. Gosain, A.; DiPietro, L.A. Aging and wound healing. *World J. Surg.* **2004**, *28*, 321–326. [[CrossRef](#)]
86. Doria, G.; Frasca, D. Regulation of cytokine production in aging mice. *Ann. N. Y. Acad. Sci.* **1994**, *741*, 299–304. [[CrossRef](#)]
87. Ershler, W.B.; Keller, E.T. Age-associated increased interleukin-6 gene expression, late-life diseases, and frailty. *Annu. Rev. Med.* **2000**, *51*, 245–270. [[CrossRef](#)]
88. Mascarucci, P.; Taub, D.; Paloma, M.A.; Dawson, H.; Roth, G.S.; Ingram, D.K.; Lane, M.A. Age-related changes in cytokine production by leukocytes in rhesus monkeys. *Aging* **2001**, *13*, 85–94. [[CrossRef](#)]
89. Ashcroft, G.S.; Horan, M.A.; Ferguson, M.W. Aging is associated with reduced deposition of specific extracellular matrix components, an up-regulation of angiogenesis, and an altered inflammatory response in a murine incisional wound healing model. *J. Investig. Dermatol.* **1997**, *108*, 430–437. [[CrossRef](#)]
90. Swift, M.E.; Kleinman, H.K.; DiPietro, L.A. Impaired wound repair and delayed angiogenesis in aged mice. *Lab. Investig.* **1999**, *79*, 1479–1487.
91. Costa, F.; Sores, R. Nicotine: A pro-angiogenic factor. *Life Sci.* **2009**, *84*, 785–790. [[CrossRef](#)] [[PubMed](#)]
92. Conklin, B.S.; Zhao, W.; Zhong, D.; Chen, C. Nicotine and cotinine up-regulate vascular endothelial growth factor expression in endothelial cells. *Am. J. Pathol.* **2002**, *160*, 413–418. [[CrossRef](#)]
93. Heeschen, C.; Jang, J.J.; Weis, M.; Pathak, A.; Kaji, S.; Hu, R.S.; Tsao, P.S.; Johnson, H.L.; Cooke, J.P. Nicotine stimulates angiogenesis and promotes tumor growth and atherosclerosis. *Nat. Med.* **2001**, *7*, 833–839. [[CrossRef](#)] [[PubMed](#)]

94. Jacobi, J.; Jang, J.J.; Sundram, U.; Dayoub, H.; Fajardo, L.F.; Cooke, J.P. Nicotine accelerates angiogenesis and wound healing in genetically diabetic mice. *Am. J. Pathol.* **2002**, *161*, 97–104. [[CrossRef](#)]
95. Mousa, S.; Mousa, S.A. Cellular and molecular mechanisms of nicotine's pro-angiogenesis activity and its potential impact on cancer. *J. Cell Biochem.* **2006**, *97*, 1370–1378. [[CrossRef](#)]



© 2020 by the authors. Licensee MDPI, Basel, Switzerland. This article is an open access article distributed under the terms and conditions of the Creative Commons Attribution (CC BY) license (<http://creativecommons.org/licenses/by/4.0/>).



Article

Effect of Hypoxia Preconditioned Secretomes on Lymphangiogenic and Angiogenic Sprouting: An in Vitro Analysis

Philipp Moog¹, Rahmin Schams¹, Alexander Schneider^{1,2}, Arndt F. Schilling³, Hans-Günther Machens^{1,*}, Ektoras Hadjipanayi^{1,†} and Ulf Dornseifer^{1,2,†}

¹ Experimental Plastic Surgery, Clinic for Plastic, Reconstructive and Hand Surgery, Klinikum Rechts der Isar, Technische Universität München, D-81675 Munich, Germany; philippmoog@web.de (P.M.); rahmin@gmx.de (R.S.); schneider@gmx.at (A.S.); e.hadjipanayi@googlemail.com (E.H.); ulf.dornseifer@isarklinikum.de (U.D.)

² Department of Plastic, Reconstructive and Aesthetic Surgery, Isar Klinikum, D-80331 Munich, Germany

³ Department of Trauma Surgery, Orthopedics and Plastic Surgery, Universitätsmedizin Göttingen, D-37075 Göttingen, Germany; arndt.schilling@med.uni-goettingen.de

* Correspondence: Hans-Guenther.Machens@mri.tum.de

† These two authors contributed equally to this work.

Received: 30 August 2020; Accepted: 19 September 2020; Published: 20 September 2020

Abstract: Hypoxia Preconditioned Plasma (HPP) and Serum (HPS) are two blood-derived autologous growth factor compositions that are being clinically employed as tools for promoting tissue regeneration, and have been extensively examined for their angiogenic activity. As yet, their ability to stimulate/support lymphangiogenesis remains unknown, although this is an important but often-neglected process in wound healing and tissue repair. Here we set out to characterize the potential of hypoxia preconditioned secretomes as promoters of angiogenic and lymphangiogenic sprouting in vitro. We first analysed HPP/HPS in terms of pro- (VEGF-C) and anti- (TSP-1, PF-4) angiogenic/lymphangiogenic growth factor concentration, before testing their ability to stimulate microvessel sprouting in the mouse aortic ring assay and lymphatic sprouting in the thoracic duct ring assay. The origin of lymphatic structures was validated with lymph-specific immunohistochemical staining (Anti-LYVE-1) and lymphatic vessel-associated protein (polydorn) quantification in culture supernatants. HPP/HPS induced greater angiogenic and lymphatic sprouting compared to non-hypoxia preconditioned samples (normal plasma/serum), a response that was compatible with their higher VEGF-C concentration. These findings demonstrate that hypoxia preconditioned blood-derived secretomes have the ability to not only support sprouting angiogenesis, but also lymphangiogenesis, which underlines their multimodal regenerative potential.

Keywords: adipose-derived stem cells; adipose-derived cell suspension; peripheral blood cells; blood-derived therapy; hypoxia; angiogenesis; hypoxia preconditioned plasma; hypoxia preconditioned serum; lymphangiogenesis; lymphatic regeneration

1. Introduction

Complete restoration of physiological tissue architecture is the ultimate goal of regenerative medicine [1]. In humans, restorative responses following dramatic injuries or chronic wounds are limited, generally leading to poor wound healing with scarring, rather than full regeneration of traumatized body parts [1]. Considering the fact that wounds naturally heal via a set of complex and interactive processes, including hemostasis, inflammation, proliferation, and remodeling [2–4], gives an idea of the complexity of tissue repair. Research on regenerative treatments commonly focuses on stimulating angiogenesis (formation of new blood vessels) and improving tissue perfusion, in

order to provide an adequate supply of oxygen/nutrients to the wound bed, which forms an absolute prerequisite for optimal cellular functions. It is gradually becoming apparent, however, that modern regenerative strategies must employ a multimodal approach that reaches beyond angiogenesis, also targeting other important processes involved in reparation of injured tissue.

Unlike angiogenesis, lymphangiogenesis is often neglected in the context of tissue regeneration, and has been so far poorly studied. Nonetheless, the importance of a sufficient lymphatic network for optimal tissue metabolism and an intact immune response must not be underestimated. The main function of the lymphatic vasculature is interstitial fluid drainage [5], which is important for fluid homeostasis, immune cell surveillance and trafficking, and lipid absorption [5–10]. In inflammatory settings, lymphangiogenesis facilitates the resolution of tissue edema and promotes macrophage and dendritic cell mobilization [11–14]. If the local immune response is delayed, or interstitial edema reduces cellular gas exchange and nutrition (by increasing diffusion distance), the wound healing process is ultimately impaired [6,15,16].

Despite the lack of an adequate body of research work, it is becoming increasingly evident that the complex cell-growth factor interactions, which are known to play catalytic roles in angiogenesis, appear to be involved in lymphangiogenesis as well [17]. For example, the VEGF family of protein factors, i.e., VEGF-A, -C, and -D can induce the outgrowth of lymphatic vessels [18], while VEGF-C/VEGFR-3 signaling is a primary mediator of lymphangiogenesis [11,19]. Moreover, the angiogenesis-related growth factors fibroblast growth factor 2 (FGF-2), insulin-like growth factor 1 (IGF-1), IGF-2, hepatocyte growth factor (HGF), endothelin-1 (ET-1), and PDGF-B have all been reported to induce lymphangiogenesis in different contexts [5,20]. Some studies have also pointed to the regulatory effects of TSP-1 and PF-4 as key endogenous inhibitors of lymphangiogenesis, through the inhibition of lymphatic endothelial cell migration and proliferation [21,22].

Our previous work has provided strong evidence that hypoxia preconditioned blood-derived secretomes could constitute a new generation of autologous and bioactive injectable/topical compositions that can supply the necessary biochemical signals for stimulating angiogenesis and driving wound healing to completion [23–28]. These angiogenic compositions can be obtained through the method of Extracorporeal Wound Simulation (EWS), using peripheral (venous) blood [23–29]. The ability to condition PBCs under the same environmental conditions encountered within a wound, i.e., physiological temperature and hypoxia, offers an easy way to optimize the angiogenic potential of Hypoxia Preconditioned Plasma (HPP) and Hypoxia Preconditioned Serum (HPS), which can be differentially prepared by adjusting blood coagulation prior to hypoxic conditioning [23–30]. More specifically, we have shown that the angiogenic potential of blood-derived secretomes is defined by the complex stoichiometry of their component pro- and anti-angiogenic factor proteins, rather than the concentration of one or more individual growth factors [28,29]. These secretomes have also been extensively examined for their angiogenic activity, showing that they are able to induce microvessel formation and sprouting *in vitro*, as well as promote wound healing *in vivo* [23,27,28]. The angiogenic potency of hypoxia preconditioned secretomes is further highlighted by the fact that they maintain their pro-angiogenic activity *in vitro*, even when they are prepared from peripheral blood that is obtained from patients who receive oral anticoagulation due to underlying vascular pathology or who suffer from diabetes mellitus [30].

To our knowledge, the lymphangiogenic potential of hypoxia preconditioned blood-derived secretomes remains unknown. Provided that there seems to be a significant overlap between the cellular/growth factor processes and regulatory pathways involved in angiogenesis and lymphangiogenesis, it is indeed possible that these secretomes might also have the capacity to stimulate the formation of lymphatic vessels. In the current study, we aimed to characterize the proteomic composition of hypoxia preconditioned plasma (HPP) and serum (HPS), in terms of key pro- and anti-angiogenic protein factors that may be involved in lymphangiogenesis (VEGF, PF-4, TSP-1), and analyze their ability to promote angiogenic and lymphangiogenic sprouting *in vitro*. Beyond providing useful insights into the clinical utility of these therapeutic blood-derived products, this work

could also enhance our scientific understanding on the biological processes that physiologically link angiogenesis with lymphangiogenesis.

2. Experimental Setup

2.1. Ethical Approval

All blood donors provided written informed consent as directed by the ethics committee of the Technical University Munich, Germany, which approved this study (File Nr.: 497/16S; Amendment, date of approval: 11 November 2016).

2.2. Preparation of Blood Plasma/Serum and Hypoxia Preconditioned Plasma (HPP)/Serum (HPS) Samples

Peripheral venous blood (20 mL) was collected from young healthy non-smoking subjects ($n = 5$), who were not taking any medication and without known comorbidities, in a 30 mL polypropylene syringe (Omnifix[®], Braun AG, Melsungen, Germany) that contained no additive for normal serum and HPS preparation or was pre-filled with 1-mL heparin (Medunasal[®], Heparin 500 I.U. 5-mL ampoules, Sintetica[®], Münster, Germany) for normal plasma and HPP preparation, under sterile and standardized conditions (Blood Collection Set $0.8 \times 19 \text{ mm} \times 178 \text{ mm}$; Safety-Lok, CE 0050, BD Vacutainer, BD, Franklin Lakes, NJ, USA). For normal plasma/serum preparation, following passive sedimentation for 60 min at room temperature ($25 \text{ }^\circ\text{C}$, no centrifugation) the blood was separated into three layers, from bottom to top: red blood cell component (RBCs), clot/buffy coat, and serum/plasma, so that the top layer (serum or plasma) could be filtered into a new syringe. For HPP/HPS preparation, following blood sampling a $0.2\text{-}\mu\text{m}$ pore filter was attached to the syringe (Sterifix[®], CE 0123, Braun AG, Melsungen, Germany), before adding 5 mL of air into the syringe through the filter, by withdrawing the plunger. Subsequently, the filter was removed, and the capped syringe was placed upright in an incubator ($37 \text{ }^\circ\text{C}/5\% \text{ CO}_2$). Incubation was carried out for 4 days (blood incubation time), without any prior centrifugation. Pericellular (local) hypoxia ($\sim 1\% \text{ O}_2$) was generated *in situ* through cell-mediated O_2 consumption, by controlling the blood volume per unit area ($\text{BVUA} > 1 \text{ mL}/\text{cm}^2$) in the blood-containing syringe, and consequently, the PBC seeding density [25,29,30]. After 4 days, the blood was passively separated into three layers, from bottom to top: red blood cell (RBC) component, buffy coat/clot, and HPP/HPS, so that the top layer comprising hypoxia preconditioned plasma or serum could be filtered ($0.2\text{-}\mu\text{m}$ pore filter, Sterifix[®], Braun AG, Melsungen, Germany) into a new syringe, removing cells/cellular debris.

2.3. Preparation of Adipose-Derived Cell Suspension (ADCS)

ADCS is known for its pro-angiogenic and lymphangiogenic activity [31–34], therefore it was selected as a positive control for this study. According to manufacturer's (ARC Processing System, InGeneron Inc., Houston, TX, USA) instructions and a previously published protocol [35], adipose tissue was dissected from female adult mice, (approximately 10–12 g) using appropriate surgical techniques into a sterile container and then manually minced until average piece size was approximately 2 mm or less. The minced adipose tissue was transferred into a sterile tube and lactated ringer (preheated to $39 \text{ }^\circ\text{C}$) was added to a fill level of 30 mL. Then 2.5 mL of the reconstituted Matrase reagent (ARC System, In Generon Inc., Houston, TX, USA) was added to the tube containing the adipose tissue. The tube was inverted several times to mix thoroughly and placed in an inverted position into the processing system for repetitive acceleration and deceleration for 30 min at $39 \text{ }^\circ\text{C}$. Processing resulted in three layers: a thin layer of oil on the top, a milky adipose layer in the middle, and an aqueous layer on the bottom. Then the tube assembly was inverted, so that the tube was on the top and the filter (Steriflip Filter) (ARC Processing System, InGeneron Inc., Houston, TX, USA) at the bottom, for allowing separation of the different layers for 1 min. The filtered material was then centrifuged again ($600 \times g$ for 5 min). After centrifugation, a pellet of red and white colored cells formed at the bottom with distinct aqueous, adipose, and oil layers settling above. Supernatants were decanted (aqueous,

adipose, and oil layers) into a sterile waste container. Then 40 mL lactated ringer was added to the cell pellet and centrifuged again ($600\times g$ for 5 min). The decanting and washing of the cell pellet, in a manner as described above was repeated to get adipose-derived cells. Then lactated ringer solution was added, using the 3 mL syringe (ARC Processing System, InGeneron Inc., Houston, TX, USA) and a new 18 G needle, very gently to the cell pellet at the bottom of the tube. The final cell product was drawn slowly in and out of the 3 mL syringe (ARC Processing System, InGeneron Inc., Houston, TX, USA), three times to break up cell clumps. After this final isolation step, adipose-derived cells (ADCs) were resuspended in Dulbecco's Modified Eagle's Medium (D-MEM without serum, Life Technologies, Paisley, UK) to reach a cell concentration of 3500 cells per mL. Cell counts were determined using the CASY Cell Counter & Analyzer (OLS OMNI Life Science GmbH & Co KG, Bremen, Germany), as described by the manufacturer's protocol. Then adipose-derived cell suspension (ADCS) was ready for testing, without any further conditioning.

2.4. Quantitative Analysis of VEGF-C, TSP-1, PF-4 Concentration in Blood-Derived Secretomes

For analysis of protein factor concentration, blood-derived secretomes (hypoxia preconditioned plasma (HPP) and serum (HPS), normal plasma and serum), were sampled following 4 days incubation and analyzed by ELISA for VEGF-C, TSP-1, PF-4 (R&D Systems, Inc., Minneapolis, MN, USA), according to manufacturer's instructions. Five samples were tested per condition.

2.5. Analysis of the Effect of Blood-Derived Secretomes on Microvessel Sprouting In Vitro

Blood-derived secretomes (hypoxia preconditioned plasma (HPP) and serum (HPS), normal plasma and serum), were tested in the mouse aortic ring assay, in order to assess their ability to induce microvessel sprouting. Aortic rings were dissected from female adult mice as previously described [36], underwent overnight serum starvation in opti-MEM reduced serum medium (Life Technologies, Darmstadt, Germany), before being embedded into Matrigel bilayer matrix (50 μ L/layer in 96-well plates) (BD, Heidelberg, Germany). Secretomes and control media samples (VEGF 90 ng/mL, ADCS; positive controls/phosphate buffered saline (PBS); negative control) samples were added (150 μ L/well) to the rings, before culturing them in a 5% CO₂/37 °C incubator. Medium change was carried out every 3 days, while rings were observed with phase contrast microscopy at 0, 3, 6 and 8 days and photographed, with all four quarters per ring analyzed for sprouting (sprouting was defined as the formation of structures of connected cells that were attached, at their base, to the ring). Furthermore, tube length was quantified after a culture period of 8 days using image analysis using ImageJ software (NIH, Bethesda, MD, USA). At least three aortic rings were tested per condition.

2.6. Analysis of the Effect of Blood-Derived Secretomes on Lymphatic Vessel Sprouting In Vitro

To assess the ability of blood-derived secretomes (hypoxia preconditioned plasma (HPP) and serum (HPS), normal plasma and serum) to induce lymphatic vessel sprouting, these were tested in the thoracic duct ring assay. Thoracic duct rings were dissected from female adult mice (Figure 1) as previously described [37], underwent overnight serum starvation in opti-MEM reduced serum medium (Life Technologies, Darmstadt, Germany), before being embedded into Matrigel bilayer matrix (50 μ L/layer in 96-well plates) (BD, Heidelberg, Germany). Secretomes and control media samples (heat-decomplemented fetal calf serum (FCS 20%) (GIBCO FCS, Thermo Fisher, Wien, Austria); ADCS; positive controls/phosphate buffered saline (PBS); negative control) were added (150 μ L/well) to the rings, before culturing them in a 5% CO₂/37 °C incubator. Medium change was carried out every 2 days, while rings were observed with phase contrast microscopy at 0, 2, 4, 6 and 8 days and photographed, with all 4 quarters per ring analyzed for sprouting (sprouting was defined as the formation of structures of connected cells that were attached, at their base, to the ring). Furthermore, tube length was quantified after a culture period of 8 days using image analysis with ImageJ software (NIH, Bethesda, MD, USA). At least three thoracic duct rings were tested per condition.

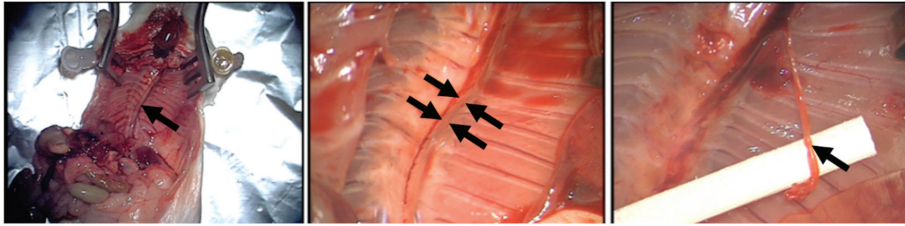


Figure 1. Thoracic Duct Ring Assay. Surgical removal of the thoracic duct, the main lymphatic vessel, under microscopic magnification. The aorta has already been excised and prepared for use in the aortic ring assay. Black arrow(s) show(s) thoracic duct.

2.7. Immunohistochemical Staining of Lymphatic Sprouts

Lymphatic sprouts were stained with anti-lymphatic vessel endothelial hyaluronan receptor-1 (Anti-LYVE-1-antibody) (Abcam, Cambridge, MA, USA), a specific lymphatic endothelial cell marker, according to the manufacturer's instructions. The staining was supplemented with nuclear DAPI counterstain (Abcam; Cambridge, MA, USA), according to the manufacturer's instructions. At least three thoracic duct rings were tested per condition.

2.8. Quantitative Analysis of Polydom Concentration in Thoracic Duct Ring Assay

Thoracic duct ring assay culture supernatants were sampled following medium change at 2 and 8 days and analyzed by ELISA for polydom/svep1, a cell-adhesion receptor involved in lymphangiogenesis [38,39], according to the manufacturer's (MyBioSource; San Diego, CA, USA) instructions. Three samples were tested per condition.

2.9. Statistical Analysis

Five subjects were tested for each experimental condition. Data are expressed as mean \pm standard deviation, as noted. Statistical analysis was carried out using Student's independent t-test, when a maximum of two groups was compared, or one-way ANOVA with Bonferroni adjustment, accompanied by post-hoc pairwise comparisons for analysis of more than two groups, using SPSS 14 software (version 14, IBM, Ehningen, Germany). The probability of a type one error was set to 5% ($\alpha = 0.05$), unless otherwise noted.

3. Results

3.1. Quantitative Analysis of pro- (VEGF-C) and anti- (TSP-1, PF-4) Angiogenic/Lymphangiogenic Growth Factor Concentration in Hypoxia Preconditioned Blood-Derived Secretomes

To establish a growth factor concentration baseline, we first quantitatively analyzed via ELISA the concentration of key angiogenesis-related protein factors in normal plasma and serum, and compared them to their hypoxia-conditioned counterparts. As shown in Figure 2, the concentration of VEGF-C in hypoxia preconditioned plasma (HPP) and hypoxia preconditioned serum (HPS) showed a 3- to 5-fold increase compared to baseline level in fresh plasma ($p = 0.19$) and fresh serum ($p = 0.0459$), respectively. No significant difference was observed between HPP and HPS VEGF-C level ($p = 0.3$). The concentration of the platelet-derived angiogenic inhibitors TSP-1 and PF-4 in fresh plasma and HPP was significantly lower than that in HPS ($p < 0.05$), indicating that the process of blood conditioning used for HPP preparation did not promote significant platelet activation. Furthermore, the concentration of TSP-1, but not PF-4, in HPS was significantly higher compared to that in fresh serum ($p < 0.05$).

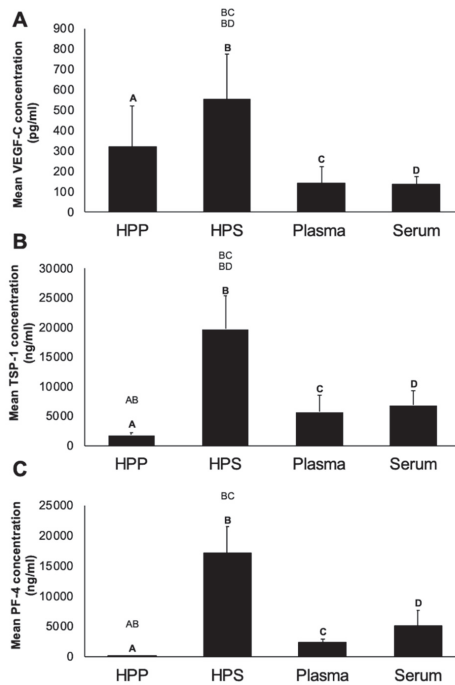


Figure 2. Quantitative analysis of pro- (VEGF-C) and anti- (TSP-1, PF-4) angiogenic/lymphangiogenic growth factor concentration in blood-derived secretomes. Plots showing the concentration of (A) VEGF-C (pg/mL), (B) TSP-1 (ng/mL), (C) PF-4 (ng/mL) in hypoxia preconditioned plasma (HPP) and serum (HPS), as well as fresh plasma and serum obtained from 5 young, healthy subjects as analysed by ELISA. Capital letter pairs over plots indicate statistical comparison of corresponding data points. For all pair comparisons, $p < 0.05$, unless otherwise indicated. Error bars represent s.d. ($n = 5$).

3.2. Analysis of the Ability of Hypoxia Preconditioned Blood-Derived Secretomes to induce Angiogenic Sprouting In Vitro

Having assessed the growth factor composition of hypoxia preconditioned blood-derived secretomes, in terms of key pro- and anti-angiogenic protein factors, an analysis of microvessel sprouting was carried out using the mouse aortic ring assay. In all secretome cultures, we observed a trend for an increasing number of sprouts as culture duration increased from 3 to 6 and 8 days (Figure 3A,B). Hypoxic preconditioning of blood-derived secretomes resulted in a higher sprout number and length, which could initially be seen as a significant difference between HPP and fresh plasma cultures at 3 days, with the difference persisting up to 8 days (Figure 3A–C) ($p < 0.05$). Similarly, HPS appeared to generate more vascular sprouts than fresh serum, at all time points examined, although such differences were not statistically significant due to a high standard deviation between samples. The pro-angiogenic effect of hypoxic conditioning was also evident in the greater number of sprouts induced by HPP compared to pure recombinant VEGF (pos. control). Specifically, there were approx. 5 times more sprouts in HPP cultures than in VEGF cultures on day 8 ($p < 0.05$). Due to the known ability of adipose-derived cell suspension (ADCS) to induce both angiogenic and lymphatic sprouting in vitro and in vivo [31,32,40,41], this was also investigated in addition to VEGF, as positive control in sprouting assays. ADCS appeared to have a similar activity as VEGF, and it was found to induce 3–5 times less sprouts than hypoxia preconditioned secretomes (Figure 3A,B). This difference was particularly evident in day 3 and day 8 cultures, where it was significant compared to HPP cultures ($p < 0.05$).

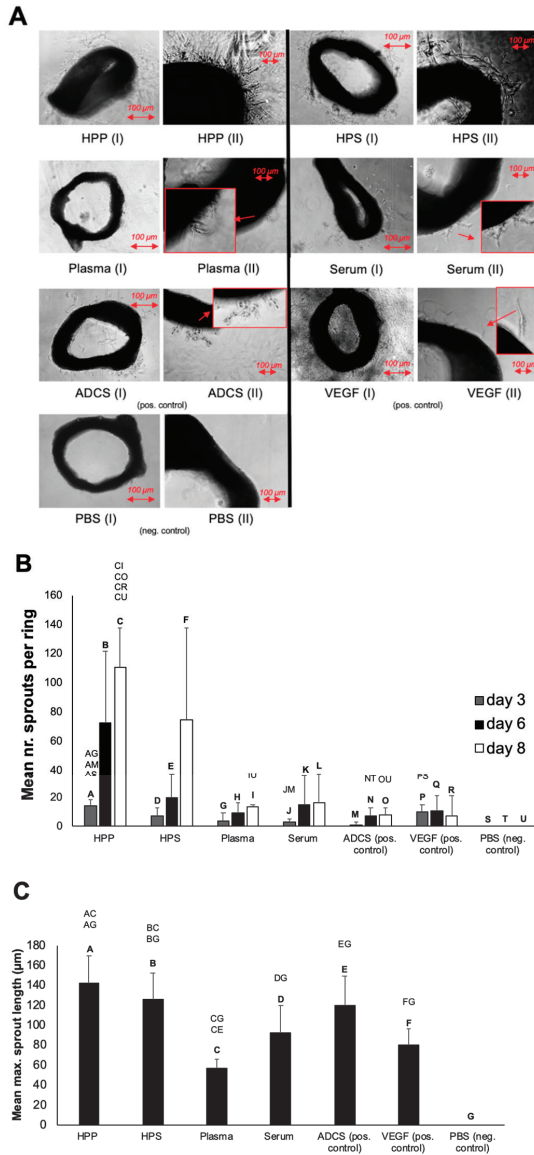


Figure 3. Effect of blood-derived secretomes on microvessel sprouting in the aortic ring assay. (A) Panel showing representative images of angiogenic sprouting assays (8 days culture), carried out in the presence of hypoxia preconditioned blood-derived secretomes (hypoxia preconditioned plasma (HPP) and serum (HPS)), normal plasma and serum, as well as positive controls (adipose-derived cell suspension (ADCS) and vascular endothelial growth factor (VEGF)) and negative control (phosphate buffered saline (PBS)) samples. Photographs were taken using a 10× (I) and a 20× (II) magnification. Enlarged image sections are indicated by red insets (Bars = 100 µm). (B) Plot showing the mean number of sprouts per ring over a culture duration of 3, 6 and 8 days ($n = 3$). (C) Plot showing the mean maximum sprout length following a culture period of 8 days. Capital letter pairs over plots indicate statistical comparison of corresponding data points. For all pair comparisons, $p < 0.05$, unless otherwise indicated. Error bars represent s.d. ($n = 3$).

3.3. Qualitative and Quantitative Validation of the Lymphatic Sprouting Assay

Lymphatic sprouting was tested in the thoracic duct ring assay. Due to the technical difficulty associated with thoracic duct preparation, we first wanted to confirm the lymphatic origin of sprouts in the thoracic duct ring assay, through lymphoid-specific immunohistochemical staining and by lymphoid-specific protein (polydom) quantification, before proceeding to a quantitative assessment of lymphatic sprouting in blood-derived secretome cultures.

As a first method for validating the lymphatic origin of sprouts observed in the thoracic duct ring assay, we examined sprouts for the presence of LYVE-1 (lymphatic vessel endothelial hyaluronan receptor-1), one of the most specific and widely used lymphatic endothelial markers that is located in lymph nodes and in the luminal/adluminal surfaces of lymphatic vessels [14,40]. Specific immunohistochemical staining (Anti-LYVE-1) of sprouts indicated lymphatic structures in HPP/HPS cultures and positive control (ADCS, FCS) cultures, while minimal to no lymphatic sprouting was observed in fresh plasma/serum cultures, as well as negative control (PBS) cultures (Figure 4A). In all culture conditions, thoracic duct rings stained positively (green staining) for LYVE-1, confirming their true lymphoid origin.

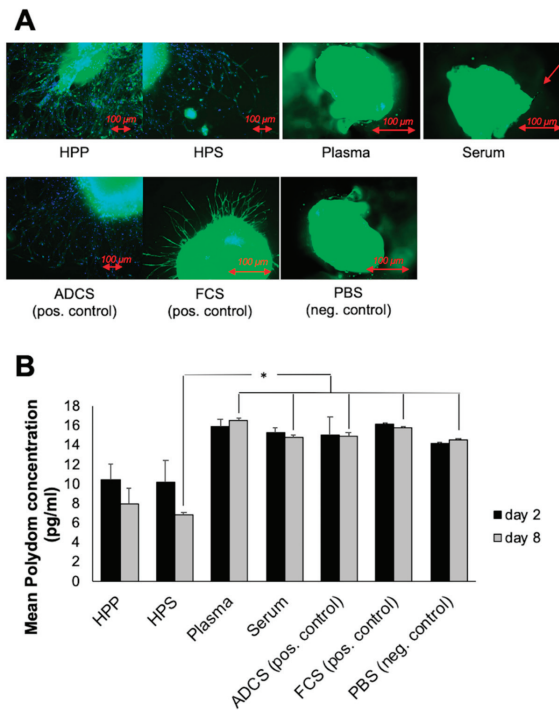


Figure 4. Validation of the lymphatic sprouting assay. **(A)** Panel showing representative images of immunohistochemical staining of thoracic duct rings with Anti-LYVE-1 (anti-lymphatic vessel endothelial hyaluronan receptor-1) (colored green) and DAPI (colored blue) in lymphatic sprouting assays (8 days), carried out in the presence of blood-derived secretomes (hypoxia preconditioned plasma (HPP) and serum (HPS), normal plasma and serum), as well as positive controls (adipose-derived cell suspension (ADCS) and fetal calf serum (FCS)) and negative control (phosphate buffered saline (PBS)) samples (Bars = 100 μ m). **(B)** Quantitative analysis of polydom in thoracic duct ring assays. Plot showing the polydom concentration (pg/ml), measured in culture supernatants obtained following medium change in thoracic duct ring assays at 2 and 8 days. (* $p < 0.05$). Error bars represent s.d. ($n = 3$).

Polydom (also called Sveg 1), a large extracellular matrix protein (>300 kDa) comprising Sushi, von Willebrand factor type A, EGF and pentraxin domain-containing protein 1, is a high-affinity ligand for integrin $\alpha 9\beta 1$, a cell adhesion receptor involved in lymphangiogenesis [38,39]. We hypothesized that polydom protein would passively be released into the culture medium, provided that true lymphoid tissue was cultivated. The polydom concentration of culture supernatants was determined by ELISA on day 2 and day 8, following medium change. As can be seen in Figure 4B, polydom was detected in all culture supernatants, while there were no significant differences between 2 and 8 days of culture for any of the blood-derived secretomes tested, suggesting an early and steady release. HPP/HPS culture supernatants appeared to have almost half the polydom concentration of fresh plasma/serum and positive/negative control cultures. This difference was indeed significant for 8 days HPS cultures ($p < 0.05$). This data, together with the fact that polydom was also present in negative control (PBS) cultures, confirmed the lymphatic origin of the observed sprouts, while also suggesting that polydom leakage into the assay supernatant was more closely correlated with the presence of thoracic duct rings rather than with the degree of lymphatic sprouting.

3.4. Analysis of the Ability of Hypoxia Preconditioned Blood-Derived Secretomes to induce Lymphatic Sprouting In Vitro

Following this double validation method, a quantitative evaluation of the ability of blood-derived secretomes to induce lymphatic sprouting in thoracic duct ring assay in vitro cultures was carried out. Sprouts were analyzed using light microscopy. None of the secretomes tested appeared to induce sprouting on day 2 (Figure 5A,B). While lymphatic sprouting was first observed at 6 days in HPP cultures, HPS generated sprouts after only 4 days (Figure 5B). Importantly, at both these time points, HPP- and HPS-induced sprouting was significantly greater than what was observed in fresh plasma and serum cultures, respectively ($p < 0.05$). Interestingly, while no sprouting was observed in fresh plasma cultures, at any time point, a small number of sprouts could be seen in day 8 serum cultures, further pointing to the higher effectiveness of serum, compared to plasma, in stimulating lymphatic sprouting in vitro. While HPP showed steady sprouting from 6 to 8 days, HPS cultures saw a decline, reaching one third of the day 4 peak after 8 days, a level comparable to HPP cultures (Figure 5B).

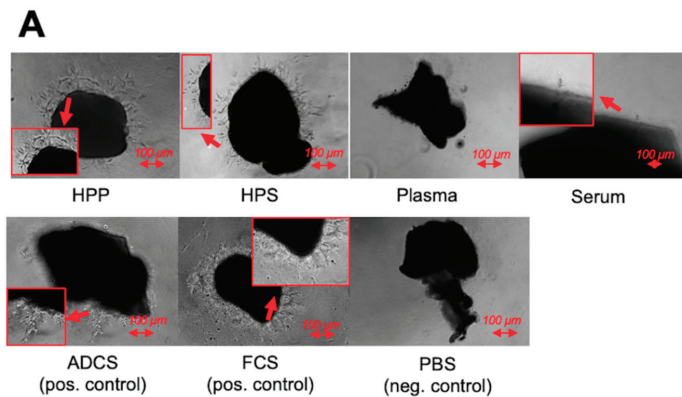


Figure 5. Cont.

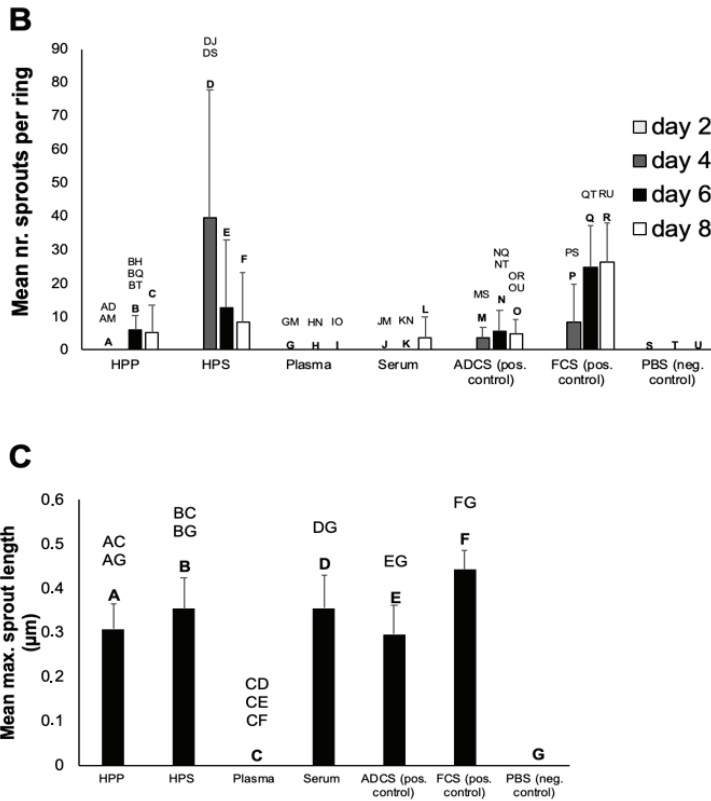


Figure 5. Effect of blood-derived secretomes on lymphatic sprouting in the thoracic duct ring assay. (A) Panel showing representative images of thoracic duct ring cultures (8 days culture), carried out in the presence of blood-derived secretomes (hypoxia preconditioned plasma (HPP) and serum (HPS), normal plasma and serum), as well as positive controls (adipose-derived cell suspension (ADCS) and fetal calf serum (FCS)), and negative control (phosphate buffered saline (PBS)) samples. Enlarged image sections are indicated by red insets. (Bars = 100 µm). (B) Plot showing the mean number of lymphatic sprouts formed in different culture conditions (2, 4, 6 and 8 days culture), as described above ($n = 3$). (C) Plot showing the mean maximum lymphatic sprout length (µm) after a culture period of 8 days ($n = 3$). Capital letter pairs over plots indicate statistical comparison of corresponding data points. For all pair comparisons, $p < 0.05$, unless otherwise indicated.

In this experiment we included adipose-derived cell suspension (ADCS), a secretome with lymphangiogenic properties [34], and fetal calf serum (FCS), a powerful lymphangiogenic stimulator [10], as positive controls. ADCS stimulated steady sprouting from the 4th culture day onwards, while sprout numbers were always higher than those observed in negative control (PBS) cultures ($p < 0.05$) (Figure 5A,B). In contrast to HPP cultures, which elicited comparable sprouting as ADCS cultures at day 6 and day 8, HPS appeared to outperform ADCS at these time points, although differences were not significant due to a large standard deviation present between HPS samples. This relative difference seen between HPP and HPS cultures was also evident when comparing them with FCS, which itself appeared to induce a stronger response compared to ADCS (Figure 5B). Indeed, while HPS was found to be equally potent as FCS at 6 and 8 culture days, HPP promoted significantly less sprouts than FCS on day 6 ($p < 0.05$) (Figure 5B).

Examination of lymphatic sprout length at 8 days culture revealed that HPP- and HPS-induced sprouts had a comparable length as those induced by fresh serum, ADCS and FCS, and significantly greater length than sprouts generated in fresh plasma cultures ($p < 0.05$) (Figure 5C), suggesting that the initiation of lymphatic sprouting and the degree of sprout extension are differentially-regulated processes.

4. Discussion

Hypoxia preconditioned blood-derived secretomes represent a new generation of autologous growth factor preparations [23–28,30] that can be produced through extracorporeal conditioning of peripheral blood cells (PBCs) under wound-simulating conditions, namely physiological temperature and hypoxia [25,26]. We had previously demonstrated that hypoxia preconditioned plasma (HPP) and serum (HPS) supply angiogenesis-specific signaling, similar to that naturally produced within the wound microenvironment [23,28]. HPP and HPS organically differ with respect to their protein factor composition, since they correlate with distinct wound healing phases, the former having a direct correlation with the hypoxia-induced, angiogenesis-driven proliferative phase, while the latter also incorporating the platelet-derived hemostatic phase [25,27,28]. The clinical utility of these secretomes harnesses their angiogenic activity, despite their differences, since they can both provide a useful tool for stimulating microvessel sprouting and new vessel formation on demand [23,27,28]. As such, they could play an important role in a modern therapeutic strategy that aims to improve local tissue perfusion and accelerate wound healing where this is delayed or stagnant.

The main thesis of this work is based on the notion, however, that regenerative wound therapy means more than just stimulating angiogenesis. Although angiogenesis appears to be the key driver of tissue repair and regeneration, lymphangiogenesis is of equal importance. Without sufficient lymphatic drainage of the interstitium, perivascular edema progressively impedes nutrient and oxygen supply, leading to cellular damage. Furthermore, lymphatic regeneration plays an important role in the inflammatory process of wound healing, by assisting the removal of local debris and inflammatory cells. Given the fact that angiogenesis and lymphangiogenesis are two complementary processes, compositions that have been shown capable of stimulating angiogenesis, such as hypoxia preconditioned blood-secretomes [23–28], might also support the formation of new lymphatic vessels. The findings of this study appear to support this hypothesis.

Quantitative analysis of angiogenic/lymphangiogenic growth factor concentration in blood-derived secretomes showed an increased concentration of VEGF-C in hypoxia preconditioned plasma (HPP) and hypoxia preconditioned serum (HPS) compared to their baseline level in fresh plasma and fresh serum, respectively (Figure 2A). It is known that, similar to blood vessel formation, the growth of lymphatic vessels is primarily mediated by vascular endothelial growth factor VEGF-C/VEGFR-3 signaling [11,19]. The current data verifies the positive effect of hypoxic conditioning on optimizing the pro-angiogenic/lymphangiogenic composition of blood-derived secretomes, shown here by the significant increase in HPS VEGF level compared to normal serum, and the significantly lower concentration of platelet-derived angiogenic inhibitors TSP-1 and PF-4 in HPP compared to HPS (Figure 2). While it has been reported that angiogenic inhibitors may have some elective effects on the formation of blood vessels, it remains unclear whether they also have additional inhibitory effects on lymphangiogenesis [42]. Our data showed a greater concentration of TSP-1 in HPS, compared to normal serum, suggesting that hypoxia-induced upregulation of TSP-1 was responsible for reaching a level beyond what is normally achieved through platelet activation. Various studies have demonstrated that TSP-1 acts as an inhibitor of inflammatory lymphangiogenesis *in vitro* and *in vivo* [18,21]. For example, exposure of macrophages to TSP-1 suppresses the expression of lymphangiogenic factors (VEGF-C and VEGF-D), while the absence of TSP-1 leads to a significant increase in lymphangiogenesis in a model of inflammation [18]. The identification of TSP-1 as an endogenous inhibitor of lymphangiogenesis opens new avenues for understanding the complex interaction between this process and angiogenesis. Of equal importance, we found a significantly lower PF-4 concentration in HPP compared to HPS

(Figure 2C). The literature suggests that PF-4 is able to dose-dependent inhibit the migration and proliferation of lymphatic endothelial cells [22]. Further work is required before clarifying whether the relative advantage of HPS, in having a higher VEGF concentration than HPP, is partly or even fully offset by its higher concentration of inhibitory factors, such as TSP-1 and PF-4, when considering the secretomes' bioactivity in the context of lymphangiogenesis.

Hypoxia preconditioned blood-derived secretomes (HPP, HPS) appeared to promote stronger microvessel sprouting in the aortic ring assay compared to normal plasma and serum (Figure 3A). The pro-angiogenic effect of hypoxic conditioning, also evident in a significantly higher number of HPP-induced sprouts compared to ADCS and pure VEGF (pos. controls) (Figure 3B), was in line with the ELISA results. There were no significant differences in sprout number or length between HPP and HPS (Figure 3B,C), suggesting that while pro-angiogenic factors, such as VEGF, are important for angiogenic sprouting, this process is not directly inhibited/limited by the presence of anti-angiogenic factors, e.g., TSP-1, PF-4, in agreement with our previous findings [28,29].

In order to more precisely quantify the lymphatic sprouting response in cultured thoracic duct rings, that were obtained through a technically demanding microsurgical preparation, the lymphatic origin of capillary-like structures observed to emerge from rings was first assessed with Anti-LYVE-1 immunohistochemical staining (Figure 4A), before quantifying the lymph-specific polydom concentration in culture supernatants (Figure 4B). Polydom is a large extracellular matrix protein of >300 kDa expressed in cultured bone marrow stromal cells and a high-affinity ligand for integrin $\alpha 9\beta 1$, a cell adhesion receptor involved in lymphangiogenesis [38], which affects remodeling of lymphatic vessels in both mouse and zebrafish [38]. However, its physiological function remains unclear [38,39]. Here, a lower polydom concentration was recorded in HPP/HPS culture supernatants, a finding that is inherently difficult to explain. Provided that these secretomes promoted stronger lymphatic sprouting compared to normal plasma/serum and PBS negative control, as it was directly evident by immunohistochemical analysis (Figure 4A), it is indeed possible that in these cultures there was less unbound polydom protein available for leaking into the medium, which further implies that polydom may be involved in lymphatic sprouting. Further studies are required, however, before this basic hypothesis can be properly tested, which will also aid the understanding of the exact function of polydom in lymphangiogenesis.

Following this double validation method, we analyzed the ability of hypoxia preconditioned blood-derived secretomes to induce lymphatic sprouting in the thoracic duct ring assay. Like angiogenic sprouting, lymphatic sprouting is a complex process that depends on multiple cellular events, including cellular outgrowth from a preexisting lymphatic vessel, endothelial cell proliferation, migration and differentiation into capillary structures [37]. The thoracic duct ring assay forms an adaptation of the aortic ring assay, that has proved to be a useful tool for investigating sprouting angiogenesis [36,37,43], and was therefore also applied here. Our hypothesis that hypoxia preconditioned secretomes support lymphatic sprouting could be confirmed by the finding that both HPP and HPS induced more sprouting than non-hypoxia preconditioned secretomes (normal plasma and serum), as well as negative control PBS samples (Figure 5A,B). Importantly, the HPS-induced response was not weaker than that elicited by the lymphangiogenic stimulators FCS and ADCS [31,37], used here as positive controls (Figure 3B). In contrast, there appeared to be a delay in the HPP-induced response, which could first be observed on day 6 (i.e., later than 4 days, as for HPS), while the number of lymphatic sprouts was significantly lower than in FCS cultures (Figure 5B). It can therefore be concluded that HPS has a greater lymphatic sprouting activity than HPP, at least in vitro (note: it is unlikely that any difference seen was due to residual heparin in HPP, since we have previously shown that heparin does not either promote or inhibit angiogenic sprouting [28]). When attempting to understand why this might be the case, it is important to consider that lymphatic regeneration most likely begins/takes place during the inflammatory phase of wound healing (as also highlighted by the day 4 induction of sprouting in HPS cultures), and therefore likely requires platelet-derived signaling. This suggests that the presence of inhibitory factors, such as TSP-1 and PF-4, in HPS is not only counterproductive towards lymphatic

sprouting, but very likely a key pre-requisite for an optimal response. Indeed, we could previously show that blocking PF-4 activity in the wound microenvironment using anti-PF-4 appeared to inhibit, rather than enhance angiogenic sprouting [29], which could mechanistically be explained through the regulation of matrix remodelling by MMPs expressed in vascular endothelial cells [44]. It appears then that PF-4 may exert an inhibitory effect on angiogenic sprouting at higher concentrations, but a minimum amount of this factor is nonetheless necessary for initiation of the sprouting process [29]. Our current findings point to the idea that this might also hold true for lymphatic sprouting. Admittedly, further work is necessary for better understanding the role of TPS-1 and PF-4 in lymphangiogenesis.

5. Conclusion

The data presented here provide supporting evidence to our previous findings, and offer further insight into the clinical utility of hypoxia preconditioned blood-derived secretomes as a tool for stimulating lymphangiogenesis. Our results suggest that HPS may be a better alternative to HPP when choosing an autologous growth factor composition to promote lymphatic sprouting, and by extension lymphatic vessel regeneration. Importantly, this work contributes to the idea that angiogenesis and lymphangiogenesis have symbiotic roles in wound healing and tissue repair, since they both appear to rely on overlapping growth factor mechanisms.

Author Contributions: Conceptualization, P.M., A.F.S., E.H., U.D.; methodology, P.M., R.S., A.S., E.H., U.D.; software, P.M., R.S., A.S., E.H., U.D.; validation, P.M., R.S., A.S.; formal analysis, P.M., R.S., A.S., E.H., U.D.; investigation, P.M., R.S., A.S.; resources, H.-G.M.; data curation, P.M., R.S., A.S., U.D.; writing—original draft preparation, P.M., E.H., U.D.; writing—review and editing, P.M., E.H., U.D.; visualization, P.M., E.H., U.D.; supervision, E.H., U.D.; project administration, H.-G.M., E.H., U.D.; funding acquisition, H.-G.M. All authors have read and agreed to the published version of the manuscript.

Funding: This research received no external funding.

Conflicts of Interest: The authors declare no conflict of interest. The blood donors involved in this study do not have any direct relationship or dependency relationship with the project leader. This study was carried out under the umbrella of the EmaCure Project (for more info please visit www.emacure.org).

Abbreviations

ADCS	adipose-derived cell suspension
ASC	adipose-derived stem cells
EWS	extracorporeal wound simulation
FCS	fetal calf serum
HPP	hypoxia preconditioned plasma
HPS	hypoxia preconditioned serum
LYVE-1	lymphatic vessel endothelial hyaluronan receptor-1
PBC	peripheral blood cells
PBS	phosphate buffered saline
PF-4	platelet factor-4
TSP-1	thrombospondin-1
VEGF	vascular endothelial growth factor
FGF	fibroblast growth factor
MMP	matrix metalloproteinase

References

- Owlarn, S.; Klenner, F.; Schmidt, D.; Rabert, F.; Tomasso, A.; Reuter, H.; Mulaw, M.A.; Moritz, S.; Gentile, L.; Weidinger, G.; et al. Generic wound signals initiate regeneration in missing-tissue contexts. *Nat. Commun.* **2017**, *8*, 2282. [[CrossRef](#)] [[PubMed](#)]
- Zhang, L.; Yin, H.; Lei, X.; Lau, J.N.Y.; Yuan, M.; Wang, X.; Zhang, F.; Zhou, F.; Qi, S.; Shu, B.; et al. A systematic review and meta-analysis of clinical effectiveness and safety of hydrogel dressings in the management of skin wounds. *Front. Bioeng. Biotechnol.* **2019**, *7*, 342. [[CrossRef](#)] [[PubMed](#)]

3. Han, G.; Ceilley, R. Chronic wound healing: A review of current management and treatments. *Adv. Ther.* **2017**, *34*, 599–610. [[CrossRef](#)] [[PubMed](#)]
4. Shi, C.; Wang, C.; Liu, H.; Li, Q.; Li, R.; Zhang, Y.; Liu, Y.; Shao, Y.; Wang, J. Selection of appropriate wound dressing for various wounds. *Front. Bioeng. Biotechnol.* **2020**, *8*, 182. [[CrossRef](#)] [[PubMed](#)]
5. Tammela, T.; Alitalo, K. Lymphangiogenesis: Molecular mechanisms and future promise. *Cell* **2010**, *140*, 460–476. [[CrossRef](#)] [[PubMed](#)]
6. Alderfer, A.; Wei, A.; Hanjaya-Putra, D. Lymphatic tissue engineering and regeneration. *J. Biol. Eng.* **2018**, *12*, 32. [[CrossRef](#)]
7. Skobe, M.; Detmar, M. Structure, function, and molecular control of the skin lymphatic system. *J. Investig. Dermatol. Symp. Proc.* **2000**, *5*, 14–19. [[CrossRef](#)] [[PubMed](#)]
8. Wiig, H.; Swartz, M. Interstitial fluid and lymph formation and transport: Physiological regulation and roles in inflammation and cancer. *Physiol. Rev.* **2012**, *92*, 1005–1060. [[CrossRef](#)]
9. Schapper, M.; Jeltsch, M.; Rohringer, S.; Redl, H.; Holthöner, W. Lymphatic vessels in regenerative medicine and tissue engineering. *Tissue Eng. Part B Rev.* **2016**, *22*, 395–407. [[CrossRef](#)]
10. Dixon, J.B.; Raghunathan, S.; Swartz, M.A. A tissue-engineered model of the intestinal lacteal for evaluating lipid transport by lymphatics. *Biotechnol. Bioeng.* **2009**, *103*, 1224–1235. [[CrossRef](#)]
11. Alitalo, K. The lymphatic vasculature in disease. *Nat. Med.* **2011**, *17*, 1371–1380. [[CrossRef](#)] [[PubMed](#)]
12. Baluk, P.; Tammela, T.; Ator, E.; Lyubynska, N.; Achen, M.G.; Hicklin, D.J.; Jeltsch, M.; Petrova, T.V.; Pytowski, B.; Stacker, S.A.; et al. Pathogenesis of persistent lymphatic vessel hyperplasia in chronic airway inflammation. *J. Clin. Invest.* **2005**, *115*, 247–257. [[CrossRef](#)] [[PubMed](#)]
13. Kataru, R.P.; Jung, K.; Jang, C.; Yang, H.; Schwendener, R.A.; Baik, J.E.; Han, S.H.; Alitalo, K.; Koh, G.H. Critical role of CD11b+ macrophages and VEGF in inflammatory lymphangiogenesis, antigen clearance and inflammation resolution. *Blood* **2009**, *113*, 5650–5659. [[CrossRef](#)] [[PubMed](#)]
14. Huggenberger, R.; Siddiqui, S.S.; Brander, D.; Ullmann, S.; Zimmermann, K.; Antsiferova, M.; Werner, S.; Alitalo, K.; Detmar, M. An important role of lymphatic vessel activation in limiting acute inflammation. *Blood* **2011**, *117*, 4667–4678. [[CrossRef](#)] [[PubMed](#)]
15. Marino, D.; Luginbühl, J.; Scola, S.; Meuli, M.; Reichmann, E. Bioengineering dermo-epidermal skin grafts with blood and lymphatic capillaries. *Sci. Transl. Med.* **2014**, *6*, 221. [[CrossRef](#)]
16. Hanjaya-Putra, D.; Shen, Y.I.; Wilson, A.; Fox-Talbot, K.; Khetan, S.; Burdick, J.A.; Steenbergen, C.; Gerecht, S. Integration and regression of implanted engineered human vascular networks during deep wound healing. *Stem. Cells Transl. Med.* **2013**, *2*, 297–306. [[CrossRef](#)]
17. Tammela, T.; Enholm, B.; Alitalo, K.; Paavonen, K. The biology of vascular endothelial growth factors. *Cardiovasc Res.* **2005**, *65*, 550–563. [[CrossRef](#)]
18. Cursiefen, C.; Maruyama, K.; Bock, F.; Saban, D.; Sadrai, Z.; Lawler, J.; Dana, R.; Masli, S. Thrombospondin 1 inhibits inflammatory lymphangiogenesis by CD36 ligation on monocytes. *J. Exp. Med.* **2011**, *208*, 1083–1092. [[CrossRef](#)]
19. Wong, B.W. Lymphatic vessels in solid organ transplantation and immunobiology. *Am. J. Transplant.* **2020**, *20*, 1992–2000. [[CrossRef](#)]
20. Karpanen, T.; Alitalo, K. Molecular biology and pathology of lymphangiogenesis. *Annu. Rev. Pathol.* **2007**, *3*, 367–397. [[CrossRef](#)]
21. Schöllhorn, L.; Bock, F.; Cursiefen, C. Thrombospondin-1 as a regulator of corneal inflammation and lymphangiogenesis: Effects on dry eye disease and corneal graft immunology. *J. Ocul. Pharmacol. Ther.* **2015**, *31*, 376–385. [[CrossRef](#)] [[PubMed](#)]
22. Shao, X.J.; Xie, F.M. Influence of angiogenesis inhibitors, endostatin and PF-4, on lymphangiogenesis. *Lymphology* **2005**, *38*, 1–8. [[PubMed](#)]
23. Hadjipanayi, E.; Bauer, A.T.; Moog, P.; Salgin, B.; Kükrek, H.; Fersch, B.; Hopfner, U.; Meissner, T.; Schlüter, A.; Ninkovic, M.; et al. Cell-free carrier system for localised delivery of peripheral blood cell-derived engineered factor signaling: Towards development of a one-step device for autologous angiogenic therapy. *J. Control. Release* **2013**, *169*, 91–102. [[CrossRef](#)] [[PubMed](#)]
24. Hadjipanayi, E.; Schilling, A.F. Hypoxia-based strategies for angiogenic induction. *Organog. Landes Biosci.* **2013**, *9*, 1–12. [[CrossRef](#)] [[PubMed](#)]
25. Hadjipanayi, E.; Schilling, A.F. Regeneration through autologous hypoxia preconditioned plasma. *Organogenesis* **2014**, *10*, 164–169. [[CrossRef](#)] [[PubMed](#)]

26. Hadjipanayi, E.; Bekeran, S.; Moog, P. Extracorporeal wound simulation as a foundation for tissue repair and regeneration therapies. *Int. J. Transpl. Plast. Surg.* **2018**, *2*, 1–10.
27. Hadjipanayi, E.; Moog, P.; Bekeran, S.; Kirchhoff, K.; Bereznoi, A.; Aguirre, J.; Bauer, A.T.; Kükrek, H.; Schmauss, D.; Hopfner, U.; et al. In vitro characterization of hypoxia preconditioned serum (HPS)-fibrin hydrogels: Basis for an injectable biomimetic tissue regeneration therapy. *J. Funct. Biomater.* **2019**, *13*, 22. [[CrossRef](#)]
28. Moog, P.; Kirchhoff, K.; Bekeran, S.; Bauer, A.T.; Isenburg, S.; Dornseifer, U.; Machens, H.G.; Schilling, A.F.; Hadjipanayi, E. Comparative evaluation of the angiogenic potential of hypoxia preconditioned blood-derived secretomes and platelet-rich plasma: An in vitro analysis. *Biomedicines* **2020**, *8*, 16. [[CrossRef](#)]
29. Hadjipanayi, E.; Kuhn, P.H.; Moog, P.; Bauer, A.T.; Kuekrek, H.; Mirzoyan, L.; Hummel, A.; Kirchhoff, K.; Salgin, B.; Isenburg, S.; et al. The fibrin matrix regulates angiogenic responses within the hemostatic microenvironment through biochemical control. *PLoS ONE* **2015**, *10*, 1–20. [[CrossRef](#)]
30. Moog, P.; Jensch, M.; Hughes, J.; Salgin, B.; Dornseifer, U.; Machens, H.G.; Schilling, A.F.; Hadjipanayi, E. Use of oral anticoagulation and diabetes do not inhibit the angiogenic potential of hypoxia preconditioned blood-derived secretomes. *Biomedicines* **2020**, *8*, 283. [[CrossRef](#)]
31. Saijo, H.; Suzuki, K.; Yoshimoto, H.; Imamura, Y.; Yamashita, S.; Tanaka, K. Paracrine effects of adipose-derived stem cells promote lymphangiogenesis in irradiated lymphatic endothelial cells. *Plast. Reconstr. Surg.* **2019**, *143*, 1189–1200. [[CrossRef](#)] [[PubMed](#)]
32. Mazini, L.; Rochette, L.; Admou, B.; Amal, S.; Malka, G. Hopes and limits of Adipose-Derived Stem Cells (ADSCs) and Mesenchymal Stem Cells (MSCs) in wound healing. *Int. J. Mol. Sci.* **2020**, *21*, 1306. [[CrossRef](#)] [[PubMed](#)]
33. Bachmann, S.; Jennewein, M.; Bubel, M.; Guthörl, S.; Pohlemann, T.; Oberringer, M. Interacting adipose-derived stem cells and microvascular endothelial cells provide a beneficial milieu for soft tissue healing. *Mol. Biol. Rep.* **2019**, *47*, 111–122. [[CrossRef](#)] [[PubMed](#)]
34. Komaki, M.; Numata, Y.; Morioka, C.; Honda, I.; Tooi, M.; Yokoyama, N.; Ayame, H.; Iwasaki, K.; Taki, A.; Oshima, N. Exosomes of human placenta-derived mesenchymal stem cells stimulate angiogenesis. *Stem. Cell Res. Ther.* **2017**, *8*, 219. [[CrossRef](#)] [[PubMed](#)]
35. Winnier, G.E.; Valnzuela, N.; Alt, C.; Alt, E.U. Isolation of adipose tissue derived regenerative cells from human subcutaneous tissue with or without the use of an enzymatic reagent. *PLoS ONE* **2018**, *14*, 1–24. [[CrossRef](#)] [[PubMed](#)]
36. Baker, M.; Robinson, S.D.; Lechertier, T.; Barber, P.R.; Tavora, B.; D’Amico, G.; Jones, D.T.; Vojnovic, B.; HodiVala-Dilke, K. Use of the mouse aortic ring assay to study angiogenesis. *Nat. Protoc.* **2011**, *7*, 89–104. [[CrossRef](#)]
37. Bruyère, F.; Melen-La, L.; Berndt, S.; Peulen, O.; Foidart, J.M.; Noël, A. The lymphatic ring assay: A 3D-culture model of lymphangiogenesis. *Protoc. Exch. (Nat. Publ. Group)* **2016**, 1–18. [[CrossRef](#)]
38. Morooka, N.; Futaki, S.; Sato-Nishiuchi, R.; Nishino, M.; Totani, Y.; Shimono, C.; Nakano, I.; Nakajima, H.; Mochizuki, N.; Sekiguchi, K. Polydom is an extracellular matrix protein involved in lymphatic vessel remodeling. *Circ. Res.* **2017**, *120*, 1276–1288. [[CrossRef](#)]
39. Karpanen, T.; Padberg, Y.; van de Pavert, S.A.; Dierkes, C.; Morooka, N.; Peterson-Maduro, J.; van de Hoek, G.; Adrian, M.; Mochizuki, N.; Sekiguchi, K.; et al. An evolutionarily conserved role for polydom/svep1 during lymphatic vessel formation. *Circ. Res.* **2017**, *120*, 1263–1275. [[CrossRef](#)]
40. Liu, Y.; Cox, S.R.; Morita, T.; Kourembanas, S. Hypoxia regulates vascular endothelial growth factor gene expression in endothelial cells. Identification of a 5′ enhancer. *Circ. Res.* **1995**, *77*, 638–643. [[CrossRef](#)]
41. Sumi, M.; Sata, M.; Toya, N.; Yanaga, K.; Ohki, T.; Nagai, R. Transplantation of adipose stromal cells, but not mature adipocytes, augments ischemia-induced angiogenesis. *Life Sci.* **2007**, *80*, 559–565. [[CrossRef](#)] [[PubMed](#)]
42. Hawighorst, T. Angiogenesis, lymphangiogenesis, and tumor progression. *Zent. Gynakol* **2002**, *124*, 497–505.

43. Nicosia, R.F.; Ottinetti, A. Growth of microvessels in serum- free matrix culture of rat aorta. A quantitative assay of angiogenesis in vitro. *Lab Invest.* **1990**, *63*, 115–122. [[PubMed](#)]
44. Klein-Soyer, C.; Duhamel-Clerin, E.; Ravanat, C.; Orvain, C.; Lanza, F.; Cazenave, J.P. PF4 inhibits thrombin-stimulated MMP-1 and MMP-3 metalloproteinase expression in human vascular endothelial cells. *C R Acad. Sci.* **1997**, *320*, 857–868. [[CrossRef](#)]



© 2020 by the authors. Licensee MDPI, Basel, Switzerland. This article is an open access article distributed under the terms and conditions of the Creative Commons Attribution (CC BY) license (<http://creativecommons.org/licenses/by/4.0/>).



Article

Febuxostat, a Xanthine Oxidase Inhibitor, Decreased Macrophage Matrix Metalloproteinase Expression in Hypoxia

Shuoyu Wei ¹, Takayuki Isagawa ^{1,2,*}, Masamichi Eguchi ¹, Daisuke Sato ¹, Hiroto Tsukano ³, Keishi Miyata ³, Yuichi Oike ³, Norihiko Takeda ⁴, Satoshi Ikeda ¹, Hiroaki Kawano ¹ and Koji Maemura ^{1,*}

¹ Department of Cardiovascular Medicine, Nagasaki University Graduate School of Biomedical Sciences, Sakamoto, Nagasaki 852-8501, Japan; bb55316008@ms.nagasaki-u.ac.jp (S.W.); masa5555@nagasaki-u.ac.jp (M.E.); daisukes@nagasaki-u.ac.jp (D.S.); siked@nagasaki-u.ac.jp (S.I.); hkawano@nagasaki-u.ac.jp (H.K.)

² Center for Data Science, Jichi Medical University, Shimotsuke, Tochigi 329-0498, Japan

³ Department of Molecular Genetics, Graduate School of Medical Sciences, Kumamoto University, Chuo-ku, Kumamoto 860-8556, Japan; chukano@sings.jp (H.T.); hully@gpo.kumamoto-u.ac.jp (K.M.); oike@gpo.kumamoto-u.ac.jp (Y.O.)

⁴ Division of Cardiology and Metabolism, Center for Molecular Medicine, Jichi Medical University, Shimotsuke, Tochigi 329-0498, Japan; ntakeda-ky@jichi.ac.jp

* Correspondence: i-takayuki13@jichi.ac.jp (T.I.); maemura@nagasaki-u.ac.jp (K.M.)

Received: 9 October 2020; Accepted: 30 October 2020; Published: 3 November 2020

Abstract: Macrophages in the atheroma region produce matrix metalloproteinases (MMPs) and decrease plaque stability. Tissue oxygen tension decreases in the arterial wall of the atherosclerotic region. Hypoxia inducible factor (HIF)-1 α plays a critical role in the transcriptional activation of hypoxia inducible genes. However, the precise roles of HIF-1 α independent pathways in hypoxic responses are largely unknown. Xanthine oxidase (XO) is an enzyme that utilizes molecular oxygen and produces reactive oxygen species (ROS). Here, we show that ROS derived from XO increases MMP-3, -10, and -13 expression in murine macrophages. We found that the transcript levels of macrophage MMP-3, -10, and -13 were increased in hypoxic conditions. Hypoxia induced MMP expression in HIF-1 α deficient macrophages. *N*-acetylcysteine (NAC) or febuxostat, an XO inhibitor, suppressed MMP expression in murine macrophages. Febuxostat decreased the incidence of plaque rupture in apolipoprotein-E-deficient mice. Our results indicate that febuxostat stabilized atherosclerotic plaque via suppressing the activities of macrophage MMP-9 and -13. Febuxostat administration is a potential therapeutic option in the management of atherosclerotic patients.

Keywords: hypoxia; macrophage; matrix metalloproteinase; atherosclerotic plaque rupture; oxidative stress; xanthine oxidase

1. Introduction

The incidence rate of cardiovascular events, including ischemic heart diseases and stroke, is increasing annually worldwide. Thrombosis caused by atherosclerotic plaque rupture leads to acute myocardial infarction, unstable angina, and sudden death from ischemic heart disease, known as acute coronary syndrome [1–3]. Therefore, it is important to understand the mechanisms of atherosclerotic plaque vulnerability and rupture to prevent acute coronary syndrome. The features of plaque vulnerability include a large necrotic core, high infiltration of inflammatory macrophages, and a thin fibrous cap composed of a small number of collagen fibers. Macrophages are immune cells abundant in atherosclerotic lesions, and they play pivotal roles in the initiation and progression of

atherosclerosis. Plaque macrophages express matrix metalloproteinases (MMPs) and weaken the fibrous cap of plaque by degrading extracellular matrix molecules [4,5]. Plaques with a weakened fibrous cap may rupture and cause thrombosis.

Hypoxic environments in plaque lesions have been shown to accelerate atherosclerosis progression [6,7]. The arterial wall of an atherosclerotic plaque is thickened as atherosclerosis progresses; therefore, the diffusion efficiency of oxygen is reduced [8]. In parallel, the oxygen consumption within atherosclerotic plaque lesions is increased by the metabolic activation of infiltrated immune cells, leading to hypoxia [9,10]. It has been suggested that hypoxia activates the expression and secretion of MMPs in atherosclerotic lesions and contributes to plaque instability by degrading extracellular matrix proteins [7,11]. Hypoxia has been shown to produce reactive oxygen species (ROS) [12–15], leading to the development of atherosclerosis, ischemia-reperfusion injury, cardiomyopathy, and heart failure. Hypoxia inducible factor (HIF)-1 α plays an integral role during the transcriptional response to hypoxia [16]. We and others have previously shown that HIF signaling significantly modulates macrophage functions, including cytokine production and migratory capacity [17–19]. Xanthine oxidase (XO) is an oxygen-consuming enzyme that oxidizes hypoxanthine or xanthine and produces ROS. While local oxygen tension could affect XO activity and ROS production, the roles of XO in macrophage function are not yet fully elucidated.

In this study, we tested the roles of XO in macrophage activation using an XO inhibitor, febuxostat. Febuxostat suppressed hypoxic induction of MMP-3, -10, and -13 in murine macrophages. Furthermore, febuxostat reduced the incidence of atherosclerotic plaque rupture in apolipoprotein-E (apoE) deficient mice. These results demonstrate that febuxostat administration is a potential therapeutic option in the management of atheromatous patients as it suppresses macrophage MMP activities.

2. Results

2.1. Hypoxic Stimulation-Induced mRNA Expression of MMP-3, -10, and -13 in Thioglycollate-Elicited Peritoneal Macrophages (TEPMs) in a HIF-1 α -Independent Manner

Macrophages in atherosclerotic plaque are exposed to hypoxic conditions [20]. Therefore, to examine the expression level of various MMP mRNAs under hypoxic conditions (1% oxygen concentration), primary TEPMs were isolated from mice. It was found that mRNAs of MMP-3, -10, and -13 were significantly increased under hypoxia (Figure 1), whereas the expression of other MMPs was unaffected (Figure 1 and data not shown). HIF-1 α is the central regulator of the cellular response to hypoxia. Thus, to examine whether HIF-1 α was involved in hypoxia-induced elevation of these MMP gene expressions, primary TEPMs were isolated from hematopoietic/endothelial-specific HIF-1 α knockout mice (*HIF-1 α ^{fllox/fllox}; Tie2-cre^{+/-}* mice; HIF-1 α KO) or cre-negative littermate controls. *Pgk1* mRNA, well-known as a HIF-1 α target gene, was significantly reduced in HIF-1 α KO TEPMs (Figure 2a). However, MMP-3, -10, and -13 mRNAs were induced under hypoxic conditions in HIF-1 α KO TEPMs, as in wild-type TEPMs (Figure 2a,b). These results showed that hypoxia increased MMP-3, -10, and -13 mRNAs in a HIF-1 α -independent manner.

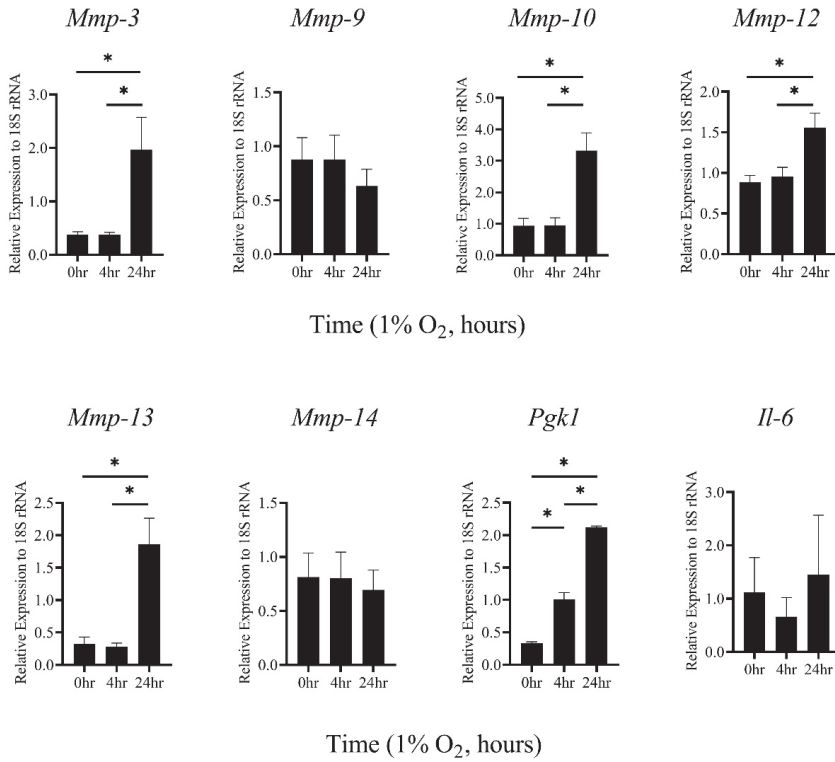


Figure 1. *MMP-3*, *-10*, and *-13* mRNAs in TEPMs are induced by hypoxia. TEPMs were exposed to hypoxia (1% O₂), and the relative expression level of *MMPs* mRNAs was analyzed. Data are the means and SE of at least three independent experiments. The one-way ANOVA and Tukey’s multiple comparisons test were performed for the statistical analysis. * *p* < 0.05.

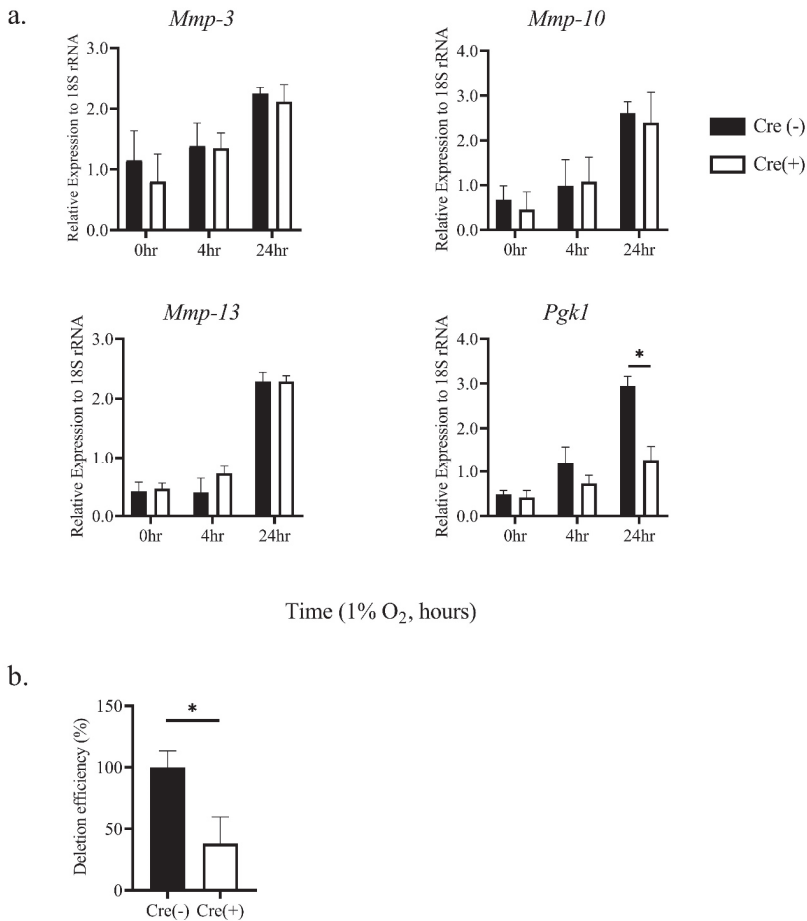


Figure 2. Hypoxic induction of *MMP-3*, *-10*, and *-13* mRNAs is independent of HIF-1 α activity. (a) TEPMs were isolated from hematopoietic/endothelial-specific *HIF-1 α* knockout mice (Cre (+)) or cre-negative littermates (Cre (-)) as a control. TEPMs were exposed to hypoxia (1% O₂), and the relative expression levels of *MMP-3*, *-10*, and *-13* mRNAs were analyzed. Quantitative PCR analysis was repeated in at least three independent experiments. The two-way ANOVA and Tukey’s multiple comparisons test were performed for the statistical analysis. * $p < 0.05$. (b) The deletion efficiency of *HIF-1 α* mRNA in TEPMs was examined. Data are the means and SE of at least three independent experiments. The unpaired *t*-test was performed for the statistical analysis. * $p < 0.05$.

2.2. The Induction of *MMP-3* and *-10* mRNAs by Hypoxia Was Dependent on ROS Generated through XO Activity

Cells cultured under hypoxic conditions have elevated intracellular ROS [12,21]. We hypothesized that such elevated ROS in TEPMs might be responsible for the increased expression of *MMP-3*, *-10*, and *-13* mRNAs. To test this, we asked whether the ROS scavenger *N*-acetyl-L-cysteine (NAC) could attenuate the expression of these MMPs under hypoxic conditions. The treatment with NAC significantly suppressed hypoxic elevation of *MMP-3*, *-10*, and *-13* mRNAs (Figure 3a). It is well-known that intracellular ROS is mainly derived from mitochondria, NADPH oxidase, and xanthine oxidase (XO) [22,23]. To identify which ROS sources were involved in the up-regulation of *MMP-3*, *-10*, and *-13* mRNAs under hypoxic conditions, selective inhibitions of mitochondrial ROS with Mito-TEMPO,

NADPH oxidase with VAS2870, and XO with febuxostat were performed. While *MMP-13* was not suppressed by any inhibitors, hypoxic induction of *MMP-3* and *-10* mRNAs was significantly suppressed by febuxostat, but not Mito-TEMPO and VAS2870 (Figure 3b–d). Moreover, ROS signaling by XO under hypoxia did not affect the accumulation and transcriptional activity of HIF-1 α protein (Supplementary Figure S1a–c). These findings suggest that ROS derived from XO contributes to the hypoxia-induced elevation of *MMP-3* and *-10* mRNAs in TEPMs independent of HIF-1 α signaling.

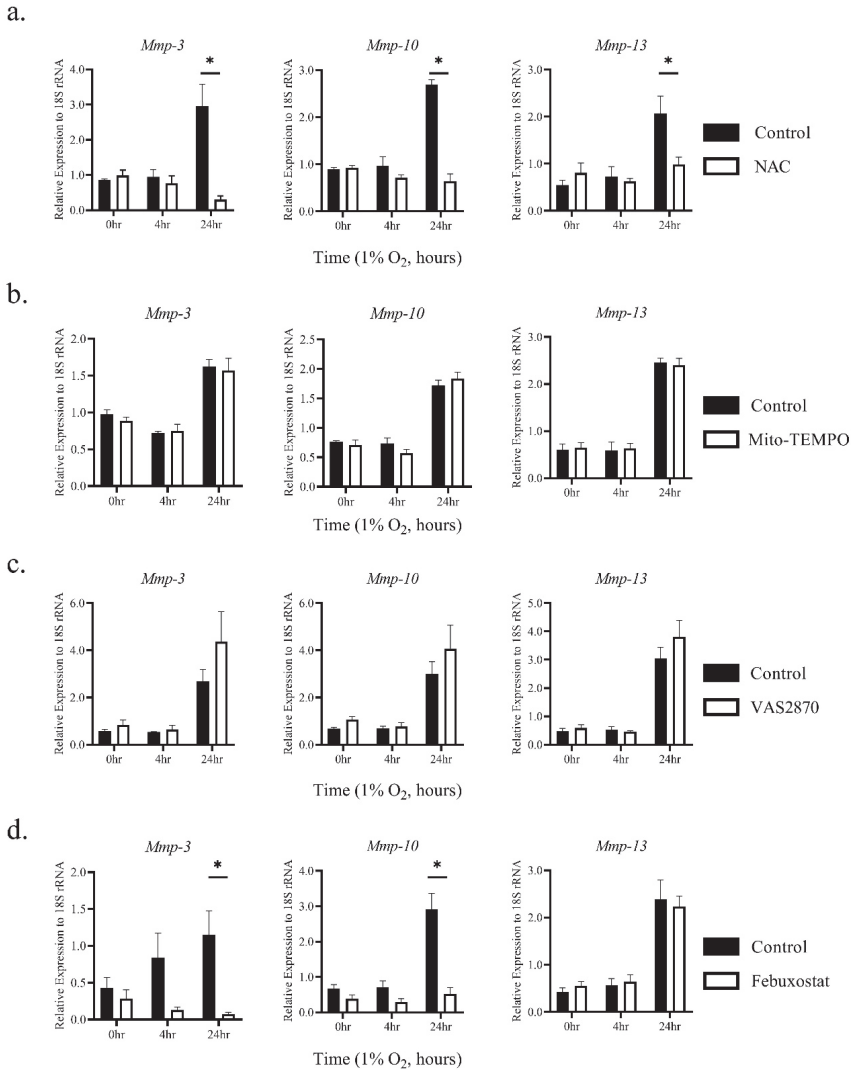
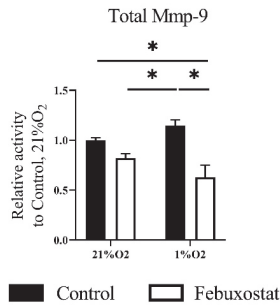


Figure 3. Hypoxia induces *MMP-3* and *MMP-10* mRNAs in TEPMs through reactive oxygen species (ROS) derived from xanthine oxidase (XO). TEPMs were exposed to hypoxia (1% O₂) after pretreatment with dimethyl sulfoxide (DMSO) (control), (a) 10 mM *N*-Acetyl-L-cysteine (NAC) (anti-oxidant), (b) 50 μ M Mito-TEMPO, (c) 2 μ M VAS2870, or (d) 50 μ M febuxostat for 1 h. Data are the means and SE of at least three independent experiments. The two-way ANOVA and Tukey’s multiple comparisons test were performed for the statistical analysis. * $p < 0.05$.

2.3. Hypoxia Activates MMPs via ROS Derived from XO

It was previously reported that MMP-3 and -10, also known as stromelysin-1 and 2, digest several extracellular matrix proteins but not interstitial collagen. Furthermore, these MMPs participate in proMMP activation for tissue remodeling. Stromelysin-1 (MMP-3) activates gelatinase B (MMP-9) in vascular smooth muscle cells (VSMCs), and contributes to neointima formation [24]. On the other hand, Stromelysin-2 (MMP-10) is expressed in macrophages. MMP-10-deficient macrophages reduce collagenolytic activity, particularly MMP-13 [25]. Therefore, to examine the hypothesis that febuxostat attenuates collagenolytic and gelatinolytic activity in macrophages, we measured MMP activity in culture media of macrophages by in-gel zymography [9,26]. The zymographic analysis showed that febuxostat significantly suppressed collagenolytic and gelatinolytic activity in macrophages (Figure 4a,b). These results suggest that inhibition of XO signaling attenuated the activity of collagenase and gelatinase in TEPMs.

a.



b.

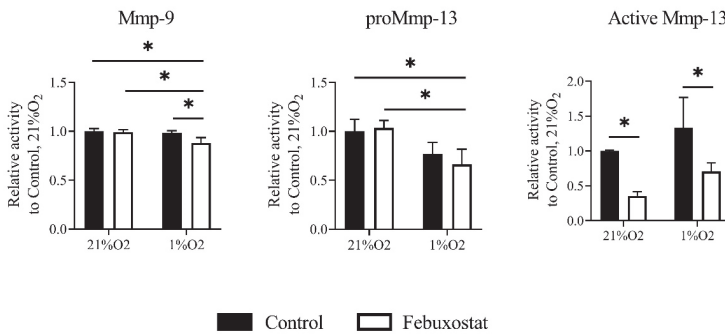


Figure 4. Inhibition of ROS production by XO attenuates gelatinolytic and collagenolytic activity in TEPMs. TEPMs were cultured under normoxic (21% O₂) and hypoxic (1% O₂) conditions in the presence of DMSO (control) or 50 μM febuxostat. MMP activity in the supernatants was assayed by in-gel zymography. (a) The activities of MMP-9 was assayed by gelatin zymography. (b) The activities of MMP-9 and 13 were assayed by collagen zymography. The quantification of MMP activity was performed using a densitometry analytic tool (Supplementary Figure S2). Data are expressed as the means ± SD of three independent experiments. The two-way ANOVA and Tukey’s multiple comparisons test were performed for the statistical analysis. * $p < 0.05$.

2.4. XO Inhibitor Suppresses the Rupture of Atherosclerotic Plaques in Mice

MMP production from macrophages contributes to atherosclerotic plaque instability and rupture [4]. It was examined whether XO signaling contributed to the vulnerability of atherosclerotic plaques using an atherosclerotic plaque rupture mouse model generated by the ligation and cuff placement method (Figure 5a) [27]. Atherosclerotic lesions were formed (Figure 5b) as follows: 15 mg/L febuxostat was continuously administered to these mice via their drinking water for 32 days. The mice were then euthanized to perform histological analyses. As shown in Figure 5c, the average number of plaque rupture lesions was significantly decreased in mice that drank the water containing febuxostat. These findings suggest that XO activity contributed to the instability of atherosclerotic plaques through MMP.

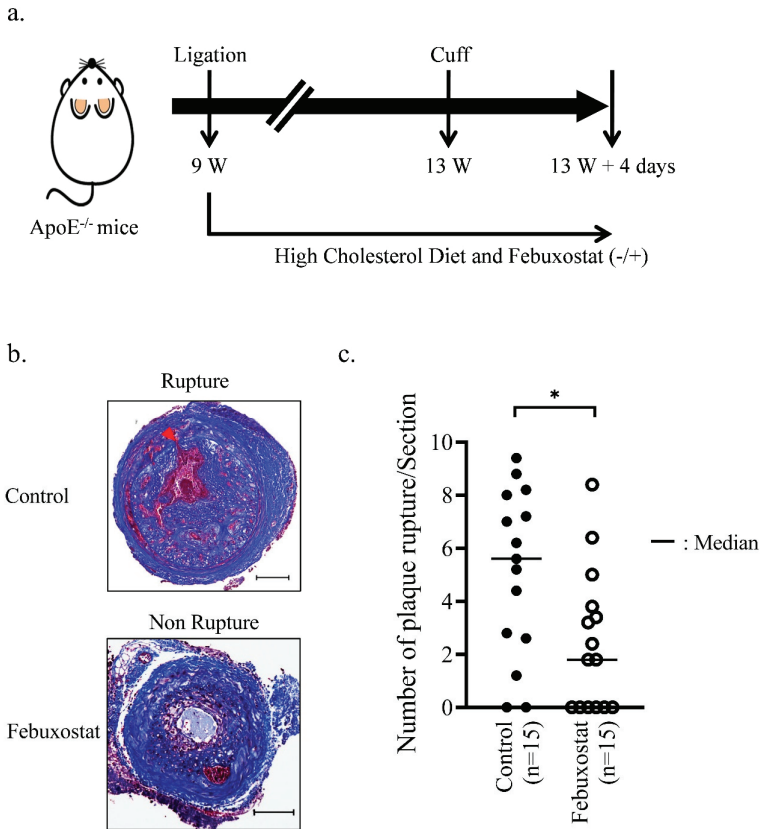


Figure 5. Febuxostat treatment reduces rupture events of the common carotid artery. (a) Schematic diagram of the operation for the atherosclerotic plaque rupture model. After the carotid artery ligation, mice were divided into the experimental and the control groups, and then fed a high-cholesterol diet. The experimental group was given drinking water containing 0.015 mg/mL of febuxostat. (b) Representative images of pathological alterations in the plaque rupture mouse model. Masson’s trichrome staining were performed using sections of the common carotid artery from *ApoE*^{-/-} male mice fed a high-cholesterol diet for 4 weeks after ligation. Representative photographs show non-ruptured and ruptured vessels. The black bar indicates 100 μ m. (c) The number of plaque ruptures was quantitatively analyzed by counting the number of internal elastic lamina breaks (arrowhead) in the Febuxostat group ($n = 15$) and the Control group ($n = 15$). The Mann-Whitney U test was used to compare differences between the control group and Febuxostat group. * $p < 0.05$.

3. Discussion

It is well understood that inflammatory macrophages contribute to atherosclerotic plaques' formation and vulnerability [28]. The microenvironment in atherosclerotic plaques contains various oxidized lipids and cytokines. Macrophages are exposed to these stimuli, resulting in the inflammatory phenotype. These inflammatory macrophages express and secrete pro-inflammatory cytokines and MMPs. Macrophages in atherosclerotic lesions have strong proteolytic activity and cause the vulnerability and rupture of plaques. At the same time, it has also been reported that the macrophage-rich region in human carotid atherosclerotic lesions is a hypoxic environment [20]. Therefore, macrophages within atherosclerotic plaques are exposed to not only inflammatory but also hypoxic environments. However, little is known about whether hypoxic stress on macrophages affects atherosclerotic plaque progression.

The present study reveals that hypoxic stress to macrophages induces the expression of *MMP-3*, *-10*, and *-13* mRNAs, and activates gelatinolytic and collagenolytic activity. It was previously reported that *MMP-3*, *-10*, and *-13* were involved in the development of atherosclerotic lesions and plaque progression [29–32]. *MMP-3* was one of the first MMPs identified in atherosclerotic plaques, and it is expressed in macrophages, as well as lymphocytes and activated VSMCs [5]. The *MMP-3* knockout mice showed a reduction in intimal growth caused by the ligation of carotid arteries. *MMP-10* expression in the atherosclerotic lesion is mainly localized in macrophage-like cells, and it is necessary for collagenolytic activity. *MMP-10/ApoE* double knockout (DKO) mice show decreased atherosclerotic lesion size and plaque calcification. *MMP-13* mRNA was abundantly expressed in macrophages. *MMP-13/ApoE* DKO mice showed the accumulation of collagen in the plaque and resulted in plaque stabilization. These previous reports and the present study suggest that hypoxic signaling in macrophages causes instability and rupture of atherosclerotic plaques by expressing *MMP-3*, *-10*, and *-13*.

Intriguingly, the hypoxic induction of *MMP-3* and *-10* mRNAs was dependent on ROS generated by XO, but not HIF-1 α , which is known as the central regulator of the hypoxic response. Previous studies have reported that hypoxia activates p38/SAPK2, JNK/SAPK, and Akt/PKB signaling [33–35]. In addition, it has been reported that ROS also activates p38, JNK, and Akt kinases [36,37]. Actually, we confirmed that inhibitors of p38 and JNK suppress the hypoxic induction of *MMP-3*, *-10*, and *-13* mRNAs (data not shown). Therefore, we consider that ROS production under the hypoxic condition induces *MMP-3*, *-10*, and *-13* mRNAs via the activation of these kinases.

At the same time, it is known that ROS interacts with the Cys thiol within the catalytic domain of MMPs, which disrupts the interaction with the catalytic Zn²⁺ ion and leads to autocatalytic activation. Previous studies report that ROS activates various proMMPs, including *MMP-1*, *MMP-2*, *MMP-7*, *MMP-8*, and *MMP-9* [38–43]. Therefore, there is a possibility that our in-gel zymographic analysis shows the activation of gelatinase and collagenase by not only *MMP-3* and *-10* but also ROS as the direct effect. Further investigations are needed to elucidate the detailed mechanisms of the hypoxic induction and activation of these MMPs.

Moreover, febuxostat significantly inhibited the production of *MMP-9* and the activation of *MMP-13* even under normoxic conditions. Previous studies reported that ROS activates MMP secretion [44,45]. In general, the mitochondria respiratory chain (MRC) consumes most oxygen in cells, and 2–4% of total oxygen consumption goes toward the generation of ROS instead of ATP synthesis [46]. Therefore, mitochondria constitutively produce ROS. A recent study has reported that inhibition of xanthine oxidase (XDH/XO) by febuxostat causes the increment of intracellular ATP by purine salvage pathway and reduces the production of ROS from MRC under normoxic conditions [47]. Thus, febuxostat may affect the production and activation of MMPs by reducing ROS derived from MRC under normoxic conditions. However, future studies are required to uncover the precise mechanism of inhibitory effects of febuxostat on MMP expression without transcriptional regulations.

Using the atherosclerotic plaque rupture mouse model, this study demonstrated that febuxostat administration significantly reduced the number of plaque ruptures. Febuxostat also attenuated

collagenolytic (MMP-13) and gelatinolytic activity (MMP-9) in the culture media of macrophages. These results may indicate that the hypoxic environment accelerates atherosclerotic plaque vulnerability and rupture by activating MMPs via XO. Previous clinical trials reported that the administration of allopurinol, a purine inhibitor of XO, was associated with a lower rate of stroke and cardiac events [48,49]. Febuxostat, a nonpurine inhibitor of XO, as well as allopurinol, is used for the management of hyperuricemia in patients with gout [50]. In addition to these beneficial effects, this study suggests that the administration of an XO inhibitor could be useful for suppressing atherosclerotic plaque instability and rupture in patients.

4. Materials and Methods

4.1. Cell Culture

TEPMs were prepared from 7-week-old C57BL/6J mice by the intraperitoneal injection of 3% thioglycollate media (Fluka, Sigma-Aldrich, St Louis, MO, USA). On day 4, TEPMs were collected by peritoneal lavage with 10 mL of PBS(-) and isolated using the adherent method. TEPMs were seeded onto ϕ 6-cm dishes at 4×10^6 /dish and grown in RPMI1640 (WAKO, Osaka, Japan) containing 10% fetal bovine serum (Sigma-Aldrich, St Louis, MO, USA) at 37 °C in 5% CO₂. TEPMs were treated by the following inhibitors at the indicated concentrations in each experiment: *N*-acetyl-L-cysteine (NAC) (10 mM), Mito-TEMPO (50 μ M), VAS2870 (2 μ M), and febuxostat (50 μ M). In all experiments, TEPMs were pretreated with these inhibitors for 1 h before stimulation by hypoxia. NAC, Mito-TEMPO, and VAS2870 were purchased from Sigma-Aldrich (St Louis, MO, USA). Febuxostat was provided by Teijin Pharma Ltd., Tokyo, Japan.

4.2. Hypoxia Treatment

Cells were placed in a personal CO₂ multi-gas incubator (Model APM-30D, ASTEC, Fukuoka, Japan) calibrated to maintain a hypoxic atmosphere (1% O₂, 5% CO₂, and 94% N₂) under a continuous flow of nitrogen. A standard tissue culture incubator was used for a normoxic environment (21% O₂, 5% CO₂).

4.3. Mouse Models of Atherosclerotic Plaque Rupture

All animal experiments were approved by the Institutional Animal Care Committee of Nagasaki University (approval number: 1701251356). B6.129P2-*ApoE*^{tm1Unc}/J (*ApoE*^{-/-}) mice were kindly provided by Dr. J. Aruga (Nagasaki University, Nagasaki, Japan). To generate mouse models of atherosclerotic plaque rupture, 9-week-old male *ApoE*^{-/-} mice were fed a standard diet. The left common carotid artery of these mice was dissected and ligated proximal to the bifurcation under anesthesia. After the ligation, the mice were randomly divided into two groups, including the experimental group (febuxostat) and the normal control group (Control), and fed a high-cholesterol diet (Oriental Yeast, Tokyo, Japan). The experimental group was given drinking water containing 0.015 mg/mL of febuxostat after the ligation. At 4 weeks after the ligation of the left common carotid artery, a polyethylene cuff (length 2 mm) was placed around the left common carotid artery tightly adjacent to the site of ligation. At 4 days after cuff placement, mice were anesthetized and injected intraperitoneally with heparin. Lesions were then obtained after perfusion from the left ventricle using a normal saline solution. The vessels after cuff removal were isolated and fixed in 10% formalin overnight.

4.4. Histological and Immunohistochemical Staining

For staining, vessels were fixed in 4% formaldehyde and embedded in paraffin. Specimens were serially sectioned at 5 μ m intervals and mounted on three consecutive slides with 60- μ m intervals on glass slides. Two slides were individually stained with hematoxylin and eosin (H&E) and Masson's trichrome stains. Five serial, identically stained slides were selected from the middle part of the cuff

placement site of each vessel to count the number of internal elastic lamina breaks. The number of ruptures was taken as the average of 5 sections.

4.5. Quantitative Real-Time RT-PCR Analysis

Total RNA was purified from culture cells using the RNeasy Mini Kit (Qiagen, Thermo Fisher Scientific, Inc., Waltham, MA, USA). Complementary DNA (cDNA) was synthesized using the ReverTra Ace[®] qPCR RT Master Mix (TOYOBO, Osaka, Japan). Quantitative real-time PCR (qPCR) was performed using the THUNDERBIRD[®] SYBR[®] qPCR MIX kit (TOYOBO, Osaka, Japan). A melting curve analysis was performed to confirm the detection of a single PCR product. We performed the standard curve method for the quantitative analysis of qPCR. Then, 5, 25, 125, and 625-fold dilutions of a sample were prepared for each gene. The standard curve was drawn from the Ct values of the samples. The expression levels of each sample were calculated using the standard curve. The relative abundance of all genes of interest was normalized to the housekeeping control 18S ribosomal RNA (18S rRNA). The primer sequences of the analyzed genes are shown as follows: *MMP-3* (NCBI accession number NM_010809.2): forward 5'-TGCAGCTCTACTTTGTTCTTTGA-3', reverse 5'-AGAGATTGCGCCAAAAGTG-3'. *MMP-9* (NCBI accession number NM_013599.4): forward 5'-CGACATAGACGGCATCCAG-3', reverse 5'-CTGTCCGGCTGTGGTTCAGT-3'. *MMP-10* (NCBI accession number NM_019471.3): forward 5'-GAGTCTGGCTCATGCCTACC-3', reverse 5'-CAGGAATAAGTTGGTCCCTGA-3'. *MMP-12* (NCBI accession number NM_008605.3): forward 5'-TGATGCTGTCACAACAGTGG-3', reverse 5'-GTAATGTTGGTGGCTGGACTC-3'. *MMP-13* (NCBI accession number NM_008607.2): forward 5'-TGGACCTTCTGGTCTTCTGG-3', reverse 5'-ATGGGCAGCAACAATAAACA-3'. *MMP-14* (NCBI accession number NM_008608.4): forward 5'-GAGAACTTCGTGTGCCTGA-3', reverse 5'-CTTTGTGGGTGACCCGACT-3'. *Pgk1* (NCBI accession number NM_008828.3): forward 5'-CTGTGGTACTGAGAGCAGCAAGA-3', reverse 5'-CAGGACCATTCCAAACAATCTG-3'. *IL6* (NCBI accession number NM_031168.2): forward 5'-GATGGATGCTACCAAACCTGGAT-3', reverse 5'-CCAGGTAGCTATGGTACTCCAGA-3'. *18S rRNA* (NCBI accession number NR_003278.3 forward 5'-GCAATTATCCCCATGAACG-3', reverse 5'-GGGACTTAATCAACGCAAGC-3'.

4.6. Zymography and Quantification

TEPMs were exposed to hypoxia for 24 h in the presence or absence of febusostat, and supernatants were collected. Cell supernatants were clarified by brief centrifugation and concentrated using the Amicon Ultra-2, 3-kDa nominal molecular mass cutoff filters (Millipore, Billerica, MA, USA). The protein concentration of supernatants was determined by the BCA Protein Assay kit (Pierce, Thermo Fisher Scientific, Inc.). Equal amounts (5 µg/well) were loaded onto 10% zymogram plus (gelatin) protein gels (Novex; Thermo Fisher Scientific, Inc., Waltham, MA, USA) for the gelatin zymogram or 10% SDS-PAGE containing 0.6 mg/mL rat type I collagen (Gibco, Thermo Fisher Scientific, Inc., Waltham, MA, USA) for the collagen zymogram, and run for 90 min under a constant voltage of 125 V. Gels were incubated in a renaturing buffer (Novex; Thermo Fisher Scientific, Inc., Waltham, MA, USA), followed by incubation at 37 °C for 24 h in developing buffer (Novex; Thermo Fisher Scientific, Inc., Waltham, MA, USA). Gels were stained with the SimplyBlue SafeStain (Invitrogen, Thermo Fisher Scientific, Inc., Waltham, MA, USA). Zymograms were analyzed by densitometry analysis using the ChemiDoc Touch Imaging System (BIO RAD Laboratories Inc., Hercules, CA, USA) (Supplementary Figure S2).

4.7. Statistical Analysis

All data are shown as means with SD. Comparisons between two groups were performed using the unpaired *t*-test. *p* values of less than 0.05 were considered significant. Differences among more than two groups were analyzed using one-way or two-way ANOVA followed by Dunn's multiple comparisons test or Tukey's multiple comparisons test.

Supplementary Materials: The following are available online at <http://www.mdpi.com/2227-9059/8/11/470/s1>.

Author Contributions: Conceptualization, T.I. and K.M. (Koji Maemura); formal analysis, T.I. and S.W.; funding acquisition, T.I. and K.M. (Koji Maemura); methodology, M.E., D.S., H.T., K.M. (Keishi Miyata) and H.K.; project administration, T.I.; Resources, K.M. (Koji Maemura); supervision, T.I.; writing—original draft, T.I. and S.W.; writing—review and editing, Y.O., N.T., S.I., H.K. and K.M. (Koji Maemura). All authors have read and agreed to the published version of the manuscript.

Funding: This work was supported by Grants-in-Aid for Scientific Research (No. 19K08542 to T.I. and No. 17K09592 to K.M. (Koji Maemura)) from the Japanese Ministry of Education, Culture, Sports, Science and Technology (MEXT).

Acknowledgments: The authors are grateful to Saori Usui and Miho Kawakatsu for their technical assistance.

Conflicts of Interest: Author K.M. has received honoraria and research grants from Teijin Pharma (Tokyo, Japan) and Sanwa Kagaku Kenkyusho (Nagoya, Japan). The sponsors had no role in the design, execution, interpretation, or writing of the study. The remaining authors declare no competing interest.

References

1. Hansson, G.K. Inflammation, atherosclerosis, and coronary artery disease. *N. Engl. J. Med.* **2005**, *352*, 1685–1695. [[CrossRef](#)]
2. Libby, P. Inflammation in atherosclerosis. *Nature* **2002**, *420*, 868–874. [[CrossRef](#)]
3. Ross, R. Atherosclerosis—An inflammatory disease. *N. Engl. J. Med.* **1999**, *340*, 115–126. [[CrossRef](#)]
4. Newby, A.C. Metalloproteinase production from macrophages—A perfect storm leading to atherosclerotic plaque rupture and myocardial infarction. *Exp. Physiol.* **2016**, *101*, 1327–1337. [[CrossRef](#)] [[PubMed](#)]
5. Galis, Z.S.; Sukhova, G.K.; Lark, M.W.; Libby, P. Increased expression of matrix metalloproteinases and matrix degrading activity in vulnerable regions of human atherosclerotic plaques. *J. Clin. Investig.* **1994**, *94*, 2493–2503. [[CrossRef](#)]
6. Aarup, A.; Pedersen, T.X.; Junker, N.; Christoffersen, C.; Bartels, E.D.; Madsen, M.; Nielsen, C.H.; Nielsen, L.B. Hypoxia-Inducible Factor-1 α Expression in Macrophages Promotes Development of Atherosclerosis. *Arterioscler. Thromb. Vasc. Biol.* **2016**, *36*, 1782–1790. [[CrossRef](#)] [[PubMed](#)]
7. Nakano, D.; Hayashi, T.; Tazawa, N.; Yamashita, C.; Inamoto, S.; Okuda, N.; Mori, T.; Sohmiya, K.; Kitaura, Y.; Okada, Y.; et al. Chronic hypoxia accelerates the progression of atherosclerosis in apolipoprotein E-knockout mice. *Hypertens. Res.* **2005**, *28*, 837–845. [[CrossRef](#)] [[PubMed](#)]
8. Carmeliet, P.; Jain, R.K. Angiogenesis in cancer and other diseases. *Nature* **2000**, *407*, 249–257. [[CrossRef](#)] [[PubMed](#)]
9. Montero, I.; Orbe, J.; Varo, N.; Beloqui, O.; Monreal, J.I.; Rodriguez, J.A.; Diez, J.; Libby, P.; Paramo, J.A. C-reactive protein induces matrix metalloproteinase-1 and -10 in human endothelial cells: Implications for clinical and subclinical atherosclerosis. *J. Am. Coll. Cardiol.* **2006**, *47*, 1369–1378. [[CrossRef](#)] [[PubMed](#)]
10. Parma, L.; Baganha, F.; Quax, P.H.A.; de Vries, M.R. Plaque angiogenesis and intraplaque hemorrhage in atherosclerosis. *Eur. J. Pharm.* **2017**, *816*, 107–115. [[CrossRef](#)] [[PubMed](#)]
11. Abbas, A.; Aukrust, P.; Russell, D.; Krohg-Sorensen, K.; Almas, T.; Bundgaard, D.; Bjerkeli, V.; Sagen, E.L.; Michelsen, A.E.; Dahl, T.B.; et al. Matrix metalloproteinase 7 is associated with symptomatic lesions and adverse events in patients with carotid atherosclerosis. *PLoS ONE* **2014**, *9*, e84935. [[CrossRef](#)]
12. Bell, E.L.; Klimova, T.A.; Eisenbart, J.; Moraes, C.T.; Murphy, M.P.; Budinger, G.R.; Chandel, N.S. The Qo site of the mitochondrial complex III is required for the transduction of hypoxic signaling via reactive oxygen species production. *J. Cell Biol.* **2007**, *177*, 1029–1036. [[CrossRef](#)] [[PubMed](#)]
13. Rathore, R.; Zheng, Y.M.; Niu, C.F.; Liu, Q.H.; Korde, A.; Ho, Y.S.; Wang, Y.X. Hypoxia activates NADPH oxidase to increase [ROS] $_i$ and [Ca $^{2+}$] $_i$ through the mitochondrial ROS-PKCEpsilon signaling axis in pulmonary artery smooth muscle cells. *Free Radic. Biol. Med.* **2008**, *45*, 1223–1231. [[CrossRef](#)] [[PubMed](#)]
14. Kelley, E.E.; Hock, T.; Khoo, N.K.; Richardson, G.R.; Johnson, K.K.; Powell, P.C.; Giles, G.I.; Agarwal, A.; Lancaster, J.R., Jr.; Tarpey, M.M. Moderate hypoxia induces xanthine oxidoreductase activity in arterial endothelial cells. *Free Radic. Biol. Med.* **2006**, *40*, 952–959. [[CrossRef](#)] [[PubMed](#)]
15. Kelley, E.E.; Khoo, N.K.; Hundley, N.J.; Malik, U.Z.; Freeman, B.A.; Tarpey, M.M. Hydrogen peroxide is the major oxidant product of xanthine oxidase. *Free Radic. Biol. Med.* **2010**, *48*, 493–498. [[CrossRef](#)]
16. Wang, G.L.; Semenza, G.L. General involvement of hypoxia-inducible factor 1 in transcriptional response to hypoxia. *Proc. Natl. Acad. Sci. USA* **1993**, *90*, 4304–4308. [[CrossRef](#)]

17. Takeda, N.; O’Dea, E.L.; Doedens, A.; Kim, J.W.; Weidemann, A.; Stockmann, C.; Asagiri, M.; Simon, M.C.; Hoffmann, A.; Johnson, R.S. Differential activation and antagonistic function of HIF- α isoforms in macrophages are essential for NO homeostasis. *Genes Dev.* **2010**, *24*, 491–501. [[CrossRef](#)]
18. Semba, H.; Takeda, N.; Isagawa, T.; Sugiura, Y.; Honda, K.; Wake, M.; Miyazawa, H.; Yamaguchi, Y.; Miura, M.; Jenkins, D.M.; et al. HIF-1 α -PDK1 axis-induced active glycolysis plays an essential role in macrophage migratory capacity. *Nat. Commun.* **2016**, *7*, 11635. [[CrossRef](#)]
19. Abe, H.; Takeda, N.; Isagawa, T.; Semba, H.; Nishimura, S.; Morioka, M.S.; Nakagama, Y.; Sato, T.; Soma, K.; Koyama, K.; et al. Macrophage hypoxia signaling regulates cardiac fibrosis via Oncostatin M. *Nat. Commun.* **2019**, *10*, 2824. [[CrossRef](#)]
20. Sluimer, J.C.; Gasc, J.M.; van Wanroij, J.L.; Kisters, N.; Groeneweg, M.; Sollewijn Gelpke, M.D.; Cleutjens, J.P.; van den Akker, L.H.; Corvol, P.; Wouters, B.G.; et al. Hypoxia, hypoxia-inducible transcription factor, and macrophages in human atherosclerotic plaques are correlated with intraplaque angiogenesis. *J. Am. Coll. Cardiol.* **2008**, *51*, 1258–1265. [[CrossRef](#)]
21. Azimi, I.; Petersen, R.M.; Thompson, E.W.; Roberts-Thomson, S.J.; Monteith, G.R. Hypoxia-induced reactive oxygen species mediate N-cadherin and SERPINE1 expression, EGFR signalling and motility in MDA-MB-468 breast cancer cells. *Sci. Rep.* **2017**, *7*, 15140. [[CrossRef](#)]
22. Brown, D.I.; Griendling, K.K. Regulation of signal transduction by reactive oxygen species in the cardiovascular system. *Circ. Res.* **2015**, *116*, 531–549. [[CrossRef](#)] [[PubMed](#)]
23. Nathan, C.; Cunningham-Bussell, A. Beyond oxidative stress: An immunologist’s guide to reactive oxygen species. *Nat. Rev. Immunol.* **2013**, *13*, 349–361. [[CrossRef](#)]
24. Johnson, J.L.; Dwivedi, A.; Somerville, M.; George, S.J.; Newby, A.C. Matrix metalloproteinase (MMP)-3 activates MMP-9 mediated vascular smooth muscle cell migration and neointima formation in mice. *Arterioscler. Thromb. Vasc. Biol.* **2011**, *31*, e35–e44. [[CrossRef](#)]
25. Rohani, M.G.; McMahan, R.S.; Razumova, M.V.; Hertz, A.L.; Cieslewicz, M.; Pun, S.H.; Regnier, M.; Wang, Y.; Birkland, T.P.; Parks, W.C. MMP-10 Regulates Collagenolytic Activity of Alternatively Activated Resident Macrophages. *J. Investig. Dermatol.* **2015**, *135*, 2377–2384. [[CrossRef](#)] [[PubMed](#)]
26. Geurts, N.; Becker-Pauly, C.; Martens, E.; Proost, P.; Van den Steen, P.E.; Stocker, W.; Opdenakker, G. Meprins process matrix metalloproteinase-9 (MMP-9)/gelatinase B and enhance the activation kinetics by MMP-3. *FEBS Lett.* **2012**, *586*, 4264–4269. [[CrossRef](#)] [[PubMed](#)]
27. Sasaki, T.; Kuzuya, M.; Nakamura, K.; Cheng, X.W.; Shibata, T.; Sato, K.; Iguchi, A. A simple method of plaque rupture induction in apolipoprotein E-deficient mice. *Arterioscler. Thromb. Vasc. Biol.* **2006**, *26*, 1304–1309. [[CrossRef](#)] [[PubMed](#)]
28. Di Gregoli, K.; Johnson, J.L. Role of colony-stimulating factors in atherosclerosis. *Curr. Opin. Lipidol.* **2012**, *23*, 412–421. [[CrossRef](#)] [[PubMed](#)]
29. Johnson, J.L.; George, S.J.; Newby, A.C.; Jackson, C.L. Divergent effects of matrix metalloproteinases 3, 7, 9, and 12 on atherosclerotic plaque stability in mouse brachiocephalic arteries. *Proc. Natl. Acad. Sci. USA* **2005**, *102*, 15575–15580. [[CrossRef](#)]
30. Quillard, T.; Tesmenitsky, Y.; Croce, K.; Travers, R.; Shvartz, E.; Koskinas, K.C.; Sukhova, G.K.; Aikawa, E.; Aikawa, M.; Libby, P. Selective inhibition of matrix metalloproteinase-13 increases collagen content of established mouse atherosclerosis. *Arterioscler. Thromb. Vasc. Biol.* **2011**, *31*, 2464–2472. [[CrossRef](#)]
31. Purroy, A.; Roncal, C.; Orbe, J.; Meilhac, O.; Belzunce, M.; Zalba, G.; Villa-Bellosta, R.; Andres, V.; Parks, W.C.; Paramo, J.A.; et al. Matrix metalloproteinase-10 deficiency delays atherosclerosis progression and plaque calcification. *Atherosclerosis* **2018**, *278*, 124–134. [[CrossRef](#)]
32. Silence, J.; Lupu, F.; Collen, D.; Lijnen, H.R. Persistence of atherosclerotic plaque but reduced aneurysm formation in mice with stromelysin-1 (MMP-3) gene inactivation. *Arterioscler. Thromb. Vasc. Biol.* **2001**, *21*, 1440–1445. [[CrossRef](#)]
33. Conrad, P.W.; Rust, R.T.; Han, J.; Millhorn, D.E.; Beitner-Johnson, D. Selective activation of p38 α and p38 γ by hypoxia. Role in regulation of cyclin D1 by hypoxia in PC12 cells. *J. Biol. Chem.* **1999**, *274*, 23570–23576. [[CrossRef](#)]
34. Beitner-Johnson, D.; Rust, R.T.; Hsieh, T.C.; Millhorn, D.E. Hypoxia activates Akt and induces phosphorylation of GSK-3 in PC12 cells. *Cell Signal.* **2001**, *13*, 23–27. [[CrossRef](#)]

35. Minet, E.; Michel, G.; Mottet, D.; Piret, J.P.; Barbieux, A.; Raes, M.; Michiels, C. c-JUN gene induction and AP-1 activity is regulated by a JNK-dependent pathway in hypoxic HepG2 cells. *Exp. Cell Res.* **2001**, *265*, 114–124. [[CrossRef](#)]
36. Torres, M.; Forman, H.J. Redox signaling and the MAP kinase pathways. *Biofactors* **2003**, *17*, 287–296. [[CrossRef](#)] [[PubMed](#)]
37. Kim, J.H.; Na, H.J.; Kim, C.K.; Kim, J.Y.; Ha, K.S.; Lee, H.; Chung, H.T.; Kwon, H.J.; Kwon, Y.G.; Kim, Y.M. The non-provitamin A carotenoid, lutein, inhibits NF-kappaB-dependent gene expression through redox-based regulation of the phosphatidylinositol 3-kinase/PTEN/Akt and NF-kappaB-inducing kinase pathways: Role of H₂O₂ in NF-kappaB activation. *Free Radic. Biol. Med.* **2008**, *45*, 885–896. [[CrossRef](#)]
38. Fu, X.; Kassim, S.Y.; Parks, W.C.; Heinecke, J.W. Hypochlorous acid oxygenates the cysteine switch domain of pro-matrilysin (MMP-7). A mechanism for matrix metalloproteinase activation and atherosclerotic plaque rupture by myeloperoxidase. *J. Biol. Chem.* **2001**, *276*, 41279–41287. [[CrossRef](#)]
39. Meli, D.N.; Christen, S.; Leib, S.L. Matrix metalloproteinase-9 in pneumococcal meningitis: Activation via an oxidative pathway. *J. Infect. Dis.* **2003**, *187*, 1411–1415. [[CrossRef](#)]
40. Peppin, G.J.; Weiss, S.J. Activation of the endogenous metalloproteinase, gelatinase, by triggered human neutrophils. *Proc. Natl. Acad. Sci. USA* **1986**, *83*, 4322–4326. [[CrossRef](#)]
41. Saari, H.; Sorsa, T.; Lindy, O.; Suomalainen, K.; Halinen, S.; Konttinen, Y.T. Reactive oxygen species as regulators of human neutrophil and fibroblast interstitial collagenases. *Int. J. Tissue React.* **1992**, *14*, 113–120. [[PubMed](#)]
42. Weiss, S.J.; Peppin, G.; Ortiz, X.; Ragsdale, C.; Test, S.T. Oxidative autoactivation of latent collagenase by human neutrophils. *Science* **1985**, *227*, 747–749. [[CrossRef](#)]
43. Viappiani, S.; Nicolescu, A.C.; Holt, A.; Sawicki, G.; Crawford, B.D.; Leon, H.; van Mulligen, T.; Schulz, R. Activation and modulation of 72kDa matrix metalloproteinase-2 by peroxynitrite and glutathione. *Biochem. Pharmacol.* **2009**, *77*, 826–834. [[CrossRef](#)]
44. Ma, C.H.; Wu, C.H.; Jou, I.M.; Tu, Y.K.; Hung, C.H.; Hsieh, P.L.; Tsai, K.L. PKR activation causes inflammation and MMP-13 secretion in human degenerated articular chondrocytes. *Redox Biol.* **2018**, *14*, 72–81. [[CrossRef](#)]
45. Mori, K.; Uchida, T.; Yoshie, T.; Mizote, Y.; Ishikawa, F.; Katsuyama, M.; Shibamura, M. A mitochondrial ROS pathway controls matrix metalloproteinase 9 levels and invasive properties in RAS-activated cancer cells. *FEBS J.* **2019**, *286*, 459–478. [[CrossRef](#)] [[PubMed](#)]
46. Peterson, C.M.; Johannsen, D.L.; Ravussin, E. Skeletal muscle mitochondria and aging: A review. *J. Aging Res.* **2012**, *2012*, 194821. [[CrossRef](#)]
47. Nomura, J.; Kobayashi, T.; So, A.; Busso, N. Febuxostat, a Xanthine Oxidoreductase Inhibitor, Decreases NLRP3-dependent Inflammation in Macrophages by Activating the Purine Salvage Pathway and Restoring Cellular Bioenergetics. *Sci. Rep.* **2019**, *9*, 17314. [[CrossRef](#)] [[PubMed](#)]
48. MacIsaac, R.L.; Salatzki, J.; Higgins, P.; Walters, M.R.; Padmanabhan, S.; Dominiczak, A.F.; Touyz, R.M.; Dawson, J. Allopurinol and Cardiovascular Outcomes in Adults with Hypertension. *Hypertension* **2016**, *67*, 535–540. [[CrossRef](#)]
49. Noman, A.; Ang, D.S.; Ogston, S.; Lang, C.C.; Struthers, A.D. Effect of high-dose allopurinol on exercise in patients with chronic stable angina: A randomised, placebo controlled crossover trial. *Lancet* **2010**, *375*, 2161–2167. [[CrossRef](#)]
50. Love, B.L.; Barrons, R.; Veverka, A.; Snider, K.M. Urate-lowering therapy for gout: Focus on febuxostat. *Pharmacotherapy* **2010**, *30*, 594–608. [[CrossRef](#)]

Publisher’s Note: MDPI stays neutral with regard to jurisdictional claims in published maps and institutional affiliations.



© 2020 by the authors. Licensee MDPI, Basel, Switzerland. This article is an open access article distributed under the terms and conditions of the Creative Commons Attribution (CC BY) license (<http://creativecommons.org/licenses/by/4.0/>).



Review

Hypoxia/HIF Modulates Immune Responses

Yuling Chen¹ and Timo Gaber^{1,2,*}

¹ Charité—Universitätsmedizin Berlin, Corporate Member of Freie Universität Berlin, Humboldt-Universität zu Berlin, Berlin Institute of Health, Department of Rheumatology and Clinical Immunology, Charitéplatz 1, 10117 Berlin, Germany; yuling.chen@charite.de

² German Rheumatism Research Centre (DRFZ) Berlin, a Leibniz Institute, Charitéplatz 1, 10117 Berlin, Germany

* Correspondence: timo.gaber@charite.de; Tel.: +49-30-450-513364

Abstract: Oxygen availability varies throughout the human body in health and disease. Under physiological conditions, oxygen availability drops from the lungs over the blood stream towards the different tissues into the cells and the mitochondrial cavities leading to physiological low oxygen conditions or physiological hypoxia in all organs including primary lymphoid organs. Moreover, immune cells travel throughout the body searching for damaged cells and foreign antigens facing a variety of oxygen levels. Consequently, physiological hypoxia impacts immune cell function finally controlling innate and adaptive immune response mainly by transcriptional regulation via hypoxia-inducible factors (HIFs). Under pathophysiological conditions such as found in inflammation, injury, infection, ischemia and cancer, severe hypoxia can alter immune cells leading to dysfunctional immune response finally leading to tissue damage, cancer progression and autoimmunity. Here we summarize the effects of physiological and pathophysiological hypoxia on innate and adaptive immune activity, we provide an overview on the control of immune response by cellular hypoxia-induced pathways with focus on the role of HIFs and discuss the opportunity to target hypoxia-sensitive pathways for the treatment of cancer and autoimmunity.

Keywords: hypoxia; HIF; T cells; B cells; monocytes; macrophages; neutrophils; ILC; oxygen

Citation: Chen, Y.; Gaber, T. Hypoxia/HIF Modulates Immune Responses. *Biomedicines* **2021**, *9*, 260. <https://doi.org/10.3390/biomedicines9030260>

Academic Editor: Kiichi Hirota

Received: 28 January 2021

Accepted: 25 February 2021

Published: 5 March 2021

Publisher's Note: MDPI stays neutral with regard to jurisdictional claims in published maps and institutional affiliations.



Copyright: © 2021 by the authors. Licensee MDPI, Basel, Switzerland. This article is an open access article distributed under the terms and conditions of the Creative Commons Attribution (CC BY) license (<https://creativecommons.org/licenses/by/4.0/>).

1. Introduction

Immune cells and proper immune response require focal sites of immune cell development, maturation, activation, tolerance, and longevity also defined as immunological niches bearing a certain microenvironment to maintain immune homeostasis [1]. These organs and tissues include the bone marrow, placenta, intestinal mucosa, renal medulla, secondary lymphoid organs, and the thymus [2,3]. In tissue pathology, sites of high immunological activity lead to inflammation and as a result tissue dysfunction bearing certain pathological microenvironment features. These pathological sites include infected, inflamed, and ischemic tissues and tumors [4–7]. Of note, sites of immune activity with distinct microenvironmental entities can broadly range between a state of immune homeostasis and a state of immune pathology. Under certain conditions of severe and disorganized immune activity, inflammation can perpetuate as a result of immune dysfunction leading to autoimmunity or culminates into inflammation-driven tumor development [8]. Microenvironmental conditions at sites of physiological and pathological immune activity play a key role in the development of effective immune response and pathological immune dysfunction by modulation of immune cell function. Understanding the impact of the microenvironment in sites of immune activity and adaptation mechanisms in immune cell reprogramming may yield into new therapeutic treatment strategies against a dysfunctional immune response as found in autoimmunity and cancer. At sites of immune activity under physiological and pathophysiological circumstances, immune cells become highly metabolically active and activate bystander cells and surrounding tissue. As a result, microenvironmental features

rapidly change by increasing the amount and number of humoral factors, metabolites and a decrease in oxygen leading to a state of hypoxia—a condition where cellular oxygen demand exceeds the oxygen supply [9,10]. Constant supply of oxygen is a prerequisite for the energy homeostasis of respiring cells. Oxygen plays a vital role in all eukaryotes, being the terminal electron acceptor of the mitochondrial electron transport chain, which finally feeds the proton gradient for the generation of ATP via oxidative phosphorylation. If the constant supply with oxygen does not anymore meet the requirements of cells, hypoxic conditions will be established and, if sustained, these conditions will ultimately result in cell death. Hypoxia arises in a variety of immunological situations under physiological and pathophysiological immune activity [10,11].

2. Physiological Hypoxia Influences Immunity

Fundamental principle of the vasculature is to supply all organs, tissues and cells with oxygen and nutrients according to their needs and to dispose of refuse (carbon dioxide and metabolic products) establishing a balance between supply and consumption which is unique for the respective organ, tissue and cell. With regard to oxygen, its availability to the cells in the human body depends on various factors, such as (i) oxygen uptake, (ii) the transport capacity of the blood, (iii) the transport of the oxygen carrier, i.e., vascularization, and finally (iv) cell respiration itself.

Even under physiological conditions oxygen partial pressure (pO₂) varies throughout the human body (Figure 1) [12–15]. Arterial blood owns an average oxygen partial pressure of ~80–100 mmHg which corresponds to an oxygen air-content (O₂ air-content) at sea level of 10–12.5%. The extreme values are 100 mmHg in the pulmonary veins and 40 mmHg in the pulmonary arteries. The tissue oxygen partial pressure varies depending on the tissue anatomy and function in the range of 30–50 mmHg (~3–6% O₂ air-content) dropping to a cellular range of 9.9–19 mmHg (~1–2% O₂ air-content) and further to a mitochondrial pO₂ of <9.9 mmHg (~1% O₂ air-content) [13]. Consequently, current standardized cell culture conditions are oriented towards of atmospheric pO₂ with oxygen concentrations 2–5 times higher than physiologically relevant, which are ignoring in vivo situation [12,13].

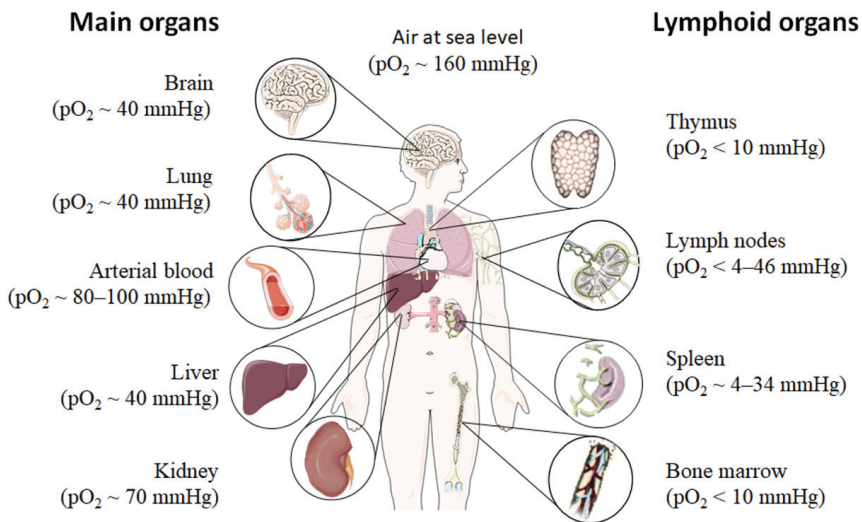


Figure 1. Oxygen partial pressure (pO₂) varies throughout the human body from main organs to lymphoid tissues. Figure was modified from Servier Medical Art, licensed under a Creative Common Attribution 3.0 Generic License [16].

Low pO₂ have been detected in various compartments of healthy and inflamed tissues as well as in tumors, often as a characteristic of tissue architecture, vascularization and

microenvironment [1]. Tissues and cells vary in their (i) circulatory distance from lung oxygenation (ii) density, functionality and relative proximity of/to their capillary network (iii) oxygen consuming microenvironmental, (iv) the rate of oxygen consumption within the cells and thus in pO_2 leading to distinct thresholds and susceptibilities to hypoxia [12,14,15]. However, at a cellular level, hypoxia and hypoxic responses generally occur at a pO_2 ~7–10 mmHg (~1% O_2 air-content) [17].

Although most tissues of the body are provided with a level of oxygen that exceeds the basal metabolic requirements, in some tissues, the pO_2 is comparatively low, which results in regions of “physiological hypoxia” [1]. Such regions can occur in the intestinal outermost mucosal surface where a controlled oxygen gradient establishes as a result of anatomical features such as juxtapositioning of the mucosal surface to the anoxic gut lumen and the functional countercurrent oxygen exchange system in the intestinal villi [18]. In kidney, oxygen gradients are necessary for organ function which is to maximize the concentration of urine by counter-current exchange of oxygen in the renal medulla [13,19]. Moreover, oxygen gradients are important for the synthesis of erythropoietin (EPO) in kidney and liver [20]. In the developmental process of the placenta and the fetus, physiological hypoxia can be observed in several regions due to constant outgrowing of the existing local blood supply [21]. If blood supply is limited due to the lack of vasculature such as found in the eye’s retina but also in the outer layer of the skin, the epidermis, ‘physiological hypoxia’ has been demonstrated to be well established [21,22]. Moreover, the major organs of the immune system, including bone marrow ($pO_2 < 10$ mmHg) [23,24], thymus ($pO_2 < 10$ mmHg) [24–26], spleen ($pO_2 \sim 4$ –34 mmHg) [26,27], and lymph nodes ($pO_2 < 4$ –46 mmHg) [28], exhibit regions of immune activity with locally significantly lower pO_2 than surrounding tissues and even lower than inhaled air. These hypoxic regions are of functional importance because they impact immunity by providing a niche for hematopoietic stem cells (HSCs) in the bone marrow, where hypoxia maintains the self-renewal capacity of HSCs favors a slow turnover of HSCs and sustains survival by promoting their quiescence [29–32] or an environment for the antigen challenging of B cells in germinal centers (GCs), where hypoxia increase glycolytic metabolism supporting the generation and expansion of antigen-specific GC B cells and the production of high-affinity immunoglobulin G (IgG) antibodies [33,34].

3. Pathophysiological Hypoxia Shapes Immune Response

Hypoxia also exists in pathophysiological states, which are more severe and confused as compared to physiological hypoxia [35] (Figure 2). Solid tumor microenvironment is one of the well-known typical pathophysiological immunological hypoxia caused by an imbalance between oxygen supply and oxygen demand [36]. The rapidly proliferating tumor cells are outgrowing from the vascular network, which limits the diffusion of oxygen into the intratumor microenvironment leading to hypoxia. In the hypoxic microenvironment of the tumor induces proangiogenic factors, such as vascular endothelial growth factor (VEGF), and promotes tumor vascularization and growth. However, the tumor’s blood vessels are usually irregularly structured and poorly functional, and also tend to form clots and local edema, aggravating local hypoxia. Moreover, the tumor induced neovasculature has gaps between endothelial cells resulting in that tumor cells leak into bloodstream and disseminate [37–39]. The hypoxic milieu recruits myeloid-derived suppressor cells (MDSCs) to the primary tumor site by activating the transcription of chemokine ligand in cancer cells [40] and promoting ectonucleoside triphosphate diphosphohydrolase 2 (ENTPD2/CD39L1) [41]. MDSCs play a key role in tumor immunosuppression by inhibition of anti-tumor T cell effector function. Usually MDSCs inhibit antigen-specific CD8+ T cells in lymphoid organs thereby reducing collateral damage and controlling effector function, but MDSCs at the tumor site preferentially differentiate into tumor associated macrophages (TAMs) facilitated by the hypoxic tumor microenvironment inhibiting not only antigen-specific but also nonspecific T cell activity [42]. Furthermore, the hypoxic microenvironment increases the expression programmed death ligand 1 (PD-L1) on MD-

SCs, which is when blocked resulting in enhanced MDSC-mediated T cell activation [43] evidencing hypoxia-mediated suppression of anti-tumor T cell effector function supporting tumor development [44–46].

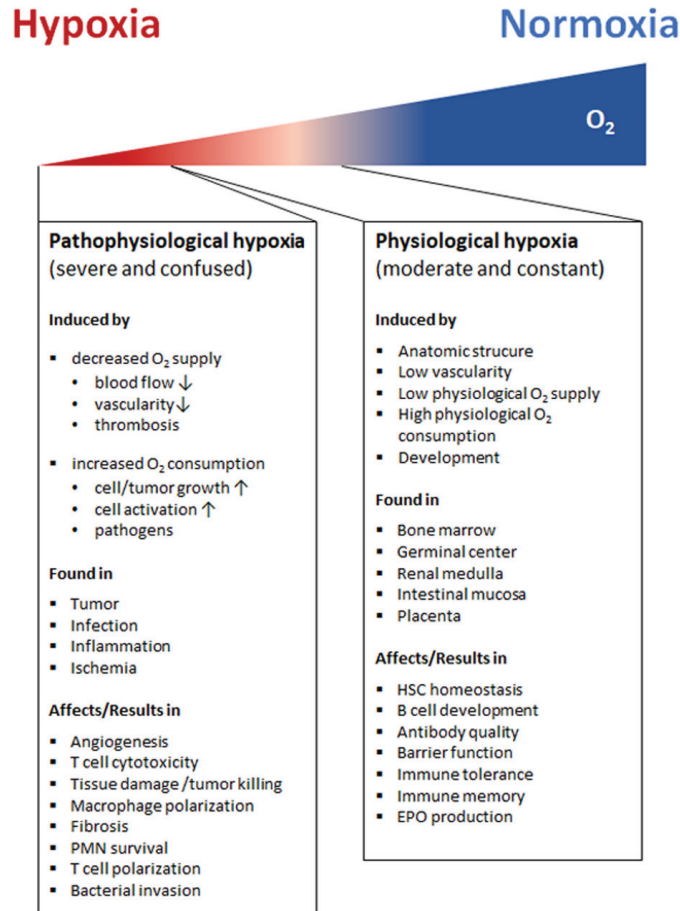


Figure 2. Hypoxia arises in a variety of immunological situations under physiological and pathophysiological immune activity. Physiological hypoxia which is attributed to be moderate and constant is caused by, e.g., oxygen gradients as a result of developmental processes, anatomic structure and functional composition. The factors contributing to physiological hypoxia differ in specific organs such as in primary and secondary lymphoid organs. Here, physiological hypoxia regulates the function of immune cells supporting beneficial immune activity (light red right panel). The pathophysiological hypoxia is usually attributed to be severe and confused, which is caused by a variety of factors in different diseases (dark red left panel). (↑: induced or up-regulated, ↓: reduced or down-regulated. PMN, polymorphonuclear neutrophils; EPO, erythropoietin; HSC, hematopoietic stem cell).

Apart from the hypoxic tumor sites, hypoxic areas may appear as a consequence of infection with pathogenic bacteria, viruses, fungi, and protozoa [47–50]. Many factors contribute to the establishment of an hypoxic environment including an increased oxygen consumption by inflamed resident cells, infiltrating immune cells and pathogens as well as a decreased oxygen supply caused by the combination of vascular pathology and microthrombosis [51]. In this scenario, the hypoxic microenvironment protects the host

by decreasing host cell death and reducing pathogenicity of invaders, while deleterious effects such as increases in antibiotic resistance and bacterial invasion make hypoxia a double-edged sword [52–54].

However, sites of inflammation undergo significant shifts in metabolic activity leading to O₂ deficiency, which is defined as “inflammatory hypoxia” [35,55]. The reasons for this kind of hypoxia include the increase in oxygen consumption by infiltration and transmigration of immune cells such as monocytes and polymorphonuclear neutrophils (PMN), by local T and B cell proliferation, by activation of oxygenase, such as oxidases, monooxygenases and dioxygenases, and the immunometabolic switch in effector cells itself. The influence of inflammatory hypoxia on the severity of inflammation is particularly tissue-specific and depends on the composition and distribution of the involved cell types, the local microenvironment, the duration and severity of hypoxia [56]. The induction of hypoxia by tissue infiltrating PMNs for instance in the intestinal epithelia ameliorates colitis [56], while in the lung enhances the severity of lung injury [57].

Blocking the blood supplying vessels by thrombus, embolus, or other blockages and followed by the subsequent restoration of perfusion and concomitant reoxygenation leads to ischemia and reperfusion injuring the demanding tissue [58]. Ischemia and reperfusion often occur in small capillaries of cerebral, coronary, or peripheral arteries [59] and is one of the leading causes of morbidity and mortality. Imbalance of oxygen supply and demand during ischemia and reperfusion leads to tissue hypoxia and immune cell attraction, which trigger inflammation and result in the tissue damage in ischemic disease [60,61].

4. Hypoxia-Inducible Factors (HIF's): Structure, Function, and Regulation

Hypoxia itself influences cellular behavior in different ways ranging from reduction of oxidative phosphorylation to induction of glycolysis leading to lactate production and acidification of the cellular microenvironment. Cells respond to these changes by inducing a certain specific transcriptional program induced by a variety of transcription factors.

4.1. HIF's—“Master Regulators” of Cellular Response to Hypoxia

The key regulator of hypoxia-induced transcriptional changes in all metazoan—also termed as “master regulator” of the adaptive transcriptional response to hypoxia—is the heterodimeric hypoxia inducible factor family of transcription factors (HIF's) [62,63]. Three members namely HIF-1, HIF-2 and HIF-3 belong to this family, bearing distinct functional activities and specificities. The best characterized transcriptional factor today of the cellular hypoxic response is the HIF-1 which binds to hypoxia response elements (HREs) in the promoters of a variety of genes to activate a transcriptional program that is directed towards adaptation to hypoxia by inducing a metabolic shift towards glycolysis, promoting oxygen transport, cell migration, the re-establishment of oxygen supply by inducing angiogenesis and vasculogenesis [64,65]. Although several of these targets are conserved in different cell types, HIF-1 also confers a variety of cell-type specific transcriptional responses towards a hypoxic environment [65] (Figure 3).

The HIFs are mainly composed of two basic helix-loop-helix (bHLH) proteins which dimerize via a PAS (Per, AHR/ARNT, Sim) domain, as defined by sequence homology to the *Drosophila* Per and Sim proteins and the mammalian aryl hydrocarbon receptor (AHR) and aryl hydrocarbon receptor nuclear translocator (ARNT) proteins [66,67] to form the transcription factor HIF (Figure 3A). The heterodimeric HIF consists of an oxygen-dependent alpha-subunit (stabilized under hypoxia) and a constitutively expressed beta-subunit (HIF-1 β or ARNT). Three α subunits have been described so far: HIF-1 α , HIF-2 α , and HIF-3 α . While HIF-1 α and HIF-2 α are well characterized, relatively little is known about HIF-3 α [68–72]. HIF-1 α regulation itself ranges from transcriptional to translational and posttranslational level [73].

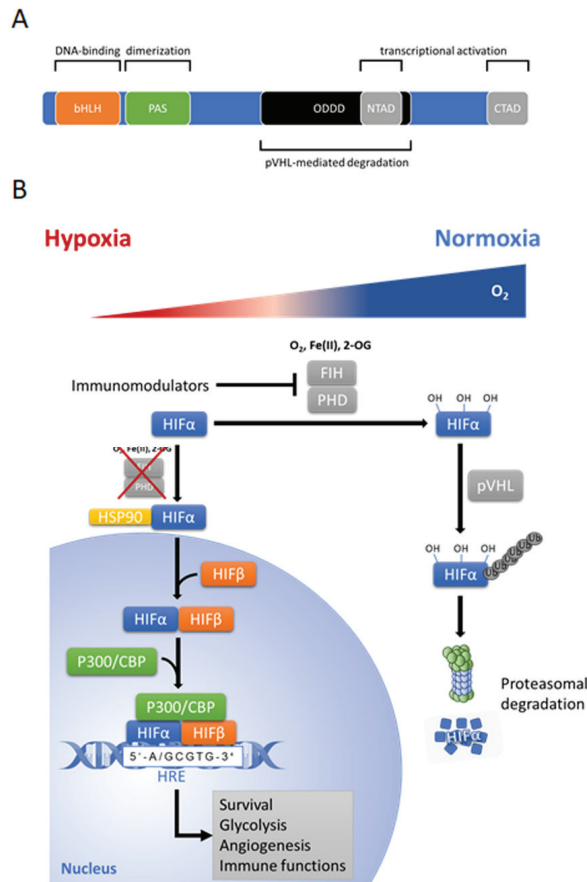


Figure 3. (A) Structure of hypoxia-inducible factor (HIF)-1 α /HIF-2 α subunit. Basic helix-loop-helix (bHLH) domain of HIF- α mediates DNA binding, and PAS domain is required for heterodimerization of the subunits. N-terminal transactivation domain (N-TAD) and the C-terminal transactivation domain (C-TAD) are transactivation domains for activation of HIF target genes. The N-TAD is responsible for the stability and target gene specificity and overlaps with the oxygen-dependent degradation domain (ODDD). The C-TAD interacts with coactivators activating gene transcription. Protein von Hippel–Lindau (pVHL)-mediated degradation of HIF- α needs hydroxylation of two proline residues in (ODDD). (B) Cellular HIF- α regulation under hypoxic (red shaded area of triangle) and normoxia conditions (blue shaded area of triangle). In hypoxia, HIF- α subunit translocates into nucleus and dimerizes with constitutively expressed HIF- β subunit, then recruits the transcriptional coactivator p300 and CREB (cAMP response element binding)-binding protein (CBP) to form a complex, which binds to hypoxic response elements (HRE) on DNA and triggers HIF-dependent transcriptional response. Under normoxic condition, when cellular oxygen supply exceeds demand, HIF- α is hydroxylated on prolyl residues by prolyl hydroxylase domain proteins (PHDs), which are members of 2-oxoglutarate (2-OG)-dependent dioxygenase superfamily and function in the presence of substrates and co-factors: oxygen (O₂), 2-oxoglutarate (2-OG), ferrous iron [Fe (II)] and ascorbate. Hydroxylation facilitates the interaction with the tumor suppressor protein von Hippel–Lindau (pVHL), which recruits an E3-ubiquitin-ligase complex tagging HIF by polyubiquitination for proteasomal degradation via the 26S proteasome. Furthermore, factor-inhibiting HIF (FIH) hydroxylates HIF and inhibits the transcriptional activation of HIF by preventing recruitment of the transcriptional coactivators p300 and CBP. Figure was modified from Servier Medical Art, licensed under a Creative Common Attribution 3.0 Generic License [16].

In the presence of sufficient oxygen, when cellular oxygen supply exceeds demand, HIF- α becomes hydroxylated on prolyl residues (402 and/or 564 in HIF-1 α , 405 and/or 531 in HIF-2 α) by dioxygenases termed prolyl hydroxylase domain proteins (PHD1-3) (Figure 3B) [74]. Hydroxylation facilitates the interaction with the tumor suppressor protein von Hippel–Lindau (pVHL), which recruits an E3-ubiquitin-ligase complex tagging HIF by polyubiquitination for proteasomal degradation via the 26S proteasome [75–77]. Furthermore, a second dioxygenase termed the factor-inhibiting HIF (FIH) hydroxylates HIF on an asparagine residue (Asn-803 in HIF-1 α) and inhibits the transcriptional activation of HIF by blocking the interaction with the transcriptional coactivators p300 and CREB (cAMP response element binding)-binding protein (CBP) [68,74,78,79].

Under hypoxic conditions where the oxygen demand exceeds the supply, and/or due to a redox imbalance, dioxygenase activity of the PHDs and FIH is attenuated and HIF- α becomes stabilized and de-repressed, respectively. Once stabilized, HIF- α translocates into the nucleus, dimerizes with the constitutively expressed ARNT, recruits transcriptional coactivators (p300/CBP) and binds to HREs activating the cell-specific adaptation program towards hypoxia [10,68,74].

Two transcriptionally active HIFs, HIF-1 and HIF-2 confer the transcriptional activation and cellular adaptation under hypoxic conditions being distinguished by their α -subunits (HIF-1 α and HIF-2 α). Although both bind the HIF-1 β , they demonstrate a distinct tissue expression profile with overlapping but also distinct functions [63,79,80]. In immunity, HIF-1 seems to be expressed in virtually all innate and adaptive immune cell populations including myeloid lineages including monocytes, macrophages and neutrophils [80,81], dendritic cells [82], T cells and B cells and NK cells and innate lymphoid cells (ILCs) (reviewed in [83–85]) while HIF-2 has been demonstrated in certain immune cells such as in tumor-associated macrophages, in vitro expanded CD8+ T cells and in response to cytokines and hypoxia (reviewed in [85,86]).

Dynamics of HIF-1 α /HIF-2 α stabilization vary with regard to acute, chronic and cyclic or intermittent hypoxia [87]. Notably, cyclic hypoxia is characterized by periodic exposure to cycles of hypoxia and reoxygenation (H–R cycles). Interestingly, several in vitro studies revealed that cyclic hypoxia increased HIF-1 α levels to a greater extent than chronic hypoxia by e.g., ROS-mediated stabilization of HIF-1 α [88,89], while chronic hypoxia showed a greater extent of HIF-2 α stabilization as compared to cyclic hypoxia [90,91].

In addition to the O₂-dependent HIF degradation pathway, there are some other pathways that activate posttranslational degradation of HIF- α in an O₂-independent way. For example, the tumor suppressor p53 binds HIF-1 α and does recruit mouse double minute 2 homolog (Mdm2) mediated ubiquitination and proteasomal degradation of HIF-1 α in an oxygen-independent manner [92]. Another example is given by IF-1 α degradation via an oxygen-independent E3 ubiquitin ligase using heat shock protein 90 (Hsp90) inhibitors [93]. Furthermore, HIF stability has been demonstrated to be susceptible to high partial pressure of CO₂ (hypercapnia) which reduces intracellular pH and promotes lysosomal degradation of HIF- α subunits [94]. The lysosomal degradation pathway of HIF- α subunits has been also identified in the regulation of cell cycle progression by the physical and functional interaction of cyclin dependent kinases with HIF- α subunits [95,96].

Apart from the O₂-independent posttranslational and translation regulation of HIF's, HIF- α can be induced by a variety of inflammatory stimuli such as bacterial products (e.g., lipopolysaccharide or LPS), TNF- α and IL-1 β which can lead to the activation of pathways successively engaging phosphatidylinositol 3-kinase (PI3K), Protein kinase B (PKB), also known as Akt and the highly conserved Ser/Thr kinase mammalian target of rapamycin (mTOR) [97–99] and/or the mitogen activated protein kinases (MAPK) pathways. These pathways promote cap-dependent translation of HIF-1 α mRNA [100] or induce transcription factor nuclear factor kappa-light-chain-enhancer of activated B cells (NF κ B)-dependent upregulation of HIF expression and activity [101–105]. Beside NF κ B- and mTOR-dependent regulation of HIF, other pathways directly or indirectly control HIF and the HIF-pathway such as reactive oxygen and nitrogen species (ROS and RNS) [106–108].

Increased mitochondria-derived ROS levels during hypoxia mainly promote the stabilization of HIF- α subunits by inactivation of PHDs [109,110]. Full enzymatic activity of PHDs requires substrates and cofactors, such as ascorbate and ferrous iron [Fe (II)], which could be depleted by increased ROS [110]. ROS mediates the oxidation of cysteine residues, which form the catalytic site of PHD2, leading to generation of inactivated PHD2 homodimerization [109]. ROS also increases HIF-1 α by other mechanism including the activation of the HIF-1 α promoter via a functional NF κ B-site [111] and inhibition of the hydroxylase domain of FIH [112]. Nitric oxide (NO) plays a paradoxical role in modulating HIF stability. High concentrations of NO (>1 μ M) stabilizes HIF-1 α under both hypoxic and normoxic conditions, but lower concentration of NO (<400 nM) facilitates HIF-1 α degradation under hypoxic conditions [113]. This could be explained by the fact that under hypoxic conditions oxygen is redistributed toward oxygen-sensing hydroxylases such as PHDs and FIH due to NO-mediated inhibition of oxygen consumption by the mitochondrial cytochrome c oxidase (complex IV) [114]. Furthermore, NO might also induce directly the expression of PHDs [115,116].

4.2. Cellular Response to Hypoxia Beyond HIF's

Cellular responses initiated by hypoxia governs a variety of cellular changes including signaling cascades, transcriptional, translational, and posttranslational changes as well as changes in metabolite pattern. Apart from HIF's, several other transcription factors are involved in the cellular hypoxic response [117]. Most important with a certain role in intermittent hypoxia or cycling hypoxia (hypoxia reoxygenation cycles) is the activation of the transcription factor nuclear factor kappa-light-chain-enhancer of activated B cells (NF κ B) [118], inducing transcription of many genes in the response to inflammatory stimuli as mentioned above including Hif-1 α itself [118,119].

Moreover, the hypoxic response also includes the posttranscriptional regulation of gene expression via hypoxic-elicited microRNAs (hypoxamiR) including the master hypoxamiR miR-210. The latter is capable to simultaneously regulate the expression of multiple target genes in order to fine-tune the adaptive response of cells to hypoxia. HypoxamiR do this by regulation of HIF itself and, thus, cellular adaptation to low oxygen availability including the metabolic reprogramming, DNA repair, apoptosis, and angiogenesis [120–124].

Hypoxia-induced changes on transcriptional levels are relatively well understood, but hypoxia-induced responses on translation are not yet well demonstrated. The latter includes the downregulation of oxidative stress-induced misfolded and unfolded proteins caused by endoplasmic reticulum (ER) stress [125] and upregulation of essential proteins for cell survival [38].

Hypoxia-induced repression of protein translation occurs on different levels:

- Inhibition of cap-dependent translation initiation is mediated by the unfolded protein response (UPR) sensor, PERK (protein kinase RNA-like ER kinase), which phosphorylates the eukaryotic initiation factor 2 (eIF2 α) attenuating protein synthesis [126,127].
- Hypoxia-induced repression of protein synthesis during peptide elongation and termination is mediated via suppression of eukaryotic elongation factors (eEFs) [128–131].
- Hypoxia-mediated accumulation of abnormal proteins at the ER activates IRE1 (inositol-requiring protein 1) and ATF6 (activating transcription factor 6) to deal with ER stress by facilitating protein-folding and maintaining cell survival [38,132].

Additionally, short-time exposure to hypoxia (30min) inhibits mTOR, which is the main regulator of cap-dependent translation and its effectors: eukaryotic translation initiation factor 4E (eIF4E)-binding proteins (4E-BPs), p70 S6 kinase, rpS6, and eukaryotic translation initiation factor 4G (eIF4G). This effect is independent of ATP levels, ATP:ADP ratios, and HIF1 α [133]. However, in chronic hypoxia mTOR complex 1 (mTORC1) is repressed by AMPK (AMP-activated protein kinase) and REDD1 (regulated in development and DNA damage response 1). Hypoxia-induced upregulation of REDD1 and activation of the energy-sensor AMPK promotes activation of the TSC1/2 complex and then represses mTORC1 signaling and/or leads to eEF2 inhibition [134–136]. Thus, hypoxia-mediated

inhibition of mTORC1 suppresses mRNA translation through many pathways, such as (i) activation of 4E-BPs, or (ii) inactivation of eEF2 [131,137].

To maintain specific gene expression and their translation under hypoxia, such as the expression of HIF target genes, mechanisms have evolved to circumvent hypoxia-induced global translational inhibition. These mechanisms mainly include the use of internal ribosome entry site (IRES)-mediated translation [138,139], hypoxic eIF4F(H)-mediated translation [140], the RNA-binding protein RBM4 and the cap-binding eIF4E2-mediated translation [141,142], as well as signal recognition particle (SRP)-dependent mRNA localization-mediated translation [143].

4.3. Mitochondrial Response to Hypoxia

Hypoxia reduces the cells oxygen consumption by inhibiting mitochondrial function and structural integrity including the electron flux via the electron transport chain (ETC) to the terminal electron acceptor oxygen (Figure 4).

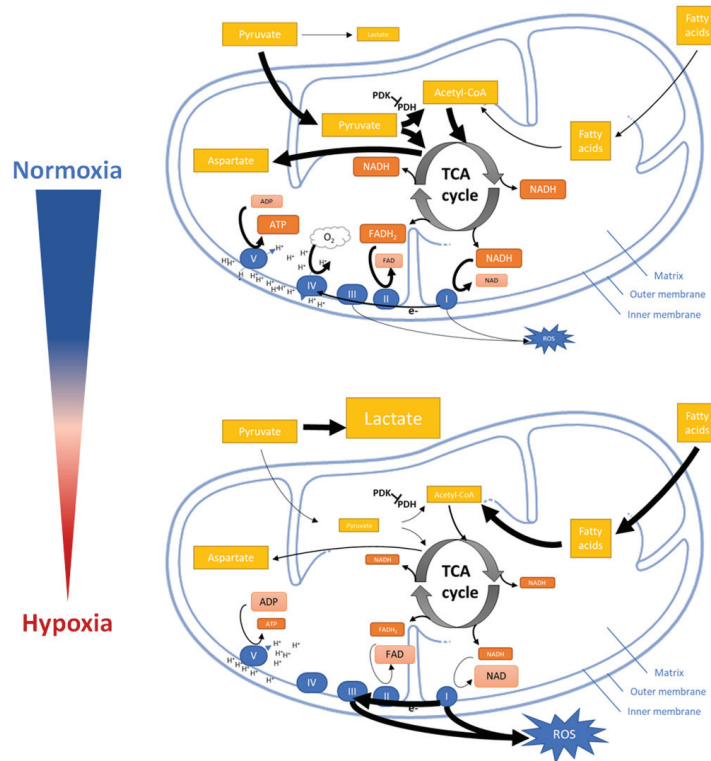


Figure 4. Impact of hypoxia on mitochondrial functions. Under normoxia, pyruvate is shifted into the mitochondria and catalyzed to Acetyl coenzyme A (Acetyl-CoA) as a substrate for the TCA cycle (tricarboxylic acid cycle) to synthesize energy-rich reductants (NADH and FADH₂) which drive the electron flux through the ETC and provide Aspartate. Under hypoxia, pyruvate is catalyzed to lactate while only few amounts of Acetyl-CoA are provided by fatty acid oxidation to the TCA. Only low amounts of energy-rich reductants and ATP are produced. The lack of the final electron acceptor (oxygen) leads to ROS generation during electron flux through the ETC. (Large arrows indicate higher flux; smaller arrows indicate lower flux; larger icons indicate higher amounts of intermediates; smaller icons indicate lower amounts of intermediates). Figure was modified from Servier Medical Art, licensed under a Creative Common Attribution 3.0 Generic License [16].

Initially, hypoxia promotes the conversion of pyruvate into lactate but reduces the entry of pyruvate into the TCA cycle (tricarboxylic acid cycle) and its conversion to acetyl-CoA [144–146]. The reduction of acetyl-CoA which usually fuels the TCA cycle now leads to a reduction of energy intermediates and metabolites such as nicotinamide adenine dinucleotide (NAD) and flavin adenine dinucleotide (FAD) resulting in NADH and FADH₂ (oxidized by the ETC to finally generate ATP) as well as aspartate (consumed in the process of nucleotide synthesis and essential for cell proliferation) [147]. Besides limiting supply of NADH and FADH₂ for ETC, hypoxia also modifies ETC by regulation the activity of mitochondrial complexes [38].

Mitochondrial complex I and III of ETC are major sites of ROS production [145]. Although decreased ETC flux might be supposed to attenuate hypoxic ROS generation in general [148–150]. Paradoxically, hypoxia increase ROS production, which in turn stabilizing HIF-1 α [151]. Recent studies demonstrated that the mitochondrial Na⁺/Ca²⁺ exchanger (NCLX) is activated under hypoxia leading to a mitochondrial increase in Na⁺. Accumulation of Na⁺ reduces the mitochondrial inner membrane fluidity and thus, the mobility of free ubiquinone. The immobile free ubiquinone leads to an increase of semiquinone at the Qo site of the mitochondrial complex III increasing the production of ROS under hypoxia [152]. Finally, hypoxia promotes mitochondrial fission mediated by mitochondrial protein fission 1 (FIS1) and activates mitophagy [153–155]. However, the mechanisms underlying how hypoxia modulates mitochondrial fission and mitophagy are not yet understood.

To compensate for reducing energy supply from mitochondrial metabolism, hypoxic cells also undergo a variety of metabolic changes to adapt to changes in the environment, such as enhancing glycolysis, glutaminolysis, fatty acid synthesis and serine synthesis pathway activity; decreasing pentose phosphate pathway activity, gluconeogenesis, nucleotide synthesis, fatty acids β -oxidation, lipid desaturation. Most of these mechanisms of metabolic reprogramming involve the regulation and modulation by the HIF- and the AMPK-pathway [38]. Additionally, hypoxic energy starvation inhibits mTOR independent of HIF and AMPK which increases over time [133,135,136]. As already mentioned, other hypoxia-responsive pathways include endoplasmic reticulum (ER) stress and NF κ B pathways [102,119,156,157].

5. Hypoxia-Inducible Factors in the Regulation of Immune Response

Immune cells face a variety of states of oxygen availability from luxury oxygen supply in the vasculature to hypoxic sites of immunological activity and severe hypoxic pathological sites of inflammation where they have to remain functionally active. Using gain and loss of function of individual HIF subunits and their regulators (PHDs) in distinct immune cell subtypes using transgenic mice, have gained deep insights into the impact of HIF's in immune response (reviewed in [158]).

5.1. HIFs in Myeloid Cell Function

Neutrophil granulocytes belong to the first line of defense which—recruited by macrophages—migrate from the circulation to sites of infection and inflammation into a pathophysiological hypoxic environment where their main function is to kill pathogens via the production of ROS (thereby reducing oxygen thus aggravating hypoxia), the formation of neutrophil extracellular DNA traps, the release of antimicrobial substances and proinflammatory cytokines like TNF- α , IL-1 β , interferons for the recruitment and activation of other immune cells [159,160]. Furthermore, neutrophilic respiratory burst can reduce immune activity by contributing to “inflammatory hypoxia” and a decrease in neutrophil invasion which results in an effective inflammatory resolution in a murine model of intestinal inflammation [56]. However, the role of HIF-1 α in neutrophils during this scenario remains unclear [161] (Table 1).

Table 1. HIF-mediated effects in myeloid cells.

Cell type	HIF Mediated Effects	Ref.
eutrophil granulocytes	HIF-1: survival ↑, glycolysis ↑, effector function ↑, (adhesion ↑, migration ↑, production of antimicrobial peptides ↑, formation of DNA traps ↑, phagocytosis ↑, oxidative burst ↑)	[9,80,81,162,163]
	HIF-2: survival ↑	[164]
Mast cells, basophils and eosinophils	HIF-1: survival ↑, effector function ↑ (synthesis of IL-8, TNF-α, VEGF, and IL-4 following TLR and/or IgE activation), eosinophil chemotaxis ↑	[165–169]
	HIF-2: eosinophil chemotaxis ↓	[166]
Monocytes/Macrophages	HIF-1: survival ↑, effector function ↑ (release pro-inflammatory TNF-α, IL-1β, IL-12 and IL-6, iNOS activity ↑ and NO production, phagocytosis)↑, glycolysis ↑, M1 polarization	[81,170–172]
	HIF-2: arginase-1 ↑, M2 polarization, phagocytosis ↓, proinflammatory cytokine/chemokine (IL-1β, IL-12, TNF-α, IL-6, IFN-γ, and CXCL2) expression, migration	[163,170,171,173]
Dendritic cells	HIF-1: survival ↑, glycolysis ↑, induction of regulatory T cells ↑, effector function ↑ (migration ↑, proper DC-mediated cytotoxic T cell activation, differentiation ↑)	[174–177]
	HIF-2: unknown	

↑: induced or up-regulated, ↓: reduced or down-regulated.

Furthermore, it has been demonstrated that activation of the HIF-1 pathway in neutrophils increases their survival and effector function (enhancement of $\beta 2$ integrin expression and migration, production of antimicrobial peptides, the formation of DNA traps, phagocytosis and oxidative burst) and induces metabolic reprogramming by inducing the Warburg effect for the generation of ATP [9,80,81,162,163,178]. Moreover, a similar importance of neutrophilic HIF-2 for survival, inflammation and tissue injury has been demonstrated by Thompson et al. [164]. Interestingly, in patients with inflammatory diseases HIF-2 is elevated in neutrophils. Thus, activation of HIF-1 and HIF-2 can be considered to enhance a proinflammatory phenotype in neutrophils.

In contrast to neutrophils, granula-rich mast cells, basophils and eosinophils play a central role in Th2-mediated allergic reactions and in the protection against parasite and microbial infections. Again, HIF-1 α stabilization in these cells remains important for survival and function as demonstrated in mice and humans, providing energy by HIF-1 α

mediated metabolic re-programming towards a glycolytic and controlling effector function by the synthesis of IL-8, TNF- α , VEGF, and IL-4 following TLR and/or IgE activation, the formation of DNA traps and chemotactic capacity [165–169].

The main actors of the innate immune response are the proinflammatory classically activated macrophages (M1-type) which belong to the first line of defense against foreign pathogens e.g., bacterial infection. M1 macrophages release pro-inflammatory cytokines such as TNF- α , IL-1 β and IL-6 and produce large amounts of ROS by NADPH oxidase (further reducing oxygen availability promoting hypoxia) and nitric oxide (NO) via inducible nitric oxide synthase (iNOS) [179]. Conversely, alternatively activated macrophages (M2-type) facilitate wound healing and support tissue repair and regeneration by anti-inflammatory and proangiogenic activity producing arginase-1 (Arg-1), VEGF and IL10 [179–182]. M1- and M2-type macrophages differ also metabolically [183]. While short-lived M1 macrophages primarily rely on glycolysis and own reduced flux through the electron transport abolishing oxidative phosphorylation [184], M2 macrophages reduce their glycolytic flux [185] and make use of fatty acid oxidation and oxidative phosphorylation [186].

In M1 macrophages, the TCA cycle halts and intermediates such as citrate and succinate accumulate [184]. Succinate is oxidized by succinate dehydrogenase, thereby elevating mitochondrial ROS which contributes to the stabilization and increased activity of HIF-1 α [182,185,186]. Secondly, LPS-induced succinate stabilizes HIF-1 α and enhances IL-1 β production [187]. Interestingly, both, HIF-1 and HIF-2, contribute to an increase in bactericidal activity, myeloid cell infiltration and an increase in acute inflammatory responses of M1 macrophages [81,163,173,188], but it seems that mainly HIF-1 is essential for the regulation of glycolytic capacity in myeloid cells feeding the cellular ATP pool which promotes myeloid cell survival, aggregation, motility, invasiveness, and bacterial killing [81], while HIF-2 modulates macrophage migration without altering intracellular ATP levels [188]. Moreover, HIF-1 has been demonstrated to be induced by Th1 cytokines in M1 macrophage polarization, whereas HIF-2 is induced by Th2 cytokines during an M2 response [171]. In contrast, using a model of sterile tissue damage Gondin et. al. demonstrated that M2 polarization is independent of either HIF isoform [170] assuming that only HIF-1 mediated metabolic reprogramming contributes to M1 polarization while the role of HIF-2 remains to be elucidated.

Dendritic cells (DCs) facilitate antigen-specific T-cell activation after recognition of invading pathogens or endogenous danger signals by their pattern recognition receptors (e.g., TLRs) [189]. Upon activation DCs increase glycolysis activate iNOS and NO production thereby inhibiting the electron flux through the electron transport chain [190]. Thus it is not surprising that HIF-1 has been shown to promote cell survival of mature DCs, DC migration, differentiation and proper DC-mediated cytotoxic T cell activation (involving IFN- α and - β production) and induction of regulatory T cells (Tregs) while inhibiting survival of immature DCs [174–177]. We can conclude from these data that proper innate immune response needs functional HIF's at least to mediate metabolic re-programming.

5.2. HIFs in Adaptive Immunity

The adaptive immune response against cancer and infections is controlled and orchestrated by the T cell compartment. T cells originate from lymphoid progenitors in the bone marrow and mature in the cortex of the thymus, which is known to be hypoxic [25] into various subpopulations of helper CD4⁺ T cells and CD8⁺ cytotoxic T cells [191] (Table 2). Forced stabilization of HIF's by deletion of VHL in thymocytes dramatically decreased thymic cellularity [192]. Additional deletion of HIF-1 α restored thymocyte development suggesting a role of HIF-1 α but not HIF-2 α and the hypoxia pathway in lymphocyte development [192]. Conversely, forced stabilization of HIF's does not affect neutrophil and monocyte development [81]. However, these mature but naïve T cells are metabolic quiescent and rely on oxidative phosphorylation of glucose and lipids to maintain cellular homeostasis [193].

Upon antigen challenging, naive T cells undergo metabolic reprogramming towards aerobic glycolysis and glutamine catabolism and differentiate into different subpopulations of effector T cells thereby generating an immune memory [193,194]. Depending on their environmental cues, CD4⁺ T cells can differentiate into subpopulations such as Tregs, Th1, Th2, or Th17 cells, which have distinct metabolic patterns and immunological functions [193,194].

A prerequisite for effector T cell differentiation (such as Th1, Th2, or Th17 cells) is the upregulation of glycolysis whereas Tregs display increased lipid oxidation and oxidative phosphorylation [193]. Inhibition of glycolysis and/or glutaminolysis or forcing the utilization of fatty acids instead results in inhibition of effector T cell differentiation, T cell anergy or shifting the effector T cells towards regulatory T cell lineage [193,194].

Table 2. HIF-mediated effects in lymphoid cells.

Cell Type	HIF Mediated Effects	Ref.
CD4 ⁺ T cells	HIF-1: survival ↑, glycolysis ↑, Th17 differentiation and effector function↑, Th1 differentiation ↑, effector function ↓ (IFN-γ↓), Treg differentiation↓, Tr1 differentiation ↓	[192,195–202]
	HIF-2: Treg differentiation ↓	[203]
CD8 ⁺ T cells	HIF-1: survival ↑ glycolysis ↑ effector function ↑ (anti-viral infection ↑, antitumor capacity ↑; IL-13 ↑) CD8 ⁺ T _C 2 cell differentiation ↑ effector molecule↑	[27,204–207]
	HIF-2: survival ↑ effector function ↑ (IFN-γ and TNF-α ↑)	[208]
B cells	HIF-1: survival ↑, glycolysis ↑, cell cycle ↑, effector function (IgG and IgM antibodies↓, IL-10 ↑), chemotherapeutic antitumor effect ↓	[209–211]
	HIF-2: unknown	

↑: induced or up-regulated, ↓: reduced or down-regulated.

HIF-1α has been demonstrated to play a crucial role in regulating development, survival, proliferation, and differentiation in murine and human T cells [192,195,199,200]. Activation of HIF-1 further promotes the metabolic reprogramming towards glycolysis thereby enhancing effector cell function. As one result, HIF-1α shifts the balance from Tregs to effector Th17 cells by (i) promotion of glycolysis [200] but also (ii) by binding of the Treg-specific transcription factor Foxp3 and its subsequent degradation favoring pro-inflammatory effector Th17 cells which drive inflammation and can lead to autoimmunity [199,200]. Moreover, HIF-1 itself is further upregulated by STAT3 and induces transcription of the gene encoding the retinoic acid-related orphan receptor γt (RORγt) [199]. Of note, RORγt is the key transcription factor that drives Th17 differentiation [212]. Finally, HIF-1 has been demonstrated to promote the longevity of Th17 cells by controlling Notch

signaling and antiapoptotic gene expression which could be abrogated by HIF-1 inhibition using echinomycin treatment [213].

Apart from deleting VHL, HIF-1 mediated overexpression of miR-210 finally promotes autoimmunity (psoriasis-like inflammation) by inducing Th1 and Th17 cell differentiation [124]. Conversely, HIF-1 α is not only enhancing miR-210, but also controlled in a negative feedback by miR-210 itself [123], an effect that is considered to be more important in Th1 cells. Here, HIF-1 negatively regulates Th1 function by reducing their capacity to produce IFN- γ [122]. Finally, the role of HIF-1 and miR-210 in Th17 and Th1 needs further investigations while studies on the role of HIF's in Th2 cell response are still missing. Apart from HIF-1 α which enhances Th17 differentiation and inhibits Treg cell differentiation, HIF-2 α may also determine the fate of T cells. Although its expression was not sufficient in other Th subsets, HIF-2 α was required for IL-9 expression in Th9 cells. Furthermore, miR-15b and miR-16 suppressed HIF-2 α expression in Treg cells [203].

When focusing on Tregs, the impact of hypoxia and HIF's is still less clear. Although HIF-1 has been reported to tip the balance of Th17/Tregs towards Th17 cells [199,200], some reports demonstrated that hypoxia enhances Treg abundance through HIF-1 α -dependent regulation of FoxP3, thus, limiting inflammation [214,215]. Thus, hypoxia and HIF-1 α in T cells constrain T-cell-mediated inflammation supporting earlier findings [216–218]. In this line, T cell-specific HIF-1 α KO mice has been demonstrated to result in severe intestinal inflammation with an upregulation of Th1 and Th17 cells [219]. Conversely, Foxp3-restricted VHL deletion in mice augmented HIF-1 α -induced glycolytic reprogramming and IFN- γ production and converted Treg cells into Th1-like effector T cells instead of Th17 cells which finally results in massive uncontrolled inflammation during dextran sulfate sodium (DSS)-induced colitis [220].

However, Foxp3-negative type I regulatory T cells (Tr1 cells), which own the capacity to attenuate Th17 cells are regulated by HIF-1 α which controls the early metabolic reprogramming of human and murine Tr1 cells [196–198,201].

In the GC, activated extrafollicular CD4⁺ T cells and follicular T helper (Tfh) promote humoral immunity of B cells. HIF-1 α depletion from CD4⁺ T cells reduces the frequencies of antigen-specific GC B cells, Tfh cells, Tfh/T follicular regulatory (Tfr) ratio, cytokine production (IFN- γ , IL-4), and overall antigen-specific antibody after immunization of sheep red blood cells (SRBC); while deficiency of HIF-1 α and HIF-2 α leading to further decrease in Tfh cells, Tfh/Tfr ratio, cytokine production and overall antigen-specific antibody. In contrast to this, after hapten-carrier immunization deficiency of HIF-1 α has no effect on affinity maturation, while both deficiency of HIF-1 α and HIF-2 α lead to affinity maturation defects [202].

Effector CD8⁺ T cells or cytotoxic T lymphocytes (CTLs) are crucial mediators of cell-mediated immunity and play an essential role in the control of infections and cancer by the production and release of perforin and granzyme [221]. Hypoxia and HIF-1 favors the development of highly cytotoxic CD8⁺ T cells upon activation by facilitating metabolic reprogramming towards glucose uptake and glycolysis through the upregulation of numerous glycolytic enzymes while enhancing the expression of effector molecules such as granzymes and perforin [27,207]. Although both HIF-1 α and HIF-2 α are essential for controlling the survival, differentiation, and proliferation of human and murine CD8⁺ T cells [205], only HIF-1 α , but not HIF-2 α , was essential for the effector state in CD8⁺ T cells providing antitumor capacity [204]. Although rapid induction glycolysis, which is known to be facilitated by HIF-1, has been demonstrated to enhance effector memory CD8⁺ T cell function [206], limiting glycolytic flux and the expression of HIF-1 during activation of CD8⁺ T cells further enhanced the generation of long-lived memory CD8⁺ T cells and antitumor functionality [222], which was supported by the finding that commitment of CD8⁺ T cells to a highly glycolysis-driven metabolic program favored short-lived effector memory cells while negatively affecting long-lived memory populations [223]. A recent study on terminally differentiated tissue-resident T cells (CD69⁺CD103⁺–D8⁺ T cells) of the

human liver demonstrated that reduction of HIF-2 α expression suppressed production of IFN- γ and TNF- α and increased TCR-induced cell death [208].

During chronic infection, the destructive capacity of CTLs is progressively dampened leading to ‘exhaustion’ which may be due induction of disease tolerance as a defense strategy [224,225]. Although stabilizing HIF’s by deletion of VHL lead to lethal CTL-mediated immunopathology during chronic infection bypasses T cell ‘exhaustion’ leading to an enhanced control of viral infection and tumor growth [226]. Moreover, hypoxia also enhance CD8⁺ type 2 cytotoxic T (T_C2) -mediated inflammation and airway hyper-responsiveness via IL-4/HIF-1 α -axis [227]. Finally, hypoxic CD8⁺T-cells demonstrate an increased capacity to persist, to proliferate, and to enhance antitumor efficacy upon a HIF-1 α -dependent increase of metabolite S-2-hydroxyglutarate (S-2HG) production modifying epigenome [205].

In summary, these data demonstrate an important role for hypoxia and HIF-1-mediated signaling and metabolic reprogramming in the regulation of T cell function.

B cells play a crucial role in humoral immunity [228]. Upon their differentiation into plasmablasts and plasma cells B cells confer humoral immunity-by the secretion of antibodies protecting the host against an unlimited variety of pathogens. As effector cells, B cells are also involved in antigen presentation [228]. Moreover, B cells possess also immunomodulatory function by the secretion of anti-inflammatory cytokines such as IL-35, TGF- β and IL-10 [229–234]. Defects in B cell development leads to immune dysfunction resulting in immunodeficiency, allergy, autoimmunity and cancer [229,235].

Hypoxia and the HIF-1 α pathway have been demonstrated to play a vital role in B cell activation, survival, proliferation, cell cycle arrest, development, effector and regulatory function [209,210,236,237]. In detail, B cell activation through B cell antigen receptor (BCR) induces upregulation of HIF-1 α expression [209]. HIF-1 α has been demonstrated to be essential for hypoxia-induced cell cycle arrest [237] and to be responsible for hypoxia-induced upregulation of two pore domain subfamily K member 5 potassium channels thereby augmenting Ca²⁺ signaling in B cells which is essential for number of cellular functions including proliferation, survival, and cytokine production [236]. In Hif1a/Rag2-deficient chimeric mice display B cell lineage defects including abnormalities in peritoneal B1 cells and high levels of IgG and IgM antibodies directed against dsDNA, a phenotype of autoimmunity [210]. Moreover, ablation of Hif1a, but not Hif2a in B cells impairs IL-10 production and the switch to glycolytic metabolism as well as CD1d^{hi}CD5⁺ B cells expansion [209]. Ultimately, lack of Hif1a results in an exacerbated collagen-induced arthritis and experimental autoimmune encephalomyelitis [209]. HIF-1 α along with p-STAT3 enhanced CD11b transcription in a DSS-induced colitis model. The latter commits regulatory function to B cells and is involved in protective activity in experimental inflammatory bowel disease (IBD) [238–240]. However, HIF-1 α deficiency in B cells improves the chemotherapeutic antitumor effect by inhibiting CD19⁺ extracellular vesicles (EV) production [100]. CD19⁺ EVs hydrolyze ATP from tumor cells into adenosine which inhibits CD8 T cell antitumor response (see Table 2) [211].

In germinal centers (GCs), antigen challenging of B cells results in proliferation, expression of high-affinity antibodies, antibody class switching, and B cell memory. GC light zones have been demonstrated to be hypoxic [33]. GC hypoxia and HIF signaling increase glycolytic metabolism but reduced B cell proliferation, increased B cell death, impairs antibody class switching to IgG2c antibody isotype. Interestingly, constitutive activation and stabilization of HIF-1 α induces B-cell proliferation, decreases antigen-specific GC B cells and impairs the generation of high-affinity IgG antibodies [33,34]. However, in hypoxic conditions the generation and maintenance of GC B cells has been demonstrated to rely on HIF-mediated increase of glycolysis and mitochondrial biogenesis for growth and proliferation [241]. In this line, blocking glucose uptake by deletion of glucose transporter 1 decreased B cell proliferation and impaired antibody production [242].

5.3. HIFs in Innate Lymphoid Immune Response

The innate lymphoid immune response is mediated by NK cells and so called innate lymphoid cells (ILCs). These tissue-resident immune cells do not express T cell receptors although they share similarities with CD4+ T cells and CTLs. ILCs are positioned at barrier surfaces to rapidly respond invading pathogens by local expansion to effectively initiate an immune response before adaptive immunity is engaged [243]. These areas are typically not well oxygenated at least when it comes to inflammation. Thus, it is essential that they own proper mechanisms to adapt to hypoxic conditions (Table 3).

Table 3. HIF-mediated effects in innate lymphoid cells.

Cell Type	HIF Mediated Effects	Ref.
Innate lymphoid cells (ILC2)	HIF-1: late-stage maturation and function of ILC2s via targeting IL-33-ST2 pathway	[244]
	HIF-2: unknown	
NK cells	HIF-1: tumor growth ↑ (angiogenesis↑, VEGFR-1↑) tumor cell killing ↑, INF-γ ↓, OCR/ECAR ratio ↓	[245,246]
	HIF-2: unknown	

↑: induced or up-regulated, ↓: reduced or down-regulated.

ILCs can be classified into three different groups, namely group 1 ILCs (including ILC1s and NK cells), group 2 ILCs and group 3 ILCs (including lymphoid tissue inducer cells, natural cytotoxicity receptor positive and negative cells), based on their similarity to Th cell subsets in terms of their expression of key transcription factors and cytokine production [247]. ILCs protect against infectious pathogens such as helminths, viruses, intracellular parasite and protozoa, extracellular bacteria and fungi, and demonstrate functional plasticity depending on their inflammatory microenvironment [247].

Together with ILC1s, NK cells constitute group 1 ILCs, which protect against intracellular pathogens and are characterized by their capacity to produce interferon-γ and their functional dependence on the transcription factor T-bet [248]. NK cells commit cytotoxic activity releasing granzymes and perforins bearing anticancer and antiviral activity [249]. Like Th2 cells, group 2 ILCs are characterized by the need for Gata-3 and a Th2 cytokine profile to facilitate immune response against extracellular microorganisms [247].

Group 3 ILCs share similarities with Th17 cells by expressing RORγt and are implicated in tissue homeostasis, repair and inflammation [247]. All ILCs have been implicated when dysregulated leading to chronic inflammation and autoimmune diseases such as spondylarthritis (SpA), psoriasis and IBD [247].

Similar to CTLs, NK cells infiltrate hypoxic tumor areas in order to kill malignant cells. Loss of HIF-1 impaired tumor cell killing but still inhibited tumor growth by exacerbated VEGF-driven angiogenesis due to a reduced infiltration of NK cells that express angiostatic soluble VEGFR-1 [246]. However, hypoxia has also been demonstrated to impair NK cell cytotoxicity [250,251]. This seems surprising since tumor hypoxia inhibits NK cell function although these cells undergo metabolic reprogramming upon activation of effector function (IFN-γ production and granzyme B expression) from the quiescent state to glycolysis via the metabolic checkpoint kinase mTOR (in similarity to T cells) [252–254]. Interestingly metabolic reprogramming was only induced upon sustained activation but not after short-term priming [255]. Single cell RNA sequencing of mouse tumor-infiltrating NK cells identified Hif1a to be upregulated in the hypoxic microenvironment of solid tumors while conditional deletion of Hif1a^{-/-} in tumor-infiltrating NK cells activated the

NFκB pathway, elevated expression of activation markers, effector molecule and increased INF-γ production in correlation with elevated oxygen consumption rate/extracellular acidification rate (OCR/ECAR) ratio finally reducing tumor growth [245].

In ILC2s deletion of VHL and stabilization of HIF's caused a decrease in mature ILC2 numbers in peripheral nonlymphoid tissues without affecting early-stage bone marrow ILC2s, resulting in reduced type 2 immune responses. The decrease in mature ILC2 numbers results from HIF-1 mediated reduction of IL-33 receptor (ST2) expression [244].

However, how hypoxia and the HIF signaling pathway modulates function and metabolism of ILCs and NK cells in the setting of tumor biology and autoimmunity requires further research.

6. Extracellular Signals Regulating HIF's in Immune Cells Apart from Hypoxia

Hypoxia and its impact on the stability of HIF and activity of HIF signaling fundamentally influences immune cell function in a cell-type specific manner. The temporal, spatial and dynamic nature of hypoxia differently impacts the immune cell function and response in a cell type specific manner. Under physiological conditions the temporal and spatial oxygen availability for cells and tissues remains constant. Although the degree of hypoxia varies between different tissues and from oxygen supplying capillaries to the cavities of mitochondrial lacuna, established oxygen gradients maintain stable and sustained allowing temporal and spatial limited fluctuations of the oxygen gradient [1].

Beside hypoxia, other extracellular microenvironmental factors (such as pathogens, cytokines, metabolic enzymes and metabolites) contribute to the induction and stabilization of HIF's in immune cells (Figure 5). Under normoxia, Gram-positive and Gram-negative bacterial components induce HIF-1α expression and stabilization in mouse bone marrow-derived macrophages [163]. Treatment of macrophages with lipopolysaccharide (LPS), a major component of the outer membrane of Gram-negative bacteria, and associated activation of Toll-like receptors (TLRs) in macrophages, increases HIF-1α expression and leads to its stabilization by multiple pathways, such as PI3K pathway [256], p44/42 MAPK and NFκB pathway, but also by activation of pyruvate kinase M2 (PKM2) [257], and by accumulation of succinate after glutaminolysis [187,258]. Interestingly, the glycolytic enzyme pyruvate kinase M2 (PKM2) has been demonstrated to shape the cellular response to hypoxia thereby affecting the immune response. PKM2 controls the rate-limiting step of glycolysis and supports glycolysis and the biosynthetic processes [257,259,260]. Furthermore, in LPS-stimulated monocytes PKM2 has been demonstrated to translocate to the nucleus and to interact with HIF-1α thereby inducing the expression of inflammatory genes such as the expression of *IL1B*, *STAT3*, *HMGB1* (encoding IL-1β, signal transducer and activator of transcription, and high mobility group box 1) [257,259–263]. Furthermore, tumor necrosis factor-α (TNF-α) and interferon-γ (IFN-γ) are capable to increase HIF-1α mRNA expression in macrophages [264], while IL-4 and IL-13 increase HIF-2α mRNA abundance [171]. Moreover, oxidized low-density lipoprotein (oxLDL) induces HIF-1α accumulation by a ROS-dependent pathway in human macrophages [265]. Recent findings revealed that atheroma plaque homogenates increased human macrophages' HIF-1α by forming liver-X-receptor (LXR)-HIF-1α-complexes on HIF-1α- and IL-1β-promoter-regions promoting inflammation in atherosclerosis [266]. Activation of mast cells with the calcium ionophore ionomycin enhanced HIF-1α gene and protein expression by activating calcineurin-dependent dephosphorylation of nuclear factor of activated T-cells (NFAT) thereby unleashing NFAT-dependent transcription [267]. Additionally, anti-IgE induces accumulation of HIF-1α protein in human basophils by activating extracellular regulated kinase (ERK) and p38 MAPK [169]. In mDC, neutralization of thymic stromal lymphopoietin (TSLP) and its receptor (TSLPR) during stimulation augments HIF-1α leading to an increased IL-1β expression [268].

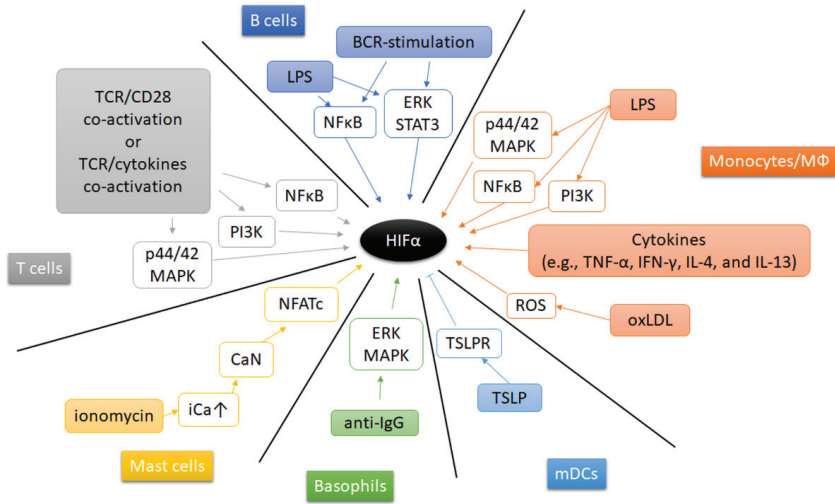


Figure 5. Extracellular regulation of HIF- α . A schematic summarizing the mechanisms underlying the regulation of HIF α activity under diverse physiological and pathological conditions. Arrow indicates activation, and bar-headed line indicates inhibition.

Adaptive immune cells can also regulate HIF-1 α in an oxygen-independent manner. Engagement of the T cell receptor (TCR) induces HIF-1 α expression and accumulation in proinflammatory T helper 17 (Th17) and Th1 cells. Th17-polarizing conditions, presence of transforming growth factor- β (TGF- β) and IL-6, further enhance HIF-1 α expression in a Stat3-dependent manner [199,200]. Moreover, TGF- β - and IL-23-induced HIF-1 α to upregulate miR-210 expression, which promotes helper T (Th) 17 and Th1 cell differentiation [124]. However, CD4+T cell activation requires mitochondrial ROS [269]. The latter is well-known to induce and stabilize HIF- α [107,109,110]. Similar to PKM2 in monocytes, glycolytic enzyme activation may constitute another mechanism of HIF induction in T cell immune response. In brief, GAPDH binds to AU-rich 3' UTR of several genes including *IFNG*, *IL2*, and *HIF1A* mRNA in glycolytic inactive naive and memory T cells. Upon T cell stimulation, glycolysis becomes activated occupying GAPDH thereby releasing *IFNG*, *IL2*, and *HIF1A* mRNA leading to effector cytokine production [74] and an elevated HIF-1 α expression [75]. In CD8+ T cell, TCR-mediated signals can also mediate an increased abundance of both HIF-1 α and HIF-2 α which can be modulated by cytokines (e.g., IL-4, IL-2) [226]. HIF-1 α mRNA and protein can be induced after LPS stimulation by NF κ B pathway and BCR-stimulation via ERK-STAT3 pathway in B cells [209].

7. Summary and Outlook: How to Treat by Targeting HIF to Modulate Immunity

As outlined above, hypoxia and the HIF-response have a variety of implications on immune activity in physiological and pathophysiological context influencing the initiation and propagation of immune response and contributing to the development of immune dysfunction in autoimmunity and cancer. Thus, it is likely, that the hypoxia responsive pathways including HIF's and PHDs could serve as promising therapeutic targets for pharmacological interventions.

Because of its significant impact on inflammation and immune-mediated inflammatory diseases (IMIDs) including autoimmune diseases and cancer, HIF-1 α could serve as a promising therapeutic target. Unraveling the molecular mechanisms of the HIF-1 α pathway and the evidence on the capacity of current treatment strategies to target this process may open novel therapeutic avenue to treat IMIDs. In fact, targeting HIF-1 α in animal models of autoimmune diseases and cancer has yielded encouraging results and new pharmacological

approaches. Consequently, a fast-developing domain of drug discovery has emerged targeting HIF-1 α and/or HIF-2 α to reduce or inhibit its transcriptional activity.

On the other hand, pharmacologic strategies to induce HIF stabilization have recently been tested in patients thereby setting the stage to use PHD inhibitors to treat patients suffering from diseases, such as chronic kidney disease and limb ischemia where the hyporesponsiveness of the HIF pathway has been observed [270]. Other potential clinical applications of HIF stabilizers include inflammatory hypoxia, such as occurs in the setting of inflammatory bowel disease, including ulcerative colitis and Crohn disease (CD). Here, activation of HIF induces intestinal barrier-protective genes (e.g., multidrug resistance gene-1, intestinal trefoil factor, CD73) and ensures mucosal integrity during colitis in vivo [271]. Dimethylxalylglycine (DMOG), a pan-PHD inhibitor, has been demonstrated to be profoundly protective after intraperitoneal injection in a model of dextran-sodium sulfate colitis [272]. Targeted delivery of DMOG to the colon provides local protection not only resulting the same efficacy at a 40-fold lower dose as intraperitoneal injection, but also reduced systemic side effects in the treatment of colitis [273]. Pan-PHD inhibitors, FG-4497 [274] and TRC160334 [275], and HIF-1 isoform-predominant PHD inhibitor, such as AKB-4924 [56,276], also showed an attenuation of inflammation in murine colitis. Furthermore, regulation of IL-12p40 by HIF induced via AKB-4924 controls Th1/Th17 responses to prevent mucosal inflammation [277]. Importantly, HIF-2 α , which can promote the inflammatory response and impair intestinal barrier integrity, constitutes a pathogenic mechanism in ulcerative colitis [278]. Due to the different role of HIF-1 α and HIF-2 α in ulcerative colitis, the balancing mechanisms of these subunits during therapeutic intervention to treat colitis needs to be further investigated [279]. Furthermore, in Crohn disease, another IBD, increased HIF-1 α protein plays a major role in adherent-invasive *E. coli* (AIEC) induced inflammatory disorders of the gastrointestinal tract [280]. When targeting HIF pathways, HIF-1 seems to be a friend in the treatment of ulcerative colitis but a foe in other autoimmune-mediated pathogenesises such as Crohn disease, systemic lupus erythematosus, rheumatoid arthritis, and psoriasis [281].

Hypoxia and the induction of HIF within the tumor microenvironment has been demonstrated to promote cancer progression, metastasis, and therapy resistance by (i) reducing anti-tumor effector immune cells such as cytotoxic T cells, nature killer cells, and cytokines and/or (ii) increasing immunosuppressive cells such as Tregs and tumor-associated macrophages owing a M2 macrophage phenotype, the expression of immunosuppressive cytokines and inhibitory immune checkpoint molecules such as programmed death 1 (PD-1) receptor or Cytotoxic T-Lymphocyte-Associated protein 4 (CTLA-4) [282]. Many small molecules, which regulate each regulatory step of HIF- α -mediated gene expression in tumor cells from its (i) gene expression, (ii) protein translation, (iii) HIF- α stabilization, (iv) dimerization, and (v) DNA binding as well as (vi) HIF- α -mediated transcription of target genes have been developed. They are in majority targeting/inhibiting HIF-1 α [270,283,284] instead of HIF-2 α [285]. Apart from directly inhibiting HIF-1/2 α , many molecules act on HIF-1/2-related signaling pathways, such as the PI3K/AKT/mTOR pathway, leading to indirect inhibition of HIF-1/2 α [270,283,286]. However, HIF-1/2 regulation pathways are very complicated and contain interacting signaling networks. Thus, unspecific inhibition of HIF might result in unexpected side effects. Recently, selective HIF-2 α allosteric inhibitors PT2385 and PT2977, which weaken heterodimerization with HIF-1 β by selectively binding to HIF-2 α -PAS-B domain [287], showed 66% and 80% of disease control rate and were well tolerated in phase I/II study of renal cell carcinomas (RCCs) [288–290]. A Phase III trial of monotherapy PT2977 in a population with previously treated RCC is planned and some clinical trials of selective HIF-2 α inhibitors are underway (Table 4).

Table 4. Summary of select ongoing clinical trials of HIF-2 α inhibitors in cancer.

Compound/Drug Name	Objective	Type of Cancer	Phase	NCT Number
PT2977 (MK6482) (Inhibition of HIF-2 heterodimerization)	Tumor response	advanced solid tumors/ccRCC /specified solid tumors/glioblastoma (GBM)	I	NCT02974738
	ORR	Advanced or metastatic ccRCC	II	NCT03634540
	ORR	VHL-Associated Renal Cell Carcinoma	II	NCT03401788
PT2385 (Inhibition of HIF-2 heterodimerization)	MTD (Part 1: PT2385; Part 2: PT2385 + nivolumab; Part 3: PT2385 + cabozantinib)	Advanced ccRCC	I	NCT02293980
	Tumor radiographic response	Recurrent GBM	II	NCT03216499
	ORR	VHL disease-associated ccRCC	II	NCT03108066
ARO-HIF2 (Neutralization of HIF2A mRNA)	AEs; RP2D	ccRCC	I	NCT04169711

NCT National Clinical Trial (clinicaltrials.gov, accessed on 25 February 2021), RCC, renal cell carcinoma; ccRCC, clear cell renal carcinoma; GBM, glioblastoma; ORR, objective response rate; VHL, Von Hippel-Lindau; MTD, maximum tolerated dose; AEs, adverse events; RP2D, recommended phase 2 dose; PFS, progression-free survival.

It is noteworthy that HIF- α actually improves effector function of many immune cells as explained before. Taking advantage of this knowledge, by selectively upregulating HIF- α in immune cells under conditions of a hypoxic tumor microenvironment may foster their tumor killing capacity; an effect which might provide a novel approach in the treatment of cancer.

Chronic kidney disease, ischemic disease and ulcerative colitis are beneficial from HIF stabilizer therapy, while cancers can be suppressed by HIF inhibitor therapy. In clinical application, the therapeutic window of HIF targeting should be exquisitely balanced. For example, the elderly tends to suffer from cancers and might be beneficial from HIF inhibitor, but this population is probably accompanied by ischemic heart disease which could be treated by HIF stabilizer. Pan-HIF inhibitor and stabilizer may have severe side effects, thereby their clinical application is limited. In these circumstances, local treatment and selectively HIF-1 or HIF-2 targeting medicine might provide therapeutic potential.

Although many clinical trials have confirmed that both HIF inhibitor and stabilizer can be used for clinical disease therapy, due to its widespread expression and wide impact on cell survival and function, the clinical benefits and side effects of drugs targeting HIF must be further carried out in specific disease context.

These and other findings reported and reviewed here suggest that targeting HIF-1 α could be a useful strategy for autoimmune diseases therapies.

Author Contributions: Conceptualization, T.G.; writing—original draft preparation, T.G. and Y.C.; writing—review and editing, T.G. and Y.C.; visualization, T.G.; supervision, T.G.; project administration, T.G.; funding acquisition, T.G. All authors have read and agreed to the published version of the manuscript.

Funding: The work of T.G. was funded by the German Research Foundation (353142848, grant approval 07/2017). The APC was funded by the German Research Foundation (DFG) and the Open Access Publication Fund of Charité-Universitätsmedizin Berlin.

Institutional Review Board Statement: Not applicable.

Informed Consent Statement: Not applicable.

Data Availability Statement: Not applicable.

Conflicts of Interest: The authors declare no conflict of interest. The funders had no role in the writing of the manuscript, or in the decision to publish the manuscript.

References

- Taylor, C.T.; Colgan, S.P. Regulation of immunity and inflammation by hypoxia in immunological niches. *Nat. Rev. Immunol.* **2017**, *17*, 774. [CrossRef]
- Beerman, I.; Luis, T.C.; Singbrant, S.; Lo Celso, C.; Mendez-Ferrer, S. The evolving view of the hematopoietic stem cell niche. *Exp. Hematol.* **2017**, *50*, 22–26. [CrossRef] [PubMed]
- Shah, D.K.; Zuniga-Pflucker, J.C. An overview of the intrathymic intricacies of T cell development. *J. Immunol.* **2014**, *192*, 4017–4023. [CrossRef] [PubMed]
- Lin, E.W.; Karakasheva, T.A.; Hicks, P.D.; Bass, A.J.; Rustgi, A.K. The tumor microenvironment in esophageal cancer. *Oncogene* **2016**, *35*, 5337–5349. [CrossRef]
- Maru, Y. The lung metastatic niche. *J. Mol. Med. (Berl)* **2015**, *93*, 1185–1192. [CrossRef]
- Biswas, S.; Davis, H.; Irshad, S.; Sandberg, T.; Worthley, D.; Leedham, S. Microenvironmental control of stem cell fate in intestinal homeostasis and disease. *J. Pathol.* **2015**, *237*, 135–145. [CrossRef] [PubMed]
- Hallenbeck, J.M.; Hansson, G.K.; Becker, K.J. Immunology of ischemic vascular disease: Plaque to attack. *Trends Immunol.* **2005**, *26*, 550–556. [CrossRef]
- Multhoff, G.; Molls, M.; Radons, J. Chronic inflammation in cancer development. *Front. Immunol.* **2011**, *2*, 98. [CrossRef]
- Lin, N.; Simon, M.C. Hypoxia-inducible factors: Key regulators of myeloid cells during inflammation. *J. Clin. Investig.* **2016**, *126*, 3661–3671. [CrossRef] [PubMed]
- Taylor, C.T.; Doherty, G.; Fallon, P.G.; Cummins, E.P. Hypoxia-dependent regulation of inflammatory pathways in immune cells. *J. Clin. Investig.* **2016**, *126*, 3716–3724. [CrossRef]
- Scholz, C.C.; Taylor, C.T. Targeting the HIF pathway in inflammation and immunity. *Curr. Opin. Pharmacol.* **2013**, *13*, 646–653. [CrossRef] [PubMed]
- McNamee, E.N.; Kornis Johnson, D.; Homann, D.; Clambey, E.T. Hypoxia and hypoxia-inducible factors as regulators of T cell development, differentiation, and function. *Immunol. Res.* **2013**, *55*, 58–70. [CrossRef] [PubMed]
- Carreau, A.; El Hafny-Rahbi, B.; Matejuk, A.; Grillon, C.; Kieda, C. Why is the partial oxygen pressure of human tissues a crucial parameter? Small molecules and hypoxia. *J. Cell Mol. Med.* **2011**, *15*, 1239–1253. [CrossRef]
- Boveris, D.L.; Boveris, A. Oxygen delivery to the tissues and mitochondrial respiration. *Front. Biosci.* **2007**, *12*, 1014–1023. [CrossRef]
- Leach, R.M.; Treacher, D.F. Oxygen transport-2. Tissue hypoxia. *BMJ* **1998**, *317*, 1370–1373. [CrossRef]
- Available online: <http://smart.servier.com/> (accessed on 1 March 2021).
- Jiang, B.H.; Semenza, G.L.; Bauer, C.; Marti, H.H. Hypoxia-inducible factor 1 levels vary exponentially over a physiologically relevant range of O₂ tension. *Am. J. Physiol.* **1996**, *271*, C1172–C1180. [CrossRef] [PubMed]
- Glover, L.E.; Lee, J.S.; Colgan, S.P. Oxygen metabolism and barrier regulation in the intestinal mucosa. *J. Clin. Investig.* **2016**, *126*, 3680–3688. [CrossRef]
- Maxwell, P.H.; Ferguson, D.J.; Nicholls, L.G.; Iredale, J.P.; Pugh, C.W.; Johnson, M.H.; Ratcliffe, P.J. Sites of erythropoietin production. *Kidney Int.* **1997**, *51*, 393–401. [CrossRef]
- Haase, V.H. Regulation of erythropoiesis by hypoxia-inducible factors. *Blood Rev.* **2013**, *27*, 41–53. [CrossRef]
- Macklin, P.S.; McAuliffe, J.; Pugh, C.W.; Yamamoto, A. Hypoxia and HIF pathway in cancer and the placenta. *Placenta* **2017**, *56*, 8–13. [CrossRef]
- Wang, W.; Winlove, C.P.; Michel, C.C. Oxygen partial pressure in outer layers of skin of human finger nail folds. *J. Physiol.* **2003**, *549*, 855–863. [CrossRef]
- Takubo, K.; Goda, N.; Yamada, W.; Iriuchishima, H.; Ikeda, E.; Kubota, Y.; Shima, H.; Johnson, R.S.; Hirao, A.; Suematsu, M.; et al. Regulation of the HIF-1 α level is essential for hematopoietic stem cells. *Cell Stem Cell* **2010**, *7*, 391–402. [CrossRef]
- Parmar, K.; Mauch, P.; Vergilio, J.A.; Sackstein, R.; Down, J.D. Distribution of hematopoietic stem cells in the bone marrow according to regional hypoxia. *Proc. Natl. Acad. Sci. USA* **2007**, *104*, 5431–5436. [CrossRef]
- Hale, L.P.; Braun, R.D.; Gwinn, W.M.; Greer, P.K.; Dewhirst, M.W. Hypoxia in the thymus: Role of oxygen tension in thymocyte survival. *Am. J. Physiol. Heart Circ. Physiol.* **2002**, *282*, H1467–H1477. [CrossRef]
- Braun, R.D.; Lanzen, J.L.; Snyder, S.A.; Dewhirst, M.W. Comparison of tumor and normal tissue oxygen tension measurements using OxyLite or microelectrodes in rodents. *Am. J. Physiol. Heart Circ. Physiol.* **2001**, *280*, H2533–H2544. [CrossRef]
- Caldwell, C.C.; Kojima, H.; Lukashev, D.; Armstrong, J.; Farber, M.; Apasov, S.G.; Sitkovsky, M.V. Differential effects of physiologically relevant hypoxic conditions on T lymphocyte development and effector functions. *J. Immunol.* **2001**, *167*, 6140–6149. [CrossRef]
- Huang, J.H.; Cardenas-Navia, L.I.; Caldwell, C.C.; Plumb, T.J.; Radu, C.G.; Rocha, P.N.; Wilder, T.; Bromberg, J.S.; Cronstein, B.N.; Sitkovsky, M.; et al. Requirements for T lymphocyte migration in explanted lymph nodes. *J. Immunol.* **2007**, *178*, 7747–7755. [CrossRef] [PubMed]
- Eliasson, P.; Rehn, M.; Hammar, P.; Larsson, P.; Sirenko, O.; Flippin, L.A.; Cammenga, J.; Jonsson, J.I. Hypoxia mediates low cell-cycle activity and increases the proportion of long-term-reconstituting hematopoietic stem cells during in vitro culture. *Exp. Hematol.* **2010**, *38*, 301.e302–310.e302. [CrossRef] [PubMed]
- Hermitte, F.; Brunet de la Grange, P.; Belloc, F.; Praloran, V.; Ivanovic, Z. Very low O₂ concentration (0.1%) favors G₀ return of dividing CD34+ cells. *Stem Cells* **2006**, *24*, 65–73. [CrossRef] [PubMed]

31. Ivanovic, Z.; Hermitte, F.; Brunet de la Grange, P.; Dazey, B.; Belloc, F.; Lacombe, F.; Vezon, G.; Praloran, V. Simultaneous maintenance of human cord blood SCID-repopulating cells and expansion of committed progenitors at low O₂ concentration (3%). *Stem Cells* **2004**, *22*, 716–724. [[CrossRef](#)]
32. Cipolleschi, M.G.; Dello Sbarba, P.; Olivotto, M. The role of hypoxia in the maintenance of hematopoietic stem cells. *Blood* **1993**, *82*, 2031–2037. [[CrossRef](#)]
33. Cho, S.H.; Raybuck, A.L.; Stengel, K.; Wei, M.; Beck, T.C.; Volanakis, E.; Thomas, J.W.; Hiebert, S.; Haase, V.H.; Boothby, M.R. Germinal centre hypoxia and regulation of antibody qualities by a hypoxia response system. *Nature* **2016**, *537*, 234–238. [[CrossRef](#)]
34. Abbott, R.K.; Thayer, M.; Labuda, J.; Silva, M.; Philbrook, P.; Cain, D.W.; Kojima, H.; Hatfield, S.; Sethumadhavan, S.; Ohta, A.; et al. Germinal Center Hypoxia Potentiates Immunoglobulin Class Switch Recombination. *J. Immunol.* **2016**, *197*, 4014–4020. [[CrossRef](#)] [[PubMed](#)]
35. Colgan, S.P.; Campbell, E.L.; Kominsky, D.J. Hypoxia and Mucosal Inflammation. *Annu. Rev. Pathol.* **2016**, *11*, 77–100. [[CrossRef](#)] [[PubMed](#)]
36. Labiano, S.; Palazon, A.; Melero, I. Immune response regulation in the tumor microenvironment by hypoxia. *Semin. Oncol.* **2015**, *42*, 378–386. [[CrossRef](#)] [[PubMed](#)]
37. Unwith, S.; Zhao, H.; Hennah, L.; Ma, D. The potential role of HIF on tumour progression and dissemination. *Int. J. Cancer* **2015**, *136*, 2491–2503. [[CrossRef](#)]
38. Lee, P.; Chandel, N.S.; Simon, M.C. Cellular adaptation to hypoxia through hypoxia inducible factors and beyond. *Nat. Rev. Mol. Cell Biol.* **2020**, *21*, 268–283. [[CrossRef](#)]
39. Krock, B.L.; Skuli, N.; Simon, M.C. Hypoxia-induced angiogenesis: Good and evil. *Genes Cancer* **2011**, *2*, 1117–1133. [[CrossRef](#)]
40. Chiu, D.K.; Xu, I.M.; Lai, R.K.; Tse, A.P.; Wei, L.L.; Koh, H.Y.; Li, L.L.; Lee, D.; Lo, R.C.; Wong, C.M.; et al. Hypoxia induces myeloid-derived suppressor cell recruitment to hepatocellular carcinoma through chemokine (C-C motif) ligand 26. *Hepatology* **2016**, *64*, 797–813. [[CrossRef](#)]
41. Chiu, D.K.; Tse, A.P.; Xu, I.M.; Di Cui, J.; Lai, R.K.; Li, L.L.; Koh, H.Y.; Tsang, F.H.; Wei, L.L.; Wong, C.M.; et al. Hypoxia inducible factor HIF-1 promotes myeloid-derived suppressor cells accumulation through ENTPD2/CD39L1 in hepatocellular carcinoma. *Nat. Commun* **2017**, *8*, 517. [[CrossRef](#)]
42. Corzo, C.A.; Condamine, T.; Lu, L.; Cotter, M.J.; Youn, J.I.; Cheng, P.; Cho, H.I.; Celis, E.; Quiceno, D.G.; Padhya, T.; et al. HIF-1 α regulates function and differentiation of myeloid-derived suppressor cells in the tumor microenvironment. *J. Exp. Med.* **2010**, *207*, 2439–2453. [[CrossRef](#)] [[PubMed](#)]
43. Noman, M.Z.; Desantis, G.; Janji, B.; Hasmim, M.; Karray, S.; Dessen, P.; Bronte, V.; Chouaib, S. PD-L1 is a novel direct target of HIF-1 α , and its blockade under hypoxia enhanced MDSC-mediated T cell activation. *J. Exp. Med.* **2014**, *211*, 781–790. [[CrossRef](#)]
44. Doedens, A.L.; Stockmann, C.; Rubinstein, M.P.; Liao, D.; Zhang, N.; DeNardo, D.G.; Coussens, L.M.; Karin, M.; Goldrath, A.W.; Johnson, R.S. Macrophage expression of hypoxia-inducible factor-1 α suppresses T-cell function and promotes tumor progression. *Cancer Res.* **2010**, *70*, 7465–7475. [[CrossRef](#)]
45. Loeffler, D.A.; Keng, P.C.; Baggs, R.B.; Lord, E.M. Lymphocytic infiltration and cytotoxicity under hypoxic conditions in the EMT6 mouse mammary tumor. *Int J. Cancer* **1990**, *45*, 462–467. [[CrossRef](#)] [[PubMed](#)]
46. Mazurek, J. Diagnostic and therapeutic role of a psychiatrist in a diagnostic and therapeutic team in a de-habituating ward. *Psychiatr. Pol.* **1975**, *9*, 349–350. [[PubMed](#)]
47. Yousaf, I.; Kaeppler, J.; Frost, S.; Seymour, L.W.; Jacobus, E.J. Attenuation of the Hypoxia Inducible Factor Pathway after Oncolytic Adenovirus Infection Coincides with Decreased Vessel Perfusion. *Cancers* **2020**, *12*, 851. [[CrossRef](#)] [[PubMed](#)]
48. Devraj, G.; Beerlage, C.; Brune, B.; Kempf, V.A. Hypoxia and HIF-1 activation in bacterial infections. *Microbes Infect.* **2017**, *19*, 144–156. [[CrossRef](#)]
49. Friedrich, D.; Fecher, R.A.; Rupp, J.; Deepe, G.S., Jr. Impact of HIF-1 α and hypoxia on fungal growth characteristics and fungal immunity. *Microbes Infect.* **2017**, *19*, 204–209. [[CrossRef](#)] [[PubMed](#)]
50. Werth, N.; Beerlage, C.; Rosenberger, C.; Yazdi, A.S.; Edelmann, M.; Amr, A.; Bernhardt, W.; von Eiff, C.; Becker, K.; Schafer, A.; et al. Activation of hypoxia inducible factor 1 is a general phenomenon in infections with human pathogens. *PLoS ONE* **2010**, *5*, e11576. [[CrossRef](#)] [[PubMed](#)]
51. Schaffer, K.; Taylor, C.T. The impact of hypoxia on bacterial infection. *FEBS J.* **2015**, *282*, 2260–2266. [[CrossRef](#)]
52. Schaible, B.; McClean, S.; Selfridge, A.; Broquet, A.; Asehounne, K.; Taylor, C.T.; Schaffer, K. Hypoxia modulates infection of epithelial cells by *Pseudomonas aeruginosa*. *PLoS ONE* **2013**, *8*, e56491. [[CrossRef](#)]
53. Zeitouni, N.E.; Chotikatum, S.; von Kockritz-Blickwede, M.; Naim, H.Y. The impact of hypoxia on intestinal epithelial cell functions: Consequences for invasion by bacterial pathogens. *Mol. Cell. Pediatr.* **2016**, *3*, 14. [[CrossRef](#)] [[PubMed](#)]
54. Schaible, B.; Taylor, C.T.; Schaffer, K. Hypoxia increases antibiotic resistance in *Pseudomonas aeruginosa* through altering the composition of multidrug efflux pumps. *Antimicrob. Agents Chemother.* **2012**, *56*, 2114–2118. [[CrossRef](#)]
55. Karhausen, J.; Haase, V.H.; Colgan, S.P. Inflammatory hypoxia: Role of hypoxia-inducible factor. *Cell Cycle* **2005**, *4*, 256–258. [[CrossRef](#)]

56. Campbell, E.L.; Bruyninckx, W.J.; Kelly, C.J.; Glover, L.E.; McNamee, E.N.; Bowers, B.E.; Bayless, A.J.; Scully, M.; Saeedi, B.J.; Golden-Mason, L.; et al. Transmigrating neutrophils shape the mucosal microenvironment through localized oxygen depletion to influence resolution of inflammation. *Immunity* **2014**, *40*, 66–77. [[CrossRef](#)] [[PubMed](#)]
57. Liu, Z.; Bone, N.; Jiang, S.; Park, D.W.; Tadie, J.M.; Deshane, J.; Rodriguez, C.A.; Pittet, J.F.; Abraham, E.; Zmijewski, J.W. AMP-Activated Protein Kinase and Glycogen Synthase Kinase 3beta Modulate the Severity of Sepsis-Induced Lung Injury. *Mol. Med.* **2016**, *21*, 937–950. [[CrossRef](#)]
58. Eltzschig, H.K.; Eckle, T. Ischemia and reperfusion—from mechanism to translation. *Nat. Med.* **2011**, *17*, 1391–1401. [[CrossRef](#)] [[PubMed](#)]
59. Harten, S.K.; Ashcroft, M.; Maxwell, P.H. Prolyl hydroxylase domain inhibitors: A route to HIF activation and neuroprotection. *Antioxid. Redox Signal.* **2010**, *12*, 459–480. [[CrossRef](#)]
60. Jian, Z.; Liu, R.; Zhu, X.; Smerin, D.; Zhong, Y.; Gu, L.; Fang, W.; Xiong, X. The Involvement and Therapy Target of Immune Cells After Ischemic Stroke. *Front. Immunol.* **2019**, *10*, 2167. [[CrossRef](#)] [[PubMed](#)]
61. Eltzschig, H.K.; Carmeliet, P. Hypoxia and inflammation. *N. Engl. J. Med.* **2011**, *364*, 656–665. [[CrossRef](#)] [[PubMed](#)]
62. Semenza, G.L. Hypoxia-inducible factors in physiology and medicine. *Cell* **2012**, *148*, 399–408. [[CrossRef](#)]
63. Semenza, G.L. Hypoxia-inducible factor 1: Master regulator of O₂ homeostasis. *Curr. Opin. Genet. Dev.* **1998**, *8*, 588–594. [[CrossRef](#)]
64. Schodel, J.; Oikonomopoulos, S.; Ragoussis, J.; Pugh, C.W.; Ratcliffe, P.J.; Mole, D.R. High-resolution genome-wide mapping of HIF-binding sites by ChIP-seq. *Blood* **2011**, *117*, e207–e217. [[CrossRef](#)] [[PubMed](#)]
65. Wenger, R.H.; Stiehl, D.P.; Camenisch, G. Integration of oxygen signaling at the consensus HRE. *Sci. STKE* **2005**, *2005*, re12. [[CrossRef](#)]
66. Wang, G.L.; Jiang, B.H.; Rue, E.A.; Semenza, G.L. Hypoxia-inducible factor 1 is a basic-helix-loop-helix-PAS heterodimer regulated by cellular O₂ tension. *Proc. Natl. Acad. Sci. USA* **1995**, *92*, 5510–5514. [[CrossRef](#)] [[PubMed](#)]
67. Hogenesch, J.B.; Chan, W.K.; Jackiw, V.H.; Brown, R.C.; Gu, Y.Z.; Pray-Grant, M.; Perdew, G.H.; Bradfield, C.A. Characterization of a subset of the basic-helix-loop-helix-PAS superfamily that interacts with components of the dioxin signaling pathway. *J. Biol. Chem.* **1997**, *272*, 8581–8593. [[CrossRef](#)]
68. Kaelin, W.G., Jr.; Ratcliffe, P.J. Oxygen sensing by metazoans: The central role of the HIF hydroxylase pathway. *Mol. Cell* **2008**, *30*, 393–402. [[CrossRef](#)]
69. Gu, Y.Z.; Moran, S.M.; Hogenesch, J.B.; Wartman, L.; Bradfield, C.A. Molecular characterization and chromosomal localization of a third alpha-class hypoxia inducible factor subunit, HIF3alpha. *Gene Expr.* **1998**, *7*, 205–213. [[PubMed](#)]
70. Makino, Y.; Uenishi, R.; Okamoto, K.; Isoe, T.; Hosono, O.; Tanaka, H.; Kanopka, A.; Poellinger, L.; Haneda, M.; Morimoto, C. Transcriptional up-regulation of inhibitory PAS domain protein gene expression by hypoxia-inducible factor 1 (HIF-1): A negative feedback regulatory circuit in HIF-1-mediated signaling in hypoxic cells. *J. Biol. Chem.* **2007**, *282*, 14073–14082. [[CrossRef](#)]
71. Makino, Y.; Kanopka, A.; Wilson, W.J.; Tanaka, H.; Poellinger, L. Inhibitory PAS domain protein (IPAS) is a hypoxia-inducible splicing variant of the hypoxia-inducible factor-3alpha locus. *J. Biol. Chem.* **2002**, *277*, 32405–32408. [[CrossRef](#)]
72. Makino, Y.; Cao, R.; Svensson, K.; Bertilsson, G.; Asman, M.; Tanaka, H.; Cao, Y.; Berkenstam, A.; Poellinger, L. Inhibitory PAS domain protein is a negative regulator of hypoxia-inducible gene expression. *Nature* **2001**, *414*, 550–554. [[CrossRef](#)] [[PubMed](#)]
73. Semenza, G.L. Regulation of oxygen homeostasis by hypoxia-inducible factor 1. *Physiology (Bethesda)* **2009**, *24*, 97–106. [[CrossRef](#)] [[PubMed](#)]
74. Kaelin, W.G. Proline hydroxylation and gene expression. *Annu. Rev. Biochem.* **2005**, *74*, 115–128. [[CrossRef](#)] [[PubMed](#)]
75. Yu, F.; White, S.B.; Zhao, Q.; Lee, F.S. HIF-1alpha binding to VHL is regulated by stimulus-sensitive proline hydroxylation. *Proc. Natl. Acad. Sci. USA* **2001**, *98*, 9630–9635. [[CrossRef](#)]
76. Ivan, M.; Kondo, K.; Yang, H.; Kim, W.; Valiando, J.; Ohh, M.; Salic, A.; Asara, J.M.; Lane, W.S.; Kaelin, W.G., Jr. HIF1alpha targeted for VHL-mediated destruction by proline hydroxylation: Implications for O₂ sensing. *Science* **2001**, *292*, 464–468. [[CrossRef](#)]
77. Jaakkola, P.; Mole, D.R.; Tian, Y.M.; Wilson, M.I.; Gielbert, J.; Gaskell, S.J.; von Kriegsheim, A.; Hebestreit, H.F.; Mukherji, M.; Schofield, C.J.; et al. Targeting of HIF-1alpha to the von Hippel-Lindau ubiquitylation complex by O₂-regulated prolyl hydroxylation. *Science* **2001**, *292*, 468–472. [[CrossRef](#)]
78. Lando, D.; Peet, D.J.; Whelan, D.A.; Gorman, J.J.; Whitelaw, M.L. Asparagine hydroxylation of the HIF transactivation domain a hypoxic switch. *Science* **2002**, *295*, 858–861. [[CrossRef](#)]
79. Mahon, P.C.; Hirota, K.; Semenza, G.L. FIH-1: A novel protein that interacts with HIF-1alpha and VHL to mediate repression of HIF-1 transcriptional activity. *Genes Dev.* **2001**, *15*, 2675–2686. [[CrossRef](#)]
80. Walmsley, S.R.; Print, C.; Farahi, N.; Peyssonnaud, C.; Johnson, R.S.; Cramer, T.; Sobolewski, A.; Condliffe, A.M.; Cowburn, A.S.; Johnson, N.; et al. Hypoxia-induced neutrophil survival is mediated by HIF-1alpha-dependent NF-kappaB activity. *J. Exp. Med.* **2005**, *201*, 105–115. [[CrossRef](#)]
81. Cramer, T.; Yamanishi, Y.; Clausen, B.E.; Forster, I.; Pawlinski, R.; Mackman, N.; Haase, V.H.; Jaenisch, R.; Corr, M.; Nizet, V.; et al. HIF-1alpha is essential for myeloid cell-mediated inflammation. *Cell* **2003**, *112*, 645–657. [[CrossRef](#)]
82. Jantsch, J.; Chakravortty, D.; Turza, N.; Prechtel, A.T.; Buchholz, B.; Gerlach, R.G.; Volke, M.; Glasner, J.; Warnecke, C.; Wiesener, M.S.; et al. Hypoxia and hypoxia-inducible factor-1 alpha modulate lipopolysaccharide-induced dendritic cell activation and function. *J. Immunol.* **2008**, *180*, 4697–4705. [[CrossRef](#)]
83. Burrows, N.; Maxwell, P.H. Hypoxia and B cells. *Exp. Cell Res.* **2017**, *356*, 197–203. [[CrossRef](#)]

84. Tao, J.H.; Barbi, J.; Pan, F. Hypoxia-inducible factors in T lymphocyte differentiation and function. A Review in the Theme: Cellular Responses to Hypoxia. *Am. J. Physiol. Cell Physiol.* **2015**, *309*, C580–C589. [[CrossRef](#)] [[PubMed](#)]
85. Palazon, A.; Goldrath, A.W.; Nizet, V.; Johnson, R.S. HIF transcription factors, inflammation, and immunity. *Immunity* **2014**, *41*, 518–528. [[CrossRef](#)]
86. Zinkernagel, A.S.; Johnson, R.S.; Nizet, V. Hypoxia inducible factor (HIF) function in innate immunity and infection. *J. Mol. Med. (Berl.)* **2007**, *85*, 1339–1346. [[CrossRef](#)]
87. Saxena, K.; Jolly, M.K. Acute vs. Chronic vs. Cyclic Hypoxia: Their Differential Dynamics, Molecular Mechanisms, and Effects on Tumor Progression. *Biomolecules* **2019**, *9*, 339. [[CrossRef](#)] [[PubMed](#)]
88. Hsieh, C.H.; Lee, C.H.; Liang, J.A.; Yu, C.Y.; Shyu, W.C. Cycling hypoxia increases U87 glioma cell radioresistance via ROS induced higher and long-term HIF-1 signal transduction activity. *Oncol. Rep.* **2010**, *24*, 1629–1636. [[CrossRef](#)] [[PubMed](#)]
89. Galanis, A.; Pappa, A.; Giannakakis, A.; Lanitis, E.; Dangaj, D.; Sandaltzopoulos, R. Reactive oxygen species and HIF-1 signalling in cancer. *Cancer Lett.* **2008**, *266*, 12–20. [[CrossRef](#)] [[PubMed](#)]
90. Nanduri, J.; Vaddi, D.R.; Khan, S.A.; Wang, N.; Makrenko, V.; Prabhakar, N.R. Xanthine oxidase mediates hypoxia-inducible factor-2alpha degradation by intermittent hypoxia. *PLoS ONE* **2013**, *8*, e75838. [[CrossRef](#)]
91. Nanduri, J.; Wang, N.; Yuan, G.; Khan, S.A.; Souvannakitti, D.; Peng, Y.J.; Kumar, G.K.; Garcia, J.A.; Prabhakar, N.R. Intermittent hypoxia degrades HIF-2alpha via calpains resulting in oxidative stress: Implications for recurrent apnea-induced morbidities. *Proc. Natl. Acad. Sci. USA* **2009**, *106*, 1199–1204. [[CrossRef](#)]
92. Ravi, R.; Mookerjee, B.; Bhujwalla, Z.M.; Sutter, C.H.; Artemov, D.; Zeng, Q.; Dillehay, L.E.; Madan, A.; Semenza, G.L.; Bedi, A. Regulation of tumor angiogenesis by p53-induced degradation of hypoxia-inducible factor 1alpha. *Genes Dev.* **2000**, *14*, 34–44.
93. Isaacs, J.S.; Jung, Y.J.; Mimnaugh, E.G.; Martinez, A.; Cuttitta, F.; Neckers, L.M. Hsp90 regulates a von Hippel Lindau-independent hypoxia-inducible factor-1 alpha-degradative pathway. *J. Biol. Chem.* **2002**, *277*, 29936–29944. [[CrossRef](#)]
94. Selfridge, A.C.; Cavadas, M.A.; Scholz, C.C.; Campbell, E.L.; Welch, L.C.; Lecuona, E.; Colgan, S.P.; Barrett, K.E.; Sporn, P.H.; Sznajder, J.I.; et al. Hypercapnia Suppresses the HIF-dependent Adaptive Response to Hypoxia. *J. Biol. Chem.* **2016**, *291*, 11800–11808. [[CrossRef](#)]
95. Hubbi, M.E.; Gilkes, D.M.; Hu, H.; Kshitz, Ahmed, I.; Semenza, G.L. Cyclin-dependent kinases regulate lysosomal degradation of hypoxia-inducible factor 1alpha to promote cell-cycle progression. *Proc. Natl. Acad. Sci. USA* **2014**, *111*, E3325–E3334. [[CrossRef](#)]
96. Hubbi, M.E.; Semenza, G.L. An essential role for chaperone-mediated autophagy in cell cycle progression. *Autophagy* **2015**, *11*, 850–851. [[CrossRef](#)]
97. Bernardi, R.; Guernah, I.; Jin, D.; Grisendi, S.; Alimonti, A.; Teruya-Feldstein, J.; Cordon-Cardo, C.; Simon, M.C.; Rafii, S.; Pandolfi, P.P. PML inhibits HIF-1alpha translation and neoangiogenesis through repression of mTOR. *Nature* **2006**, *442*, 779–785. [[CrossRef](#)]
98. Brugarolas, J.B.; Vazquez, F.; Reddy, A.; Sellers, W.R.; Kaelin, W.G., Jr. TSC2 regulates VEGF through mTOR-dependent and-independent pathways. *Cancer Cell* **2003**, *4*, 147–158. [[CrossRef](#)]
99. Hudson, C.C.; Liu, M.; Chiang, G.G.; Otterness, D.M.; Loomis, D.C.; Kaper, F.; Giaccia, A.J.; Abraham, R.T. Regulation of hypoxia-inducible factor 1alpha expression and function by the mammalian target of rapamycin. *Mol. Cell Biol.* **2002**, *22*, 7004–7014. [[CrossRef](#)] [[PubMed](#)]
100. Sacks, D.; Baxter, B.; Campbell, B.C.; Carpenter, J.S.; Cognard, C.; Dippel, D.; Eesa, M.; Fischer, U.; Hausegger, K.; Hirsch, J.A.; et al. Multisociety Consensus Quality Improvement Revised Consensus Statement for Endovascular Therapy of Acute Ischemic Stroke. *Int. J. Stroke* **2018**, *13*, 612–632. [[CrossRef](#)] [[PubMed](#)]
101. Fang, H.Y.; Hughes, R.; Murdoch, C.; Coffelt, S.B.; Biswas, S.K.; Harris, A.L.; Johnson, R.S.; Imityaz, H.Z.; Simon, M.C.; Fredlund, E.; et al. Hypoxia-inducible factors 1 and 2 are important transcriptional effectors in primary macrophages experiencing hypoxia. *Blood* **2009**, *114*, 844–859. [[CrossRef](#)]
102. Rius, J.; Guma, M.; Schachtrup, C.; Akassoglou, K.; Zinkernagel, A.S.; Nizet, V.; Johnson, R.S.; Haddad, G.G.; Karin, M. NF-kappaB links innate immunity to the hypoxic response through transcriptional regulation of HIF-1alpha. *Nature* **2008**, *453*, 807–811. [[CrossRef](#)]
103. Jung, Y.J.; Isaacs, J.S.; Lee, S.; Trepel, J.; Neckers, L. IL-1beta-mediated up-regulation of HIF-1alpha via an NFkappaB/COX-2 pathway identifies HIF-1 as a critical link between inflammation and oncogenesis. *FASEB J.* **2003**, *17*, 2115–2117. [[CrossRef](#)]
104. Zhou, J.; Schmid, T.; Brune, B. Tumor necrosis factor-alpha causes accumulation of a ubiquitinated form of hypoxia inducible factor-1alpha through a nuclear factor-kappaB-dependent pathway. *Mol. Biol. Cell* **2003**, *14*, 2216–2225. [[CrossRef](#)]
105. Jung, Y.; Isaacs, J.S.; Lee, S.; Trepel, J.; Liu, Z.G.; Neckers, L. Hypoxia-inducible factor induction by tumour necrosis factor in normoxic cells requires receptor-interacting protein-dependent nuclear factor kappa B activation. *Biochem. J.* **2003**, *370*, 1011–1017. [[CrossRef](#)]
106. Nishi, K.; Oda, T.; Takabuchi, S.; Oda, S.; Fukuda, K.; Adachi, T.; Semenza, G.L.; Shingu, K.; Hirota, K. LPS induces hypoxia-inducible factor 1 activation in macrophage-differentiated cells in a reactive oxygen species-dependent manner. *Antioxid. Redox Signal.* **2008**, *10*, 983–995. [[CrossRef](#)]
107. Brunelle, J.K.; Bell, E.L.; Quesada, N.M.; Vercauteren, K.; Tiranti, V.; Zeviani, M.; Scarpulla, R.C.; Chandel, N.S. Oxygen sensing requires mitochondrial ROS but not oxidative phosphorylation. *Cell Metab.* **2005**, *1*, 409–414. [[CrossRef](#)]
108. Chandel, N.S.; McClintock, D.S.; Feliciano, C.E.; Wood, T.M.; Melendez, J.A.; Rodriguez, A.M.; Schumacker, P.T. Reactive oxygen species generated at mitochondrial complex III stabilize hypoxia-inducible factor-1alpha during hypoxia: A mechanism of O2 sensing. *J. Biol. Chem.* **2000**, *275*, 25130–25138. [[CrossRef](#)]

109. Lee, G.; Won, H.S.; Lee, Y.M.; Choi, J.W.; Oh, T.I.; Jang, J.H.; Choi, D.K.; Lim, B.O.; Kim, Y.J.; Park, J.W.; et al. Oxidative Dimerization of PHD2 is Responsible for its Inactivation and Contributes to Metabolic Reprogramming via HIF-1 α Activation. *Sci. Rep.* **2016**, *6*, 18928. [[CrossRef](#)] [[PubMed](#)]
110. Li, Y.N.; Xi, M.M.; Guo, Y.; Hai, C.X.; Yang, W.L.; Qin, X.J. NADPH oxidase-mitochondria axis-derived ROS mediate arsenite-induced HIF-1 α stabilization by inhibiting prolyl hydroxylases activity. *Toxicol. Lett.* **2014**, *224*, 165–174. [[CrossRef](#)] [[PubMed](#)]
111. Bonello, S.; Zahringer, C.; BelAiba, R.S.; Djordjevic, T.; Hess, J.; Michiels, C.; Kietzmann, T.; Grolach, A. Reactive oxygen species activate the HIF-1 α promoter via a functional NF κ B site. *Arterioscler. Thromb. Vasc. Biol.* **2007**, *27*, 755–761. [[CrossRef](#)] [[PubMed](#)]
112. Masson, N.; Singleton, R.S.; Sekirnik, R.; Trudgian, D.C.; Ambrose, L.J.; Miranda, M.X.; Tian, Y.M.; Kessler, B.M.; Schofield, C.J.; Ratcliffe, P.J. The FIH hydroxylase is a cellular peroxide sensor that modulates HIF transcriptional activity. *EMBO Rep.* **2012**, *13*, 251–257. [[CrossRef](#)]
113. Mateo, J.; Garcia-Lecea, M.; Cadenas, S.; Hernandez, C.; Moncada, S. Regulation of hypoxia-inducible factor-1 α by nitric oxide through mitochondria-dependent and -independent pathways. *Biochem. J.* **2003**, *376*, 537–544. [[CrossRef](#)]
114. Sebastiani, G.D.; Passiu, G. The current outlook in the therapy of autoimmune diseases. *Ann. Ital. Med. Int.* **1992**, *7*, 95–101.
115. Berchner-Pfannschmidt, U.; Tug, S.; Trinidad, B.; Oehme, F.; Yamac, H.; Wotzlaw, C.; Flamme, I.; Fandrey, J. Nuclear oxygen sensing: Induction of endogenous prolyl-hydroxylase 2 activity by hypoxia and nitric oxide. *J. Biol. Chem.* **2008**, *283*, 31745–31753. [[CrossRef](#)] [[PubMed](#)]
116. Berchner-Pfannschmidt, U.; Yamac, H.; Trinidad, B.; Fandrey, J. Nitric oxide modulates oxygen sensing by hypoxia-inducible factor 1-dependent induction of prolyl hydroxylase 2. *J. Biol. Chem.* **2007**, *282*, 1788–1796. [[CrossRef](#)] [[PubMed](#)]
117. Cummins, E.P.; Taylor, C.T. Hypoxia-responsive transcription factors. *Pflugers Arch.* **2005**, *450*, 363–371. [[CrossRef](#)] [[PubMed](#)]
118. Taylor, C.T.; Cummins, E.P. The role of NF- κ B in hypoxia-induced gene expression. *Ann. N. Y. Acad. Sci.* **2009**, *1177*, 178–184. [[CrossRef](#)]
119. Cummins, E.P.; Berra, E.; Comerford, K.M.; Ginouves, A.; Fitzgerald, K.T.; Seeballuck, F.; Godson, C.; Nielsen, J.E.; Moynagh, P.; Pouyssegur, J.; et al. Prolyl hydroxylase-1 negatively regulates I κ B kinase- β , giving insight into hypoxia-induced NF κ B activity. *Proc. Natl. Acad. Sci. USA* **2006**, *103*, 18154–18159. [[CrossRef](#)]
120. Bertero, T.; Rezzonico, R.; Pottier, N.; Mari, B. Impact of MicroRNAs in the Cellular Response to Hypoxia. *Int. Rev. Cell Mol. Biol.* **2017**, *333*, 91–158. [[CrossRef](#)]
121. Nallamshetty, S.; Chan, S.Y.; Loscalzo, J. Hypoxia: A master regulator of microRNA biogenesis and activity. *Free Radic. Biol. Med.* **2013**, *64*, 20–30. [[CrossRef](#)]
122. Shehade, H.; Acolty, V.; Moser, M.; Oldenhove, G. Cutting Edge: Hypoxia-Inducible Factor 1 Negatively Regulates Th1 Function. *J. Immunol.* **2015**, *195*, 1372–1376. [[CrossRef](#)]
123. Wang, H.; Flach, H.; Onizawa, M.; Wei, L.; McManus, M.T.; Weiss, A. Negative regulation of Hif1 α expression and TH17 differentiation by the hypoxia-regulated microRNA miR-210. *Nat. Immunol.* **2014**, *15*, 393–401. [[CrossRef](#)] [[PubMed](#)]
124. Wu, R.; Zeng, J.; Yuan, J.; Deng, X.; Huang, Y.; Chen, L.; Zhang, P.; Feng, H.; Liu, Z.; Wang, Z.; et al. MicroRNA-210 overexpression promotes psoriasis-like inflammation by inducing Th1 and Th17 cell differentiation. *J. Clin. Investig.* **2018**, *128*, 2551–2568. [[CrossRef](#)] [[PubMed](#)]
125. Feldman, D.E.; Chauhan, V.; Koong, A.C. The unfolded protein response: A novel component of the hypoxic stress response in tumors. *Mol. Cancer Res.* **2005**, *3*, 597–605. [[CrossRef](#)] [[PubMed](#)]
126. Jackson, R.J.; Hellen, C.U.; Pestova, T.V. The mechanism of eukaryotic translation initiation and principles of its regulation. *Nat. Rev. Mol. Cell Biol.* **2010**, *11*, 113–127. [[CrossRef](#)]
127. Brewer, J.W.; Diehl, J.A. PERK mediates cell-cycle exit during the mammalian unfolded protein response. *Proc. Natl. Acad. Sci. USA* **2000**, *97*, 12625–12630. [[CrossRef](#)] [[PubMed](#)]
128. Moore, C.E.; Mikolajek, H.; Regufe da Mota, S.; Wang, X.; Kenney, J.W.; Werner, J.M.; Proud, C.G. Elongation Factor 2 Kinase Is Regulated by Proline Hydroxylation and Protects Cells during Hypoxia. *Mol. Cell Biol.* **2015**, *35*, 1788–1804. [[CrossRef](#)]
129. Feng, T.; Yamamoto, A.; Wilkins, S.E.; Sokolova, E.; Yates, L.A.; Munzel, M.; Singh, P.; Hopkinson, R.J.; Fischer, R.; Cockman, M.E.; et al. Optimal translational termination requires C4 lysyl hydroxylation of eRF1. *Mol. Cell* **2014**, *53*, 645–654. [[CrossRef](#)]
130. Romero-Ruiz, A.; Bautista, L.; Navarro, V.; Heras-Garvin, A.; March-Diaz, R.; Castellano, A.; Gomez-Diaz, R.; Castro, M.J.; Berra, E.; Lopez-Barneo, J.; et al. Prolyl hydroxylase-dependent modulation of eukaryotic elongation factor 2 activity and protein translation under acute hypoxia. *J. Biol. Chem.* **2012**, *287*, 9651–9658. [[CrossRef](#)]
131. Connolly, E.; Braunstein, S.; Formenti, S.; Schneider, R.J. Hypoxia inhibits protein synthesis through a 4E-BP1 and elongation factor 2 kinase pathway controlled by mTOR and uncoupled in breast cancer cells. *Mol. Cell Biol.* **2006**, *26*, 3955–3965. [[CrossRef](#)]
132. Hetz, C. The unfolded protein response: Controlling cell fate decisions under ER stress and beyond. *Nat. Rev. Mol. Cell Biol.* **2012**, *13*, 89–102. [[CrossRef](#)]
133. Arsham, A.M.; Howell, J.J.; Simon, M.C. A novel hypoxia-inducible factor-independent hypoxic response regulating mammalian target of rapamycin and its targets. *J. Biol. Chem.* **2003**, *278*, 29655–29660. [[CrossRef](#)] [[PubMed](#)]
134. Sofer, A.; Lei, K.; Johannessen, C.M.; Ellisen, L.W. Regulation of mTOR and cell growth in response to energy stress by REDD1. *Mol. Cell Biol.* **2005**, *25*, 5834–5845. [[CrossRef](#)] [[PubMed](#)]

135. Brugarolas, J.; Lei, K.; Hurley, R.L.; Manning, B.D.; Reiling, J.H.; Hafen, E.; Witters, L.A.; Ellisen, L.W.; Kaelin, W.G., Jr. Regulation of mTOR function in response to hypoxia by REDD1 and the TSC1/TSC2 tumor suppressor complex. *Genes Dev.* **2004**, *18*, 2893–2904. [[CrossRef](#)] [[PubMed](#)]
136. Liu, L.; Cash, T.P.; Jones, R.G.; Keith, B.; Thompson, C.B.; Simon, M.C. Hypoxia-induced energy stress regulates mRNA translation and cell growth. *Mol. Cell* **2006**, *21*, 521–531. [[CrossRef](#)] [[PubMed](#)]
137. Ding, M.; Van der Kwast, T.H.; Vellanki, R.N.; Foltz, W.D.; McKee, T.D.; Sonenberg, N.; Pandolfi, P.P.; Koritzinsky, M.; Wouters, B.G. The mTOR Targets 4E-BP1/2 Restrain Tumor Growth and Promote Hypoxia Tolerance in PTEN-driven Prostate Cancer. *Mol. Cancer Res.* **2018**, *16*, 682–695. [[CrossRef](#)] [[PubMed](#)]
138. King, H.A.; Cobbold, L.C.; Willis, A.E. The role of IRES trans-acting factors in regulating translation initiation. *Biochem. Soc. Trans.* **2010**, *38*, 1581–1586. [[CrossRef](#)]
139. Kozak, M. A second look at cellular mRNA sequences said to function as internal ribosome entry sites. *Nucleic Acids Res.* **2005**, *33*, 6593–6602. [[CrossRef](#)]
140. Ho, J.J.D.; Wang, M.; Audas, T.E.; Kwon, D.; Carlsson, S.K.; Timpano, S.; Evagelou, S.L.; Brothers, S.; Gonzalgo, M.L.; Krieger, J.R.; et al. Systemic Reprogramming of Translation Efficiencies on Oxygen Stimulus. *Cell Rep.* **2016**, *14*, 1293–1300. [[CrossRef](#)]
141. Uniacke, J.; Perera, J.K.; Lachance, G.; Francisco, C.B.; Lee, S. Cancer cells exploit eIF4E2-directed synthesis of hypoxia response proteins to drive tumor progression. *Cancer Res.* **2014**, *74*, 1379–1389. [[CrossRef](#)]
142. Uniacke, J.; Holterman, C.E.; Lachance, G.; Franovic, A.; Jacob, M.D.; Fabian, M.R.; Payette, J.; Holcik, M.; Pause, A.; Lee, S. An oxygen-regulated switch in the protein synthesis machinery. *Nature* **2012**, *486*, 126–129. [[CrossRef](#)] [[PubMed](#)]
143. Cui, X.A.; Palazzo, A.F. Localization of mRNAs to the endoplasmic reticulum. *Wiley Interdiscip. Rev. RNA* **2014**, *5*, 481–492. [[CrossRef](#)] [[PubMed](#)]
144. Papandreou, I.; Cairns, R.A.; Fontana, L.; Lim, A.L.; Denko, N.C. HIF-1 mediates adaptation to hypoxia by actively downregulating mitochondrial oxygen consumption. *Cell Metab.* **2006**, *3*, 187–197. [[CrossRef](#)] [[PubMed](#)]
145. Kim, J.W.; Tchernyshyov, I.; Semenza, G.L.; Dang, C.V. HIF-1-mediated expression of pyruvate dehydrogenase kinase: A metabolic switch required for cellular adaptation to hypoxia. *Cell Metab.* **2006**, *3*, 177–185. [[CrossRef](#)]
146. Iyer, N.V.; Kotch, L.E.; Agani, F.; Leung, S.W.; Laughner, E.; Wenger, R.H.; Gassmann, M.; Gearhart, J.D.; Lawler, A.M.; Yu, A.Y.; et al. Cellular and developmental control of O₂ homeostasis by hypoxia-inducible factor 1 alpha. *Genes Dev.* **1998**, *12*, 149–162. [[CrossRef](#)]
147. Garcia-Bermudez, J.; Baudrier, L.; La, K.; Zhu, X.G.; Fidelin, J.; Sviderskiy, V.O.; Papagiannakopoulos, T.; Molina, H.; Snuderl, M.; Lewis, C.A.; et al. Aspartate is a limiting metabolite for cancer cell proliferation under hypoxia and in tumours. *Nat. Cell Biol.* **2018**, *20*, 775–781. [[CrossRef](#)]
148. Schulz, T.J.; Zarse, K.; Voigt, A.; Urban, N.; Birringer, M.; Ristow, M. Glucose restriction extends *Caenorhabditis elegans* life span by inducing mitochondrial respiration and increasing oxidative stress. *Cell Metab.* **2007**, *6*, 280–293. [[CrossRef](#)]
149. Bell, E.L.; Klimova, T.A.; Eisenbart, J.; Schumacker, P.T.; Chandel, N.S. Mitochondrial reactive oxygen species trigger hypoxia-inducible factor-dependent extension of the replicative life span during hypoxia. *Mol. Cell Biol.* **2007**, *27*, 5737–5745. [[CrossRef](#)]
150. Liu, X.; Jiang, N.; Hughes, B.; Bigras, E.; Shoubridge, E.; Hekimi, S. Evolutionary conservation of the clk-1-dependent mechanism of longevity: Loss of mcl1 increases cellular fitness and lifespan in mice. *Genes Dev.* **2005**, *19*, 2424–2434. [[CrossRef](#)]
151. Solaini, G.; Baracca, A.; Lenaz, G.; Sgarbi, G. Hypoxia and mitochondrial oxidative metabolism. *Biochim. Biophys. Acta* **2010**, *1797*, 1171–1177. [[CrossRef](#)]
152. Hermansanz-Agustin, P.; Choya-Foces, C.; Carregal-Romero, S.; Ramos, E.; Oliva, T.; Villa-Pina, T.; Moreno, L.; Izquierdo-Alvarez, A.; Cabrera-Garcia, J.D.; Cortes, A.; et al. Na(+) controls hypoxic signalling by the mitochondrial respiratory chain. *Nature* **2020**, *586*, 287–291. [[CrossRef](#)] [[PubMed](#)]
153. Liu, Q.; Zhang, D.; Hu, D.; Zhou, X.; Zhou, Y. The role of mitochondria in NLRP3 inflammasome activation. *Mol. Immunol.* **2018**, *103*, 115–124. [[CrossRef](#)] [[PubMed](#)]
154. Liu, L.; Feng, D.; Chen, G.; Chen, M.; Zheng, Q.; Song, P.; Ma, Q.; Zhu, C.; Wang, R.; Qi, W.; et al. Mitochondrial outer-membrane protein FUNDC1 mediates hypoxia-induced mitophagy in mammalian cells. *Nat. Cell Biol.* **2012**, *14*, 177–185. [[CrossRef](#)] [[PubMed](#)]
155. Kim, H.; Scimia, M.C.; Wilkinson, D.; Trelles, R.D.; Wood, M.R.; Bowtell, D.; Dillin, A.; Mercola, M.; Ronai, Z.A. Fine-tuning of Drp1/Fis1 availability by AKAP121/Siah2 regulates mitochondrial adaptation to hypoxia. *Mol. Cell* **2011**, *44*, 532–544. [[CrossRef](#)] [[PubMed](#)]
156. Safronova, O.; Pluemsampant, S.; Nakahama, K.; Morita, I. Regulation of chemokine gene expression by hypoxia via cooperative activation of NF-kappaB and histone deacetylase. *Int. J. Biochem. Cell Biol.* **2009**, *41*, 2270–2280. [[CrossRef](#)] [[PubMed](#)]
157. Koumenis, C.; Naczki, C.; Koritzinsky, M.; Rastani, S.; Diehl, A.; Sonenberg, N.; Koromilas, A.; Wouters, B.G. Regulation of protein synthesis by hypoxia via activation of the endoplasmic reticulum kinase PERK and phosphorylation of the translation initiation factor eIF2alpha. *Mol. Cell Biol.* **2002**, *22*, 7405–7416. [[CrossRef](#)] [[PubMed](#)]
158. Krzywinska, E.; Stockmann, C. Hypoxia, Metabolism and Immune Cell Function. *Biomedicines* **2018**, *6*, 56. [[CrossRef](#)]
159. Amulic, B.; Cazalet, C.; Hayes, G.L.; Metzler, K.D.; Zychlinsky, A. Neutrophil function: From mechanisms to disease. *Annu. Rev. Immunol.* **2012**, *30*, 459–489. [[CrossRef](#)]

160. Brinkmann, V.; Reichard, U.; Goosmann, C.; Fauler, B.; Uhlemann, Y.; Weiss, D.S.; Weinrauch, Y.; Zychlinsky, A. Neutrophil extracellular traps kill bacteria. *Science* **2004**, *303*, 1532–1535. [[CrossRef](#)]
161. Wera, O.; Lancellotti, P.; Oury, C. The Dual Role of Neutrophils in Inflammatory Bowel Diseases. *J. Clin. Med.* **2016**, *5*, 118. [[CrossRef](#)]
162. Harris, A.J.; Thompson, A.R.; Whyte, M.K.; Walmsley, S.R. HIF-mediated innate immune responses: Cell signaling and therapeutic implications. *Hypoxia (Auckl)* **2014**, *2*, 47–58. [[CrossRef](#)]
163. Peyssonnaud, C.; Datta, V.; Cramer, T.; Doedens, A.; Theodorakis, E.A.; Gallo, R.L.; Hurtado-Ziola, N.; Nizet, V.; Johnson, R.S. HIF-1 α expression regulates the bactericidal capacity of phagocytes. *J. Clin. Investig.* **2005**, *115*, 1806–1815. [[CrossRef](#)] [[PubMed](#)]
164. Thompson, A.A.; Elks, P.M.; Marriott, H.M.; Eamsamang, S.; Higgins, K.R.; Lewis, A.; Williams, L.; Parmar, S.; Shaw, G.; McGrath, E.E.; et al. Hypoxia-inducible factor 2 α regulates key neutrophil functions in humans, mice, and zebrafish. *Blood* **2014**, *123*, 366–376. [[CrossRef](#)]
165. Mollerherm, H.; von Kockritz-Blickwede, M.; Branitzki-Heinemann, K. Antimicrobial Activity of Mast Cells: Role and Relevance of Extracellular DNA Traps. *Front. Immunol.* **2016**, *7*, 265. [[CrossRef](#)]
166. Crotty Alexander, L.E.; Akong-Moore, K.; Feldstein, S.; Johansson, P.; Nguyen, A.; McEachern, E.K.; Niciata, S.; Cowburn, A.S.; Olson, J.; Cho, J.Y.; et al. Myeloid cell HIF-1 α regulates asthma airway resistance and eosinophil function. *J. Mol. Med. (Berl.)* **2013**, *91*, 637–644. [[CrossRef](#)]
167. Sumbayev, V.V.; Yasinska, I.; Oniku, A.E.; Streatfield, C.L.; Gibbs, B.F. Involvement of hypoxia-inducible factor-1 in the inflammatory responses of human LAD2 mast cells and basophils. *PLoS ONE* **2012**, *7*, e34259. [[CrossRef](#)]
168. Nissim Ben Efraim, A.H.; Eliashar, R.; Levi-Schaffer, F. Hypoxia modulates human eosinophil function. *Clin. Mol. Allergy* **2010**, *8*, 10. [[CrossRef](#)]
169. Sumbayev, V.V.; Nicholas, S.A.; Streatfield, C.L.; Gibbs, B.F. Involvement of hypoxia-inducible factor-1 HIF(1 α) in IgE-mediated primary human basophil responses. *Eur. J. Immunol.* **2009**, *39*, 3511–3519. [[CrossRef](#)] [[PubMed](#)]
170. Gondin, J.; Theret, M.; Duhamel, G.; Pegan, K.; Mathieu, J.R.; Peyssonnaud, C.; Cuvellier, S.; Lacroche, C.; Chazaud, B.; Bendahan, D.; et al. Myeloid HIFs are dispensable for resolution of inflammation during skeletal muscle regeneration. *J. Immunol.* **2015**, *194*, 3389–3399. [[CrossRef](#)] [[PubMed](#)]
171. Takeda, N.; O’Dea, E.L.; Doedens, A.; Kim, J.W.; Weidemann, A.; Stockmann, C.; Asagiri, M.; Simon, M.C.; Hoffmann, A.; Johnson, R.S. Differential activation and antagonistic function of HIF-1 α isoforms in macrophages are essential for NO homeostasis. *Genes Dev.* **2010**, *24*, 491–501. [[CrossRef](#)]
172. Peyssonnaud, C.; Cejudo-Martin, P.; Doedens, A.; Zinkernagel, A.S.; Johnson, R.S.; Nizet, V. Cutting edge: Essential role of hypoxia inducible factor-1 α in development of lipopolysaccharide-induced sepsis. *J. Immunol.* **2007**, *178*, 7516–7519. [[CrossRef](#)]
173. Dehn, S.; DeBerge, M.; Yeap, X.Y.; Yvan-Charvet, L.; Fang, D.; Eltzschig, H.K.; Miller, S.D.; Thorp, E.B. HIF-2 α in Resting Macrophages Tempers Mitochondrial Reactive Oxygen Species To Selectively Repress MARCO-Dependent Phagocytosis. *J. Immunol.* **2016**, *197*, 3639–3649. [[CrossRef](#)]
174. Fluck, K.; Breves, G.; Fandrey, J.; Winning, S. Hypoxia-inducible factor 1 in dendritic cells is crucial for the activation of protective regulatory T cells in murine colitis. *Mucosal Immunol.* **2016**, *9*, 379–390. [[CrossRef](#)]
175. Wobben, R.; Husecken, Y.; Lodewick, C.; Gibbert, K.; Fandrey, J.; Winning, S. Role of hypoxia inducible factor-1 α for interferon synthesis in mouse dendritic cells. *Biol. Chem.* **2013**, *394*, 495–505. [[CrossRef](#)]
176. Kohler, T.; Reizis, B.; Johnson, R.S.; Weighardt, H.; Forster, I. Influence of hypoxia-inducible factor 1 α on dendritic cell differentiation and migration. *Eur. J. Immunol.* **2012**, *42*, 1226–1236. [[CrossRef](#)]
177. Naldini, A.; Morena, E.; Pucci, A.; Miglietta, D.; Riboldi, E.; Sozzani, S.; Carraro, F. Hypoxia affects dendritic cell survival: Role of the hypoxia-inducible factor-1 α and lipopolysaccharide. *J. Cell Physiol.* **2012**, *227*, 587–595. [[CrossRef](#)] [[PubMed](#)]
178. Kong, T.; Eltzschig, H.K.; Karhausen, J.; Colgan, S.P.; Shelley, C.S. Leukocyte adhesion during hypoxia is mediated by HIF-1-dependent induction of beta2 integrin gene expression. *Proc. Natl. Acad. Sci. USA* **2004**, *101*, 10440–10445. [[CrossRef](#)]
179. Mantovani, A.; Biswas, S.K.; Galdiero, M.R.; Sica, A.; Locati, M. Macrophage plasticity and polarization in tissue repair and remodelling. *J. Pathol.* **2013**, *229*, 176–185. [[CrossRef](#)] [[PubMed](#)]
180. Sica, A.; Mantovani, A. Macrophage plasticity and polarization: In vivo veritas. *J. Clin. Investig.* **2012**, *122*, 787–795. [[CrossRef](#)] [[PubMed](#)]
181. Galli, S.J.; Borregaard, N.; Wynn, T.A. Phenotypic and functional plasticity of cells of innate immunity: Macrophages, mast cells and neutrophils. *Nat. Immunol.* **2011**, *12*, 1035–1044. [[CrossRef](#)]
182. Gordon, S. Alternative activation of macrophages. *Nat. Rev. Immunol.* **2003**, *3*, 23–35. [[CrossRef](#)] [[PubMed](#)]
183. Mills, E.L.; O’Neill, L.A. Reprogramming mitochondrial metabolism in macrophages as an anti-inflammatory signal. *Eur. J. Immunol.* **2016**, *46*, 13–21. [[CrossRef](#)] [[PubMed](#)]
184. Jha, A.K.; Huang, S.C.; Sergushichev, A.; Lampropoulou, V.; Ivanova, Y.; Loginicheva, E.; Chmielewski, K.; Stewart, K.M.; Ashall, J.; Everts, B.; et al. Network integration of parallel metabolic and transcriptional data reveals metabolic modules that regulate macrophage polarization. *Immunity* **2015**, *42*, 419–430. [[CrossRef](#)] [[PubMed](#)]
185. Rodriguez-Prados, J.C.; Traves, P.G.; Cuenca, J.; Rico, D.; Aragones, J.; Martin-Sanz, P.; Cascante, M.; Bosca, L. Substrate fate in activated macrophages: A comparison between innate, classic, and alternative activation. *J. Immunol.* **2010**, *185*, 605–614. [[CrossRef](#)]

186. O'Neill, L.A.; Hardie, D.G. Metabolism of inflammation limited by AMPK and pseudo-starvation. *Nature* **2013**, *493*, 346–355. [[CrossRef](#)] [[PubMed](#)]
187. Tannahill, G.M.; Curtis, A.M.; Adamik, J.; Palsson-McDermott, E.M.; McGettrick, A.F.; Goel, G.; Frezza, C.; Bernard, N.J.; Kelly, B.; Foley, N.H.; et al. Succinate is an inflammatory signal that induces IL-1 β through HIF-1 α . *Nature* **2013**, *496*, 238–242. [[CrossRef](#)] [[PubMed](#)]
188. Imtiyaz, H.Z.; Williams, E.P.; Hickey, M.M.; Patel, S.A.; Durham, A.C.; Yuan, L.J.; Hammond, R.; Gimotty, P.A.; Keith, B.; Simon, M.C. Hypoxia-inducible factor 2 α regulates macrophage function in mouse models of acute and tumor inflammation. *J. Clin. Investig.* **2010**, *120*, 2699–2714. [[CrossRef](#)]
189. Kelly, B.; O'Neill, L.A. Metabolic reprogramming in macrophages and dendritic cells in innate immunity. *Cell Res.* **2015**, *25*, 771–784. [[CrossRef](#)]
190. Everts, B.; Amiel, E.; Huang, S.C.; Smith, A.M.; Chang, C.H.; Lam, W.Y.; Redmann, V.; Freitas, T.C.; Blagih, J.; van der Windt, G.J.; et al. TLR-driven early glycolytic reprogramming via the kinases TBK1-IRK3varepsilon supports the anabolic demands of dendritic cell activation. *Nat. Immunol.* **2014**, *15*, 323–332. [[CrossRef](#)] [[PubMed](#)]
191. Masopust, D.; Schenkel, J.M. The integration of T cell migration, differentiation and function. *Nat. Rev. Immunol.* **2013**, *13*, 309–320. [[CrossRef](#)] [[PubMed](#)]
192. Biju, M.P.; Neumann, A.K.; Bensinger, S.J.; Johnson, R.S.; Turka, L.A.; Haase, V.H. Vhlh gene deletion induces Hif-1-mediated cell death in thymocytes. *Mol. Cell Biol.* **2004**, *24*, 9038–9047. [[CrossRef](#)]
193. Gaber, T.; Chen, Y.; Krauss, P.L.; Buttgerit, F. Metabolism of T Lymphocytes in Health and Disease. *Int. Rev. Cell Mol. Biol.* **2019**, *342*, 95–148. [[CrossRef](#)]
194. Gaber, T.; Strehl, C.; Buttgerit, F. Metabolic regulation of inflammation. *Nat. Rev. Rheumatol.* **2017**, *13*, 267–279. [[CrossRef](#)]
195. Makino, Y.; Nakamura, H.; Ikeda, E.; Ohnuma, K.; Yamauchi, K.; Yabe, Y.; Poellinger, L.; Okada, Y.; Morimoto, C.; Tanaka, H. Hypoxia-inducible factor regulates survival of antigen receptor-driven T cells. *J. Immunol.* **2003**, *171*, 6534–6540. [[CrossRef](#)]
196. Brockmann, L.; Soukou, S.; Steglich, B.; Czarnewski, P.; Zhao, L.; Wende, S.; Bedke, T.; Ergen, C.; Manthey, C.; Agalioti, T.; et al. Molecular and functional heterogeneity of IL-10-producing CD4(+) T cells. *Nat. Commun.* **2018**, *9*, 5457. [[CrossRef](#)] [[PubMed](#)]
197. Mascanfroni, I.D.; Takenaka, M.C.; Yeste, A.; Patel, B.; Wu, Y.; Kenison, J.E.; Siddiqui, S.; Basso, A.S.; Otterbein, L.E.; Pardoll, D.M.; et al. Metabolic control of type 1 regulatory T cell differentiation by AHR and HIF1- α . *Nat. Med.* **2015**, *21*, 638–646. [[CrossRef](#)]
198. Pot, C.; Apetoh, L.; Awasthi, A.; Kuchroo, V.K. Induction of regulatory Tr1 cells and inhibition of T(H)17 cells by IL-27. *Semin. Immunol.* **2011**, *23*, 438–445. [[CrossRef](#)]
199. Dang, E.V.; Barbi, J.; Yang, H.Y.; Jinasena, D.; Yu, H.; Zheng, Y.; Bordman, Z.; Fu, J.; Kim, Y.; Yen, H.R.; et al. Control of T(H)17/T(reg) balance by hypoxia-inducible factor 1. *Cell* **2011**, *146*, 772–784. [[CrossRef](#)]
200. Shi, L.Z.; Wang, R.; Huang, G.; Vogel, P.; Neale, G.; Green, D.R.; Chi, H. HIF1 α -dependent glycolytic pathway orchestrates a metabolic checkpoint for the differentiation of TH17 and Treg cells. *J. Exp. Med.* **2011**, *208*, 1367–1376. [[CrossRef](#)] [[PubMed](#)]
201. Roncarolo, M.G.; Gregori, S.; Battaglia, M.; Bacchetta, R.; Fleischhauer, K.; Levings, M.K. Interleukin-10-secreting type 1 regulatory T cells in rodents and humans. *Immunol. Rev.* **2006**, *212*, 28–50. [[CrossRef](#)] [[PubMed](#)]
202. Cho, S.H.; Raybuck, A.L.; Blagih, J.; Kemboi, E.; Haase, V.H.; Jones, R.G.; Boothby, M.R. Hypoxia-inducible factors in CD4(+) T cells promote metabolism, switch cytokine secretion, and T cell help in humoral immunity. *Proc. Natl. Acad. Sci. USA* **2019**, *116*, 8975–8984. [[CrossRef](#)]
203. Singh, Y.; Garden, O.A.; Lang, F.; Cobb, B.S. MicroRNAs regulate T-cell production of interleukin-9 and identify hypoxia-inducible factor-2 α as an important regulator of T helper 9 and regulatory T-cell differentiation. *Immunology* **2016**, *149*, 74–86. [[CrossRef](#)] [[PubMed](#)]
204. Palazon, A.; Tyrakis, P.A.; Macias, D.; Velica, P.; Rundqvist, H.; Fitzpatrick, S.; Vojnovic, N.; Phan, A.T.; Loman, N.; Hedenfalk, I.; et al. An HIF-1 α /VEGF-A Axis in Cytotoxic T Cells Regulates Tumor Progression. *Cancer Cell* **2017**, *32*, 669–683. [[CrossRef](#)] [[PubMed](#)]
205. Tyrakis, P.A.; Palazon, A.; Macias, D.; Lee, K.L.; Phan, A.T.; Velica, P.; You, J.; Chia, G.S.; Sim, J.; Doedens, A.; et al. S-2-hydroxyglutarate regulates CD8(+) T-lymphocyte fate. *Nature* **2016**, *540*, 236–241. [[CrossRef](#)]
206. Gubser, P.M.; Bantug, G.R.; Razik, L.; Fischer, M.; Dimeloe, S.; Hoenger, G.; Durovic, B.; Jauch, A.; Hess, C. Rapid effector function of memory CD8+ T cells requires an immediate-early glycolytic switch. *Nat. Immunol.* **2013**, *14*, 1064–1072. [[CrossRef](#)] [[PubMed](#)]
207. Finlay, D.K.; Rosenzweig, E.; Sinclair, L.V.; Feijoo-Carnero, C.; Hukelmann, J.L.; Rolf, J.; Panteleev, A.A.; Okkenhaug, K.; Cantrell, D.A. PDK1 regulation of mTOR and hypoxia-inducible factor 1 integrate metabolism and migration of CD8+ T cells. *J. Exp. Med.* **2012**, *209*, 2441–2453. [[CrossRef](#)]
208. Kim, J.H.; Han, J.W.; Choi, Y.J.; Rha, M.S.; Koh, J.Y.; Kim, K.H.; Kim, C.G.; Lee, Y.J.; Kim, A.R.; Park, J.; et al. Functions of human liver CD69(+)/CD103(-)CD8(+) T cells depend on HIF-2 α activity in healthy and pathologic livers. *J. Hepatol.* **2020**, *72*, 1170–1181. [[CrossRef](#)]
209. Meng, X.; Grottsch, B.; Luo, Y.; Knaup, K.X.; Wiesener, M.S.; Chen, X.X.; Jantsch, J.; Fillatreau, S.; Schett, G.; Bozec, A. Hypoxia-inducible factor-1 α is a critical transcription factor for IL-10-producing B cells in autoimmune disease. *Nat. Commun.* **2018**, *9*, 251. [[CrossRef](#)] [[PubMed](#)]

210. Kojima, H.; Gu, H.; Nomura, S.; Caldwell, C.C.; Kobata, T.; Carmeliet, P.; Semenza, G.L.; Sitkovsky, M.V. Abnormal B lymphocyte development and autoimmunity in hypoxia-inducible factor 1alpha-deficient chimeric mice. *Proc. Natl. Acad. Sci. USA* **2002**, *99*, 2170–2174. [[CrossRef](#)] [[PubMed](#)]
211. Zhang, F.; Li, R.; Yang, Y.; Shi, C.; Shen, Y.; Lu, C.; Chen, Y.; Zhou, W.; Lin, A.; Yu, L.; et al. Specific Decrease in B-Cell-Derived Extracellular Vesicles Enhances Post-Chemotherapeutic CD8(+) T Cell Responses. *Immunity* **2019**, *50*, 738–750. [[CrossRef](#)] [[PubMed](#)]
212. Ivanov, I.I.; McKenzie, B.S.; Zhou, L.; Tadokoro, C.E.; Lepelley, A.; Lafaille, J.J.; Cua, D.J.; Littman, D.R. The orphan nuclear receptor RORgammat directs the differentiation program of proinflammatory IL-17+ T helper cells. *Cell* **2006**, *126*, 1121–1133. [[CrossRef](#)]
213. Kryczek, I.; Zhao, E.; Liu, Y.; Wang, Y.; Vatan, L.; Szeliga, W.; Moyer, J.; Klimczak, A.; Lange, A.; Zou, W. Human TH17 cells are long-lived effector memory cells. *Sci. Transl. Med.* **2011**, *3*, 104ra100. [[CrossRef](#)] [[PubMed](#)]
214. Clambey, E.T.; McNamee, E.N.; Westrich, J.A.; Glover, L.E.; Campbell, E.L.; Jedlicka, P.; de Zoeten, E.F.; Cambier, J.C.; Stenmark, K.R.; Colgan, S.P.; et al. Hypoxia-inducible factor-1 alpha-dependent induction of FoxP3 drives regulatory T-cell abundance and function during inflammatory hypoxia of the mucosa. *Proc. Natl. Acad. Sci. USA* **2012**, *109*, E2784–E2793. [[CrossRef](#)]
215. Ben-Shoshan, J.; Maysel-Auslender, S.; Mor, A.; Keren, G.; George, J. Hypoxia controls CD4+CD25+ regulatory T-cell homeostasis via hypoxia-inducible factor-1alpha. *Eur. J. Immunol.* **2008**, *38*, 2412–2418. [[CrossRef](#)] [[PubMed](#)]
216. Georgiev, P.; Belikoff, B.G.; Hatfield, S.; Ohta, A.; Sitkovsky, M.V.; Lukashov, D. Genetic deletion of the HIF-1alpha isoform I.1 in T cells enhances antibacterial immunity and improves survival in a murine peritonitis model. *Eur. J. Immunol.* **2013**, *43*, 655–666. [[CrossRef](#)]
217. Thiel, M.; Caldwell, C.C.; Kreth, S.; Kuboki, S.; Chen, P.; Smith, P.; Ohta, A.; Lentsch, A.B.; Lukashov, D.; Sitkovsky, M.V. Targeted deletion of HIF-1alpha gene in T cells prevents their inhibition in hypoxic inflamed tissues and improves septic mice survival. *PLoS ONE* **2007**, *2*, e853. [[CrossRef](#)]
218. Lukashov, D.; Klebanov, B.; Kojima, H.; Grinberg, A.; Ohta, A.; Berenfeld, L.; Wenger, R.H.; Ohta, A.; Sitkovsky, M. Cutting edge: Hypoxia-inducible factor 1alpha and its activation-inducible short isoform I.1 negatively regulate functions of CD4+ and CD8+ T lymphocytes. *J. Immunol.* **2006**, *177*, 4962–4965. [[CrossRef](#)] [[PubMed](#)]
219. Higashiyama, M.; Hokari, R.; Hozumi, H.; Kurihara, C.; Ueda, T.; Watanabe, C.; Tomita, K.; Nakamura, M.; Komoto, S.; Okada, Y.; et al. HIF-1 in T cells ameliorated dextran sodium sulfate-induced murine colitis. *J. Leukoc. Biol.* **2012**, *91*, 901–909. [[CrossRef](#)]
220. Lee, J.H.; Elly, C.; Park, Y.; Liu, Y.C. E3 Ubiquitin Ligase VHL Regulates Hypoxia-Inducible Factor-1alpha to Maintain Regulatory T Cell Stability and Suppressive Capacity. *Immunity* **2015**, *42*, 1062–1074. [[CrossRef](#)]
221. Harty, J.T.; Tvinnereim, A.R.; White, D.W. CD8+ T cell effector mechanisms in resistance to infection. *Annu. Rev. Immunol.* **2000**, *18*, 275–308. [[CrossRef](#)]
222. Sukumar, M.; Liu, J.; Ji, Y.; Subramanian, M.; Crompton, J.G.; Yu, Z.; Roychoudhuri, R.; Palmer, D.C.; Muranski, P.; Karoly, E.D.; et al. Inhibiting glycolytic metabolism enhances CD8+ T cell memory and antitumor function. *J. Clin. Investig.* **2013**, *123*, 4479–4488. [[CrossRef](#)]
223. Pollizzi, K.N.; Patel, C.H.; Sun, I.H.; Oh, M.H.; Waickman, A.T.; Wen, J.; Delgoffe, G.M.; Powell, J.D. mTORC1 and mTORC2 selectively regulate CD8(+) T cell differentiation. *J. Clin. Investig.* **2015**, *125*, 2090–2108. [[CrossRef](#)] [[PubMed](#)]
224. Frebel, H.; Nindl, V.; Schuepbach, R.A.; Braunschweiler, T.; Richter, K.; Vogel, J.; Wagner, C.A.; Loffing-Cueni, D.; Kurrer, M.; Ludwig, B.; et al. Programmed death 1 protects from fatal circulatory failure during systemic virus infection of mice. *J. Exp. Med.* **2012**, *209*, 2485–2499. [[CrossRef](#)]
225. Medzhitov, R.; Schneider, D.S.; Soares, M.P. Disease tolerance as a defense strategy. *Science* **2012**, *335*, 936–941. [[CrossRef](#)] [[PubMed](#)]
226. Doedens, A.L.; Phan, A.T.; Stradner, M.H.; Fujimoto, J.K.; Nguyen, J.V.; Yang, E.; Johnson, R.S.; Goldrath, A.W. Hypoxia-inducible factors enhance the effector responses of CD8(+) T cells to persistent antigen. *Nat. Immunol.* **2013**, *14*, 1173–1182. [[CrossRef](#)]
227. Ning, F.; Takeda, K.; Schedel, M.; Domenico, J.; Joetham, A.; Gelfand, E.W. Hypoxia Enhances CD8+ Tc2 Dependent Airway Hyperresponsiveness and Inflammation Through Hypoxia Inducible Factor 1alpha. *J. Allergy Clin. Immunol.* **2019**. [[CrossRef](#)]
228. Lund, F.E.; Randall, T.D. Effector and regulatory B cells: Modulators of CD4+ T cell immunity. *Nat. Rev. Immunol.* **2010**, *10*, 236–247. [[CrossRef](#)] [[PubMed](#)]
229. Hoffman, W.; Lakkis, F.G.; Chalasani, G. B Cells, Antibodies, and More. *Clin. J. Am. Soc. Nephrol.* **2016**, *11*, 137–154. [[CrossRef](#)] [[PubMed](#)]
230. Rosser, E.C.; Mauri, C. Regulatory B cells: Origin, phenotype, and function. *Immunity* **2015**, *42*, 607–612. [[CrossRef](#)]
231. Lee, K.M.; Stott, R.T.; Zhao, G.; SooHoo, J.; Xiong, W.; Lian, M.M.; Fitzgerald, L.; Shi, S.; Akrawi, E.; Lei, J.; et al. TGF-beta-producing regulatory B cells induce regulatory T cells and promote transplantation tolerance. *Eur. J. Immunol.* **2014**, *44*, 1728–1736. [[CrossRef](#)] [[PubMed](#)]
232. Shen, P.; Roch, T.; Lampropoulou, V.; O'Connor, R.A.; Stervbo, U.; Hilgenberg, E.; Ries, S.; Dang, V.D.; Jaimes, Y.; Daridon, C.; et al. IL-35-producing B cells are critical regulators of immunity during autoimmune and infectious diseases. *Nature* **2014**, *507*, 366–370. [[CrossRef](#)]
233. Kalampokis, I.; Yoshizaki, A.; Tedder, T.F. IL-10-producing regulatory B cells (B10 cells) in autoimmune disease. *Arthritis Res. Ther.* **2013**, *15* (Suppl. 1), S1. [[CrossRef](#)] [[PubMed](#)]

234. Mauri, C.; Bosma, A. Immune regulatory function of B cells. *Annu. Rev. Immunol.* **2012**, *30*, 221–241. [[CrossRef](#)]
235. Pieper, K.; Grimmacher, B.; Eibel, H. B-cell biology and development. *J. Allergy Clin. Immunol.* **2013**, *131*, 959–971. [[CrossRef](#)] [[PubMed](#)]
236. Shin, D.H.; Lin, H.; Zheng, H.; Kim, K.S.; Kim, J.Y.; Chun, Y.S.; Park, J.W.; Nam, J.H.; Kim, W.K.; Zhang, Y.H.; et al. HIF-1 α -mediated upregulation of TASK-2 K(+) channels augments Ca(2)(+) signaling in mouse B cells under hypoxia. *J. Immunol.* **2014**, *193*, 4924–4933. [[CrossRef](#)]
237. Goda, N.; Ryan, H.E.; Khadivi, B.; McNulty, W.; Rickert, R.C.; Johnson, R.S. Hypoxia-inducible factor 1 α is essential for cell cycle arrest during hypoxia. *Mol. Cell Biol.* **2003**, *23*, 359–369. [[CrossRef](#)]
238. Qian, T.; Hong, J.; Wang, L.; Wang, Z.; Lu, Z.; Li, Y.; Liu, R.; Chu, Y. Regulation of CD11b by HIF-1 α and the STAT3 signaling pathway contributes to the immunosuppressive function of B cells in inflammatory bowel disease. *Mol. Immunol.* **2019**, *111*, 162–171. [[CrossRef](#)]
239. Wang, Z.; Zhang, H.; Liu, R.; Qian, T.; Liu, J.; Huang, E.; Lu, Z.; Zhao, C.; Wang, L.; Chu, Y. Peyer's patches-derived CD11b(+) B cells recruit regulatory T cells through CXCL9 in dextran sulphate sodium-induced colitis. *Immunology* **2018**, *155*, 356–366. [[CrossRef](#)] [[PubMed](#)]
240. Liu, X.; Jiang, X.; Liu, R.; Wang, L.; Qian, T.; Zheng, Y.; Deng, Y.; Huang, E.; Xu, F.; Wang, J.Y.; et al. B cells expressing CD11b effectively inhibit CD4+ T-cell responses and ameliorate experimental autoimmune hepatitis in mice. *Hepatology* **2015**, *62*, 1563–1575. [[CrossRef](#)]
241. Jellusova, J.; Cato, M.H.; Apgar, J.R.; Ramezani-Rad, P.; Leung, C.R.; Chen, C.; Richardson, A.D.; Conner, E.M.; Benschop, R.J.; Woodgett, J.R.; et al. Gsk3 is a metabolic checkpoint regulator in B cells. *Nat. Immunol.* **2017**, *18*, 303–312. [[CrossRef](#)] [[PubMed](#)]
242. Caro-Maldonado, A.; Wang, R.; Nichols, A.G.; Kuraoka, M.; Milasta, S.; Sun, L.D.; Gavin, A.L.; Abel, E.D.; Kelsoe, G.; Metabolic reprogramming is required for antibody production that is suppressed in anergic but exaggerated in chronically BAFF-exposed B cells. *J. Immunol.* **2014**, *192*, 3626–3633. [[CrossRef](#)] [[PubMed](#)]
243. Shikhagaie, M.M.; Germar, K.; Bal, S.M.; Ros, X.R.; Spits, H. Innate lymphoid cells in autoimmunity: Emerging regulators in rheumatic diseases. *Nat. Rev. Rheumatol.* **2017**, *13*, 164–173. [[CrossRef](#)] [[PubMed](#)]
244. Li, Q.; Li, D.; Zhang, X.; Wan, Q.; Zhang, W.; Zheng, M.; Zou, L.; Elly, C.; Lee, J.H.; Liu, Y.C. E3 Ligase VHL Promotes Group 2 Innate Lymphoid Cell Maturation and Function via Glycolysis Inhibition and Induction of Interleukin-33 Receptor. *Immunity* **2018**, *48*, 258–270. [[CrossRef](#)]
245. Ni, J.; Wang, X.; Stojanovic, A.; Zhang, Q.; Wincher, M.; Buhler, L.; Arnold, A.; Correia, M.P.; Winkler, M.; Koch, P.S.; et al. Single-Cell RNA Sequencing of Tumor-Infiltrating NK Cells Reveals that Inhibition of Transcription Factor HIF-1 α Unleashes NK Cell Activity. *Immunity* **2020**, *52*, 1075.e1078–1087.e1078. [[CrossRef](#)] [[PubMed](#)]
246. Krzywinska, E.; Kantari-Mimoun, C.; Kerdiles, Y.; Sobbecki, M.; Isagawa, T.; Gotthardt, D.; Castells, M.; Haubold, J.; Millien, C.; Viel, T.; et al. Loss of HIF-1 α in natural killer cells inhibits tumour growth by stimulating non-productive angiogenesis. *Nat. Commun.* **2017**, *8*, 1597. [[CrossRef](#)] [[PubMed](#)]
247. Spits, H.; Artis, D.; Colonna, M.; Diefenbach, A.; Di Santo, J.P.; Eberl, G.; Koyasu, S.; Locksley, R.M.; McKenzie, A.N.; Mebius, R.E.; et al. Innate lymphoid cells—a proposal for uniform nomenclature. *Nat. Rev. Immunol.* **2013**, *13*, 145–149. [[CrossRef](#)]
248. Spits, H.; Bernink, J.H.; Lanier, L. NK cells and type 1 innate lymphoid cells: Partners in host defense. *Nat. Immunol.* **2016**, *17*, 758–764. [[CrossRef](#)]
249. Viel, S.; Marçais, A.; Guimaraes, F.S.; Loftus, R.; Rabilloud, J.; Grau, M.; Degouve, S.; Djebali, S.; Sanlaville, A.; Charrier, E.; et al. TGF- β inhibits the activation and functions of NK cells by repressing the mTOR pathway. *Sci. Signal.* **2016**, *9*, ra19. [[CrossRef](#)] [[PubMed](#)]
250. Berchem, G.; Noman, M.Z.; Bosseler, M.; Paggetti, J.; Baconnais, S.; Le Cam, E.; Nanbakhsh, A.; Moussay, E.; Mami-Chouaib, F.; Janji, B.; et al. Hypoxic tumor-derived microvesicles negatively regulate NK cell function by a mechanism involving TGF- β and miR23a transfer. *Oncoimmunology* **2016**, *5*, e1062968. [[CrossRef](#)]
251. Sarkar, S.; Germeraad, W.T.; Rouschop, K.M.; Steeghs, E.M.; van Gelder, M.; Bos, G.M.; Wieten, L. Hypoxia induced impairment of NK cell cytotoxicity against multiple myeloma can be overcome by IL-2 activation of the NK cells. *PLoS ONE* **2013**, *8*, e64835. [[CrossRef](#)]
252. Marçais, A.; Cherfils-Vicini, J.; Viant, C.; Degouve, S.; Viel, S.; Fenis, A.; Rabilloud, J.; Mayol, K.; Tavares, A.; Bienvenu, J.; et al. The metabolic checkpoint kinase mTOR is essential for IL-15 signaling during the development and activation of NK cells. *Nat. Immunol.* **2014**, *15*, 749–757. [[CrossRef](#)] [[PubMed](#)]
253. Donnelly, R.P.; Loftus, R.M.; Keating, S.E.; Liou, K.T.; Biron, C.A.; Gardiner, C.M.; Finlay, D.K. mTORC1-dependent metabolic reprogramming is a prerequisite for NK cell effector function. *J. Immunol.* **2014**, *193*, 4477–4484. [[CrossRef](#)] [[PubMed](#)]
254. Keating, S.E.; Zaiatz-Bittencourt, V.; Loftus, R.M.; Keane, C.; Brennan, K.; Finlay, D.K.; Gardiner, C.M. Metabolic Reprogramming Supports IFN- γ Production by CD56bright NK Cells. *J. Immunol.* **2016**, *196*, 2552–2560. [[CrossRef](#)]
255. Velasquez, S.Y.; Killian, D.; Schulte, J.; Sticht, C.; Thiel, M.; Lindner, H.A. Short Term Hypoxia Synergizes with Interleukin 15 Priming in Driving Glycolytic Gene Transcription and Supports Human Natural Killer Cell Activities. *J. Biol. Chem.* **2016**, *291*, 12960–12977. [[CrossRef](#)] [[PubMed](#)]
256. Blouin, C.C.; Page, E.L.; Soucy, G.M.; Richard, D.E. Hypoxic gene activation by lipopolysaccharide in macrophages: Implication of hypoxia-inducible factor 1 α . *Blood* **2004**, *103*, 1124–1130. [[CrossRef](#)]

257. Palsson-McDermott, E.M.; Curtis, A.M.; Goel, G.; Lauterbach, M.A.; Sheedy, F.J.; Gleeson, L.E.; van den Bosch, M.W.; Quinn, S.R.; Domingo-Fernandez, R.; Johnston, D.G.; et al. Pyruvate kinase M2 regulates Hif-1 α activity and IL-1 β induction and is a critical determinant of the warburg effect in LPS-activated macrophages. *Cell Metab.* **2015**, *21*, 65–80. [[CrossRef](#)]
258. Mills, E.L.; Kelly, B.; Logan, A.; Costa, A.S.H.; Varma, M.; Bryant, C.E.; Tourlomousis, P.; Dabritz, J.H.M.; Gottlieb, E.; Latorre, I.; et al. Succinate Dehydrogenase Supports Metabolic Repurposing of Mitochondria to Drive Inflammatory Macrophages. *Cell* **2016**, *167*, 457–470. [[CrossRef](#)]
259. Luo, W.; Hu, H.; Chang, R.; Zhong, J.; Knabel, M.; O’Meally, R.; Cole, R.N.; Pandey, A.; Semenza, G.L. Pyruvate kinase M2 is a PHD3-stimulated coactivator for hypoxia-inducible factor 1. *Cell* **2011**, *145*, 732–744. [[CrossRef](#)]
260. Shirai, T.; Nazarewicz, R.R.; Wallis, B.B.; Yanes, R.E.; Watanabe, R.; Hilhorst, M.; Tian, L.; Harrison, D.G.; Giacomini, J.C.; Assimes, T.L.; et al. The glycolytic enzyme PKM2 bridges metabolic and inflammatory dysfunction in coronary artery disease. *J. Exp. Med.* **2016**, *213*, 337–354. [[CrossRef](#)] [[PubMed](#)]
261. Yang, P.; Li, Z.; Li, H.; Lu, Y.; Wu, H.; Li, Z. Pyruvate kinase M2 accelerates pro-inflammatory cytokine secretion and cell proliferation induced by lipopolysaccharide in colorectal cancer. *Cell Signal.* **2015**, *27*, 1525–1532. [[CrossRef](#)]
262. Yang, L.; Xie, M.; Yang, M.; Yu, Y.; Zhu, S.; Hou, W.; Kang, R.; Lotze, M.T.; Billiar, T.R.; Wang, H.; et al. PKM2 regulates the Warburg effect and promotes HMGB1 release in sepsis. *Nat. Commun.* **2014**, *5*, 4436. [[CrossRef](#)] [[PubMed](#)]
263. Andersson, U.; Wang, H.; Palmblad, K.; Aveberger, A.C.; Bloom, O.; Erlandsson-Harris, H.; Janson, A.; Kokkola, R.; Zhang, M.; Yang, H.; et al. High mobility group 1 protein (HMG-1) stimulates proinflammatory cytokine synthesis in human monocytes. *J. Exp. Med.* **2000**, *192*, 565–570. [[CrossRef](#)] [[PubMed](#)]
264. Albina, J.E.; Mastrofrancesco, B.; Vessella, J.A.; Louis, C.A.; Henry, W.L., Jr.; Reichner, J.S. HIF-1 expression in healing wounds: HIF-1 α induction in primary inflammatory cells by TNF- α . *Am. J. Physiol. Cell Physiol.* **2001**, *281*, C1971–C1977. [[CrossRef](#)] [[PubMed](#)]
265. Shatrov, V.A.; Sumbayev, V.V.; Zhou, J.; Brune, B. Oxidized low-density lipoprotein (oxLDL) triggers hypoxia-inducible factor-1 α (HIF-1 α) accumulation via redox-dependent mechanisms. *Blood* **2003**, *101*, 4847–4849. [[CrossRef](#)] [[PubMed](#)]
266. Menegaut, L.; Thomas, C.; Jalil, A.; Julla, J.B.; Magnani, C.; Ceroi, A.; Basmaciyan, L.; Dumont, A.; Le Goff, W.; Mathew, M.J.; et al. Interplay between Liver X Receptor and Hypoxia Inducible Factor 1 α Potentiates Interleukin-1 β Production in Human Macrophages. *Cell Rep.* **2020**, *31*, 107665. [[CrossRef](#)]
267. Walczak-Drzewiecka, A.; Ratajewski, M.; Wagner, W.; Dastyk, J. HIF-1 α is up-regulated in activated mast cells by a process that involves calcineurin and NFAT. *J. Immunol.* **2008**, *181*, 1665–1672. [[CrossRef](#)]
268. Elder, M.J.; Webster, S.J.; Fitzmaurice, T.J.; Shaunak, A.S.D.; Steinmetz, M.; Chee, R.; Mallat, Z.; Cohen, E.S.; Williams, D.L.; Gaston, J.S.H.; et al. Dendritic Cell-Derived TSLP Negatively Regulates HIF-1 α and IL-1 β During Dectin-1 Signaling. *Front. Immunol.* **2019**, *10*, 921. [[CrossRef](#)]
269. Sena, L.A.; Li, S.; Jairaman, A.; Prakriya, M.; Ezponda, T.; Hildeman, D.A.; Wang, C.R.; Schumacker, P.T.; Licht, J.D.; Perlman, H.; et al. Mitochondria are required for antigen-specific T cell activation through reactive oxygen species signaling. *Immunity* **2013**, *38*, 225–236. [[CrossRef](#)]
270. Semenza, G.L. Pharmacologic Targeting of Hypoxia-Inducible Factors. *Annu. Rev. Pharmacol. Toxicol.* **2019**, *59*, 379–403. [[CrossRef](#)]
271. Karhausen, J.; Furuta, G.T.; Tomaszewski, J.E.; Johnson, R.S.; Colgan, S.P.; Haase, V.H. Epithelial hypoxia-inducible factor-1 is protective in murine experimental colitis. *J. Clin. Investig.* **2004**, *114*, 1098–1106. [[CrossRef](#)]
272. Cummins, E.P.; Seeballuck, F.; Keely, S.J.; Mangan, N.E.; Callanan, J.J.; Fallon, P.G.; Taylor, C.T. The hydroxylase inhibitor dimethylxalylglycine is protective in a murine model of colitis. *Gastroenterology* **2008**, *134*, 156–165. [[CrossRef](#)] [[PubMed](#)]
273. Tambuwala, M.M.; Manresa, M.C.; Cummins, E.P.; Aversa, V.; Coulter, I.S.; Taylor, C.T. Targeted delivery of the hydroxylase inhibitor DMOG provides enhanced efficacy with reduced systemic exposure in a murine model of colitis. *J. Control. Release* **2015**, *217*, 221–227. [[CrossRef](#)]
274. Robinson, A.; Keely, S.; Karhausen, J.; Gerich, M.E.; Furuta, G.T.; Colgan, S.P. Mucosal protection by hypoxia-inducible factor prolyl hydroxylase inhibition. *Gastroenterology* **2008**, *134*, 145–155. [[CrossRef](#)]
275. Gupta, R.; Chaudhary, A.R.; Shah, B.N.; Jadhav, A.V.; Zambad, S.P.; Gupta, R.C.; Deshpande, S.; Chauthaiwale, V.; Dutt, C. Therapeutic treatment with a novel hypoxia-inducible factor hydroxylase inhibitor (TRC160334) ameliorates murine colitis. *Clin. Exp. Gastroenterol.* **2014**, *7*, 13–23. [[CrossRef](#)] [[PubMed](#)]
276. Keely, S.; Campbell, E.L.; Baird, A.W.; Hansbro, P.M.; Shalwitz, R.A.; Kotsakis, A.; McNamee, E.N.; Eltzschig, H.K.; Kominsky, D.J.; Colgan, S.P. Contribution of epithelial innate immunity to systemic protection afforded by prolyl hydroxylase inhibition in murine colitis. *Mucosal Immunol.* **2014**, *7*, 114–123. [[CrossRef](#)] [[PubMed](#)]
277. Marks, E.; Naudin, C.; Nolan, G.; Goggins, B.J.; Burns, G.; Mateer, S.W.; Latimore, J.K.; Minahan, K.; Plank, M.; Foster, P.S.; et al. Regulation of IL-12p40 by HIF controls Th1/Th17 responses to prevent mucosal inflammation. *Mucosal Immunol.* **2017**, *10*, 1224–1236. [[CrossRef](#)]
278. Xue, X.; Ramakrishnan, S.; Anderson, E.; Taylor, M.; Zimmermann, E.M.; Spence, J.R.; Huang, S.; Greenson, J.K.; Shah, Y.M. Endothelial PAS domain protein 1 activates the inflammatory response in the intestinal epithelium to promote colitis in mice. *Gastroenterology* **2013**, *145*, 831–841. [[CrossRef](#)]
279. Shah, Y.M. The role of hypoxia in intestinal inflammation. *Mol. Cell Pediatr.* **2016**, *3*, 1. [[CrossRef](#)]

280. Mimouna, S.; Goncalves, D.; Barnich, N.; Darfeuille-Michaud, A.; Hofman, P.; Vouret-Craviari, V. Crohn disease-associated *Escherichia coli* promote gastrointestinal inflammatory disorders by activation of HIF-dependent responses. *Gut Microbes* **2011**, *2*, 335–346. [[CrossRef](#)]
281. Guan, S.Y.; Leng, R.X.; Tao, J.H.; Li, X.P.; Ye, D.Q.; Olsen, N.; Zheng, S.G.; Pan, H.F. Hypoxia-inducible factor-1alpha: A promising therapeutic target for autoimmune diseases. *Expert Opin. Ther. Targets* **2017**, *21*, 715–723. [[CrossRef](#)] [[PubMed](#)]
282. Walsh, J.C.; Lebedev, A.; Aten, E.; Madsen, K.; Marciano, L.; Kolb, H.C. The clinical importance of assessing tumor hypoxia: Relationship of tumor hypoxia to prognosis and therapeutic opportunities. *Antioxid. Redox Signal.* **2014**, *21*, 1516–1554. [[CrossRef](#)] [[PubMed](#)]
283. Tang, W.; Zhao, G. Small molecules targeting HIF-1alpha pathway for cancer therapy in recent years. *Bioorg. Med. Chem.* **2020**, *28*, 115235. [[CrossRef](#)] [[PubMed](#)]
284. Albadari, N.; Deng, S.; Li, W. The transcriptional factors HIF-1 and HIF-2 and their novel inhibitors in cancer therapy. *Expert Opin. Drug Discov.* **2019**, *14*, 667–682. [[CrossRef](#)] [[PubMed](#)]
285. Yu, Y.; Yu, Q.; Zhang, X. Allosteric inhibition of HIF-2alpha as a novel therapy for clear cell renal cell carcinoma. *Drug Discov. Today* **2019**, *24*, 2332–2340. [[CrossRef](#)]
286. Fallah, J.; Rini, B.I. HIF Inhibitors: Status of Current Clinical Development. *Curr. Oncol. Rep.* **2019**, *21*, 6. [[CrossRef](#)]
287. Wu, D.; Su, X.; Lu, J.; Li, S.; Hood, B.L.; Vasile, S.; Potluri, N.; Diao, X.; Kim, Y.; Khorasanizadeh, S.; et al. Bidirectional modulation of HIF-2 activity through chemical ligands. *Nat. Chem. Biol.* **2019**, *15*, 367–376. [[CrossRef](#)] [[PubMed](#)]
288. Courtney, K.D.; Infante, J.R.; Lam, E.T.; Figlin, R.A.; Rini, B.I.; Brugarolas, J.; Zojwalla, N.J.; Lowe, A.M.; Wang, K.; Wallace, E.M.; et al. Phase I Dose-Escalation Trial of PT2385, a First-in-Class Hypoxia-Inducible Factor-2alpha Antagonist in Patients With Previously Treated Advanced Clear Cell Renal Cell Carcinoma. *J. Clin. Oncol.* **2018**, *36*, 867–874. [[CrossRef](#)]
289. Choueiri, T.K.; Plimack, E.R.; Bauer, T.M.; Merchan, J.R.; Papadopoulos, K.P.; McDermott, D.F.; Michaelson, M.D.; Appleman, L.J.; Thameke, S.; Zojwalla, N.J.; et al. Phase I/II study of the oral HIF-2 α inhibitor MK-6482 in patients with advanced clear cell renal cell carcinoma (RCC). *J. Clin. Oncol.* **2020**, *38*, 611. [[CrossRef](#)]
290. Xu, R.; Wang, K.; Rizzi, J.P.; Huang, H.; Grina, J.A.; Schlachter, S.T.; Wang, B.; Wehn, P.M.; Yang, H.; Dixon, D.D.; et al. 3-[(1S,2S,3R)-2,3-Difluoro-1-hydroxy-7-methylsulfonylindane-4-yl]oxy-5-fluorobenzo nitrile (PT2977), a Hypoxia-Inducible Factor 2alpha (HIF-2alpha) Inhibitor for the Treatment of Clear Cell Renal Cell Carcinoma. *J. Med. Chem.* **2019**, *62*, 6876–6893. [[CrossRef](#)] [[PubMed](#)]



Review

HIF- α Prolyl Hydroxylase Inhibitors and Their Implications for Biomedicine: A Comprehensive Review

Kiichi Hirota

Department of Human Stress Response Science, Institute of Biomedical Science, Kansai Medical University, Hirakata, Osaka 573-1010, Japan; khirota-kyt@umin.ac.jp; Tel.: +81-72-804-2526

Abstract: Oxygen is essential for the maintenance of the body. Living organisms have evolved systems to secure an oxygen environment to be proper. Hypoxia-inducible factor (HIF) plays an essential role in this process; it is a transcription factor that mediates erythropoietin (EPO) induction at the transcriptional level under hypoxic environment. After successful cDNA cloning in 1995, a line of studies were conducted for elucidating the molecular mechanism of HIF activation in response to hypoxia. In 2001, cDNA cloning of dioxygenases acting on prolines and asparagine residues, which play essential roles in this process, was reported. HIF-prolyl hydroxylases (PHs) are molecules that constitute the core molecular mechanism of detecting a decrease in the partial pressure of oxygen, or hypoxia, in the cells; they can be called oxygen sensors. In this review, I discuss the process of molecular cloning of HIF and HIF-PH, which explains hypoxia-induced EPO expression; the development of HIF-PH inhibitors that artificially or exogenously activate HIF by inhibiting HIF-PH; and the significance and implications of medical intervention using HIF-PH inhibitors.

Keywords: hypoxia; transcription factor; hypoxia-inducible factor 1; HIF-1; hypoxia sensing; HIF-PH inhibitor

Citation: Hirota, K. HIF- α Prolyl Hydroxylase Inhibitors and Their Implications for Biomedicine: A Comprehensive Review. *Biomedicines* **2021**, *9*, 468. <https://doi.org/10.3390/biomedicines9050468>

Academic Editor: Shaker A. Mousa

Received: 5 April 2021

Accepted: 23 April 2021

Published: 24 April 2021

Publisher's Note: MDPI stays neutral with regard to jurisdictional claims in published maps and institutional affiliations.



Copyright: © 2021 by the author. Licensee MDPI, Basel, Switzerland. This article is an open access article distributed under the terms and conditions of the Creative Commons Attribution (CC BY) license (<https://creativecommons.org/licenses/by/4.0/>).

1. Introduction

Chronic kidney disease (CKD), cancers, inflammatory diseases, nutritional deficiencies, genetic disorders, and drugs may cause anemia. Erythropoiesis-stimulating agents (ESAs), including recombinant erythropoietin (EPO) analogs, have been used for treating anemia associated with CKD through compensating for decreased EPO [1–3]. However, resistance and tolerance to these drugs have been shown to develop, and high doses of ESAs can cause side effects such as cardiovascular diseases [4].

Anemia is a condition in which the blood is unable to deliver sufficient amounts of oxygen to the tissues because of insufficient number of red blood cells (RBCs), which are the oxygen carriers in the blood, and insufficient hemoglobin, which holds molecular oxygen in the RBCs [5–7]. Oxygen is essential for the maintenance of the body [8]. Since there is no biosynthetic system for oxygen in the body, the supply of oxygen to the organism depends solely on the supply from the outside world, usually through gas exchange in the lungs. For oxygen to be distributed throughout the body in this manner, blood vessels must be lined throughout the body, RBCs must be produced appropriately, oxygen must be delivered in a hemoglobin-bound state to the cells that require oxygen, and the transported oxygen must be consumed appropriately [9,10]. Living organisms have evolutionarily constructed the systems for the purpose [8,10]. Hypoxia-inducible factor (HIF) plays an essential role in this process; it is a transcription factor that was genetically isolated while elucidating the molecular mechanism through which EPO is induced at the transcriptional level in hypoxia [11]. After successful cDNA cloning in 1995 [12–14], studies were conducted to elucidate the molecular mechanism through which HIF is activated in response to hypoxia. In 2001, the cloning of dioxygenases or hydroxylases acting on proline and asparagine residues, which play an important role in this process, was reported [15–18]. In particular, the enzyme that hydroxylates the proline residues of the HIF- α subunit is a dioxygenase or

hydroxylase whose substrates are the HIF- α subunit, α -ketoglutarate (2-oxoglutarate: 2-OG), and molecular oxygen (O_2); its cofactors are divalent iron (Fe^{2+}) and ascorbic acid. Thus, HIF-prolyl hydroxylases (HIF-PHs) constitute the core molecular mechanism of detecting a decrease in the partial pressure of oxygen, or hypoxia, in the cells; they can be called oxygen sensors [19,20].

Various strategies have been developed for inducing HIF activation under normoxic conditions, such as chelation of divalent iron and cobalt ion treatment. Certain 2-OG analogs have been reported to activate HIF. Pharmacological inhibition of HIF-PHs increases EPO and DMT1 (ferrous ion membrane transport protein 1)/Nramp2 (NRAMP metal ion transporter 2) in the intestinal epithelium and decreases hepcidin production in the liver, thereby improving iron metabolism *in vivo* and potentially leading to efficient treatment of not only CDK-induced anemia but also anemia associated with chronic diseases [11,21–23].

In this review, I describe the process of molecular cloning of HIF and HIF-PH, which explains the induction of EPO expression by hypoxia; the development of HIF-PH inhibitors (HIF-PHIs) that artificially activate HIF by inhibiting HIF-PH; medical interventions that utilize HIF-PHIs; and the implications and significance of these interventions [24,25]. In addition, this review will specifically describe HIF-PHIs, which are currently prescribed in medical practice, and explain its biological effects in addition to its anemia-alleviating effects in relation to its molecular mechanism.

2. Sensing of Hypoxia and Execution of the Hypoxic Gene Responses

The body has evolved systems for monitoring oxygen concentration in various organs and tissues and for responding to deviations in oxygen partial pressure. The hypoxic response of living organisms is diverse and multilayered, reflecting the fact that oxygen is essential for life support [8,26].

There is a system that signals a decrease in the partial pressure of arterial blood oxygen to the respiratory center in brainstem via carotid body-glossopharyngeal nerve and aortic body-vagus nerve [27]. In this system, glomus type I cells in the carotid body serve as hypoxia sensor cells. In addition, small pulmonary arteries contract in response to alveolar hypoxia (hypoxic pulmonary vasoconstriction) [28]. In this case, the alveolar epithelium may act as hypoxia sensor cells. Thus, these hypoxic responses act through specific mechanisms for sensing hypoxia. Hypoxic signaling in glomus type I cells and the pulmonary artery smooth muscle is mediated by potassium channel-calcium channel coupling. However, the molecular mechanisms through which hypoxic signaling is mediated by these channels remain unclear. The study of hypoxic response has been preceded by electrophysiological studies, which included the above-mentioned study on the involvement of ion channels. Studies using classical biochemical methods have a long history; however, molecular biology methods were not introduced until the 1990s. An important turning point in this research was the isolation of the gene for HIF-1, which was identified as a transcription factor involved in the hypoxic induction of EPO [20,29].

3. Exploration of the Mechanism of Erythropoietin (EPO) Production Induction

In the early 1990s, it was assumed that circulating factors stimulating hematopoiesis were present in the serum of phlebotomized rabbits, as demonstrated by parabiosis experiments in rats in 1950 [30]. The name erythropoietin was proposed for this hypothetical liquid factor; however, the molecular mechanism underlying its induction was unknown. At that time, this factor was hypothesized to be secreted by the pituitary gland. In 1957, EPO was shown to be produced by the kidneys [31–33]. In 1977, Miyake and his colleagues succeeded in purifying EPO from a large amount of urine from a patient with aplastic anemia [34]. EPO acts on the erythroid progenitor cells in the bone marrow to promote their differentiation and proliferation into RBCs. In 1985, EPO gene cloning was successfully developed [35], paving the way for the production of large amounts of EPO through

genetic engineering. Additionally, approximately 30 years ago, a therapeutic method was established for administering EPO produced exogenously through genetic engineering.

Until recently, there was debate regarding the sites and cells involved in EPO production. The candidates included the juxtaglomerular apparatus, proximal tubules of the kidney, and vascular endothelial cells. Finally, an elegant analysis using genetically modified mice revealed tubulointerstitial cells in the kidney. There is a consensus that EPO secreted into the bloodstream is produced primarily by renal EPO-producing (REP) cells, with supplementary production in the liver. Although there are reports of EPO production in the brain, it is believed that EPO acts as a paracrine factor rather than being secreted into the circulating blood [36].

In recent years, therapeutic approaches have emerged that induce EPO production *in vivo* through the administration of exogenous small-molecule compounds, namely HIF-prolyl hydroxylase inhibitors (PHIs); five HIF-PHI agents are available for prescription in clinical practice in Japan.

Research on the regulation of EPO expression is interlinked with research on hypoxia-induced gene responses. Erythropoiesis has been observed to be stimulated in hypoxic environments. This phenomenon can be applied to sports medicine through high-altitude training. The increase in RBCs, hemoglobin, and blood volume improves the body's ability to carry more oxygen in the blood, leading to an increase in endurance (aerobic exercise capacity). Effective utilization of oxygen by the muscles is improved by the development of skeletal muscle capillaries and increased concentrations of the oxygen storage protein myoglobin, as well as the induction of enzymes involved in oxidative phosphorylation in the mitochondria and increased mitochondrial mass [37]. This a topic that needs further research as there are conflicting observations with regard to the effectiveness of high-altitude training.

Research on the molecular biology of hypoxia-induced gene response began in the late 1980s. In 1987, a research group at Harvard University demonstrated that a human hepatocarcinoma-derived established cell line produced EPO in response to hypoxia [38]. They found that not only hypoxia but also iron chelators and CoCl_2 stimulate EPO production in cells [38–40].

Thus, the modern era of research on the biology of hypoxia-induced gene responses began with the discovery that EPO, which had been believed to be produced by specialized cells in the kidney stroma, could also be produced by established cell lines that could be grown indefinitely on a Petri dish. In other words, molecular biological methods could be adapted to this research.

4. Molecular Cloning of Hypoxia-Inducible Factor 1

Eight years later, a transcription factor involved in EPO induction under hypoxic conditions was isolated. The protein and cDNA of hypoxia-inducible factor 1 was purified and isolated in 1995 using a method in which a protein that binds to a specific DNA sequence (hypoxia response element; HRE; 5'-R(A/G)CGTG-3') on the EPO gene was purified from established cell line HeLa cells [12–14].

HIF-1 is a transcription factor consisting of an α subunit (HIF-1 α) and a β subunit (HIF-1 β) with helix-loop-helix (HLH) and Per-ARNT-SIM (PAS) domains, which are hydrophobically linked to each other to form a functional protein [12]. The activated and dimerized HIF-1 (HIF-1 α /HIF-1 β) translocates to the cell nucleus and binds to the HRE in the regulatory region of the target gene to promote the expression of the dominant gene. The expression of the HIF-1 α protein is maintained to be very low in culture under 20% oxygen conditions; however, it increases rapidly in response to a decrease in oxygen partial pressure below 5% oxygen conditions [41]. In addition, the activity of HIF as a transcription factor increases with decreasing oxygen partial pressure, independent of the change in protein expression [18]. In this scheme, HIF-1 α accumulated in the cell forms a heterodimer with HIF-1 β , and the activated HIF-1 moves into the cell nucleus, where it binds to the expression control region and promotes the expression of the target gene [20,29].

HIF-1 α , which was isolated in this manner, has been found to have the HIF-2 α and HIF-3 α family of molecules [42]. In particular, HIF-2 α is highly homologous to HIF-1 α ; however, there are certain dissimilarities in hypoxia-inducible gene expression. As discussed later, several genes that are involved in iron metabolism are regulated by HIF-2 rather than HIF-1 [42]. Surprisingly, although HIF-1 was isolated as a factor responsible for hypoxia-induced expression of EPO, it is HIF-2, not HIF-1, that is responsible for hypoxia-induced expression of EPO in the kidney [43,44].

5. Intracellular Signaling Pathways Linking Hypoxia and HIF Activation

Following the cDNA cloning of HIF-1 [13], the molecular mechanism through which HIF activity is increased under hypoxic conditions remained a major question, the solution to which was expected to resolve the larger problem of how cells sense and signal a decrease in the partial pressure of oxygen.

A major turning point in the elucidation of this mechanism was the discovery that the HIF-1 α protein is ubiquitinated in the presence of ample oxygen and is consequently sequestered to the proteasome for degradation [45,46]. The VHL protein, which exhibits E3 ubiquitin ligase activity, plays a central role in HIF-1 α ubiquitination. The VHL gene has been identified as the causative gene in von Hippel–Lindau disease. It is a tumor suppressor gene, and the deficiency of this gene causes hemangioblastoma of the brain and retina and renal cell carcinoma [47–50]. The VHL protein is a component of a protein complex that includes elongin B, elongin C, and cullin-2. Nevertheless, the molecular mechanism of HIF-1 α ubiquitination, caused by the decrease in oxygen partial pressure, was unclear.

Under conditions of sufficient oxygen, the newly translated HIF-1 α protein from the mRNA undergoes hydroxylation at the proline residues, which results in hydroxylated-proline residue-dependent ubiquitination by the VHL system and transport to the proteasome, the intracellular protein destruction machinery, for degradation [51,52]. HIF-1 α and its family member HIF-2 α are regulated in a similar manner [53,54]. However, it was reported that the transcriptional activity of HIF-1 α and HIF-2 α is regulated by the hydroxylation of asparagine residues, which are conserved across species in the transcriptional domain of HIF-1 α , in addition to protein stabilization [18]. In the hydroxylated state, association with basic transcription factors such as p300 is inhibited, and sufficient transcriptional activity is not achieved. Exposure to hypoxia decreases the hydroxylation of asparagine residues and renews transcriptional activity.

In other words, under hypoxia, the hydroxylation of proline and asparagine residues is inhibited, protein destruction is reduced, and HIF-1 α accumulates in the cell, allowing it to associate with basic transcription factors such as p300, leading to activation (Figure 1).

In 2001, results were published regarding molecular cloning of oxygenase (dioxygenase) using 2-OG, molecular oxygen, and the HIF-1 protein as the substrate for hydroxylation [15–17].

6. Genetic Cloning of Enzymes Modifying HIF- α Hydroxylation (PHDs and FIH-1)

The cDNAs of the oxygenases were isolated. Three isozymes of proline hydroxylase were designated as prolyl hydroxylase domain (PHD)1-3 [15] and an asparagine residue hydroxylase as a factor inhibiting HIF (FIH)-1 [16,17]. The regulation of intracellular accumulation of HIF- α protein including HIF-1 α and HIF-2 α and the TAD (trans activation domain) transcriptional activity of HIF- α by PHD and FIH-1, respectively, are mediated by the hydroxylation of amino acid residues [17]. It has been proposed that the enzymatic activity of PHD decreases in response to a decrease in oxygen concentration and the protein expression of HIF- α increases. Subsequently, when the oxygen concentration decreases further, the enzymatic activity of FIH-1 decreases, p300 binds to TAD, and the transcriptional activity of HIF increases to its maximum activity [17,18]. Three PHD genes have been identified in mammals, and each gene product is believed to perform a specific function, as they differ with respect to the organ of expression and subcellular localization [15,55–57].

In vitro experiments have shown that all three PHD genes hydroxylate specific proline residues of HIF- α [55]. In in vivo conditions, however, PHD2 is the major proline hydroxylase for HIF- α ; it has been shown to be essential for biogenesis through gene disruption experiments [55]. PHD1 and PHD2 also negatively regulates the HIF-mediated hypoxia response by hydroxylating the proline residues of HIF- α [58]. The enzymatic properties of the recombinant proteins were analyzed, and these enzymes were clearly identified as dioxygenases that hydroxylate proline or asparagine residues; they require molecular oxygen, 2-OG, Fe²⁺, and ascorbic acid as substrates [55–57] (Figure 2).

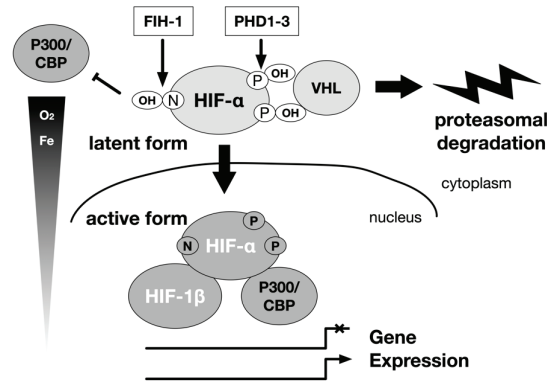


Figure 1. Regulation of α subunits of HIF-1 and HIF-2 by hydroxylation. The main stream of HIF-1 and HIF-2 activation is carried out by the hydroxylase of the HIF- α subunit. The hydroxylation is carried out by the prolyl hydroxylase domain (PHD) protein and the factor inhibiting HIF-1 (FIH-1) protein. Oxygen is the substrate of these enzymes. A decrease in the concentration of the substrate oxygen leads to a decrease in the hydroxylation reaction, and the HIF-1 α and HIF-2 α are spared from destruction in the proteasome. Then, the HIF- α protein accumulates in the cell, becomes active as a transcription factor. They form a heterodimer with the HIF-1 β subunit, and translocate from the cytoplasm to the nucleus to regulate gene expression. The intracellular elements that affect this reaction can be regulators of HIF-1 activity independent of oxygen partial pressure. P: proline, N: asparagine.

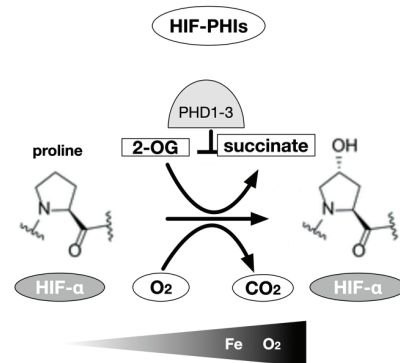


Figure 2. HIF- α prolyl hydroxylase. The hydroxylation of proline residues is an enzymatic reaction using 2-oxoglutarate as a substrate in addition to HIF-1 α or HIF-2 α subunits and molecular oxygen. Three types of prolyl hydroxylase domains are known in humans, but in most cells, PHD2 is mainly involved. Theoretically, chelation of the coenzyme Fe (II) also inhibits the activity of the enzyme, but the inhibitors currently used in clinical medicine work in competition with 2-OG to inhibit this enzyme.

Notably, molecular oxygen is the substrate for these enzymatic reactions. The signal of a decrease in the partial pressure of oxygen as the substrate leads to a decrease of the activity of the oxygenase, resulting in a decrease in the ratio of hydroxylated HIF- α translated from the mRNA and an increase in the ratio of HIF- α recognized and bound by VHL [47]. VHL does not exhibit E3 ligase activity under hypoxia, and the ratio of ubiquitinated HIF- α decreases; consequently, the destruction of HIF is inhibited, and the dimer with HIF-1 β protein is translocated to the nucleus where it acts as a transcription factor [59,60].

In their monumental paper published in 2001, Epstein et al. investigated the hydroxylation-modifying activity of HIF-1 α using recombinant PHD1 protein generated in *Escherichia coli* through the in vitro transcription-translation method [15]. The activity of PHD1 has been shown to be suppressed in response to a change from 21% to 0% oxygen, simultaneously with the decrease in oxygen partial pressure.

Myllyharju et al. determined that the *K_m* for PHD oxygen was 230–250 μ M and that for FIH-1 was 90 μ M, using a 20 amino-acid residue polypeptide as a substrate for a recombinant protein produced in insect cells. These results provide consistent evidence that PHD functions as an intracellular oxygen sensor, at least in the regulation of HIF-1 activity [58,61] (Table 1).

Table 1. Enzymatic properties of HIF- α prolyl and asparaginyl hydroxylases [61,62]

Gene Name	Enzyme	Substrate			<i>K_m</i> (μ M)			
		Pro-402	Pro-564	O ₂	2-OG	Ascorbate	Fe (II)	
<i>EGLN1</i>	PHD2	+	+	230	60	170	0.03	
<i>EGLN2</i>	PHD1	+	+	250	60	180	0.1	
<i>EGLN3</i>	PHD3	–	+	230	55	140	0.03	
<i>HIF1AN</i>	FIH-1		Asp-803	90	25	260	0.5	

Decreased oxygen partial pressure leads to decreased VHL-mediated ubiquitination, resulting in a shift in the balance between protein destruction and translation, and a scheme or “dogma” of intracellular accumulation of HIF-1 α protein [55].

7. Development of HIF-PHIs for Clinical Use

In the process of elucidating the molecular biological properties of HIFs, several small-molecule compounds have been observed to cause intracellular accumulation of HIF- α protein and increase transcriptional activity independent of the oxygen concentration or even under normoxic conditions [55,56,63]. Salts of Co²⁺, Cu²⁺, and Ni²⁺ were found to have hydroxylase inhibitory activity as antagonist of Fe²⁺ [38–40]. In addition, iron chelators such as deferoxamine mesylate, 3,4-dihydroxybenzoic acid, 1,10-phenanthroline, and quercetin were found exhibit enzyme inhibition [55,56,63]. These low molecular weight compounds have been found to activate HIF through the inhibition of prolyl and asparaginyl hydroxylases. However, these compounds are not specific HIF- α hydroxylase inhibitors. They also inhibit iron-dependent pathways in addition to HIF- α hydroxylase inhibition and may cause undue toxicity.

Characterization of the enzymes following the isolation of hydroxylase cDNA in 2001 has provided various insights into the effects of conventional HIF activators in terms of their effects on hydroxylase [55,57].

Dimethyloxalylglycine (DMOG), has been used as an HIF activator since early early research on HIF, primarily in basic experiments. DMOG is an antagonist of 2-OG, and it inhibits HIF-hydroxylases, including PHDs and FIH-1. Thus, the development and design of PHIs began with the synthesis of 2-OG analogs. N-oxalylglycine (NOG) was the first reported 2-OG mimetic molecule; however, DMOG, a precursor of NOG with the cell permeability of NOG, has been frequently used as a tool compound in research [63].

The synthesis of 2-OG analogs was the first approach employed in the design of PH inhibitors. Most molecules that have advanced to clinical use are 2-OG derivatives.

The active site-targeted inhibitors identified in this class exhibit strong binding interactions with hydrophobic residues in the 2-OG pocket. 2-OG mimics, such as NOG, allowed PHs and HIF binding, whereas larger heterocyclic inhibitors, such as FG-2216, stabilize the closed conformational structure and prevent binding of the substrate to the PHs [64,65]. Most PH inhibitors are composed of three structural features based on ligand-protein interactions. The first feature is a bidentate coordination site on the iron atom. The second important feature is a carboxylic acid that forms a salt bridge with the Arg383 side chain. The third attribute is a hydrogen bond acceptor for the phenolic hydroxyl of Tyr303 [55,63,66].

There are more than sixty 2-OG-dependent hydroxylases in the body; however, the inhibitors on the market are more than 1000 times more specific for PHD1-3 than for FIH-1, and the inhibition of HDACs and other enzymes is negligible [58].

There are five HIF-PHIs that have completed Phase III trials and are now being marketed and prescribed in clinical practice in Japan: daprodustat, roxadustat, vadadustat, molidustat, and enarodustat (Figure 3). Desidustat (ZYAN1) and JNJ-429045343, which is under preclinical development, are new drugs under development. Although there are recognized class effects, each has a different molecular structure, half-life, and adverse event profile, and there is diversity in PHs selectivity.

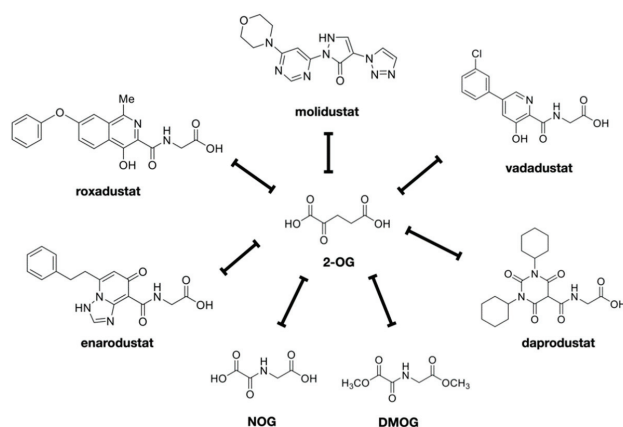


Figure 3. HIF-PHIs available in clinical field. HIF-PH inhibitors were shown. These are all competitive inhibitors of 2-OG. NOG and DMOG are the prototypes of these drugs. Daprodustat, enarodustat, molidustat, molidustat, and vadadustat are the inhibitors currently used in clinical medicine in Japan.

There is also diversity in PHs selectivity. For example, molidustat mainly inhibits PHD2, daprodustat inhibits PHD2 and PHD3, while roxadustat seems to inhibit all three PHDs. It remains to be seen whether such selectivity affects the malignancy risk of individual PHDs. Among various drugs that have been developed, at least five HIF-PHIs, approved for the treatment of renal anemia in Japan, are being used in clinical practice as of 2021 [24].

The recombinant protein of HIF-PHs including PHD1-3 has become available, laying the foundation for the assay and development of inhibitors [58,67]. On the basis of the general assay for 2-OG-hydroxylase activity, various assays have been proposed and reported for HIF-hydroxylase activity [68], including assays based on 2-OG/O₂ consumption and succinate/CO₂ production [69–71] and cell-based assays including the classical manual method of detecting HIF-1 α /2 α proteins with specific antibodies and using HRE-reporters has been proposed [72]. Other cell-based assays are based on measuring changes in the expression of well-characterized HIF transcriptional targets, such as EPO. A recent advancement has been the development of HIF-1 α hydroxylation site-specific antibodies,

which allow semi-quantitative analysis of the relative efficiency of intracellular PHDs and FIH-1-catalyzed HIF- α hydroxylation [73–79].

In addition, cell-based assays have been developed. Additionally, the classical manual method of detecting HIF-1 α /2 α proteins with specific antibodies and using HRE-reporters has been proposed [72]. Other cell-based assays are based on measuring changes in the expression of well-characterized HIF transcriptional targets, such as EPO. A recent advancement has been the development of HIF-1 α hydroxylation site-specific antibodies, which allow semi-quantitative analysis of the relative efficiency of intracellular PHDs and FIH-1-catalyzed HIF- α hydroxylation [73–76].

The hydroxyproline antibody-based amplified luminescent proximity homogeneous assay (AlphaScreen assay) was adapted to FG-4592 (roxadustat), GSK1278863 (daprodustat), vadadustat, and molidustat for measuring the PHD2-catalyzed hydroxylation of the HIF-1 α peptide (HIF-1 α residues 556–574). All “clinical” inhibitors potently inhibited the activity of PHD2, with IC₅₀ values in the sub-micromolar range. Notably, molidustat (IC₅₀ = 7 nM) is more potent than roxadustat (IC₅₀ = 27 nM), vadadustat (IC₅₀ = 29 nM), and daprodustat (IC₅₀ = 67 nM), according to this assay [58]. To investigate the efficiency of inhibition of HIF-1 α prolyl hydroxylation in cells, a luciferase-based hypoxia response element (HRE) reporter assay was performed with promoters containing tandem HRE sequences using established cell lines. All inhibitors strongly induced fire luciferase activity in a dose-dependent manner after 16 h of cell treatment, with EC₅₀ values reported to be 5.1, 0.8, and 2.1 μ M for roxadustat, daprodustat, and molidustat, respectively. In contrast, the ability of vadadustat (EC₅₀ 41 μ M, 16 h treatment) to induce HIF-1 α in the HRE reporter assay was weaker than that of the other compounds specified above [58].

8. Metabolism of HIF-PHIs and Interactions with Other Drugs

HIF-PHIs are primarily eliminated through hepatic clearance, and drug interactions occur through the absorption and metabolism processes [80]. With the exception of daprodustat, concomitant use of oral drugs containing metal cations, polymeric phosphorus adsorbents, and iron agents decreases gastrointestinal absorption [81].

Several compounds have been screened as HIF-PHIs, and modifications have been made to develop compounds with good target enzyme inhibition ability, EPO production ability, cell permeability, oral absorption, and no accumulation in the body. Currently, several of these compounds are clinically used as drugs; however, there are certain differences in their pharmacokinetics. The pharmacokinetic characteristics of HIF-PH translation are summarized in the Table 2; hepatic metabolism involves CYPs and conjugating enzymes, transporters mediate transport in and out of hepatocytes, and renal interaction involves organic anion transporters (OATs).

With respect to metabolism, the effects of metabolic enzymes and transporter inhibitors are known; for example, the blood concentrations of roxadustat and daprodustat are increased by the concomitant use of CYP2C8 inhibitors. In addition, HIF-PHIs inhibit transporters in the liver and kidney, which may enhance the effects of concomitant drugs. Therefore, when applying HIF-PHIs, it is necessary to evaluate drug interactions occurring via these mechanisms (Table 2).

Roxadustat is taken up by organic anion transporting polypeptide (OATP) 1B1 in hepatocytes, hydroxylated by CYP2C8 or conjugated to a sulfate group, and glucuronosylated by uridine diphosphate glucuronosyltransferase (UGT) 1A9 [82,83]. Vadadustat is glucuronosylated by UGT1A1, and its contribution to metabolism is small. Solubility increases with increase in pH; however, no effect has been observed with the concomitant use of proton pump inhibitors [84]. Daprodustat is metabolized by CYP2C8, and its blood concentration increases with the concomitant use of CYP2C8 inhibitors [81]. The half-life of daprodustat is shorter than that of other HIF-PHIs. No effects of diet or phosphorus adsorbents were observed. Gemfibrozil, a CYP2C8 inhibitor, increased the AUC of daprodustat by 18.6 folds. Enarodustat is hardly sensitive to metabolism and is not affected by CYP or other factors [85]. It is primarily eliminated through hepatic clearance, excreted in

the bile, and circulated in the intestinal tract; its apparent elimination half-life is relatively long [86]. Molidustat is primarily glucuronidated by UGT1A1, and approximately 85% of the administered dose is recovered in the urine as N-glucuronidated metabolites [87–90].

Table 2. Pharmacologic profiles of HIF-PHIs.

Drug	Absorption	Excretion Rate of Unchanged Substance in Urine	Half Life (h)	Major Metabolic Pathways	Ref.
Roxadustat	40~80%	1%	12~15	CYP2C8, UGT1A9	[82]
Vadadustat	>75%	<1%	4~7	UGT1A1/1A9	[84,91]
Dapurodustat	65%	<0.05%	1~7	CYP2C8	[81,92]
Enarodustat	41.70%	27~61%	~11	Less susceptible to metabolism	[85,93]
Molidustat	59%	4%	4~10	UGT1A1/1A9	[88,89]

9. Regulatory Mechanism of Erythropoiesis

EPO is a major external factor for erythropoiesis during the differentiation and maturation of erythroid lineage cells from hematopoietic stem cells [94]. EPO is secreted from the kidney by hypoxia, and EPO acts on the EPO receptor (EPOR) of erythroblast progenitor cells; EPOR is present in the plasma membrane as a homodimer. Signaling from EPO to EPOR includes the JAK2/STAT5-, PI3K/Akt-, and MAP kinase-mediated pathways. The JAK2/STAT5-mediated pathway is particularly important. When EPO binds to EPOR, the three-dimensional structure of EPOR changes, and the bound JAK2 is autophosphorylated. The phosphorylated JAK2 phosphorylates the tyrosine residue of EPOR, which causes the phosphorylation of STAT5, which is transferred to the nucleus; STAT5 acts as a transcription factor in cooperation with GATA-1 [95]. Signals from EPOR inhibit apoptosis and increase the expression of genes required for erythroid differentiation. EPOR promotes the proliferation of erythroleukemia cell lines and various tumor cells. In contrast to anemia, polycythemia involves an abnormal increase in the number of RBCs. Polycythemia vera and familial erythrocytosis are two types of polycythemia caused by genetic abnormalities. In polycythemia vera, the V617F mutation in the JAK2 gene in hematopoietic stem cells homeostatically activates cell proliferation signals, including the EPOR, leading to an increase in the number of cells in the three lineages erythrocytes, granulocytes, and platelets [95–97]. In addition to polycythemia vera, this mutation is often found in myeloproliferative tumors, such as primary myelofibrosis and essential thrombocythemia. Four types of familial erythrocytosis have additionally been reported. Type 1 is caused by a genetic abnormality of EPOR, resulting in increased reactivity to EPO and an increased erythrocyte count [98]. The serum EPO concentration was low. Type 2 is common in the Chuvash region of the Volga River basin in Russia, where the Turkic peoples live. It is caused by mutations in the VHL gene [99,100]. The mutant VHL protein is unable to bind to E3 ubiquitin ligase and HIF-1, which inhibits the degradation of HIF α and increases the expression of HIF target genes such as EPO, glucose transporters, transferrin, transferrin receptor 1 (TFR1), and VEGF. The Hb level can be over 20 g/dL; blood pressure is low; and the frequency of myocardial infarction, thrombosis, and spinal cord hemangioma is high. Unlike in type 1, serum EPO concentration is increased in type 2. Type 3 is caused by mutations in the PHD2 (*EGLN1*) gene [101,102]. Type 4 is caused by mutations in the HIF2A (*EPAS1*) gene; the mutant HIF-2 α protein is not degraded, resulting in increased expression of EPO and erythrocytosis [103]. Additionally, serum EPO concentration increases. Thus, various reports indicate that activation of the HIF pathway can lead to improvement of anemia. Thus, the focus of research moved in the direction of artificially modifying PH activity.

10. Renal Anemia Due to CKD

Anemia caused primarily by renal failure is defined as renal anemia [104–106]. REP cells are localized in the interstitium of normal kidneys [43,107]. They are widely distributed from the outer layer of the tubulointerstitial medulla to the cortex, and they border

interstitial capillaries [108,109]. Near the REP cells are tubular epithelial cells that consume large amounts of oxygen during urine reabsorption. Thus, the oxygen environment in the paratesticular capillaries is variable. Not all REP cells produce EPO uniformly, and some cells express EPO genes in a flexible and sensitive response to oxygen concentration [36]. HIF-2 is a regulator of this system. Under hypoxia, HIF induces EPO gene expression, whereas under normoxia, oxygen and proline hydroxylase bind to the HIF-2 α protein, which is rapidly degraded and which does not stimulate EPO production in the REP cells. Interstitial fibrosis secondary to renal failure is a major pathomorphological finding in renal injury, and REP cells that are transformed from fibroblasts to myofibroblast-like cells play a major role in interstitial fibrosis. Myofibroblasts play a major role in fibrosis, and a study tracing the origin of renal myofibroblasts determined that half of them were derived from stromal fibroblasts, 35% from the bone marrow, 10% from endothelial cells, and 5% from epithelial cells [110–112]. In addition, studies in animal models have shown that many of the myofibroblasts are transformed from cells that originally exhibited the properties of REP cells; when REP cells are transformed, they strongly express α -smooth muscle actin, leading to progressive fibrosis. In the fibrotic area, capillaries around the tubules drop out; additionally, tissue oxygen and nucleic acids are disturbed.

Fibrosis further lowers the partial pressure of oxygen in the kidneys. However, although the partial pressure of oxygen is lowered, the transformed REP cells lose their ability to produce EPO [36]. Thus, at the stage of renal interstitial fibrosis, even if the oxygen concentration decreases, EPO production is insufficient, resulting in a lack of oxygenated hemoglobin; the remaining tubular cells do not receive enough oxygen because the tubules consume high amounts of oxygen. This is the pathophysiology of renal anemia [36].

Uremic substances induce oxidative stress and inflammatory cytokines; impair iron utilization via hepcidin; and affect HIF activation.

As of 2016, the number of patients with end-stage renal failure reached 3.73 million worldwide; this figure is increasing at a rate of 5–6% per year. This includes 2.65 million on hemodialysis, 340,000 on peritoneal dialysis, and 740,000 on renal transplantation, with all treatment modes increasing at a rate of 5–6% per year.

The frequency and severity of renal anemia worsens with the development of renal dysfunction.

Chronic anemia has been shown to exacerbate renal dysfunction, increase cardiovascular complications, and adversely affect life expectancy because of the development of organ damage due to ischemia, leading to the cardiac-renal-anemia syndrome.

11. HIF-PHIs as a Treatment for Renal Anemia

Absorption of orally administered HIF-PHIs from the intestinal tract can result in HIF activation in most cells in the body. HIF-PHIs are clinically used for the treatment of renal anemia [24,25,113].

Treatment of renal anemia improves quality of life, which is impaired due to poor exercise tolerance caused by chronic anemia; additionally, it has been shown to exhibit organ protective effects. For example, therapeutic intervention with ESA from the early stage of CKD, which has become a serious problem, is expected to not only improve the quality of life of the patients and avoid blood transfusion but also to improve life prognosis through organ protection, including prevention of progression of renal dysfunction.

When ESAs were introduced into the clinic in the 1980s, their effectiveness in improving anemia was confirmed, and several clinical studies were conducted primarily in Europe and the United States to establish safe and effective treatment guidelines [114]. However, contrary to expectations, there have been reports of increased adverse events such as cardiovascular complications or no improvement in prognosis when high hemoglobin levels were used as the target for correction [115]. However, the target Hb levels in these clinical trials were approximately 11 g/dL and 13 g/dL or higher; compared to Hb levels of approximately 11 g/dL, there was no additional prognostic effect even if the Hb levels were improved to a level equivalent to that of healthy subjects [115,116]. These results suggest

that continued administration of high-dose ESAs to patients with a low hematopoietic response to ESAs may increase the risk of life-threatening events. In response to these results, Western countries, which had been aiming for normal Hb levels, took a turn and revised their targets downward. The KDIGO (The Kidney Disease Improving Global Outcomes) guideline published in 2012 states that with regard to the upper limit of targets for patients with conservative CKD, it is desirable not to administer ESAs to maintain Hb levels above 11.5 g/dL. If the Hb level is less than 10.0 g/dL, the decision to initiate ESA therapy should be individualized on the basis of the rate of decline in Hb concentration, response to prior iron therapy, risk of needing a blood transfusion, risks associated with ESA therapy, and the presence or absence of symptoms associated with anemia [117,118]. This does not mean that uniform criteria should be set. In addition, for HD patients, it was stated that it is desirable to start ESA therapy when the Hb level does not fall below 9.0 g/dL, as it is not reasonable to maintain Hb levels above 11.5 g/dL [116]. It is now advocated that renal anemia should be managed with adequate iron supplementation followed by ESA or HIF-PHIs [24,116]. The target hemoglobin level for CKD in the conservative phase is 11–13 g/dL and that for CKD in the hemodialysis phase is 10–12 g/dL. The target Hb level was determined and treated according to the pathology of each individual case [24,116].

As mentioned above, the canonical target of HIF-PHIs for EPO production is the renal interstitial REP cells, which stabilize HIF-1 α and HIF-2 α and induce endogenous EPO expression to promote erythropoiesis [119,120]. HIF-PHIs have been reported to increase EPO production in patients undergoing hemodialysis even after the removal of both kidneys, and PHD1-3 inhibition in hepatocytes restores EPO production, suggesting that EPO production in organs other than the kidney, including the liver, may contribute to the improvement of anemia.

HIF-PHIs may additionally contribute to the improvement of anemia by improving iron metabolism. Hepcidin, a peptide hormone produced in the liver, plays a central role in regulating iron metabolism by turning over and recycling iron in the body inhibitors. The iron-supply mechanism includes transferrin receptor 2 (TFR2), hepcidin/ferroportin (FPN), and iron regulatory protein (IRP), which sense changes in intracellular iron concentration. IRP creates a feedback mechanism that ultimately maintains a constant level of serum iron and hemoglobin. During evolution, iron was a difficult element to ingest, and humans were believed to have been iron starved. Therefore, humans do not have a system for excreting iron. The iron required by the body is absorbed through the intestinal tract. Orally ingested inorganic iron is taken into the body via DMT1 (divalent metal transporter 1) in the duodenal epithelium, while heme iron is taken into the body via HCP-1 (heme carrier protein 1). The expression of DMT1 and FPN is regulated by IRP through sensing the amount of intracellular divalent iron. As the iron concentration increases during absorption (mucosal uptake), DMT1 expression decreases, and new absorption is restricted. In contrast, mucosal transfer of iron into the blood is mediated by FPN, which is regulated by hepcidin. As serum hepcidin levels increase, intestinal iron absorption decreases. In renal anemia, oral iron is believed to be ineffective, and injections should be utilized; the cause of this ineffectiveness is increased serum hepcidin levels (Figure 4).

In CDK patients, hepcidin levels are elevated due to decreased excretion and chronic inflammation. Hepcidin internalizes and degrades ferroportin, the only iron efflux protein present *in vivo*, thereby inhibiting iron absorption from the intestinal epithelium, iron release from hepatocytes, and iron cycling from macrophages. This results in increased serum iron concentration and intracellular iron and impaired iron utilization in the bone marrow.

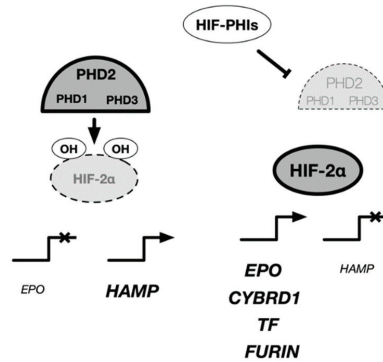


Figure 4. Regulatory mechanism of EPO and iron metabolism-related genes in cells. HIF-PH inhibitors have been prescribed for the treatment of renal anemia. The target cells of HIF-PH inhibitors include Rep cells located in the kidney, liver, and intestinal epithelial cells, where activation of HIF-2 rather than HIF-1 induces expression of various genes related to EPO and iron metabolism. In the liver, HIF-2 is known to have an inhibitory effect on hepcidin expression. EPO: erythropoietin, HAMP: hepcidin, CYBRD1: Dcytb, TF:transferrin, FURIN: furin.

In addition, transferrin and transferrin receptors, which are involved in iron transport, are target genes of HIF-1, and the expression of DMT1 and Dcytb, which are involved in intestinal iron absorption, are regulated by HIF-2 (Table 3).

Table 3. HIFs target genes involved in iron homeostasis.

Protein	Gene	HIF1/HIF2	Function	Ref.
Ceruloplasmin	<i>CP</i>	HIF-1	ferroxidase	[121]
Duodenal cytochrome b	<i>CYBRD1</i>	HIF-2	Ferric reductase	[122]
Erythropoietin	<i>EPO</i>	HIF-2	promote red blood cell production	[36,123]
Ferrochelatase	<i>FECH</i>	HIF-1	Heme synthesis	[124]
Furin	<i>FURIN</i>	HIF-1	subtilisin-like proprotein convertase	[125–127]
Hepcidin	<i>HAMP</i>	HIF-2	maintenance of iron homeostasis	[128,129]
Heme oxygenase-1	<i>HMOX1</i>	HIF-1	Heme degradation	[121]
Aconitase	<i>IRP1</i>	HIF-1	Cellular iron sensing	[130]
Transferrin	<i>TF</i>	HIF-1	Serum iron transporter	[131,132]
Transferrin receptor	<i>TFRC</i>	HIF-1	Cellular iron uptake	[121]

In particular, it has been reported that hepcidin production is increased under inflammatory conditions, causing ESA resistance because iron stores are not available for hematopoiesis.

Previous clinical trials have shown that patients with high CRP require larger doses of ESAs to maintain the same Hb level than those with low CRP levels; however, there is no difference in the dose of roxadustat required, regardless of the CRP level.

Regarding the effect of iron metabolism, the required dose of ESAs was reported to be higher in iron-deficient patients with low TSAT and ferritin levels than that in iron-deficient patients with TSAT and ferritin levels above the guideline recommendations; in contrast, the difference in dosing was minor with roxadustat [133–136].

Thus, HIF-PH inhibitors may contribute to the improvement of anemia by stimulating EPO production and altering iron metabolism in favor of hematopoiesis.

12. Nephroprotective Effects of HIF-PHIs

HIF-PHIs are expected to be effective in treating other diseases and conditions, including acute kidney injury (AKI) and renal transplantation [137,138].

In AKI, hypoxia caused by renal ischemia leads to functional decline of tubular epithelial cells, resulting in degeneration and necrosis [139–142]. Urothelial epithelial cells are oxygen-consuming cells with abundant mitochondria that require a large amount of oxygen for the reabsorption and secretion of substances [143]. This indicates that they are vulnerable to hypoxia [144–146].

In kidney transplantation, artificial ischemic AKI occurs during the removal of the transplanted kidney from the donor. After transplantation into the recipient, the resumption of blood flow causes ischemia-reperfusion injury to the transplanted kidney [147–150].

AKI and renal ischemia-reperfusion cause various physiological changes, including oxidative stress updating, inflammatory cytokine release, mitochondrial dysfunction, autophagic dysfunction, and hyperglycemia. During the anastomosis in kidney transplantation procedure, the transplanted kidney from the donor was maintained at a low temperature.

AKI in the kidney induces activation of HIFs in tubular epithelial cells and renal vasculature. This is believed to be a biological defense response.

HIFs have been reported to act as a protective mechanism for tubular epithelial cells in AKI by decreasing ROS and retaining glycogen [151].

Theoretically, HIF-PHI may protect against AKI or renal ischemia-reperfusion by activating HIF [152,153]. Cisplatin nephropathy in mice induced by roxadustat resulted in apoptosis and suppression of pro-inflammatory cytokines, indicating nephroprotection. In a report on the effect of the HIF-PHI roxadustat on AKI in cisplatin nephropathy [154], HIF-PHI improved renal function based on KIM-1 and NGAL levels as well as HIF-1 activation, suggesting that roxadustat induces profound changes in renal metabolism [155]. It is suggested that enalodustat may exert nephroprotective effects by altering energy-related metabolic metabolism in tubular cells [151].

In a rat ischemia-reperfusion model, the group pre-treated with daprodustat showed less renal interstitial fibrosis and interstitial inflammatory response after ischemia-reperfusion and less anemia deterioration than the control group [156]. FG-4497 administration to transplant donor rats improved the prognosis of transplanted grafts; upregulation of AgtPI4 and HO-1, inhibition of apoptosis, and activation of antioxidant pathways were observed in the renal tubular epithelium of the grafts [156].

These experimental results suggest that HIF-PHIs, when administered to renal transplant recipients or donors in advance, are promising nephroprotective agents against transient AKI or renal ischemia-reperfusion injury that occurs after renal transplantation. Renal expression of HIF has been reported to be associated with renal transplant rejection.

It may be used as a diagnostic pathological marker for rejection or as a prognostic marker for grafts.

13. Diverse Effects of HIF-PHIs

HIF-PHIs constitute a treatment for renal anemia with a completely new mechanism of action. Unlike conventional ESAs, which are injectable drugs that act specifically on the hematopoietic system, HIF-PHIs are oral drugs that may also have systemic effects. However, there is a concern regarding the possibility of side effects caused by the activation of defense mechanisms by HIF in conditions where angiogenesis plays a role in disease progression, such as cancer and retinal diseases. In addition to these theoretical concerns, adverse events have been reported in clinical trials.

13.1. Ischemia

Organ ischemia, or reduced blood flow, is a major clinical problem caused by diseases of the circulatory system. These ischemia may occur artificially as an interruption or bypass of circulation due to the needs of the surgical technique during surgery. All organs of the

body can be affected, but in particular, the ischemia of brain, heart, kidneys, and extremities are the most clinically problematic. Ischemia can be acute in time (sudden decrease in blood flow within minutes to hours) or chronic (gradual decrease in blood flow over weeks to years). Tissue hypoxia is a common feature of ischemia, but the condition is complicated by decreased supply and discharge of metabolites. In these conditions, activation of the HIF system occurs, but the extent of this effect varies within and between ischemic tissues. Administration of HIF-PHI under these conditions is expected to increase HIF activity at a time that is precipitated by a decrease in blood flow, thereby enhancing endogenous defense and repair responses.

Multiple studies have been conducted to determine whether exogenous activation of HIFs can improve the outcome of experimental ischemia in various animal models [22,157–160]. The results of the majority of these studies suggest that HIF activation leads to improvement in pathology, at least in the short term. In models of cerebral ischemia, treatment immediately before or immediately after arterial occlusion has improved outcomes as assessed by infarct volume. Studies of coronary artery ligation have demonstrated the benefits of HIF-PHI administration, both in terms of reduction in infarct size and (when treated after ischemia) improvement in ventricular function [161–163].

Overall, a great number of ischemic protective mechanisms have been attributed to specific HIF target genes. These include genes involved in reprogramming cellular metabolism, affecting apoptosis/survival pathways, and altering vascular permeability. Others act on a longer time scale, such as angiogenesis and reperfusion, tissue repair, stem cell activation and homing, and matrix remodeling. However, it is still largely unknown which of these mechanisms mediate the effects observed in different ischemic models.

13.2. Inflammation

Inflammation is triggered in many diseases and plays an important role in the progression of the disease. Inflammation is caused by multiple factors, including responses to pathogens, tissue damage, and immune dysregulation, and is essentially a progressive condition. The high cytokine and chemokine environment and hypoxia induced by inflammation together lead to the activation of HIFs, which in turn have multiple effects on immune and inflammatory cells, including differentiation, apoptosis, and effects on cytokine production. Under a variety of circumstances, induction of HIF-1 has been reported to activate pro-inflammatory Th17 T cells by upregulating and co-activating the transcription factor ROR- γ t and activating anti-inflammatory agents [164]. For example, activation of HIF may promote enhanced barrier function [165] and epithelial-mesenchymal transition [166] under various circumstances. On the other hand, however, artificial activation of HIF has been reported to improve the prognosis of various inflammatory models.

In an ulcerative colitis model in mice induced by administration of trinitrobenzene sulfonic acid, treatment with the HIF-PH inhibitors FG-4497 and AKB-4924 resulted in therapeutic effects based on weight loss, colon shortening, and reduced histological injury [160,167,168]. Mechanisms for this protective effect were proposed, including HIF-1-mediated improvement of epithelial barrier function and healing, and reduction of the inflammatory response. In another study of acute lung injury in mice, FG-4497 resulted in a decrease in leukocyte infiltration and was associated with increased survival of individuals [169]. The mechanism of protection in this study was proposed to be HIF-2-dependent induction of the vascular endothelial protein tyrosine phosphatase, leading to an increase in the integrity of the vascular barrier in the lung. Some studies have examined the effects of HIF-PHI on inflammation associated with bacterial infections; GSK360A was reported to alleviate elevated blood lactate levels and increase survival in a mouse model of endotoxin shock. It has been proposed that this effect is mediated by inhibition of the Cori cycle in the liver [170].

14. Adverse Effects of HIF-PHIs

14.1. Iron Deficiency

HIF-PH inhibitors cause a decrease in ferritin and an increase in TIBC after administration due to their complete effect on iron metabolism; administration of HIF-PHIs in iron-deficient patients may lead to iron deficiency, which reduces the effect of iron deficiency on anemia and causes iron deficiency symptoms in the bones, skin, and mucous membranes.

14.2. Cancers and Malignant Tumors

Clinical and animal studies of HIF-PH inhibitors have provided no evidence that HIF-PH inhibitors increase the incidence of renal cancer or other malignancies [90,119,120,133–135]. However, it cannot be denied that HIF activation by HIF-PH inhibitors may promote the proliferation, invasion, and metastatic potential of cells that have already undergone malignant transformation. It is important to note that HIF-1, but not HIF-2, is associated with the activity of malignant genes in tumors, and that activation of HIFs, particularly HIF-1, appears to be associated with the spread of metastases in breast, prostate, lung, bone, and colorectal cancers [171]. Nevertheless, HIF-2 has also been identified in malignant hepatocellular cell lines *in vitro* and is involved in the activation of cancer stem cell factors and is strongly associated with metastasis and even poor prognosis of various tumors [172]. In most kidney cancers, the VHL tumor suppressor gene is mutated or inactivated, resulting in the activation of the transcription factor HIF and upregulation of multiple genes downstream of HIF that are involved in cancer cell proliferation, invasion, and metastasis. In addition to renal cancer, increased expression of the HIF-1 α protein has been positively correlated with cancer progression and metastasis in several solid tumors. The malignant transformation of cells requires the accumulation of driver gene mutations that play a decisive role in this process. Currently, there is no evidence that HIF-PHIs promote this process [173]. However, the effects of HIF activation on events such as mitosis, metastasis, and migration of cancerous cells are well predicted for the reasons described above. In addition, patients with the highest risk of kidney disease should be evaluated and followed up with appropriate imaging studies, such as MRI, contrast-enhanced CT, and ultrasound, before and after HIF-PHIs are administered and at least once a year after administration.

Nevertheless, normalization of tumor blood vessels is considered a useful therapeutic strategy to improve the tumor tissue environment [24].

On the basis of these findings, we investigated whether HIF-PHIs induce tumor vascular normalization and contribute to the improvement of the tumor tissue environment and found that administration of HIF-PHIs altered the vascular structure in tumor tissue [174]. In particular, fluorescent immunostaining of tumor tissues using CD31, a marker of vascular endothelial cells, showed that CD31 positivity per unit area of tumor tissue sections increased significantly after treatment with HIF-PHIs. A significant increase was observed in the evaluation of vessel length. A decrease in the number of vessels per unit area was observed during the evaluation of vessel density in the tumor tissue. These results suggest that HIF-PHIs suppress irregular branching and prolong the length of a single blood vessel in the tissue, reducing the specific characteristics of tumor vessels, such as irregular meandering and branching [174]. In addition, extravascular leakage was reduced in HIF-PHI-treated tissues. These results suggest that HIF-PHIs not only induce structural changes in blood vessels but also functionally improve normal blood vessels. These results suggest that HIF-PHI-induced vascular normalization improves the drug delivery efficiency of anticancer drugs and enhances anticancer drug sensitivity. In addition, HIF-PHIs have been reported to restore the immune responsiveness of immune cells in tumors by improving the tumor-specific tissue environment, resulting in therapeutic effects mediated by immune cells [175].

14.3. Diabetic Retinopathy and Age-Related Macular Degeneration

HIF-1 α and VEGF induced by HIF-1 α are closely related to the development and progression of diabetic retinopathy and age-related macular degeneration (AMD). HIF-PHIs may increase the expression of VEGF and angiogenesis through the activation of HIF. There are concerns that stabilization of HIF may exacerbate retinal lesions, especially diabetic retinopathy, which is a common complication in dialysis patients. However, no clinical study reported to date has been associated with worsening of retinopathy, and the results of clinical trials indicate that retinal hemorrhage was as frequent in the HIF-PHI group as in ESA group for all drugs [90,119,120,133–135]. However, it has been suggested that VEGF may be expressed locally in the retina and that it may act in an autocrine and paracrine manner; EPO itself is suggested to be associated with retinopathy. In addition, several clinical trials have excluded patients at high risk of retinal hemorrhage; therefore, caution should be exercised during the use of HIF-PHIs to ensure that retinopathy does not worsen, especially in patients who already have retinopathy.

14.4. Thromboembolism

Since thromboembolism can be caused by a sudden increase in the viscosity of the blood, the rate of increase in hemoglobin levels should not exceed 0.5 g/dL/week. To this end, the dose of HIF-PHIs should be increased gradually, with appropriate intervals between increases, in accordance with the label of the respective drug [25,176]. Since iron deficiency itself has been reported to be a risk factor for thromboembolism, iron deficiency should be avoided [25,177,178]. Signs and symptoms of suspected thromboembolism should be closely monitored during treatment. Specific suspected symptoms include significant left-right difference in leg edema (suspicion of deep vein thrombosis), poor bleeding out of the vascular access (precursor of vascular access occlusion), transient ischemic attack (precursor of cerebral infarction), and sudden onset of rapid loss of vision or blurred vision (suspicion of retinal vein occlusion). If these symptoms occur, in addition to the evaluation of hemoglobin level, FDP, vascular access echocardiography, brain MRI, and ophthalmologic evaluation should be performed as soon as possible, and immediate action should be taken. If these symptoms clearly increase after initiation of HIF-PHIs, the inhibitor treatment should be discontinued.

HIF-1 activation by hypoxia promotes vascular calcification by transforming smooth muscle cells into osteoblast-like cells, and some CKD patients exhibit significant vascular calcification; therefore, care should be taken when administering HIF-PHIs [179].

14.5. Pulmonary Hypertension

Studies using patients with mutations in HIF-related genes and animal models have indicated that constant activation of HIF signaling may exacerbate pulmonary hypertension [180]. Considering the characteristics of the pulmonary vascular response to oxygenation, the risk of developing pulmonary hypertension due to administration of HIF-PHIs should be carefully considered. When HIF-PHIs are administered, patients should be carefully interviewed to ensure that exercise tolerance is not impaired. In addition, electrocardiography and echocardiography should be performed periodically to check for right ventricular strain findings. In particular, if peak tricuspid regurgitation velocities of 3.4 m or more per second occur, referral to a cardiologist should be considered. The use of HIF-PH inhibitors in patients who have already developed pulmonary hypertension should be considered with extreme caution. Although the relationship between HIF-PHIs and cardiovascular events in Japanese patients is unclear at this time, in animal studies, constant activation of HIF signaling has been reported to cause heart failure [181–188]. When HIF-PHIs are administered, it is recommended that chest radiography and echocardiography be performed periodically. It should be noted that the BNP levels in the blood may be directly induced by the administration of HIF-PHIs, as well as by renal function [189].

14.6. Polycystic Kidney Disease (PCKD)

HIF-1 α has been reported to be involved in the enlargement of renal scales in an animal model of advanced polycystic kidney disease [190]. In contrast, there was no increase in the number of renal scales in a mild animal model of polycystic kidney disease [191]. It is not known whether HIF-PHIs induce further HIF activation in patients with multiple cysts; local HIF activation in the kidney has been reported to occur because of reduced blood flow caused by compression by the polycysts. However, because of the short duration of the trial, further long-term evaluation is necessary to determine the effect.

The development of hepatic dysfunction is a significant issue; in fact, the HIF-PHI FG-2216, which was clinically developed in 2008, was withdrawn from the market owing to the development of fatal liver failure in one patient.

HIF has been reported to be associated with hepatic fibrosis and inflammation in nonalcoholic fatty liver disease; therefore, abnormal liver function should be closely monitored [192–194].

14.7. Hyperkalemia

A phase III clinical trial in China reported a significant increase in hyperkalemia and metabolic acidosis complications in both conservative CKD patients and hemodialysis patients treated with roxadustat [119,120]. Additionally, daprodustat clinical trials reported a significant increase in hyperkalemia, as a side effect, in hemodialysis patients [195]. We cannot rule out the possibility that this side effect is a class effect of HIF-PHI. However, the incidence of hyperkalemia was comparable between the roxadustat and control groups when analyzed using data. In addition, several studies have reported a higher incidence of hyperkalemia in the HIF-PHIs group, but definitive conclusions about this side effect have not yet been reached. Considering that hyperkalemia is a common and life-threatening complication, especially in patients with kidney disease, it is necessary to monitor serum potassium regularly after initiation of HIF-PHIs as well as during treatment.

15. Establishment of Resistance

Clearly, our body has a built-in negative feedback mechanism to prevent HIF from being constantly activated. The HIF system forms a negative feedback loop [196,197]. HIF-1 activation has been observed to repress HIF-dependent gene responses through the induction of PHD2 and PHD3 mRNA expression [198,199].

HIF-PHIs activate HIF and may induce the mRNA and protein expression of PHD2 and PHD3 independent of the oxygen concentration. If HIF-PHIs trigger this feedback loop and alter EPO induction and iron metabolism-related gene expression, long-term use may lead to resistance against HIF-PHIs.

16. Conclusions

HIF-PHIs activate HIF-1 and HIF-2 by exogenously triggering the hypoxia-responsive gene response in the body. It has been shown that HIF activation stimulates EPO production by REP cells and improves the oxygen-carrying capacity of the blood through proliferation of erythrocytes by increasing the efficiency of iron metabolism. Currently, five orally administered HIF-PHIs are available for the treatment of renal anemia in clinical practice. It is necessary to continue to carefully study their adverse effects on malignancy and retinopathy and the currently unknown effects of their long-term use.

Funding: This work was supported by a research grant from the Kansai Medical University (KMU) research consortium and the branding program as a world-leading research university on intractable immune and allergic diseases from MEXT Japan.

Institutional Review Board Statement: Not applicable.

Informed Consent Statement: Not applicable.

Data Availability Statement: This study did not report any data.

Acknowledgments: I would like to thank Hideko Nagasawa at Gifu Pharmaceutical University for drawing the chemical formulas.

Conflicts of Interest: The author declares no conflict of interest.

References

- Nagel, S.; Talbot, N.P.; Mecinovic, J.; Smith, T.G.; Buchan, A.M.; Schofield, C.J. Therapeutic manipulation of the HIF hydroxylases. *Antioxid. Redox Signal.* **2010**, *12*, 481–501. [[CrossRef](#)]
- Thavarajah, S.; Choi, M.J. The Use of Erythropoiesis-Stimulating Agents in Patients With CKD and Cancer: A Clinical Approach. *Am. J. Kidney Dis.* **2019**, *74*, 667–674. [[CrossRef](#)] [[PubMed](#)]
- Edmonston, D.; Wolf, M. FGF23 at the crossroads of phosphate, iron economy and erythropoiesis. *Nat. Rev. Nephrol.* **2020**, *16*, 7–19. [[CrossRef](#)]
- Del Vecchio, L.; Minutolo, R. ESA, Iron Therapy and New Drugs: Are There New Perspectives in the Treatment of Anaemia? *J. Clin. Med.* **2021**, *10*, 839. [[CrossRef](#)]
- Camaschella, C. Iron-deficiency anemia. *N. Engl. J. Med.* **2015**, *372*, 1832–1843. [[CrossRef](#)] [[PubMed](#)]
- Ganz, T. Anemia of Inflammation. *N. Engl. J. Med.* **2019**, *381*, 1148–1157. [[CrossRef](#)]
- Kaplan, J. Roxadustat and Anemia of Chronic Kidney Disease. *N. Engl. J. Med.* **2019**, *381*, 1070–1072. [[CrossRef](#)] [[PubMed](#)]
- Semenza, G.L. Life with oxygen. *Science* **2007**, *318*, 62–64. [[CrossRef](#)]
- Semenza, G.L. Perspectives on oxygen sensing. *Cell* **1999**, *98*, 281–284. [[CrossRef](#)]
- Semenza, G.L. HIF-1 and human disease: One highly involved factor. *Genes Dev.* **2000**, *14*, 1983–1991.
- Hirota, K. Basic Biology of Hypoxic Responses Mediated by the Transcription Factor HIFs and its Implication for Medicine. *Biomedicines* **2020**, *8*, 32. [[CrossRef](#)] [[PubMed](#)]
- Wang, G.; Semenza, G. Purification and characterization of hypoxia-inducible factor 1. *J. Biol. Chem.* **1995**, *270*, 1230–1237. [[CrossRef](#)] [[PubMed](#)]
- Wang, G.; Jiang, B.; Rue, E.; Semenza, G. Hypoxia-inducible factor 1 is a basic-helix-loop-helix-PAS heterodimer regulated by cellular O₂ tension. *Proc. Natl. Acad. Sci. USA* **1995**, *92*, 5510–5514. [[CrossRef](#)] [[PubMed](#)]
- Wang, G.; Semenza, G. Characterization of hypoxia-inducible factor 1 and regulation of DNA binding activity by hypoxia. *J. Biol. Chem.* **1993**, *268*, 21513–21518. [[CrossRef](#)]
- Epstein, A.; Gleadle, J.; McNeill, L.; Hewitson, K.; O'Rourke, J.; Mole, D.; Mukherji, M.; Metzen, E.; Wilson, M.; Dhanda, A.; et al. C. elegans EGL-9 and mammalian homologs define a family of dioxygenases that regulate HIF by prolyl hydroxylation. *Cell* **2001**, *107*, 43–54. [[CrossRef](#)]
- Mahon, P.C.; Hirota, K.; Semenza, G.L. FIH-1: A novel protein that interacts with HIF-1 α and VHL to mediate repression of HIF-1 transcriptional activity. *Genes Dev.* **2001**, *15*, 2675–2686. [[CrossRef](#)]
- Lando, D.; Peet, D.J.; Gorman, J.J.; Whelan, D.A.; Whitelaw, M.L.; Bruick, R.K. FIH-1 is an asparaginyl hydroxylase enzyme that regulates the transcriptional activity of hypoxia-inducible factor. *Genes Dev.* **2002**, *16*, 1466–1471. [[CrossRef](#)]
- Lando, D.; Peet, D.J.; Whelan, D.A.; Gorman, J.J.; Whitelaw, M.L. Asparagine hydroxylation of the HIF transactivation domain a hypoxic switch. *Science* **2002**, *295*, 858–861. [[CrossRef](#)]
- Fandrey, J.; Schodel, J.; Eckardt, K.U.; Katschinski, D.M.; Wenger, R.H. Now a Nobel gas: Oxygen. *Pflügers Arch.* **2019**. [[CrossRef](#)]
- West, J.B. Physiological Effects of Chronic Hypoxia. *N. Engl. J. Med.* **2017**, *376*, 1965–1971. [[CrossRef](#)]
- Gilreath, J.A.; Rodgers, G.M. How I treat cancer-associated anemia. *Blood* **2020**, *136*, 801–813. [[CrossRef](#)]
- Bishop, T.; Ratcliffe, P.J. HIF hydroxylase pathways in cardiovascular physiology and medicine. *Circ. Res.* **2015**, *117*, 65–79. [[CrossRef](#)] [[PubMed](#)]
- Hirota, K. An intimate crosstalk between iron homeostasis and oxygen metabolism regulated by the hypoxia-inducible factors (HIFs). *Free Radic. Biol. Med.* **2019**, *133*, 118–129. [[CrossRef](#)]
- Yap, D.Y.H.; McMahon, L.P.; Hao, C.M.; Hu, N.; Okada, H.; Suzuki, Y.; Kim, S.G.; Lim, S.K.; Vareesangthip, K.; Hung, C.C.; et al. Recommendations by the Asian Pacific society of nephrology (APSN) on the appropriate use of HIF-PH inhibitors. *Nephrology* **2020**. [[CrossRef](#)]
- Gupta, N.; Wish, J.B. Hypoxia-Inducible Factor Prolyl Hydroxylase Inhibitors: A Potential New Treatment for Anemia in Patients With CKD. *Am. J. Kidney Dis.* **2017**, *69*, 815–826. [[CrossRef](#)]
- Ho, V.T.; Bunn, H.F. Effects of transition metals on the expression of the erythropoietin gene: Further evidence that the oxygen sensor is a heme protein. *Biochem. Biophys. Res. Commun.* **1996**, *223*, 175–180. [[CrossRef](#)]
- Weir, E.K.; Lopez-Barneo, J.; Buckler, K.J.; Archer, S.L. Acute oxygen-sensing mechanisms. *N. Engl. J. Med.* **2005**, *353*, 2042–2055. [[CrossRef](#)]
- Prabhakar, N.R.; Peng, Y.J. Oxygen Sensing by the Carotid Body: Past and Present. *Adv. Exp. Med. Biol.* **2017**, *977*, 3–8. [[CrossRef](#)]
- Simon, M.C. The Hypoxia Response Pathways—Hats Off! *N. Engl. J. Med.* **2016**, *375*, 1687–1689. [[CrossRef](#)] [[PubMed](#)]
- Reissmann, K.R. Studies on the mechanism of erythropoietic stimulation in parabiotic rats during hypoxia. *Blood* **1950**, *5*, 372–380. [[CrossRef](#)]
- Fried, W.; Goldwasser, E.; Jacobson, L.O.; Plzak, L.F. Studies on erythropoiesis. III. Factors controlling erythropoietin production. *Proc. Soc. Exp. Biol. Med.* **1957**, *94*, 237–241. [[CrossRef](#)]

32. Jacobson, L.O.; Goldwasser, E.; Fried, W.; Plzak, L.F. Studies on erythropoiesis. VII. The role of the kidney in the production of erythropoietin. *Trans. Soc. Assoc. Am. Physicians* **1957**, *70*, 305–317.
33. Goldwasser, E.; Fried, W.; Jacobson, L.O. Studies on erythropoiesis. VIII. The effect of nephrectomy on response to hypoxic anoxia. *J. Lab. Clin. Med.* **1958**, *52*, 375–378.
34. Miyake, T.; Kung, C.K.; Goldwasser, E. Purification of human erythropoietin. *J. Biol. Chem.* **1977**, *252*, 5558–5564. [[CrossRef](#)]
35. Jacobs, K.; Shoemaker, C.; Rudersdorf, R.; Neill, S.D.; Kaufman, R.J.; Mufson, A.; Seehra, J.; Jones, S.S.; Hewick, R.; Fritsch, E.F.; et al. Isolation and characterization of genomic and cDNA clones of human erythropoietin. *Nature* **1985**, *313*, 806–810. [[CrossRef](#)] [[PubMed](#)]
36. Suzuki, N.; Yamamoto, M. Roles of renal erythropoietin-producing (REP) cells in the maintenance of systemic oxygen homeostasis. *Pflug. Arch.* **2016**, *468*, 3–12. [[CrossRef](#)] [[PubMed](#)]
37. Hawley, J.A.; Lundby, C.; Cotter, J.D.; Burke, L.M. Maximizing Cellular Adaptation to Endurance Exercise in Skeletal Muscle. *Metab. Cell Metab.* **2018**, *27*, 962–976. [[CrossRef](#)]
38. Goldberg, M.A.; Glass, G.A.; Cunningham, J.M.; Bunn, H.F. The regulated expression of erythropoietin by two human hepatoma cell lines. *Proc. Natl. Acad. Sci. USA* **1987**, *84*, 7972–7976. [[CrossRef](#)] [[PubMed](#)]
39. Goldwasser, E.; Jacobson, L.O.; Fried, W.; Plzak, L.F. Studies on erythropoiesis. V. The effect of cobalt on the production of erythropoietin. *Blood* **1958**, *13*, 55–60. [[CrossRef](#)]
40. Goldberg, M.A.; Dunning, S.P.; Bunn, H.F. Regulation of the erythropoietin gene: Evidence that the oxygen sensor is a heme protein. *Science* **1988**, *242*, 1412–1415. [[CrossRef](#)]
41. Jiang, B.H.; Semenza, G.L.; Bauer, C.; Marti, H.H. Hypoxia-inducible factor 1 levels vary exponentially over a physiologically relevant range of O₂ tension. *Am. J. Physiol.* **1996**, *271*, C1172–C1180. [[CrossRef](#)]
42. Keith, B.; Johnson, R.S.; Simon, M.C. HIF1alpha and HIF2alpha: Sibling rivalry in hypoxic tumour growth and progression. *Nat. Rev. Cancer* **2011**, *12*, 9–22. [[CrossRef](#)]
43. Suzuki, N. Erythropoietin gene expression: Developmental-stage specificity, cell-type specificity, and hypoxia inducibility. *Tohoku J. Exp. Med.* **2015**, *235*, 233–240. [[CrossRef](#)]
44. Suzuki, N.; Gradin, K.; Poellinger, L.; Yamamoto, M. Regulation of hypoxia-inducible gene expression after HIF activation. *Exp. Cell Res.* **2017**, *356*, 182–186. [[CrossRef](#)] [[PubMed](#)]
45. Salceda, S.; Caro, J. Hypoxia-inducible factor 1alpha (HIF-1alpha) protein is rapidly degraded by the ubiquitin-proteasome system under normoxic conditions. Its stabilization by hypoxia depends on redox-induced changes. *J. Biol. Chem.* **1997**, *272*, 22642–22647. [[CrossRef](#)] [[PubMed](#)]
46. Kallio, P.J.; Wilson, W.J.; O'Brien, S.; Makino, Y.; Poellinger, L. Regulation of the hypoxia-inducible transcription factor 1alpha by the ubiquitin-proteasome pathway. *J. Biol. Chem.* **1999**, *274*, 6519–6525. [[CrossRef](#)] [[PubMed](#)]
47. Maxwell, P.H.; Wiesener, M.S.; Chang, G.W.; Clifford, S.C.; Vaux, E.C.; Cockman, M.E.; Wykoff, C.C.; Pugh, C.W.; Maher, E.R.; Ratcliffe, P.J. The tumour suppressor protein VHL targets hypoxia-inducible factors for oxygen-dependent proteolysis. *Nature* **1999**, *399*, 271–275. [[CrossRef](#)]
48. Srinivas, V.; Zhang, L.P.; Zhu, X.H.; Caro, J. Characterization of an oxygen/redox-dependent degradation domain of hypoxia-inducible factor alpha (HIF-alpha) proteins. *Biochem. Biophys. Res. Commun.* **1999**, *260*, 557–561. [[CrossRef](#)]
49. Srinivas, V.; Zhu, X.; Salceda, S.; Nakamura, R.; Caro, J. Hypoxia-inducible factor 1alpha (HIF-1alpha) is a non-heme iron protein. Implications for oxygen sensing. *J. Biol. Chem.* **1999**, *274*, 1180. [[CrossRef](#)]
50. Cockman, M.E.; Masson, N.; Mole, D.R.; Jaakkola, P.; Chang, G.W.; Clifford, S.C.; Maher, E.R.; Pugh, C.W.; Ratcliffe, P.J.; Maxwell, P.H. Hypoxia inducible factor-alpha binding and ubiquitylation by the von Hippel-Lindau tumor suppressor protein. *J. Biol. Chem.* **2000**, *275*, 25733–25741. [[CrossRef](#)]
51. Ivan, M.; Kondo, K.; Yang, H.; Kim, W.; Valiano, J.; Ohh, M.; Salic, A.; Asara, J.M.; Lane, W.S.; Kaelin, W.G., Jr. HIF1alpha targeted for VHL-mediated destruction by proline hydroxylation: Implications for O₂ sensing. *Science* **2001**, *292*, 464–468. [[CrossRef](#)]
52. Jaakkola, P.; Mole, D.R.; Tian, Y.M.; Wilson, M.I.; Gielbert, J.; Gaskell, S.J.; von Kriegsheim, A.; Hebestreit, H.F.; Mukherji, M.; Schofield, C.J.; et al. Targeting of HIF-1alpha to the von Hippel-Lindau ubiquitylation complex by O₂-regulated prolyl hydroxylation. *Science* **2001**, *292*, 468–472. [[CrossRef](#)] [[PubMed](#)]
53. Krek, W. VHL takes HIF's breath away. *Nat. Cell Biol.* **2000**, *2*, E121–E123. [[CrossRef](#)] [[PubMed](#)]
54. Ohh, M.; Park, C.W.; Ivan, M.; Hoffman, M.A.; Kim, T.Y.; Huang, L.E.; Pavletich, N.; Chau, V.; Kaelin, W.G. Ubiquitination of hypoxia-inducible factor requires direct binding to the beta-domain of the von Hippel-Lindau protein. *Nat. Cell Biol.* **2000**, *2*, 423–427. [[CrossRef](#)] [[PubMed](#)]
55. Schofield, C.J.; Ratcliffe, P.J. Oxygen sensing by HIF hydroxylases. *Nat. Rev. Mol. Cell Biol.* **2004**, *5*, 343–354. [[CrossRef](#)]
56. Wilkins, S.E.; Abboud, M.I.; Hancock, R.L.; Schofield, C.J. Targeting Protein-Protein Interactions in the HIF System. *ChemMedChem* **2016**, *11*, 773–786. [[CrossRef](#)]
57. Hirota, K.; Semenza, G.L. Regulation of hypoxia-inducible factor 1 by prolyl and asparaginyl hydroxylases. *Biochem. Biophys. Res. Commun.* **2005**, *338*, 610–616. [[CrossRef](#)]
58. Yeh, T.L.; Leissing, T.M.; Abboud, M.I.; Thinnies, C.C.; Atasoylu, O.; Holt-Martyn, J.P.; Zhang, D.; Tumber, A.; Lippl, K.; Lohans, C.T.; et al. Molecular and cellular mechanisms of HIF prolyl hydroxylase inhibitors in clinical trials. *Chem. Sci.* **2017**, *8*, 7651–7668. [[CrossRef](#)] [[PubMed](#)]

59. Iwai, K.; Yamanaka, K.; Kamura, T.; Minato, N.; Conaway, R.C.; Conaway, J.W.; Klausner, R.D.; Pause, A. Identification of the von Hippel-lindau tumor-suppressor protein as part of an active E3 ubiquitin ligase complex. *Proc. Natl. Acad. Sci. USA* **1999**, *96*, 12436–12441. [[CrossRef](#)]
60. Kamura, T.; Sato, S.; Iwai, K.; Czyzyk-Krzeska, M.; Conaway, R.C.; Conaway, J.W. Activation of HIF1alpha ubiquitination by a reconstituted von Hippel-Lindau (VHL) tumor suppressor complex. *Proc. Natl. Acad. Sci. USA* **2000**, *97*, 10430–10435. [[CrossRef](#)]
61. Hirsila, M.; Koivunen, P.; Gunzler, V.; Kivirikko, K.I.; Myllyharju, J. Characterization of the human prolyl 4-hydroxylases that modify the hypoxia-inducible factor. *J. Biol. Chem.* **2003**, *278*, 30772–30780. [[CrossRef](#)]
62. Koivunen, P.; Hirsila, M.; Gunzler, V.; Kivirikko, K.I.; Myllyharju, J. Catalytic properties of the asparaginyl hydroxylase (FIH) in the oxygen sensing pathway are distinct from those of its prolyl 4-hydroxylases. *J. Biol. Chem.* **2004**, *279*, 9899–9904. [[CrossRef](#)] [[PubMed](#)]
63. Joharapurkar, A.A.; Pandya, V.B.; Patel, V.J.; Desai, R.C.; Jain, M.R. Prolyl Hydroxylase Inhibitors: A Breakthrough in the Therapy of Anemia Associated with Chronic Diseases. *J. Med. Chem.* **2018**, *61*, 6964–6982. [[CrossRef](#)]
64. Hsieh, M.M.; Linde, N.S.; Wynter, A.; Metzger, M.; Wong, C.; Langsetmo, I.; Lin, A.; Smith, R.; Rodgers, G.P.; Donahue, R.E.; et al. HIF prolyl hydroxylase inhibition results in endogenous erythropoietin induction, erythrocytosis, and modest fetal hemoglobin expression in rhesus macaques. *Blood* **2007**, *110*, 2140–2147. [[CrossRef](#)] [[PubMed](#)]
65. Cases, A. The latest advances in kidney diseases and related disorders. *Drug News Perspect.* **2007**, *20*, 647–654.
66. Chan, M.C.; Holt-Martyn, J.P.; Schofield, C.J.; Ratcliffe, P.J. Pharmacological targeting of the HIF hydroxylases—A new field in medicine development. *Mol. Aspects Med.* **2016**, *47–48*, 54–75. [[CrossRef](#)]
67. Hewitson, K.S.; Schofield, C.J.; Ratcliffe, P.J. Hypoxia-inducible factor prolyl-hydroxylase: Purification and assays of PHD2. *Methods Enzymol.* **2007**, *435*, 25–42. [[CrossRef](#)]
68. Rose, N.R.; McDonough, M.A.; King, O.N.; Kawamura, A.; Schofield, C.J. Inhibition of 2-oxoglutarate dependent oxygenases. *Chem. Soc. Rev.* **2011**, *40*, 4364–4397. [[CrossRef](#)]
69. Ehrismann, D.; Flashman, E.; Genn, D.N.; Mathioudakis, N.; Hewitson, K.S.; Ratcliffe, P.J.; Schofield, C.J. Studies on the activity of the hypoxia-inducible-factor hydroxylases using an oxygen consumption assay. *Biochem. J.* **2007**, *401*, 227–234. [[CrossRef](#)]
70. Kaule, G.; Gunzler, V. Assay for 2-oxoglutarate decarboxylating enzymes based on the determination of [1-14C]succinate: Application to prolyl 4-hydroxylase. *Anal. Biochem.* **1990**, *184*, 291–297. [[CrossRef](#)]
71. McNeill, L.A.; Hewitson, K.S.; Claridge, T.D.; Seibel, J.F.; Horsfall, L.E.; Schofield, C.J. Hypoxia-inducible factor asparaginyl hydroxylase (FIH-1) catalyses hydroxylation at the beta-carbon of asparagine-803. *Biochem. J.* **2002**, *367*, 571–575. [[CrossRef](#)] [[PubMed](#)]
72. Smirnova, N.A.; Rakhman, I.; Moroz, N.; Basso, M.; Payappilly, J.; Kazakov, S.; Hernandez-Guzman, F.; Gaisina, I.N.; Kozikowski, A.P.; Ratan, R.R.; et al. Utilization of an in vivo reporter for high throughput identification of branched small molecule regulators of hypoxic adaptation. *Chem. Biol.* **2010**, *17*, 380–391. [[CrossRef](#)]
73. Chan, M.C.; Atasoylu, O.; Hodson, E.; Tumber, A.; Leung, I.K.; Chowdhury, R.; Gomez-Perez, V.; Demetriades, M.; Rydzik, A.M.; Holt-Martyn, J.; et al. Potent and Selective Triazole-Based Inhibitors of the Hypoxia-Inducible Factor Prolyl-Hydroxylases with Activity in the Murine Brain. *PLoS ONE* **2015**, *10*, e0132004. [[CrossRef](#)] [[PubMed](#)]
74. Lee, S.H.; Jeong Hee, M.; Eun Ah, C.; Ryu, S.E.; Myung Kyu, L. Monoclonal antibody-based screening assay for factor inhibiting hypoxia-inducible factor inhibitors. *J. Biomol. Screen.* **2008**, *13*, 494–503. [[CrossRef](#)]
75. Snell, C.E.; Turley, H.; McIntyre, A.; Li, D.; Masiero, M.; Schofield, C.J.; Gatter, K.C.; Harris, A.L.; Pezzella, F. Proline-hydroxylated hypoxia-inducible factor 1alpha (HIF-1alpha) upregulation in human tumours. *PLoS ONE* **2014**, *9*, e88955. [[CrossRef](#)] [[PubMed](#)]
76. Tian, Y.M.; Yeoh, K.K.; Lee, M.K.; Eriksson, T.; Kessler, B.M.; Kramer, H.B.; Edelman, M.J.; Willam, C.; Pugh, C.W.; Schofield, C.J.; et al. Differential sensitivity of hypoxia inducible factor hydroxylation sites to hypoxia and hydroxylase inhibitors. *J. Biol. Chem.* **2011**, *286*, 13041–13051. [[CrossRef](#)] [[PubMed](#)]
77. Chowdhury, R.; Candela-Lena, J.I.; Chan, M.C.; Greenald, D.J.; Yeoh, K.K.; Tian, Y.M.; McDonough, M.A.; Tumber, A.; Rose, N.R.; Conejo-Garcia, A.; et al. Selective small molecule probes for the hypoxia inducible factor (HIF) prolyl hydroxylases. *ACS Chem. Biol.* **2013**, *8*, 1488–1496. [[CrossRef](#)] [[PubMed](#)]
78. Hewitson, K.S.; Lienard, B.M.; McDonough, M.A.; Clifton, I.J.; Butler, D.; Soares, A.S.; Oldham, N.J.; McNeill, L.A.; Schofield, C.J. Structural and mechanistic studies on the inhibition of the hypoxia-inducible transcription factor hydroxylases by tricarboxylic acid cycle intermediates. *J. Biol. Chem.* **2007**, *282*, 3293–3301. [[CrossRef](#)]
79. Oehme, F.; Jonghaus, W.; Narouzz-Ott, L.; Huetter, J.; Flamme, I. A nonradioactive 96-well plate assay for the detection of hypoxia-inducible factor prolyl hydroxylase activity. *Anal. Biochem.* **2004**, *330*, 74–80. [[CrossRef](#)]
80. Zheng, Q.; Yang, H.; Sun, L.; Wei, R.; Fu, X.; Wang, Y.; Huang, Y.; Liu, Y.N.; Liu, W.J. Efficacy and safety of HIF prolyl-hydroxylase inhibitor vs epoetin and darbepoetin for anemia in chronic kidney disease patients not undergoing dialysis: A network meta-analysis. *Pharmacol. Res.* **2020**, *159*, 105020. [[CrossRef](#)]
81. Dhillon, S. Daprodustat: First Approval. *Drugs* **2020**, *80*, 1491–1497. [[CrossRef](#)] [[PubMed](#)]
82. Dhillon, S. Roxadustat: First Global Approval. *Drugs* **2019**, *79*, 563–572. [[CrossRef](#)]
83. Backman, J.T.; Filppula, A.M.; Niemi, M.; Neuvonen, P.J. Role of Cytochrome P450 2C8 in Drug Metabolism and Interactions. *Pharmacol. Rev.* **2016**, *68*, 168–241. [[CrossRef](#)]
84. Markham, A. Vadadustat: First Approval. *Drugs* **2020**, *80*, 1365–1371. [[CrossRef](#)] [[PubMed](#)]
85. Markham, A. Enarodustat: First Approval. *Drugs* **2020**. [[CrossRef](#)]

86. Pai, S.M.; Connaire, J.; Yamada, H.; Enya, S.; Gerhardt, B.; Maekawa, M.; Tanaka, H.; Koretomo, R.; Ishikawa, T. A Mass Balance Study of (14) C-Labeled JTZ-951 (Enarodustat), a Novel Orally Available Erythropoiesis-Stimulating Agent, in Patients With End-Stage Renal Disease on Hemodialysis. *Clin. Pharmacol. Drug Dev.* **2020**, *9*, 728–741. [[CrossRef](#)] [[PubMed](#)]
87. van der Mey, D.; Gerisch, M.; Jungmann, N.A.; Kaiser, A.; Yoshikawa, K.; Schulz, S.; Radtke, M.; Lentini, S. Drug-drug interaction of atazanavir on UGT1A1-mediated glucuronidation of molidustat in human. *Basic Clin. Pharmacol. Toxicol.* **2020**. [[CrossRef](#)]
88. Lentini, S.; van der Mey, D.; Kern, A.; Thuss, U.; Kaiser, A.; Matsuno, K.; Gerisch, M. Absorption, distribution, metabolism and excretion of molidustat in healthy participants. *Basic Clin. Pharmacol. Toxicol.* **2020**, *127*, 221–233. [[CrossRef](#)]
89. Lentini, S.; Kaiser, A.; Kapsa, S.; Matsuno, K.; van der Mey, D. Effects of oral iron and calcium supplement on the pharmacokinetics and pharmacodynamics of molidustat: An oral HIF-PH inhibitor for the treatment of renal anaemia. *Eur. J. Clin. Pharmacol.* **2020**, *76*, 185–197. [[CrossRef](#)]
90. Akizawa, T.; Taguchi, M.; Matsuda, Y.; Iekushi, K.; Yamada, T.; Yamamoto, H. Molidustat for the treatment of renal anaemia in patients with dialysis-dependent chronic kidney disease: Design and rationale of three phase III studies. *BMJ Open* **2019**, *9*, e026602. [[CrossRef](#)]
91. Haase, V.H. HIF-prolyl hydroxylases as therapeutic targets in erythropoiesis and iron metabolism. *Hemodial. Int.* **2017**, *21* (Suppl. S1), S110–S124. [[CrossRef](#)]
92. Caltabiano, S.; Mahar, K.M.; Lister, K.; Tenero, D.; Ravindranath, R.; Cizman, B.; Cobitz, A.R. The drug interaction potential of daprostadustat when coadministered with pioglitazone, rosuvastatin, or trimethoprim in healthy subjects. *Pharmacol. Res. Perspect.* **2018**, *6*, e00327. [[CrossRef](#)] [[PubMed](#)]
93. Fukui, K.; Shinozaki, Y.; Kobayashi, H.; Deai, K.; Yoshiuchi, H.; Matsui, T.; Matsuo, A.; Matsushita, M.; Tanaka, T.; Nangaku, M. JTZ-951 (enarodustat), a hypoxia-inducible factor prolyl hydroxylase inhibitor, stabilizes HIF- α protein and induces erythropoiesis without effects on the function of vascular endothelial growth factor. *Eur. J. Pharmacol.* **2019**, *859*, 172532. [[CrossRef](#)] [[PubMed](#)]
94. Palis, J.; Segel, G.B. Developmental biology of erythropoiesis. *Blood Rev.* **1998**, *12*, 106–114. [[CrossRef](#)]
95. Baxter, E.J.; Scott, L.M.; Campbell, P.J.; East, C.; Fourouclas, N.; Swanton, S.; Vassiliou, G.S.; Bench, A.J.; Boyd, E.M.; Curtin, N.; et al. Acquired mutation of the tyrosine kinase JAK2 in human myeloproliferative disorders. *Lancet* **2005**, *365*, 1054–1061. [[CrossRef](#)]
96. Kralovics, R.; Passamonti, F.; Buser, A.S.; Teo, S.S.; Tiedt, R.; Passweg, J.R.; Tichelli, A.; Cazzola, M.; Skoda, R.C. A gain-of-function mutation of JAK2 in myeloproliferative disorders. *N. Engl. J. Med.* **2005**, *352*, 1779–1790. [[CrossRef](#)]
97. James, C.; Ugo, V.; Le Couedic, J.P.; Staerk, J.; Delhommeau, F.; Lacout, C.; Garcon, L.; Raslova, H.; Berger, R.; Bennaceur-Griscelli, A.; et al. A unique clonal JAK2 mutation leading to constitutive signalling causes polycythaemia vera. *Nature* **2005**, *434*, 1144–1148. [[CrossRef](#)]
98. de la Chapelle, A.; Sistonen, P.; Lehvaslaiho, H.; Ikkala, E.; Juvonen, E. Familial erythrocytosis genetically linked to erythropoietin receptor gene. *Lancet* **1993**, *341*, 82–84. [[CrossRef](#)]
99. Ang, S.O.; Stockton, D.W.; Hirota, K.; Gordeuk, V.R.; Jelinek, J.; Sergueeva, A.I.; Maxwell, P.H.; Semenza, G.L.; Prchal, J.T. Oxygen sensing and Chuvash polycythemia. *Exp. Hematol.* **2002**, *30*, 43.
100. Ang, S.O.; Chen, H.; Hirota, K.; Gordeuk, V.R.; Jelinek, J.; Guan, Y.; Liu, E.; Sergueeva, A.I.; Miasnikova, G.Y.; Mole, D.; et al. Disruption of oxygen homeostasis underlies congenital Chuvash polycythemia. *Nat. Genet.* **2002**, *32*, 614–621. [[CrossRef](#)]
101. Percy, M.J.; Zhao, Q.; Flores, A.; Harrison, C.; Lappin, T.R.; Maxwell, P.H.; McMullin, M.F.; Lee, F.S. A family with erythrocytosis establishes a role for prolyl hydroxylase domain protein 2 in oxygen homeostasis. *Proc. Natl. Acad. Sci. USA* **2006**, *103*, 654–659. [[CrossRef](#)]
102. Percy, M.J.; Furlow, P.W.; Beer, P.A.; Lappin, T.R.; McMullin, M.F.; Lee, F.S. A novel erythrocytosis-associated PHD2 mutation suggests the location of a HIF binding groove. *Blood* **2007**, *110*, 2193–2196. [[CrossRef](#)]
103. Percy, M.J.; Furlow, P.W.; Lucas, G.S.; Li, X.; Lappin, T.R.; McMullin, M.F.; Lee, F.S. A gain-of-function mutation in the HIF2A gene in familial erythrocytosis. *N. Engl. J. Med.* **2008**, *358*, 162–168. [[CrossRef](#)]
104. Nangaku, M.; Eckardt, K.U. Pathogenesis of renal anemia. *Semin. Nephrol.* **2006**, *26*, 261–268. [[CrossRef](#)]
105. Yamazaki, T.; Mimura, I.; Tanaka, T.; Nangaku, M. Treatment of Diabetic Kidney Disease: Current and Future. *Diabetes Metab. J.* **2021**, *45*, 11–26. [[CrossRef](#)] [[PubMed](#)]
106. Mimura, I.; Tanaka, T.; Nangaku, M. How the Target Hemoglobin of Renal Anemia Should Be. *Nephron* **2015**, *131*, 202–209. [[CrossRef](#)] [[PubMed](#)]
107. Souma, T.; Suzuki, N.; Yamamoto, M. Renal erythropoietin-producing cells in health and disease. *Front. Physiol.* **2015**, *6*, 167. [[CrossRef](#)]
108. Pan, X.; Suzuki, N.; Hirano, I.; Yamazaki, S.; Minegishi, N.; Yamamoto, M. Isolation and characterization of renal erythropoietin-producing cells from genetically produced anemia mice. *PLoS ONE* **2011**, *6*, e25839. [[CrossRef](#)]
109. Obara, N.; Suzuki, N.; Kim, K.; Nagasawa, T.; Imagawa, S.; Yamamoto, M. Repression via the GATA box is essential for tissue-specific erythropoietin gene expression. *Blood* **2008**, *111*, 5223–5232. [[CrossRef](#)] [[PubMed](#)]
110. LeBleu, V.S.; Taduri, G.; O’Connell, J.; Teng, Y.; Cooke, V.G.; Woda, C.; Sugimoto, H.; Kalluri, R. Origin and function of myofibroblasts in kidney fibrosis. *Nat. Med.* **2013**, *19*, 1047–1053. [[CrossRef](#)] [[PubMed](#)]

111. Souma, T.; Nezu, M.; Nakano, D.; Yamazaki, S.; Hirano, I.; Sekine, H.; Dan, T.; Takeda, K.; Fong, G.H.; Nishiyama, A.; et al. Erythropoietin Synthesis in Renal Myofibroblasts Is Restored by Activation of Hypoxia Signaling. *J. Am. Soc. Nephrol.* **2016**, *27*, 428–438. [[CrossRef](#)]
112. Asada, N.; Takase, M.; Nakamura, J.; Oguchi, A.; Asada, M.; Suzuki, N.; Yamamura, K.; Nagoshi, N.; Shibata, S.; Rao, T.N.; et al. Dysfunction of fibroblasts of extrarenal origin underlies renal fibrosis and renal anemia in mice. *J. Clin. Investig.* **2011**, *121*, 3981–3990. [[CrossRef](#)]
113. Souza, E.; Cho, K.H.; Harris, S.T.; Flindt, N.R.; Watt, R.K.; Pai, A.B. Hypoxia-inducible factor prolyl hydroxylase inhibitors: A paradigm shift for treatment of anemia in chronic kidney disease? *Expert Opin. Investig. Drugs* **2020**, *29*, 831–844. [[CrossRef](#)] [[PubMed](#)]
114. Aapro, M.; Gascon, P.; Patel, K.; Rodgers, G.M.; Fung, S.; Arantes, L.H., Jr.; Wish, J. Erythropoiesis-Stimulating Agents in the Management of Anemia in Chronic Kidney Disease or Cancer: A Historical Perspective. *Front. Pharmacol.* **2018**, *9*, 1498. [[CrossRef](#)] [[PubMed](#)]
115. Bazeley, J.; Wish, J.B. The Evolution of Target Hemoglobin Levels in Anemia of Chronic Kidney Disease. *Adv. Chronic Kidney Dis.* **2019**, *26*, 229–236. [[CrossRef](#)] [[PubMed](#)]
116. Bohlius, J.; Bohlke, K.; Castelli, R.; Djulbegovic, B.; Lustberg, M.B.; Martino, M.; Mountzios, G.; Peswani, N.; Porter, L.; Tanaka, T.N.; et al. Management of cancer-associated anemia with erythropoiesis-stimulating agents: ASCO/ASH clinical practice guideline update. *Blood Adv.* **2019**, *3*, 1197–1210. [[CrossRef](#)]
117. KDIGO. KDIGO Clinical Practice Guideline for Anemia in Chronic Kidney Disease. *Kidney Int. Suppl.* **2012**, *2*, 279.
118. Drueke, T.B.; Parfrey, P.S. Summary of the KDIGO guideline on anemia and comment: Reading between the (guide)line(s). *Kidney Int.* **2012**, *82*, 952–960. [[CrossRef](#)]
119. Chen, N.; Hao, C.; Peng, X.; Lin, H.; Yin, A.; Hao, L.; Tao, Y.; Liang, X.; Liu, Z.; Xing, C.; et al. Roxadustat for Anemia in Patients with Kidney Disease Not Receiving Dialysis. *N. Engl. J. Med.* **2019**, *381*, 1001–1010. [[CrossRef](#)]
120. Chen, N.; Hao, C.; Liu, B.C.; Lin, H.; Wang, C.; Xing, C.; Liang, X.; Jiang, G.; Liu, Z.; Li, X.; et al. Roxadustat Treatment for Anemia in Patients Undergoing Long-Term Dialysis. *N. Engl. J. Med.* **2019**, *381*, 1011–1022. [[CrossRef](#)]
121. Peyssonnaud, C.; Nizet, V.; Johnson, R.S. Role of the hypoxia inducible factors HIF in iron metabolism. *Cell Cycle* **2008**, *7*, 28–32. [[CrossRef](#)]
122. Peyssonnaud, C.; Zinkernagel, A.S.; Schuepbach, R.A.; Rankin, E.; Vaulont, S.; Haase, V.H.; Nizet, V.; Johnson, R.S. Regulation of iron homeostasis by the hypoxia-inducible transcription factors (HIFs). *J. Clin. Investig.* **2007**, *117*, 1926–1932. [[CrossRef](#)]
123. Suzuki, N.; Hirano, I.; Pan, X.; Minegishi, N.; Yamamoto, M. Erythropoietin production in neuroepithelial and neural crest cells during primitive erythropoiesis. *Nat. Commun.* **2013**, *4*, 2902. [[CrossRef](#)]
124. Liu, Y.L.; Ang, S.O.; Weigent, D.A.; Prchal, J.T.; Bloomer, J.R. Regulation of ferrochelatase gene expression by hypoxia. *Life Sci.* **2004**, *75*, 2035–2043. [[CrossRef](#)] [[PubMed](#)]
125. Riby, J.E.; Firestone, G.L.; Bjeldanes, L.F. 3,3'-diindolylmethane reduces levels of HIF-1 α and HIF-1 activity in hypoxic cultured human cancer cells. *Biochem. Pharmacol.* **2008**, *75*, 1858–1867. [[CrossRef](#)]
126. McMahon, S.; Grondin, F.; McDonald, P.P.; Richard, D.E.; Dubois, C.M. Hypoxia-enhanced expression of the proprotein convertase furin is mediated by hypoxia-inducible factor-1: Impact on the bioactivation of proproteins. *J. Biol. Chem.* **2005**, *280*, 6561–6569. [[CrossRef](#)]
127. Ma, J.; Evrard, S.; Badiola, I.; Siegfried, G.; Khatib, A.M. Regulation of the proprotein convertases expression and activity during regenerative angiogenesis: Role of hypoxia-inducible factor (HIF). *Eur. J. Cell Biol.* **2017**, *96*, 457–468. [[CrossRef](#)]
128. Shah, Y.M.; Matsubara, T.; Ito, S.; Yim, S.H.; Gonzalez, F.J. Intestinal hypoxia-inducible transcription factors are essential for iron absorption following iron deficiency. *Metab. Cell Metab.* **2009**, *9*, 152–164. [[CrossRef](#)] [[PubMed](#)]
129. Mastrogiannaki, M.; Matak, P.; Keith, B.; Simon, M.C.; Vaulont, S.; Peyssonnaud, C. HIF-2 α , but not HIF-1 α , promotes iron absorption in mice. *J. Clin. Investig.* **2009**, *119*, 1159–1166. [[CrossRef](#)] [[PubMed](#)]
130. Luo, Q.Q.; Qian, Z.M.; Zhou, Y.F.; Zhang, M.W.; Wang, D.; Zhu, L.; Ke, Y. Expression of Iron Regulatory Protein 1 Is Regulated not only by HIF-1 but also pCREB under Hypoxia. *Int. J. Biol. Sci.* **2016**, *12*, 1191–1202. [[CrossRef](#)]
131. Xia, X.; Lemieux, M.E.; Li, W.; Carroll, J.S.; Brown, M.; Liu, X.S.; Kung, A.L. Integrative analysis of HIF binding and transactivation reveals its role in maintaining histone methylation homeostasis. *Proc. Natl. Acad. Sci. USA* **2009**, *106*, 4260–4265. [[CrossRef](#)] [[PubMed](#)]
132. Manalo, D.J.; Rowan, A.; Lavoie, T.; Natarajan, L.; Kelly, B.D.; Ye, S.Q.; Garcia, J.G.; Semenza, G.L. Transcriptional regulation of vascular endothelial cell responses to hypoxia by HIF-1. *Blood* **2005**, *105*, 659–669. [[CrossRef](#)] [[PubMed](#)]
133. Akizawa, T.; Iwasaki, M.; Yamaguchi, Y.; Majikawa, Y.; Reusch, M. Phase 3, Randomized, Double-Blind, Active-Comparator (Darbepoetin Alfa) Study of Oral Roxadustat in CKD Patients with Anemia on Hemodialysis in Japan. *J. Am. Soc. Nephrol.* **2020**, *31*, 1628–1639. [[CrossRef](#)]
134. Akizawa, T.; Nangaku, M.; Yamaguchi, T.; Arai, M.; Koretomo, R.; Matsui, A.; Hirakata, H. A Placebo-Controlled, Randomized Trial of Enarodustat in Patients with Chronic Kidney Disease Followed by Long-Term Trial. *Am. J. Nephrol.* **2019**, *49*, 165–174. [[CrossRef](#)]
135. Akizawa, T.; Nangaku, M.; Yonekawa, T.; Okuda, N.; Kawamatsu, S.; Onoue, T.; Endo, Y.; Hara, K.; Cobitz, A.R. Efficacy and Safety of Daprodustat Compared with Darbepoetin Alfa in Japanese Hemodialysis Patients with Anemia: A Randomized, Double-Blind, Phase 3 Trial. *Clin. J. Am. Soc. Nephrol.* **2020**, *15*, 1155–1165. [[CrossRef](#)]

136. Nangaku, M.; Hamano, T.; Akizawa, T.; Tsubakihara, Y.; Nagai, R.; Okuda, N.; Kurata, K.; Nagakubo, T.; Jones, N.P.; Endo, Y.; et al. Daprostustat Compared with Epoetin Beta Pegol for Anemia in Japanese Patients Not on Dialysis: A 52-Week Randomized Open-Label Phase 3 Trial. *Am. J. Nephrol.* **2021**, 1–10. [\[CrossRef\]](#)
137. Del Vecchio, L.; Locatelli, F. Hypoxia response and acute lung and kidney injury: Possible implications for therapy of COVID-19. *Clin. Kidney J.* **2020**, *13*, 494–499. [\[CrossRef\]](#)
138. Spath, M.R.; Koehler, F.C.; Hoyer-Allo, K.J.R.; Grundmann, F.; Burst, V.; Muller, R.U. Preconditioning strategies to prevent acute kidney injury. *F1000Research* **2020**, *9*. [\[CrossRef\]](#) [\[PubMed\]](#)
139. Nangaku, M. Chronic hypoxia and tubulointerstitial injury: A final common pathway to end-stage renal failure. *J. Am. Soc. Nephrol.* **2006**, *17*, 17–25. [\[CrossRef\]](#)
140. Bullen, A.; Liu, Z.Z.; Hepokoski, M.; Li, Y.; Singh, P. Renal Oxygenation and Hemodynamics in Kidney Injury. *Nephron* **2017**, *137*, 260–263. [\[CrossRef\]](#)
141. Kawakami, T.; Mimura, I.; Shoji, K.; Tanaka, T.; Nangaku, M. Hypoxia and fibrosis in chronic kidney disease: Crossing at pericytes. *Kidney Int. Suppl.* **2014**, *4*, 107–112. [\[CrossRef\]](#) [\[PubMed\]](#)
142. Nangaku, M.; Rosenberger, C.; Heyman, S.N.; Eckardt, K.U. Regulation of hypoxia-inducible factor in kidney disease. *Clin. Exp. Pharmacol. Physiol.* **2013**, *40*, 148–157. [\[CrossRef\]](#) [\[PubMed\]](#)
143. Evans, R.G.; Smith, J.A.; Wright, C.; Gardiner, B.S.; Smith, D.W.; Cochrane, A.D. Urinary oxygen tension: A clinical window on the health of the renal medulla? *Am. J. Physiol. Regul. Integr. Comp. Physiol.* **2014**, *306*, R45–R50. [\[CrossRef\]](#)
144. Lankadeva, Y.R.; Okazaki, N.; Evans, R.G.; Bellomo, R.; May, C.N. Renal Medullary Hypoxia: A New Therapeutic Target for Septic Acute Kidney Injury? *Semin. Nephrol.* **2019**, *39*, 543–553. [\[CrossRef\]](#)
145. Heyman, S.N.; Gorelik, Y.; Zorbavel, D.; Rosenberger, C.; Abassi, Z.; Rosen, S.; Khamaisi, M. Near-drowning: New perspectives for human hypoxic acute kidney injury. *Nephrol. Dial. Transplant.* **2020**, *35*, 206–212. [\[CrossRef\]](#) [\[PubMed\]](#)
146. Mimura, I.; Nangaku, M. The suffocating kidney: Tubulointerstitial hypoxia in end-stage renal disease. *Nat. Rev. Nephrol.* **2010**, *6*, 667–678. [\[CrossRef\]](#)
147. Manotham, K.; Tanaka, T.; Matsumoto, M.; Ohse, T.; Miyata, T.; Inagi, R.; Kurokawa, K.; Fujita, T.; Nangaku, M. Evidence of tubular hypoxia in the early phase in the remnant kidney model. *J. Am. Soc. Nephrol.* **2004**, *15*, 1277–1288. [\[CrossRef\]](#)
148. Nangaku, M.; Eckardt, K.U. Hypoxia and the HIF system in kidney disease. *J. Mol. Med.* **2007**, *85*, 1325–1330. [\[CrossRef\]](#)
149. Nangaku, M. Founding papers of current nephrology: From acute kidney injury to diabetic kidney disease. *Kidney Int.* **2020**, *98*, 6–9. [\[CrossRef\]](#) [\[PubMed\]](#)
150. Honda, T.; Hirakawa, Y.; Nangaku, M. The role of oxidative stress and hypoxia in renal disease. *Kidney Res. Clin. Pract.* **2019**, *38*, 414–426. [\[CrossRef\]](#)
151. Ito, M.; Tanaka, T.; Ishii, T.; Wakashima, T.; Fukui, K.; Nangaku, M. Prolyl hydroxylase inhibition protects the kidneys from ischemia via upregulation of glycogen storage. *Kidney Int.* **2020**, *97*, 687–701. [\[CrossRef\]](#) [\[PubMed\]](#)
152. Kapitsinou, P.P.; Jaffe, J.; Michael, M.; Swan, C.E.; Duffy, K.J.; Erickson-Miller, C.L.; Haase, V.H. Preischemic targeting of HIF prolyl hydroxylation inhibits fibrosis associated with acute kidney injury. *Am. J. Physiol. Ren. Physiol.* **2012**, *302*, F1172–F1179. [\[CrossRef\]](#) [\[PubMed\]](#)
153. Kapitsinou, P.P.; Sano, H.; Michael, M.; Kobayashi, H.; Davidoff, O.; Bian, A.; Yao, B.; Zhang, M.Z.; Harris, R.C.; Duffy, K.J.; et al. Endothelial HIF-2 mediates protection and recovery from ischemic kidney injury. *J. Clin. Investig.* **2014**, *124*, 2396–2409. [\[CrossRef\]](#) [\[PubMed\]](#)
154. Li, S.; Wen, L.; Hu, X.; Wei, Q.; Dong, Z. HIF in Nephrotoxicity during Cisplatin Chemotherapy: Regulation, Function and Therapeutic Potential. *Cancers* **2021**, *13*, 180. [\[CrossRef\]](#)
155. Yang, Y.; Yu, X.; Zhang, Y.; Ding, G.; Zhu, C.; Huang, S.; Jia, Z.; Zhang, A. Hypoxia-inducible factor prolyl hydroxylase inhibitor roxadustat (FG-4592) protects against cisplatin-induced acute kidney injury. *Clin. Sci.* **2018**, *132*, 825–838. [\[CrossRef\]](#) [\[PubMed\]](#)
156. Bernhardt, W.M.; Gottmann, U.; Doyon, F.; Buchholz, B.; Campean, V.; Schodel, J.; Reisenbuechler, A.; Klaus, S.; Arend, M.; Flippin, L.; et al. Donor treatment with a PHD-inhibitor activating HIFs prevents graft injury and prolongs survival in an allogenic kidney transplant model. *Proc. Natl. Acad. Sci. USA* **2009**, *106*, 21276–21281. [\[CrossRef\]](#) [\[PubMed\]](#)
157. Fraisl, P.; Aragonès, J.; Carmeliet, P. Inhibition of oxygen sensors as a therapeutic strategy for ischaemic and inflammatory disease. *Nat. Rev. Drug Discov.* **2009**, *8*, 139–152. [\[CrossRef\]](#)
158. Eltzschig, H.K.; Eckle, T. Ischemia and reperfusion—from mechanism to translation. *Nat. Med.* **2011**, *17*, 1391–1401. [\[CrossRef\]](#)
159. Hyvärinen, J.; Hassinen, I.E.; Sormunen, R.; Maki, J.M.; Kivirikko, K.I.; Koivunen, P.; Myllyharju, J. Hearts of hypoxia-inducible factor prolyl 4-hydroxylase-2 hypomorphic mice show protection against acute ischemia-reperfusion injury. *J. Biol. Chem.* **2010**, *285*, 13646–13657. [\[CrossRef\]](#) [\[PubMed\]](#)
160. Robinson, A.; Keely, S.; Karhausen, J.; Gerich, M.E.; Furuta, G.T.; Colgan, S.P. Mucosal protection by hypoxia-inducible factor prolyl hydroxylase inhibition. *Gastroenterology* **2008**, *134*, 145–155. [\[CrossRef\]](#)
161. Vogler, M.; Zieseniss, A.; Hesse, A.R.; Levent, E.; Tiburcy, M.; Heinze, E.; Burzlafl, N.; Schley, G.; Eckardt, K.U.; Willam, C.; et al. Pre- and post-conditional inhibition of prolyl-4-hydroxylase domain enzymes protects the heart from an ischemic insult. *Pflugers Arch.* **2015**, *467*, 2141–2149. [\[CrossRef\]](#)
162. Philipp, S.; Jurgensen, J.S.; Fielitz, J.; Bernhardt, W.M.; Weidemann, A.; Schiche, A.; Pilz, B.; Dietz, R.; Regitz-Zagrosek, V.; Eckardt, K.U.; et al. Stabilization of hypoxia inducible factor rather than modulation of collagen metabolism improves cardiac function after acute myocardial infarction in rats. *Eur. J. Heart Fail.* **2006**, *8*, 347–354. [\[CrossRef\]](#)

163. Ong, S.G.; Lee, W.H.; Theodorou, L.; Kodo, K.; Lim, S.Y.; Shukla, D.H.; Briston, T.; Kiriakidis, S.; Ashcroft, M.; Davidson, S.M.; et al. HIF-1 reduces ischaemia-reperfusion injury in the heart by targeting the mitochondrial permeability transition pore. *Cardiovasc. Res.* **2014**, *104*, 24–36. [[CrossRef](#)]
164. Dang, E.V.; Barbi, J.; Yang, H.Y.; Jinasena, D.; Yu, H.; Zheng, Y.; Bordman, Z.; Fu, J.; Kim, Y.; Yen, H.R.; et al. Control of T(H)17/T(reg) balance by hypoxia-inducible factor 1. *Cell* **2011**, *146*, 772–784. [[CrossRef](#)]
165. Furuta, G.T.; Turner, J.R.; Taylor, C.T.; Hershberg, R.M.; Comerford, K.; Narravula, S.; Podolsky, D.K.; Colgan, S.P. Hypoxia-inducible factor 1-dependent induction of intestinal trefoil factor protects barrier function during hypoxia. *J. Exp. Med.* **2001**, *193*, 1027–1034. [[CrossRef](#)]
166. Higgins, D.F.; Kimura, K.; Bernhardt, W.M.; Shrimanker, N.; Akai, Y.; Hohenstein, B.; Saito, Y.; Johnson, R.S.; Kretzler, M.; Cohen, C.D.; et al. Hypoxia promotes fibrogenesis in vivo via HIF-1 stimulation of epithelial-to-mesenchymal transition. *J. Clin. Investig.* **2007**, *117*, 3810–3820. [[CrossRef](#)]
167. Keely, S.; Campbell, E.L.; Baird, A.W.; Hansbro, P.M.; Shalwitz, R.A.; Kotsakis, A.; McNamee, E.N.; Eltzschig, H.K.; Kominsky, D.J.; Colgan, S.P. Contribution of epithelial innate immunity to systemic protection afforded by prolyl hydroxylase inhibition in murine colitis. *Mucosal Immunol.* **2014**, *7*, 114–123. [[CrossRef](#)] [[PubMed](#)]
168. Marks, E.; Goggins, B.J.; Cardona, J.; Cole, S.; Minahan, K.; Mateer, S.; Walker, M.M.; Shalwitz, R.; Keely, S. Oral delivery of prolyl hydroxylase inhibitor: AKB-4924 promotes localized mucosal healing in a mouse model of colitis. *Inflamm. Bowel Dis.* **2015**, *21*, 267–275. [[CrossRef](#)]
169. Gong, H.; Rehman, J.; Tang, H.; Wary, K.; Mittal, M.; Chaturvedi, P.; Zhao, Y.Y.; Komarova, Y.A.; Vogel, S.M.; Malik, A.B. HIF2alpha signaling inhibits adherens junctional disruption in acute lung injury. *J. Clin. Investig.* **2015**, *125*, 652–664. [[CrossRef](#)] [[PubMed](#)]
170. Suhara, T.; Hishiki, T.; Kasahara, M.; Hayakawa, N.; Oyaizu, T.; Nakanishi, T.; Kubo, A.; Morisaki, H.; Kaelin, W.G., Jr.; Suematsu, M.; et al. Inhibition of the oxygen sensor PHD2 in the liver improves survival in lactic acidosis by activating the Cori cycle. *Proc. Natl. Acad. Sci. USA* **2015**, *112*, 11642–11647. [[CrossRef](#)] [[PubMed](#)]
171. Pezzuto, A.; Carico, E. Role of HIF-1 in Cancer Progression: Novel Insights. A Review. *Curr. Mol. Med.* **2018**, *18*, 343–351. [[CrossRef](#)] [[PubMed](#)]
172. Fluegen, G.; Avivar-Valderas, A.; Wang, Y.; Padgen, M.R.; Williams, J.K.; Nobre, A.R.; Calvo, V.; Cheung, J.F.; Bravo-Cordero, J.J.; Entenberg, D.; et al. Phenotypic heterogeneity of disseminated tumour cells is preset by primary tumour hypoxic microenvironments. *Nat. Cell Biol.* **2017**, *19*, 120–132. [[CrossRef](#)] [[PubMed](#)]
173. Seeley, T.W.; Sternlicht, M.D.; Klaus, S.J.; Neff, T.B.; Liu, D.Y. Induction of erythropoiesis by hypoxia-inducible factor prolyl hydroxylase inhibitors without promotion of tumor initiation, progression, or metastasis in a VEGF-sensitive model of spontaneous breast cancer. *Hypoxia* **2017**, *5*, 1–9. [[CrossRef](#)]
174. Nishide, S.; Uchida, J.; Matsunaga, S.; Tokudome, K.; Yamaguchi, T.; Kabei, K.; Moriya, T.; Miura, K.; Nakatani, T.; Tomita, S. Prolyl-hydroxylase inhibitors reconstitute tumor blood vessels in mice. *J. Pharmacol. Sci.* **2020**, *143*, 122–126. [[CrossRef](#)]
175. Nishide, S.; Matsunaga, S.; Shiota, M.; Yamaguchi, T.; Kitajima, S.; Maekawa, Y.; Takeda, N.; Tomura, M.; Uchida, J.; Miura, K.; et al. Controlling the Phenotype of Tumor-Infiltrating Macrophages via the PHD-HIF Axis Inhibits Tumor Growth in a Mouse Model. *iScience* **2019**, *19*, 940–954. [[CrossRef](#)]
176. Yamamoto, H.; Taguchi, M.; Matsuda, Y.; Iekushi, K.; Yamada, T.; Akizawa, T. Molidustat for the treatment of renal anaemia in patients with non-dialysis-dependent chronic kidney disease: Design and rationale of two phase III studies. *BMJ Open* **2019**, *9*, e026704. [[CrossRef](#)]
177. Biguzzi, E.; Siboni, S.M.; Peyvandi, F. How I treat gastrointestinal bleeding in congenital and acquired von Willebrand disease. *Blood* **2020**, *136*, 1125–1133. [[CrossRef](#)] [[PubMed](#)]
178. Reveiz, L.; Gyte, G.M.; Cuervo, L.G.; Casasbuenas, A. Treatments for iron-deficiency anaemia in pregnancy. *Cochrane Database Syst. Rev.* **2011**, CD003094. [[CrossRef](#)]
179. Mokas, S.; Lariviere, R.; Lamalice, L.; Gobeil, S.; Cornfield, D.N.; Agharazii, M.; Richard, D.E. Hypoxia-inducible factor-1 plays a role in phosphate-induced vascular smooth muscle cell calcification. *Kidney Int.* **2016**, *90*, 598–609. [[CrossRef](#)]
180. Cowburn, A.S.; Crosby, A.; Macias, D.; Branco, C.; Colaco, R.D.; Southwood, M.; Toshner, M.; Crotty Alexander, L.E.; Morrell, N.W.; Chilvers, E.R.; et al. HIF2alpha-arginase axis is essential for the development of pulmonary hypertension. *Proc. Natl. Acad. Sci. USA* **2016**, *113*, 8801–8806. [[CrossRef](#)]
181. Gale, D.P.; Harten, S.K.; Reid, C.D.; Tuddenham, E.G.; Maxwell, P.H. Autosomal dominant erythrocytosis and pulmonary arterial hypertension associated with an activating HIF2 alpha mutation. *Blood* **2008**, *112*, 919–921. [[CrossRef](#)] [[PubMed](#)]
182. Hu, C.J.; Poth, J.M.; Zhang, H.; Flockton, A.; Laux, A.; Kumar, S.; McKeon, B.; Mouradian, G.; Li, M.; Riddle, S.; et al. Suppression of HIF2 signalling attenuates the initiation of hypoxia-induced pulmonary hypertension. *Eur. Respir. J.* **2019**, *54*. [[CrossRef](#)]
183. Smith, K.A.; Waypa, G.B.; Dudley, V.J.; Budinger, G.R.S.; Abdala-Valencia, H.; Bartom, E.; Schumacker, P.T. Role of Hypoxia-Inducible Factors in Regulating Right Ventricular Function and Remodeling during Chronic Hypoxia-induced Pulmonary Hypertension. *Am. J. Respir. Cell Mol. Biol.* **2020**, *63*, 652–664. [[CrossRef](#)] [[PubMed](#)]
184. Macias, D.; Moore, S.; Crosby, A.; Southwood, M.; Du, X.; Tan, H.; Xie, S.; Vassallo, A.; Wood, A.J.T.; Wallace, E.M.; et al. Targeting HIF2alpha-ARNT hetero-dimerisation as a novel therapeutic strategy for pulmonary arterial hypertension. *Eur. Respir. J.* **2021**, *57*. [[CrossRef](#)] [[PubMed](#)]

185. Pullamsetti, S.S.; Mamazhakypov, A.; Weissmann, N.; Seeger, W.; Savai, R. Hypoxia-inducible factor signaling in pulmonary hypertension. *J. Clin. Investig.* **2020**, *130*, 5638–5651. [[CrossRef](#)]
186. Siques, P.; Brito, J.; Pena, E. Reactive Oxygen Species and Pulmonary Vasculature During Hypobaric Hypoxia. *Front. Physiol.* **2018**, *9*, 865. [[CrossRef](#)] [[PubMed](#)]
187. Urrutia, A.A.; Aragonés, J. HIF Oxygen Sensing Pathways in Lung Biology. *Biomedicines* **2018**, *6*, 68. [[CrossRef](#)]
188. Archer, S.L.; Gomberg-Maitland, M.; Maitland, M.L.; Rich, S.; Garcia, J.G.; Weir, E.K. Mitochondrial metabolism, redox signaling, and fusion: A mitochondria-ROS-HIF-1 α -Kv1.5 O₂-sensing pathway at the intersection of pulmonary hypertension and cancer. *Am. J. Physiol. Heart Circ. Physiol.* **2008**, *294*, H570–H578. [[CrossRef](#)]
189. Weidemann, A.; Klanke, B.; Wagner, M.; Volk, T.; Willam, C.; Wiesener, M.S.; Eckardt, K.U.; Warnecke, C. Hypoxia, via stabilization of the hypoxia-inducible factor HIF-1 α , is a direct and sufficient stimulus for brain-type natriuretic peptide induction. *Biochem. J.* **2008**, *409*, 233–242. [[CrossRef](#)]
190. Buchholz, B.; Schley, G.; Faria, D.; Kroening, S.; Willam, C.; Schreiber, R.; Klanke, B.; Burzlaff, N.; Jantsch, J.; Kunzelmann, K.; et al. Hypoxia-inducible factor-1 α causes renal cyst expansion through calcium-activated chloride secretion. *J. Am. Soc. Nephrol.* **2014**, *25*, 465–474. [[CrossRef](#)]
191. Raptis, V.; Bakogiannis, C.; Loutradis, C.; Boutou, A.K.; Lampropoulou, I.; Intzevidou, E.; Sioulis, A.; Balaskas, E.; Sarafidis, P.A. Levels of Endocan, Angiopoietin-2, and Hypoxia-Inducible Factor-1 α in Patients with Autosomal Dominant Polycystic Kidney Disease and Different Levels of Renal Function. *Am. J. Nephrol.* **2018**, *47*, 231–238. [[CrossRef](#)] [[PubMed](#)]
192. Chen, J.; Chen, J.; Fu, H.; Li, Y.; Wang, L.; Luo, S.; Lu, H. Hypoxia exacerbates nonalcoholic fatty liver disease via the HIF-2 α /PPAR α pathway. *Am. J. Physiol. Endocrinol. Metab.* **2019**, *317*, E710–E722. [[CrossRef](#)]
193. He, Y.; Yang, W.; Gan, L.; Liu, S.; Ni, Q.; Bi, Y.; Han, T.; Liu, Q.; Chen, H.; Hu, Y.; et al. Silencing HIF-1 α aggravates non-alcoholic fatty liver disease in vitro through inhibiting PPAR- α /ANGPTL4 signaling pathway. *Gastroenterol. Hepatol.* **2020**. [[CrossRef](#)] [[PubMed](#)]
194. Han, J.; He, Y.; Zhao, H.; Xu, X. Hypoxia inducible factor-1 promotes liver fibrosis in nonalcoholic fatty liver disease by activating PTEN/p65 signaling pathway. *J. Cell. Biochem.* **2019**, *120*, 14735–14744. [[CrossRef](#)]
195. Meadowcroft, A.M.; Cizman, B.; Holdstock, L.; Biswas, N.; Johnson, B.M.; Jones, D.; Nossuli, A.K.; Lepore, J.J.; Aarup, M.; Cobitz, A.R. Daprodustat for anemia: A 24-week, open-label, randomized controlled trial in participants on hemodialysis. *Clin. Kidney J.* **2019**, *12*, 139–148. [[CrossRef](#)] [[PubMed](#)]
196. Kobayashi, Y.; Oguro, A.; Imaoka, S. Feedback of hypoxia-inducible factor-1 α (HIF-1 α) transcriptional activity via redox factor-1 (Ref-1) induction by reactive oxygen species (ROS). *Free Radic. Res.* **2021**, 1–11. [[CrossRef](#)] [[PubMed](#)]
197. Aprelikova, O.; Chandramouli, G.V.; Wood, M.; Vasselli, J.R.; Riss, J.; Maranchie, J.K.; Linehan, W.M.; Barrett, J.C. Regulation of HIF prolyl hydroxylases by hypoxia-inducible factors. *J. Cell. Biochem.* **2004**, *92*, 491–501. [[CrossRef](#)] [[PubMed](#)]
198. Fujita, N.; Markova, D.; Anderson, D.G.; Chiba, K.; Toyama, Y.; Shapiro, I.M.; Risbud, M.V. Expression of prolyl hydroxylases (PHDs) is selectively controlled by HIF-1 and HIF-2 proteins in nucleus pulposus cells of the intervertebral disc: Distinct roles of PHD2 and PHD3 proteins in controlling HIF-1 α activity in hypoxia. *J. Biol. Chem.* **2012**, *287*, 16975–16986. [[CrossRef](#)]
199. Henze, A.T.; Riedel, J.; Diem, T.; Wenner, J.; Flamme, I.; Pouyseggur, J.; Plate, K.H.; Acker, T. Prolyl hydroxylases 2 and 3 act in gliomas as protective negative feedback regulators of hypoxia-inducible factors. *Cancer Res.* **2010**, *70*, 357–366. [[CrossRef](#)]



Article

Multi-Omic Meta-Analysis of Transcriptomes and the Bibliome Uncovers Novel Hypoxia-Inducible Genes

Yoko Ono and Hidemasa Bono *

Program of Biomedical Science, Graduate School of Integrated Sciences for Life, Hiroshima University, 3-10-23 Kagamiyama, Higashi-Hiroshima, Hiroshima 739-0046, Japan; d205302@hiroshima-u.ac.jp

* Correspondence: bonohu@hiroshima-u.ac.jp; Tel.: +81-82-424-4013

Abstract: Hypoxia is a condition in which cells, tissues, or organisms are deprived of sufficient oxygen supply. Aerobic organisms have a hypoxic response system, represented by hypoxia-inducible factor 1- α (HIF1A), to adapt to this condition. Due to publication bias, there has been little focus on genes other than well-known signature hypoxia-inducible genes. Therefore, in this study, we performed a meta-analysis to identify novel hypoxia-inducible genes. We searched publicly available transcriptome databases to obtain hypoxia-related experimental data, retrieved the metadata, and manually curated it. We selected the genes that are differentially expressed by hypoxic stimulation, and evaluated their relevance in hypoxia by performing enrichment analyses. Next, we performed a bibliometric analysis using gene2pubmed data to examine genes that have not been well studied in relation to hypoxia. Gene2pubmed data provides information about the relationship between genes and publications. We calculated and evaluated the number of reports and similarity coefficients of each gene to HIF1A, which is a representative gene in hypoxia studies. In this data-driven study, we report that several genes that were not known to be associated with hypoxia, including the G protein-coupled receptor 146 gene, are upregulated by hypoxic stimulation.

Keywords: hypoxia; RNA-seq; ChIP-seq; gene2pubmed; bibliome; meta-analysis; signature genes; *GPR146*; enrichment analysis

Citation: Ono, Y.; Bono, H. Multi-Omic Meta-Analysis of Transcriptomes and the Bibliome Uncovers Novel Hypoxia-Inducible Genes. *Biomedicines* **2021**, *9*, 582. <https://doi.org/10.3390/biomedicines9050582>

Academic Editor: Sonia Rocha

Received: 30 March 2021

Accepted: 19 May 2021

Published: 20 May 2021

Publisher's Note: MDPI stays neutral with regard to jurisdictional claims in published maps and institutional affiliations.



Copyright: © 2021 by the authors. Licensee MDPI, Basel, Switzerland. This article is an open access article distributed under the terms and conditions of the Creative Commons Attribution (CC BY) license (<https://creativecommons.org/licenses/by/4.0/>).

1. Introduction

The development of genetic engineering techniques such as genome editing have made it possible to test hypotheses that are constructed on the basis of the knowledge of each researcher, including information in the literature, by performing biological experiments. Hypothesis construction is triggered by literature surveys and the collective knowledge of researchers, and is also influenced by publication bias. For example, when the frequency with which approximately 600,000 publications annotated around 20,000 human coding genes was calculated, more than 9000 publications reported the p53 gene whereas over 600 genes were not mentioned at all [1]. In contrast, the development of microarray and high-throughput sequencing technologies has enabled the comprehensive acquisition of thousands of gene expression profiles at a time. Published transcriptome data are archived in public databases such as the Gene Expression Omnibus (GEO) of the U.S. National Center for Biotechnology Information (NCBI, Bethesda, MD, USA) [2], ArrayExpress (AE) of the European Bioinformatics Institute [3], and the Genomic Expression Archive (GEA) of the DNA Data Bank of Japan [4]. At present, although approximately 60,000 expression data series of human genes have been registered, we estimate that they are rarely used in studies. We believe that meta-analysis of these transcriptome data may provide additional insights into biology.

Among the various fields of biological research, the more well-studied the field, the greater the impact of publication bias. We considered areas where meta-analysis based on gene expression data can uncover new findings buried by publication bias. The analyses were performed by considering the following conditions: (1) hypoxia-inducible factor 1- α

(HIF1A) is a representative transcription factor involved in hypoxic stimulus-response, and (2) categorization in Gene Ontology, a database where gene expression data can easily be obtained. In our previous study, we studied hypoxic stimulus-responses using public databases [5]. Here, we performed a meta-analysis of gene expression data following the previous method. The present study is a continuation of our previous study to further build our knowledge of the hypoxic stimulus-response. In a previous report, we integrated meta-analyzed hypoxic transcriptome data with public ChIP-seq data of known human HIFs, HIF-1 and HIF-2, to gain insight into hypoxic response pathways involving direct binding of transcription factors. Due to publication bias, there has been little focus on genes other than the well-known, signature hypoxia-inducible genes. Therefore, in this study, we conducted an omic-scale analysis of bibliological data in PubMed. Bibliometric analysis is a method of analyzing biological publications and it is used in biomedical research [6]. This new type of analysis is called “bibliome, and it involves using NCBI’s gene2pubmed data, which provides information about the relationship between genes and publications, to discover novel hypoxia-inducible genes.

Oxygen is essential for respiration in aerobic organisms. Hypoxia occurs in a variety of neurological conditions such as traumatic brain injury, Alzheimer’s disease, and stroke, and is known to be responsible for some of their symptoms. In hyperbaric oxygen therapy, subjects are placed in a chamber filled with 100% oxygen gas at a pressure of 1 atm or higher, and it is mainly used to treat hypoxia-related symptoms [7]. Oxygen is used to produce ATP by oxidative phosphorylation and electron transfer systems. Hypoxia is a condition in which cells, tissues, or organisms are deprived of sufficient oxygen supply as the amount of oxygen in the blood decreases. The tissues and cells of higher organisms, including humans, have a hypoxic response system that is regulated by HIFs to adapt to the oxygen-deprived conditions caused by hypoxic stimuli.

Under normoxic conditions, HIFs are hydroxylated by the α -ketoglutarate-dependent dioxygenase factor inhibiting HIF-1 (FIH-1) and prolyl hydroxylases (PHDs), resulting in degradation by the ubiquitin–proteasome system and suppression of transcriptional activation [8,9]. However, under hypoxic conditions, the activity of PHDs and FIH-1 is reduced, and HIFs escape hydroxylation and form a complex with aryl hydrocarbon receptor nuclear translocator (ARNT) and the transcriptional co-factor CREB-binding protein to induce expression of downstream genes [10].

In this study, we focused on hypoxic stimulus-response and aimed to identify novel genes by performing meta-analysis using public databases. We selected hypoxia-inducible genes based on the gene expression ratio of approximately 500 pairs of hypoxia-stimulated samples and evaluated the similarity coefficient of each gene for HIF1A, a representative factor in hypoxia research, using gene2pubmed, which shows the relationship between genes and publications.

2. Materials and Methods

2.1. Curation of Public Gene Expression Data

To obtain the accession of hypoxia-related gene expression data from public databases, we used a graphical web tool called All of Gene Expression (AOE) [11,12]. AOE integrates metadata from not only GEO, AE, and GEA, but also RNA sequencing (RNA-seq) data that are exclusively archived in the Sequence Read Archive (SRA) [13]. We searched for a list of experimental data series related to hypoxia from GEO using the following search formulas: “hypoxia” [MeSH Terms] OR “hypoxia” [All Fields] AND “Homo sapiens” [porgn] AND “gse” [Filter]. We downloaded this list on 17 August 2020. We obtained the metadata from the Series Matrix files in GEO, from articles, or downloaded the metadata from SRA using the Python package pysradb (v 0.11.1). We then curated only the RNA-seq data into comparable sample pairs of hypoxia and normoxia (HN-pairs) [14]. The criteria for curation were that the specimens with the experimental conditions of hypoxia and normoxia should be in the same data series so as to set the HN-pair and to derive RNA-seq reads from human cell lines or tissue specimens. All relevant data were adopted if the

metadata content was certain. We collected the SRA format data from the NCBI using prefetch (version 2.9.6).

2.2. Gene Expression Quantification

Since the downloaded data were in the SRA format, we used the fasterq-dump program in SRA Toolkit [15] to convert the data into FASTQ formatted files for expression quantification. We then quantified single-end and paired-end RNA-seq reads using ikra (version 1.2.3) [16], an RNA-seq pipeline with default parameters. Ikra automates the RNA-seq data analysis process, which includes the quality control of reads (Trim Galore version 0.6.3) and transcript quantification (Salmon version 0.14.0 [17] with reference transcript sets in GENCODE release 30). We chose this workflow because it is suitable for quantifying gene expression from heterogeneous RNA-seq data obtained from various instruments and laboratories. In this study, the data acquisition and quality control processes required approximately 1 month to obtain the current dataset. Quantitative RNA-seq data are accessible at figshare [18].

2.3. Calculation of HN-Ratio and HN-Score

Based on the transcriptome data paired with hypoxia and normoxia, we calculated the ratio of expression value for each gene (termed the HN-ratio) [19]. The HN-ratio R is calculated using the following equation:

$$R = \frac{T_{hypoxia} + 1}{T_{normoxia} + 1} \quad (1)$$

where $T_{hypoxia}$ is the gene expression value described as scaled transcripts per million (scaledTPM) [20] under hypoxic conditions and $T_{normoxia}$ is scaledTPM under normoxic conditions, paired with hypoxic conditions. To reduce the effect of small variations in extremely low gene expression values, we calculated the HN-ratio by adding 1 to the denominator and numerator.

We then classified each gene into three groups based on its HN-ratio. When the HN-ratio was greater than the threshold, the gene was considered upregulated, and when the ratio was less than the inverse of the threshold, the gene was considered downregulated. If a gene was neither up- nor downregulated, it was classified as unchanged. For the classification of up- and downregulated genes, we tested 1.5- and 2-fold thresholds, and then selected the 1.5-fold threshold to classify upregulated and downregulated genes. For evaluating hypoxia-inducible genes, we calculated the HN-score for each coding gene in humans. The HN-score was calculated by subtracting the number of samples with downregulated genes from the number of samples with upregulated genes.

2.4. Enrichment Analysis

We used Metascape [21,22] and ChIP-Atlas [23,24] for Gene Set Enrichment Analysis. ChIP-Atlas is a comprehensive and integrated database for visualization and utilization of publicly available chromatin immunoprecipitation sequencing (ChIP-seq) data. In this study, we performed conventional “express analysis” using Metascape. In the ChIP-Atlas settings, we set the “Select dataset to be compared” item to “Refseq coding genes (excluding user data)” and set the other items to default.

2.5. Meta-Analysis of ChIP-Seq Data

Public ChIP-seq data were collected, curated, and pre-calculated for reuse in the ChIP-Atlas database [23,24]. In ChIP-Atlas, the category of proteins that bind to DNA is referred to as “antigens”. We used the “Target Genes” function of ChIP-Atlas to obtain average model-based analysis of ChIP-seq (MACS2) scores for three antigens at a distance of $\pm 5k$ from the transcription start site. These antigens were selected from the following genes that were shown to be related to the UP 100 genes by the ChIP-Atlas enrichment analysis: HIF1A, endothelial PAS domain-containing protein 1 (EPAS1, also known as hypoxia-

inducible factor-2 α), and ARNT. We combined the ChIP-seq data with the HN-score data described above, using the gene name to combine the two datasets.

2.6. Calculation of the Number of Publications for Each Gene and Similarity Coefficient for HIF1A

We calculated the number of publications and Simpson similarity coefficient per human gene using Python (version 3.8.6) [25]. The Simpson similarity coefficient S was calculated using the following equation:

$$S(X, Y) = \frac{|X \cap Y|}{\min(|X|, |Y|)} \quad (2)$$

where $|X \cap Y|$ is the number of PubMed IDs that overlaps between HIF1A and a gene in gene2pubmed, whereas $\min(|X|, |Y|)$ is the number of PubMed IDs of HIF1A or the gene in gene2pubmed, whichever value is less. Gene2pubmed [26] and Gene Info [26], which were required for the above calculations, were downloaded on 4 January 2021. In order to select a gene to determine whether or not hypoxia-related studies have been reported, we calculated the similarity coefficients of each gene for EPAS1 and ARNT as well as HIF1A. After reviewing the results, we determined that HIF1A was suitable.

2.7. Visualization and Integrated Functional Analysis of Genes

To generate scatter and box plots, we used TIBCO Spotfire Desktop version 11.0.0 (TIBCO Spotfire, Inc., Palo Alto, CA, USA).

3. Results

3.1. Overview

This study was performed in three main steps (Figure 1). In Step 1, we obtained the RNA-seq data related to hypoxic stimulation from public gene expression databases. After the manual curation of metadata, UP 100 and DOWN 100 gene lists related to hypoxia stimulation were obtained through the quantification of gene expression in the corresponding datasets. The UP 100 and DOWN 100 gene lists included the top 100 and bottom 100 genes according to HN-score. In Step 2, we verified hypoxia-related genes in the UP 100 and DOWN 100 gene lists, not only by enrichment analyses, but also by visualizing the HIF-related ChIP-seq peak of each gene using HN-scores. Finally, in Step 3, we investigated novel hypoxia-inducible genes using bibliometric analysis of gene2pubmed.

3.2. Curation of Hypoxic Transcriptome Data in Public Databases

Initially, we used AOE to check whether a large number of hypoxia-related data were registered. We then curated the metadata provided by the NCBI for further analysis. Next, we obtained the SRA IDs for 69 data series and 495 HN-pairs of GEO-drawn samples after integration with hypoxia-related data lists provided in previous reports and elimination of duplicates [14]. This resulted in a four-fold increase in HN-pairs compared to previous reports. In 495 HN-pair data, the hypoxic conditions ranged between 0.1% and 5% O₂ concentration, including some chemical hypoxic conditions where CoCl₂ was used to induce a hypoxia-related state under normoxic conditions. The treatment time ranged from 1 hour to a maximum of 3 months. The most common hypoxic condition among the data was 1% O₂ (266 HN-pairs, 53.7%) and 24 h of treatment (234 HN-pairs, 47.3%). The most common cell type was cancer (324 HN-pairs, 65.5%), and the most common tissue was breast cancer (112 HN-pairs, 22.6%).

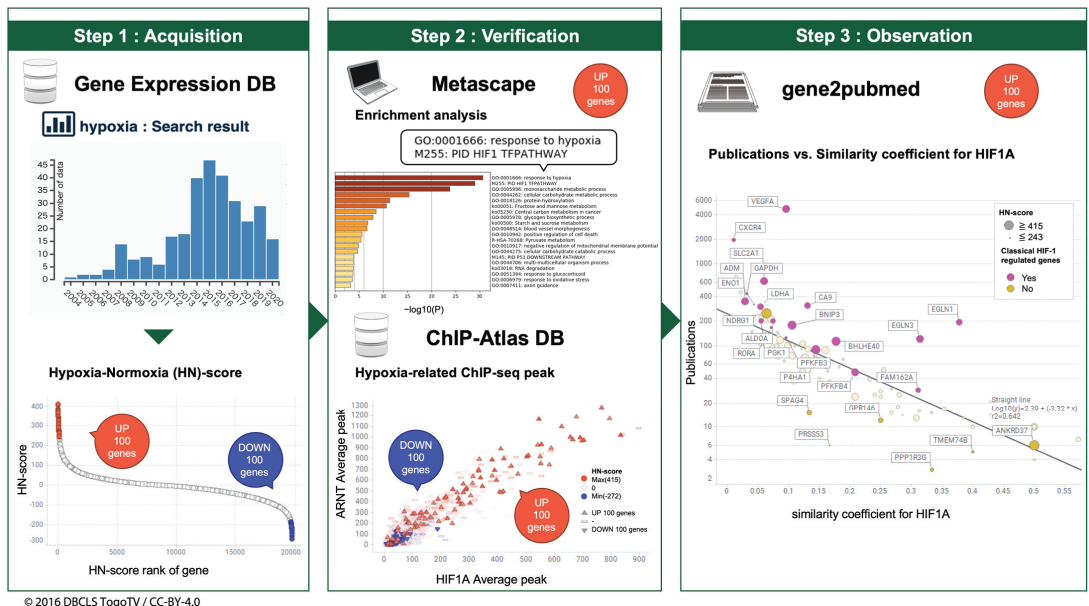


Figure 1. Schematic view of hypoxic transcriptome meta-analysis. Step 1. Evaluation and listing of upregulation and downregulation of hypoxia-inducible genes. Step 2. Confirmation of known hypoxic stimulation-related genes. Step 3. Discovery of novel genes related to hypoxic stimulus-response.

3.3. Meta-Analysis of Hypoxia-Inducible Genes

After the quantification of gene expression data obtained from RNA-seq, the number of conditions under which each gene was upregulated, downregulated, and remained unchanged was estimated on the basis of the HN-ratio. The complete lists of meta-analyzed results are accessible from figshare [27]. We calculated the HN-score of each gene to evaluate the responsiveness of each gene toward hypoxia. For example, in the case of vascular endothelial growth factor A (VEGFA), the counts showed 406 UP, 25 DOWN, and 64 unchanged, and therefore, its HN-score was 381. Full lists of counts (upregulated/downregulated/unchanged) with HN-scores for all genes are accessible from figshare [27]. We selected the top 100 [28] and bottom 100 [29] HN-scored genes and used these genes as the UP 100 and DOWN 100 gene lists, respectively, for further analysis.

3.4. Evaluation of Hypoxia-Inducible Genes

To confirm whether the UP 100 and DOWN 100 gene lists were affected by hypoxia-related regulators such as HIF1A, we performed enrichment analysis using ChIP-Atlas [23,24]. Enrichment analysis in ChIP-Atlas showed that a set of genes in the UP 100 gene list was related to hypoxia-related antigens such as HIF1A, ARNT, and EPAS1, whereas a set in the DOWN 100 gene list was related to epigenetic regulators such as Sin3A associated protein 30 (SAP30), histone deacetylase 1 (HDAC1), and MYC proto-oncogene, bHLH transcription factor (MYC), an oncogene involved in cell cycle progression (Table 1). Similarly, enrichment analysis by Metascape showed that hypoxia-related gene sets and genes related to the metabolic processes of non-coding RNAs (ncRNAs) were listed in the UP 100 and DOWN 100 gene lists, respectively (Figure 2a,b). Since it was important that the hypoxia-inducible genes were correctly evaluated by HN-score as intended in this analysis, we confirmed this not only by ChIP-Atlas enrichment analysis, but also by visualizing the high HIF-related MACS2 score of each gene with a high HN-score. The scatter plots of the mean MACS2 peaks of HIF1A, EPAS1, and ARNT, which were the top-ranked genes in the enrichment

analysis of the UP 100 gene list, were plotted. The genes with higher MACS2 peaks also had higher HN-scores (Figure 2c,d). These results indicate that the genes regulated by hypoxia-related factors are listed in the UP 100 gene list, and genes regulated by SAP30, MYC, and HDAC1 are listed in the DOWN 100 gene list.

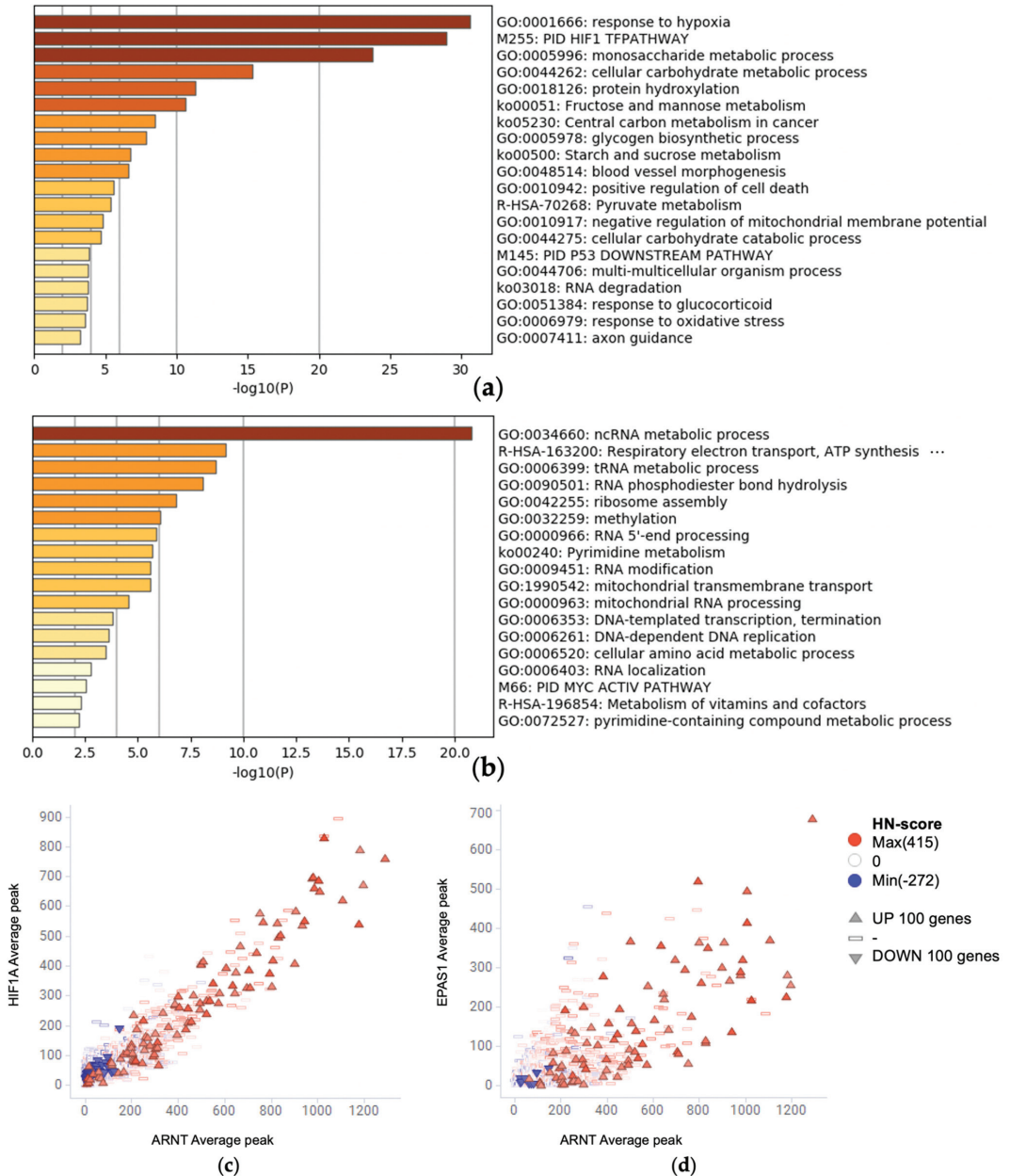


Figure 2. (a,b) Confirmation of known hypoxic stimulation-related genes. Enrichment analysis for (a) the UP 100 gene list and (b) the DOWN 100 gene list. (c,d) Scatter plot of ChIP-seq average peaks of hypoxic-related antigens, (c) HIF1A vs. ARNT and (d) EPAS1 vs. ARNT colored by HN-score.

Table 1. The result of enrichment analysis in ChIP-Atlas. Enrichment analysis in ChIP-Atlas is a search tool for target genes and colocalizing factors of a given transcription regulator.

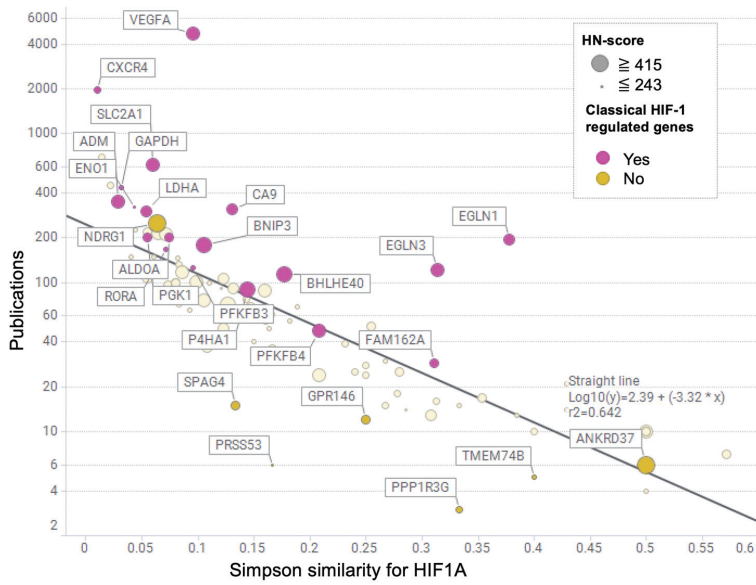
Input List	Antigen	ID	Log P-val	Log Q-val	Fold Enrichment
UP 100 gene list	HIF1A	SRX4802348	−88.8246	−84.064	35.6249
	ARNT	SRX4802353	−76.4303	−72.3686	83.3136
	EPAS1	SRX3051209	−73.1987	−69.2831	34.9928
DOWN 100 gene list	SAP30	SRX116447	−34.1844	−30.0149	4.96916
	MYC	SRX1497384	−31.4158	−27.5474	2.97453
	HDAC1	SRX186644	−27.4205	−24.1541	3.3231

3.5. Evaluation of Simpson Similarity between HIF1A and Genes

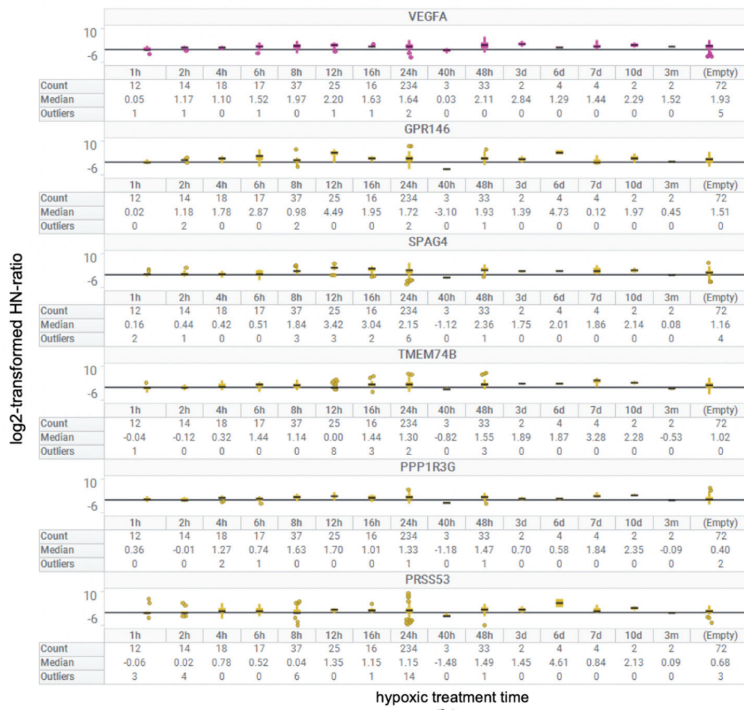
We performed bibliometric analysis, a method of analysis using biological publication information, to determine whether the genes of the UP 100 gene list had been previously studied in relation to hypoxia. We calculated the number of publications for each gene in the UP 100 gene list [30]. We also calculated the Simpson similarity coefficient between these genes and HIF1A [31]. The number of publications and Simpson similarity coefficients were visualized using a scatter plot (Figure 3a). In addition, we defined genes that were reported to be involved with HIF-1 15 years ago [32] as “Classical HIF-1 regulated genes”, and these were marked on the scatter plot. Interestingly, those classical hypoxia-inducible genes were plotted on the upper side of the regression line.

3.6. Box Plot of HN-Ratio by Treatment Time

To check the individual HN-ratio of genes with high HN-scores based on the treatment time, we visualized base-2 logarithm (log₂) transformed HN-ratios using the box plot (Figure 3b). Genes in the box plot were selected from the HIF-1-regulated gene *VEGFA*, and some genes were plotted below the regression line, such as sperm-associated antigen 4 (*SPAG4*), G protein-coupled receptor 146 (*GPR146*), protein phosphatase 1 regulatory subunit 3G (*PPP1R3G*), transmembrane protein 74B (*TMEM74B*), and serine protease 53 (*PRSS53*). The six genes visualized in the box plot showed positive HN-ratio values for the majority of the treatment time.



(a)



(b)

Figure 3. Discovery of novel genes associated with hypoxic stimulus-response. (a) Scatter plot of the number of publications vs. Simpson similarity coefficients for HIF1A in the UP 100 gene list. In this scatter plot, genes that were reported to be associated with HIF-1 15 years ago were marked as “known genes regulated by HIF-1”. (b) Box plot of log₂-transformed HN-ratio per hypoxic treatment time for some of the UP 100 genes.

4. Discussion

In this study, we identified hypoxia-inducible genes by performing metadata analysis. We reported that several genes that were not known to be associated with hypoxia, *GPR146*, *TMEM74B*, *PPP1R3G*, and *PRSS53*, were upregulated by hypoxic stimulation.

We analyzed 69 data series related to hypoxia, which were selected from the entire gene expression data registered in GEO, and obtained 495 HN-pairs, which is about four times more than previously reported [5]. In this study, 65.5% of the gene expression data were derived from cancer experiments, reflecting the demand for these data in hypoxia-related cancer research and ease of handling. We believe that each gene was evaluated without publication bias. Our study was possible because of the availability of data from public databases.

First, the Metascape and ChIP-Atlas enrichment analyses of the UP 100 gene list showed their association with hypoxia-related gene sets as expected, and hence, we concluded that HN-score helps select the hypoxia-inducible genes (Table 1, Figure 2). Thus, we decided to proceed with the analysis of the UP 100 gene list in subsequent analyses. On the other hand, Metascape enrichment analysis of the DOWN 100 gene list suggested an association with the metabolic processes of ncRNA (Figure 2b). This suggests that hypoxic stimulation may also affect the expression of ncRNAs. In this study, only the protein-coding genes of GENCODE were quantitatively analyzed, and hence, ncRNAs were excluded from this analysis. Further studies are needed to identify ncRNAs involved in hypoxic stimulation.

Gene2pubmed has been used to determine the order of genes retrieved by RefEx [33]. In this study, we used gene2pubmed to evaluate the genes that are not as well-known as hypoxia-related genes. We used gene2pubmed to calculate two variables: the number of publications per gene and the Simpson similarity coefficient for HIF1A. The Simpson similarity coefficient measures the strength of the co-occurrence of PubMed IDs associated with HIF1A or with a gene. If the Simpson similarity coefficient is close to 1, the relationship between PubMed IDs and HIF1A is considered strong; however, the lower the number of PubMed IDs on the side being compared indicates a poor relationship. For this reason, we visualized the number of publications and Simpson similarity coefficient for the genes in the UP 100 gene list in the scatter plot. In addition, we also plotted HIF-1-regulated genes [32] in this plot (Figure 3a). The Simpson similarity coefficient was lower in the case of more publications; this might be because of the fact that more relationships were revealed, and thus, the Simpson similarity coefficient is likely to be underestimated. The classical HIF-1 regulated genes scored high in the Simpson similarity coefficient and was plotted on the upper side of regression line, despite a large number of publications. The genes with a small number of publications, such as ankyrin repeat domain 37, which was reported to be regulated by HIF1A [34], were also plotted above the regression line. Therefore, we hypothesized that the genes plotted below the regression line, such as *GPR146*, *SPAG4*, *TMEM74B*, *PPP1R3G* and *PRSS53* might be considered as candidates for novel hypoxia-inducible genes. The log₂-transformed HN ratio of these genes was visualized as a box plot (Figure 3b). These genes had positive HN-ratio values, as well as genes with known hypoxic responses, such as *VEGFA*. Although some reports state that *SPAG4* is related to hypoxia [35,36], no reports were available in a PubMed search related to hypoxia-related genes other than *SPAG4*.

We focused on *GPR146* because it is a G protein-coupled receptor and therefore worth considering as a drug target and because it has a higher HN-score than other genes. In the similarity coefficient analysis using gene2pubmed, three reports on the co-occurrence of PubMed IDs between HIF1A and *GPR146* were available [37–39]. These were overall genetic analyses and did not focus on hypoxia. We confirmed that *GPR146* was upregulated, which was plotted below the regression line in the scatter plot (Figure 3a), similar to other known hypoxia-inducible genes. *GPR146* was not reported to be associated with hypoxia in the PubMed search; thus, we believe that *GPR146* is an important hypoxia-inducible gene that has not been focused on so far. In hypoxia studies using comprehensive gene

expression data [40,41], *GPR146* is included in the list of genes upregulated by hypoxic stimulation. However, according to previous reports, *GPR146* is just a gene among many hypoxia-related genes. The inhibition of GPR146 is involved in lowering cholesterol levels [42]. C-peptide, a putative ligand of GPR146, inhibited low O₂-induced ATP release in erythrocytes [43]. The biological function of GPR146 is expected to be further elucidated in future studies.

We focused on the hypoxic response and visualized the number of research reports for each gene using gene2pubmed data. We identified the novel genes by using public data containing thousands of pieces of gene expression information, which can be obtained regardless of the researcher's interest. As shown in Figure 3b, the gene expression variation at each time point was not constant. Also, the tissues and cells in each data set were different. In this study, we only made a rough evaluation of the variation in gene expression by using the collective intelligence from the public database. Further stratification analysis will be undertaken in our future work. We plan to continue using public databases to discover similar new findings. For example, we believe that the ncRNA field, where hypothesis generation is difficult due to the lack of information, has great potential for new discoveries. At present, the number of known human long ncRNA transcripts exceeds several hundred thousand [44,45]. We plan to investigate the gene expression of ncRNAs under hypoxic conditions, based on our results of the effect of hypoxia on metabolic process-related genes of ncRNA (Figure 2b).

5. Conclusions

Multi-omics analysis of the transcriptome and bibliome revealed that several genes, which were not known to be associated with hypoxia, were upregulated under hypoxic conditions.

Author Contributions: Conceptualization, Y.O., H.B.; methodology, Y.O.; software, Y.O.; validation, Y.O., H.B.; formal analysis, Y.O., H.B.; investigation, Y.O.; resources, Y.O., H.B.; data curation, Y.O.; writing—Original draft preparation, Y.O.; writing—Review and editing, H.B.; visualization, Y.O.; supervision, H.B.; project administration, H.B.; funding acquisition, H.B. All authors have read and agreed to the published version of the manuscript.

Funding: This research was supported by the Center of Innovation for Bio-Digital Transformation (BioDX), a program on the open innovation platform for industry-academia co-creation (COI-NEXT), Japan Science and Technology Agency (JST, COI-NEXT, JPMJPF2010). This research was also supported by ROIS-DS-JOINT (010RP2020) and JSPS KAKENHI Grant Number 20H03776.

Institutional Review Board Statement: Not applicable.

Informed Consent Statement: Not applicable.

Data Availability Statement: The data presented in this study are openly available in figshare [46]. Source codes to replicate the study are also freely available at GitHub under the MIT license [25].

Acknowledgments: Authors would like to thank the late Yusuke Yamada for helpful discussions in the initial stage of this study.

Conflicts of Interest: The authors declare no conflict of interest. The funders had no role in the design of the study; in the collection, analyses, or interpretation of data; in the writing of the manuscript, or in the decision to publish the results.

References

1. Carter, A.J.; Kraemer, O.; Zwick, M.; Mueller-Fahrnow, A.; Arrowsmith, C.H.; Edwards, A.M. Target 2035: Probing the Human Proteome. *Drug Discov. Today* **2019**, *24*, 2111–2115. [[CrossRef](#)]
2. Barrett, T.; Wilhite, S.E.; Ledoux, P.; Evangelista, C.; Kim, I.F.; Tomashevsky, M.; Marshall, K.A.; Phillippy, K.H.; Sherman, P.M.; Holko, M.; et al. NCBI GEO: Archive for Functional Genomics Data Sets—Update. *Nucleic Acids Res.* **2013**, *41*, D991–D995. [[CrossRef](#)]
3. Athar, A.; Füllgrabe, A.; George, N.; Iqbal, H.; Huerta, L.; Ali, A.; Snow, C.; Fonseca, N.A.; Petryszak, R.; Papatheodorou, I.; et al. ArrayExpress Update—From Bulk to Single-Cell Expression Data. *Nucleic Acids Res.* **2019**, *47*, D711–D715. [[CrossRef](#)]

4. Kodama, Y.; Mashima, J.; Kosuge, T.; Ogasawara, O. DDBJ Update: The Genomic Expression Archive (GEA) for Functional Genomics Data. *Nucleic Acids Res.* **2019**, *47*, D69–D73. [CrossRef]
5. Bono, H.; Hirota, K. Meta-Analysis of Hypoxic Transcriptomes from Public Databases. *Biomedicines* **2020**, *8*, 10. [CrossRef] [PubMed]
6. Cheung, W.A.; Ouellette, B.F.; Wasserman, W.W. Inferring Novel Gene–Disease Associations Using Medical Subject Heading Over-Representation Profiles. *Genome Med.* **2012**, *4*, 75. [CrossRef] [PubMed]
7. Fischer, I.; Barak, B. Molecular and Therapeutic Aspects of Hyperbaric Oxygen Therapy in Neurological Conditions. *Biomolecules* **2020**, *10*, 1247. [CrossRef] [PubMed]
8. Mahon, P.C.; Hirota, K.; Semenza, G.L. HIF-1: A Novel Protein That Interacts with HIF-1 α and VHL to Mediate Repression of HIF-1 Transcriptional Activity. *Genes Dev.* **2001**, *15*, 2675–2686. [CrossRef] [PubMed]
9. Jaakkola, P.; Mole, D.R.; Tian, Y.M.; Wilson, M.I.; Gielbert, J.; Gaskell, S.J.; von Kriegsheim, A.; Hebestreit, H.F.; Mukherji, M.; Schofield, C.J.; et al. Targeting of HIF- α to the von Hippel-Lindau Ubiquitylation Complex by O₂-Regulated Prolyl Hydroxylation. *Science* **2001**, *292*, 468–472. [CrossRef] [PubMed]
10. Ebert, B.L.; Bunn, H.F. Regulation of Transcription by Hypoxia Requires a Multiprotein Complex That Includes Hypoxia-Inducible Factor 1, an Adjacent Transcription Factor, and P300/CREB Binding Protein. *Mol. Cell. Biol.* **1998**, *18*, 4089–4096. [CrossRef]
11. AOE. Available online: <https://aoe.dbcls.jp/> (accessed on 27 February 2021).
12. Bono, H. All of Gene Expression (AOE): An Integrated Index for Public Gene Expression Databases. *PLoS ONE* **2020**, *15*, e0227076. [CrossRef]
13. Kodama, Y.; Shumway, M.; Leinonen, R.; on behalf of the International Nucleotide Sequence Database Collaboration. The Sequence Read Archive: Explosive Growth of Sequencing Data. *Nucleic Acids Res.* **2012**, *40*, D54–D56. [CrossRef]
14. Ono, Y. Information on Hypoxic Conditions and Samples in the Dataset Used for the Meta-Analysis. *figshare* **2021**. [CrossRef]
15. Download SRA Sequences from Entrez Search Results. Available online: <https://www.ncbi.nlm.nih.gov/sra/docs/srdownload/> (accessed on 27 February 2021).
16. Yoshiaki/Ikra: RNAseq Pipeline Centered on Salmon. Available online: <https://github.com/yoshiaki/ikra> (accessed on 27 February 2021).
17. Patro, R.; Duggal, G.; Love, M.I.; Irizarry, R.A.; Kingsford, C. Salmon Provides Fast and Bias-Aware Quantification of Transcript Expression. *Nat. Methods* **2017**, *14*, 417–419. [CrossRef]
18. Ono, Y. Quantitative Gene Expression Data of Hypoxia Experimental Data Sets. *figshare* **2021**. [CrossRef]
19. Ono, Y. Ratio of Gene Expression under Hypoxic and Normoxic Conditions (HN-Ratio). *figshare* **2021**. [CrossRef]
20. Sonesson, C.; Love, M.I.; Robinson, M.D. Differential Analyses for RNA-Seq: Transcript-Level Estimates Improve Gene-Level Inferences. *F1000Res* **2016**, *4*, 1521. [CrossRef] [PubMed]
21. Metascape. Available online: <https://metascape.org> (accessed on 27 February 2021).
22. Zhou, Y.; Zhou, B.; Pache, L.; Chang, M.; Khodabakhshi, A.H.; Tanaseichuk, O.; Benner, C.; Chanda, S.K. Metascape Provides a Biologist-Oriented Resource for the Analysis of Systems-Level Datasets. *Nat. Commun.* **2019**, *10*, 1523. [CrossRef]
23. ChIP-Atlas. Available online: <https://chip-atlas.org/> (accessed on 27 February 2021).
24. Oki, S.; Ohta, T.; Shioi, G.; Hatanaka, H.; Ogasawara, O.; Okuda, Y.; Kawaji, H.; Nakaki, R.; Sese, J.; Meno, C. ChIP-Atlas: A Data-Mining Suite Powered by Full Integration of Public ChIP-Seq Data. *EMBO Rep.* **2018**, *19*, e46255. [CrossRef] [PubMed]
25. No85j/Hypoxia_Code. Available online: https://github.com/no85j/hypoxia_code (accessed on 2 March 2021).
26. Index of /Gene/DATA. Available online: <https://ftp.ncbi.nlm.nih.gov/gene/DATA/> (accessed on 27 February 2021).
27. Ono, Y. Score Based on the Ratio of Gene Expression between Hypoxic and Normoxic Conditions (HN-Score). *figshare* **2021**. [CrossRef]
28. Ono, Y. Genelist_Top 100 Human Genes Up-Regulated under Hypoxic Conditions. *figshare* **2021**. [CrossRef]
29. Ono, Y. Genelist_Top 100 Human Genes Down-Regulated under Hypoxic Conditions. *figshare* **2021**. [CrossRef]
30. Ono, Y. Number of Publications per Human Gene. *figshare* **2021**. [CrossRef]
31. Ono, Y. Simpson Similarity of Each Human Gene to HIF1A Based on Gene2pubmed. *figshare* **2021**. [CrossRef]
32. Hirota, K.; Semenza, G.L. Regulation of Angiogenesis by Hypoxia-Inducible Factor 1. *Crit. Rev. Oncol./Hematol.* **2006**, *59*, 15–26. [CrossRef]
33. Ono, H.; Ogasawara, O.; Okubo, K.; Bono, H. RefEx, a Reference Gene Expression Dataset as a Web Tool for the Functional Analysis of Genes. *Sci. Data* **2017**, *4*, 170105. [CrossRef] [PubMed]
34. Benita, Y.; Kikuchi, H.; Smith, A.D.; Zhang, M.Q.; Chung, D.C.; Xavier, R.J. An Integrative Genomics Approach Identifies Hypoxia Inducible Factor-1 (HIF-1)-Target Genes That Form the Core Response to Hypoxia. *Nucleic Acids Res.* **2009**, *37*, 4587–4602. [CrossRef] [PubMed]
35. Shoji, K.; Murayama, T.; Mimura, I.; Wada, T.; Kume, H.; Goto, A.; Ohse, T.; Tanaka, T.; Inagi, R.; van der Hoorn, F.A.; et al. Sperm-Associated Antigen 4, a Novel Hypoxia-Inducible Factor 1 Target, Regulates Cytokinesis, and Its Expression Correlates with the Prognosis of Renal Cell Carcinoma. *Am. J. Pathol.* **2013**, *182*, 2191–2203. [CrossRef]
36. Knaup, K.X.; Monti, J.; Hackenbeck, T.; Jobst-Schwan, T.; Klanke, B.; Schietke, R.E.; Wacker, I.; Behrens, J.; Amann, K.; Eckardt, K.-U.; et al. Hypoxia Regulates the Sperm Associated Antigen 4 (SPAG4) via HIF, Which Is Expressed in Renal Clear Cell Carcinoma and Promotes Migration and Invasion in Vitro. *Mol. Carcinog.* **2014**, *53*, 970–978. [CrossRef]

37. Strausberg, R.L.; Feingold, E.A.; Grouse, L.H.; Derge, J.G.; Klausner, R.D.; Collins, F.S.; Wagner, L.; Shenmen, C.M.; Schuler, G.D.; Altschul, S.F.; et al. Generation and Initial Analysis of More than 15,000 Full-Length Human and Mouse CDNA Sequences. *Proc. Natl. Acad. Sci. USA* **2002**, *99*, 16899–16903. [[CrossRef](#)]
38. Gerhard, D.S.; Wagner, L.; Feingold, E.A.; Shenmen, C.M.; Grouse, L.H.; Schuler, G.; Klein, S.L.; Old, S.; Rasooly, R.; Good, P.; et al. The Status, Quality, and Expansion of the NIH Full-Length CDNA Project: The Mammalian Gene Collection (MGC). *Genome Res.* **2004**, *14*, 2121–2127. [[CrossRef](#)]
39. Kimura, K.; Wakamatsu, A.; Suzuki, Y.; Ota, T.; Nishikawa, T.; Yamashita, R.; Yamamoto, J.; Sekine, M.; Tsuritani, K.; Wakaguri, H.; et al. Diversification of Transcriptional Modulation: Large-Scale Identification and Characterization of Putative Alternative Promoters of Human Genes. *Genome Res.* **2006**, *16*, 55–65. [[CrossRef](#)]
40. Labrecque, M.P.; Takhar, M.K.; Nason, R.; Santacruz, S.; Tam, K.J.; Massah, S.; Haegert, A.; Bell, R.H.; Altamirano-Dimas, M.; Collins, C.C.; et al. The Retinoblastoma Protein Regulates Hypoxia-Inducible Genetic Programs, Tumor Cell Invasiveness and Neuroendocrine Differentiation in Prostate Cancer Cells. *Oncotarget* **2016**, *7*, 24284–24302. [[CrossRef](#)]
41. Qi, J.; Nakayama, K.; Cardiff, R.D.; Borowsky, A.D.; Kaul, K.; Williams, R.; Krajewski, S.; Mercola, D.; Carpenter, P.M.; Bowtell, D.; et al. Siah2-Dependent Concerted Activity of HIF and FoxA2 Regulates Formation of Neuroendocrine Phenotype and Neuroendocrine Prostate Tumors. *Cancer Cell* **2010**, *18*, 23–38. [[CrossRef](#)] [[PubMed](#)]
42. Yu, H.; Rimbart, A.; Palmer, A.E.; Toyohara, T.; Xia, Y.; Xia, F.; Ferreira, L.M.R.; Chen, Z.; Chen, T.; Loaiza, N.; et al. GPR146 Deficiency Protects Against Hypercholesterolemia and Atherosclerosis. *Cell* **2019**, *179*, 1276–1288.e14. [[CrossRef](#)] [[PubMed](#)]
43. Richards, J.P.; Yosten, G.L.C.; Kolar, G.R.; Jones, C.W.; Stephenson, A.H.; Ellsworth, M.L.; Sprague, R.S. Low O₂-Induced ATP Release from Erythrocytes of Humans with Type 2 Diabetes Is Restored by Physiological Ratios of C-Peptide and Insulin. *Am. J. Physiol. Regul. Integr. Comp. Physiol.* **2014**, *307*, R862–R868. [[CrossRef](#)]
44. Fang, S.; Zhang, L.; Guo, J.; Niu, Y.; Wu, Y.; Li, H.; Zhao, L.; Li, X.; Teng, X.; Sun, X.; et al. NONCODEV5: A Comprehensive Annotation Database for Long Non-Coding RNAs. *Nucleic Acids Res.* **2018**, *46*, D308–D314. [[CrossRef](#)]
45. Ma, L.; Cao, J.; Liu, L.; Du, Q.; Li, Z.; Zou, D.; Bajic, V.B.; Zhang, Z. LncBook: A Curated Knowledgebase of Human Long Non-Coding RNAs. *Nucleic Acids Res.* **2019**, *47*, D128–D134. [[CrossRef](#)] [[PubMed](#)]
46. Ono, Y. Multiomic Meta-Analysis of Hypoxic Stress from Public Databases. *bioRxiv* **2021**. [[CrossRef](#)]

MDPI
St. Alban-Anlage 66
4052 Basel
Switzerland
Tel. +41 61 683 77 34
Fax +41 61 302 89 18
www.mdpi.com

Biomedicines Editorial Office
E-mail: biomedicines@mdpi.com
www.mdpi.com/journal/biomedicines



MDPI
St. Alban-Anlage 66
4052 Basel
Switzerland

Tel: +41 61 683 77 34
Fax: +41 61 302 89 18

www.mdpi.com



ISBN 978-3-0365-2913-4